

Materials Horizons: From Nature to Nanomaterials

Shrikrishna Nandkishor Joshi
Pranjal Chandra *Editors*

Advanced Micro- and Nano- manufacturing Technologies

Applications in Biochemical and
Biomedical Engineering

 Springer

Materials Horizons: From Nature to Nanomaterials

Series Editor

Vijay Kumar Thakur, School of Aerospace, Transport and Manufacturing,
Cranfield University, Cranfield, UK

Materials are an indispensable part of human civilization since the inception of life on earth. With the passage of time, innumerable new materials have been explored as well as developed and the search for new innovative materials continues briskly. Keeping in mind the immense perspectives of various classes of materials, this series aims at providing a comprehensive collection of works across the breadth of materials research at cutting-edge interface of materials science with physics, chemistry, biology and engineering.

This series covers a galaxy of materials ranging from natural materials to nanomaterials. Some of the topics include but not limited to: biological materials, biomimetic materials, ceramics, composites, coatings, functional materials, glasses, inorganic materials, inorganic-organic hybrids, metals, membranes, magnetic materials, manufacturing of materials, nanomaterials, organic materials and pigments to name a few. The series provides most timely and comprehensive information on advanced synthesis, processing, characterization, manufacturing and applications in a broad range of interdisciplinary fields in science, engineering and technology.

This series accepts both authored and edited works, including textbooks, monographs, reference works, and professional books. The books in this series will provide a deep insight into the state-of-art of Materials Horizons and serve students, academic, government and industrial scientists involved in all aspects of materials research.

More information about this series at <http://www.springer.com/series/16122>

Shrikrishna Nandkishor Joshi · Pranjal Chandra
Editors

Advanced Micro- and Nano-manufacturing Technologies

Applications in Biochemical and Biomedical
Engineering

 Springer

Editors

Shrikrishna Nandkishor Joshi
Department of Mechanical Engineering
Indian Institute of Technology Guwahati
Guwahati, Assam, India

Pranjal Chandra
School of Biochemical Engineering
Indian Institute of Technology (BHU)
Varanasi
Varanasi, Uttar Pradesh, India

ISSN 2524-5384

ISSN 2524-5392 (electronic)

Materials Horizons: From Nature to Nanomaterials

ISBN 978-981-16-3644-8

ISBN 978-981-16-3645-5 (eBook)

<https://doi.org/10.1007/978-981-16-3645-5>

© The Editor(s) (if applicable) and The Author(s), under exclusive license to Springer Nature Singapore Pte Ltd. 2022

This work is subject to copyright. All rights are solely and exclusively licensed by the Publisher, whether the whole or part of the material is concerned, specifically the rights of translation, reprinting, reuse of illustrations, recitation, broadcasting, reproduction on microfilms or in any other physical way, and transmission or information storage and retrieval, electronic adaptation, computer software, or by similar or dissimilar methodology now known or hereafter developed.

The use of general descriptive names, registered names, trademarks, service marks, etc. in this publication does not imply, even in the absence of a specific statement, that such names are exempt from the relevant protective laws and regulations and therefore free for general use.

The publisher, the authors and the editors are safe to assume that the advice and information in this book are believed to be true and accurate at the date of publication. Neither the publisher nor the authors or the editors give a warranty, expressed or implied, with respect to the material contained herein or for any errors or omissions that may have been made. The publisher remains neutral with regard to jurisdictional claims in published maps and institutional affiliations.

This Springer imprint is published by the registered company Springer Nature Singapore Pte Ltd. The registered company address is: 152 Beach Road, #21-01/04 Gateway East, Singapore 189721, Singapore

Preface

Micro- and nano-manufacturing technologies deal with miniaturized fabrication techniques that create features, products, systems, and devices having dimensions in the range of nanometers to millimeters. These devices include functional segments, immobile assemblies, or both. In today's date, micro–nano-fabrication and manufacturing have become an integral part of applications in biochemical and biomedical disciplines. These applications can be majorly categorized into four domains: application in molecular biology and biochemical science, application focusing on cellular systems, prototyping of medical devices, and development of biosensors.

Micro- and nano-manufacturing structures provide a considerably improved function for conventional devices. These fabrication techniques always offer great potentials. Such enhanced and improved potentials are deliberated when these techniques are exploited appropriately to address the right types of problems. Considering the massive advancement of micro–nano-manufacturing technologies, this book attempts to provide an illustrative knowledge regarding these techniques between its two covers. It discusses vividly the principles of various advanced manufacturing technologies applied to develop different biomedical devices. Techniques including advanced microchannel fabrication, advanced finishing processes, and rapid manufacturing for configuring biomedical devices have been accounted for. The novel areas of interest considering the mediators like nanomaterials, piezoelectric nanogenerators, localized surface plasmon resonance for sensor development, and fabrication have also been discussed thoroughly. This book also collectively detailed the varying advantages presented by these techniques and how these advantages have been explored to date. We believe the chapters presented in the book cover various new dimensions of micro- and nano-manufacturing technologies and their most recent applications in biochemical and biomedical engineering. This book not only will be helpful for the students, scholars, and faculty members, but will also help the newcomers in the field and the industry experts.

Guwahati, India
Varanasi, India

Shrikrishna Nandkishor Joshi
Pranjal Chandra

Contents

1	Nanomaterials Based Biosensing: Methods and Principle of Detection	1
	Nirmal Kumar Katiyar, Gaurav Goel, and Saurav Goel	
2	Pathways to Translate the Biomedical Prototypes	29
	Tamanna Bhuyan, Surjendu Maity, Devi Rupa Saha, Nayan Mani Das, and Dipankar Bandyopadhyay	
3	Accuracy of Biosensors as Rapid Diagnostic and Biochemical Monitoring Tools for Non-communicable Diseases Management	57
	Norhafizah Muhammad, Lim Tiong Hoo, Afiqah Nabihah Ahmad, Azureen Mohamad, and Syazana Abdullah Lim	
4	Rapid Manufacturing of Biomedical Devices: Process Alternatives, Selection and Planning	77
	Sanchit Jhunjhunwala and Sajan Kapil	
5	Advanced Finishing Processes for Biomedical Applications	105
	Talwinder Singh Bedi, Ravi Kant, and Hema Gurung	
6	Advanced Microchannel Fabrication Technologies for Biomedical Devices	127
	Upasana Sarma, Pranjal Chandra, and Shrikrishna N. Joshi	
7	Droplet Microfluidics—A Tool for Biosensing and Bioengineering Applications	145
	U. Banerjee, R. Iqbal, S. Hazra, N. Satpathi, and A. K. Sen	
8	Advances in Microfluidic Techniques for Detection and Isolation of Circulating Tumor Cells	173
	K. Mirkale, R. Gaikwad, B. Majhy, G. Narendran, and A. K. Sen	

9	Localized Surface Plasmon Resonance Sensors for Biomarker Detection with On-Chip Microfluidic Devices in Point-of-Care Diagnostics	199
	S. Z. Hoque, L. Somasundaram, R. A. Samy, A. Dawane, and A. K. Sen	
10	Development of Piezoelectric Nanogenerator Based on Micro/Nanofabrication Techniques and Its Application on Medical Devices	225
	Aparna Zagabathuni and Subramani Kanagaraj	
11	Optical Biosensors Towards Point of Care Testing of Various Biochemicals	245
	Vinoth Edal Joseph and Archana Ramadoss	
12	Blood Coagulation System and Carbon-Based Nanoengineering for Biomedical Application	279
	Abhishek R. Panigrahi, Pooja Yadav, Samir K. Beura, and Sunil K. Singh	
13	Opportunities and Challenges in Medical Robotic Device Development	299
	Neha Khatri, Mukesh Kumar, and Ranjan Jha	
14	Flexible Organic Field-Effect Transistors for Biomimetic Applications	315
	Vivek Raghuwanshi and Shree Prakash Tiwari	
15	Methods for Surface Superfinishing of Prosthesis	335
	Atul Singh Rajput, Sajan Kapil, and Manas Das	
16	Principles of Advanced Manufacturing Technologies for Biomedical Devices	361
	G. L. Samuel, Lingxue Kong, Y. Arcot, and Pavan Pandit	

About the Editors



Prof. Shrikrishna Nandkishor Joshi is a Professor of Mechanical Engineering at the Indian Institute of Technology (IIT) Guwahati, India. He was a Visiting Faculty at the Asian Institute of Technology, Thailand in 2015. His research interests include micro, nano, and precision manufacturing processes with a focus on applications of lasers in manufacturing, thin-wall machining, single point diamond turning, CAD/CAM, and manufacturing automation. Prof. Joshi published more than seventy research articles in journals of international repute and conferences. He has published two books on Laser-based Manufacturing and authored more than ten book chapters. He has developed a Massive Open Online Course on “Automation in Manufacturing” and a web course on “Mechatronics and Manufacturing Automation” as part of the Government of India’s flagship project National Programme on Technology Enhanced Learning (NPTEL).



Prof. Pranjal Chandra is an Assistant Professor at the School of Biochemical Engineering, Indian Institute of Technology (BHU), Varanasi, India. He earned his Ph.D. from Pusan National University, South Korea and did post-doctoral training at Technion-Israel Institute of Technology, Israel. His research focus is highly interdisciplinary, spanning a wide range in biotechnology, nanobiosensors, material engineering, and nanomedicine. He has designed several commercially viable biosensing prototypes that can be operated for onsite analysis for biomedical diagnostics. He is a guest editor and an editorial board member of various international journals. He is author of over 100

high impact publications including research/reviews papers and invited book chapter. He has published 11 books on various aspects of biosensors/medical diagnostics. Dr. Chandra is the recipient of many prestigious awards, coveted honors, and fellowships such as: DST Ramanujan fellowship (Government of India); Early Career Research Award (ECRA) (DST, Government of India); BK-21 and NRF fellowship, South Korea; Technion Post-Doctoral Fellowship, Israel; Nano Molecular Society India Young Scientist Award; Biotech Research Society India (BRSI) Young Scientist Award; Young Engineers Award 2018; Highly Cited Corresponding authors in The Royal Society of Chemistry (RSC), Cambridge, London; Top 10% cited article in the General Chemistry Section RSC Journal, Cambridge, London, Gandhian Young Technology Innovation Award (GYTI) 2020, etc. Dr. Chandra is also listed among the world's top 2% scientist in a report by Stanford University, USA.

Chapter 1

Nanomaterials Based Biosensing: Methods and Principle of Detection



Nirmal Kumar Katiyar , Gaurav Goel , and Saurav Goel 

Abbreviations

CNT	Carbon nanotube
D	Dimensional
DNA	Deoxyribonucleic acid
FAD	Flavinadenine dinucleotide
FET	Field Effect Transistor
NPs	Nanoparticles
RI	Refractive index
SPCE	Screen Printed Carbon Electrode
SERS	Surface-enhanced Raman scattering
SPR	Surface plasmon resonance
SWCNTs	Single Wall Carbon Nanotubes

N. K. Katiyar · G. Goel (✉) · S. Goel
School of Engineering, London South Bank University, 103 Borough Road, London 1 0AA, UK
e-mail: Goelg@lsbu.ac.uk

N. K. Katiyar
e-mail: kumarn@lsbu.ac.uk

S. Goel
e-mail: Goels@lsbu.ac.uk

S. Goel
EPSRC Centre for Doctoral Training in Ultra-Precision Engineering, University of Cambridge
and Cranfield University, Bedfordshire, UK

School of Aerospace, Transport and Manufacturing, Cranfield University,
Bedfordshire MK43 0AL, UK

Department of Mechanical Engineering, Shiv Nadar University, Gautam Budh Nagar,
Chennai 201314, India

1 Introduction

Biosensing is an emerging research area that is being governed by the need to develop easy, simple, and inexpensive biosensors with instant and precise detection. Nanotechnology has brought tremendous capability to miniaturize biosensors and to make them more affordable. On the other hand, conventional methods of measurement are limited by the complexity of the process and requirement of skilled manpower and time to measure a particular change or property. A simple question one may ask, how does a sensor make life easy for humans? We can understand this through the utilization of biosensors in our daily life, such as a diabetic person can measure their glucose level instantly anywhere by herself/himself, pregnancy diagnostic kits can now be used conveniently without any prior experience and are easily affordable.

One of the simplest biosensors is the body temperature measurement sensor, which most of the people uses in their life. There are many non-bio sensors in our daily life such as a clock or a watch to record time, a mobile phone used to receive the data and voice communication including the pedometer inside it, as well as a speedometer measuring the speed of the bike. Sensors measuring a single parameter may have different working principles but they all do the same thing, i.e. measure the magnitude of certain property such as a thermometer based on Hg (Mercury) measures thermal expansion, a non-contact thermometer based on infra-red radiations popularly used recently for fast monitoring of the body temperature caused by COVID-19, and a digital thermometer based on thermistor (thermocouple) principle. All three devices have the same goal to measure temperature, as shown in Fig. 1.

Similarly, in the food and medical sectors, many biosensors are based on leveraging different working principles such as estimation of glucose in the blood sample,

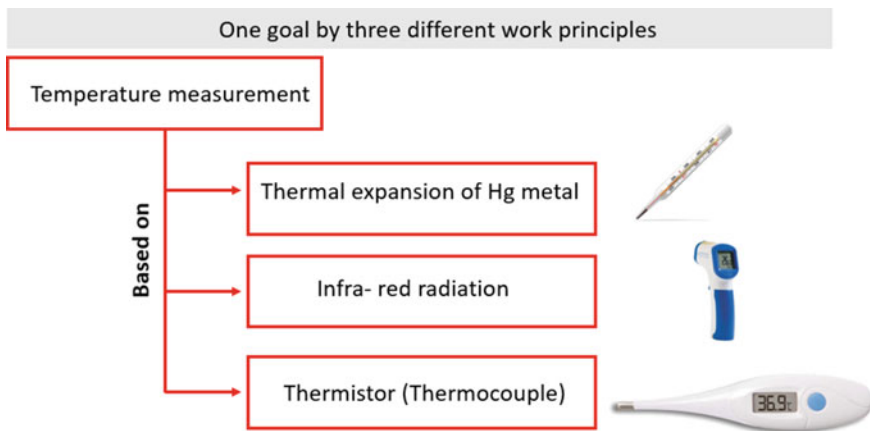


Fig. 1 Temperature measurement sensor with three different working principles

cancer cell detection, bacteria detection, DNA identification, virus detection, detection of pesticides/chemicals/antibiotics, and biological toxin level detection in food and beverages. Biosensors are becoming an integral part of our life to raise awareness and consciousness at the early stages of a process. Biosensors either detect the target analytes or provides exact measurements. Different target analytes require different biosensors, and it can be associated with different working principles. Therefore, emerging nanoscale materials have been employed in combination with newer electronic circuits to develop easy to handle nanoplatforms for sensing various types of analytes. Nanoscale integrated biosensors can work as multiplexed biosensors, or one sensor can detect more than one analyte. However, the prime goal behind the development of biosensors is to improve the lower limit of detection.

Many biosensors are being used in medical and food sectors, having different work principles such as acoustic wave biosensors, electrochemical biosensors, fluorescent paper-based sensors, electrogenerated chemiluminescence, colourimetric detection, Microbial fuel cell-based biosensor, etc. There are multiple biosensors, which are part of daily use. They can be classified into various categories such as diverse principle-based, different sectors based, and different materials based, such as paper-based biosensors, electronic biosensors, hydrogel-based sensors, etc. This chapter is limited in scope to discuss various essential principles being used in the development of biosensors utilizing nanomaterials and categorization based on nanomaterials dimensions for example zero, one, and two-dimensional nanomaterials (nanoparticles, nanofibers, and nanosheets).

2 What Makes a Sensor Good?

The quality of a biosensor depends on some of its salient features such as selectivity, stability, reproducibility, sensitivity, and linearity. Besides these properties, the sensor must be economical. Modern technology is integrated with nanoscience/technology, which makes biosensors ultrasensitive, and they can detect even a single biomolecule.

Fast detection: The quick response of a sensor has its importance, especially in point-of-care diagnostic. Also, during a life-threatening incident, the rapid response of the sensor is essential such as heartbeat monitoring, in-vivo monitoring, etc.

Selective detection: Selective detection of analytes by a biosensor is equally crucial because most of the biological samples (e.g. Blood) and food (e.g. Beverage), etc. are the pool of biochemicals. A biosensor needs to detect only the particular analytes, for which it is tuned, and it must be neutral to other interfering analytes. It is known as the selectivity of the biosensor.

Reproducibility: Reproducibility is the ability of a biosensor to produce similar or identical results every time the measurement is repeated, or we can say there is a negligible change in the result during multiple measurements.

Stability: The stability of a biosensor is an essential factor and indicates the consistency in results after a biosensor is deployed for a long time (storage/transportation). Better stability guarantees consistency, reproducible results, and precision regardless of secondary factors such as environmental conditions.

Accuracy of biosensor: The human body is prone to respond to slight chemical change. Therefore, a sensor must be accurate to quantify the measurement.

Minimum sample requirement: The sampling requirement for sensing is an important parameter and the smallest quantity requirement is the best especially in forensic science, where destructive testing and availability of samples could be very limited.

3 Methods for Biosensors Formulation

A biosensor is a device having three parts, as shown in Fig. 2, the first part being the biological recognition system, which is highly specific towards the analytes and provides quick response on interaction with analytes. The second part is a transducer, which takes the response from the recognition system, and converts it into an electric signal, which is calibrated with the standard value of the response. The third part deals with the amplification of the weak signals and displays on the controlling unit, although it is not necessary for all biosensors.

Recently developed biosensors are based on various types of nanomaterials and possess advantage due to their high surface energy to volume ratio, and delivers response on minor changes over the surface such as metallic nanoparticle change their surface plasmon response on binding with other molecules, nanowires change their frequency of vibration on binding with another biomolecule, fluorescence efficiency variation in nanosheets on the landing of analytes, etc., as shown in Fig. 3.

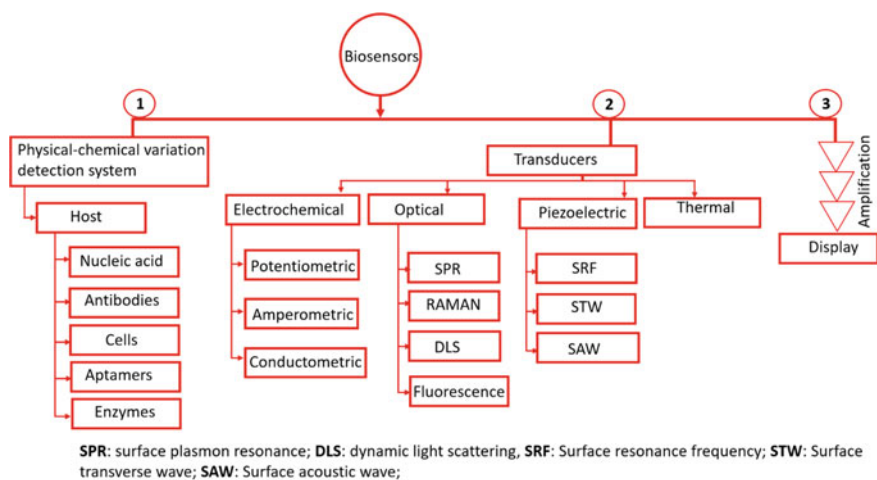


Fig. 2 Classification of biosensor parts and working principles

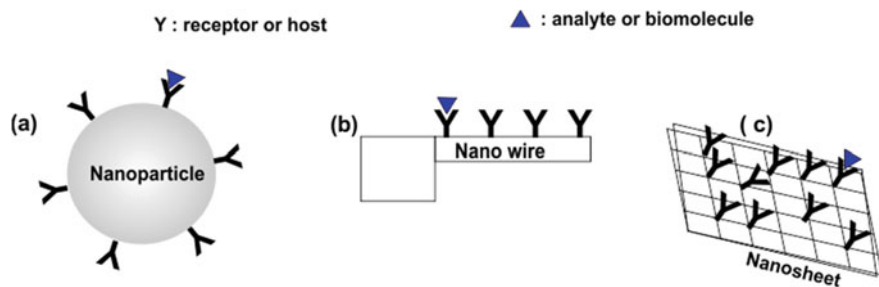


Fig. 3 Schematic of functionalization with receptor. **a** nanoparticles 0D, **b** nanowire 1D, **c** nanosheet 2D

4 Working Principle

The following sections discuss the various working principles for the different biosensors based on various nanomaterials (i.e. 0D, 1D, and, 2D). These working principles may be used individually or in combination to achieve optimum results.

4.1 Nanoparticles (0D Materials)

The materials with all three dimensions less than 100 nm are considered nanoparticles [1, 2]. They have unique and sensitive properties suitable for developing the biosensors such as high surface energy to bind with other molecules, surface plasmon resonance, etc. The nanoparticles-based biosensor is further divided into two categories: Label-based biosensor and Label-free biosensor. In the former technique, nanoparticles functionalized with the specific receptor (enzyme, fluorescence, antibody, etc.) directly bind to the analytes. On the other hand, in the Label-free technique, the nanoparticles directly interact with the analytes to give the response.

4.1.1 Surface Plasmon Resonance-Based

The surface plasmon resonance (SPR) is a versatile character of the metallic nanoparticles. This phenomenon is recognized by the collective oscillation of the valance electrons when incident electromagnetic radiation oscillation matches the surface electrons, and it appears as an absorption band, the schematic of oscillation shown in Fig. 4 [3]. The position of the absorption band is very sensitive to the dielectric constant of the surrounding medium, nanoparticle shape, size, and ligand interactions (increase or decrease surface electron density). The shifting of the band towards a lower wavelength (high energy) is referred to as a blue shift and shifting of the band towards a higher wavelength (lower energy) is referred to as redshift. The shift of

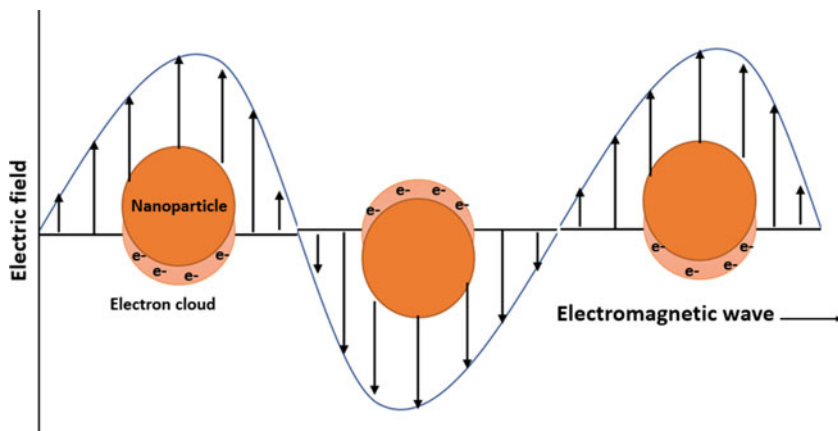


Fig. 4 Surface plasmon resonance on nanoparticles

the SPR band by more than 2 nm in the visible range (~ 500 nm wavelength) can be recorded easily. On the change of SPR band position (by analytes-nanoparticles coupling), the reaction jar reflects the colour change, which can be identified through the naked eyes, as shown in Fig. 5 [4]. A slight change of refractive index (RI) around the nanoparticle's surroundings can be detected as a signal, and this phenomenon is being utilized to develop many different types of biosensors. Similarly, a change in the size of the nanoparticle also alters the surface plasmon band and can be used for the development of the sensor. The spherical gold nanoparticles suspension having an average diameter of 10 nm appears as red colour (SPR band at 520 nm). On the other hand, silver nanoparticles suspension having the same size appears as yellow colour (SPR band at 395 nm) [5, 6]. Therefore, the core-shell nanoparticles (Au nanoparticles with Ag surface) optical properties can be tuned to the cyan-green region by altering the Ag layer thickness. Also, these nanoparticles are surface modified using engineered antibody-conjugated, which are prone to bind to harmful biotoxin staphylococcal enterotoxin A (SEA) [5, 7]. It is a small protein mostly found in staphylococcal food poisoning [8]. Therefore, a solution assay containing these nanoparticles functionalized with engineered conjugate antibody works as a biosensor; the assay changes their colour on binding with biotoxin SEA, which may be observed through naked eyes as shown in Fig. 5.

4.1.2 Surface-Enhanced Raman Scattering Based

The Surface-Enhanced Raman Scattering (SERS) is a phenomenon that enhances signal intensity by many orders of magnitude ($\sim 10^6$ – 10^{14}) and overcomes the inherent weakness of a Raman signal. It is highly sensitive and selective due to unique fingerprint spectra. Therefore, even just a single molecule [9] can be detected using this technique.

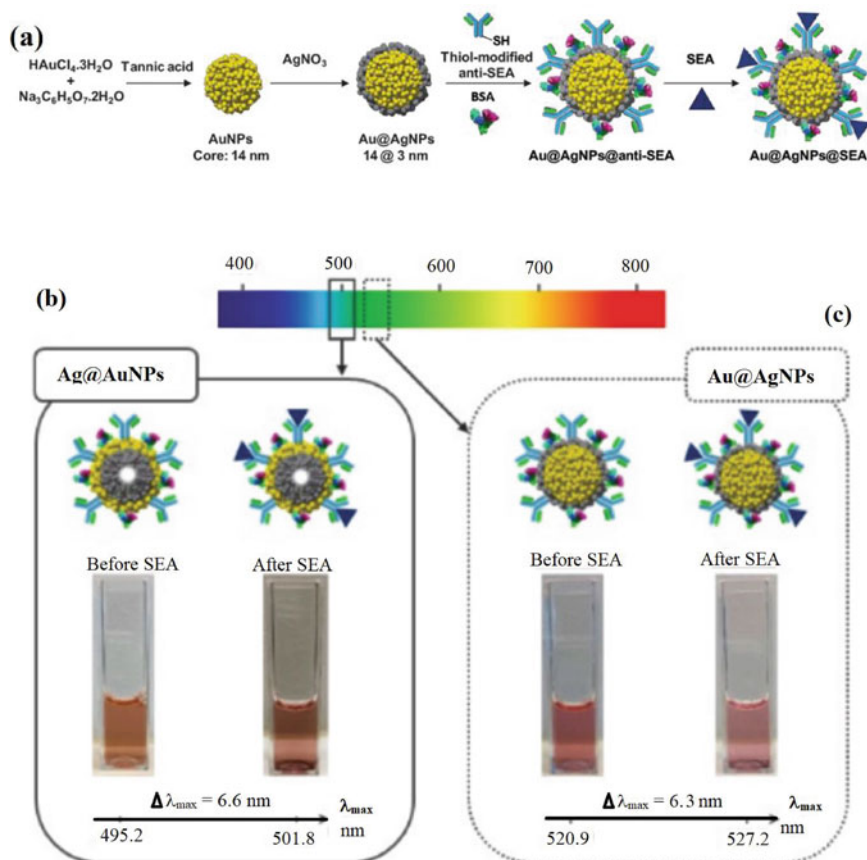


Fig. 5 a Schematic of synthesis core-shell nanoparticles (Au@AgNPs), their functionalization with conjugated-antibody, and binding with SEA, b Ag@AuNPs change in colour before and after binding with SEA, c Au@AgNPs, change in colour before and after binding (printed with the permission) [7]

SERS can be utilized for developing different biosensors such as in-vivo glucose detection [10, 11] nucleic acid and proteins [12], DNA detection [13], and rapid detection of bacteria [14, 15]. The detection methodology with label-based and label-free techniques utilizing nanoparticles is shown in Fig. 6.

4.1.3 Magnetic Nanoparticles Based

Magnetic nanoparticles-based sensing is also being actively used for biosensing since the last decade. They are alternatives to fluorescent biosensors. Magnetic nanoparticles show super magnetic behaviour at nanoscale dimensions due to a reduced

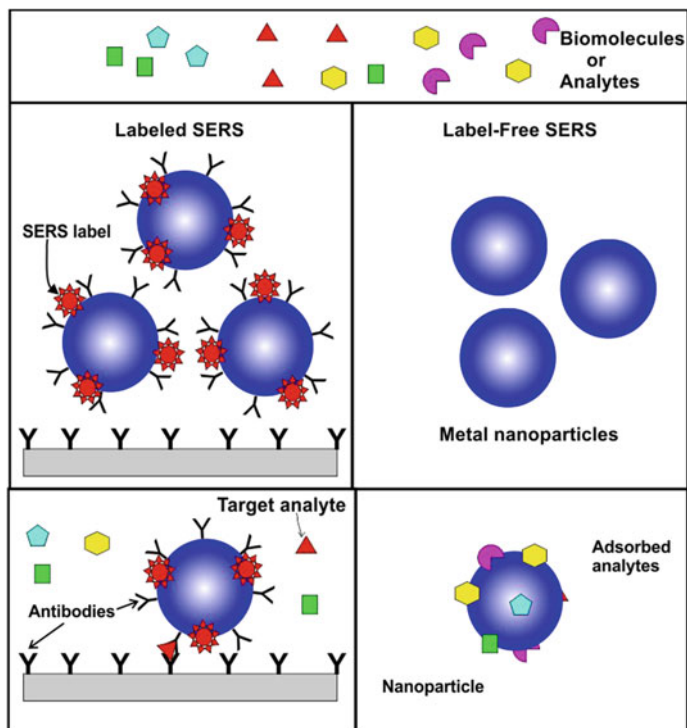


Fig. 6 Schematics of label-based and label-free surface-enhanced Raman scattering phenomena for designing biosensors

number of domains, and magnetization can flip direction instantly. However, in the case of bulk, the external magnetic field is required to demagnetize and flip the direction, as shown in Fig. 7 [16]. For nanoparticles, there is no thumb rule to determine magnetic behaviour (diamagnetic, paramagnetic, ferromagnetic) [17]. In the past few years, different types of magnetic nanoparticles are used for biosensing such as Co, Mn, Fe, Ni, Fe_2O_3 , Fe_3O_4 , FePt, FePt-Ag, CdS, etc. [18]. The magnetic behaviour of nanoparticles is now being integrated with transducers' materials, which impart analytical merits such as low limit detection, high signal to noise ratio, enhanced sensitivity, etc. [19].

The separation of analytes from a large sample or other words concentration enhancement of analytes utilizing functionalized magnetic nanoparticles is a competent technique nowadays. In this technique, a nanoparticle functionalized with the receptor directly binds with the targeted analytes in a sample. Furthermore, analytes, along with magnetic nanoparticles, separates from the solution using an external magnetic field. In this way, centrifugation can be avoided from sample preparation, which brings other impurities along with targeted analytes [17].

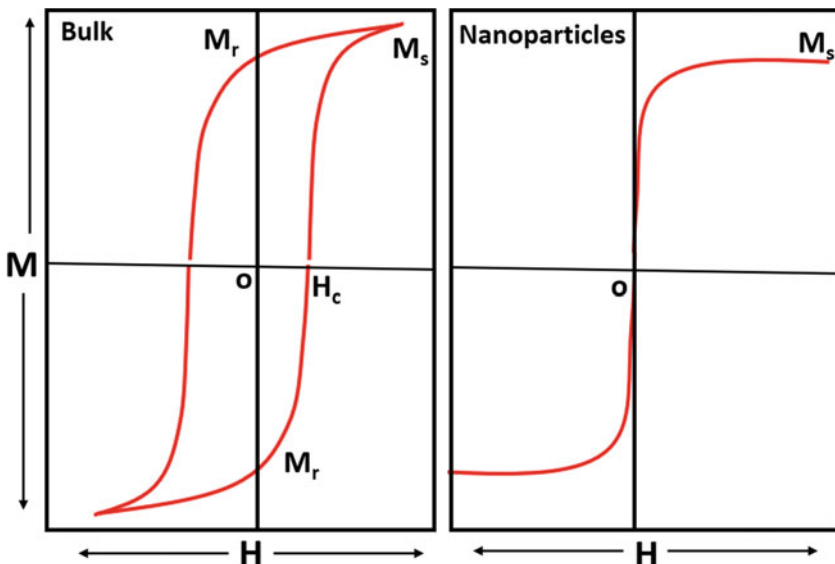


Fig. 7 Schematics of the magnetic materials hysteresis loop of bulk magnetic vs nanoparticles (M_s : magnetic saturation, M_r : remnant magnetization, H_c : coercivity)

4.2 Nanowire (1D Materials)

A nanowire is a thin wire with a diameter below 100 nm. Nanowires made from various materials such as Ag, Au, Pt, carbon nanotubes, etc. have been developed. The frequency of vibration, stress response of piezoelectric nanowire, and an array of nanowires endows with photonic properties such as wire arrangement helps to trap the light in a broad range of wavelengths, and these properties of nanowires are utilized in biosensor development.

4.2.1 Nanomechanical-Based Sensors

The deformation and vibrations in a nanowire are sensitive properties, and the utilization of these unique properties is helpful in the development of biosensors. The nanowires functionalized with the receptors are purposely made to bind with biomolecules of interest. Whenever the analytes or biomolecules bind with the receptor on nanowires, it induces the stress and nanowire bend shown by a schematic in Fig. 8. The deflection of the nanowire can be measured through optical (laser deflection, optical interferometric, etc.) or electrical techniques (piezoelectric, etc.). Similarly, whenever biomolecules land onto a nanowire, which reduces their vibration frequency due to mass increase, which can be measured through optical techniques [20, 21].

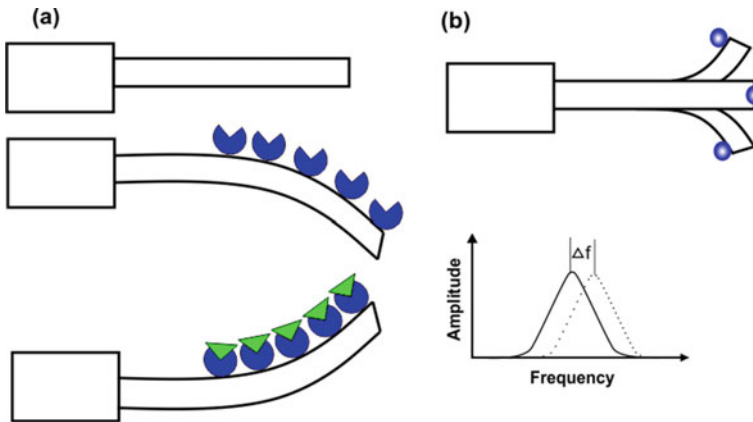


Fig. 8 Nanomechanical biosensor principle. **a** static; bending of nanowire, **b** dynamic; changing the vibration of the nanowire

4.2.2 Opto-Thermo-Mechanical Based

The working principle of Opto-thermo-mechanical based biosensor is slightly different from the thermomechanical based biosensor. In this method, the array of the nanowire is vertically planted over the silicon–silicon dioxide membrane. In this way, the high surface area achieved makes it highly sensitive to respond to even a few analyte molecules. These nanowires are capable of trapping light of broadband due to nanostructures. Also, nanowires are functionalized with the single-stranded probe DNA. When analyte molecules come in contact with a target single-stranded DNA, the relevant molecules bind together, changing the mass detected by the device. Also, the vibration frequency of nanowire changes due to the addition of mass. 90% of the laser light exposed over the surface of the array nanowire gets trapped or absorbed due to nanostructure array, which activates the efficient opto-thermomechanical excitation of the resonator. An optical signal of laser light (variation in frequency) is used to read for interpretation of the results. In this way, there is no requirement for wires to connect with the biorecognition platform [22].

4.2.3 Field-Effect Based (Semiconductor) Biosensing

A material having its conductivity between conductor and insulator is known as a semiconductor, which is defined in terms of a bandgap. Therefore, a nanowire having a bandgap and its ability to bind different analytes over the surface makes it more popular to design a wide range of biosensors. Silicon is a popular semiconductor used in most electronics applications. Cui et al. [23], reported for the first time to use the silicon nanowire building block to develop different sensors, which can detect protein, viruses, nucleic acid, etc. Silicon nanowire acts as a resistor when the number

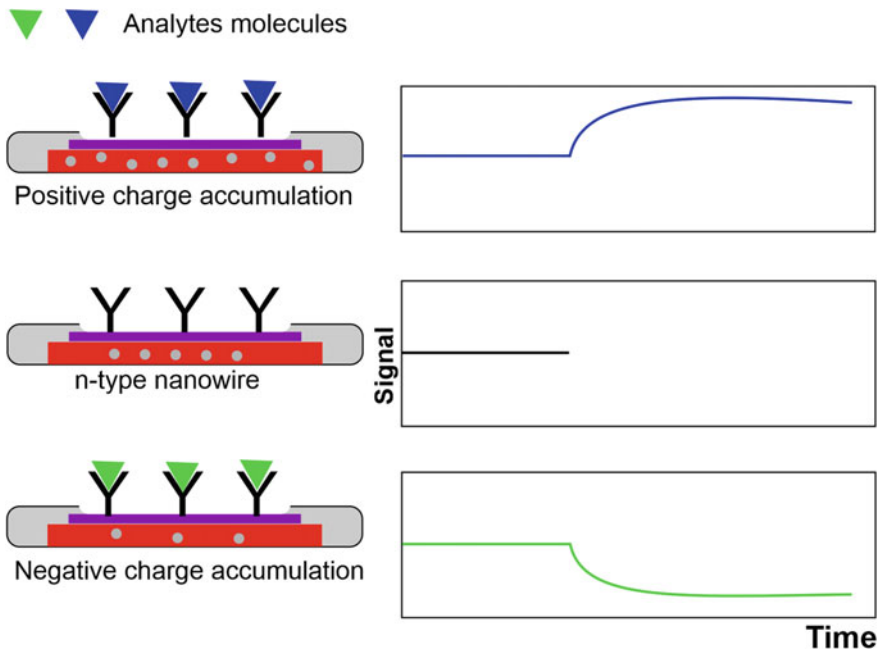


Fig. 9 Semiconductor-based nanowire biosensor configured with receptor over nanowire surface

of charge molecules binds over nanowire, and it leads to depletion or accumulation charge carrier, as shown in Fig. 9. As a result, the conductivity of the nanowire can be harnessed as a signal, and it is ultrasensitive up to a single virus/molecule detection [24, 25]. The bio-molecules induce charges in an aqueous solution (proteins, nucleic acid) that can bind easily with appropriate receptor functionalized over the surface of the nanowire [26]. The different materials nanowire used for various bio analyte detection such as silicon nanowire for gastric cancer detection from exhaled volatolome [27], troponin detection [28], Follicle-Stimulating Hormone detection [29], etc.

Similarly, the carbon nanotubes are very sensitive to response even at single-molecule interaction. There are carbon nanotubes (SWCNTs) and multi-wall carbon nanotubes (MWCNTs) being used for biosensor formulation. The SWCNTs having a high electrical transduction property and utilized paper-based chemiresistor sensor for the detection of human immunoglobulin G (HIgG) up to the picomolar level [30].

4.3 Nanosheet Based (2D)

A two-dimensional thinnest material, having a thickness of less than a few nanometers is referred to as a nanosheet or in short 2D nanostructure materials. These materials

are having unique and excellent mechanical, thermal, optical, and electrical properties that have attracted researchers to harness their properties for many applications, one of them is to develop biosensors.

4.3.1 Fluorescence-Based Biosensing

Fluorescent molecules absorb light and in turn excites the electrons of the molecules, causing them to jump to a higher energy level. Upon returning from an excited state to a ground state, the energy is released in the form of radiation or heat. The light-emitted in this process is referred to as fluorescence, and molecules are known as fluorophore. However, when the fluorophore interacts with the quencher (another molecule), the resultant complex may become non-fluorescent. A German scientist Theodor Förster proposed and explained the mechanism of two light-sensitive (donor–acceptor) molecules interaction, which may emit light or can absorb [31]. It is known as Förster (Fluorescence) resonance energy transfer (FRET). The electronically excited state of a donor may transfer energy to an acceptor via the non-radiative dipole–dipole interaction. Energy transfer efficiency is inversely proportional to the sixth power of the distance between donor and acceptor making FRET extremely sensitive to small gaps [31].

The two-dimensional nanomaterials are extensively in use for biosensing because 2D nanosheets can act as a platform, where biomolecules can easily land or adsorb and alter the fluorescence efficiency (donor–acceptor). Now a day, many 2D materials are in practice to harness fluorescence property for use in biosensing, including the use of Vanadium disulfide (VS_2) nanosheet for detection of cytochrome c.

4.3.2 Field-Effect Based (Semiconductor)

The field-effect transistor technology is a milestone in developing tiny and simplest biosensors. There are many-layered structure materials such as molybdenum disulfide (MoS_2), Graphite, Vanadium disulfide (VS_2), boron nitride (BN), tungsten disulfide (WS_2) that are easy to exfoliate in different solvents to prepare nanosheets. Additionally, graphene-based FET's are highly sensitive towards the detection of the analyte. Graphene has an extraordinary ability of the electron-transport property [32]. Therefore, graphene channels show conductivity change in response to the minor adsorption of analyte molecules on the sensor surface. Chen et al. [33] described field-effect transistor-based detection of Ebola shown in Fig. 10. The reduced graphene oxide bridge between the source and the drain electrode, and layer protected with Al_2O_3 to protect underline rGO. The gold nanoparticles conjugated with antibody immobilized over the reduced graphene oxide layer, are highly prone to bind with Ebola virus glycoproteins. Therefore, the exposure of EGP (Ebola glycoprotein), makes the dynamic response of FET measured and the drain-voltage current to decrease with time as more protein binds with the platform (see Fig. 10b). The detection limit of such a biosensor is 1 ng/ml EGP.

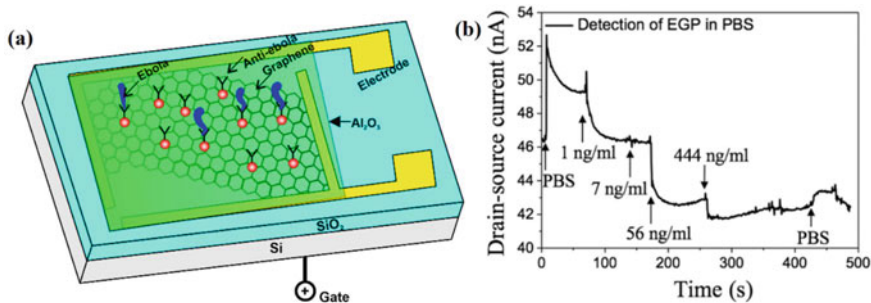


Fig. 10 **a** Schematic of reduced graphene oxide-based Field-Effect Transistor (FET) biosensor. Ebola antibody conjugated with gold nanoparticles and Al_2O_3 coating for passivation, **b** dynamic response of FET sensor on the exposure of Ebola glycoprotein (EGP) (reprinted with permission) [33]

4.3.3 Optical Biosensors

Graphene-based materials are mostly studied due to their extraordinary optical property such as surface plasmon and absorption polarization, which endowed the sensor to detect even single cells [34]. The distinction of graphene biosensors based on their electrical and optical properties are summarized in Table 1.

Surface Plasmon Based Biosensing

The best property of optical sensors is that they respond ultra-fast and gives result in real-time. The electronic properties of graphene are excellent because the Fermi surface of graphene lies in the overlapped/intersection of the empty conduction band

Table 1 Difference in electrical and optical principle-based graphene biosensor

Property	Graphene electrical biosensor	Graphene optical biosensor	References
Principle	Receptor functionalized graphene changes conductivity on binding with analytes. Monitor the drain-source conductivity in Field effect transition mode	Broad band absorption of graphene and their sensitivity with any change near to graphene surface or refractive index	[35–37]
Advantage	Fast response time High surface area Lower detection limit	Unlabelled sample Accurate detection High spatial resolution	
Disadvantage	Only measure current Sample damage	Light absorption of monolayer graphene too low. Aggregation of graphene affects the optical properties	

and the filled valence band and also in the middle of the p band, where electrons are the valence electrons and have the mobility of about $1/300$ the speed of light known as Dirac Fermion [38, 39]. These fermions show a linear energy-momentum relationship near the Dirac point, and this endowed graphene with optical resonance property at any frequency in the ultra-violet, infra-red region. Therefore, many different biosensors have been developed, in which the fibre optic sensor is the simplest. The fibre optic integrated with graphene makes use of optical fibre used for transmission of light and to receive the output. The change in intensity, wavelength, frequency, etc. after interaction with the graphene platform received through the optical fibre is analyzed [40, 41]. There are many graphene SPR based biosensors used for a variety of purposes, such as specific protein detection [42], gas detection [43], and different chemical- biological species [44].

Polarization Absorption Enhanced

Another interaction of light with graphene depends on the number of layers and prismatic total internal reflection (TIR) structure. In the graphene, the prismatic TIR structure shows the characteristic polarization absorption and broadband absorption enhancement [45]. When the refractive index of the medium increases than the graphene, it starts to show a variation in the optical power of two polarization states [34, 46]. Also, by utilization of change in polarization states, many sensitive biosensors have been designed [39].

4.3.4 Gravimetric-Based Biosensors

The natural frequency of a piezo crystal or film is inversely proportional to its thickness, and also, we can make it oscillatory due to piezoelectricity by applying electricity using a simple circuit. Also, whenever any mass is bound to the piezoelectric film, its frequency gets reduced. This method can be utilized in different modes such as resonating crystal, in which well-known quartz crystal microbalance works, surface acoustic wave mode, etc. [47]. This type of sensor sensitivity depends on the film thickness. Therefore, many piezoelectric polymer films have been developed, which can be drawn in very thin films to develop highly sensitive biosensors. The Polyvinylidene Fluoride (PVDF) polymer is one such well known piezoelectric polymer [47].

4.4 3D Nanomaterials

Bulk materials with nanophase domains or equiaxed clear grains can be called 3D nanomaterials [48]. Suppose a material has been rolled to form inside nanostructuring due to deformation; it becomes a nanomaterial. However, if we extend 2D rapheme in

the third dimension by stacking without any raphemelization between two rapheme sheets, it becomes bulk graphite. The properties of these stacked sheets are like the graphite, while it is having 2D nano rapheme sheets by its virtue. Therefore, the author's points of view are that a 3D nanomaterial will fall in the category of 0D, 1D, and 2D. It is just consolidation of nanoparticles/rods/sheets.

4.5 Electrochemical Sensor

The electrochemical sensors work as electrochemical transduction, where electrochemical reactions (oxidation–reduction) results in the transfer of electrons, which can be detected through amperometry or voltammetry. It can detect enzymes, cells, tissues, gas, ligand, etc. In principle, it is a conventional electrochemical cell containing three separate electrodes: the working electrode (WE), the counter electrode (CE), and the reference electrode (RE), and these three-electrodes can be printed on paper, polymer, etc. as shown in Fig. 11.

Nowadays, screen-printed carbon electrode (SPCE) biosensors are so famous due to easy, point-of-care, small fluid volume (analyte) [49]. The working electrode is functionalized with a biorecognition system (enzyme, etc.) utilizing nanoscale materials, and the analytes directly interact with the working electrode. As a result of this, the electrochemical cell becomes active and produces a signal.

Zelada-Guillén et al. [50] utilized carbon nanotubes as an ion-to-electron transducer, and covalently bonded aptamers for the detection of *Staphylococcus aureus*. The measurement of electromotive force (EMF) or potential, generated on the antigen–antibody interaction is known as a potentiometric biosensor. On the other hand, the measurement of the ionic strength of the solution, which affects the conductivity, is known as a conductometry biosensor [51]. Similarly, amperometric transducers measure the direct current from redox reaction under a constant potential applied to WE. The activity of the recognition element varies before and after the interaction with a target molecule. The product must be electroactive and undergoes a redox process [52]. However, if the biosensor measures the current-potential relationship, and the reference of potential at zero current applied is known as a voltammetric

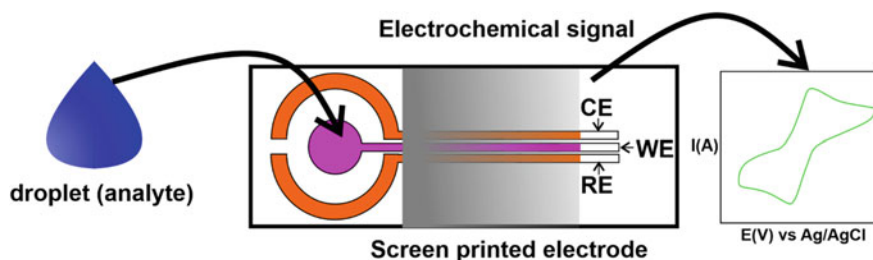
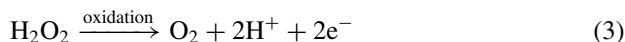
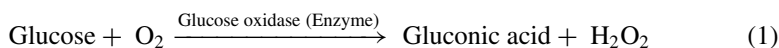


Fig. 11 Screen printed electrode-based biosensor

biosensor. Many analytes can be detected with their characteristic potentials. It has been divided into many such as cyclic voltammetry (CV), linear sweep voltammetry (LSV), and differential pulse voltammetry (DPV), etc. Currently, the most popular nanoscale materials being utilized for enhancing the sensitivity of biosensors are Au nanoparticles (NPs), Pt NPs, alloy nanoparticles, carbon nanotubes, graphene, MoS₂ nanosheet, VS₂ nanosheet. The utilization of different nanoscale materials and various working principles used for analytes detection have been summarized in Table 2.

4.6 *Electrochemical Glucose Biosensor: How Nanoscale Materials Appear to Play a Role?*

The glucose level detection in the human body is a very important task, which changes abruptly in a diabetic person, and needs careful monitoring. The electrochemical amperometric biosensors are so common in daily use. The working principle of this type of biosensor is based on a simple enzyme-catalysed reaction of glucose as follows:



Therefore, we can detect the consumption of oxygen or the generation of H₂O₂ electrochemically. The H₂O₂ oxidizes and produces electrons, and these electrons (anodic current) can be monitored electronically. These were classed as the first generation of glucose biosensors. In this process, the high potential required to apply at which other drugs may present in the blood sample becomes electroactive at such potential resulting in inaccuracy. Therefore, the influence of coexisting electroactive compounds reduced by a coating over the electrode surface with polymer layer (poly-(phenylenediamine), polyphenol, Nafion, cellulose acetate, etc.), and tuning the operational electrode potential of targeted analytes oxidation range preciously. However, the whole process depends on oxygen. Consequently, slight tension in oxygen and stoichiometry alter the sensor response [63]. Therefore, to counter this problem in a glucose biosensor, a mediator (non-physiological electron acceptor) is inserted between glucose oxidase enzyme and electrode, which carry forward electron from the reaction center to the electrode surface.

These are classed as the second-generation glucose biosensors and are based on the following equations as illustrated further in Fig. 12.

Table 2 Some biosensors researching nanoscale materials, method and analytes

Materials	Method or principle	Analytes to be measured	Lower limit of detection	Dimension of nanomaterials	References
Ag@Au core shell nanoparticles	Surface plasmon resonance	Biotoxin staphylococcal enterotoxin A (SEA)	0.2 nM	0D	[7]
FeCo nanoparticles	Giant Magnetoresistive immunosensor	Endoglin detection from urine	83 fM	0D	[53]
Carboxyl functionalized iron oxide nanoparticles	Superconducting quantum interference	breast cancer cells	10^6 cells with uncertainty 20%	0D	[54]
Manganese-doped ferrite (MnFe ₂ O ₄)	Hall Sensor	Rare cells: MDA-MB-468 cancer cells (whole blood)	Individual cell	0D	[55]
Carbon nanotube	Chemiresistor	Proteins detection	6.6 pM	1D	[30]
Polyaniline nanofibres (PANI-NF) functionalized with gold NPs	Electrochemical (Cyclic voltammetry)	DNA detection	150 pM	1D	[56]
Nickel oxide (NiO) nanofibres	Field effect	Alcohol detection	100 ppm	1D	[57]
Gold NanoWire arrays	Optical and electrocheical	Bacteria in kidney infection	10^3 cell/ml	1D	[58]
Platinum Nanowires	Electrochemical (Amperometer)	electrocatalytic reduction of hydrogen peroxide (H ₂ O ₂)	5×10^{-6} M	1D	[59]
Graphene	Field Effect Transistor	Ebola virus detection	1 ng/ml	2D	[33]
Graphene	Field Effect Transistor	Acetylcholine	2.3 M	2D	[60]
Layered titanate sheets	Electrochemical based	Catalytic reduction of H ₂ O ₂	0.6 M	2D	[61]
Flower-shaped copper oxide thin sheet	Electrochemicacal (amperometric)	Glucose	1.37 M	2D	[62]

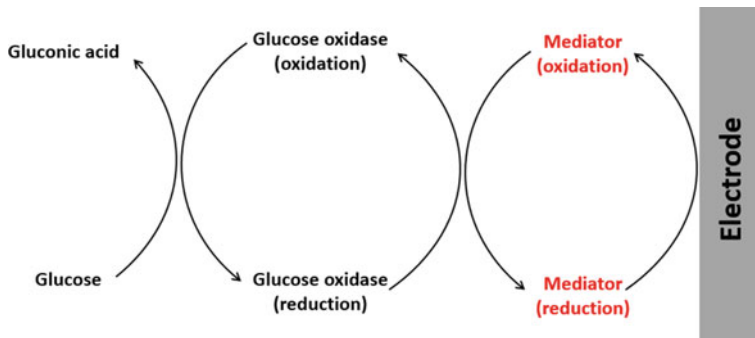
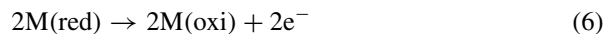
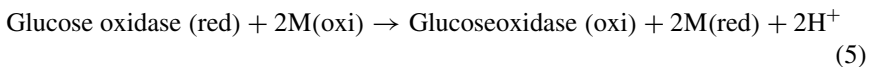
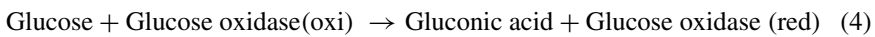


Fig. 12 Sequence of reaction occur in second-generation glucose biosensor [63]



Many mediators are being used, such as ferricyanide, conducting organic salts, quinone compounds, transition-metal complexes, phenothiazine and phenoxazine compounds, etc. which are insoluble, non-toxic, and chemically stable. The mediator is fast enough to react with enzymes and transfer electrons, but still, oxygen remains a problem due to self-diffusing. It limits the accuracy of low glucose concentration.

Further improvements in the biosensor have been made by placing wiring as nanomaterials to fast electron transfer from the centre of the redox enzyme to the electrode. It is fast communication between the redox enzyme and the electrode. Patolsky et al. [64, 65] have constituted the glucose oxidase enzyme over the carbon nanotubes, which vertically connects to the electrode, and acts as a wire to fast transfer charge, as shown in Fig. 13.

It is known as the third generation of glucose biosensors based on amperometry. Modern technology is revolutionizing very fastly. These biosensors can now be screen printed with multilayers (electrode, enzyme, mediator, binder, etc.) strips for one-time use.

5 Biological Recognition Element

The biological recognition elements are different types of receptors or bio-probes, which are highly specific towards their stimuli. The bio probes are immobilized over the surface of nanoscale materials, which can form covalent bonds with analytes

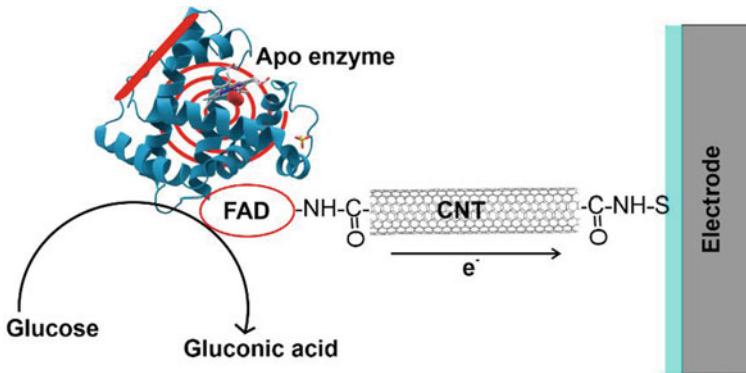


Fig. 13 Carbon nanotube (CNT) as a connector for electrical communication in glucose biosensor; (FAD: flavinadenine dinucleotide) [64]

or adsorbed and bind with Van der-Waal forces, etc., such as antibodies, enzymes, and cells. The most straightforward process is the physical adsorption of bio-probes. However, the salts, pH, and other contaminants appear as a nuisance, which creates noise in the output signals and losses in the precision quantification or detection. Contrarily, the chemical immobilization of bio-probes has attractive features, such as strong covalent bonding with nanoscale materials and is highly specific towards the target analytes; which increases precision and the probability of detection.

Each biosensor needs a unique combination of biorecognition element and transducer, which depends on the target analyte. A schematic map is shown in Fig. 14 for selecting a suitable biorecognition element.

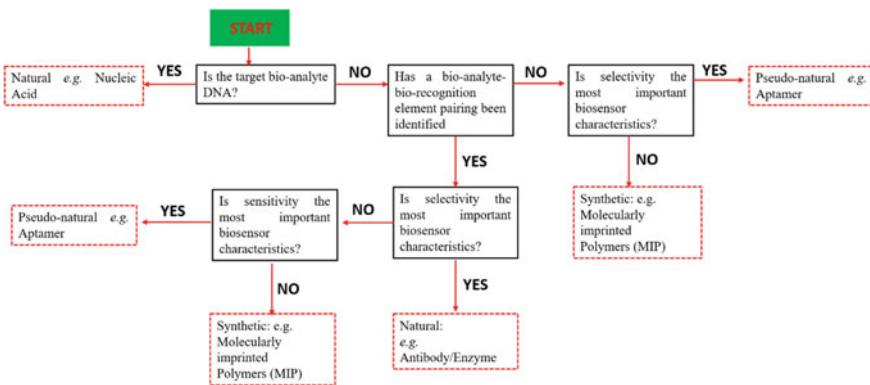


Fig. 14 Map of selecting biorecognition element for developing biosensor (reprinted with permission) [66]

Antibodies

Antibodies are different types of proteins that are largely used as biorecognition elements. They are more specific and selective towards analytes that are being used for developing various types of biosensors. The antibodies may be categorized into two kinds monoclonal and polyclonal. Monoclonal antibodies can recognize a single epitope of a target molecule, whereas polyclonal antibodies can recognize different epitopes of the same target. The antibodies are more susceptible to temperature and required to store at low temperatures. Otherwise, it gets denatured; as a result, it can lose the binding ability.

Deoxyribonucleic acid (DNA)

In modern biosensors, DNA is being used as a probe in the biorecognition platform. It is a short DNA sequence, immobilized over the transducer surface, that can interact with the specific target DNA sequence, or it can bind to a complementary DNA sequence. In the case of metal ions detection, the phosphate backbone of DNA molecules have a negative charge and easily binds with the positively charged metal ions [67].

Cells

The living cells are being used as biorecognition (bio-receptor), which is an economical alternative to enzymes and antibodies. Designing a biosensor recognition platform becomes easier by using cells in comparison to the other bio-receptors. The different types of cells with distinct functional strategies are in use for developing biosensors, as shown in Fig. 15. The cells are immobilized over the transducer in such a way; the viability of the cell does not affect, such as direct immobilization on the electrode, hydrogel entrapment, and biofilm formation, etc. [68].

Enzymes

The enzymes are biocatalytic biomolecules, which can enhance the biological reaction and also liberate the measurable product. During the biocatalytic reaction, the intermediate product to the final product formation process is easily monitored through the transducer, electrochemical transducers (amperemeter, voltammeter, etc.).

6 Challenges

There are still many challenges to developing a special type of biosensors, such as particular virus-detection biosensors. The virus is a tiny biological entity capable of destroying human body cells. Its detection at an early stage of infection has not been very much possible as yet, primarily because the affected person does not realize the asymptomatic symptoms. However, early diagnosis of virus infection/biochemical disbalance/bacterial infection, etc. can be detected through in-vivo biosensor, and

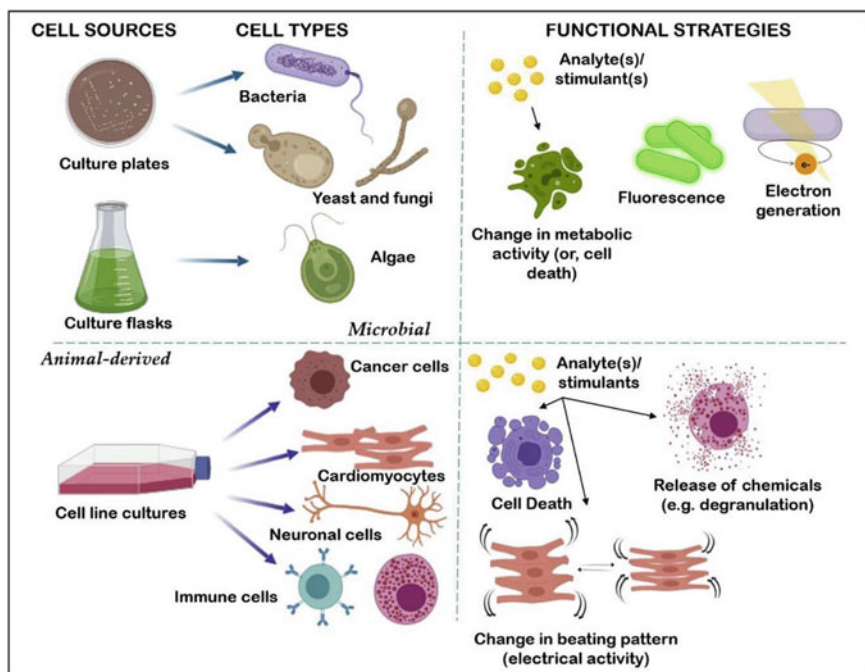


Fig. 15 Schematic showing different cell types obtained (left), and functional strategies of cell-based biosensors (right) (reprinted with permission) [68]

it will be a milestone in the clinical sector. However, the materials currently being utilized in making biosensors are foreign materials for the human body and their acceptance into the human body is still a challenge. Therefore, the utilization of materials in biosensing needs to be compatible with the human body, or the whole biosensor must be biological. Also, many biosensors are complicated and required to be stored at low temperatures. Therefore, the new technology needs to develop sensors that can be stored and operated at room temperature.

Research Data statement

Data sharing is not applicable to this article as no new data were created or analyzed in this study.

Acknowledgements Authors are very much thankful to the Research support provided by the UKRI via Grants No.: (EP/L016567/1, EP/S013652/1, EP/S036180/1, EP/T001100/1 and EP/T024607/1), Royal Academy of Engineering via Grants No. (IAPP18-19\295, TSP1332 and EXPP2021\1\277), EU Cost Actions (CA15102, CA18125, CA18224 and CA16235) and Newton Fellowship award from the Royal Society (NIF\R1\191571). SG is particularly thankful to European Regional Development Funds (ERDF) sponsored A2i project at LSBU that has catalyzed several industrial partnerships. The work used Isambard Bristol, UK supercomputing service accessed by Resource Allocation Panel (RAP) grant as well as ARCHER resources (Project e648).

Questions and Answers to Check Your Reading

Objective Types

(1) Surface plasmon resonance belongs to which type of biosensor?

- (a) Transducer (b) Recognition system
(c) Signal Amplification (d) none

Ans: Transducer

(2) What is an aptamer in a biosensor?

- (a) Transducer (b) Recognition system
(c) Signal Amplification (d) none

Ans: Recognition system

(3) Please fill in the blank. An analyte can be detected through _____ working principles.

- (a) one (b) two
(c) three (d) many

Ans: Many

(4) A nanoscale material is defined to have its _____ ?

- (a) one dimension <100 nm (b) two dimensions <100 nm
(c) three dimensions <100 nm (d) All dimensions <100 nm

Ans: one dimension <100 nm

Subjective Types

(5) What is a biosensor?

A biosensor is an analytical device, which is successfully used for the qualitative and quantitative estimation of several biologically important substances.

(6) What are the various types of biosensors?

Biosensors can be classified by their transduction mechanisms such as Electrochemical, Piezoelectrical, Thermometric, Optical, and Physical; one can also

classify them by the mode of biorecognition, e.g., enzyme-based, antibody-based, nucleic acid-based, aptamer-based and whole cell-based. Also, the transducer-based classification can be further sub-divided. For example, electrochemical biosensors can be amperometric, potentiometric, conductometric, etc. In addition, biosensors can be defined by both the recognition mode and transducer, e.g., enzyme-based electrochemical biosensors or, more specifically, enzyme-based potentiometric biosensors.

- (7) Describe the main components of biosensors and explain their function.
The biosensor consists of a biorecognition element, transducer, amplification, and display.
The biorecognition system detects the analytes; the transducer converts action of recognition system into the signal; the amplification enhances the signal strength to read easily; display shows the result.
- (8) Define precision and selectivity for a sensor.
Precision: The ability to have high reproducibility upon the repetition of measurements of the same sample. The sensor has good reproducibility of its response (low standard deviation).
Selectivity: The sensor performance towards targeted analytes. A sample has many chemical/biomolecules, but sensor detects particular analytes/biomolecules, for what it is tuned.
- (9) What are nanomechanical biosensors (cantilever biosensors)? How have these been used for biosensor development? How can the biorecognition event be transduced?
These are microfabricated finger-like transducers that can bend/oscillate (depending on the material) as a result of a physical/electrical stimulation. The bending/oscillation of these devices is proportional to their mass. Cantilever-based biosensors have been used for hybridization assay, for the screening of the effect of drugs on the growth of bacteria, for affinity (antibodies) based assay by immobilizing on the surface of the cantilever DNA probes, drugs or antibodies. Transduction can be optical or piezoelectrical. In optical, the reflection of a laser beam is used to evaluate the bending of the cantilever. In the case of piezoelectrical changes in the oscillation frequency of cantilever (made with piezoelectric material) are used to detect changes in the mass onto them.
- (10) What is an enzyme? What is the function of an enzyme, when used as a biorecognition element?
The enzymes are protein and act as a biological catalyst. In the biorecognition system, it is attached to the transducer and catalyzes analyte conversion faster and efficiently. Correlate the analyte to a measurable event (loss in a substrate or generation of a product).

- (11) What are the two main problems associated with the use of the Oxygen electrode (Clark electrode) as a transducer in the glucose electrochemical biosensor?
This is dependent on the starting concentration of oxygen in the starting solution. Use high potential: sensitive to interference from other molecules. The electrochemical reaction consumes oxygen (this can produce false positive).
- (12) What are the main advantages and disadvantages of the transducer's functionalization via the adsorption process instead of covalent bonding?
Physical adsorption is a simple and easy process. However, pH variation and other analytes in the sample create interference in the signal, which appears as noise and reduces the probability of accurate detection.

Some further unsolved problems:

- (1) Explain a label-based and a label-free biosensor.
- (2) What is meant by spectral interrogation schemes in LSP sensors?
- (3) Describe Glucose biosensors. First, second and third generation of amperometric sensors.
- (4) Achieving selectivity and sensitivity in SPR biosensors. Immobilization strategies in SPR. Improving signal for small analytes.
- (5) Describe applications of carbon nanotubes and nanowires for biosensing.

References

1. Roduner, E.: Size matters: why nanomaterials are different. *Chem. Soc. Rev.* **35**, 583–592 (2006)
2. EU commission. <https://eur-lex.europa.eu/legal-content/EN/TXT/?uri=CELEX:32011H0696> (2011)
3. Linic, S., Aslam, U., Boerigter, C., Morabito, M.: Photochemical transformations on plasmonic metal nanoparticles. *Nat Mater* **14**, 567–576 (2015)
4. Chen, P., et al.: Nanoplasmonic sensing from the human vision perspective. *Anal. Chem* **90**, 4916–4924 (2018)
5. Loiseau, A. et al.: Silver-based plasmonic nanoparticles for and their use in biosensing. *Biosensors* **9**, 78, (2019)
6. Noguez, C.: Surface plasmons on metal nanoparticles: the influence of shape and physical environment. *J. Phys. Chem. C* **111**, 3606–3619 (2007)
7. Loiseau, A. et al.: Core-shell gold/silver nanoparticles for localized surface plasmon resonance-based naked-eye toxin biosensing. *ACS Appl. Mater. Interfaces* **11**, 46462–46471, (2019)
8. K erouanton, A., et al.: Characterization of *Staphylococcus aureus* strains associated with food poisoning outbreaks in France. *Int. J. Food Microbiol* **115**, 369–375 (2007)
9. Langer, J., et al.: Present and future of surface-enhanced raman scattering. *ACS Nano* **14**, 28–117 (2020)
10. Stuart, D.A., et al.: In vivo glucose measurement by surface-enhanced raman spectroscopy. *Anal. Chem* **78**, 7211–7215 (2006)
11. Laing, S., Jamieson, L.E., Faulds, K., Graham, D.: Surface-enhanced Raman spectroscopy for in vivo biosensing. *Nat. Rev. Chem.* **1**, 0060 (2017)

12. Chao, J. et al.: Nanostructure-based surface-enhanced Raman scattering biosensors for nucleic acids and proteins. *J. Mater. Chem. B* **4**, 1757–1769, (2016)
13. Yuan, W., Ho, H.P., Lee, R.K.Y., Kong, S.K.: Surface-enhanced Raman scattering biosensor for DNA detection on nanoparticle island substrates. *Appl Opt* **48**, 4329–4337 (2009)
14. Dina, N.E., Colniță, A., Leopold, N., Haisch, C.: Rapid single-cell detection and identification of bacteria by using surface-enhanced Raman spectroscopy. *Procedia Technol.* **27**, 203–207 (2017)
15. Prakash, O., Sil, S., Verma, T., Umapathy, S.: Direct detection of bacteria using positively charged Ag/Au bimetallic nanoparticles: a label-free surface-enhanced Raman scattering study coupled with multivariate analysis. *J. Phys. Chem. C* **124**, 861–869 (2020)
16. Chen, Y.T., Kolhatkar, A.G., Zenasni, O., Xu, S. Lee, T.R.: Biosensing using magnetic particle detection techniques. *Sensors (Switzerland)* **17**, (2017)
17. Li, X.-S., Zhu, G.-T., Luo, Y.-B., Yuan, B.-F., Feng, Y.-Q.: Synthesis and applications of functionalized magnetic materials in sample preparation. *TrAc Trends Anal. Chem.* **45**, 233–247 (2013)
18. Rocha-Santos, T.A.P.: Sensors and biosensors based on magnetic nanoparticles. *TrAc Trends Anal. Chem.* **62**, 28–36 (2014)
19. Justino, C.I.L., Rocha-Santos, T.A.P., Cardoso, S., Duarte, A.C.: Strategies for enhancing the analytical performance of nanomaterial-based sensors. *TrAc Trends Anal. Chem.* **47**, 27–36 (2013)
20. Boisen, A., Dohn, S., Keller, S.S., Schmid, S., Tenje, M.: Cantilever-like micromechanical sensors. *Rep. Prog. Phys.* **74**, 036101, (2011)
21. Goeders, K.M., Colton, J.S., Bottomley, L.A.: Microcantilevers: sensing chemical interactions via mechanical motion. *Chem. Rev.* **108**, 522–542 (2008)
22. Lu, Y., Peng, S., Luo, D., Lal, A.: Low-concentration mechanical biosensor based on a photonic crystal nanowire array. *Nat. Commun.* **2**, 578 (2011)
23. Cui, Y., Lieber, C.M.: Functional nanoscale electronic devices assembled using silicon nanowire building blocks. *Science* **291**, 851 (2001)
24. Zhang, A., Lieber, C.M.: Nano-bioelectronics. *Chem. Rev.* **116**, 215–257 (2016)
25. Peretz-Soroka, H., et al.: Manipulating and monitoring on-surface biological reactions by light-triggered local pH alterations. *Nano Lett.* **15**, 4758–4768 (2015)
26. Livi, P., et al.: Monolithic integration of a silicon nanowire field-effect transistors array on a complementary metal-oxide semiconductor chip for biochemical sensor applications. *Anal. Chem.* **87**, 9982–9990 (2015)
27. Shehada, N., et al.: Ultrasensitive silicon nanowire for real-world gas sensing: noninvasive diagnosis of cancer from breath volatolome. *Nano Lett.* **15**, 1288–1295 (2015)
28. Kutovyi, Y. et al.: Origin of noise in liquid-gated Si nanowire troponin biosensors. *Nanotechnology* **29**, 175202, (2018)
29. Lee, M., et al.: Ultrasensitive electrical detection of follicle-stimulating hormone using a functionalized silicon nanowire transistor chemosensor. *ACS Appl. Mater. Interfaces* **10**, 36120–36127 (2018)
30. Pozuelo, M. et al.: Paper-based chemiresistor for detection of ultralow concentrations of protein. *Biosens. Bioelectron.* **49**, 462–465, (2013)
31. Förster, T.: Zwischenmolekulare Energiewanderung und Fluoreszenz. *Ann. Phys.* **437**, 55–75 (1948)
32. García-Miranda Ferrari, A., Foster, C.W., Brownson, D.A.C., Whitehead, K.A., Banks, C.E.: Exploring the reactivity of distinct electron transfer sites at CVD grown monolayer graphene through the selective electrodeposition of MoO₂ nanowires. *Sci. Rep.* **9**, 12814 (2019)
33. Chen, Y. et al.: Field-effect transistor biosensor for rapid detection of Ebola antigen. *Sci. Rep.* **7**, 10974, (2017)
34. Li, Z., Zhang, W., Xing, F.: Graphene optical biosensors. *Int J Mol Sci* **20**, 2461 (2019)
35. Zhu, J., Holmen, A., Chen, D.: Carbon nanomaterials in catalysis: proton affinity, chemical and electronic properties, and their catalytic consequences. *ChemCatChem* **5**, 378–401 (2013)

36. Szunerits, S., Maalouli, N., Wijaya, E., Vilcot, J.P., Boukherroub, R.: Recent advances in the development of graphene-based surface plasmon resonance (SPR) interfaces. *Anal. Bioanal. Chem.* **405**, 1435–1443 (2013)
37. Wu, L., Chu, H.S., Koh, W.S., Li, E.P.: Highly sensitive graphene biosensors based on surface plasmon resonance. *Opt. Express* **18**, 14395–14400 (2010)
38. Cao, M.-S., Wang, X.-X., Cao, W.-Q., Yuan, J.: Ultrathin graphene: electrical properties and highly efficient electromagnetic interference shielding. *J. Mater. Chem. C* **3**, 6589–6599 (2015)
39. Heersche, H.B., Jarillo-Herrero, P., Oostinga, J.B., Vandersypen, L.M.K., Morpurgo, A.F.: Bipolar supercurrent in graphene. *Nature* **446**, 56–59 (2007)
40. Kim, J.A., et al.: Graphene based fiber optic surface plasmon resonance for bio-chemical sensor applications. *Sens. Actuators B Chem.* **187**, 426–433 (2013)
41. Zhao, Y., Li, X.-g., Zhou, X. & Zhang, Y.-n.: Review on the graphene based optical fiber chemical and biological sensors. *Sens. Actuators B Chem.* **231**, 324–340, (2016)
42. Jiang, W.-S., et al.: Reduced graphene oxide-based optical sensor for detecting specific protein. *Sens. Actuators B Chem.* **249**, 142–148 (2017)
43. Liedberg, B., Nylander, C., Lunström, I.: Surface plasmon resonance for gas detection and biosensing. *Sensors and Actuators* **4**, 299–304 (1983)
44. Homola, J.: Surface plasmon resonance sensors for detection of chemical and biological species. *Chem. Rev.* **108**, 462–493 (2008)
45. Ye, Q. et al.: Polarization-dependent optical absorption of graphene under total internal reflection. *Appl. Phys. Lett.* **102**, 021912, (2013)
46. Thongrattanasiri, S., Koppens, F.H.L. García de Abajo, F.J.: Complete optical absorption in periodically patterned graphene. *Phys. Rev. Lett.* **108**, 047401, (2012)
47. Walton, P.W., O’Flaherty, M.R., Butler, M.E., Compton, P.: Gravimetric biosensors based on acoustic waves in thin polymer films. *Biosens. Bioelectron.* **8**, 401–407 (1993)
48. Ngô, C., Voorde, M.H.V.D.: In: *Nanotechnology in a nutshell*. (2014)
49. Cinti, S., Arduini, F.: Graphene-based screen-printed electrochemical (bio) sensors and their applications: efforts and criticisms. *Biosens. Bioelectron.* **89**, 107–122 (2017)
50. Zelada-Guillén, G.A., Sebastián-Avila, J.L., Blondeau, P., Riu, J., Rius, F.X.: Label-free detection of staphylococcus aureus in skin using real-time potentiometric biosensors based on carbon nanotubes and aptamers. *Biosens. Bioelectron.* **31**, 226–232 (2012)
51. Salek-Maghsoudi, A., et al.: Recent advances in biosensor technology in assessment of early diabetes biomarkers. *Biosens. Bioelectron.* **99**, 122–135 (2018)
52. Singh, S., Kaushal, A., Khare, S., Kumar, A.: DNA chip based sensor for amperometric detection of infectious pathogens. *Int. J. Biol. Macromol.* **103**, 355–359 (2017)
53. Srinivasan, B., et al.: A three-layer competition-based giant magnetoresistive assay for direct quantification of endoglin from human urine. *Anal. Chem.* **83**, 2996–3002 (2011)
54. Hathaway, H.J., et al.: Detection of breast cancer cells using targeted magnetic nanoparticles and ultra-sensitive magnetic field sensors. *Breast Cancer Res.* **13**, R108 (2011)
55. Issadore, D., et al.: Ultrasensitive clinical enumeration of rare cells ex vivo using a μ -Hall detector. *Sci. Transl. Med.* **141**, 1–22 (2012)
56. Spain, E., et al.: High sensitivity DNA detection using gold nanoparticle functionalised polyaniline nanofibres. *Biosens. Bioelectron.* **26**, 2613–2618 (2011)
57. George, G., Anandhan, S.: Synthesis and characterisation of nickel oxide nanofibre webs with alcohol sensing characteristics. *RSC Adv.* **4**, 62009–62020 (2014)
58. Basu, M. et al.: Nano-biosensor development for bacterial detection during human kidney infection: use of glycoconjugate-specific antibody-bound gold nanoWire arrays (GNWA). *Glycoconj. J.* **21**, 487–496, (2004)
59. Lu, Y., Yang, M., Qu, F., Shen, G., Yu, R.: Amperometric biosensors based on platinum nanowires. *Anal. Lett.* **40**, 875–886 (2007)
60. Fenoy, G.E., Marmisollé, W.A., Azzaroni, O., Knoll, W.: Acetylcholine biosensor based on the electrochemical functionalization of graphene field-effect transistors. *Biosens. Bioelectron.* **148**, 111796, (2020)

61. Zhang, L., Zhang, Q., Li, J.: Layered titanate nanosheets intercalated with myoglobin for direct electrochemistry. *Adv. Funct. Mater* **17**, 1958–1965 (2007)
62. Umar, A., Rahman, M.M., Al-Hajry, A., Hahn, Y.B.: Enzymatic glucose biosensor based on flower-shaped copper oxide nanostructures composed of thin nanosheets. *Electrochem. commun.* **11**, 278–281 (2009)
63. Wang, J.: Electrochemical glucose biosensors. *Chem. Rev.* **108**, 814–825 (2008)
64. Patolsky, F., Weizmann, Y., Willner, I.: Long-range electrical contacting of redox enzymes by SWCNT connectors. *Angew. Chem. Int. Ed.* **43**, 2113–2117 (2004)
65. Liu, J., Chou, A., Rahmat, W., Paddon-Row, M.N., Gooding, J.J.: Achieving direct electrical connection to glucose oxidase using aligned single walled carbon nanotube arrays. *Electroanalysis* **17**, 38–46 (2005)
66. Morales, M.A., Halpern, J.M.: Guide to selecting a biorecognition element for biosensors. *Bioconjug. Chem.* **29**, 3231–3239 (2018)
67. Peng, B., Fang, S., Tang, L., Ouyang, X., Zeng, G. In: *Nanohybrid and nanoporous materials for aquatic pollution control*. Tang, L., et al. (ed.), pp. 233–264. Elsevier, (2019)
68. Gupta, N., Renugopalakrishnan, V., Liepmann, D., Paulmurugan, R., Malhotra, B.D.: Cell-based biosensors: recent trends, challenges and future perspectives. *Biosens. Bioelectron.* **141**, 111435, (2019)

Chapter 2

Pathways to Translate the Biomedical Prototypes



Tamanna Bhuyan, Surjendu Maity, Devi Rupa Saha, Nayan Mani Das,
and Dipankar Bandyopadhyay

1 Introduction

Recent decades have witnessed remarkable technological advancements in healthcare devices that have been responsible for early and precise diagnosis, more successful treatments, and helping patients to lead healthier lives [1, 2]. However, because new technology primarily drives healthcare expenditures and product risks against benefits, a careful evaluation of primary critical paths, including product initiation, formulation, design, final validation, and product launch, is increasingly necessary for clinical practice [3–5]. The target audience for these activities is scientists, clinicians, and technologists to translate novel medical technologies from academia to the market [6, 7]. The global medical device industry is significantly technology-driven and progressing rapidly. However, in India, it is still in the nascent stage with restricted levels of availability of infrastructure, penetration, lack of trained human resources, adoption and out-of-pocket expenditures [8–10].

T. Bhuyan · S. Maity · D. R. Saha · N. M. Das · D. Bandyopadhyay (✉)
Centre for Nanotechnology, Indian Institute of Technology Guwahati, Guwahati, Assam 781039,
India

e-mail: dipban@iitg.ac.in

S. Maity

e-mail: surjendu.nano@iitg.ac.in

D. R. Saha

e-mail: drupa@iitg.ac.in

D. Bandyopadhyay

Department of Chemical Engineering, Indian Institute of Technology Guwahati, Guwahati,
Assam 781039, India

N. M. Das

Department of Physics, Sipajhar College, Darrang, Assam 784145, India

Currently, the Indian healthcare industry is significantly import-dependent, comprising only 1.7% of the world market, and valued at approximately USD 10 billion. Over the past few years, the Indian government has raised public expenditure on health to 2.5% of the Gross Domestic Product that has substantially registered a compound growth rate of 25%. As per the market evaluations, the Indian healthcare industry comprises over 800 manufacturers, of which 65% of companies having a turnover of USD 1.5 million. Interestingly, 2% of the company's turnover was measured to be more than USD 73 million, which has been expected to reach close to USD 25 billion by 2025 [11–14]. This presents an exciting opportunity to understand the nature of this industry and to play a considerable role in providing quality universal healthcare to the nation.

The path for transforming an idea into a user-centered medical product is essentially based on multiple factors, including basic research, invention, patent application, additive manufacturing, clinical testing, market trends, capitalization, regulatory requirements and commercialization [15–22]. The roadmap for prototype translation toward product commercialization comprises of six consecutive stages: (i) Initiation and risk analysis, (ii) formulation and feasibility, (iii) design and development, (iv) verification and validation, (v) product launch, and (vi) post-launch assessment [23–25].

The six stages of lifecycle to develop and commercialize user-centric medical device has been schematically represented in Fig. 1. Employing such systematized approaches ensures the development of effective and well-designed medical devices that are in tune with medical practitioners, patients, and lay caregivers. Earlier, companies adopted the licensing intellectual property when the prototype was still in the research phase. However, in recent years, the assessment of preclinical data has been made mandatory by the venture capital groups to minimize their risks before investing [15]. The funding agencies for laboratory research largely support hypothesis-driven studies and experiences high commercial risk. On the contrary, major granting agencies undergo relatively lower commercial risk while translating prototypes from the clinical-stage toward marketing [26–28].

For these reasons, planning ahead for translation is the finest way to obviate costly downfalls that can endanger long-term profits [29, 30]. Currently, numerous companies are familiar with the effects of prototype translation, while they are also curious to understand the intricacies of such transformations toward medical device industries for developing clinically effective devices [31, 32].

In view of the commercialization complexities that lead to many innovations being “lost in translation”, this chapter unpacks an overview of the methodical translational strategies to drive promising biomedical prototypes from laboratories to market. The chapter introduces the current technological trends of several commercialized biomedical sensors outlining their basic working principle, component-based classification and their impact on the healthcare industry. This chapter allows a better understanding of the strategic planning required to design medical devices for early-stage valuation and implementation. The chapter also discusses the rigorous testing needed for passing clinical trials, premarket approval process, post-market surveillance procedures and other essential regulatory regimes of the Indian medical device

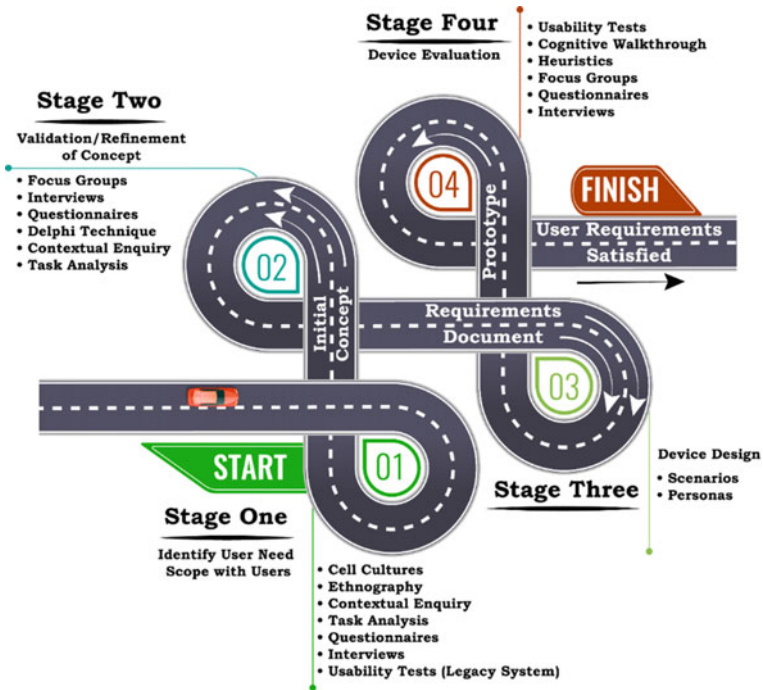


Fig. 1 The six stages of lifecycle to commercialize the user-centric medical device

industry. Through this discussion, we also highlight the gaps and challenges that exist between universities, industry partners and medical practitioners, and articulate the role of government to drive medical devices growth by combating the difficulties with prototype translation.

2 Diagnostic Biosensors: An Overview

Since the discovery of the first glucose biosensor in 1962, biosensors have progressed tremendously, leading to their vital use in almost every discipline in today’s world [33, 34]. In the past two decades, several integrated biosensors have led to the formation of sophisticated medical devices, which has increased the early detection of infections, decreasing the patient mortality rate and encouraging the researchers to imbibe more advanced technologies in the domain of biosensors [35–37].

(i) Technological Breakthroughs

Over the past few decades, the discovery of biosensors has gained tremendous attention in the field of healthcare devices. An overview of the advancements in biosensors technology till date has been summarized in Table 1 [38–45].

Table 1 A summary of a few reported biosensors

Serial No.	Year	Events
1	1962	First electrode-based biosensor for glucose detection present in biological samples
2	1970	Discovery of ISFET (Ion sensitive field effect transistor) based biosensor
3	1983	First SPR (surface plasmon resonance) based immunosensor
4	1984	Amperometric biosensor mediated with ferrocene for detection of glucose
5	1992	First hand-held-based blood biosensor
6	2008	Aptamer-antibody-based chip immunoassay to detect C-reactive protein present in spiked serum
7	2013	Detection of (HER2) human epidermal growth factor receptor-2 found in patients with breast cancer using aptamer-based electrochemical nanobiosensor
8	2014	Silicon-based optical biosensor for cancer therapy
9	2015	Detection of CTCs (circulating tumor cells) in case of breast, melanoma and prostate cancers using cluster chips
10	2016	Detection of blood glucose non-invasively using low powered lasers-based wearable biosensors
11	2017	Detection of glucose using ZnO (zinc oxide) nanorods on FTO (fluorine doped tin oxide) based biosensor
12	2018	Detection of prostate cancer biomarkers using gold nanorods-based electrochemiluminescence (ECL) aptasensors
13	2019	Functional tattoos to detect concentration and pH of albumin and glucose present in human serum
14	2020	Detection of CTCs (circulating tumor cells) present in patients suffering from neck and head cancer using cellulose nanocrystals magnetized by iron oxide NPs (nanoparticles) based biosensors

(ii) Components of Medical Biosensors

A diagnostic biosensor typically comprises an analyte, bioreceptor, transducer, electronic system, and a display, as presented in Fig. 2. Realizing the appropriate role of every biorecognition element during the preliminary developmental stages is necessary to promote novel biosensor technology's clinical success. Choosing the biorecognition elements that are sensitive to the bio-analyte concentrations facilitates the detection of diseases at an early stage [46, 47]. The performance of the biosensing elements depends on factors like transport and storage conditions. Therefore, in the initial design phase, it is vital to analyze the target bio-analyte and its corresponding biosensor utilization because an appropriate bioreceptor selection will contribute to the development of efficient biosensors [48, 49]. An early emphasis on the clinical trials during the biosensor development stage has the potential to ameliorate the accessibility of patient-centric medical devices in low-resource regions.

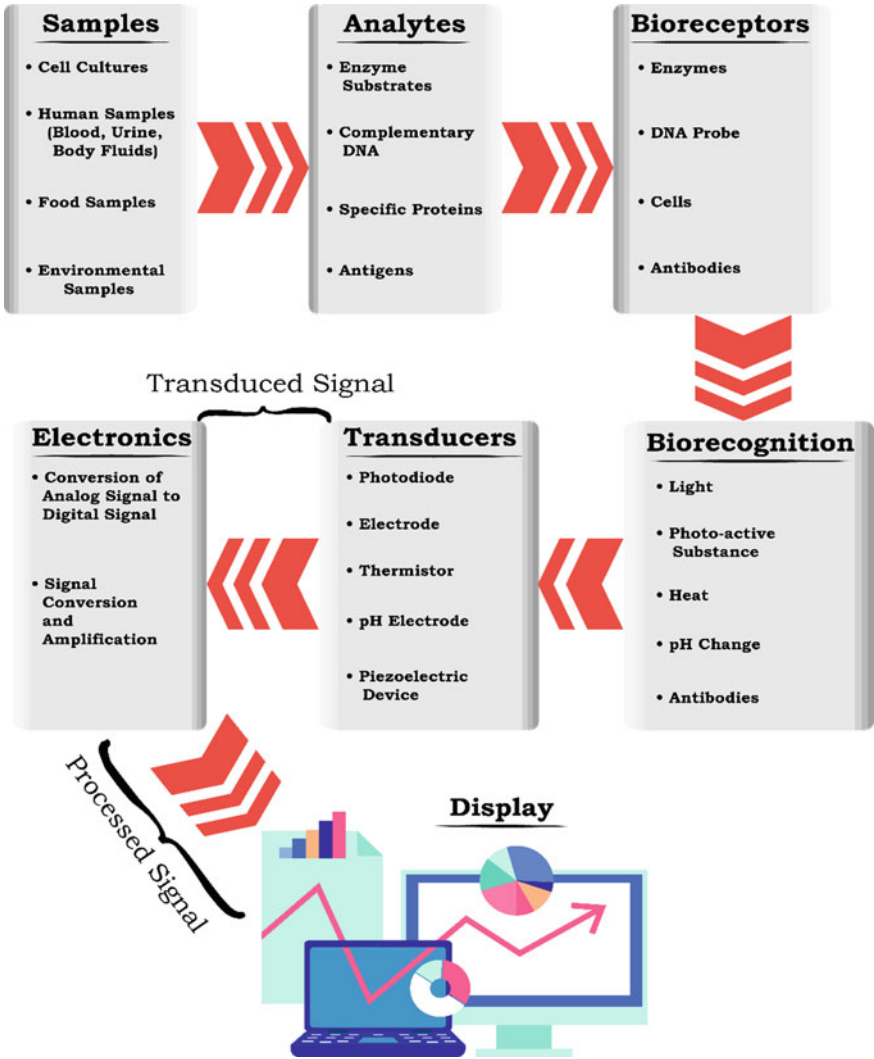


Fig. 2 Components of a diagnostic biosensor

The success of innovative biosensor development depends on an overall biosensor performance and requires a crucial understanding of selecting an optimal biorecognition element in the preliminary design stage. There are numerous biorecognition elements that range from naturally occurring to synthetic constructs [47, 50]. The pros and cons of selecting natural, pseudo-natural and synthetic biorecognition elements have been outlined in Fig. 3.

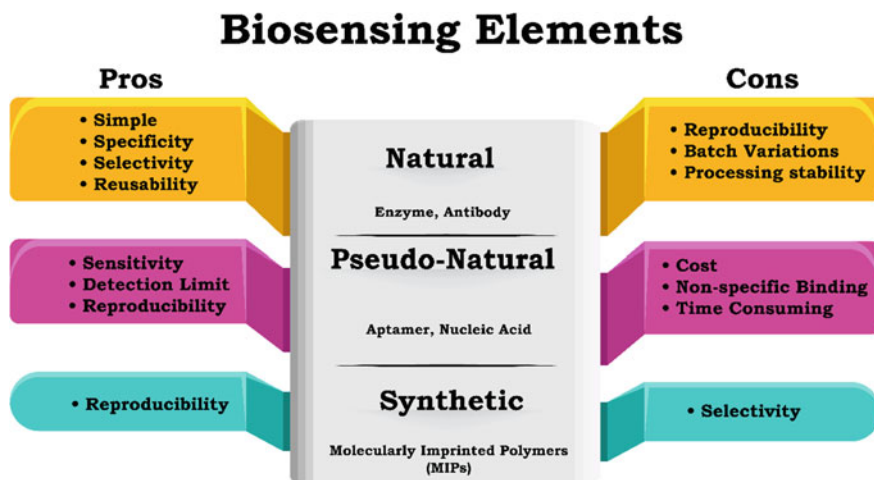


Fig. 3 Selecting various biosensing elements

(iii) Biotransducer-Based Classification

Biotransducers are components in the biosensing system that determines the stimulus discharged from the analyte-bioreceptor interactions and generates an electrical signal following electrochemical, mass, or temperature changes [51, 52]. Transducer-based biosensors are categorized based on their physicochemical transduction and are mainly of four types: electrochemical, optical, mass-based, and calorimetric, as shown in Fig. 4.

(iv) Biosensors and Healthcare

Over the past 60 years, the contributions of the biosensors have provided a greater outlook to develop highly multi-functional, and low-cost point of care testing devices to measure the medication records taken by patients. The capability of such devices to provide rapid real-time testing have not only allowed the patients to evade labor-intensive medical laboratory analyses but also have assisted the clinicians in examining minute details of the patient's health [53]. In the upcoming years, further advancements in detecting methods will lead to the design of highly sensitive sensors for disease-related sensing of biomolecules. Conclusively, it could be realized that design and development of real-time biosensors, particularly microfluidic integrated biosensors, photonics-based biosensors, and biochip integrated biosensors, would improve the efficacy of translating healthcare innovations, thus facilitating rapid estimation of sample and accurate testing [54–57].

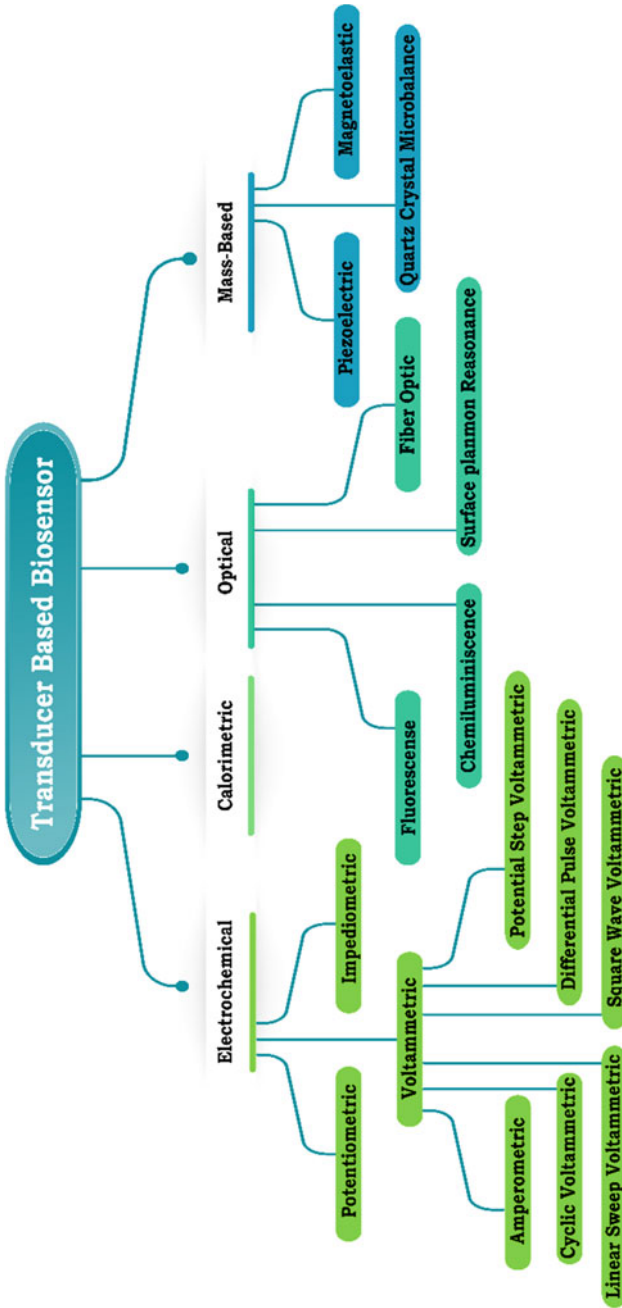


Fig. 4 Classification of transducer-based biosensors

3 Planning for Device

Transforming a laboratory-based prototype into a marketable device requires some vital and systematic planning. It is noted that the healthcare devices are directly involved with monitoring and saving human lives as well as improving the lifestyle. Therefore, the focus has been shifted toward meeting the industrial standard with high accuracy, and low interference that is possible by managing strategic planning ahead of time [58]. The process of strategic planning for prototype translation is described below.

(i) Translate Ideas to Invention

It is crucial to select the idea around the laboratory-based prototype. For that, one must survey the problems associated with the society or community. For example, the survey on the detection of diseases or any time-taking biomarker analysis through blood or urine may give you the clues for the new ideas, which might be transformed into future inventions [59–61].

(ii) Risk Analysis of Product

Once the idea or target is fixed, the risk analysis of the product becomes a pivotal factor in giving the idea a green signal. A detailed market survey should be done to analyze the potential of the device. For example, the idea must be unique, cost-effective, less time-consuming, and highly accurate. The product must have a sellable market, or the market should be created by spreading the awareness of the device. Errors related to medical devices create a genuine risk to patients that can be reduced through understanding and evaluation of device-related events [62–64].

(iii) Prototyping

The prototype should be protected by filing for Intellectual Property (IP) and patent the idea after finalizing the idea and completing the feasibility of the product in the market. This step would provide the developer with legal freedom from the competitor to develop the product. In India, the patent filing trends in the medical device domain has roughly doubled with 1104 filings in 2014, as against 640 filings in 2005. This specifies the progressive and consistent IP awareness and strategies of the foreign manufacturers to capitalize on the flourishing Indian medical device industry [63].

(iv) Laboratory Research to Prototype Development

The planning should be conducted thoroughly after analyzing the risk and marketability of the product. This step would provide information regarding the clear pathway to develop the laboratory-based product through proper research work. Besides, it reveals all the parameters associated with the development of the device and where the optimizations are required. The involvement of all kinds of accessories such as instruments, chemicals, reagents is discussed in detail. Once such searches have been performed and anticipate to protect and follow the idea, the project and preclinical research have to be separated from fundamental research projects keeping it confidential until submission of patent protection.

(v) **Formulating Budgets and Time Chart**

Formulating budgets is a very crucial entity for the development of any product. Allocation of money should be planned diligently to maintain the seamlessness of the development. For example, all the reagents, chemicals, electronics, and instruments should be bought with the allocated money. A time chart should be formed, and the weekly targets must be fixed for the entire time frame. The headroom approach holds promise for rational planning of business decisions, financial sustainability with commercial negotiations based on timing along the development cycle for a new product [65].

4 Initial Implementation Stages

Once the developer is wholly convinced with the product, which has the market to sell and is financially viable, only then they go forward with the initial implementation stage. This stage consists of writing a project for funding to set up protocols for product-related developments. The linear stage-gate model provides a comprehensive elucidation of the activities related to the development of medical devices. Some of the parameters are listed below.

(i) **Funds**

At this stage, writing the project report is the most critical work to do because it would attract funding for development. The detailed description of the device, patent or IP document, the working principle, and market survey might help the report to be more approachable to the funding agencies. Besides, the strong partnerships may be formed by signing memorandums with other companies for the developments, if needed.

(ii) **Potential Revenue**

A detailed report must be prepared to project on the potential revenue by selling the products. This may provide ideas toward the sustainability of the company and the product. Additionally, it articulates the potential market available for the device. An estimation of the potential commercial viability of medical devices can be carried out by following the Headroom approach combined with return on investment [66].

(iii) **Regulatory Compliances**

A proper investigation must be conducted for the regulatory compliance on the medical product or healthcare device, which are being developed. A medical device or product should pass all the rules set by the governing authority. Failing to do so may compromise the future of the device and deny the license to market the invention. Thus, a detailed study on regulatory compliance is required to ensure safety for the patients. Additionally, it may provide the required approval from the regulatory authority and conduct the audit to go smoothly [67].

(iv) **Quality Management System (QMS)**

QMS is the foundation of any company, which provides an excellent base to develop everything on it. ISO 13,485 is the internationally recognized standard and adopted by most of the medical device companies such as Johnson & Johnson, Novartis AG, and Abbott Laboratories. The QMS would help to standardize the procedure, forms, documents and templates that would cover all activities throughout the product development cycle, including product design, manufacturing, risk management, addressing the complaint, clinical data storage, loading and supply, among others [68].

5 Design and Development

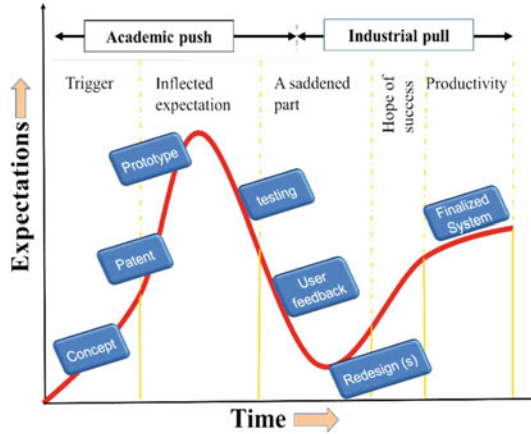
(i) **Traceability of Device Design**

A strategic approach of designing is followed while doing innovation, which at large, diverges, way beyond the concept of the product design in the context of strategy and management. Systematic management of skills, works power, workman-handling, documentation, organization, investments reliability, etc., is the part of this strategy while looking at the cutting edge approaches and developments in the strategic design deals in the case of medical devices.

- (a) **Strategic Design and Development of Product:** Inspiration, ideation and implementation are the main three spaces of the new business plan that can be developed thinking a strategic plan. Looking at the parameters, the strategic design possesses complex learning and thinking to solve a mainland problem with a correct rational approach. Thus the strategic design becomes a strategic practice, and the practitioners or the researchers literally deals in *designing a practice*. An organization now aim to perform the strategic plan keeping a view on the problem assigned to achieve “what” it is and “how” it is, which uplifts design or rather a practice, up to a strategic path than mere thinking of a purely tactical approach, hence the emergence of strategic design [69, 70]. Thus a strategic design in the case of a medical device does accumulate the feasibility, desirability, viability, design practices, principles and tools at extending while implicating the complete design [71–73].

The Gartner’s Hype Circle: Following the strategic plan for the innovation through research, the scientist found the best way to deal with the strategy and that is determined by what is called the Gartner’s hype circle [74, 75]. The study says that the hype circle seems to be very well managing while following the higher-level concepts of device program such as IT methodologies and management disciplines. In general, the Hype circles produce innumerable numbers of plan circles to track the concerned innovation maturity and future potential. Hype circles manage the decision to implement the typical progression of innovation by maintaining the trends and ideas, strategies, standards, management concepts, competencies and capabilities, as shown in Fig. 5.

Fig. 5 The Gartner’s hype model



(b) **Defining Design Inputs:** Once the strategic design is confirmed, then comes the design input. In general, the platform where the academic push and the industrial pull starts operating (Fig. 5) for satisfying the goal of innovation and marketing, respectively. The academic push is concerned with mostly the design, prototype, manufacturing and product engineering. The lab-based research work is now ready for device makers, and the designers or the architect starts thinking about the design. They undergo a lot of hits and trials in designing a perfect geometrical shape and ready to get hold of the next step of prototyping. The prototyping also needs a lot of trials, although less than the design part and finally comes with device product manufacturing with perfect engineering [76]. The design inputs go hand in hand with the development. Development is the stage where the ideas cherished are transformed into definitions and then turned into geometrical shapes. Design and development all stay with the proper market concerns, and they must be flexible to be implemented according to the relevant prevailing concepts and information. In this regard, physicians or medical practitioners can come up with really valued ideas to be implemented or incorporated once the design and development process is carried out.

The practitioners are dealing with the real public, and within the area of expertise, they are exposed to vivid ideas and shortcomings. The physicians represent the customer, and engineers implement the design engineering according to their needs, and hence the practitioners are media of data generation and the engineers innovate and develop based on real facts and requirements. Thus collecting knowledge of years of experience from the medical practitioners can deeply impact the device design and manufacturing inputs. We can now generalize that the device input and performance characteristics are used as the basis for device design, as represented in Fig. 6.

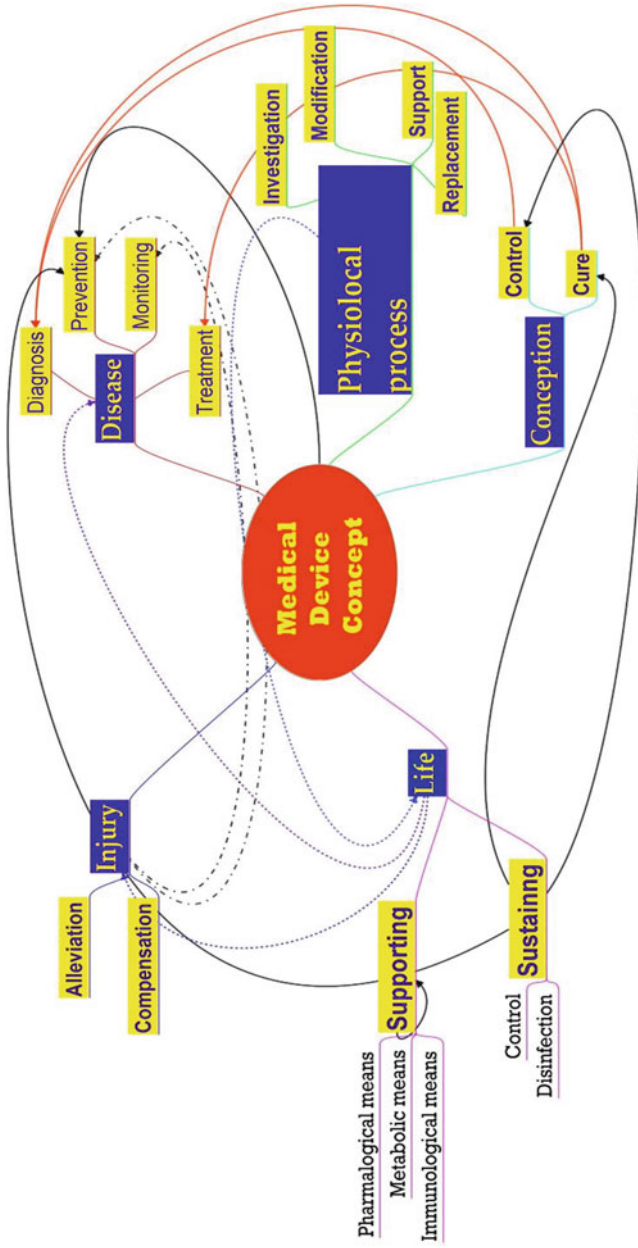


Fig. 6 The mind-map of the medical device concept

We may define the design inputs as the supersets of the following subsets, which are:

- Ensure requirements are appropriate by addressing user needs and intended use in terms that are measurable.
- One needs to address incomplete, ambiguous, or conflicting requirements.
- The document, review and approve input requirements.
- Lastly, Human factors.

(c) **Specifying Design Outputs:** The design outputs are the fruits that are gained after the successful implementation of strategic design, design input and development. These are all at a time come out with the assemblies and subassemblies of thoughts, components, parts and pieces. A successful device output is a carefully executed mission of assembled ideas and implementing them step by step with proper documentation. A similar approach has been demonstrated as a case study of translational research, as shown in Fig. 7. These documents are clearly abbreviated and further explaining the new user with proper guidance and exact work streaming to redesign the same with repetition. Such a documented idea leads to the basis of the *device master record* (DMR). Thus the DMR stands alone as the complete recipe for the new device. Further, the documented literature about the device output is described very well in the FDA 21 CFR Part 820.30(d) and ISO 13485:2016 7.3.4 state about Design Outputs [77].

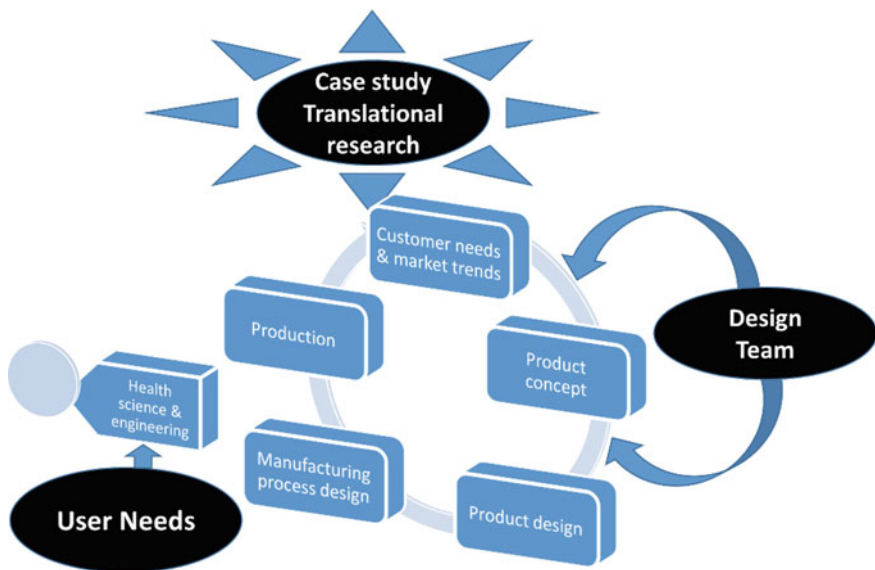


Fig. 7 The case study for translational research

- (d) **Optimization of Designs:** After successfully completing the output stage, there comes the technology transfer, and the device is ready to be marketed. At this stage, the academic push ceases to work further, and the business/market pull tries to acquire the field depending upon the market and response. Effective design transfers from the push–pull interface are feasible through rigorous product’s design documentation, selection of components and careful definition of production methods. Business pull without an ineffective or complete failure in implementing may lead to doom, causing the monetary crisis. The practice of ill-proven devices may be fatal to human society too. Newly conducted trials and modifications of design and development can lead to an increase in cost and thus making it rarely accessible. Consequently, the result of effective design transfer becomes null and void. In order to tactfully manage the marketing and to live the business, re-evaluation of design is of utmost importance. It can definitely lower the material and production cost, decrease the product time to market, increases product quality and also generate customer enthusiasm.
- (e) **Design Validation:** The term validation and verification (V&V) is a very key factor to be checked at each level from idea generation to product launch finally. Each and every point in each stage to be verified, and the marketing team, as well as the research/stakeholder team, should be ready with verified documentation or product innovation lining. The project may see changes in manpower, funding instability, user-defined problems, but V&V may find answerable to each and everyone with perfect reasoning and with common ideas. This will not let the project go astray and will also not disturb the final release. This will also ensure to establish and maintain device design correctly [78]. To grow in the market and to justify the medical cure V&V should carry on from early stages of product development and should continue throughout the product’s life cycle. The product V&V, in a nutshell, deal with the assembly drawings, inspection and test specification and manufacturing events.
- (f) **Design History File (DHF):** In order to maintain the regulatory action in the medical device distribution in the market, the manufacturing company must comply with the DHF. According to DHF guidelines, there should be a perfect compilation of record history that describes the finished device. The DHF is basically used to regulate the developed device, major components, labelling, packaging and production processes. DHF is fully required for the product developed with DMR.

6 Information to Regulatory Body

(i) Classification

Medical devices are categorized based on risk factors. Generally, in a broader group, they have been classified into four (4) major groups. However, counting risk and use and purpose the devices can have further several specific sub-groups. Following

Table 2 Classification of medical devices as approved by the central drugs standard control organization

Group	Risk factor	Items included
Group A	Low risk	Absorbent cotton wools, monitoring devices, disinfectants, etc.
Group B	Low-moderate risk	Thermometer, BP monitoring device, disinfectants, etc.
Group C	High-moderate risk	Implants, hemodialysis catheter, etc.
Group D	High risk	Angiographic guide wire, heart valve, pacemaker, etc.

are the classification as approved by Central Drugs Standard Control Organization CDSCO (New Medical Device Rules 2018), represented in Table 2.

In practice, the risk assessments are done on the basis of the experience of the healthcare professionals and also on the manufacturing guidelines as provided by the engineers. For accomplishing the risk evaluation, the different governments have different committees making policies and also the decision-making powers of the lawmakers.

(ii) Quality management system (QMS)

QMS basically adopted to standardize the medical devices in terms of the following parameters, and the organization must take into consideration the interdisciplinary quality control measures to attain those principles [79].

- (a) *Customer focus*
- (b) *Leadership*
- (c) *Engagement of people*
- (d) *Process approach*
- (e) *Continuous improvement*
- (f) *Evidence-based decision making*
- (g) *Relationship management.*

The above-mentioned doctrines are to be implemented via special training and induction programs to the staff and management authorities in order to raise the assessment scores. It also urges to be technically sound so that no one should bother about the record-keeping process. Lastly, it also emphasizes on promoting the work to the highest authority review with a stipulated period.

(iii) Registration

After the completion of the rules, regulations, assessments, validation, etc., the product now set for seeking government registration. This is very important as the cost, transparency in product details, medical regulations, in-house product use, etc., are verified and finalized in all parts of the region. The medical devices intended for use in the USA must register with the US Food and Drug Administration (FDA). In India, any medical device is notified by the MoHFW (Ministry of Health and Family Welfare) Drug and Cosmetic Act (DCA) 1940 rules.

(iv) Labelling

Labelling and specifying the instructions are of utmost importance in using the medical device. Mislabeling of medical devices can result in serious consequences for the user. According to the classification of the medical devices, they pose a threat to the end-users in low to high progression. Properly packaged such devices pose little risk to the user, handling them even if the device is hazardous. The labelling and proper packaging of the device also ensure in delivering clean, sterile and protected. In shipping, the product to distant places also requires labelling and secure packaging.

7 Product Launch

(i) Final Validation

The manufacturers must ensure that the product that has been designed will meet all the required standards and safety protocols. The DMR and DHF should be well maintained, and if required, could be checked in the response of the final product launch. Strategic design, development, manufacturing, packaging, labelling is all verified finally to get the product being ready for the market. Final trials or validation is required, which may lead to terms like the “user error” while implicating the human factors and can lead to deviation from what is intended by the manufactures.

(ii) Tenders for Public Procurement Order (PPO)

After the final validation, the next market strategy is to engage the distribution company so that the product can take the market in full swing. There are approved procedures for opening the tenders for public procurement orders (PPO). Once approved, the final transfer of assets with DMO, DHF, design, R&D works, V&V documentation is transferred to the company in support of royalty in return.

(iii) Transferring the Product Design

The overall prime focus with highly discussed but less productive action is the technology transfer. A lot of work on medical devices all around the world has been going on, but only a few see the market, and even fewer are successful. This is because technology transfer is truly very difficult and problematic. The method of presupposition measures for technology transfer has been outlined in Fig. 8.

(iv) Successful Reimbursement

Gaining success in the medical device market is not at all guaranteed, and even the different registration agencies after the approval of the product launch are not responsible for reimbursement once the product fails to gain the market. Regulatory authority only gives medical device companies the opportunity to market a device, and it does not ensure payment. For successful reimbursements need early and savvy planning while introducing new to the market, payers and providers must be enlightened about the innovative technology to be demonstrated and also should be made

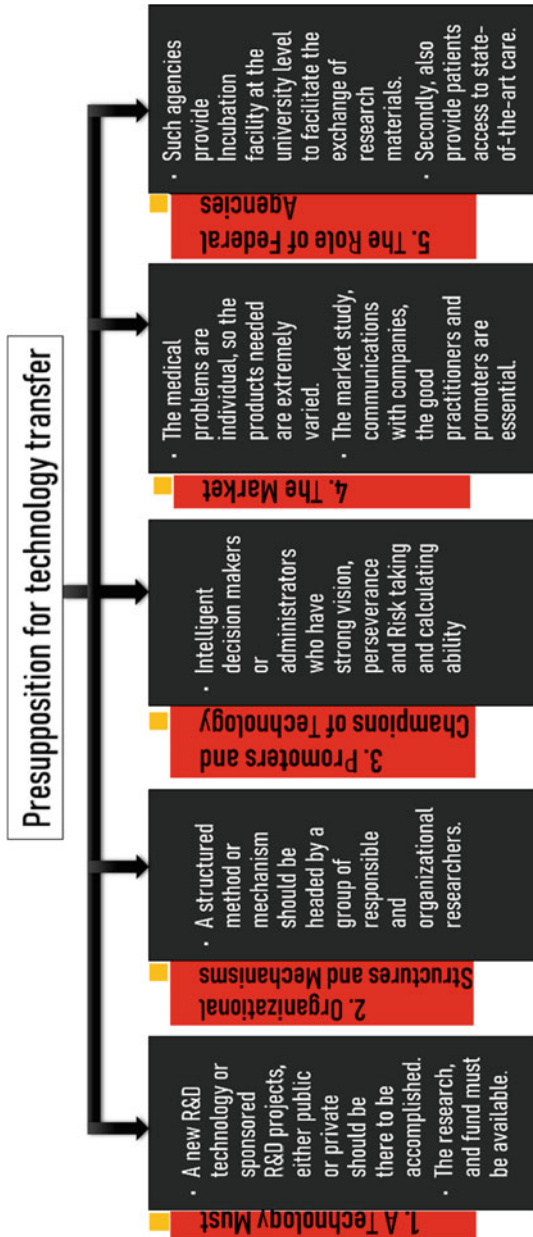


Fig. 8 Schematic diagram showing the presupposition for technology transfer

aware of clinical and economic value to be getting considered for reimbursement. Failing to have a strategic market plan by addressing the above issues may risk being stalled in the marketplace. Successful reimbursement also emphasizes study on the economic value endpoints in order to save money, time and to be hassle-free.

8 Post Product Launch

In April 2015, a guidance document was released by the Center for Devices and Radiological Health (CDRH) for assisting patient access toward safe and effective medical devices that persuades a real-time healthcare system. Such a plan of action could improve the CDRH internal systems by making the premarket review process more predictable, efficient, consistent and transparent [80, 81]. This section will focus on the relevant post-launch activities required to complete the feedback loop, which marks the beginning of the product marketing journey. Some of the major activities that can be construed as Post Market Controls by the FDA often include Post-market Surveillance (PMS), dealing with quality management and scrutinizing quality management system (QMS).

(i) Post-market Surveillance (PMS)

It refers to a system of monitoring the safety, efficacy and performance of the product carried out by the medical device manufacturers after it has been sold in the market. When it comes to product surveillance, rigorous review of post-market studies and product associated clinical trials for market approval, the medical device has to be carried out by the medical device developers. The PMS reports can be submitted by the developers tabularizing any reported failures, risks and adverse non-conformance events, stratified into whether the owner considers them to be device-related or not [82]. Also, the FDA entails device developers to carry out independent PMS compliance for Class II or Class III device that is used in paediatrics, implanted in customers for over a year, cause serious health hazard upon product malfunction, and devices envisioned for life-sustaining use outside traditional healthcare facilities [83].

The device developers conduct the PMS activity following a strictly scheduled plan after systematic collection of the database from proactive and reactive sources. PMS could respond after the occurrence of an incident, thus considered as “Reactive” and passive as they broadly execute database collection operations. PMS could also be considered as “Proactive”—as they provide data and detailed information into the real-world performance of the medical device. The PMS plan should address the utilization of available information corresponding to trend reporting, feedbacks, and details of similar available products, technical databases and records on undesirable side-effects [84]. Once the PMS planning has been achieved, the results of the collected data and the conducted corrective PMS activities need to be published in the form of a PMS Report (PMSR). The documentation of PMSR offers guidance to medical device manufacturers in drawing up the well-structured PMS plans in report

templates, implementing the PMS activities, analyzing the gathered PMS database and drawing appropriate conclusions [82].

(ii) **Quality Management System (QMS)**

A quality management system (QMS) of a medical device is a standardized system of procedures and methods encompassing entire aspects of medical device design, manufacturing, managing suppliers with risks associated, dealing with customer complaints, clinical data management, product distribution, storage, installation, servicing and labelling, among others. On the basis of device classification, the complexity of the QMS varies. For instance, different QMS implementation will be required by companies making medium-risk (Class II) or high-risk (Class III) medical devices than companies developing low risk and aseptic surgical instrument (Class I) devices. Therefore, the requirements of the quality system can govern all stages in the medical device lifecycle [68]. This is the point where medical device companies add procedures for these areas to expand their QMS with clear documentation. For medical devices, the International Organization for Standardization (ISO) (ISO 13485:1996 and ISO 13488:1996) issues the international quality system standards [85]. Once the production of a medical device is ramping up and products are being sold in multiple markets, there is an urgent need to track a variety of quality events, particularly product malfunction, addressing customer feedback and complaints, and monitoring quality issues.

(a) **Product Malfunction**

Sometimes the medical device may fail to meet certain specifications and desired levels of standards, an incidence called non-conformance terms of ISO 9001. Some of the possible causes of nonconformity include poor maintenance of an operative system, lack of robustness in quality, ineffective execution of analytical techniques, low-quality investments, overestimation in the product, and overconfidence with a lack of understanding in the system [86]. If non-conformance continues, it can lead to an overall demise of a company, as the ISO 9001 standards ensure quality and safety for the customers. The malfunctioning device should first be identified by co-workers or supervisors before the matter reaches the auditors [87].

By investigating the infraction, an auditor recognizes the level of nonconformity and resolves the issues precisely before it affects the higher goals of the company. Minor non-conformance includes low-risk situations, isolated personnel incidents, single missing records or one document alteration that does not adversely affect the operating system of the entire business. On the contrary, major non-conformance like multiple unsigned documents, many alterations to documents and huge requirement violations can obstruct the business operation at ISO 9001 standards. Minor non-conformances in the long term can compound into major nonconformities if not addressed immediately [62, 64]. A non-conformance report (NCR) can be filled out by the managers notifying the ISO 9001 requirement that is being violated, elaborating the infraction, and a detailed plan of action for fixing the issue.

(b) Addressing Customer Feedback and Complaints

An essential component of management requirements for PMS is responding to customer feedback. Most companies have a good way of addressing customer complaints, but not many are as dedicated as they should in consorting general feedback. Setting up a proactive plan for gathering feedback helps to identify complications before they turn out to be systemic. Sometimes, customers may propose unique perspectives on ergonomics, material and color that might be advantageous for the improvement of the device. Essentially, post-market issues can be “incident-driven” with immediate action requirements or “review-driven” that falls within the ISO 13485:2016 and FDA definitions of complaints with reliability issues [88].

After receiving a customer complaint, the following three particulars should be evaluated:

- Is there any requirement for submitting the reported event to regulatory bodies?
- Is there any requirement for a detailed investigation?
- Is there any requirement for additional corrective operation?

(c) Monitoring Quality Issues

The quality issue trends can be monitored and handled in real-time before they create regulatory complications by assigning investigation-related responsibilities to the relevant partners and prompt sharing of compiled data with regulators. The need for corrective actions to resolve causes of recurring nonconformities or any other undesirable situations led to an establishment of a document-intensive process named Corrective and preventive action (CAPA or simply corrective action). The CAPA has been designed by a team of quality assurance personnel and workers involved in the real surveillance of non-conformance. The structuring of CAPA requires the use of an effective 8D framework method that must be systematically investigated to identify the root cause and to eliminate further recurrence of any nonconformities. It is also mandatory to close CAPAs in a timely manner, ensuring that they do not remain open for an extended time period [89]. CAPA is an approach within many ISO business standards in association with good manufacturing practice (GMP), Hazard Analysis and Critical Control Points and Risk-based Preventive Controls (HACCP/HARPC).

As determined by the Deming-Shewhart cycle, CAPA fits into the PDCA (plan-do-check-act) philosophy that includes stages for investigation, action, review, and further action (Fig. 9). Investigations may imply simple remedies to a problem with no systemic root cause identification and additionally may conclude exclusion of any corrective or preventive actions [90]. Implementation of corrective actions is based on problem identification through staff suggestions, the management or document reviews, internal audits, and customer complaints. Correction is the step to terminate an identified nonconformity through error proofing, process redesign, modifying existing programs and improving material handling. Preventive action comprises predicting problems, self-initiated activities to avoid such occurrences and product-related analysis by the active participation of staff members [91]. Thus, execution of CAPA is the approach toward improvement and effectiveness of QMS where a medical device company sets out a CAPA process within their QMS.

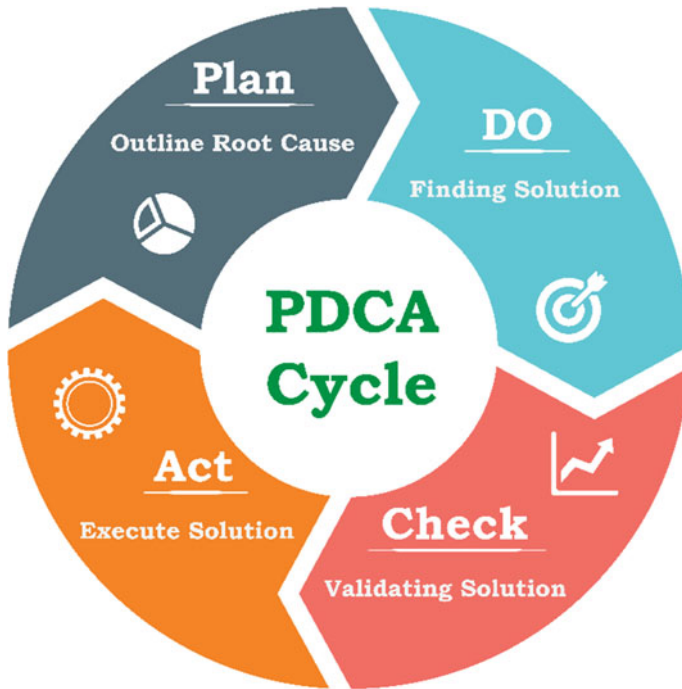


Fig. 9 Corrective and preventive action (CAPA) fits into of PDCA cycle

(iii) Examining QMS Process

The maintenance of the QMS process can be carried out by management reviews by aiding the role of executive management in assessing and examining the QMS procedures. Conducting management reviews regularly could reduce risks by improving the product quality process by measuring the improvements several times in a year and also helps to set goals between the evaluations [68].

- (a) **Clear Documentation:** An internal or external audit makes it easier to figure out where workers might lack in terms of compliance. Manufacturers and importers are required to submit reports for adverse events and device-related problems to the FDA. Such post-market surveillance tools used by FDA is Medical Device Reporting (MDR) that monitors device performance, identify safety issues, and provides product associated benefit-risk to improve patient safety [82].
- (b) **Planning Ahead:** At the beginning of the process, transactional activities including implementation, business dealings, inspections, negotiations, mergers and acquisitions should primarily be considered with a promising exit strategy and then reassessed during the product development cycle. Planning the internal audits ahead of time lowers the stress of forthcoming external audits

and provides an opportunity to perform quality gap studies, thus improving the performance of a medical device, and as such, the quality of life of customers [29, 30].

9 Preparing for ICMR Inspections

Since India is being envisaged as a global hub for translational research with growing numbers of corporate hospitals with state-of-the-art facilities, visits by foreign specialists using newer biomedical devices and techniques have been increasing. Many academic and research institutions, as well as private entrepreneurs, are actively involved in creating indigenous devices, which need to be critically tested in Indian patients for safety and efficacy. Some low technology devices seek the Indian Standards Institute (ISI) and The Bureau of Indian Standards (BIS) for premarket approval requirements. Most of the devices are being assessed by Central Excise testing specifically for taxation purposes and do not come under the strict regulatory bodies, which discourages entrepreneurs from venturing. However, these procedures are not satisfactory to ensure the quality of high technology biomedical devices, and thus only a handful of patents or propriety medical equipment are manufactured in the country. Therefore, the concept of regulatory bodies governing strict investigations of healthcare devices is relatively new in India [9, 11].

India is now aiming for imparting affordable, accurate and good quality healthcare through minimizing out-of-pocket expenditure, efficient evaluation of disease burden, surveillance, and identifying outbreaks. Appreciating the urgent need to strengthen the quality and availability of high-quality diagnostic devices in the Indian healthcare system, the Indian Council of Medical Research (ICMR) has established the National Essential Diagnostic List (NEDL). NEDL enables standardization of technologies and will help to foster research for developing new and effective diagnostics at affordable prices. It will also promote improved procurement regulation, strengthened accreditation of laboratories, and development of nationwide quality control systems, among others [92].

Besides, a proposed setup of the Indian Medical Devices Regulatory Authority (IMDRA) is being explored by the Indian Health Ministry. As for the clinical trials of medical devices, general drug-related principles should be followed, where safety analysis and premarket efficiency of the product for 1–3 years should be achieved before premarket certification. Further, a notification named “Medical Devices Rules, 2016” has been issued by the Ministry of Health and Family Welfare, Department of Health and Family Welfare, Government of India [GSR 983 (E)] on 17th October 2016 for medical devices, stating that medical devices are broadly categorized as investigational medical devices and registered or approved medical devices. It also mentions that medical devices at the clinical trial stage need approvals from both the Institutional Ethics Committee (IEC) and the Drugs Controller General of India (DCGI), while initial laboratory studies not intended for marketing the device requires only IEC approval [92].

10 Barriers for Commercialization

The medical device market in India is valued at around \$3 billion, rising 15% per year. Relatively, it is a small market to serve a 1.3 billion population that reflects minimal usage of advanced medical technology in the Indian healthcare system. Further, 75% of the medical devices sold in the country is dominated by imports and are priced out of reach for many patients. This presents an opportunity to tackle the disease burden in India by accessing appropriate healthcare technologies [93]. However, the challenges of the Indian healthcare sector that hinders commercialization include inadequate infrastructure, high cost of services and clinical trials, lack of early-stage financing, lack of trained personnel, poor regulations around manufacture and product sale, and lack of intellectual property (IP) protection. Also, receiving FDA approval for a new product can be time-consuming and very expensive [10, 94, 95].

Such obstacles can be reduced by developing a better regulatory regime for controlling the quality, safety and efficacy of devices, adequate IP enforcement, reliable funding and bridging the gap between academic researchers and business communities. Most importantly, medical technology courses should be introduced to medical and engineering students to create a synergistic pool of practitioners and skilled engineers suitable for the Indian healthcare system. The efforts of the Indian government to improve the ease of doing business by removing bureaucratic handles have been appreciated by the national medical device industry [67, 94]. It is also felt that frugal innovation is an important strength that India can offer the world that will help the nation to attract the right technology, upgrade manufacturing operations for-profits, and build local R&D capability. Furthermore, the participation of a vibrant private sector together with promising collaboration between government and industry would uplift the standards of Indian healthcare sharply in the next decade [96].

11 Summary

This chapter provides an overview of the strategies involved in designing the medical devices and how the medical device companies play a vital role in developing new healthcare devices for diagnosis and treatment. In particular, the entire discussion on the transition of healthcare technologies from academia to industry proved to be a sophisticated process. Such an innovative transition of ideas toward commercialization requires advancement in technicalities and manufacture, clinical effectiveness, regulatory approvals and market sustainability. Accordingly, active healthcare devices require a multidisciplinary team that encompasses academia, industry and clinical inputs to address the diverse areas of product development. The chapter also reviews the basic stages needed for approval of medical devices by regulatory regimes like the Food and Drug Administration. It summarizes the post-marketing procedures to avoid pitfalls and complications that may waste time and resources.

Each of the complicated attributes of medical device safety and reliability must be methodically analyzed in an accurate, documented manner. When risks are discovered, they must be evaluated, eliminated and monitored throughout by implementing control measures to ensure that no new or unexpected risks arise. In light of these considerations, a clear long-term vision for the Indian medical industry and government to work together would improve accessibility, adoption and affordability for the medical devices. The future of the “Make in India” initiative to access affordable quality healthcare depends on nurturing local innovations and the extent of changes initiated through collaborative transformation, thus making India a global hub for medical device manufacturing.

References

1. Jakimovska, K.K., Glavas-Dodov, M., Tonic-Ribarska, J., Trajkovic-Jolevska S.: Medical device risk management and its economic impact. *Maced. Pharm. Bull.* 59(1, 2), 49–60 (2013)
2. Raab, G.G., Parr, D.H.: From medical invention to clinical practice: the reimbursement challenge facing new device procedures and technology, Part 1: issues in medical device assessment. *J. Am. Coll. Radiol.* 3(9), 694–702 (2006)
3. Burns, L.R.: Growth and innovation in medical devices: a conversation with stryker chairman John Brown. *Health Aff (Millwood)*. 26(3), 436–444 (2007)
4. White, P.F., Smith, I.: Impact of newer drugs and techniques on the quality of ambulatory anesthesia. *J. Clin. Anesth.* 5(6), 3–13 (1993)
5. Ventola, C.L.: Challenges in evaluating and standardizing medical devices in health care facilities. *Pharm. Ther.* 33(6), 348–359 (2008)
6. Sanami, M., Flood, T., Hall, R., Kingscott, F., Jayne, D., Culmer, P.: Translating healthcare innovation from academia to industry. *Adv. Mech. Eng.* 9(3), 1–9 (2017)
7. Page, R., John, K.: Commercializing academic medical research: the role of the translational design. *Des. J.* 22(5), 687–705 (2019)
8. Clark, D., Dean, G., Bolton, S., Beeson, B.: Bench to bedside: the technology adoption pathway in healthcare. *Health. Technol.* 10(2), 537–545 (2020)
9. Targhotra, M., Aggarwal, G., Popli, H., Gupta, M.: Regulatory aspects of medical devices in India. *Int. J. Drug Deliv.* 9(2), 18–27 (2017)
10. Tehrani, N.: Challenges in medical device commercialization. *Int. J. Sci. Res. Eng. Dev.* 2(1), 1–5 (2019)
11. Ventrola, C.L.: Challenges in evaluating and standardizing medical devices in health care facilities. *Pharmacol. Ther.* 33(6), 348–359 (2008)
12. Shah, A.R., Goyal, R.K.: Current status of the regulation for medical devices. *Indian J. Pharm. Sci.* 70(6), 695–700 (2008)
13. Ganesan, L., Veena, R.S.: ‘Make in India’ for healthcare sector in India: a SWOT analysis on current status and future prospects. *Int. J. Health Sci. Res.* 8(2), 258–265 (2018)
14. Depuru, S., Kumar, R.R.: An outlook on India’s healthcare system with a medical case study and review on big data and its importance in healthcare. *Int. J. Sci. Res.* 5(4), 1486–1492 (2016)
15. Kleinbeck, K., Anderson, E., Ogle, M., Burmania, J., Kao, W.J.: The new (challenging) role of academia in biomaterial translational research and medical device development. *Biointerphases* 7(1), 12–15 (2012)
16. Tamsin, M., Bach, C.: The design of medical devices. *Int. J. Innov. Sci. Res.* 1(2), 127–134 (2014)
17. Ratchford, B.T.: The history of academic research in marketing and its implications for the future. *Span. J. Mark.-ESIC* 24(1), 3–36 (2020)

18. Dixit, T., Srivastava, S., Sahu, S., Selvamurthy, W.: Intellectual property evolution and innovation ecosystem as effective tools in strengthening Indian healthcare sector. *Curr. Sci.* **114**(8), 1639–1649 (2018)
19. Javid, M., Haleem, A.: Additive manufacturing applications in medical cases: a literature based review. *Alexandria J. Med.* **54**(4), 411–422 (2018)
20. Girling, A., Young, T., Brown, C., Lilford, R.: Early-stage valuation of medical devices: the role of developmental uncertainty. *Value Health* **13**(5), 585–591 (2010)
21. Stamenovic, M., Dobraca, A., Smajlovic, M.: Contemporary aspects of marketing in clinical trials including segments of IT and technology transfer. *Acta. Inform. Med.* **26**(1), 67–70 (2018)
22. Gupta, P., Janodia, M.D., Jagadish, P.C., Udupa, N.: Medical device vigilance systems: India, US, UK, and Australia. *Med. Devices (Auckl)* **3**, 67–79 (2010)
23. Ciurana, J.: Designing, prototyping and manufacturing medical devices: an overview. *Int. J. Comput. Integr. Manuf.* **27**(10), 901–918 (2014)
24. Schwartz, J., Macomber, C.: So, you think you have an idea: a practical risk reduction-conceptual model for academic translational research. *Bioengineering* **4**(29), 1–12 (2017)
25. Money, A.G., Barnett, J., Kuljis, J., Craven, M.P., Martin, J.L., Young, T.: The role of the user within the medical device design and development process: medical device manufacturers' perspectives. *BMC Med. Inform. Decis. Mak.* **11**(15), 1–12 (2011)
26. Kucklick, T.R.: *The Medical Device R&D Handbook*. CRC Press, Taylor & Francis Group, LLC, Boca Raton (2012)
27. Kimmelman, J., Henderson, V.C.: Assessing risk/benefit for trials using preclinical evidence: a proposal. *J. Med. Ethics* **42**(1), 50–53 (2016)
28. Schimmel, B.J.: The use of systematic training to minimize risk in operating medical devices. In: *Symposium record policy issues in information and communication technologies in medical applications*, pp. 165–167. IEEE., USA (1988)
29. David, Y., Jahnke, E.G.: Medical technology management: from planning to application. *Conf. Proc. IEEE Eng. Med. Biol. Soc.* 2006, 186–189 (2005)
30. Karwacka, W.: Quality assurance in medical translation. *J. Spec. Transl.* **21**, 19–34 (2014)
31. Songara, R.K., Sharma, G.N., Gupta, V., Gupta, P.: Need for harmonization of labeling of medical devices: a review. *J. Adv. Pharm. Technol. Res.* **1**(2), 127–144 (2010)
32. Bridgelal Ram, M., Grocott, P.R., Weir, H.C.: Issues and challenges of involving users in medical device development. *Health Expect.* **11**(1), 63–71 (2008)
33. Vigneshvar, S., Sudhakumari, C.C., Senthilkumaran, B., Prakash, H.: Recent advances in biosensor technology for potential applications—an overview. *Front. Bioeng. Biotechnol.* **4**(11), 1–9 (2016)
34. Mehrotra, P.: Biosensors and their applications—a review. *J. Oral. Biol. Craniofac. Res.* **6**(2), 153–159 (2016)
35. Noah, N.M., Ndangili, P.M.: Current trends of nanobiosensors for point-of-care diagnostics. *J. Anal. Methods Chem.* **2019**(2179718), 1–17 (2019)
36. Sin, M.L., Mach, K.E., Wong, P.K., Liao, J.C.: Advances and challenges in biosensor-based diagnosis of infectious diseases. *Expert Rev. Mol. Diagn.* **14**(2), 225–244 (2014)
37. Patel, S., Nanda, R., Sahoo, S., Mohapatra, E.: Biosensors in health care: the milestones achieved in their development towards lab-on-chip-analysis. *Biochem. Res. Int.* **2016**, 1–12 (2016)
38. Yoo, E.H., Lee, S.Y.: Glucose biosensors: an overview of use in clinical practice. *Sensors* **10**(5), 4558–4576 (2010)
39. Yuqing, M., Jianguo, G., Jianrong, C.: Ion sensitive field effect transducer-based biosensors. *Biotechnol. Adv.* **21**(6), 527–534 (2003)
40. Vachali, P.P., Li, B., Bartschi, A., Bernstein, P.S.: Surface plasmon resonance (SPR)-based biosensor technology for the quantitative characterization of protein-carotenoid interactions. *Arch. Biochem. Biophys.* **572**, 66–72 (2015)
41. Pultar, J., Sauer, U., Domnanich, P., Preininger, C.: Aptamer-antibody on-chip sandwich immunoassay for detection of CRP in spiked serum. *Biosens. Bioelectron.* **24**(5), 1456–1461 (2009)

42. Bezerra, G., Córdula, C., Campos, D., Nascimento, G., Oliveira, N., Seabra, M.A., Visani, V., Lucas, S., Lopes, I., Santos, J., Xavier, F.: Electrochemical aptasensor for the detection of HER2 in human serum to assist in the diagnosis of early stage breast cancer. *Anal. Bioanal. Chem.* **411**(25), 6667–6676 (2019)
43. Damborska, D., Bertok, T., Dosekova, E., Holazova, A., Lorencova, L., Kasak, P., Tkac, J.: Nanomaterial-based biosensors for detection of prostate specific antigen. *Mikrochim. Acta* **184**(9), 3049–3067 (2017)
44. Yetisen, A.K., Moreddu, R., Seifi, S., Jiang, N., Vega, K., Dong, X., Dong, J., Butt, H., Jakobi, M., Elsner, M., Koch, A.W.: Dermal tattoo biosensors for colorimetric metabolite detection. *Angew. Chem. Int.* **131**(31), 10616–10623 (2019)
45. Hazra, R.J., Kale, N., Aland, G., Qayyumi, B., Mitra, D., Jiang, L., Bajwa, D., Khandare, J., Chaturvedi, P., Quadi, M.: Cellulose mediated transferrin nanocages for enumeration of circulating tumor cells for head and neck cancer. *Sci. Rep.* **10**(1), 1–14 (2020)
46. Martinkova, P., Kostelnik, A., Valek, T., Pohanka, M.: Main streams in the construction of biosensors and their applications. *Int. J. Electrochem. Sci.* **12**(8), 7386–7403 (2017)
47. Morales, M.A., Halpern, J.A.: Guide to selecting a biorecognition element for biosensors. *Bioconjug. Chem.* **29**(10), 3231–3239 (2018)
48. Turner, A.P.: Biosensors: sense and sensibility. *Chem. Soc. Rev.* **42**(8), 3184–3196 (2013)
49. Rajpoot, K.: Recent advances and applications of biosensors in novel technology. *Biosens. J.* **6**(2), 1–12 (2017)
50. Chambers, J.P., Arulanandam, B.P., Matta, L.L., Weis, A., Valdes, J.J.: Biosensor recognition elements. *Curr. Issues Mol. Biol.* **10**, 1–12 (2008)
51. Monošík, R., Stredanský, M., Šturdík, E.: Biosensors—classification, characterization and new trends. *Acta Chim. Slov.* **5**(1), 109–120 (2012)
52. Yang, F., Ma, Y., Stanciu, S.G., Wu, A.: Transduction Process-Based Classification of Biosensors. *Nanobiosensors: From Design to Applications.* (2020)
53. Gouvea, C.: *Biosensors for Health Applications.* Intech. (2011)
54. Kim, J., Campbell, A.S., de Ávila, B.E., Wang, J.: Wearable biosensors for healthcare monitoring. *Nat. Biotechnol.* **37**(4), 389–406 (2019)
55. Luka, G., Ahmadi, A., Najjaran, H., Alocilja, E., DeRosa, M., Wolthers, K., Malki, A., Aziz, H., Althani, A., Hoorfar, M.: Microfluidics integrated biosensors: a leading technology towards lab-on-a-chip and sensing applications. *Sensors* **15**(12), 30011–30031 (2015)
56. Inan, H., Poyraz, M., Inci, F., Lifson, M.A., Baday, M., Cunningham, B.T., Demirci, U.: Photonic crystals: emerging biosensors and their promise for point-of-care applications. *Chem. Soc. Rev.* **46**(2), 366–388 (2017)
57. Ali, M.A., Mondal, K., Jiao, Y., Oren, S., Xu, Z., Sharma, A., Dong, L.: Microfluidic immuno-biochip for detection of breast cancer biomarkers using hierarchical composite of porous graphene and titanium dioxide nanofibers. *ACS Appl. Mater. Interfaces.* **8**(32), 20570–20582 (2016)
58. Baldassarre, B., Konietzko, J., Brown, P., Calabretta, G., Bocken, N., Karpen, I.O., Hultink, E.J.: Addressing the design-implementation gap of sustainable business models by prototyping: a tool for planning and executing small-scale pilots. *J. Clean. Prod.* **255**, 1–15 (2020)
59. Hagedorn, T.J., Grosse, I.R., Krishnamurty, S.: A concept ideation framework for medical device design. *J. Biomed. Inform.* **55**, 218–230 (2015)
60. Laal, M.: Innovation and medicine. *Proc. Technol.* **1**, 469–473 (2012)
61. Kelly, C.J., Young, A.J.: Promoting innovation in healthcare. *Future Healthc. J.* **4**(2), 121–125 (2017)
62. Mattox, E.: Medical devices and patient safety. *Crit. Care Nurse* **32**(4), 60–68 (2012)
63. Markan, S., Verma, Y.: Indian medical device sector: insights from patent filing trends. *BMJ Innov.* **3**(3), 167–175 (2017)
64. Wagner, U.: Risks in the application of medical devices. *Qual. Manag. Health Care* **19**(4), 304–311 (2010)
65. Girling, A.: Headroom approach to device development: current and future directions. *Int. J. Technol. Assess. Health Care* **31**(5), 331–338 (2015)

66. Markiewicz, K., van Til, J.A., Steuten, L.M., IJzerman, M.J.: Commercial viability of medical devices using headroom and return on investment calculation. *Technol. Forecast. Soc. Change* 112, 338–346 (2016)
67. Kumar, V.: Regulatory regime on Indian medical device industry—a way forward. *Innoriginal Int. J. Sci.* 5(3), 5–7 (2018)
68. Martins, E.G., de Lima, E.P., da Costa, S.E.G.: Developing a quality management system implementation process for a medical device manufacturer. *J. Manuf. Technol. Mana.* 26(7), 955–979 (2015)
69. Dorst, K.: The core of “design thinking” and its application. *Des. Stud.* 32(6), 521–532 (2011)
70. Kimbell, L.: Rethinking design thinking: Part II. *Des. Cult.* 4(2), 129–148 (2012)
71. Calabretta, G., Gemser, G., Karpen, I.: *Strategic Design: Eight Essential Practices Every Strategic Designer Must Master*. BIS Publishers, Amsterdam (2016)
72. Liedtka, J., Ogilvie, T.: Helping business managers discover their appetite for design thinking. *Des. Manag. Rev.* 23(1), 6–13 (2012)
73. Karpen, I.O., Gemser, G., Calabretta, G.: A multilevel consideration of service design conditions. *J. Serv. Theor. Pract.* 27(2), 384–407 (2017)
74. O’Leary, D.E.: Gartner’s hype cycle and information system research issues. *Int. J. Account. Inf.* 9(4), 240–252 (2008)
75. Moore, G.: *Crossing the Chasm: Marketing and Selling Disruptive Products to Mainstream Customers*. Collins Business Essentials, 3rd edn (2014)
76. Sharples, S., Martin, J., Lang, A., Craven, M., O’Neil, S., Barnett, J.: Medical device design in context: a model of user–device interaction and consequences. *Displays* 33(4–5), 221–232 (2012)
77. U.S. Food and Drug Administration, Code of Federal Regulations. CITE: 21CFR820.30, U.S. Department of Health & Human Services (2019)
78. Gupta, H.S., Zioupos, P.: Fracture of bone tissue: the ‘Hows’ and the ‘Whys.’ *Med. Eng. Phys.* 30(10), 1209–1226 (2008)
79. Hrgarek, N., Bowers, K.A.: Integrating six sigma into a quality management system in the medical device industry. *J. Inf. Organ. Sci.* 33(1), 1–12 (2009)
80. Rogers, E.M.: *Diffusion of Innovations*, 3rd edn. The Free Press (1983)
81. Santel, F., Bah, I., Kim, K., Lin, J.A., McCracken, J., Teme, A.: Assessing readability and comprehension of informed consent materials for medical device research: a survey of informed consents from FDA’s center for devices and radiological health. *Contemp. Clin. Trials Commun.* 85, 1–8 (2019)
82. Gross, T.P., Gardner, S.N.: Postmarket surveillance: ensuring the safety of marketed medical devices. *J. Biolaw. Bus.* 10(3), 41–45 (2007)
83. Van Norman, G.A.: Drugs, devices, and the FDA: Part 2. An overview of approval processes: FDA approval of medical devices. *JACC Basic Transl. Sci.* 1(4), 277–287 (2016)
84. Pane, J., Francisca, R.D., Verhamme, K.M., Orozco, M., Viroux, H., Rebollo, I., Sturkenboom, M.C.: EU postmarket surveillance plans for medical devices. *Pharmacoepidemiol. Drug Saf.* 28(9), 1155–1165 (2019)
85. Reese, P.: *Calibration in Regulated Industries: Federal Agency Use of ISO 17025 and ANSI Z540.3*. NCSL International Workshop & Symposium (2016)
86. Jain, A., Ganesh, N., Venkatesh, M.P.: Quality standards for medical devices. *Int. J. Drug Regul. Aff.* 2(4), 19–24 (2014)
87. Kohani, M., Pecht, M.: Malfunctions of medical devices due to electrostatic occurrences; big data analysis of 10 Years of the FDA’s reports. *IEEE Access* 6, 5805–5811 (2017)
88. Ogrodnik, P.J.: Chapter 12—Postmarket Surveillance. *Medical Device Design*, pp. 287–298. Academic Press (2013)
89. Raj, A.: A review on corrective action and preventive action (CAPA). *Afr. J. Pharm. Pharmacol.* 10(1), 1–6 (2016)
90. Kotvitska, A., Lebedynets, V., Karmavrova, T.: The PDCA cycle implementation at the internal audit process of quality management systems of pharmaceutical companies. *J. Pharm. Innov.* 8(2), 709–713 (2019)

91. Realyvásquez-Vargas, A., Arredondo-Soto, K.C., Carrillo-Gutiérrez, T., Ravelo, G.: Applying the plan-do-check-act (PDCA) cycle to reduce the defects in the manufacturing industry. A case study. *Appl. Sci.* **8**(11), 2181–2197 (2018)
92. Bhattacharya, S.K., Sur, D.: Ethical guidelines for biomedical research on human participants. *Indian J. Med. Res.* **126**(6), 587–589 (2007)
93. Datta, P., Selvaraj, S.: Medical devices manufacturing industry. *Econ. Political Wkly.* **54**(15), 47 (2019)
94. Shah, S.G.S., Robinson, I.: Benefits of and barriers to involving users in medical device technology development and evaluation. *Health Care* **23**(1), 131–137 (2007)
95. Mazzocchi, R.A.: Medical sensors—defining a pathway to commercialization. *ACS Sens.* **1**(10), 1167–1170 (2016)
96. Santos, I.C., Gazelle, G.S., Rocha, L.A., Tavares, J.M.R.: Medical device specificities: opportunities for a dedicated product development methodology. *Expert Rev. Med. Devices* **9**(3), 299–311 (2012)

Chapter 3

Accuracy of Biosensors as Rapid Diagnostic and Biochemical Monitoring Tools for Non-communicable Diseases Management



Norhafizah Muhammad, Lim Tiong Hoo, Afiqah Nabihah Ahmad, Azureen Mohamad, and Syazana Abdullah Lim

1 Introduction

Non-communicable diseases (NCDs) are the leading cause of death globally, and one of the major health challenges of the 21st century as they are by far the leading cause of death worldwide. According to [1], NCDs were responsible for 71% (41 million) of the 57 million global deaths in 2016. A global status report by World Health Organization (WHO) reported that the major NCDs responsible for these deaths included cardiovascular diseases (17.9 million deaths, ranked first in mortality—accounting for 44% of all NCD deaths and 31% of all global deaths), followed by cancers (9 million deaths, 22% of all NCD deaths and 16% of all global deaths); chronic respiratory diseases (3.8 million deaths, 9% of all NCD deaths and 7% of all global deaths); and diabetes (1.6 million deaths, 4% of all NCD deaths and 3% of all global deaths). A significant amount of the worldwide NCD burden is attributable to behavioural, dietary, environmental and metabolic risk factors [2, 3]. Cesare et al. reported that people who have a low socioeconomic status and those who live in poor or marginalized communities have a higher risk of dying from NCDs than advantaged groups and communities [4].

With NCDs sweeping the entire globe, followed by an increasing trend of mortality, NCDs have attracted worldwide attention as a major global health issue with the trend observed not only in the developed nations but also in developing

N. Muhammad · L. T. Hoo · A. Mohamad

Electrical and Electronic Engineering, Faculty of Engineering, Universiti Teknologi Brunei, Jalan Tungku Link, Mukim Gadong A, 1410, Bandar Seri Begawan, Brunei Darussalam

A. N. Ahmad · A. Mohamad · S. Abdullah Lim (✉)

Center of Research of Agri-Food Science and Technology, Universiti Teknologi Brunei, Jalan Tungku Link, Mukim Gadong A, 1410, Bandar Seri Begawan, Brunei Darussalam
e-mail: syazana.lim@utb.edu.bn

countries [1]. This ultimately exerts pressure on the healthcare system in treating non-communicable disease and its associated complications. Diagnosis of NCDs at early stages can significantly aid in reducing the complications from progressing to advanced stages. Moreover, an early and efficient diagnosis can greatly facilitate the identification of proper medication, or doses of medication for NCDs for a safe and effective treatment thus increasing the chance of patients' survival. A "fit-for-use" approach and non-invasive screening method couples with reliable test result are key criteria for successful treatments and preventions. One optimistic approach is to diagnose the NCDs based on the biomarkers from the vital fluids with point-of-care (POC) diagnostics devices integrated with biosensor with high capability of offering rapid results. Rapid diagnosis of clinical conditions and provision of monitoring technology is significant in preventing delays in managing NCDs. The delay of diagnosis or unavailability of laboratory testing contributes to unnecessary hospitalization, intercurrent, worsening of well-being of the patient and underreporting surveillance. A well-designed monitoring system outside the healthcare institutions can assist to reduce the financial burdens carried by government and patients. The recent advancements in the field of biosensorics, for instance, have facilitated the development of functionalized nano-biosensors which have the potential to provide all of the aforementioned characteristics as a diagnostic strategy for NCDs even in faraway or resource-limited settings. Therefore, more scientific attention is now paid towards the transition of the currently available investigative technologies into advanced biosensors as diagnostic and monitoring tools in POC tests.

Over the last few decades, a wide range of nanomaterials are used for developing biosensors due to their great sensitivity and specificity for developing various types of biosensors. Nano-biosensors are nano-scaled analytical frameworks that comprise of nano-conjugated biological materials as transducing system for the detection of minuscule quanta of any biological, chemical or physical analytes [43]. On the basis of transducer, nano-biosensors can be electrochemical (amperometric, potentiometric, impedimetric, etc.) or optical (absorption, reflection, refraction, transmission, etc.). Contrariwise, on the basis of recognition elements, nano-biosensors can be enzymatic, DNA or RNA biosensors, immunosensors (antibody, antigens or biomarkers) and whole-cell sensors (Fig. 1). Immunosensors are affinity-based analytical device that is based on an immunochemical reaction comprising of antigen or antibody as the biorecognition element that is immobilized on a transducer surface. Immunosensors are known to be highly sensitive as they can detect nanomolar to femtomolar concentrations of biomolecules [5]. Additionally, immunosensors are widely used for clinical analysis due to their high selectivity, sensitivity and specificity. In clinical diagnosis, serological POC testing analysis of patient sample was found to be more accurate, feasible, practical and advantageous than nucleic acid. This is because there is high concentrations of antibodies and antigens in biological fluids than of DNA or RNA sequences, and pre-treatment of samples is not needed. Furthermore, antibodies are chemically more stable than RNA or DNA sequences, which are vulnerable to be attacked by RNases or DNases in POC tests. In this context, POC testing mostly dedicated to development of immunosensors as diagnostic tools. Moreover, with the progression in nanotechnology and nanomaterials, development

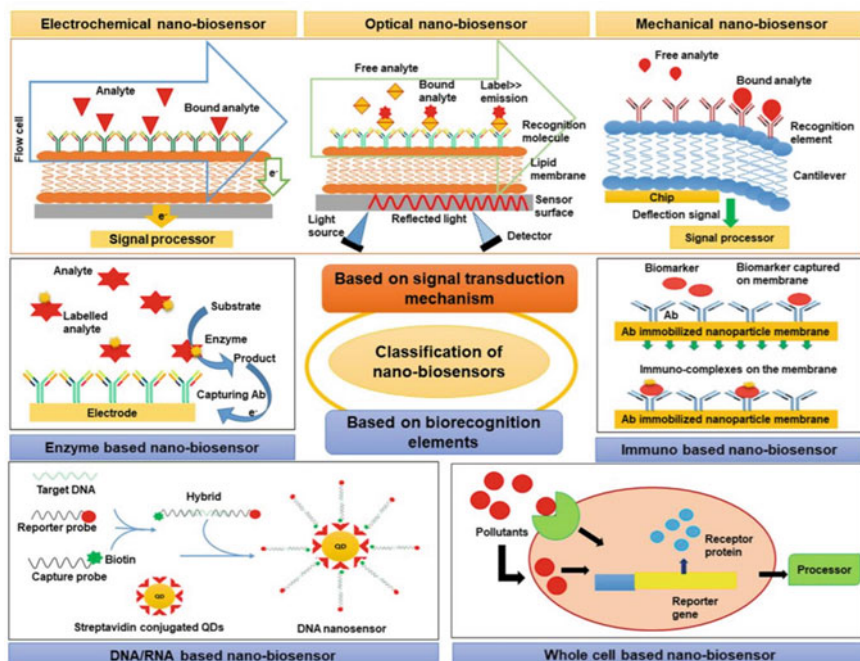


Fig. 1 Diagrammatic illustration of the different classes of biosensors based on the signal transduction mechanisms and the biorecognition molecules. (details see text. Copyright, Shandilya et al. 2019 [43])

of new matrices and strategies in POC testing has advanced. Nowadays, the development of nano-immunosensors plays a vital role in detecting in major NCDs such as cancer [6–8], diabetes [9, 10], cardiovascular diseases [11, 12] as well as chronic respiratory diseases [13].

With the integration of nanomaterials into the POC immunosensor design, there are important parameters to consider for evaluating the reliability of POC testing. The parameters are the sensitivity (the percentage of true positive results) and specificity (percentage of true negative results) of the test [14]. Furthermore, the analytical performance of the POC test is also evaluated through its imprecision, measured using the within-run coefficient of variation (CV) from the test result data of the developed POC device, and its accuracy, calculated by its means of coefficient of correlation (r) from the obtained data set from the developed POC device and the reference test [15].

In NCDs, most diseases are chronic in nature where continuous monitoring of patients is crucial as soon as symptoms appear to effectively mitigate complications and consequences of the diseases. Advancement of embedded technologies and miniaturization of electronic devices has facilitated the applications of biosensors in wireless biosensor networks (WBNs) for diagnosis and monitoring purposes. WBNs

are a collection of wearable biosensor devices that have the capability to collect physiological information and process the information in order to detect diseases and medical-related issues. Wearable biosensor device is the key in technology that can help in an early detection of illness [16] and undoubtedly will increase the life expectancy of the population especially the elderly [17]. This makes the technology becoming proactive and more affordable as the demand of biosensors in the healthcare system increases. The needs for ultra-low power consumption and reliable wireless communication from the biosensor devices for information exchange are critical for the success of the e-health monitoring. It is important that these issues are analysed and addressed.

This chapter will examine biosensor as reliable diagnostic and monitoring tools for NCDs management. The first section will be looking at recent strategies used in NCDs detection with electrochemical immunosensor as a reference and using selected examples. While there have been incremental improvements in the performance of nano-immunosensors as POC tests for various diseases, many do not meet the required sensitivity to be practically useful. Therefore, numerous efforts are being made to enhance the resolution, accuracy and miniaturization of nano-immunosensors for NCDs detection in order to fulfil a number of unmet needs in the diagnostics industry. The second part of this chapter will provide an insight to the application of WBN to medicine highlighting some of the communication issues of WBN. Due to the sharing of the radio channel with other medical devices, WBNs are prone to interference. Various solutions have been proposed to overcome the interference and improve the reliability and prolong the operations of those devices. Adaptive radio approaches that can reconfigure its communication modules according to the changes in operating environment have been proposed in order to reduce the data delivery failure and device power consumption. WBN has been applied in areas such as patient and pandemic monitoring, environmental monitoring, chemical detection and food and agriculture.

1.1 Technology for Detection of Non-Communicable Diseases

1.1.1 Cancer Diagnosis

The diagnosis of cancer commonly involves the detection of elevated level of cancer biomarkers in biological fluids such as serum. Current screening, testing and monitoring of cancer progress can be done by costly, bulky and time-consuming equipment that often requires technical expertise to run these tests. For cancer diagnosis, early detection of cancer biomarkers, which can be in nano-concentrations in the circulation [18], is favourable to avoid late stages of the condition and allow early intervention. An ultrasensitive POC immunosensor testing with high precision is desired for detecting specific cancer biomarkers as there are a panel of cancer biomarkers

specific to each kind of cancers. This has led to the development of multiplex testing that can save time, reagents, sample and the cost of the tests for a complete diagnosis of cancer.

Gao and colleagues reported a multiplex measurement of twelve biomarkers [19]: alpha-feto protein (AFP), carcinoembryonic antigen (CEA), cytokeratin 19 fragment (CYFRA-21-1), neuron-specific enolase (NSE), β -human chorionic gonadotropin (β -hCG), squamous cell carcinoma (SCC), pepsinogen I (PG I), pepsinogen II (PG II), total prostate-specific antigen (total PSA), free PSA, thyroglobulin (Tg) and carbohydrate antigen 19-9 (CA19-9). In their POC testing strategy, they integrated a giant magnetic resistance (GMR) sensor chip, which is layered with multiple nanomaterials consisting of SiO₂, Ts, PtMn, CoFe, Cu, NiFe and Al₂O₃ nanomaterials, magnetic nano-beads label and combining microfluidic technology. 50 μ L of serum sample was dropped onto the sample channel, and the samples move through microfluidic action into the GMR chip containing the detecting antibodies. Biotinylated capture antibodies were then introduced into the system through microfluidic channels and bind to the captured analytes. The biotinylated antibodies in turn bind to the magnetic nano-beads. The captured magnetic nano-beads created stray magnetic field and reduced the magnetic field, which changed the resistance of the GMR chip sensor. The resistance was measured and mapped into the domain of the specific analyte concentration. The sensor used a magnetic immunosensor analyser for an automated data processing and setting calibration curves. They reported that the results can be transmitted via Wi-Fi network; thus, the POC testing results can be accessed easily by the technician and clinician. The assay was able to detect 12 cancer biomarkers in about 15 min to generate its final results. Each of the twelve biomarkers was able to be detected in the nanogram range with precision of less than 10% CV. Furthermore, the accuracy of the GMR POC immunosensor has good correlation coefficient ($r = 0.95$) to commercial immunosensors for the detection of the twelve tumour markers [19].

1.1.2 Cardiovascular Diagnosis

Cardiovascular disease is a leading cause of mortality for NCDs globally. Acute myocardial infarction (AMI) is the most threatening of all the cardiovascular diseases, whereby it inflicts the myocardium with irreversible damage. The damage leads to the release of the cardiac biomarker, cardiac troponin I (cTnI), which stayed in the bloodstream within 90 min of the onset of AMI [45]. Rapid and accurate diagnosis of an acute myocardial infarction or heart attack is essential to immediately execute an intervention and treatment. However, conventional laboratory testing for cTnI has a long turn-around time and requires expensive and bulky machines. In this regard, POC testing is favourable as it can provide an immediate or short testing time when the patient was first encountered, albeit the physiological concentration of cTnI in the bloodstream is very low (0.01–0.1 ng/mL) [20]. Since troponin has different isotopes for different types of muscles (Troponin *T*, *C* and *I*), thus, a very cardiac-specific and sensitive POC test becomes more crucial.

Although cTnI biomarker is very specific to AMI, a panel of cardiac biomarkers, such as myoglobin, CK-MB and troponin *T*, would provide better results to predict the actual risk of the AMI after onset of symptoms [21]. The ability to filter actual AMI cases can allow patients to be discharged and easing the financial burden of the healthcare system or beds in the hospital [44].

Lim and colleagues constructed a rapid multiplex cardiac biomarker POC test based on paper microfluidic device [22]. Three biomarkers were detected, and each biomarker detected was assigned a colour as optical labels using gold, silver and gold nano-urchin nanoparticles. The colour was evaluated using a camera, and the intensity was quantitatively measured. The limit of detection of GPBB, CK-MB and cTnT was measured at 0.5 ng/mL, 0.5 ng/mL and 0.05 ng/mL, respectively. The assay was done within 5 minutes, and the immunosensor was described to have precision in the acceptable range of > 10% to < 20% for each biomarker. The accuracy of the POC immunosensor was also measured with excellent correlation coefficient (r) of 0.962.

1.1.3 Diabetes

Type 2 diabetes (T2D) is one of the most common and important disorders affecting the world's population. The rise of T2D occurrence has been closely related to the increasing incidence of obesity causing not only government billions of dollars in medical bills, medication and blood glucose assays but also work loss. T2D can be typified by insulin resistance due to the loss of sensitivity to insulin [23]. Adipokines are a type of cytokines secreted by adipose tissues and often used as an indicator for insulin resistance and prediction of T2D recurrence [24].

ELISA kits are typically used to quantify adiponectin in blood circulating levels, albeit this method is time-consuming. An immunosensor based on sandwich configuration was developed to detect adipokines using a hybrid of reduced graphene oxide-carboxymethylcellulose as a detection platform. Immobilization of the anti-adipokines was carried out in an oriented manner that resulted in a detection limit of 61 ng/mL and linear plot ranging within 0.5–10.0 $\mu\text{g/mL}$ [25].

Retinol Binding Protein 4 (RBP4), a type of adipokines, is a highly potential biomarker for management an early stage of diabetes. Ojeda et al. reported an electrochemical immunosensor for the detection of RBP4 for POC application. In their design, screen-printed carbon electrodes with functionalized double-walled carbon nanotubes were employed for oriented immobilization of antibody. A linear range between 0.05 and 10 $\mu\text{g/mL}$ with a detection limit of 14.5 ng/mL was achieved. In comparison with the output produced by ELISA kits, their results displayed better reproducibility, stability and selectivity [26].

2 Communication Technology for Biosensor

This section will provide an overview on WBN and its functionalities to readers. The subsequent sections will show the use of WBNs in remote patient monitoring application, architectural design of WBNs followed by highlights of the challenges and communication issues in WBN, and possible solutions to mitigate the failures in biosensor communications will also be presented.

2.1 Architecture of Wireless Biosensor Networks

WBN is a group of independent biosensor nodes that can communicate wirelessly over a limited range using pre-defined frequency and bandwidth. These biosensor nodes are usually attached or ingested to the human body. Each node can read medical signals such as the electrocardiogram (ECG), pulse rate, blood pressure, temperature and blood count, depending on method of deployment. WBNs can improve healthcare delivery, diagnostic monitoring and disease tracking and related medical procedures [27]. The main goal of WBNs is to provide continuous monitoring of the patients' data and the states of health to healthcare personnel. These data can show a patient's physiological information of vital organs and remotely provide feedback. The transmission of the data needs to be continuously and in real time.

According to Lai et al. and Hayajneh et al., the design of WBNs is based on wireless sensor networks (WSNs) used in monitoring smart city and wildlife [27, 28]. They exhibit the same characteristics in terms of deployment approach, density, size, energy utilization and data transmission. In WBNs, the deployment of nodes is usually attached on or around the human body, and the numbers of nodes can reach up to a few dozens. Each of the biosensor nodes needs to ensure the accuracy of collected data with a guaranteed data delivery [27]. The size of the nodes must be small so that it can be attached discretely on any part of the body. These devices are usually battery powered, and the data transmission rate will depend on the location of nodes. For health applications in WBNs, the networks must be robust, secured and reliable with low latency [28]. Hence, it is necessary to understand the architecture of the WBNs in order to provide a guaranteed communication networks.

Figure 2 shows the general architecture of WBNs in the healthcare application, which consists of a network of biosensing nodes, aggregation or sink nodes, base station and radio communication channel [27]. Different biosensors such as ECG sensor plate, blood pressure sensor, respiration sensor, EMG sensor, temperature sensor, visual sensor, accelerator and gyroscope can be connected to the biosensor nodes. The architecture in Fig. 2 shows that the biosensor nodes and the sink node can either be worn or implanted to the human body. During the data sensing and transmission, the sink node will collect the physiological data from the biosensor nodes and transmit them to the base station and finally to the doctor or clinicians. These nodes usually have limited power as they are usually battery powered. According to Lai

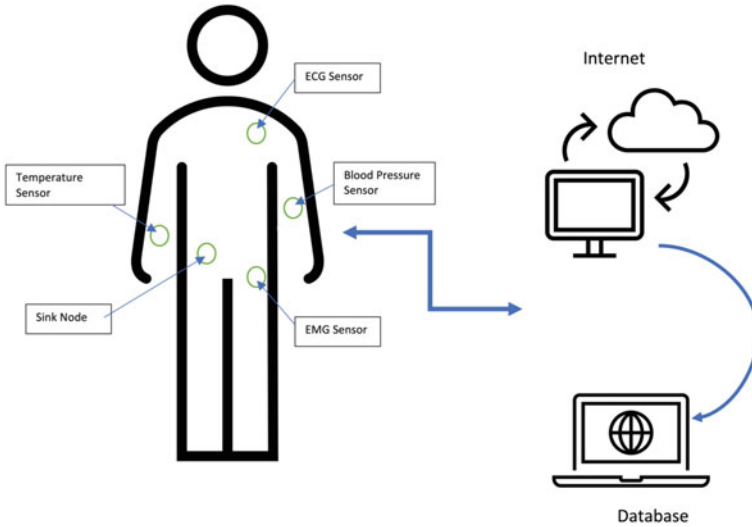


Fig. 2 Architecture of a body sensor network (details see text. Copyright

et al., the nodes usually consume more energy during data transmission compared to data sensing [27]. Hence, it is important to reduce the number of data transmission performed by the nodes.

2.2 Communication Architecture

To understand the operation of data transmission in WBNs, there is a that need to understand the communication architecture of WBNs. WBNs communication architecture follows a three-tier network of communication as shown in Fig. 3. Tier 1 is called the intra-BAN, it involves a personal communication between the biosensing nodes, and the sink node where the data received by the sink node will be aggregated. The second tier (Tier 2) is called the inter-BAN, and this tier is responsible for data processing, aggregation and storage of the data generated. Finally, the third tier (Tier 3) is called the extra-BAN. This tier consists of the integration of wide-area network (WAN) and local-area network (LAN) technologies, where the responsibility is to transmit or broadcast the transmission data to the central server.

The reliability and efficiency of WBN will depend on the system respond, where the response needs to be quickly and accurately propagated during the transmission of data between the nodes [29]. The gateway node should also be able to recognize the high-level and low-level language algorithms. This will give efficient capturing and retransmission of data [30]. Eventually, the selecting the components of the WBN system, topologies, protocols and the algorithms is needed in designing and applying the WBN systems.

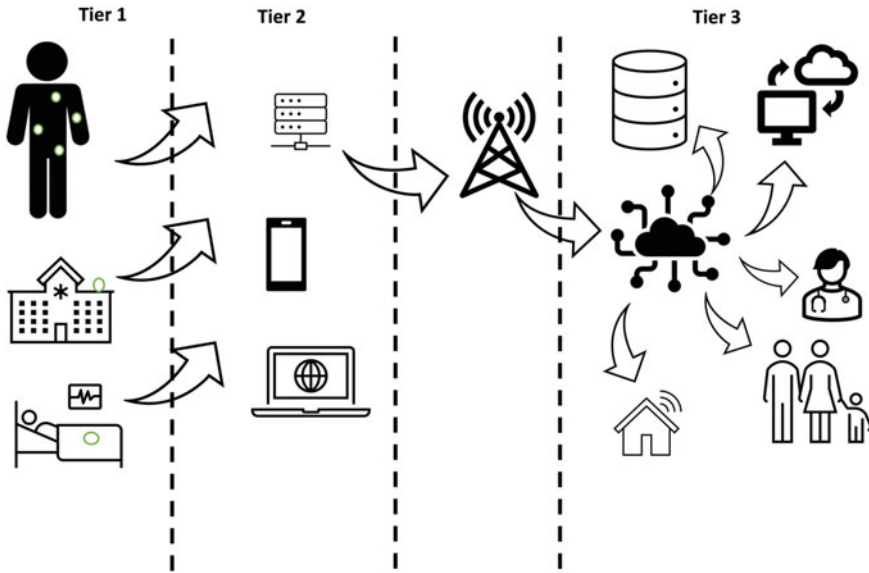


Fig. 3 Three-tier network of communication in WBNs

2.3 Communication Protocol Layer

According to Lai et al., the WBNs communication architecture follows the protocols layer approaches used in the computer networks [27]. It consists of the application, network topology and routing, medium access control and physical radio communication as shown in Fig. 4. The use of layering in WBN protocol helps to simplify the design of the WBN communication architecture, assist in troubleshooting and ease the upgrade process. It shares many similar features with WSNs such as the network architecture, radio transmission technology, communication protocols, energy control and network security. In order to improve the efficiency of the biosensor networks, there are factors need to take into consideration when designing the WBN based on the layered shown in Fig. 4. The protocols stack will be furthered explain in the next sub-section.

Fig. 4 WBNs-layered protocol stack

Application
Network topology & Routing
Medium Access Control
Physical Layer

2.3.1 Physical Layer

The physical layer is found at the bottom layer of the stack. This layer is responsible for the preparation of the raw data transmission in the node. It provides data signal encoding and decoding, preamble or header generation and removal, bit transmission and reception and the specification of transmission medium [27]. It addresses the needs for a simple but robust modulation, transmission and receiving techniques using the ultra-wide band (UWB) as a physical layer of WBANs [31]. The UWB has the advantage of low energy consumption, good co-operation with existing 5G network and a range large enough to support the entire body.

2.3.2 Medium Access Control Layer

The medium access control (MAC) layer is responsible for ensuring the transmission to achieve maximum throughput and minimum delay with maximize network life-time. These can be done by reducing energy wastage due to transmission collisions, idle listening, overhearing and packet cost [27]. Lai et al. and Khan et al. highlighted that there are three classes of protocols in MAC layer, namely schedule protocol, contention protocol and contention-schedule protocol [27, 32].

In schedule protocol, the transmission is divided into several slot of time. At each slot, a node will be assigned to transmit within the assigned slot. This schedule protocol is known as the time division multiple access (TDMA), a very energy efficient as a node that can operate at a reduced power consumption when it is not transmitting. In addition, there is no contention, idle listening and overhearing problem [27]. However, there is a need for the node to perform time synchronization, and this can be difficult to achieve.

In contention protocol or random access, collision sense media access with collision avoidance (CSMA/CA) is widely used for a short-range wireless communication network [32]. A node using this protocol will check the availability of the transmission channel whether it is free or not. If the channel is free, the node will send out the packets. However, when two nodes try to transmit at the same time, packets collision will occur on the network. As a result, each node will retransmission until the packet successfully transmit. This can increase the power consumption and cause unnecessary utilization on the networks.

Finally, for a contention schedule protocol, a combination between the contention and schedule protocols is used. This protocol applies the round-robin scheme where nodes are polled in a sequential manner. Sensor nodes can join or depart a network by simply sending a message to the controller centre [31]. The packet transmission and packet queuing are affected depending on the size of the nodes and traffic volume of a network. This protocol can provide better energy efficiency, higher capacity utilization and less delay [27].

2.3.3 Network Topology and Routing Layer

The network topology and routing are responsible for the addressing and forwarding of the packet in a multi-nodes environment. The way the nodes are connected in the networks dictates the network topology of WBNs. There are two types of hardware devices used in WBNs, namely reduced functionality device (RFD) and full functionality device (FFD) [33–36]. RFD allows the device to act as an end device and communicate with the PAN coordinator. As for the full functionality device FFD, this device can operate as the PAN coordinator, end device and an ordinary coordinator. These two devices can support three types of network topologies (star, tree and peer-to-peer) as shown in Fig. 5. In a star topology, devices can only communicate with the network coordinator, which is the RFD. In peer-to-peer topology, any of the devices can act as FFD and RFD as long as it is within the range. The combination of both the star and peer-to-peer topologies leads to the formation of mesh topology. The topology of the networks will affect the type of routing protocol used in the networks and their overall network performance such as the power consumption, traffic load, node robustness, selection of transmission access protocol and forwarding of the packets to the clinician [27].

Table 1 shows the performance of the WBNs based on the parameters in different types of network topologies [27].

Fig. 5 Network topologies of WBNs

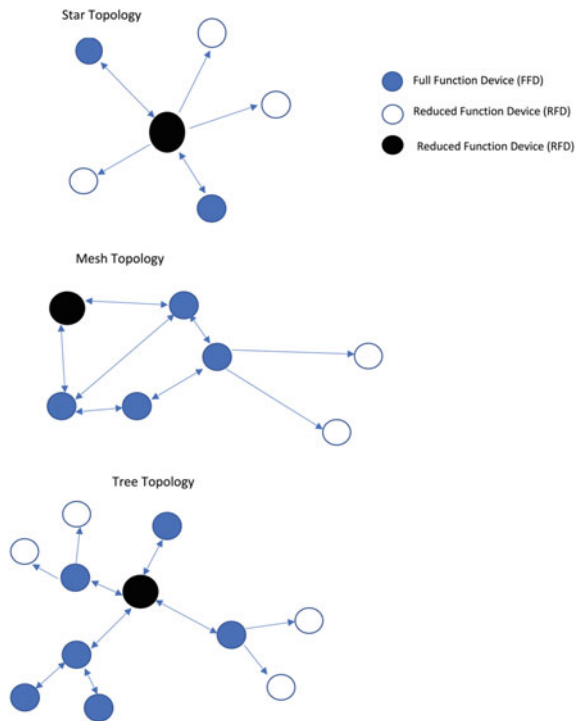


Table 1 Performance comparison between star topology and mesh topology

	Star topology	Mesh topology
Path loss	Nodes on the same side with low path loss. Nodes on the different sides with high path loss	Reducing path loss caused by diffraction through multiple hops
Radio transmission range	Not suitable for small radio propagation range	Adjusting radio propagation range by changing the number of nodes
Energy consumption	Nodes closer to sink node consumes lower power	The nodes nearer to sink node consume more energy, as they have to forward not only their data but also data from other nodes
Transmission delay	Sensors connect with sink node directly take the least possible delay in transmission	Nodes closest to sink node get their data quickly, without any intermediate delay
Inter-user interference	Nodes farther away from sink node need higher power to transmit data with more interference to other nodes	As each node only transmits to its neighbours, the energy of transmission is low and hence smaller interference
Node failure and mobility	Only the failed is affected and the rest nodes of network perform well	The whole network including nodes with errors need to be reset

In the WBNs, the communication architecture layers need to follow a standardize specification in order to ensure inter-operability between different network technologies [36]. The WBNs follow the IEEE 802.15.4 standard specification that specifies the physical and MAC layers of the network. IEEE 802.15.4 is a simple packet data protocol designed for lightweight wireless networks [38]. The main advantages are long battery life, selectable latency for controllers, sensors, remote monitoring and portable electronics [38]. Pai and Kavitha (2014) also mentioned reasons of using the IEEE 802.15.4 that it is well layered and can provide a combination of link management mechanism that can be enabled selectively depending on the user configuration [35]. This can guarantee data confidentiality and integrity. However, according to Salayma et al., the existing standard failed to support the need of applications in terms of the following issues: reliability, low power, the variety of traffic flows and coexistence [36]. This is mainly because in the WBAN, the number of sensor nodes that are wearable or implanted on or in human can be reached to a few dozen nodes. So, the IEEE 802.15 group introduced task group 6 in the standard technology, IEEE 802.15.6. This kind of standard can support an array of applications with a range of requirements such as data rates and channel bandwidths [36].

2.3.4 Application Layer

This application layer provides the interface in managing the WBN. This layer has different types of software that can be built and used in response to the type of sensing task. The main function of the application layer is to ensure secure environment for accessing sensitive medical data.

Since the demand of the advancement of WBN increases, there are many types of applications that spans from entertainment to sport and even in military. According to Le and Moh [39], the applications of WBN can be categorized into two fields; there are medical and non- medical approach [39]. In the medical approach, this involved in the remote monitoring, physiological feedback and rehabilitations. The authors also mentioned the application of WBN in the non-medical approach such as use for monitoring fitness, performance and notifying the management [39].

2.4 Challenges in Designing WBNs

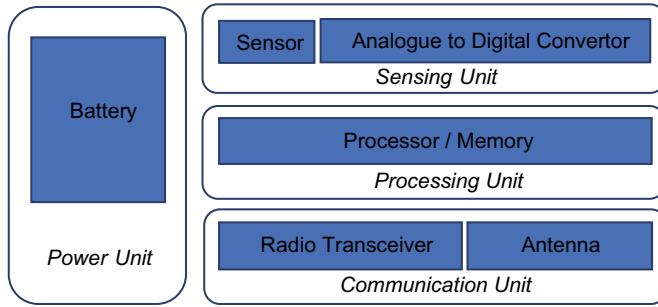
When designing WBNs, there are many factors that need to take into considerations such as fault tolerance, scalability, operating environment, hardware constraints, transmission media and power consumption [40].

Fault tolerance deals with the reliability of the networks. When a node failed due to lack of power, physical and environmental interference, it can affect the fault tolerance of the network. Fault tolerance can be measured by the quality of the link or by the efficiency of end-to-end communication [36]. When WBNs is applied in medical applications, they need to be fault tolerance. They must provide high-quality delivery service in order to avoid packet loss or delays resulting in a fatality especially in emergency cases [36].

During the deployment of WBNs, the number of biosensor nodes can reach up to hundreds with the availability of nano-biotechnology depending on the application use. According to Hayajneh et al., the biosensor node can join and leave the network as new nodes are added [28]. The protocol should also be able to support the physical dynamic change in the network topology as the number of nodes increases.

As shown in Fig. 6, the biosensor node consists of four basic components, namely the power unit, sensing unit, processing unit and communication unit. The power unit can be powered by using the battery or even the solar or kinetic movement. The sensing unit consists of biosensors and analogue to digital converter (ADC). The sensed data is fed to the processing unit, before it stores in the memory. The processor manages the sensing tasks. Finally, the communication unit allows the node to connect to other nodes.

As the main task of a biosensor node is to detect data, process and transmit the data, it is necessary to ensure that there is sufficient power supply to operate the node. The power consumption is divided into three phases: sensing, communication and data processing. The node is usually battery powered, and it is important that the



INCREASES.

Fig. 6 Sensor node architecture

design of the operation of WBNs must be energy efficient to prolong the operations of the networks.

2.5 Issues of WBAN in Healthcare System

The main goal of WBNs is to provide continuous long-term monitoring the patient's medical health care without effecting his/her daily activities. As mentioned in the introduction, interference can occur during the implementation of WBNs. When there is interference in the network, sensors will not be able to continue normal operation leading to loss of critical information [41]. It can affect the performance, reliability and sensor lifetime as more retransmission occurs.

There are two types of interference: inter-WBNs and intra-WBNs [39, 42]. Inter-interference can occur between the nodes within same network. While the inter-interference occurs in a multiple network available around the surrounding, it can be divided into mutual and cross-type of interferences. In mutual, interference happens due to overlapping of signal transmission from another WBAN. The cross-interference is caused by another wireless technologies in transmission and receiving signal using the same frequency as the nodes of WBNs.

2.6 Interference in WBNs

Sarra et al. stated that interference reduces the reliability of WBNs as it can affect the transmission of packet between nodes and reduce the packet delivery rate and data rate [41]. As these interferences increase, packet delivery rate dropped further due to collision. The interference can also affect the network throughput where the presence of another wireless technology such as Wi-Fi can interfere with the WBNs communication as they share the same radio frequency [39]. This causes the signal

to degrade. Other aspects such as packet size can equally increase the probability of collision in the network [28].

According to Le and Moh [39], the types of wireless specification implemented in the node can also cause interference depending on which specification is more superior [39]. For instance, IEEE 802.15.6 the standard is superior to the IEEE 802.15.4 as it consumes more energy in the carrier sense multiple access with collision avoidance compared to IEEE 802.15.4. Shaik et al. made a comparison between the wireless specifications and its applications [42]. They show that the Bluetooth technology is not a suitable in the application of WBNs in health monitoring, because of low range of operation and high-power consumption. While IEEE 802.15.4 used by Zigbee has a better performance than the Bluetooth in terms of power consumptions, but the limitations are Zigbee have a higher rate of delay and inadequate of quality of services (QoS). IEEE 802.15.11 standard is used by Wi-Fi and has the best security, QoS and data transmission rate.

Hence, there is a need to over the interference in WBNs to ensure the quality of services provided by the networks.

2.7 Interference Mitigation

There are several proposed solutions in mitigating the interference with the main purpose on minimizing these interference effects, namely time spacing, frequency spacing, code diversity, standard modifications, standard adaptation and hybrid solution [28]. The two common approaches used in interference mitigation are the MAC approach and low power approach [39, 42]. In the MAC approach, it can reduce the number of collisions using random access protocol in the CSMA/CA architecture. The CSMA/CA helps to provide a flexible and reliable monitoring and data delivery [32]. On other hand, low power transmission can help to reduce the probability of interference between nodes while providing a high resistance against interference in WBNs compared to the standard Wi-Fi [28]. It has the capability to interoperate with the standard Wi-Fi and WBNs.

Another MAC approach calls collection tree protocol (CTP) are developed and tested in WBNs [41]. This protocol can improve the reliability, connectivity and battery life. Their experimental results showed that the transmission power, data transmission frequency and packet size were different under the real and heavy interferences. However, there was no dominating scheme in mitigation interferences [39]. Shaik et al. highlighted that adopting different interference mitigation techniques in the design of WBNs is important to ensure continuous operations [42].

3 Conclusions and Future Directions

NCDs are one of the main causes of mortality affecting millions of lives globally. The proportion of the world population affected is so significantly high to an extent that most countries are spending a high percentage of their budget to treat complications caused by NCDs. Hospitalization and medical treatment are a big burden to healthcare institutions, patients and their family members. A new strategy is therefore required and crucial to relief these financial burdens through the employment of thorough and consistence monitoring at the comfort of their own home. The construction of POC tests features miniaturization, portability, simplicity, rapid testing time, cost effective to a constraint healthcare economy, sensitive detection and reliable monitoring of the disease. With the integration of nanotechnology into immunosensors, POC testing has been revolutionized into more rapid, greater detection range and improved sensitivity of sensors. Despite the substantial breakthrough, there are still pressing issues related to the practical application on POC testing in clinical diagnosis that needed to be addressed such as reagents used in POC tests. The stability of the reagents is used in POC devices, and the optimal condition for the reagent storage still require further optimisation. Simplicity and portability of POC devices implement the integration of pre-stored reagents into the devices. Most microfluidic POC devices develop reagent storage into their POC devices without the introduction of manual introduction of reagent into the device, minimizing contamination and ease the usage. Furthermore, benefits of POC nano-immunosensors are demonstrated into prototypes primarily on the research level and not exploited for commercialisation. Thus, future improvement and innovations in creation of stable reagents to overcome the issue are desirable. Another limitation in clinical testing is the acquirement of sample for diagnosis. Most diagnosis testing requires blood sample, which present a painful process. Nowadays, research has explored other non-invasive samples such as saliva, urine or sweat, as an alternative to blood.

With respect to communication technology, the effect of the current COVID-19 pandemic situation has driven telemedicine and wireless technology to achieve new undertakings and swift improvement for a rapid personalized health report. Portable wireless POC devices have broadened the landscape for POC diagnosis. This could provide convenience for patients as there is no need of travelling to see the doctor to receive the results and in turn save the time and cost for both patients and clinicians. A set of sensors can be allocated to patients associated to their disease with a suitable mobile application. Data collected from these sensors would then be processed and information be communicated to healthcare personnel for further assessment. Although WNBs are in rapid development in the wireless technology, the study of mitigating of WBAN interference is still developing. Based on the related works, the parameters including coupling strength, period of time, the transmission power and transmission rate in the networks play important role in improving the throughput, the reliability and energy consumption. With ongoing works being actively carried out, the future in biosensor wireless technology will

allow patients to have better access to an efficient and reliable care outside hospitals in managing and prevention of NCDs.

References

1. World Health Organization.: Noncommunicable Diseases Country Profiles 2018. World Health Organization. <https://apps.who.int/iris/handle/10665/274512>. License: CC BY-NC-SA 3.0 IGO (2018)
2. Danaei, G., Hoorn, S.V., Lopez, A.D., Murray, C.J., Ezzati, M.: Causes of cancer in the world: Comparative risk assessment of nine behavioural and environmental risk factors. *The Lancet* **366**, 1784–1793 (2005)
3. Ezzati, M., Lopez, A.D., Rodgers, A., Hoorn, S.V., Murray, C.J.: Selected major risk factors and global and regional burden of disease. *The Lancet* **360**, 1347–1360 (2002)
4. Cesare, M., Khang, Y., Asaria, P., Blakely, T., Cowan, M.J., Farzadfar, F., Guerrero, R., Ikeda, N., Kyobutungi, C., Msyamboza, K.P., Oum, S., Lynch, J.W., Marmot, M.G., Ezzati, M.: Inequalities in non-communicable diseases and effective responses. *Lancet* **381**, 585–597 (2013)
5. Malhotra, B.D., Ali, M.A.: Nanomaterials in biosensors. *Nanomaterials Biosens.* 1–74 (2018)
6. Chakkarapani, S.K., Sun, Y., Kang, S.H.: Ultrasensitive norovirus nanoimmunosensor based on concurrent axial super-localization of ellipsoidal point spread function by 3D light sheet microscopy. *Sens. Actuators B Chem.* **284**, 81–90 (2019)
7. Ju, S., Chakkarapani, S.K., Lee, S., Kang, S.H.: Supersensitive single-particle plasmonic scattering-based cancer antigen 125 nanoimmunosensor by enhanced dark-field microscopy with dual-detection mode. *Sens. Actuators B Chem.* **245**, 1015–1022 (2017)
8. Prasad, K.S., Cao, X., Gao, N., Jin, Q., Sanjay, S.T., Henao-Pabon, G., Li, X.: A low-cost nanomaterial-based electrochemical immunosensor on paper for high-sensitivity early detection of pancreatic cancer. *Sens. Actuators B Chem.* **305**, 127516 (2020)
9. Torabi, R., Ghourchian, H.: Ultrasensitive nano-aptasensor for monitoring retinol binding protein 4 as a biomarker for diabetes prognosis at early stages. *Sci. Rep.* **10**, 1–10 (2020)
10. Wang, X., Su, J., Zeng, D., Liu, G., Liu, L., Xu, Y., Wang, C., Liu, X., Wang, L., Mi, X.: Gold nano-flowers (Au NFs) modified screen-printed carbon electrode electrochemical biosensor for label-free and quantitative detection of glycated hemoglobin. *Talanta* **201**, 119–125 (2019)
11. Rezaei, B., Shoushtari, A.M., Rabiee, M., Uzun, L., Mak, W.C., Turner, A.P.: An electrochemical immunosensor for cardiac Troponin I using electrospun carboxylated multi-walled carbon nanotube-whiskered nanofibres. *Talanta* **182**, 178–186 (2018)
12. Singh, S., Tuteja, S.K., Sillu, D., Deep, A., Suri, C.R.: Gold nanoparticles-reduced graphene oxide based electrochemical immunosensor for the cardiac biomarker myoglobin. *Microchim. Acta* **183**, 1729–1738 (2016)
13. Selyanchyn, R., Wakamatsu, S., Hayashi, K., L.S.: A Nano-thin film-based prototype QCM sensor array for monitoring human breath and respiratory patterns. *Sensors* **15**, 18834–18850 (2015)
14. McNerney, R., Daley, P.: Towards a point-of-care test for active tuberculosis: obstacles and opportunities. *Nat. Rev. Microbiol.* **9**, 204–213 (2011)
15. Pezzuto, F., Scarano, A., Marini, C., Rossi, G., Stocchi, R., Di Cerbo, A., Di Cerbo, A.: Assessing the reliability of commercially available point of care in various clinical fields. *Open Public Health J.* **12**, 342–368 (2019)
16. Milenkovic, A., Otto, C., Jovanoa, E.: Wireless sensor network for personal health monitoring: issues and an implementation. *Article Commun. Aug 2006* (2006)
17. Farhat, S., Mahto, S., Ghosh, S.: Wireless sensor networks in health care system. *Int. J. Res. Eng. Technol. Sci.* **VII**(Feb 2017) (2017)

18. Mosayebi, R., Ahmadzadeh, A., Wicke, W., Jamali, V., Schober, R., Nasiri-Kenari, M.: Early cancer detection in blood vessels using mobile nanosensors. *IEEE Trans. Nanobiosci.* **18**, 103–116 (2019)
19. Gao, Y., Huo, W., Zhang, L., Lian, J., Tao, W., Song, C., Tang, J., Shi, S., Gao, Y.: Multiplex measurement of twelve tumor markers using a GMR multi-biomarker immunoassay biosensor. *Biosens. Bioelectron.* **123**, 204–210 (2019)
20. Tu, D., Dean, J., Holderby, A., Schechinger, M., Coté, G.L.: Development of a paper microfluidic surface enhanced Raman scattering assay for cardiac troponin I, In: *Proceeding of the SPIE* (2020)
21. Newby, L.K., Goldmann, B.U., Ohman, E.M.: Troponin: an important prognostic marker and risk-stratification tool in non-ST-segment elevation acute coronary syndromes. *J. Am. Coll. Cardiol.* **41**, S31–S36 (2003)
22. Lim, W.Y., Thevarajah, T.M., Goh, B.T., Khor, S.M.: Paper microfluidic device for early diagnosis and prognosis of acute myocardial infarction via quantitative multiplex cardiac biomarker detection. *Biosens. Bioelectron.* **128**, 176–185 (2019)
23. García-Jiménez, C., Gutiérrez-Salmerón, M., Chocarro-Calvo, A., García-Martínez, J.M., Castaño, A., De la Vieja, A.: From obesity to diabetes and cancer: epidemiological links and role of therapies. *Br. J. Cancer* **114**, 716–722 (2016)
24. Jung, U.J., Choi, M.S.: Obesity and its metabolic complications: the role of adipokines and the relationship between obesity, inflammation, insulin resistance, dyslipidemia and nonalcoholic fatty liver disease. *Int. J. Mol. Sci.* **15**, 6184–6223 (2014)
25. Arenas, C., Sánchez-Tirado, E., Ojeda, I., Gómez-Suárez, C.A., González-Cortés, A., Villalonga, R., Pingarrón, J.M.: An electrochemical immunosensor for adiponectin using reduced graphene oxide–carboxymethylcellulose hybrid as electrode scaffold. *Sens. Actuators B Chem.* **223**, 89–94 (2016)
26. Ojeda, I., Barrejón, M., Arellano, L., González-Cortés, A., Yáñez-Sedeño, P., Langa, F., Pingarrón, J.M.: Grafted-double walled carbon nanotubes as electrochemical platforms for immobilization of antibodies using a metallic-complex chelating polymer: application to the determination of adiponectin cytokine in serum. *Biosens. Bioelectron.* **74**, 24–29 (2015)
27. Lai, X., Liu, Q., Wang, W., Zhou, G., Han, G.: A survey of body sensor networks. *Sensors* **13**, 5406–5447 (2013)
28. Hayajneh, T., Almashaqah, G., Ullah, S., Vasilakos, A.V.: *A Survey of Wireless Technologies Coexistence in WBAN: Analysis and Open Research Issues*. Springer Science & Business Media, New York (2014)
29. Bhanumathi, V., Sangeetha, C.P.: A guide for the selection of routing protocols in WBAN for Healthcare applications. *Human- centric Comput. Inf. Sci.* **7**(24) (2017)
30. Pramanik, P.K.D., Nayyar, A., Pareek, G.: WBAN: driving e- healthcare beyond telemedicine to remote health monitoring. In: *Telemedicine Technologies: Big data, Deep Learning, Robotics, Mobile and Remote Applications for Global Healthcare*, pp. 89–119 (2019)
31. Ragesh, G.K., Baskaran, K.: A survey on futuristic health care systems: WBANs. In: *International Conference on Communication Technology and System Design*. *Procedia Engineering*, vol. 30, pp. 889–896 (2012)
32. Khan, J.Y., Yuce, M.R., Bulgar, G., Harding, B.: *Wireless body area network (WBAN) design techniques and performance evaluation*. Springer Science + Business Media, LLC (2010)
33. Azzouz, B.B., Abdesselam, B., Mohamed, B., Nacer, A.: A new reinforced MAC protocol for lifetime prolongation of reliable wireless body area network. *ECTI Trans. Electr. Eng. Electron. Commun.* **16**(2) (2018)
34. Farhad, A., Zia, Y., Farid, S., Hussain, F.B.: D-MAC: a dynamic MAC algorithm for the body sensor networks based on IEEE802.15.4. *Int. J. Comput. Sci. Net. Secur.* **16**, 29 (2016)
35. Pai, S.R., Kavitha, C.: Channel modelling and optimization of wireless body area network (WBAN). *Int. J. Comput. Sci. Inf. Technol.* **5**, 2762–2766 (2014)
36. Salayma, M., Al-Dubai, A., Romdhani, I.: Wireless body area network (WBAN) a survey on reliability, fault tolerance and technologies coexistence. *ACM Comput. Surv.* **50**, 1–38 (2017)

37. Garg, V.K.: *Wireless Communication and Networking* 1st Edition Elsevier's Science & Technology, pp. 689–690. Elsevier India (2007)
38. Jassim, S.I., Nourildean, S.W.: IEEE 802.15.4 ZigBee- based wireless sensor network in medical application. *Iraqi J. Sci.* **53**, 1055–1066 (2012)
39. Le, T.T.T., Moh, S.: Interference mitigation schemes for wireless body area sensor networks: a comparative study. *Sensors* 13805–13838 (2015)
40. Akyildiz, I.F., Su, W., Sankarasubramaniam, C.E.: *Wireless sensor networks: a survey*. Elsevier Sci. Comput. Netw. **38**, 393–422 (2002)
41. Sarra, E., Moun gla, H., Benayoune, S., Mehaoua, A.: Coexistence improvement of wearable body area network (WBAN). In: *Medical Environment IEEE ICC. Wireless Communications Symposium* (2014)
42. Shaik, M.F., Lakshmi, V., Komanapalli, N., Subashini, M.S.: *A Comparative Study of Interference and Mitigation Techniques in Wireless Body Area Networks*. Springer Science Business Media, LLC (2017)
43. Shandilya, R., Bhargava, A., Bunkar, N., Tiwari, R., Goryacheva, I.Y., Mishra, P.K.: Nanobiosensors: point-of-care approaches for cancer diagnostics. *Biosens. Bioelectron.* **130**, 147–165 (2019)
44. Jacob, R., Khan, M.: Cardiac biomarkers: what Is and what can be. *Indian J. Cardiovasc. Dis. Women - WINCARS.* **03**, 240–244 (2018)
45. Vasatova, M., Pudil, R., Horacek, J.M., Buchler, T.: Current applications of cardiac troponin T for the diagnosis of myocardial damage. *Adv. Clin. Chem.* **61**, 33–65 (2013)
46. Li, M., Lou, W., Ren, K.: Data security and privacy in wireless body area networks. *IEEE Wireless Commun.* **17** (1), 51–58

Chapter 4

Rapid Manufacturing of Biomedical Devices: Process Alternatives, Selection and Planning



Sanchit Jhunjunwala and Sajan Kapil

1 Introduction

The increase of interest and subsequent investment in biomedical applications has implied exponential advancements in their design, functionality, and scope of medical value. With a deepening understanding of human physiology, it has become easier to develop solutions for problems encountered by medical professionals in treating patients suffering from a wide variety of conditions. These rapid advancements in biomedical engineering have implied immense strain on the limitations of conventional methods of design implementation, most prominently those of manufacturing. The ever-expanding complexity of designs has pushed the boundaries of manufacturing methodologies into exploring newer frontiers, previously deemed unreliable for quality-intensive applications such as biomedical devices. One such frontier is that of *Rapid Manufacturing (RM)*, whereby the flexibility and relative adolescence of the technology has implied high adaptability for unconventional applications. The characteristics of mass customization, developmental efficacy, ease of prototyping and material efficiency—all notably attributed to RM—make it an obvious candidate for interest in the biomedical production industry. This chapter deals with the rapid manufacturing of numerous biomedical applications, ranging from implantable objects such as stents, and ingestible materials such as pharmacological products, to external instruments such as surgical equipment, and devices such as ventilators. Therefore, a broad definition of biomedical applications suitable hereby is that of entities that assist in the healthcare of human beings, such as medical processes for effective treatment of patients and the physiological and mental well-being of their

S. Jhunjunwala · S. Kapil (✉)

Department of Mechanical Engineering, Indian Institute of Technology Guwahati, Guwahati, India

e-mail: sajan.kapil@iitg.ac.in

S. Jhunjunwala

e-mail: sanchit.jhun@iitg.ac.in

© The Author(s), under exclusive license to Springer Nature Singapore Pte Ltd. 2022

S. N. Joshi and P. Chandra (eds.), *Advanced Micro- and Nano-manufacturing*

Technologies, Materials Horizons: From Nature to Nanomaterials,

https://doi.org/10.1007/978-981-16-3645-5_4

users. The flow of this discussion begins with the definitions, classes, and instances of both—biomedical devices and RM technologies, in the first and second sections, respectively. The classifications aim to provide a bird's eye view of the fields of development, to also allow for an effective understanding of the scope of discussion. This is followed by a listing of the types of RM technologies with allied technologies. Thereafter, the process planning required for the efficient production of parts using RM techniques is discussed. This is followed by an investigation into the challenges encountered with the industrial deployment of RM to produce biomedical devices. Finally, the scope of developments in existing and upcoming manufacturing technologies relevant to biomedical applications has been discussed.

2 Biomedical Devices

Biomedical devices, as per standard conventions, however, may be defined as appliances (machines, software, reagents or materials) intended for the use of human beings in (i) diagnosis, prevention, monitoring, compensation or treatment, of a disease, injury or disability; (ii) investigation, replacement, modification, control, support or sustenance of life, any anatomical system or any physiological process; (iii) treatment or disinfection of medical devices.

The above definition [1] requires that the device does not achieve its primary intended action by pharmacological, immunological, or metabolic means, thus ruling out drugs or any other pharmaceutical materials. However, given the capabilities of RM technologies, it is important to note that such pharmacological applications are not beyond the scope of RM [2] and thus the term biomedical devices and other relevant phrases used hereafter, for the purpose of this chapter is inclusive of ingestible and otherwise administered drugs as well.

2.1 *Classification of Biomedical Devices and Systems*

There are several ways biomedical devices may be classified, depending on the characteristics being compared. Government regulators, within their jurisdictions, classify these products in consideration of the risk factor involved with their usage and deployment, such as the United States Food and Drug Administration (USFDA) which defines three classes of medical devices (I, II, III) [3], or the Danish Medicines Agency which has a total of four categories (I, IIA, IIB, III) [4]. Here, categories are defined based on the control required over the quality and maintenance of the device, with the risks associated with each class usually increasing with the class number. Similarly, such applications may also be segregated based on the nature of their deployment, thus aiding the choice of treatment methodology and whether or not a device may be considered for involvement in a certain medical procedure. The classification may be based upon the level of interaction of the device with the

patient, whether it is a supplementary device necessary as an auxiliary tool during the treatment, or if it behaves as an integral component of the treatment framework. For instance, the USFDA defines 16 ‘panels’ of devices [5], with each corresponding to a field of medicine or biomedical applications such as cardiovascular devices, neurological devices, orthopaedic devices, etc.

The intent for the classification of these devices is important for the appropriate style of categorization and, therefore, for the correct set of categories to be defined. Given this chapter’s context, the classification made hereby depends on the application and manufacturing characteristics of the associated fields of biomedical engineering. It is difficult to precisely define the term biomedical manufacturing because a versatile and robust definition would require accommodation of prospects associated with the rapid research and development associated with the healthcare industry. The optimal definition would be to deem it to be the manufacturing of devices, tools, and other products that are used in the healthcare and associated activities of human beings.

As illustrated in Fig. 1, the classification may be layered into three levels—fields of research, subsequent areas of application, and resulting products. Given that some products may require nonphysical production such as software and services, the current discussion focuses only on those that require manufacturing, examples of which have been indicated in italic stylization. Instances within each layer may depend upon multiple elements from the previous layer for their implementation, which has been indicated with the help of arrowhead connectors in Fig. 1.

2.2 Custom and Stock Device Design

Perhaps one of the most important distinctions across biomedical devices, in the context of their manufacturability, is the necessity for customization. Stock versions of a product refer to conventionally mass-producible, identical components produced with minimum to no tolerance for variations across batches. Custom products refer to those produced in adherence to the specifications of the customer, with the purposes of a specific end-user being addressed by the design variations.

As has been observed with the production of components using *Additive Manufacturing (AM)* techniques, the cost of production per component is constant over the increasing number of components to be produced, in contrast to conventional manufacturing, where the costs reduce with the increase in volume [6] (see Fig. 2). Therefore, AM is relatively economical for products requiring smaller numbers of identical components, such as customizable products, while conventional processes such as casting and forming, are preferable for mass production. In consideration of these cost consequences, devices and their components are optimized for their design in accordance with statistical data about user specifications, to the maximum extent possible. This allows for low costs and high repeatability of the mass production of stock components, which are made available in a limited number of different sizes, with their corresponding quantities being statistically optimized. For an instance of

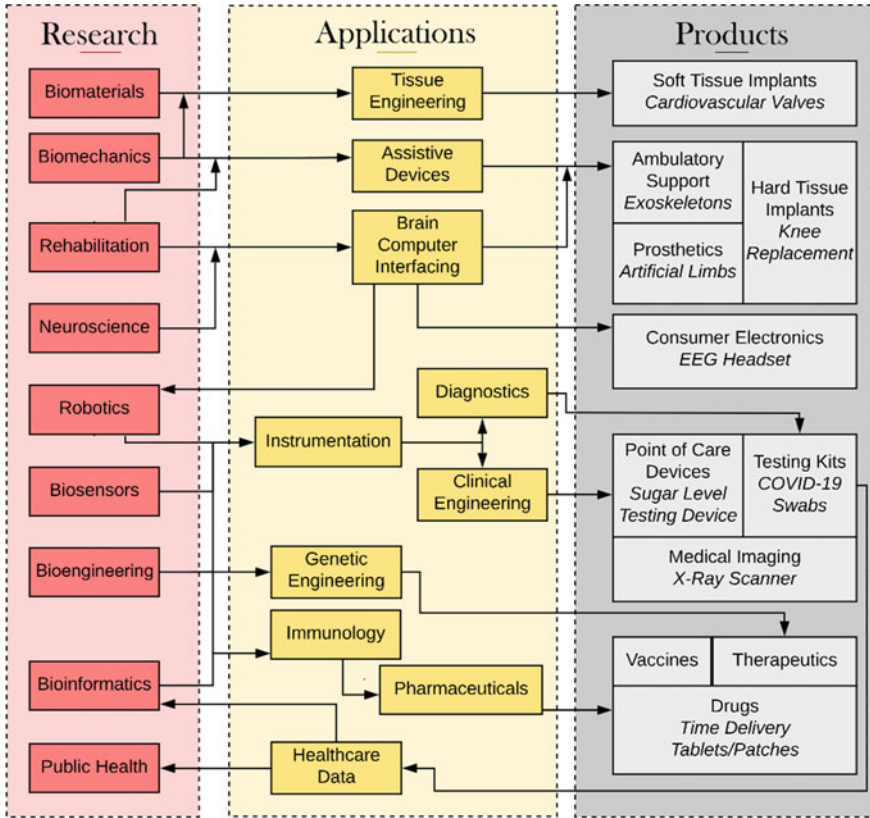


Fig. 1 Classification of biomedical devices based on research area, application, and products

biomedical relevance, stent-grafts used in endovascular aneurysm repair have been found to be identical in terms of procedure and outcome, regardless of whether they were *Customized Stent Grafts (CSGs)* or *Standardized Stent Grafts (SSGs)* [7].

However, it becomes necessary for customization to be enabled in applications that require patient-specific design parameters such as optimized dimensions, calibrated surface profiles, and even personal aesthetic choices. For example, customized knee implants have been found to provide better outcomes at the same procedural costs while also reducing the necessity of post-procedural treatment and follow-up care [8]. In the case of orthodontic procedures, the advantages of customized products such as dental prostheses, along with regulatory freedom by virtue of low associated risk factors, have made customization widely popular among establishments as well as users. It ensures a shortened procedural and production time durations, high precision, and therefore enhanced overall comfort [9]. In certain upcoming and developmental applications, customized deliverables are at the centre of research assumptions. In the case of 3D printed pharmaceuticals such as time-delivery drugs, the product concept itself relies upon customizability of the build to provide novel functionalities such as

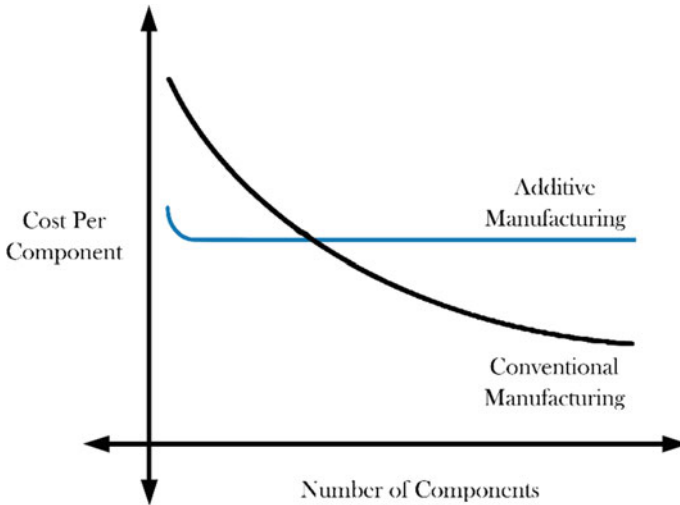


Fig. 2 Variation in cost per component with number of components fabricated by additive manufacturing and conventional manufacturing processes [6]

user-specific dosage and temporal dosage control [10]. Applications may also require customization as an inherently fundamental step of production such as in the case of synthetic tissues and organs, where it would be crucial for the build to accurately adhere to the requirements of the patient's body [11].

Therefore, *Rapid Manufacturing (RM)* is a subject of substantial as well as increasing interest within the field of biomedical engineering due to its fundamental advantages over other manufacturing technologies. The following sections discuss these RM techniques in a general context to highlight the scope and implications of its employment in fabricating the biomedical devices.

3 Rapid Manufacturing

Rapid Manufacturing (RM) is a term that has been defined in a multitude of ways, which reflects its vast scope of application. A substantial number of academics have debated the use of this term. The author has defined the RM as follows:

Rapid Manufacturing may refer to a manufacturing process or combination/hybridization of manufacturing processes that can speed-up the mass/batch/unit production of customized/stock components, in comparison to other prevalent methods of producing the same.

The demand for rapidity in production stems from the need to deliver products faster and cheaper, while also catering to growing requirements of bleeding-edge updated designs and customizability. This can be achieved by reducing the time and costs associated with the manufacturing of the product.

However, the translation of a component from concept to product is a process comprised of several stages before and after manufacturing, with each stage having its own time duration and cost considerations. The developmental and design stages comprise research, professional feedback, prototyping, and other formative steps which constitute the development cost of the product. The production stage comprises of two cost types: variable costs (associated with the material inventory, purchased parts, and labour), and fixed costs (associated with tooling and overheads). The final stage, which is that of the sales and marketing itself, incurs an expenditure of its own, which adds together with the other preceding costs to give the total cost of the product.

Firstly, the costs can be reduced by cutting down on manufacturing expenses. The overheads and tooling are time-dependent costs, which can, therefore, be reduced by increasing the rate of production, without increasing the tooling costs. Second, one of the major factors upon which the developmental costs depend is the prototype production. The cost and time associated with the manufacturing of prototypes heavily impact the economic considerations of the development stage, ultimately adding to the cost of the product itself. Finally, even though the marketing stage is beyond the purview of RM, the characteristics offered—primarily that of customization—are helpful to the process of building customer interest and confidence. Moreover, the time associated with each stage combines to give the total time taken for a product to come to market, a factor that is increasingly crucial within intensely competitive markets.

The central technology applied hereby is an automated fabrication process to produce a part specified on a *Computer-Aided Design (CAD)* platform that may either be used directly to produce the final components or may be used to produce tooling for another manufacturing process. A relevant classification of RM has been provided in the next subsection.

3.1 Classification of Rapid Manufacturing Processes

Broadly, there are two routes for producing the end components rapidly - direct and indirect, as visualized in Fig. 3. In the case of direct RM routes, the end products are fabricated directly using an appropriate, subtractive, forming, additive, or hybrid manufacturing process. In indirect RM routes, the injection moulding tools, casting moulds/patterns, are fabricated to speed-up the casting (for metal parts) and injection moulding (for non-metal parts) processes.

Subtractive processes refer to the production of the objects by removing the material from a raw-stock. A CNC (computer numerical control) machining process falls into the category of direct routes of RM. The development of intelligent *Computer-Aided Manufacturing (CAM)* packages for *Computer-Aided Process Planning (CAPP)* helps in producing the parts rapidly [12].

Forming processes such as incremental forming [13], and laser forming [14] are emerging manufacturing processes for fabricating products, rapidly, without the requirement for any specific tooling.

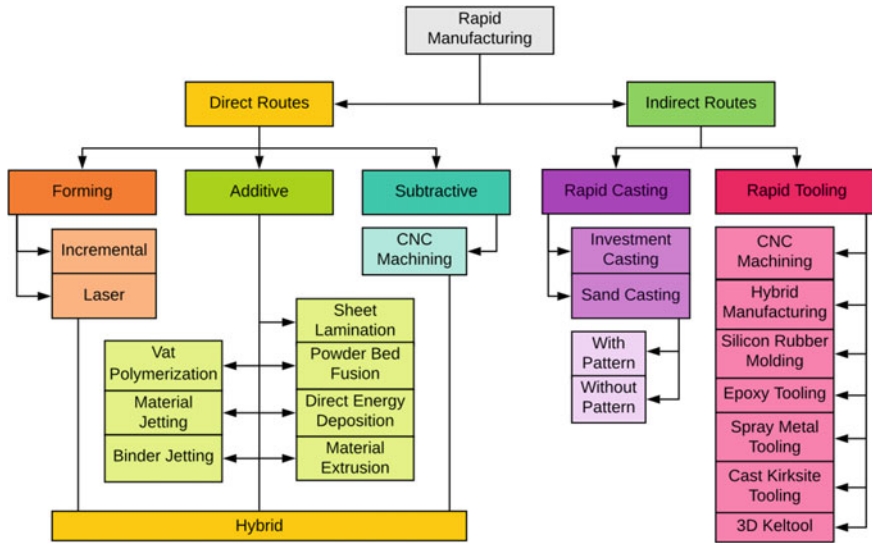


Fig. 3 Classification of rapid manufacturing

Additive manufacturing refers to the automatic production of three-dimensional objects from a CAD model by adding together layers, droplets, beads, and other elemental forms of material, with the help of joining and processes such as fusion, glueing, sintering, polymerization, etc. As per ASME, the AM processes are classified into 7 categories [15] viz., (i) Vat-photopolymerization (ii) Material Jetting (iii) Binder Jetting (iv) Material Extrusion (v) Sheet Lamination (vi) Powder-Bed Fusion and (vii) Directed Energy Deposition. Total automation is the primary advantage of AM processes, which leads to the quick realization of complicated objects.

Hybrid processes refer to combinations of two or more direct RM techniques that have been fully coupled to improve part quality while overcoming their individual limitations, synergistically. This definition implies that the combined processes, once fully coupled, may not be decoupled during the resulting hybrid process, thus ruling out pre and post-production processes. The synergy of these processes implies that the resulting hybrid process has enhanced capabilities, which cannot be achieved from the individual processes by themselves, thus overall improving the quality of the part and the performance of the process.

Rapid Casting (RC) technologies are the indirect RM routes in which appropriate AM techniques are used to produce the patterns, cores, or the moulds, which in turn are used to produce the metal casting.

Rapid Tooling (RT) technologies are also indirect RM routes but for producing non-metallic components. In this category, the moulds/dies are fabricated. AM techniques are used to produce the patterns, die/injection-moulds, which in turn are used to produce the non-metal parts in bulk.

Automated subtractive methods such as CNC machining have been the convention for nearly a half a century, and the ongoing advancements are relevant only at extreme scales of component dimensions such as micro and nanofabrication, which are well discussed in academic spheres. On the other hand, rapid forming methods such as single point incremental formation (SPIF) [16] and laser forming have emerged only very recently are at present limited in their applicability to medical device manufacturing.

However, additive manufacturing is currently in its developmental prime, with rapid advancements on all scales of dimensions from nanofabrication to microfabrication, even unto civilian constructions; and has been established as a reliable manufacturing technique for biomedical production to a certain extent. It is also a fundamental technology upon which both rapid casting and rapid tooling depend, alongside machining. Therefore, the bulk of this text deals with RM in the context of the AM technologies that enable its implementation, along with the allied technologies that complement the limitations and requirements of additive production methods.

3.2 Allied Technologies

RM processes use a variety of allied technologies to achieve speed and quality of production. The allied technologies are generally grouped into three categories viz., pre-build processes, in-situ build processes, and post-build processes. These allied technologies are summarized in Fig. 4. In pre-build processes, a CAD model is prepared, with the help of *Computer-Aided Engineering (CAE)* tools, whereby geometry definition and feature analysis tools help optimize the design. The file is then converted to a compatible format, and a tool path is generated using an associated CAM software package. In some cases, the existing products are to be reproduced then an appropriate reverse engineering technique is used to scan the object and create the CAD model. The in-situ build processes are used to enhance the functionality of the parts produced by an RM process. The processes fall into this category are such as embedding inserts [17], cold working after every layer [18], laser shock peening [19], machining in-between a certain number of layers [20], etc. The post-build processes used for removing the support material, improving the surface quality (polishing, machining [21]), improving interior quality (thermal and pressure treatments) [22].

3.3 Implications of Rapid Manufacturing

Usage of production technology has direct and indirect implications on the produced component, in terms of design, physical properties, quality, and other aspects of the product such as costs and marketing. These can be categorized into the following.

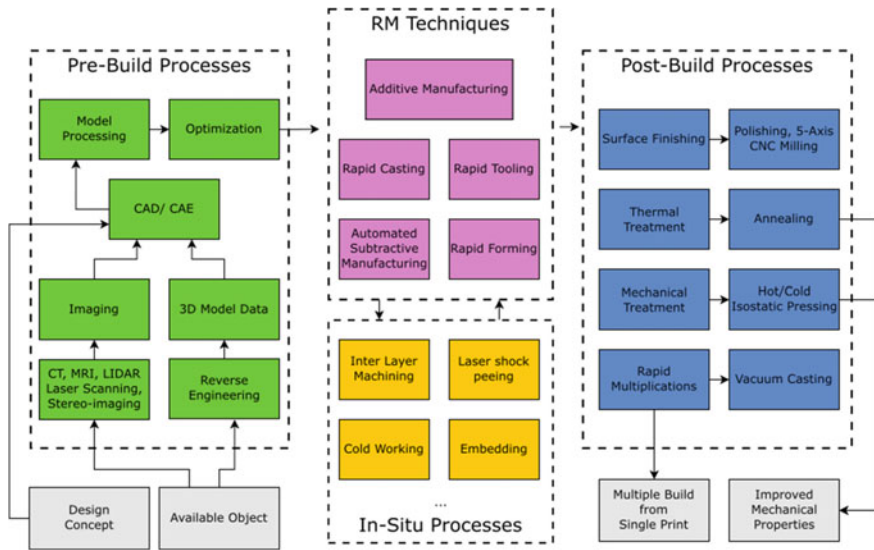


Fig. 4 Integration of manufacturing processes (light grey) with allied technologies (dark grey) for enhanced build characteristics of speed, quality, and cost

3.3.1 Design Implications

The primary advantage of RM arises from its employment of AM, which implies maximum independence of the design process from manufacturing constraints. The product need not be tweaked for ensuring manufacturability or even logistical feasibility. With most AM technologies, if the design can be geometrically represented, it can be printed. This allows a level of geometric flexibility with the design, which is practically unheard of in other fields of manufacturing.

3.3.2 Process Implications

The absence of tools, jigs, and fixtures implies that there are no extra components that need to be made for every batch of the product. This implies that the scalability of production only depends on the trade-off between product cost and demand, generally going upwards with growth in demand. However, the process inherently requires the digitization of resources and the education of operating staff. Further, the involvement of allied technologies implies an increase in already long build times, with frequent interruptions in the build process. For instance, the inclusion of subtractive processes such as machining, in between layers or segments of an AM build would imply the generation of shrapnel from the previous layer, which can neither be recycled (thus adding to material wastages) nor can it be left as is, since the particles may interfere with further layers. Thus it becomes important to introduce a cleaning sweep with every iteration of the machining process, further extending the build time.

3.3.3 Product Implications

One of the primary driving factors for investment in RM is its ability to implement customizations in design, at no/less increased costs of production. This implies greater adherence to customer-specific requirements and enhanced user experience. Therefore, some RM processes can also be used as a platform to achieve mass production of customized products [23]. For efficient mass production of the complicated metallic and non-metallic parts, indirect RM routes rapid casting [24] and rapid tooling [25] can be used, respectively. Products with assembly without joints, lattice structure, non-linear internal ducts, *Functionally Graded Materials (FGMs)* can be easily fabricated through RM. However, AM technologies are notorious for their mechanical properties, especially in the case of fused filament fabrication of plastic and sintering-based metallic builds.

4 Rapid Manufacturing of Biomedical Devices

RM technologies have been closely associated both in development as well as application, with biomedical engineering. Among the publications relevant to RM technologies, between 1980 and 2010, 15% of all papers and patents have been specifically about biomedical engineering. For reference, this share of percentage is only second to general mechanical engineering topics which primarily relate to technology development itself, and it is closely tied in place with computer science (16.4%) and material science (14.4%) related topics, which themselves reference a number of biomedical applications either as their intended outcomes or as a scope of application [26].

4.1 Biomedical Fields of Rapid Manufacturing Application

With advances in production quality improving feasibility and thus aiding the expansion of applicability, RM has found use in numerous fields of biomedical engineering ranging from diagnostic and research-centric fields such as radiology, imaging, medical informatics, testing disposables, molecular biology, anatomical and surgical modelling, to treatment-related fields such as surgical tooling, orthopaedics, internal medicine, neurology, pharmaceuticals, immunology, and even veterinary usage.

As shown in Fig. 5, biomodelling for diagnostics as well as surgical training and planning employ AM technologies for the obvious benefits such as design freedom, 3D reconstruction fidelity, and definable colour representation. This is possible with technologies such as multiple extruders based *Fused Deposition Modelling (FDM)*, polyjet, and pigmented resin deposition [26].

In the area of implantable devices, AM has already been accepted and established to a large extent, given its inherent advantages. In orthodontic applications especially,

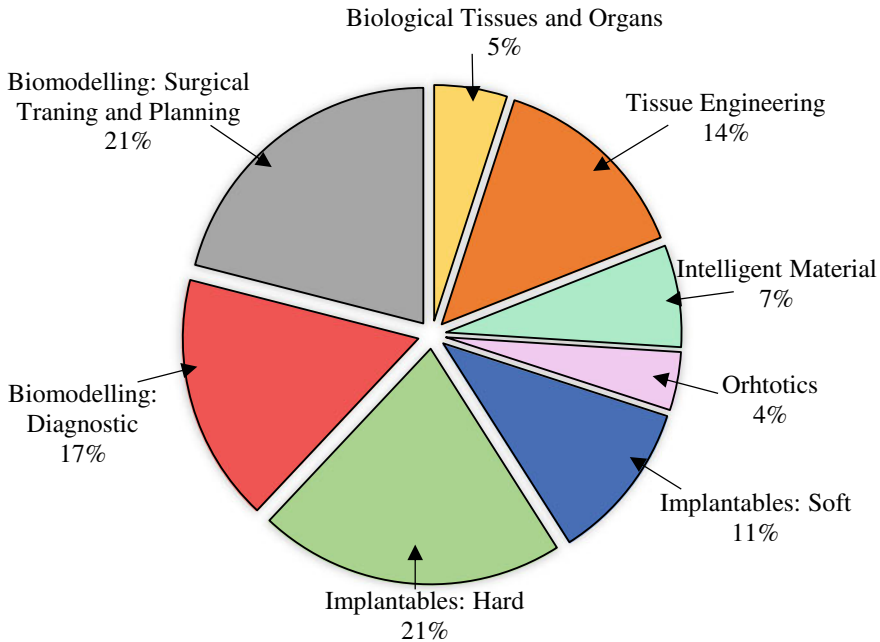


Fig. 5 Application of additive manufacturing in the different domains of biomedical engineering [26]

given the low risks associated with dental surgeries and the heightening customer demands for aesthetics and customization in dental implants, rapid technologies have found extensive application. Additive manufacturing processes such as SLM are known to be capable of improving the osteocompatibility of component surfaces [27], and as a result, bone tissue implants make use of technologies such as Powder-Bed Fusion (PBF). Therefore, hard tissue replacement which requires the direct manufacturing of implantable devices consists of a 21% share of all applications of rapid manufacturing in biomedical devices [26]. Otherwise, in fields of tissue engineering, applicability still remains low and limited to research whereby most experimental apparatuses make use of animal models for testing.

Extensive applications have been found in orthotics, used for complimentary support to external physiological systems, such as limbs and joints for performance assistance and improvement [28]. This is because the materials need not interact with chemically sensitive tissue, and most products can be used as wearable, separated by a layer of skin-suitable material such as foams and fabrics. The flexibility in design and customizability provided by rapid manufacturing makes it feasible to make patient-specific products such as foot-sole rests, shin and calf pads, fracture casts, and spinal orthoses.

4.2 Process Planning

Process planning is an important step in the transition from design to product, regardless of whether the manufacturing technology used for production is conventional or rapid. It is in the preparation of this plan, where a majority of the challenges to be faced in production are highlighted, so that necessary adjustments to either the manufacturing sequence, material selection, process selection, or even the design itself, may be made to allow for an optimal and viable product.

In the case of RM, such planning becomes necessary rather than beneficial. This is primarily because of the involvement of multiple pre and post-build processes which complement and enable the central manufacturing process. Further, such a plan is feasible to implement as a CAPP, with an appropriate Boolean formulation of the same.

Process flows for RM of a product are generally divisible into three phases, as shown in Fig. 6. The first phase involves the development of the product itself. From the conception of an idea and its deliberation with experts and professionals from relevant fields, through the development of the concept which requires a study of the market, review of scientific literature, the definition of functionalities, and comparison followed by registration of intellectual property, to the steps preceding design (e.g. *Reverse Engineering (RE)*); the first phase covers the preparation of an implementable concept of the product from a mere idea. While most manufacturing technologies would not require such a preliminary phase to be involved in the production plan of a product, with rapid manufacturing, the development process is integral to the overall flow. This is a natural outcome of the fact that most rapid manufacturing technologies evolved from rapid prototyping techniques. Therefore, the back and forth between advanced stages of production and the design and development process itself, is much more feasible with such techniques. For example, the imaging required to prepare the scaffolds in the first implementation iteration of the design is a developmental process, conventionally. However, the mass customization enabled by rapid manufacturing allows for this step to be revisited with every iteration for adjustments to the basic design, to allow for patient-specific products to be made. Upon finalization of product specifications, which are derived from the study and concluded with the functional definition from the development phase, the process moves to the second phase, that of design. Here, the design is visualized and documented with every iteration of prototyping and testing. Prototypes are of two kinds: virtual and physical. While virtual prototypes are tested in computational environments (in-silico) and are substantially more cost-effective, especially with improvements in simulation technologies, physical prototypes are necessitated by regulatory procedures, because of their inherent confidence in repeatability. This phase is highly iterative, with the majority of such iterations gradually shifting towards virtual prototypes. Upon finalization, the design geometry is documented as a CAD model and transferred to the next and final phase of production, manufacturing itself. This transition from geometry to part is facilitated by a CAM system. The provided design geometry file is first converted to an appropriate format, the most notable of which

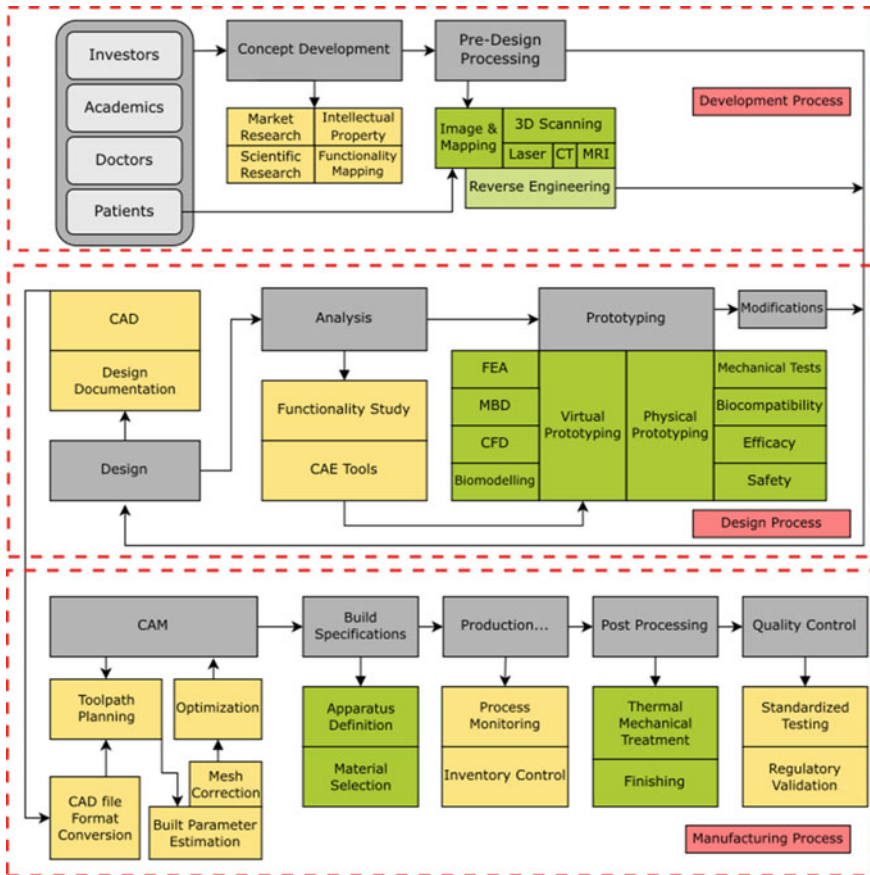


Fig. 6 Process planning for three different phases (viz., development, design, and manufacturing) of realizing the biomedical devices

is the STL format (.stl) which essentially stores the geometry as triangulated points on the surfaces of the parts. The main function of a CAM system is to convert a given standard geometry file into a toolpath. A toolpath file contains a geometry along which the end effector of an automated manufacturing apparatus, such as an FDM printer, or a CNC router, must travel to deposit or remove the substrate substance. Based on the generated toolpath and properties of the build apparatus (e.g. Resolution, feed rate, layer height, etc.) the build parameters (e.g. time of build, surface roughness, etc.) may be calculated. By iterating between multiple instances of adjusted geometry meshes and resultant build parameters, the toolpath may be optimized before being forwarded to the apparatus. Once the apparatus and the feed material have been defined, in accordance with the in-situ processes associated, the production commences with a monitoring system to account for detectable deviations

from the projected process outcome. Hereafter, the post-processing of the substrate is carried out, which is followed by quality control.

This final phase of manufacturing involves the choice of appropriate combinations of manufacturing techniques. The selection and sequencing of these processes are crucial for effective rapid production. The choice of the central RM process can be made from those discussed in Sect. 3.1, which can be used appropriately for fabricating biomedical devices.

Direct routes are suitable for customized products and mass customization for some cases, while indirect routes are suitable for mass production of stock components. Indirect processes can be chosen from simply based on whether the required final product is metallic or non-metallic. Rapid Casting processes are used for reproducing metallic components, while rapid tooling is used for mass-producing non-metallic components.

Within direct routes of RM, the subdivided choices may be made based on mechanical aspects of the substrate part, such as geometry, finish, billet type, etc. For instance, rapid forming techniques are used for sheet metal billets, while subtractive processes such as CNC machining may provide high surface finish, but for relatively simple geometries. For complex geometries, streamlined mass customization, ease of intermittent processing, functionally graded or modified internal cross sections, multiple materials, etc., it is best to use additive manufacturing techniques. Given the vast palette of choices available within AM technologies, the process of making this choice is described in the following subsection.

4.3 Selection of an Appropriate AM Technology

The primary selection of an appropriate AM process may be made on the basis of the type of feedstock that can be used, which translates to the choice of material already made for the product. Further, specific technologies may be chosen from on the basis of their build characteristics, precedents of usage in biomedical device production, allowed materials, etc., as indicated in Table 1. There are three important criteria involved in arriving at a decision for the choice of an AM technology:

4.3.1 Raw Material

Depending upon the mechanical properties and other important factors such as biocompatibility, once the material for the biomedical component has been determined, it is required that the processes as available in the literature, shown in Table 1, be analyzed for compatibility with the chosen material. For example, while metals such as chromium alloys may be used to manufacture a product using SLM, a process such as SLS may not be used for such material.

Table 1 Overview of additive manufacturing techniques for biomedical devices and applications

Feedstock material	Process type	AM technology	Product vendors	Materials	Prevalent use cases	Build characteristics		
						Resolution	Advantages	Limitations
Liquid	Vat polymerization	Stereolithography apparatus (SLA) Digital light processing (DLP)	3D systems, USA	Photopolymers, bio-resins	Surgical guides, tissue engineering, cell containing hydrogels, orthopaedic models, dental implant guides and models, hearing aids [29–34]	1.2–200 μm	High resolution and accuracy, allows for suspension of other materials such as alumina and hydroxyapatite to form parts	Limited material options, IP heavy material costs
			Cubital, Israel					
			Envisiontec, Germany					
			Schultheiss, Germany					
Material jetting	Material jetting	Multi-jet modeling (MIM)	Objet, Israel (now Stratays, USA)	Polymers (HDPE, photopolymers, Polypropylene, PMMA, ABS, PC), bio inks, plastics, wax, ceramics, nanoparticles	Dental casts and implant guides, medical models, optics, bioprinting of cell culture scaffolds, soft tissue and organ development [35–37]	20–100 μm	Low material wastage, multiple colours in the same build process	Support material requirements, limited choice of materials (only polymers and waxes)
			3D systems, USA					
			Projet					
			Solid scape, USA					

(continued)

Table 1 (continued)

Feedstock material	Process type	AM technology		Product vendors	Materials	Prevalent use cases	Build characteristics		Limitations
		Desktop prototyping	Fused deposition modelling (FDM) Fused filament fabrication (FFF)				Resolution	Advantages	
Solid wire	Material extrusion		Stratasys, USA	Polymers (ABS, Nylon, PC, AB), thermoplastics, hydrogels, ceramics, bioinks	Instrumentation, prototyping, consumer devices, testing kits, cell culture scaffold bioprinting, rigid and soft models for surgical planning [35, 38, 39]	100–200 µm	Cost-efficient process, relatively common in deployment, easily accessible materials (ABS, PLA)	Dependence on nozzle radius for good build quality, low speed, contact pressure required (for ironing effect for better quality)	
			RepRap, open-source global collaboration						
Direct energy deposition	Arc welding		Sciaky, USA	Metals (Ti alloys, Co alloys, Ti-Ni alloys, 316L stainless steel, ceramic, composites, nylon)	Porous implants for accelerated healing, to build large parts, repair existing components, otherwise limited usage in biomedical applications [40, 41]	250–500 µm	Fast process, the porosity of components to allow for better healing via biological fixation, can alter mechanical properties simply by changing build orientation and geometry, multi-material incorporation	Expensive may require post-process machining	
			DMG Mori, Japan						
			Optomec, USA						

(continued)

Table 1 (continued)

Feedstock material	Process type	AM technology	Product vendors	Materials	Prevalent use cases	Build characteristics		
						Resolution	Advantages	Limitations
Solid powder	Powder bed fusion	Selective laser melting (SLM)	SLM, Germany	Metal powders	Tissue engineering scaffolds, drug delivery vehicles, Hard tissue implants (dental, orthopaedic, craniofacial), fixations and models requiring defined lattices, temporary and degradable rigid implants [42, 43]	100–200 μm	Small machines, extensive options for materials, no solvents required	Quality dependence on powder grain size, expensive, Post process-intensive, Low speed, structurally lacking materials, limited workspace sizes
		Selective laser/EB sintering (SLS)	EoS' DMLS, Germany Arcam, Sweden	Thermoplastics, metal powder, ceramics, sand Metals				
Binder jetting	3D printing (3DP)	Multijet raster Type	Z-Corp, USA	Polymers (ABS, PA, PC)	Hard and mineralized structures, anatomical modelling, coloured prints, degradable (Fe alloys) metal implants [44–46]	50–400 μm	Multiple materials supported, fast process, the variant powder-binder ratio for variant product properties	Post-processing required for clean builds, structurally unreliable
			ExOne, USA	Sand, metal, ceramics				
			Hoeganas, Sweden	metal				

(continued)

Table 1 (continued)

Feedstock material	Process type	AM technology		Product vendors	Materials	Prevalent use cases	Build characteristics		Limitations
		Laminated object manufacturing	Sheet-based cutting				Resolution	Advantages	
Solid sheet	Sheet lamination	Laminated object manufacturing	Laser-based sheet cutting	Helisys, USA	Plastic, paper	Macroscopic anatomical modelling, Orthopaedic modelling, limited implant manufacturing, otherwise limited biomedical usage [47–50]	~1 mm	Ease of material handling does not involve melting or sintering thus limiting shrinkage and distortion of finished parts, good surface finish, the possibility of prefabricated structures such as honeycombs	Finish may be bad for paper-based LOM, heavy material wastage and labour time for decubing processes, limited research on the application in biomedical devices
		Ultrasonic consolidation	Shear-based sheet cutting	Kira, Japan	Plastic, paper				
				Solid DIMENSION, USA	Ceramics, metals				

4.3.2 Layer Thickness

Upon definition of product deliverables, properties such as the build Resolution and surface finish may be used further to determine the optimal AM process suitable for production. For instance, the swabs for a viral testing kit may be manufactured using FDM, instead of SLA as they do not require great dimensional accuracy. Whereas, knee implants are generally constructed using SLM given the ability to form surfaces that enhance the biocompatibility of the implant with the surrounding bone tissue.

4.3.3 Support Mechanism

Overhanging features within a geometry refer to those parts of the substrate component being printed, which do not have layers of material directly underneath them. Such features may occur naturally in design geometries but may be minimized with the help of an optimal orientation of the component during the build, with respect to the direction of the build. However, in certain cases, it becomes impossible to completely eliminate such features, which can cause problems in most AM processes. These are issues of lack of inherent support to freshly printed layers of substrate, causing the layer to sag, drop or break under a load of gravity. Such an issue may be fixed with the help of temporary features added to the build geometry, called support mechanisms. However, such structures add material usage (unrecyclable and thus wastages) and removal time (to rid the substrate of the temporary support features), while also interfering with the surface finish of the product. The issue may be circumvented with the choice of appropriate build directions for the product, perhaps even multiple, for different features of the same build. Depending on the prevalence of overhangs, the required surface finish and build time, an appropriate trade-off may be made between the design geometry and the AM process, to minimize the amount of support scaffolding required.

4.4 *Selection of Allied Processes*

As visualized in Fig. 4, allied technologies are used before, during or after the build of the component. The pre-build processes are used to develop the design for the part to be produced, most prominent of which are reverse engineering techniques such as 3D scanning. Imaging techniques may be used to generate either the product geometry itself—as is done in conventional reverse engineering—or it may be used to generate the contour of the environment within which the product must function. For example, the production of prosthetics is heavily dependent on the surface geometry of the patient's affected limb. A scanning method may allow for an accurate representation of the limb, which can enable an optimal fit of the produced prosthetic, upon the patient. Apart from such customization, pre-build processes also allow for analysis and optimization of the design geometry for maximized efficiency of production.

In-situ processes are primarily used for improving the mechanical properties of the build, as it progresses. This allows access to the internal sections of the final part, as the layers may be processed in numerous ways, in accordance with desired final properties. Interlayer machining allows for maximum assurance of geometry fidelity to the original design, while processes such as cold working and laser shock peening improve the interior material properties of the final build. In the case of embedded inserts being required, sections of the part otherwise accessible can be planted with the required external components and sealed. Post-processing may also be employed to improve the number of product properties. For example, isostatic pressing (hot or cold) is employed to provide the part with increased strength and resistance to fatigue or creep. The selection of these processes may be made on the basis of desired product properties, and the advantages and caveats associated with each such technology, as indicated in Table 2.

5 Challenges in Rapid Manufacturing of Biomedical Devices

Rapid manufacturing is among the newest technologies in the upcoming, let alone in the field of manufacturing. Therefore, there are several issues with the deployment of such a technology for the industrial production of components, especially those with stringent quality control parameters, as in the case of biomedical devices. As a result, the RM of these products encounters many challenges right from the initial fabrication. Thereafter, problems are also faced during post-processing as well as where the allied technologies interact with these products. The finished product itself has to overcome a number of management-related hurdles before being brought to the market and, therefore, to the end-user. There can be two broad categories of such challenges: those that arise within the production process itself, and those that affect the management of the product (see Fig. 7).

5.1 *Process Related Challenges*

The production of biomedical applications requires adherence to standards set by domestic or international regulatory authorities. These regulations are built upon the characteristics of the product, such as its biocompatibility, lifespan, biodegradability, etc. One of the challenges faced is the limited and tedious choice of binders used in the build process [51]. The binders that can be chosen are further reduced in variety due to the additional requirement of biocompatibility, making it difficult for certain materials to be manufactured with ease, driving up costs. For instance, in the case of implantables, it becomes increasingly necessary to prioritize organic materials, which tend to affect plastic parts of the building apparatus [52]. Along

Table 2 Overview of allied technologies

Precedence	Technology	Description	Advantages	Limitations
Pre build	Reverse engineering	Reproduction of design from existing products	Reduces design and development time and costs	May result in intellectual property related legal issues
	Model processing	Data reduction, object segmentation for gluing, editing, and repair of models and lattice	Optimizes generated CAM file for efficient build processing	Skill intensive and non-repetitive
	OptiLOM	Analysis and Optimization	Increases efficiency of the build pipeline	Skill intensive and non-repetitive
	CAD/CAE	Efficient and effective design translation, design optimization	Virtual prototype testing and iterative improvement	Skill intensive and non-repetitive
	Imaging	A systematic understanding of ground truth and user requirement with 3D measurements and automatic modelling	Eases and streamlines the design generation and documentation process with accurate data	Expensive equipment and skilled operation
In situ	Micro RP and Nanomanufacturing	Use of suitable technologies to append micro and nano-scaled features onto the build	Allows monolithic implementation of trans-scale features, such as micro-features on macro-components	Expensive instrumentation, materials and process reconfiguration
	Embedding PCB inserts	For inbuilt electronics and embedded	Allows seamless integration without auxiliary joining components such as nuts and bolts	Increases build time and interruptions, may reduce inter-layer bonding strength
	Cold working	Done after every layer	Increases quality of inter-layer interaction while reducing defects present in individual layers, preventing them from propagating or causing structural weakness	Time-consuming additional process, which may also reduce or eliminate desirable layer properties such as porosity

(continued)

Table 2 (continued)

Precedence	Technology	Description	Advantages	Limitations
Post build	Machining	Done after every layer	Increases quality of layer adhesion and compensates feed-rate errors and bumps	Generates waste shrapnel which is unrecyclable and difficult (but necessary) to remove before the next layer is deposited
	Surface Finishing	Via polishing or machining such as 5-axis milling	Increases quality of surface finish and provides desired surface properties	Requires high-end machining apparatus to provide significant improvement in quality
	Interior quality	Thermal or pressure based treatments such as isostatic pressing	Increases the otherwise lacking mechanical properties such as strength and fatigue/creep resistance	HIP/CIP machines are very expensive both to set up and operate
	Multiplication via rapid replication	Multiple pieces via indirect methods such as vacuum casting	Reduces time required for tooling, while eliminating the requirement of multiple build times	Labour intensive process

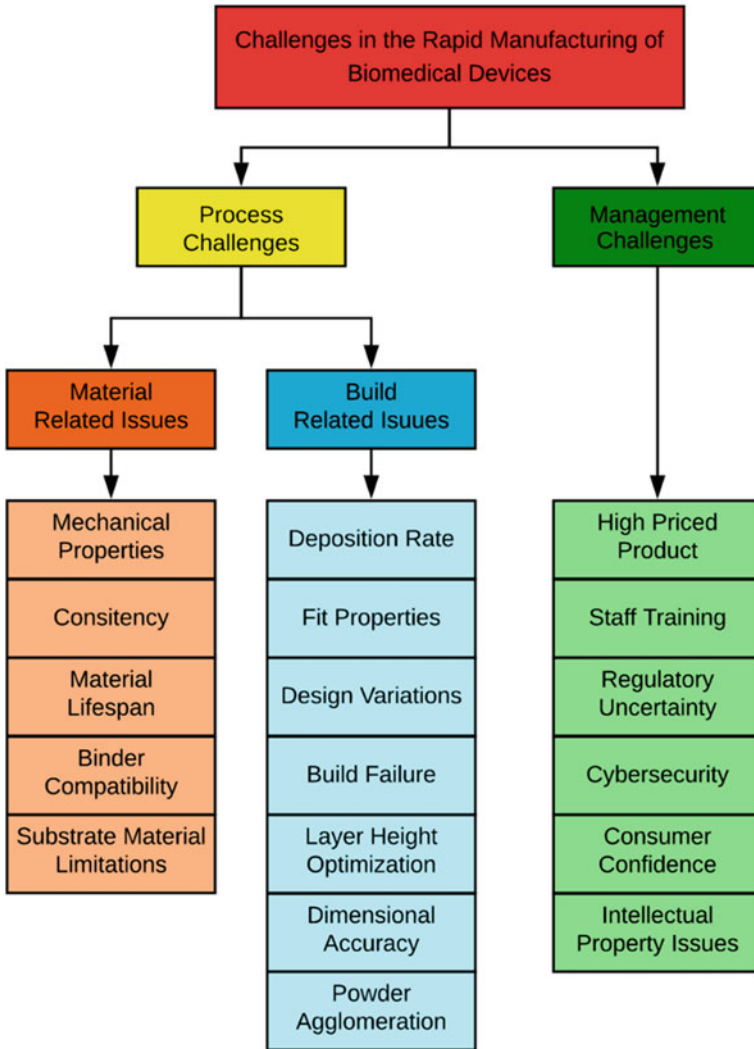


Fig. 7 The challenges encountered during the rapid manufacturing of the biomedical devices

with the binders, the materials themselves are more constrained in terms of choice. Moreover, the poor mechanical properties of the final product are a challenge as there must be adequate tensile and compressive strength, once the print has been finished. Dimensional accuracy and its changes through and after the print as a result of shrinkage must be addressed. Depending on the state of the fitting, whether there is an underfit or overfit, the final product may encounter defects, where the nozzle size plays an important role in defining print properties such as structure and accuracy.

In the case of powder bed technologies, to avoid density fluctuation and powder agglomeration [53], the powder distribution must be ensured for evenness [54].

Operational procedures with scaled industrial implementation of rapid prototyping technologies also encounter a number of issues. The optimization between production rate capacity and layer thickness and, therefore, print resolution [55], is one with heavy considerations of quality and build time. The already prevalent problem of costly substrate materials accentuated the short lifespan of biocompatible materials, thus making inventory control crucial as expired materials may cause brittleness, cracking, discolouration, and even incompatibility with biological environments [56]. Even though customization is an important aspect of rapid manufacturing, it presents the issue of dependence on the iterative design and redesign process, since techniques such as group technology may not be employed to streamline the process plan. The control parameters and code of the automated build apparatus are at a constant threat of failure from programming bugs and connectivity issues, resulting in build failures [56].

5.2 Management-Related Challenges

The introduction of novel technologies, including the many aspects of RM, such as AM technologies, computer-aided process planning, etc. involve investment in training and re-education of staff [57]. Moreover, the digitalization of the entire process pipeline implies that it is also vulnerable to cyber threats [58]. The nascency of regulatory guidelines makes it challenging to adhere to them, along with patenting and other IP processes that enhance the risks of legal issues [59]. The inherent costs of development, customizable design, material prices, which are themselves IP heavy, marketing digitization and cybersecurity, and legal fees imply high prices of the final products [60].

6 Conclusion

The major improvements in rapid manufacturing that remain are speed, mechanical properties, and material costs. Only upon the overcoming of these challenges can the term rapid manufacturing be truly applicable to the current combinations of additive and allied technologies. With continuous advancements, the cost of manufacturing hardware shall reduce. More importantly, there have been promising outcomes in the development of improved 3D printing methods in the recent past, with technologies such as HARP (High Area Rapid Printing) which utilizes larger workspaces and effective heat transfer mechanisms to provide increased speeds of production [61], and techniques such as computed axial lithography are providing more efficient ways of energy deposition and polymerization, which results in truly solid, smooth, and possibly flexible builds [62]. A number of technologies have already

been employed for first usage cases in biomedical applications. Two-photon polymerization, a technique that employs a non-linear optical process, provides higher resolutions as a result of more localized polymerization initiations and has been demonstrated to manufacture microscale medical devices such as tissue growth scaffolds and microneedle arrays [63]. Interference lithography, a technique that uses interference from lightwave superposition to produce regular patterns, has been successfully used to produce structures on micro and nano-scaled, such as micro sieves, nanopillars, and 3D photonic crystals [64]. In metal substrate technologies such as SLS, recent advances have enabled higher resolution and lower stiffness of the printed part, which allows for applications to soft tissue engineering applications [65]. In the case of FDM based fabrications, the major advancements are in the increase of variety of filament options, given the relative freedom of choice associated with injection moulding. Therefore, in one instance, precision injection moulding has been combined with a gantry to allow for an increased range of substrate materials [66].

Therefore, rapid manufacturing is of growing importance to the realization of biomedical engineering advances. As designs become more sophisticated, the manufacturing methodologies employed to produce them would need to keep up in order to reduce the gap between scientific development and market availability. Rapid manufacturing, with its characteristics of design freedom, material efficiency, and customizability, allows for the same, both technologically and financially. The challenges faced in RM of biomedical devices have gradually translated to exponential rates of development of involved technologies. In the coming decades, especially the immediate on, the employment of RM in the biomedical space shall be interesting to witness.

References

1. Global Harmonization Task Force.: Definition of the Terms 'Medical Device' and 'In Vitro Diagnostic (IVD) Medical Device'. Study Group 1 (2012)
2. Norman, J et al.: A new chapter in pharmaceutical manufacturing: 3D-printed drug products. *Adv. Drug Deliv. Rev.* **108**, 39–50 (2017)
3. FDA, US.: Classify Your Medical Device (2014)
4. Danish Medicines Agency, Denmark.: Medical Devices (2020)
5. US Food and Drug Administration.: Device classification panels (2014)
6. Busachi, A. et al.: A review of additive manufacturing technology and cost estimation techniques for the defence sector. *CIRP J. Manufact. Sci. Technol.* **19**, 117–128 (2017)
7. Chuter, T.A.M., et al.: The transition from custom-made to standardized multibranched thoracoabdominal aortic stent grafts. *J. Vascular Surg* **54.3**, 660–668 (2011)
8. Culler, S.D., Martin, G.M., Swearingen, A.: Comparison of adverse events rates and hospital cost between customized individually made implants and standard off-the-shelf implants for total knee arthroplasty. *Arthroplasty Today* **3**(4), 257–263 (2017)
9. Osman, R.B., et al.: 3D-printing zirconia implants; a dream or a reality? An in-vitro study evaluating the dimensional accuracy, surface topography and mechanical properties of printed zirconia implant and discs. *J. Mech. Behav. Biomed. Mater.* **75**, 521–528 (2017)

10. Solanki, N.G., et al.: Formulation of 3D printed tablet for rapid drug release by fused deposition modeling: screening polymers for drug release, drug-polymer miscibility and printability. *J. Pharm. Sci.* **107.1**, 390–401 (2018)
11. Neves, L.S., et al.: Current approaches and future perspectives on strategies for the development of personalized tissue engineering therapies. *Expert Rev. Precision Med. Drug Dev.* **1.1**, 93–108 (2016)
12. Xu, X.W., et al.: STEP-compliant NC research: the search for intelligent CAD/CAPP/CAM/CNC integration. *Int. J. Prod. Res.* **43.17**, 3703–3743 (2005)
13. Martins, P.A.F., et al.: Theory of single point incremental forming. *CIRP Ann.* **57(1)**, 247–252 (2008)
14. Geiger, M., Vollertsen, F.: The mechanisms of laser forming. *CIRP Ann.* **42(1)**, 301–304 (1993)
15. ASTM Committee F42 on Additive Manufacturing Technologies, and ASTM Committee F42 on Additive Manufacturing Technologies. Subcommittee F42. 91 on Terminology. Standard terminology for additive manufacturing technologies. *Astm International* (2012)
16. Saidi, B., et al.: Experimental and numerical study on force reduction in SPIF by using response surface. In: *International Conference Design and Modeling of Mechanical Systems*. Springer, Cham (2017)
17. Aguilera, E., et al.: 3D printing of electro mechanical systems. In: *Proceedings of the Solid Freeform Fabrication Symposium* (2013)
18. Gu, J., et al.: The effect of inter-layer cold working and post-deposition heat treatment on porosity in additively manufactured aluminum alloys. *J. Mater. Process. Technol.* **230**, 26–34 (2016)
19. Guo, W. et al.: Laser shock peening of laser additive manufactured Ti6Al4V titanium alloy. *Surf. Coat. Technol.* **349**, 503–510 (2018)
20. Dilip, J.J.S., et al.: Use of friction surfacing for additive manufacturing. *Mater. Manuf. Process.* **28(2)**, 189–194 (2013)
21. Karunakaran, K.P., et al.: Low cost integration of additive and subtractive processes for hybrid layered manufacturing. *Robot. Comput. Integr. Manuf.* **26(5)**, 490–499 (2010)
22. Chen, C. et al.: Effect of hot isostatic pressing (HIP) on microstructure and mechanical properties of Ti6Al4V alloy fabricated by cold spray additive manufacturing. *Add. Manuf.* **27**, 595–605 (2019)
23. Reeves, P., Tuck, C., Hague, R.: Additive manufacturing for mass customization. In: *Mass Customization*, pp. 275–289. Springer, London (2011)
24. Chhabra, M., Singh, R.: Rapid casting solutions: a review. *Rapid Prototyping J.* (2011)
25. Karapatis, N.P., Van Griethuysen, J.P.S., Glardon, R.: Direct rapid tooling: a review of current research. *Rapid Prototyping J.* (1998)
26. Lantada, A.D., Pilar, L.M.: Rapid prototyping for biomedical engineering: current capabilities and challenges. *Ann. Rev. Biomed. Eng.* **14**, 73–96 (2012)
27. Bandyopadhyay, A., et al.: Direct comparison of additively manufactured porous titanium and tantalum implants towards in vivo osseointegration. *Addit. Manufact* **28**, 259–266 (2019)
28. Varga, P., et al.: Novel PLA-CaCO₃ composites in additive manufacturing of upper limb casts and orthotics—A feasibility study. *Mater. Res. Express* **6.4**, 045317 (2019)
29. Ozan, O., et al.: Clinical accuracy of 3 different types of computed tomography-derived stereolithographic surgical guides in implant placement. *J. Oral Maxillofac. Surg.* **67.2**, 394–401 (2009)
30. Kamran, M., Saxena, A.: A comprehensive study on 3D printing technology. *MIT Int. J. Mech. Eng.* **6(2)**, 63–69 (2016)
31. Mano, J.F., et al.: Natural origin biodegradable systems in tissue engineering and regenerative medicine: present status and some moving trends. *J. R. Soc. Interface* **4(17)**, 999–1030 (2007)
32. Cohen, A., et al.: Mandibular reconstruction using stereolithographic 3-dimensional printing modeling technology. *Oral Surg. Oral Med. Oral Pathol. Oral Radiol. Endodontol.* **108.5**, 661–666 (2009)
33. Whitley III, D., et al.: In-office fabrication of dental implant surgical guides using desktop stereolithographic printing and implant treatment planning software: a clinical report. *J. Prosthet. Dent.* **118.3**, 256–263 (2017)

34. Patel, D.K., et al.: Highly stretchable and UV curable elastomers for digital light processing based 3D printing. *Adv. Mater.* **29.15**, 1606000 (2017)
35. Aimar, A., Augusto, P., Bernardo, I.: The role of 3D printing in medical applications: a state of the art. *J. Healthc. Eng.* (2019)
36. Ibrahim, D., et al.: Dimensional error of selective laser sintering, three-dimensional printing and PolyJet™ models in the reproduction of mandibular anatomy. *J. Cranio-Maxillofac. Surg.* **37.3**, 167–173 (2009)
37. Alamán, J., et al.: Inkjet printing of functional materials for optical and photonic applications. *Materials* **9.11**, 910 (2016)
38. Tanaka, K.S., Lightdale-Miric, N.: Advances in 3D-printed pediatric prostheses for upper extremity differences. *JBJS* **98**(15), 1320–1326 (2016)
39. Larrañeta, E., Juan, D.-R., Dimitrios, A.L.: Additive manufacturing can assist in the fight against COVID-19 and other pandemics and impact on the global supply chain. *3D Printing Addit. Manufac.* (2020)
40. Trevisan, F., et al.: Additive manufacturing of titanium alloys in the biomedical field: processes, properties and applications. *J. Appl. Biomater. Funct. Mater.* **16.2**, 57–67 (2018)
41. Kaierle, S., et al.: Review on laser deposition welding: from micro to macro. *Phys. Procedia* **39**, 336–345 (2012)
42. Duan, B., Wang, M.: Selective laser sintering and its application in biomedical engineering. *MRS Bull.* **36**(12), 998 (2011)
43. Sing, S.L., et al.: Laser and electron-beam powder-bed additive manufacturing of metallic implants: a review on processes, materials and designs. *J. Orthop. Res.* **34.3**, 369–385 (2016)
44. Ahangar, P., et al.: Current biomedical applications of 3D printing and additive manufacturing. *Appl. Sci.* **9.8**, 1713 (2019)
45. Matsumoto, J.S., et al.: Three-dimensional physical modeling: applications and experience at Mayo Clinic. *Radiographics* **35.7**, 1989–2006 (2015)
46. Hong, D., et al.: Binder-jetting 3D printing and alloy development of new biodegradable Fe-Mn-Ca/Mg alloys. *Acta Biomater.* **45**, 375–386 (2016)
47. Webb, P.A.: A review of rapid prototyping (RP) techniques in the medical and biomedical sector. *J. Med. Eng. Technol.* **24**(4), 149–153 (2000)
48. Auricchio, F., Marconi, S.: 3D printing: clinical applications in orthopaedics and traumatology. *EFORT Open Rev.* **1**(5), 121–127 (2016)
49. Mueller, B., Kochan, D.: Laminated object manufacturing for rapid tooling and patternmaking in foundry industry. *Comput. Ind.* **39**(1), 47–53 (1999)
50. Dhavalikar P., Lan, Z., Kar, R., Salhadar, K., Gaharwar, A.K., Cosgriff-Hernandez E. In: Wagner, W.R., Sakiyama-Elbert, S.E., Zhang, G., Yaszemski, M.J. (eds.) 1.4.8—Biomedical Applications of Additive Manufacturing, *Biomaterials Science (Fourth Edition)*. Academic Press (2020)
51. Bogue, R.: 3D printing: the dawn of a new era in manufacturing? *Assembly Autom.* (2013)
52. Bose, S., Vahabzadeh, S., Bandyopadhyay, A.: Bone tissue engineering using 3D printing. *Mater. Today* **16**(12), 496–504 (2013)
53. Pires, I., et al.: Characterization of sintered hydroxyapatite samples produced by 3D printing. *Rapid Prototyping J.* (2014)
54. Vasireddi, R., Bikramjit, B.: Conceptual design of three-dimensional scaffolds of powder-based materials for bone tissue engineering applications. *Rapid Prototyping J.* (2015)
55. Yan, Q., et al.: A review of 3D printing technology for medical applications. *Engineering* **4.5**, 729–742 (2018)
56. Shahrubudin, N., et al.: Challenges of 3D printing technology for manufacturing biomedical products: a case study of Malaysian manufacturing firms. *Heliyon* **6.4**, e03734 (2020)
57. Sandström, C.: Adopting 3D printing for manufacturing—The case of the hearing aid industry. *Ratio Working Pap.* 262, 1–20 (2015)
58. Sturm, L.D., et al.: Cyber-physical vulnerabilities in additive manufacturing systems: a case study attack on the. STL file with human subjects. *J. Manuf. Syst.* **44**, 154–164 (2017)

59. Pavlovich, M.J., Hunsberger, J., Atala, A.: Biofabrication: a secret weapon to advance manufacturing, economies, and healthcare. *Trends Biotechnol.* **34**(9), 679–680 (2016)
60. Emelogu, A., et al.: Additive manufacturing of biomedical implants: a feasibility assessment via supply-chain cost analysis. *Addit. Manufac.* **11**, 97–113 (2016)
61. Walker, D.A., Hedrick, J.L., Mirkin, C.A.: Rapid, large-volume, thermally controlled 3D printing using a mobile liquid interface. *Science* **366**(6463), 360–364 (2019)
62. Kelly, B., et al.: Computed axial lithography (CAL): toward single step 3D printing of arbitrary geometries. arXiv preprint [arXiv:1705.05893](https://arxiv.org/abs/1705.05893) (2017)
63. Raimondi, M.T., et al.: Two-photon laser polymerization: from fundamentals to biomedical application in tissue engineering and regenerative medicine. *J. Appl. Biomater. Funct. Mater.* **10.1**, 56–66 (2012)
64. Prenen, A.M., et al.: Monodisperse, polymeric nano- and microsieves produced with interference holography. *Adv. Mater.* **21.17**, 1751–1755 (2009)
65. Yeong, W.Y., et al.: Porous polycaprolactone scaffold for cardiac tissue engineering fabricated by selective laser sintering. *Acta Biomater.* **6**(6), 2028–2034 (2010)
66. Von Zeppelin, D., Manka, M.: ARBURG plastic freeforming. *Eng. Biomater.* **20.143**, spec. iss (2017)

Chapter 5

Advanced Finishing Processes for Biomedical Applications



Talwinder Singh Bedi , Ravi Kant , and Hema Gurung 

1 Introduction

Nanofinishing is an ultra-precision finishing process for enhancing a material's surface characteristics by obtaining nanometer order surface finish using different finishing processes [1]. Conventional finishing processes such as grinding and lapping are commonly used in industries to finish various components. Nanofinishing is related to surface integrity and one of the most challenging tasks for any manufacturing industry due to the complexities involved in process selection, control, monitoring, job fixing, measurement, repetition, and spot locating [2]. Nanofinishing of freeform/complex surfaces is more challenging than the flat and cylindrical surfaces because of the need of specific tool orientation, tool path, and tool geometry [3]. Nanofinishing can provide many advantages such as low frictional and wear losses between mating parts, longer fatigue life, improved hardness, better process quality control, negligible backlash in assembly, improved corrosion and chemical resistance, bacteria resistance, excellent optical properties, improved appearance, better wettability, hydrophobic characteristics of the surface, and improved electrical properties [4, 5].

T. S. Bedi
Assistant Professor, Desh Bhagat University, Mandi Gobindgarh, Punjab 147301, India

R. Kant (✉)
Department of Mechanical Engineering, Indian Institute of Technology Ropar, Rupnagar, Punjab 140001, India
e-mail: ravi.kant@iitrpr.ac.in

H. Gurung
Department of Mechanical Engineering, Thapar Institute of Engineering and Technology, Patiala, Punjab 147004, India

Researchers are developing products and materials with higher functionality and more extended durability for biomedical, aerospace, automotive, optics and electronics, sensors, and defense industries [6]. Biomedical implants market was raised by \$35 billion in 2019 and is expected to garner \$116 billion by 2022 [7]. Orthopedic, pacing devices, stents, spinal and dentist implants contribute a higher share in the current market. The artificial orthopedic implants such as hip, shoulder, or knee joints act as structural aids in the human body. Freeform implant structure is normally screwed to bones [8]. These implants are made of biocompatible materials such as stainless steel, titanium alloys, chromium alloys, ceramics, and polymers materials. International standards say that the biomedical implant's surface roughness should be less than 100 nm for proper functioning and longer service life [9]. It is because the biomedical implants have frequent relative motion with mating parts, which can result in deformation, surface erosion, and chipping of the implants over time [10, 11]. These deformed/worn-out implants can cause joints dislocation, stiffening, and squeaky noises, causing inconvenience to the human body. Therefore, enhancing a biomedical implant's surface integrity is highly considerable for its better operative functionality [12, 13].

Conventional finishing processes are suitable for finishing the easily accessible areas of freeform surfaces and can finish within a limited range of surface roughness. These processes are not suitable for mass production of nanofinished components due to rigid tool geometry, low repeatability, slow processing, and high production cost. These processes cannot deal with complex shapes due to poor accessibility of tools on the interior, inclined, and curved surfaces. It may result in non-uniform roughness across the finished surface. However, uniform surface finishing is an essential factor for the satisfactory performance of biomedical implants, which is convenient to obtain using a flexible tool that has easy and uniform accessibility at different regions of complex surfaces. In this chapter, various finishing processes, their applications, and advantages are discussed in the biomedical industry perspective.

2 Applications and Advantages of Nanofinishing in the Biomedical Industry

Biomedical implants used in the shoulder, hip (stem and ball joint), knee (femur and tibia), ankle, and finger joints are complex and continuously move inside the human body. These implants often wear out due to friction between two parts in relative motion and require replacement after some time. The biomedical industry requires parts with high surface quality in order to increase their operational life. Some of the benefits which arise with a high surface finish of biomedical implants are as follows:

- Reduction of wear and friction between joints.
- Reduction in the dislocation of joints.
- A defect-free surface can be achieved.
- Operative functionality of joints may be increased.

The finishing processes like electron discharge machining (EDM), sand blasting, and bonnet polishing are not suitable for finishing inaccessible areas of complex surfaces used in biomedical implants. High-quality surface finishing of these inaccessible complex surfaces requires advanced technology, which would ultimately increase the manufacturing cost. However, for their better operational life, the nanofinishing is more important than the manufacturing cost. Nanofinishing of biomedical implants can be obtained using various finishing processes which are discussed in the following sections.

3 Finishing Processes for Biomedical Implants

Finishing processes shown in Fig. 1 have been developed for nanofinishing of complex surfaces used in biomedical, optics, semiconductor, automotive, and aerospace industries. These finishing processes provide better surface accuracy by overcoming limitations of the conventional finishing processes. The main advantages of these finishing processes are as follows:

- Uses a flexible tool that can alter shape according to the nature of the workpiece.
- Produces surface with closer tolerances.
- The mirror finish surface can be achieved on complex surfaces.
- Surface defects are less.
- Fast processing, high productivity, lower cost of production, etc.

3.1 Abrasive Flow Finishing (AFF)

AFF is initially introduced in the year 1960 by Extrude Hones Corporation (USA), which is mainly used for finishing a wide range of engineering components used in aerospace, biomedical, automotive, and defense [14, 15]. The principle behind AFF is to use a large number of cutting edges of abrasive particles with indistinct orientation and geometry. This process is used for deburring, finishing, and removing the recast layer from the workpiece surface. The inaccessible areas of freeform surface can be finished more effectively with AFF.

AFF consists of a cylinder into which the piston reciprocates, as shown in Fig. 1a. A carrier fluid is placed inside the cylinder, which moves as the piston reciprocates. The carrier fluid comprises an abrasive slurry and polymeric medium [16]. The important parameters to control the process are extrusion pressure, number of finishing cycles, and traveling length [17]. The workpiece is placed inside the cylinder so that the carrier fluid moves across the workpiece surface when the piston reciprocates. The sharper edges of abrasive particles inside the carrier fluid are responsible for high-level finishing. The surface irregularities such as out of roughness, lays, deep scratches, and large bumps cannot be removed by AFF because there is no control of abrading forces produced by abrasive particles during the finishing operation [18].

Sarkar and Jain [19] performed experiments on AFF to finish a stainless steel knee joint. Abrasive particle size and extrusion pressure were taken as controlling

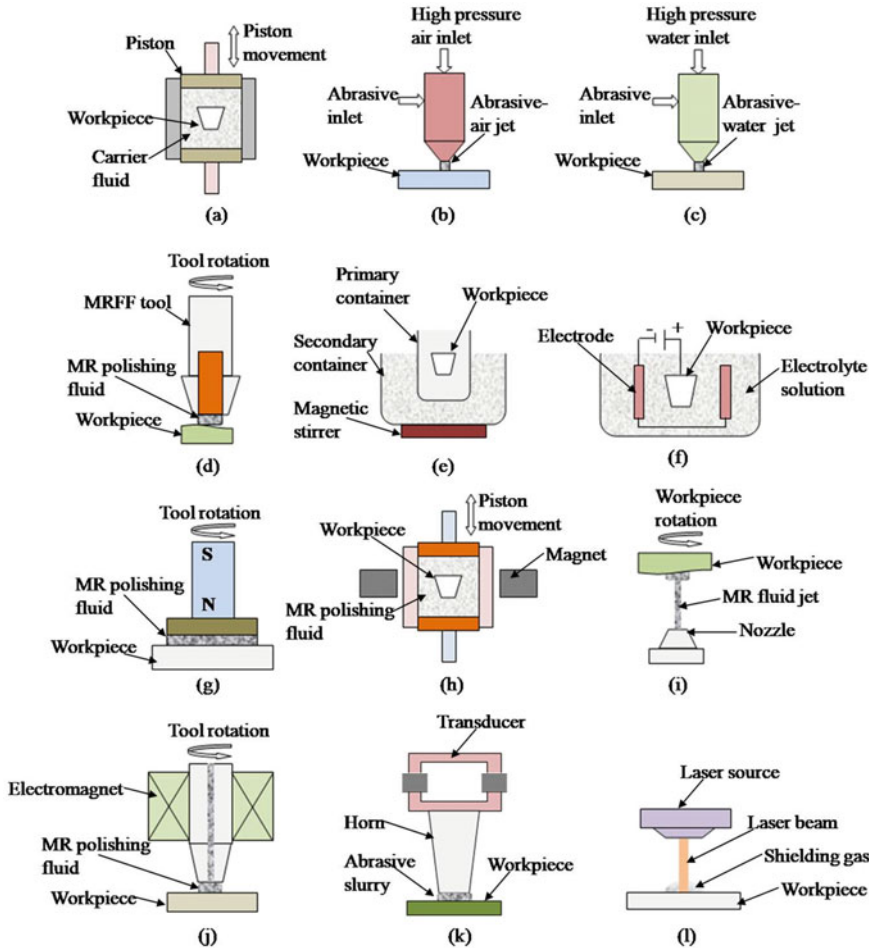


Fig. 1 Finishing processes for biomedical implants **a** abrasive flow finishing (AFF), **b** abrasive jet finishing (AJF), **c** abrasive water jet finishing (AWJF), **d** magnetorheological fluid-based finishing (MRFF), **e** chemical polishing (CP), **f** electrolysis-based polishing (EBP), **g** chemo-mechanical magnetorheological finishing (CMMRF), **h** magnetorheological abrasive flow finishing (MRAFF), **i** magnetorheological jet finishing (MRJF), **j** ball end magnetorheological finishing (BEMRF), **k** ultrasonic polishing (UP), and **l** laser polishing (LP)

parameters. The finishing was carried out on different knee joint faces with the number of finishing cycles as 1500. Results reported surface roughness (R_a) between 42.9 and 50.5 nm with SiC mesh size of 1500 and extrusion pressure of 24 bars.

Subramanian et al. [20] worked on AFF for finishing a hip joint made of Co-Cr alloy. Results showed that the surface roughness (R_a) reduced from an initial 56 nm to 11 nm with an extrusion pressure of 14 MPa, SiC abrasive size of 800, and number of finishing cycles of 500. Singh et al. [21] conducted experiments on stainless steel

surgical tubes which are typically used in biological applications. The finishing was performed to avoid the probability of the failure of tubes due to corrosion and wear. The surface roughness (R_a) was decreased to 31 nm from its initial value of 650 nm with an extrusion pressure of 5 MPa, the number of finishing cycles of 550, and SiC abrasive concentration of 55%. Singh and Sankar [22] used AFF for precision finishing of stainless steel microholes used in drug-eluting stents. These microholes are used for releasing drugs from the human body. Results revealed that the surface roughness (R_a) can be reduced from 1400 to 150 nm with an extrusion pressure of 4 MPa, SiC abrasive concentration of 55%, and number of finishing cycles of 6.

3.2 Abrasive Jet-Based Finishing

In abrasive jet-based finishing, the material is finished by high-speed narrow jet of abrasive particles accelerated by pressurized air or water stream [23]. The abrasive jet-based finishing can be divided into two categories:

- **Abrasive jet finishing (AJF):** The schematic of abrasive jet finishing is shown in Fig. 1b. In this process, the abrasive particles are accelerated by the pressurized air/gas.
- **Abrasive water jet finishing (AWJF):** The schematic of abrasive water jet finishing is shown in Fig. 1c. In this process, the abrasive particles are accelerated by the pressurized water.

These processes are used to machine various biomedical components and to enhance the surface quality of biomedical implants. The abrasive jet-based finishing offers many advantages such as (1) negligible detrimental effects on the implant surface because of no chatter and heat involved, (2) low setup, maintenance, and operating cost, and (3) higher material removal rate [24]. However, the abrasive particles must be selected with care because they may impinge into the surface and cause bioincompatible surfaces with sharp edges of abrasives directing outside.

Seo et al. [25] worked on abrasive water jet finishing of titanium alloy (Ti-6Al-4V) and found that the surface roughness (R_a) reduced to 1.89 μm from its initial value of 5 μm with jet pressure of 207 MPa, stand-off distance of 4 mm, traverse speed of 0.7 mm/s, and SiC grit number of 100. Shiou et al. [26] worked on abrasive jet finishing of bulk metallic glass using SiC abrasive particles and found that the surface roughness (R_a) decreased to 16 nm from an initial value of 675 nm with process parameters as stand-off distance of 15 mm, jet pressure of 2 kg/cm^2 , and polishing time of 60 min.

3.3 Magnetorheological Fluid-Based Finishing (MRFF)

MRFF process is developed for nanofinishing of engineering materials used in optics, biomedical, automotive, mold, and dies making. This process uses a smart fluid called magnetorheological (MR) polishing fluid which is synthesized by mixing abrasive and iron particles in a viscoelastic base medium. The viscoelastic base medium is a mixer of carrier liquid (heavy paraffin oil or mineral oil or vegetable oil) and additives (grease or glycerol). MR polishing fluid becomes active under the effect of magnetic field. The iron particle of MR polishing fluid adheres to the magnet and grips the non-magnetic abrasive particles by their chain structures. The sharper edges of these abrasive particles are responsible for surface finishing.

The schematic of MRFF for finishing of a freeform surface is shown in Fig. 1d [27]. MRFF tool is made in the shape of a circular cross section. The upper part of the tool is mounted on a computer-controlled milling machine so that when the machine spindle rotates and reciprocates, the tool follows the same path. The permanent magnet is used in the lower part for stiffening and retaining the MR polishing fluid. During finishing, the MR polishing fluid creates a flexible brush along the direction of magnetic fluxes at different feed rates, as shown in Fig. 2 [28]. The working gap between tool and workpiece is adjusted by providing the reciprocating motion to the tool. The workpiece is mounted on X – Y axis slides through a precision vice. The linear movement along X – Y axis is provided to finish a desired area. The material is removed as a result of mechanical abrasion.

Sidpara and Jain [27] developed MRFF for enhancing the surface quality of stainless steel knee joint. Initially, the knee joint roughness (R_a) was between 147 nm to 524 nm which reduced to 21.7 nm and 37.4 nm, when machined with water and chemical-based MR polishing fluid, respectively, using input parameters as: tool rotation of 1000 rpm, working gap of 1 mm, workpiece feed rate of 4 mm/min, and finishing time of 16.4 h.

Sidpara and Jain [28] showed that the tangential and normal finishing forces significantly reduce with the increase in workpiece surface curvature and increase with the increase in tool rotation and workpiece feed. Barman and Das [29] worked on finishing of a titanium alloy knee joint and showed that the surface roughness (R_a)

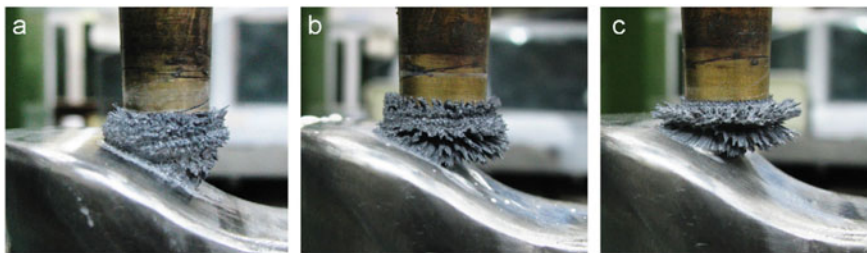


Fig. 2 Condition of MR polishing fluid brush at different feed rates **a** 1 mm/min, **b** 3 mm/min, and **c** 5 mm/min ($\theta = 25^\circ$ and $S = 700$ RPM) [28] (with permission, Copyright Elsevier)

can be reduced to 20 nm from an initial value of 120 nm with optimum parameters, i.e., tool speed of 901 rpm, working gap of 0.6 mm, and finishing time of 4.65 h.

3.4 Chemical Polishing (CP)

A schematic for the chemical polishing of specimen is shown in Fig. 1e. In this process, the workpiece is submerged into an acidic or alkaline solution contained in a chemically inert container such as high density polyethylene (HDPE) container. The finishing of the components takes place as a result of chemical erosion of material. The material either dissolves into the chemical solution, or converts into gas and evaporates into the environment, or forms a solid sludge and settles at the bottom of the container, based on the chemical reaction between the workpiece and chemical solution. Many times, the workpiece is subsequently submerged into a secondary container which consists of ice bath to maintain the solution temperature. It helps to maintain or alter the surface properties as per the requirements. A magnetic stirrer may be used to circulate the solution [30]. Metal ions diffuse more on the convex surface than the concave surface, leading to the flattening and smoothing of the workpiece. This process is suitable for producing a high finish glossy surface. This process does not use DC current so the setup, operating and maintenance costs are low. Other advantages include simple process, no need for skilled labor, processing of many components simultaneously, suitable for almost all materials, no distortion during processing, suitable for any shape and size, and independent of thermal and mechanical properties of the material. Balyakin et al. [31] used chemical polishing to finish a biocompatible Ti-6Al-4V alloy by submerging it into a salt solution which contained a mixer of NH_4F -HF and NH_2OH -HCl along with nitric acid and found that the surface roughness (R_a) was reduced from an initial value of 4.6 μm to 0.38 μm . Bazuidenhout et al. [30] worked on chemical polishing of Ti-6Al-4V using HF- HNO_3 solutions and observed that the surface roughness (R_a) was reduced to $0.99 \pm 0.11 \mu\text{m}$ from an initial value of $10.92 \pm 1.405 \mu\text{m}$.

3.5 Electrolysis-Based Polishing (EBP)

Electrolysis is a process that uses DC current to drive a chemical reaction and separates the elements from the workpiece materials using an electrolytic cell. The schematic of electrolysis-based polishing is shown in Fig. 1f. Electric current flows from one electrode to another through an electrically conducting solution called electrolyte. The electrodes coupled with negative and positive terminals of the battery are known as cathode and anode, respectively. The workpiece is made anode, and the tool is made cathode. When an electric current is passed through the electrodes, the positively charged cations are attracted by the cathode and the negatively charged anions are attracted by the anode. The polishing occurs due to the continuous removal

of positively charged metal ions from the anode [32]. An ion is removed from the position on the workpiece electrode, where it finds minimum current flow resistance. Electrolysis-based polishing can be divided into two categories:

- **Electro-chemical polishing (ECP):** In electro-chemical polishing, the particles removed from the workpiece (anode) get deposited on the tool (cathode) surface. This may result in decrease in the operational life of the tool.
- **Electro-polishing (EP):** In electro-polishing, the particles removed from the workpiece (anode) get dissolved into the electrolyte solution. The electrolyte should have salt of the workpiece (anode) material as an electrolyte, for example, for machining of copper, copper salt should be used as an electrolyte.

Wexell et al. [33] worked on electro-polishing of screw-shaped titanium implant. Titanium implant achieved a superior surface finish, and a thin oxide layer was formed on the surface which is preferable for bone formation and remodeling. Dobberthin et al. [34] compared the performance of drag grinding and electro-chemical polishing during nanofinishing of femoral heads for hip endoprosthesis made of CoCrMo material. The sulfuric acid was used as an electrolyte solution for electro-chemical polishing. Results reported that the electro-chemical polishing provides a better surface quality as compared to drag grinding as shown in Fig. 3.

Han and Fang [35] studied the effect of water concentration during electro-polishing of 316L steel. The authors used sulfuric acid-free electrolyte which

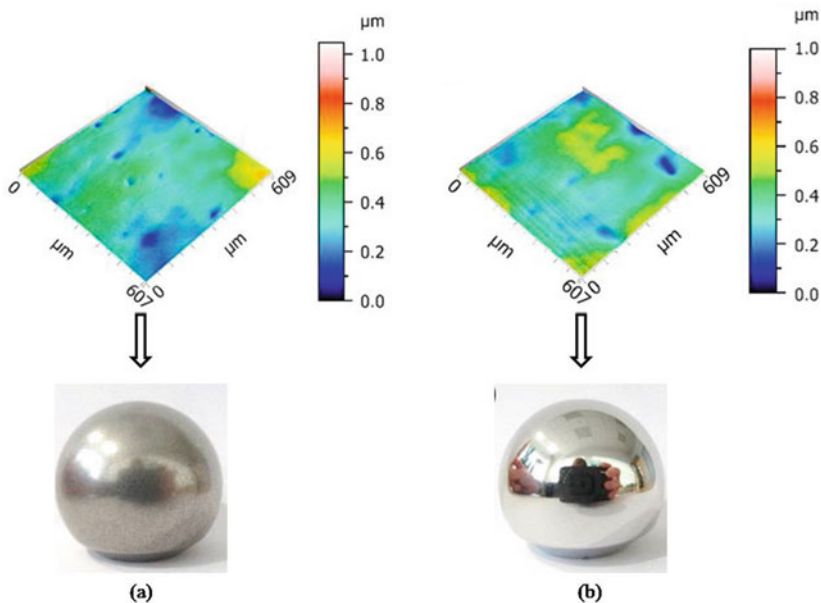


Fig. 3 Surface topography and actual photograph of femoral heads for hip endoprosthesis after **a** drag grinding and **b** electro-chemical polishing [34] (with permission, Copyright Elsevier)

consisted of a mixer of phosphoric acid, water, and glycerol. Results showed that the material removal rate increases with an increase in water concentration and current density.

3.6 Chemo-Mechanical Magnetorheological Finishing (CMMRF)

CMMRF shown in Fig. 1g is a chemo-mechanical finishing process which works on the combination of chemical erosion and magnetorheological-based mechanical abrasion [36]. This process is used to produce a surface roughness (R_a) in the range of 0.5 nm [37]. It consists of a cylindrical permanent magnet, which is fixed vertically to the spindle of CNC milling. CMMRF tool is reciprocated and rotated as per the feed given by the CNC milling. The workpiece is fixed on the machine table through a precision vice. The working gap between tool and workpiece is set by providing a reciprocating motion to the tool. MR polishing fluid is inserted between the working gap. Under the influence of magnetic field, iron particles present in the MR polishing fluid adhere to the magnet surface, form chains, and grip the abrasive particles. These active abrasive particles are responsible for precise surface finishing of workpiece materials [38].

Liang et al. [39] worked on CMMRF with different polishing slurry pads for enhancing the surface quality of single-crystal SiC, which is mainly used in semiconductor and biomedical components. They obtained a minimum surface roughness (R_a) of 0.60 nm with S5 slurry (mixture of abrasive particles, iron particles, glycerin, and deionized water), having magnetic pole rotation of 60 rpm and workpiece rotation of 350 rpm. Ranjan et al. [40] performed experiments on stainless steel workpiece, using MR polishing fluid as a mixture of silica abrasive, iron particles, glycerol, and deionized water. The surface roughness (S_q) was reduced up to 1.07 nm from an initial roughness of 375 nm with process parameters: tool rotation of 300 rpm, workpiece feed of 10 mm/min, working gap of 0.8 mm, and finishing time of 2.45 h.

3.7 Magnetorheological Abrasive Flow Finishing (MRAFF)

MRAFF process is developed for enhancing the performance of abrasive flow finishing (AFF) [41]. This process is suitable for finishing freeform and intricate internal surfaces made up of non-ferromagnetic materials such as brass, stainless steel, and copper. In MRAFF, the abrading forces can be controlled by varying the magnetizing current in electromagnets. The schematic of MRAFF for finishing of a freeform surface is shown in Fig. 1h. It consists of two pistons placed opposite to each other inside a vertical cylindrical frame. MR polishing fluid and workpiece are

inserted inside the cylindrical frame. Electromagnets are placed outside the cylindrical frame to activate the MR polishing fluid [42]. When the electromagnet is powered ON, the MR polishing fluid becomes stiffer and forms chains inside the cylindrical frame. The moving pistons provide the reciprocating motion to the MR polishing fluid. The active abrasive particles reciprocate over the workpiece surface because of the workpiece's non-ferromagnetic nature [41]. The continuous movement of abrasive particles removes the roughness peaks from the workpiece surface. The main advantage of MRAFF is that it can uniformly finish the inaccessible areas of any freeform surface, which is either impossible or very difficult with other competitive processes. Jha and Jain [41] developed MRAFF for precise finishing of freeform surfaces. They performed experiments on stainless steel workpiece with 200 finishing cycles using a mixer of SiC abrasives, iron particles, grease, and heavy paraffin oil as MR polishing fluid. They found that the percentage change in surface roughness (R_a) increases with the increase in magnetic flux density as shown in Fig. 4.

Jha and Jain [42] studied the effect of MR polishing fluid with different iron particles (CS and HS grades) on the final surface roughness (R_a). It was observed that the CS grade iron particles lead to a better surface finish in comparison with HS grade iron particles when finishing is carried out for 200 cycles with a magnetic flux density of 0.531 T. Results showed that a surface roughness (R_a) of 170 nm and 240 nm could be obtained with CS and HS grade iron particles, respectively, while processing on stainless steel workpiece with initial roughness of 280 nm. Das et al.

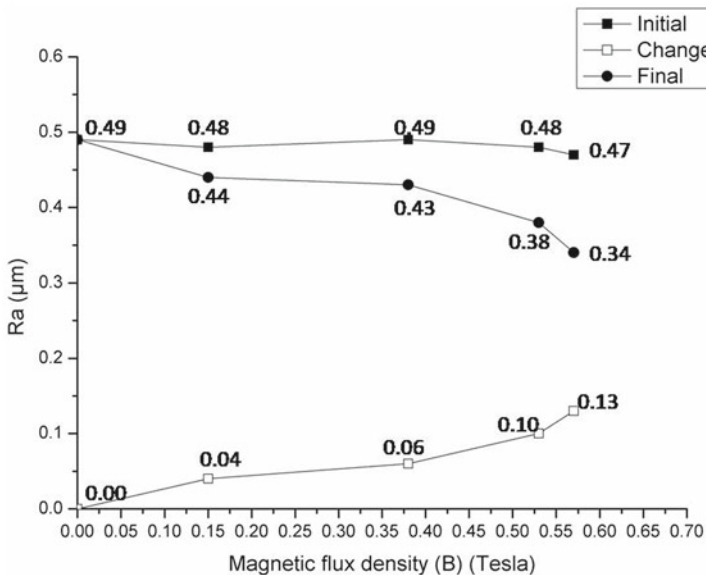


Fig. 4 Plot between magnetic flux density and surface roughness (R_a) [41] (Redrawn, with permission, Copyright Elsevier)

[43] developed a theoretical model to determine the effect of magnetizing current and number of finishing cycles on final surface roughness.

MRAFF is modified slightly to increase the shearing tendency of abrasive particles and is named rotational–magnetorheological abrasive flow finishing (R-MRAFF) [44]. In R-MRAFF process, the arrangement is made to revolve the electromagnet, which is placed outside the cylindrical frame. During finishing, the reciprocating piston moves the MR polishing fluid in a vertical direction, whereas the revolving electromagnet provides rotational motion to the MR polishing fluid. Magnetized MR polishing fluid forms a chain structure along the direction of magnetic field. These iron particles chain structures finally grip and push the non-magnetic abrasive particles toward the workpiece surface. Under this effect, the shearing tendency of abrasive particles increases to perform a uniform nanofinishing on the workpiece surface.

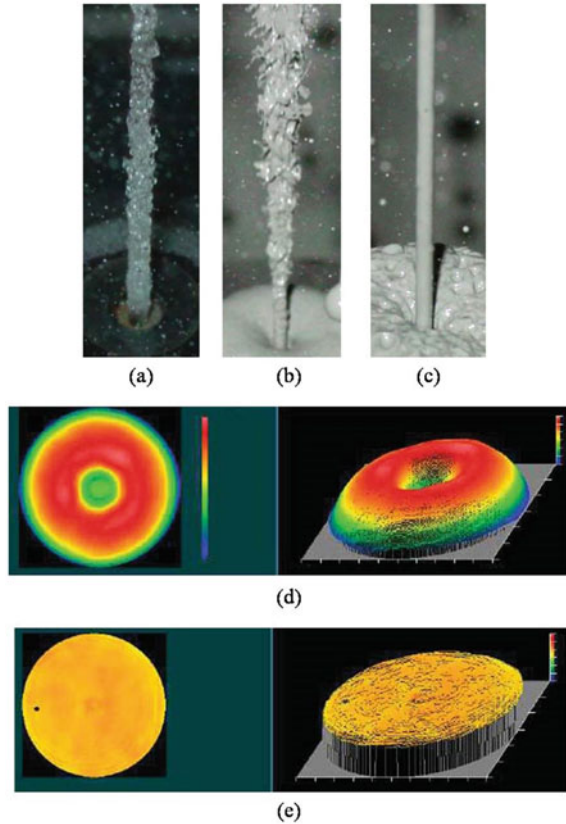
Das et al. [45] compared MRAFF and R-MRAFF processes to finish a stainless steel workpiece. It was observed that the surface roughness (R_a) can be reduced to 200 nm and 110 nm from an initial surface roughness of 260 nm with MRAFF and R-MRAFF process, respectively, when processed with the number of finishing cycles of 660, extrusion pressure of 38.92 bar, and magnet speed of 67 rpm.

Nagdeve et al. [46] worked on R-MRAFF for nanofinishing of knee joint made up of Co–Cr–Mo alloy. They developed an inverse replica fixture for holding the knee joint during the finishing process. A mixer of B_4C abrasives, iron particles, and base fluid was used as an MR polishing fluid. Results showed that the surface roughness (R_a) was reduced to 78 nm from an initial value of 172 nm and 89 nm from an initial value of 178 nm in X -direction and Y -direction, respectively, after overall finishing for 10.35 h. Nagdeve et al. [47] developed a negative replica fixture for holding the knee joint made of stainless steel. The knee joint was completely inserted inside the fixture and provided with some working gap for the movement of MR polishing fluid. The fixture was placed inside R-MRAFF setup for finishing. They were able to reduce the surface finish up to 26 nm using the developed fixture. Later, they optimized the input parameters to finish the Co–Cr–Mo alloy knee joint with R-MRAFF process [48]. Using optimum parameters, they could obtain the surface roughness (R_a) of 50 nm from an initial roughness of 190.5 nm within 2 h of finishing time.

3.8 Magnetorheological Jet Finishing (MRJF)

MRJF process shown in Fig. 1i is developed for nanofinishing of freeform, conformal, and steep concave surfaces used in mold and die, optics, or biomedical industries [49]. It consists of MR shaper and electromagnets, which are fixed vertically on the CNC machine table. The workpiece is mounted on the machine spindle through a specially made fixture. The spindle rotates and reciprocates as per the feed given to the CNC machine. The reciprocating motion of the spindle controls the stand-off distance between MR shaper and workpiece. When the magnetic field is turned OFF, MR polishing fluid coming out from the shaper behaves like liquid paste, as

Fig. 5 **a** Water coming out from MR shaper, **b** MR polishing fluid coming out from MR shaper behaves like liquid paste when the magnetic field is turned OFF, **c** MR polishing fluid coming out from MR shaper becomes stiffer and forms a thick paste when the magnetic field is turned ON, **d** initial surface error on the workpiece surface, and **e** final finished surface with processed with MRJF [49] (with permission, Copyright Elsevier)



shown in Fig. 5b, while in the presence of a magnetic field, it becomes stiffer and forms like a thick paste, as shown in Fig. 5c. During finishing, MR polishing fluid strikes the workpiece surface at very high velocity, and the material is removed by abrasion action [50]. Kordonski et al. [50] developed MRJF process to finish concave-shaped fused glass silica. The workpiece was inserted inside the specially designed concave fixture. MR polishing fluid was sprayed onto the workpiece surface with a jet velocity of 18.6 m/min and stand-off distance of 50 mm. The surface roughness (R_q) was reduced to 0.65 nm from an initial value of 470 nm. Tricard et al. [49] worked on dome-shaped glass specimens used in optics and biomedical industries. Experiments were conducted with a jet velocity of 20 m/s, and a jet hole of 2.4 mm and the surface roughness (R_q) was reduced to 6 nm from an initial value of 73.4 nm, as shown in Fig. 5d, e.

3.9 Ball End Magnetorheological Finishing (BEMRF)

BEMRF process is developed for fine finishing of 3D complex surfaces made up of ferromagnetic and non-ferromagnetic materials. This process finds applications in tooling, molds and dies, optics, and biomedical industries [51]. This process, as shown in Fig. 1j, consists of a C-shaped bracket on which a tool is mounted. BEMRF tool consists of a hollow cylindrical core, electromagnetic coils, and a cooling chamber. Electromagnet coils are wound around the hollow cylindrical core using an aluminum bobbin. A cooling arrangement is provided to avoid overheating of these electromagnetic coils [52]. MR polishing fluid continuously flows inside the hollow cylindrical core by means of a peristaltic pump. In the presence of a magnetic field, MR polishing fluid becomes stiffer at the ball end of the hollow cylindrical core [53]. The workpiece is mounted on the X - Y axis linear slides through a precision vice. Magnetically active MR polishing fluid is rotated onto the workpiece surface by means of a servo motor. The material is removed in the form of microchips by abrasion action, and a fine surface finishing is achieved. Singh et al. [54] worked on BEMRF for nanofinishing of 3D complex surfaces using a mixer of SiC abrasives, iron powder, heavy paraffin oil, and grease as MR polishing fluid. Finite element analysis results on the distribution of magnetic flux for finishing of 30° inclined surface is shown in Fig. 6a, b. The experimental setup of finishing 30° inclined surface by stiffened MR polishing fluid is shown in Fig. 6c. Results showed that the surface roughness (R_a) reduces significantly under process condition: magnetizing current of 4 A, core rotational speed of 500 rpm, and finishing time of 2 h, as shown in Fig. 6d.

Kumar and Singh [55] used a solid rotating core-based BEMRF tool for precise finishing of BK7 glass, which is commonly used in optics and biomedical industries. MR polishing fluid consisted of CeO_2 abrasives, iron particles, and deionized water during the finishing operation. The surface roughness (R_a) was reduced to 17 nm from 41 nm with a core rotational speed of 300 rpm, magnetizing current of 1 A, and finishing time of 90 min. Kumar et al. [56] worked on BEMRF tool for nanofinishing of polylactic acid (PLA) material, which is biocompatible for making medical implants and optimized the % vol. of Al_2O_3 abrasives and iron particles in MR polishing fluid. The optimum value was found as 16.7% vol. of abrasives, 25% vol. of iron particles, and 58.83% of distilled water.

3.10 Ultrasonic Polishing (UP)

Ultrasonic polishing is a material removal process used for both metallic and non-metallic materials [57]. The schematic of ultrasonic finishing process is shown in Fig. 1k. In ultrasonic finishing, a high-frequency (greater than 15 kHz) electrical power is converted into mechanical vibrations using a transducer, which are then transmitted to the tool through a horn (i.e., an energy focusing device). The horn vibrates the tool along its longitudinal axis. The abrasive slurry (a mixture of abrasive

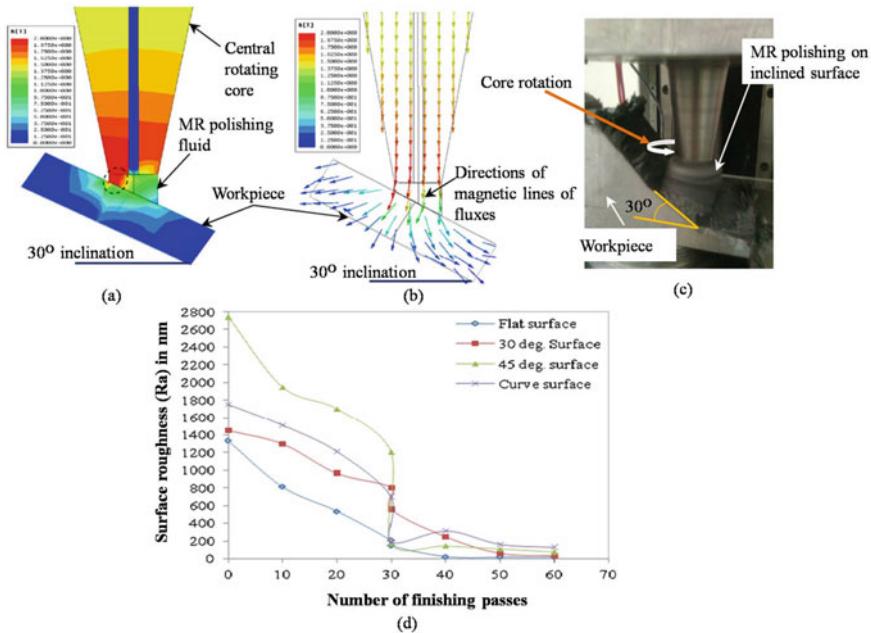


Fig. 6 **a** Finite element analysis for distribution of magnetic flux density in a working gap of 30° inclined surface, **b** representation of flow of magnetic lines of forces in a working gap of 30° inclined surface, **c** photograph of finishing the 30° inclined surface of typical 3D workpiece by stiffened MR polishing fluid, and **d** effect of number of finishing passes on surface roughness value of the 3D workpiece [54] (with permission, Copyright Elsevier)

particles and carrier media like water or oil) is continuously supplied in the working gap between the tool and workpiece surfaces. The tool vibration causes the abrasive particles to hit on the workpiece surface at a very high speed. Thus, the material is removed by abrasive particles with a combination of microcutting and brittle fracture [58]. Researchers have developed hybrid processes using ultrasonic vibrations in conjunction with other finishing processes.

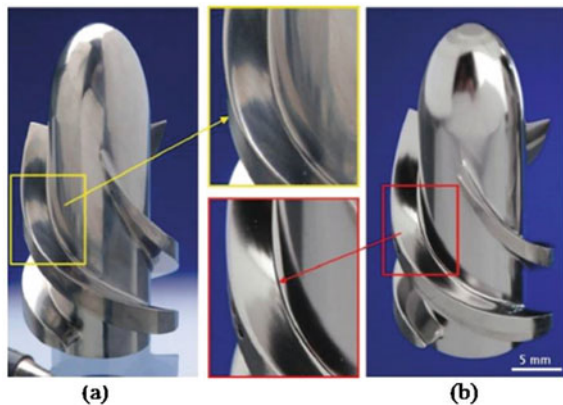
Choi et al. [59] worked on ultrasonic vibration-assisted grinding and compared the grinding forces for finishing of three different biocompatible materials, i.e., Ti-6Al-4V, FCD700, and S45C. It was observed that the grinding forces were reduced with an increase in the ultrasonic vibration frequency and feed rate. Zheng et al. [60] worked on ultrasonic vibration-assisted grinding of sintered zirconia ceramics, popularly used in the dental applications. They found that the friction coefficient and wear rate decreased with the application of ultrasonic vibrations compared to the diamond grinding.

3.11 Laser Polishing (LP)

Laser polishing is a new and emerging technique to smoothen the workpiece surface using high-intensity laser beam. A short pulse laser is used to get lower roughness while a continuous beam leads to a higher surface roughness but higher polishing speed [61]. The schematic of laser polishing is shown in Fig. 11. Laser beam with controlled parameters is irradiated on the workpiece surface. The material is smoothened mainly by melting and distributing the molten material in the surroundings region, without removing any material from the workpiece surface [62, 63]. In some cases, the roughness peaks are removed by local ablation of the material using a high power density laser beam. However, it is not preferred due to low process efficiency and slow processing of the workpiece. The inert shield gas is used to prevent contamination of the molten pool. Advantages of laser polishing include complete automation, high processing speed, good repeatability, shape retention ability, non-contact processing, and ability to process any surface orientation of the workpiece. The important controlling parameters are the laser power density, beam wavelength, pulse duration, angle of incidence, scanning speed and workpiece material, and surface properties.

Perry et al. [64] worked on laser polishing for enhancing the surface quality of Ti-6Al-4V alloy workpiece, which is widely used in biomedical implants. The authors performed experiments on a square-shaped Ti-6Al-4V workpiece using Nd:YAG laser and reduced the surface roughness (R_a) to 70 nm from initial value of 206 nm. Temmler et al. [65] improved surface quality of outlet flow guide vane of left ventricular assist device made up of Ti-6Al-4V using laser polishing process, as shown in Fig. 7. Giorgi et al. [62] used laser for micropolishing of stainless steel and found that the surface roughness and waviness can be reduced up to 50% which enhances antibacterial properties of the workpiece surface.

Fig. 7 Photograph of outlet flow guide vane of left ventricular assist device having **a** manually prepolished surface and **b** laser polished surface [65] (with permission, Copyright John Wiley and Sons)



Various finishing processes suitable for improving the surface quality of biomedical implants are discussed in this chapter. Table 1 presents a comparative evaluation of various finishing processes in terms of processing cost, material removal rate (MRR), and limitation of the process.

Table 1 Comparative evaluation of various finishing processes

Finishing technique	Surface roughness (R_a)	Processing cost	Material removal rate (MRR)	Limitations
Grinding/lapping	<450 nm	Low	High	<ul style="list-style-type: none"> • Tool is not flexible • Lesser control over the finishing forces • Produces various surface defects such as cavities, deeper scratches, etc.
Abrasive flow finishing (AFF)	<200 nm	Moderate	Slow	<ul style="list-style-type: none"> • Higher initial cost • Limited variety of work material can be finished • Not suitable for finishing of hollow cavities in complex shaped workpiece
Abrasive jet-based finishing (AJBF)	>1 μ m	Low	High	<ul style="list-style-type: none"> • Not suitable for producing a uniform surface finishing
Magnetorheological fluid-based finishing (MRFF)	20–37.4 nm	Moderate	Slow	<ul style="list-style-type: none"> • Not suitable for finishing the inaccessible areas of complex shaped workpiece
Chemical polishing (CP)	<400 nm	Low	Moderate	<ul style="list-style-type: none"> • Larger surface defects cannot be removed • Not suitable for uniform surface polishing • Not suitable for chemically inert materials

(continued)

Table 1 (continued)

Finishing technique	Surface roughness (R_a)	Processing cost	Material removal rate (MRR)	Limitations
Electrolysis-based polishing (EBP)	200–300 nm	Low	Moderate	<ul style="list-style-type: none"> • Not suitable for attaining a better surface polishing • Cannot remove the rough surface defects • Not suitable for all metals and alloys
Chemo-mechanical magnetorheological abrasive flow finishing (CMMRF)	<10 nm	Moderate	More	<ul style="list-style-type: none"> • High initial cost • Less effective for ferromagnetic materials
Magnetorheological abrasive flow finishing (MRAFF)	50–175 nm	Moderate	Slow	<ul style="list-style-type: none"> • The surface defects such as deeper grooves and higher cavities cannot be easily removed • Needs a specially designed fixture to hold the complex shaped workpiece • Only suitable for non-ferromagnetic workpiece
Magnetorheological jet finishing (MRJF)	<50 nm	Moderate	Slow	<ul style="list-style-type: none"> • Requires a continuous flow of polishing fluid onto the workpiece during the finishing operation. This may result in wastage of MR polishing fluid
Ball end magnetorheological finishing (BEMRF)	17–80 nm	Moderate	Slow	<ul style="list-style-type: none"> • Better suited for spot finishing • Tool is not suitable to finish the inaccessible areas of complex surfaces

(continued)

Table 1 (continued)

Finishing technique	Surface roughness (R_a)	Processing cost	Material removal rate (MRR)	Limitations
Ultrasonic polishing (UP)	>500 nm	Moderate	Slow	<ul style="list-style-type: none"> • Cannot remove the rough surface defects • Less suitable to finish the complex geometry and ductile materials
Laser polishing (LP)	<150 nm	High	Moderate	<ul style="list-style-type: none"> • High initial cost • Under atmospheric conditions, the oxidation of work material takes place • Material properties changes under high temperature conditions • Not suitable for transparent and reflective materials

4 Conclusions

Biomedical industries are growing very fast because of the tremendous increase in demand for implants across the globe. However, customer requirements are also increasing, and it is becoming difficult to meet the customers' satisfaction level because of the need for a super-finished surface, customized design, and usage of advanced materials. This is the reason, the industries are trying to reform; especially, they are upgrading their manufacturing units. Modern manufacturing systems are able to meet the customer's requirements and increase the functionality and operational life of the products. This chapter has presented a recent development in the finishing processes which are useful for biomedical applications. The important processes discussed include abrasive flow polishing, abrasive jet polishing, magnetorheological polishing, chemical polishing, electrolysis-based polishing, ultrasonic polishing, laser polishing, and hybrid polishing processes. These processes are suitable for nanofinishing of biomedical implants. These processes are compared and their advantages, applications, and limitations are discussed in detail. Uniform nanofinishing of complex surfaces used in biomedical implants is still a challenging task, and the biomedical industries are struggling to overcome many challenging for

example poor efficiency, low productivity, high production cost, no suitable process for all kind of materials and shapes, distortion in desired surface properties, and poor repeatability. Many researchers across the globe are working hard on various aspects including development of materials, processes, and technologies to address these issues. Modeling these processes is difficult and researchers are working hard to develop new models that are very accurate for wide range of process parameters. Modeling and optimization are essential to meet future needs for machine learning, artificial intelligence, and Industry 4.0. The research trends show that this area is going to grow at a fast rate.

References

1. Bedi, T.S., Singh, A.K.: Magnetorheological methods for nanofinishing—a review. *Part. Sci. Technol.* **34**(4), 412–422 (2016)
2. Jain, V.K.: Abrasive-based nano-finishing techniques: an overview. *Mach. Sci. Technol.* **12**, 257–294 (2008)
3. Jain, V.K.: Magnetic field assisted abrasive based micro-/nanofinishing. *J. Mater. Process. Technol.* **209**, 6022–6038 (2009)
4. Jain, V.K., Kumar, V., Sankar, M.R.: Experimental study and empirical modeling of magnetic abrasive finishing on ferromagnetic and non-ferromagnetic materials. *Int. J. Precis. Technol.* **3**(1), 91–104 (2012)
5. Zhong, Z.W.: Recent advances in polishing of advanced materials. *Mater. Manuf. Processes* **23**(5), 449–456 (2008)
6. Sankar, M.R., Jain, V.K., Ramkumar, J.: Abrasive flow machining (AFM): an overview. Indo-US workshop on smart machine tools, intelligent machining systems and multi-scale manufacturing, December (2008)
7. Goldsmith, A.A.J., Dowson, D., Issac, G.H., Lancaster, J.G.: A comparative joint simulator study of the wear of metal-on-metal and alternative material combinations in hip replacements. *Proc. Inst. Mech. Eng. Part H: J. Eng. Med.* **214**(1), 39–47 (2000)
8. Hosseinzadeh, H.R.S., Eajazi, A., Shahi, A.S.: The bearing surfaces in total hip arthroplasty-options, material characteristics and selection. *Recent Adv. Arthroplasty.* <https://doi.org/10.5772/26362> (2012)
9. ASTM standard: F 2083-11 standard specifications for total knee prosthesis, pp. 1–9. <https://doi.org/10.1520/F2083-11.2>
10. Dalury, D.F., Pomeroy, D.L., Gorab, R.S., Adams, M.J.: Why are total knee arthroplasties being revised? *J. Arthroplast* **28**, 120–121 (2013)
11. Blunt, L., Charlton, P., Beaucamp, A., Jiang, X.: The application of optics polishing to free form knee implants. In: *Proceedings of the 6th Euspen International Conference*, pp. 1–4, Baden, Austria (2006)
12. Brecher, C., Tuecks, R., Zunke, R., Wenzel, C.: Development of a force controlled orbital polishing head for free form surface finishing. *Prod. Eng. Res. Devel.* **4**, 269–277 (2010)
13. Cheung, C.F., Ho, L.T., Charlton, P., Kong, L.B., To, S., Lee, W.B.: Analysis of surface generation in the ultra precision polishing of freeform surfaces. *Proc. Inst. Mech. Eng. Part B: J. Eng. Manuf.* **224**, 59–73 (2010)
14. Loveless, T.R., Williams, R.E., Rajurkar, K.P.: A study of the effects of abrasive-flow finishing on various machined surfaces. *J. Mater. Process. Technol.* **47**, 133–151 (1994)
15. Tzeng, H.J., Van, B.H., Hsu, R.T., Lin, Y.C.: Self-modulating abrasive medium and its application to abrasive flow machining for finishing micro channel surfaces. *Int. J. Adv. Manuf. Technol.* **32**(11–12), 1163–1169 (2007)

16. Rhoades, L.J., Kohut, T.A., Nokovich, N.P.: Unidirectional abrasive flow machining, Patent number 5367833 (1994)
17. Li, J., Liu, W., Yang, L., Tian, C., Zhang, S.: A method of motion control about micro-hole abrasive flow machining based on Delphi language. In: Proceeding of the International Conference on Mechatronics and Automation, pp. 9–12, Changchun, China (2009)
18. Walia, R.S., Shan, H.S., Kumar, P.: Parametric optimization of centrifugal force-assisted abrasive flow machining (CFAAFM) by the Taguchi method. *Mater. Manuf. Processes* **21**, 375–382 (2006)
19. Sarkar, M., Jain, V.K.: Nanofinishing of freeform surfaces using abrasive flow finishing process. *Proc. Inst. Mech. Eng. Part B: J. Eng. Manuf.* **231**(9), 1501–1515 (2015)
20. Subramanian, K.T., Balashanmugam, N., Kumar, P.V.S.: Nanometric finishing on biomedical implants by abrasive flow finishing. *J. Inst. Eng. (India): Ser. C* **97**, 55–61 (2016)
21. Singh, S., Sankar, M.R., Jain, V.K.: Simulation and experimental investigations into abrasive flow nanofinishing of surgical steel tubes. *Mach. Sci. Technol.* **22**(3), 454–475 (2018)
22. Singh, S., Sankar, M.R.: Development of polymer abrasive medium for nanofinishing of micro-holes on surgical stainless steel using abrasive flow machining process. *Proc. Inst. Mech. Eng. Part B: J. Eng. Manuf.* **234**(3), 355–370 (2019)
23. Folkes, J.: Waterjet-an innovative tool for manufacturing. *J. Mater. Process. Technol.* **209**, 6181–6189 (2009)
24. Kovacevic, R., Hashish, M., Mohan, R., Ramulu, M., Kim, T.J., Geskin, E.S.: State of the art of research and development in abrasive water jet machining. *J. Manuf. Sci. Eng.* **119**, 776–785 (1997)
25. Seo, Y.W., Ramulu, M., Kim, D.: Machinability of titanium alloy (Ti-6Al-4V) by abrasive waterjets. *Proc. Inst. Mech. Eng. Part B: J. Eng. Manuf.* **217**(12), 1709–1721 (2003)
26. Shiou, F.J., Loc, P.H., Dang, N.H.: Surface finish of bulk metallic glass using sequential abrasive jet polishing and annealing processes. *Int. J. Adv. Manuf. Technol.* **66**, 1523–1533 (2013)
27. Sidpara, A., Jain, V.K.: Nanofinishing of freeform surfaces of prosthetic knee joint implant. *Proc. Inst. Mech. Eng. Part B: J. Eng. Manuf.* **226**(11), 1833–1846 (2012)
28. Sidpara, A., Jain, V.K.: Analysis of forces on the freeform surface in magnetorheological fluid based finishing process. *Int. J. Mach. Tools Manuf.* **69**, 1–10 (2013)
29. Barman, A., Das, M.: Magnetic field assisted finishing process for super-finished Ti alloy implant and its 3D surface characterization. *J. Micromanuf.* **1**(2), 154–169 (2018)
30. Bazuidenhout, M., Haar, G.T., Becker, T., Rudolph, S., Damm, O., Sacks, N.: The effect of HF-HNO₃ chemical polishing on the surface roughness and fatigue life of laser powder bed fusion produced Ti6Al4V. *Mater. Today Commun.* **25**, 101396 (2020)
31. Balyakin, A., Goncharov, E., Zhechenko, E.: The effect of preprocessor on surface quality in the chemical polishing of parts from titanium alloy produced by SLM. *Mater. Today Proc.* **19**(5), 2291–2294 (2019)
32. Asgari, V., Noormohammadi, M., Ramazani, A., Almasikashi, M.: A new approach to electro-polishing of pure Ti foil in acidic solution at room temperature for the formation of ordered and rod TiO₂ nanotube arrays. *Corros. Sci.* **136**, 38–46 (2018)
33. Wexell, C.L., Shah, F.A., Ericson, L., Matic, A., Palmquist, A., Thomsen, P.: Electro-polished titanium implants with a mirror-like surface support osseointegration and bone remodeling. *Adv. Mater. Sci. Eng.* **1750105**, 1–10 (2016)
34. Dobberthina, C., Mullera, R., Meichsnera, G., Welzela, F., Oschatzchena, M.H.: Experimental analysis of the shape accuracy in electro-chemical polishing of femoral heads for hip endoprosthesis. *Proc. Manuf.* **47**, 719–724 (2020)
35. Han, W., Fang, F.: Two step electro polishing of 316L stainless steel in a sulfuric acid-free electrolyte. *J. Mater. Process. Technol.* **279**, 116558 (2020)
36. Ghai, V., Ranjan, P., Batish, A., Singh, H.: Atomic-level finishing of aluminium alloy by chemo-mechanical magnetorheological finishing (CMMRF) for optical applications. *J. Manuf. Process.* **32**, 635–643 (2018)
37. Wanga, H., Songa, Z., Konga, W.L.H.: Effect of hydrogen peroxide concentration on surface micro-roughness of silicon wafer after final polishing. *Microelectron. Eng.* **88**(6), 1010–1015 (2011)

38. Ranjan, P., Balasubramaniam, R., Suri, V.K.: Modelling and simulation of chemo-mechanical magnetorheological finishing (CMMRF) process. *Int. J. Precis. Technol.* **4**(3/4), 230–246 (2014)
39. Liang, H., Lu, J., Pan, J., Yan, Q.: Material removal process of single-crystal SiC in chemical-magnetorheological compound finishing. *Int. J. Adv. Manuf. Technol.* **94**, 2939–2948 (2017)
40. Ranjan, P., Balasubramaniam, R., Suri, V.K.: Investigations into the mechanism of material removal and surface modification at atomic scale on stainless steel using molecular dynamic simulation. *Phil. Mag.* **98**(16), 1437–1469 (2018)
41. Jha, S., Jain, V.K.: Design and development of the magnetorheological abrasive flow finishing (MRAFF) process. *Int. J. Mach. Tools Manuf.* **44**, 1019–1029 (2004)
42. Jha, S., Jain, V.K.: Modeling and simulation of surface roughness in magnetorheological abrasive flow finishing (MRAFF) process. *Wear* **261**, 856–866 (2006)
43. Das, M., Jain, V.K., Ghoshdastidar, P.S.: Analysis of magnetorheological abrasive flow finishing (MRAFF) process. *Int. J. Adv. Manuf. Technol.* **38**, 613–621 (2008)
44. Das, M., Jain, V.K., Ghoshdastidar, P.S.: The out-of-roundness of the internal surfaces of stainless steel tubes finished by the rotational–magnetorheological abrasive flow finishing process. *Mater. Manuf. Processes* **26**(8), 1073–1084 (2011)
45. Das, M., Jain, V.K., Ghoshdastidar, P.S.: Nanofinishing of flat workpiece using rotational-magnetorheological abrasive flow finishing (R-MRAFF) process. *Int. J. Adv. Manuf. Technol.* **62**(1), 405–420 (2012)
46. Nagdeve, L., Jain, V.K., Ramkumar, J.: Preliminary investigations into nano-finishing of freeform surface (femoral) using inverse replica fixture. *Int. J. Adv. Manuf. Technol.* **100**, 1081–1092 (2017)
47. Nagdeve, L., Jain, V.K., Ramkumar, J.: Differential finishing of freeform surfaces (knee joint) using R-MRAFF process and negative replica of workpiece as a fixture. *Mach. Sci. Technol.* **22**(4), 671–695 (2018)
48. Nagdeve, L., Jain, V.K., Ramkumar, J.: Optimization of process parameters in nanofinishing of Co–Cr–Mo alloy knee joint. *Mater. Manuf. Processes* **35**(9), 985–992 (2020)
49. Tricard, M., Kordonski, W.I., Shorey, A.B.: Magnetorheological jet finishing of conformal, freeform and steep concave optics. *CIRP Ann.* **55**(1), 309–312 (2006)
50. Kordonski, W.I., Shorey, A.B., Tricard, M.: Magnetorheological jet finishing technology. *Trans. ASME* **128**, 20–26 (2006)
51. Singh, A.K., Jha, S., Pandey, P.M.: Design and development of nanofinishing process for 3D surfaces using ball end MR finishing tool. *Int. J. Mach. Tools Manuf.* **51**, 142–151 (2011)
52. Singh, A.K., Jha, S., Pandey, P.M.: Mechanism of material removal in ball end magnetorheological finishing process. *Wear* **302**, 1180–1191 (2013)
53. Singh, A.K., Jha, S., Pandey, P.M.: Parametric analysis of an improved ball end magnetorheological finishing process. *Proc. Inst. Mech. Eng. Part B: J. Eng. Manuf.* **226**(9), 1550–1563 (2012)
54. Singh, A.K., Jha, S., Pandey, P.M.: Nanofinishing of a typical 3D ferromagnetic workpiece using a ball end magnetorheological finishing process. *Int. J. Mach. Tools Manuf.* **63**, 21–31 (2012)
55. Kumar, S., Singh, A.K.: Magnetorheological nanofinishing of BK7 used for lens manufacturing. *Mater. Manuf. Processes* **33**(11), 1188–1196 (2018)
56. Kumar, A., Alam, Z., Khan, D.A., Jha, S.: Nanofinishing of FDM-fabricated components using ball end magnetorheological finishing process. *Mater. Manuf. Processes* **34**(2), 232–242 (2018)
57. Weller, E.J.: Non-traditional machining processes. *Society of Manufacturing Engineers* 15–71 (1984)
58. Miller, G.E.: Special theory of ultrasonic machining. *J. Appl. Phys.* **28**(2), 149–156 (1957)
59. Choi, Y.J., Park, K.H., Hong, Y.H., Kim, K.T., Lee, S.W., Choi, H.Z.: Effect of ultrasonic vibration in grinding: horn design and experiment. *Int. J. Precis. Eng. Manuf.* **14**(11), 1873–1879 (2013)
60. Zheng, K., Li, Z., Liao, W., Xiao, X.: Friction and wear performance on ultrasonic vibration assisted grinding dental zirconia ceramics against natural tooth. *J. Braz. Soc. Mech. Sci. Eng.* **39**, 833–843 (2017)

61. Nusser, C., Wehrmann, I., Willenborg, E.: Influence of intensity distribution and pulse duration on laser micro polishing. *Phys. Proc.* **12**, 462–471 (2011)
62. Giorgia, C.D., Furlana, V., Demira, A.G., Tallarita, E., Candianib, G., Previtala, B.: Laser micro polishing of stainless steel for antibacterial surface applications. *Proc. CIRP* **46**, 88–93 (2016)
63. Krishnan, A., Fang, F.: Review on mechanism and process of surface polishing using lasers. *Front. Mech. Eng.* **14**(3), 299–319 (2019)
64. Perry, T.L., Werschmoeller, D., Li, X., Pfefferkorn, F.E., Duffie, N.A.: Pulsed laser polishing of micro-milled Ti6Al4V samples. *J. Manuf. Process.* **11**, 74–81 (2009)
65. Temmler, A., Graichen, K., Donath, J.: Laser polishing of components for left ventricular assist devices. *Laser Mater. Process.* **7**(2), 53–57 (2010)

Chapter 6

Advanced Microchannel Fabrication Technologies for Biomedical Devices



Upasana Sarma , Pranjal Chandra , and Shrikrishna N. Joshi 

1 Introduction

Microchannels are simple and distinct patterns engineered into biomaterials allowing controlled flow or transport of solutes through it. It can handle small volumes of solutes and manipulate micron and submicron size particles flowing through it [1]. As such, microchannels have discovered its widespread application in biomedical devices. It necessitates a minute amount of samples and can run a complete process in a very short time. The microchannel-based lab-on-a-chips such as microfluidic devices [2], electrofluidic devices [3], circuit patterning [4] and microreactors [5] are some of the emerging onsite clinical applications that can be used as a personalized diagnostic device [6]. The microchannel is an indispensable part of such technology. In a biomedical device, the samples' concentration has a direct effect on the chemical reactions and the ability to detect sample molecules such as proteins and DNA. The use of a microchannel enables the concentrating of the samples in one specific area, and hence, it became the key to the success of many biomedical devices [1]. Moreover, microchannel-based biomedical devices have many advantages like reducing human errors, cost-efficient, low volume and higher sensitivity. They are also commonly

U. Sarma · S. N. Joshi (✉)

Department of Mechanical Engineering, Indian Institute of Technology Guwahati, Guwahati
781039, India

e-mail: snj@iitg.ac.in

U. Sarma

e-mail: upasana.sarma@iitg.ac.in

P. Chandra

School of Biochemical Engineering, Indian Institute of Technology (BHU), Varanasi 221005,
India

e-mail: pranjal.bce@iitbhu.ac.in

© The Author(s), under exclusive license to Springer Nature Singapore Pte Ltd. 2022

127

S. N. Joshi and P. Chandra (eds.), *Advanced Micro- and Nano-manufacturing*

Technologies, Materials Horizons: From Nature to Nanomaterials,

https://doi.org/10.1007/978-981-16-3645-5_6

used in delivering the drugs directly into the target cell, so that no healthy cells get harmed [7].

Microchannels can be fabricated by conventional and non-conventional techniques like microwire moulding, lithography, imprinting, laser processing, etc. Correspondingly, microchannels are prepared on a variety of materials like glass [8], metals like stainless steel [9], polymers like polycarbonate (PC) [10], polydimethylsiloxane (PDMS) [11], polymethylmethacrylate (PMMA) [12], etc. Techniques and materials used for the fabrication of microchannels mostly depend on the application of the microchannels. Nevertheless, most of the biomedical devices demand the use of transparent materials with high visibility and optical properties. The glass is one of the most trending materials due to its high transparency over a wide range of wavelength. Also, glass has excellent resistance to chemical reactions, high thermal stability and high hardness. Thus, glass is used for microchannel fabrication. Also, PC's inherent impact strength, dimensional stability, optical clarity and eco-friendly nature make it ideal for the medical device industries. Its dimensional stability makes them valuable for tube connectors. Its ability to transmit light in a large range of wavelength makes it effective in visual monitoring of blood or other biological fluids. PC plate is used in the manufacturing of microfluidic devices that can capture colorectal cancer cells from one of the most common types of human malignant tumours [10]. It is also used in developing urethane (polycarbonate urethane, PCU) that acts as the bearing material in the orthopedic prosthesis, knee prosthesis [13], etc. Such urethane has higher resistance and stability compared to polyester and polyether urethanes. PDMS's distinguished properties make it an essential material for microchannels too. It is optically transparent, electrically and thermally insulating, and impermeable to water and organic solvents [11].

Besides, the channels can be classified in many ways. Mehendale [14] categorized the channels based on the dimension of the channels, for instance, 1–100 μm as microchannels, 100–1 mm as mesochannels, 1–6 mm as compact passages and >6 mm as conventional passages. Further, Kandilkar [15] classified the channels based on the hydraulic diameter of the channels, as shown in Table 1.

Considering the various types of channels and the different materials used for its fabrication, literature reports many techniques for the fabrication of the channels, viz. microwire moulding [16, 17], injection moulding [18], compression moulding [19], imprinting [20], lithography [21–24], micromilling [25], abrasive jet machining

Table 1 Classification of channels based on hydraulic diameter

Type of channel	Hydraulic diameter (D_h)
Conventional channel	$D_h \geq 3 \text{ mm}$
Minichannel	$3 \text{ mm} \geq D_h > 200 \mu\text{m}$
Microchannel	$200 \mu\text{m} \geq D_h > 10 \mu\text{m}$
Transition microchannel	$10 \mu\text{m} \geq D_h > 1 \mu\text{m}$
Transition nanochannel	$1 \mu\text{m} \geq D_h > 0.1 \mu\text{m}$
Molecular nanochannel	$0.1 \mu\text{m} \geq D_h$

[26], chemical etching [27], plasma etching [28], laser-based machining [9], etc. Though the techniques mentioned above can process various materials, they have limited applicability, like photolithography requires high vacuum condition. Chemical etching is hazardous as the etching material contains atoms of lead or sodium, that may result in formation of non-volatile halogen compounds. Abrasive jet machining [3] results in a rough surface and are limited to larger components. Ultra-sonic machining requires complex set-up. Laser processing has, however, proved its capability in fabricating clean and uniform channels and is cost-effective.

In the present study, discussions on the operation principles of some of the microchannel fabrication technologies, their process parameters and process capabilities have been presented. It has been found that laser has certain advantages over the other fabrication technologies and as such, discussion on the laser fabrication technology of microchannel is presented in detail. Moreover, some of the experimental results of microchannel formation and development of a thermally bonded closed microchannel have also been presented. This chapter also signifies the diverse applications of the microchannels.

2 Overview of Various Microchannel Fabrication Technologies

The fabrication technologies of the microchannels have a strong impact on the ability to implant the microchannels into a small-sized biomedical device. Consequently, the different technologies used for microchannel fabrication on a variety of materials and various applications have been studied by many researchers all over the world and the list is ceaseless. They are fabricated by both conventional and non-conventional techniques like micromilling, dry and wet etching, microwire moulding, lithography, injection moulding, electrospinning, imprinting, laser processing, laser-induced plasma-assisted ablation (LIPAA), etc. A graphical representation of the overview of the various technologies used for the fabrication of microchannels on a variety of materials and its applications is given in Fig. 1.

Although there are many techniques being used in the industry, some of them are predominantly being used viz. microwire moulding, lithography, imprinting, direct laser micromachining and laser-induced plasma-assisted ablation (LIPAA). These processes have been discussed in the following sections.

3 Microwire Moulding

Wire moulding is a simple and flexible technique for microchannel fabrication. This technique utilizes the concept of embedding a microwire into a degassed polymer and later, removing the wire after the curing of the polymer. Depending on the strategy of

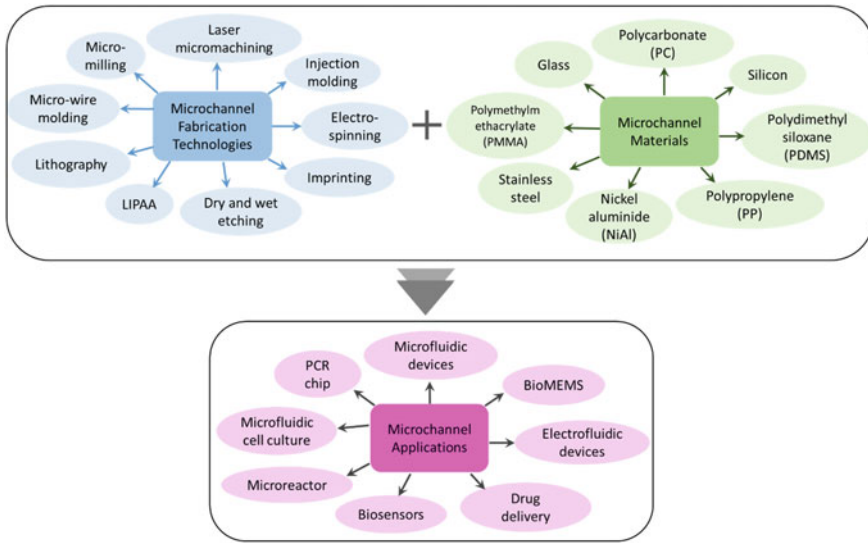
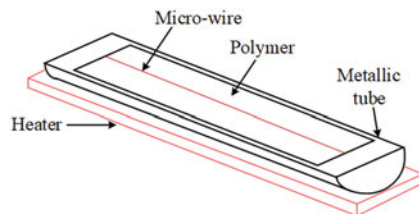


Fig. 1 Graphical representation of the overview of the various technologies used for the fabrication of microchannels on a variety of materials and its applications

the process, the key resources required in this technique are polymers (on which the microchannel is intended to be fabricated), microwires, a mould of metallic tube and a heating source. Here, the mould of metallic tube is taken to be of internal diameter approximately 5 mm. The tube is attached with an electric heater to the bottom of it for heating and temperature control. The temperature is maintained depending on the melting point temperature of the polymer. Wires of varying diameter are used in this method. Wires of any shape are fixed to both the end of the mould. The degassed polymer mixture is poured into the moulding cavity where the wire acts as the axis of the mould. The mould is then closed under hydraulic pressure, and the excess degassed polymer material is removed. The mould is held closed until the polymer is cured. Later, on curing the polymer, the mould is opened and the wire is pulled of the polymer and hence the microchannel is obtained. Figure 2 shows a schematic representation of the wire moulding process.

Fig. 2 Set-up for wire moulding technique using metallic tube and heater



The process of microwire moulding offers various advantages for microchannel fabrication. The flexibility of the microwire used in the process enables generation of microchannels of various cross sections as well as a variety of junctions like Y, T, etc. The moulds can be reused to fabricate hundreds of microchannels which assures the consistency in the shape and size of the microchannels produced. The process moreover has a shorter cycle time for channel fabrication compared to other processes.

But, certain difficulties are also faced while using the process. For complex shaped microchannels, the complexity of the mould design makes the tooling cost expensive. Besides, when the mould is closed under hydraulic pressure, the excess material flows out of the mould and gets wasted. Thus, material wastage is high in this method. Mould maintenance and its cleaning is again a hectic task, thus making the process time-consuming.

Several literatures have reported the use of this wire moulding technique for microchannel fabrication. Effati and Pourabbas [16] explained a quick method for the design and fabrication of 3D microchannel by the technique of microwire moulding. Microchannels on PDMS were fabricated using Nylon and metallic wires of diameter ranging from 150 to 800 μm . The technique provides the possibility to fabricate microchannels with different cross sections. The same technique of wire moulding has also been utilized by Kumar et al. [17] for fabricating microchannels in PDMS casting using copper wire of 0.21 mm diameter. Two different types of inlet sections (L and T types) have been constructed by the technique. YueFei et al. [29] utilized the conventional moulding capability of polydimethylsiloxane (PDMS) for microchannel fabrication by the wire moulding process. It was possible to generate different types of topological structures of the microchannels due to the smooth surface, high-intensity and high flexibility of the wires.

4 Lithography Technology

Lithography is mainly a printing process that is based on the basic idea of the immiscibility of oil or grease with water. It is simple technique and is the most widely used fabrication technique for microchannels. The key steps involved in the process are coating, baking, exposing and development [21]. In most cases, surface conditioning precedes the step of the surface coating. It prepares the substrate surface to accept the photoresist by providing a clean surface. The substrate is then placed on a vacuum chuck and the resist is applied by the method of spin coating. The speed of the chuck determines the thickness of the resist applied. The thickness of the spin coated layer is usually kept equal to the height of the microchannel. Two types of resists are available, namely positive resist and negative resist. In the positive resist, the portion exposed to the light becomes more soluble, while in the negative resist, the portion exposed to the light gets hardened. It is then soft-baked to remove the excess solvents and later cooled to room temperature. The coated substrate is then covered with a mask that has the required pattern on it. Then, it is exposed to a wavelength (light)

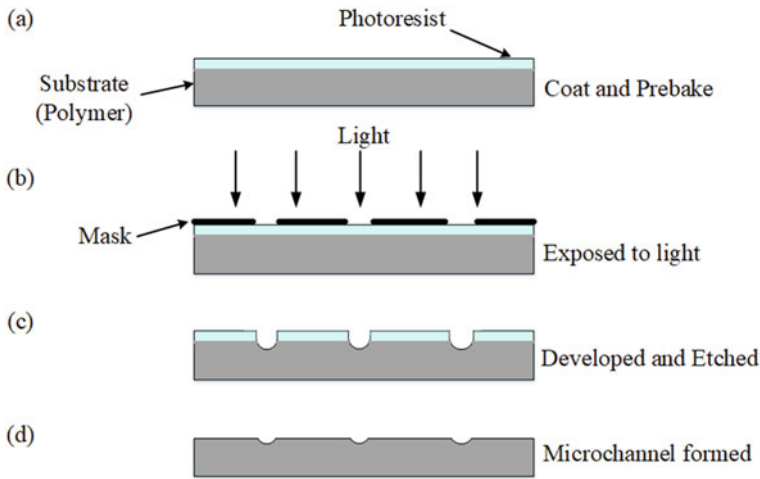


Fig. 3 Stepwise lithographic process involving steps like **a** coating and prebaking the substrate, **b** exposing the substrate to light, **c** etching the substrate in suitable solution and **d** final development of the microchannel

travelling through the mask, that the resist is designed for. In the region exposed, the resist undergoes a chemical reaction with the light. The substrate is then etched in a suitable solution, and thus, the microchannel is finally formed. A simple description of the method is shown in Fig. 3.

The process of lithography however has certain pros and cons depending on its purpose of use. The main advantage of the process is that it can create clear, smooth and sharp microchannels on a variety of materials. Also, channels of any length and three-dimensional microstructures can easily be produced using the process of lithography. It is a cost-effective process when used for fabricating microchannels in large batches.

However, there are certain disadvantages that are faced during the lithography process. It is a slow process when compared to other microchannel fabrication technologies. Further, it does not prove itself to be a cost-effective process when run for small batches and requires skilled personnel to run the process. The process requires a clean environment and its maintenance cost is excessive. Also, distortion of the patterns may result in poor alignment of the microchannels.

Literature reports various applications of the lithography technique for microchannel fabrication. Yao et al. [21] performed the lithography process based on an inconsistent combination of resists and standard lithography facilities. They fabricated microchannels using both one resist layer and multiple resist layers and also demonstrated fluid delivery through the channel. McUsic et al. [30] also reported the use of lithography process for the fabrication of bioinspired pattern microchannel scaffolds. They used patterned silicon master and PDMS negative mould casting. The fabricated channels were used for directing the morphogenesis and differentiating the retinal cells derived from mice and human embryonic stem cells. Also, Laviano

et al. [31] presented the same technique of lithography to produce an inclined array of microchannel. Further, they demonstrated how it could be utilized to produce a precise vortex flow in a well-controlled environment. Wang et al. [32] used two cycles of photolithographic and chemical wet etching for the fabrication of microchannel arrays and also capillary connecting channels on glass substrate. The channels after the completion of the fabrication process were treated with plasma using a plasma cleaner for surface cleaning. They were then bonded with a cover plate by dropping ultrapure water at the edge of the substrates. Thus, channels on different materials and of different dimensions can be made utilizing the lithographic technique.

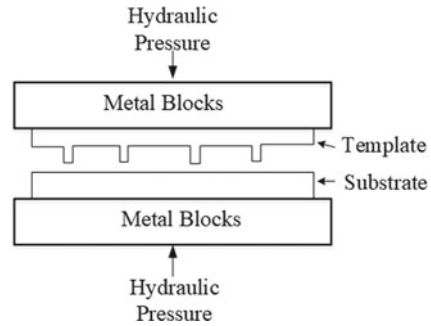
5 Embossing or Imprinting Technology

Embossing or imprinting is a technique of creating different structures like microchannel in polymeric matrices, which are complementary to a template in size and shape. It is a simple and cost-effective process that takes into consideration the versatility of the materials to be imprinted. In this method, a template is first prepared on a silicon substrate mostly by the photolithography method. They are characterized using an optical microscope to determine the effect of the imprinting procedure. The template is then coated with a solution containing biomolecules. It is one of the simplest methods where the template is brought in contact with the plastic or polymer substrate. The plastic or the polymer material is however cleaned and dried before bringing to contact with the silicon template. The whole arrangement of this polymer substrate and the silicon template is then sandwiched between two metallic blocks. The imprinting time depends on the material to be imprinted and also on the temperature and pressure applied between the two metallic blocks. The process when carried out at room temperature, the pressure and time required are high, while performing the process at a high temperature requires less time and pressure. The metallic blocks are subjected to a hydraulic press, varying the pressure between 450 and 2700 psi at room temperature [20]. On releasing the pressure, open microchannels are formed on the substrate. The difference in the dimension of the template before and after the imprinting process is generally less than 1%, which indicates the absence of detrimental effect on the fabricated microchannels. Figure 4 shows the schematic of the imprinting technique.

The technique of embossing or imprinting, however, has certain advantages and disadvantages during the fabrication of microchannels. The technique of embossing or imprinting being an easy and low-cost fabrication process makes it an ideal process for fabrication of microchannels. Moreover, two-sided microchannels can be fabricated utilizing templates on both sides of the polymer. It provides high mechanical stability and also gives a high reproducibility rate.

The technique of embossing or imprinting is however accompanied by certain disadvantages too. In this process, defects in the microchannels may be generated during demoulding and also, the template formation step is a time-consuming procedure. All three parameters, namely time, temperature and pressure, have to be

Fig. 4 Schematic representation of the imprinting technique using metal blocks and hydraulic pressure



kept in firm observations. Difficulties are faced in manufacturing three-dimensional microstructures. And slow mass transport and permanent entrapment of the material into the metal blocks lead to the heterogeneous distribution of material and also inadequate properties.

Researchers have carried out several experiments on fabricating microchannels by the technique of embossing or imprinting. Xu et al. [20] adopted the room-temperature imprinting method for microchannel fabrication on a variety of plastic substrates. They showed that the use of this method improved the device yield from approximately ten devices to above 100 devices per template. Indeed, the number of devices produced by the single template showed a variation of less than even 2%. Zhai et al. [33] presented the fabrication thin glass/PDMS microfluidic coupled with a monolithic capillary column. In the fabrication process, they utilized a copper mould with a microchannel network imprinted on it. Lei and Tong [34] also carried out the technique of imprinting for microchannel fabrication. They, instead of utilizing a conventional mould with microchannel embedded on it as the template, used a stainless steel wire mould of outer diameter 105 μm , making the technique more flexible.

6 Laser Direct Machining

Laser direct machining is a thermal process considering its material removal mechanism. The material removal in this process takes place due to the thermal energy converted from the light energy of a highly coherent beam of photons. When a laser beam irradiates a material, a fraction of the laser energy (light energy) gets absorbed, while the remaining part gets reflected. The absorbed portion of the energy gets converted to heat energy instantaneously and leads to a rise in temperature in the irradiated zone. When the laser energy is sufficiently high enough, it further leads to the melting and vaporization of the material. The vapour thus formed from the vaporization induces a recoil pressure at the surface of the melt pool, which results in melt ejection and hence, lastly the material removal is obtained. Thus, from the above discussion, it is clear that laser has to be used on materials that are capable

of absorbing laser energy. But on the other hand, most microchannels demand the use of transparent materials due to its high visibility. High transparency of the transparent material does not allow laser energy to be absorbed and hence, it is difficult to machine transparent material by a laser. Nevertheless, ultrashort lasers are capable of processing transparent materials as it produces highly localized light field that is absorbed into the transparent material by nonlinear absorption and is sufficient enough to ionize any atom. Similar to ultrashort lasers, short-wavelength lasers also have the ability to process transparent materials. It is due to the low transmissibility of most of the transparent materials at short wavelength.

Laser micromachining has proved itself to be a promising tool in fabricating microchannels. The main advantage of laser micromachining lies in its speed and precision. It is a contactless machining process, thus has no direct impact on the material. Also, complex microstructures can be machined very easily without the use of any solvents or chemicals.

However, certain disadvantages are faced during the process. Only short wavelength and shorter pulse are capable of machining transparent materials. Additionally, equipment is expensive when compared to other fabrication technologies. Also, for operating the laser machine, skilled personnel are needed and the material removal rate of the laser machining process is very low.

Literature reports various works on direct laser machining for microchannel fabrication. The capability of the lasers to provide an efficient and economical way of fabricating microchannels make it the most widely used technique for microchannel fabrication. McCann presented the fabrication of microchannels on cyclic olefin polymer using an industrial 1064 nm Nd: YAG laser [35]. They demonstrated the ability to vary the channel width and channel depth by varying the laser fluence. Prakash and Kumar [12] fabricated rectangular cross-sectional microchannels on PMMA by CO₂ laser. They described how with the application of a mask, microchannels with U-shape cross section and rectangular cross section could be fabricated by a CO₂ laser. In addition to this, they also showed that this technique could provide better control of channel dimensions and also, better surface quality of the microchannels. Wu et al. [36] also tried to overcome the difficulty of fabricating trapezoidal cross-sectional microchannels by CO₂ laser. Multipass translational method was utilized and was observed that the technique was able to produce clean bottom microchannels. Microchannel fabrication on alumina using Nd: YAG laser writing was presented by Mohammed et al. [37]. They selected the best inputs of process parameters for fabricating microchannels by optimization using RSM and Lipschitz sampling. It was found that laser intensity and pulse overlap are the major controlling parameters in microchannel fabrication. Likewise, Singh et al. [38] reported the fabrication of microchannels on transparent polycarbonate (PC) by using nanosecond Nd: YAG laser and further, produced closed channels by the method of thermal bonding. They studied the effect of the laser fluence and the number of laser scans on the channel width, depth and its cross section. It was observed that laser fluence below the ablation threshold resulted in bulging and bubble formation. However, due to the incubation effect, ablation on the polycarbonate material was induced by repeated laser shots.

Though the above-mentioned techniques are capable of machining microchannels on a variety of materials, they have certain limitations too. Microwire moulding, despite being a flexible method, has a higher volume of waste due to the overflow of the degassed polymer from the mould. Also, the mould complexity and its maintenance make it an expensive and time-consuming process, while the disadvantage of using lithography for microchannel fabrication is that the substrate usually absorbs the development solution. Moreover, its requirement of a room preventing UV radiation makes it an expensive process. Limitations in the imprinting technique arise due to the slow mass transport and permanent entrapment of the material into the metal blocks, leading to the heterogeneous distribution of material and also inadequate properties. Laser direct machining has however been found as a promising tool if it is applied with proper setting of laser parameters such as wavelength and laser power. It is known that laser beam must be highly absorbed to achieve ablation. For high absorption, short wavelength (high energy photons) and short pulse width in the subpicosecond range were first attempted, but such laser faced difficulties due to its high capital cost. Also, small beam diameter results in low material removal rate and slow scanning process. For research and other applications, the development of a new fabrication technique of glass was desired, and hence, in 1998 a group of Japanese scientists invented laser-induced plasma-assisted mechanism, which can be used to process transparent materials.

7 Laser-Induced Plasma-Assisted Ablation (LIPAA)

For microchannel fabrication using lasers, it is essential that the laser must be highly absorbed by the material. Materials preferred for fabricating microchannel are mostly transparent materials like glass, polycarbonates, etc., due to its high visibility. High transparency of such material does not absorb the laser energy and as such, it passes through the material leading to no thermal effect on the transparent material. Such materials are absorptive at a very low wavelength and also at shorter pulse. Laser processing of transparent materials with long-pulsed and long-wavelength lasers is thus quite difficult to achieve. But, with the method of laser-induced plasma-assisted ablation (LIPAA), longer pulses and longer wavelength lasers have the potential to process transparent materials. In the LIPAA process, an additional absorbing layer is placed on the rear side of the transparent material. Based on the medium of the absorbing layer, the LIPAA process can be classified into three categories (i) Laser-Induced Backside Wet Etching (LIBWE), (ii) Laser-Induced Backside Dry Etching (LIBDE) and (iii) Laser Etching at a Surfaced-Adsorbed Layer (LESAL) [14]. In LIBWE, a highly absorbing solvent for the used laser wavelength is applied at the rear side of the transparent material. It is characterized by a low etching rate, low surface roughness and incubation effect. In LESAL, a thin absorbing layer is continuously formed on the rear side of the transparent material by adsorbing hydrocarbon products from a gaseous organic medium. It is characterized by a very low etching rate, low surface roughness and incubation effects. And in LIBDE, a thin metal is placed

behind the transparent material. It is characterized by a high etching rate and no incubation effects are found.

LIPAA is a high potential ablation technique where transparent materials are ablated with the aid of plasma formed on the irradiation of the absorbing medium (say metal) by the incoming laser beam. In this method, a transparent material and a metal sheet are arranged one above the other. The transparent substrate is chosen such that it is transparent for the laser beam wavelength. The laser beam passes through the substrate and irradiates the target metal placed behind. The laser fluence for this method is set above the ablation threshold of the target metal and below the ablation threshold of the transparent material. When the peak power density exceeds the ionization threshold potential of the metal surface, the metal surface melts and gets vaporized. The vapour again interacts with the incoming laser beam and results in the ionization of the vapour particles, leading to the formation of dense and optically opaque plasma. The plasma generated flies towards the substrate at a high speed of approximately 10^4 m/s [15]. They further absorb the energy of the incoming laser beam through the laser-plasma interaction process [16]. As a result, the plasma gets expanded and has a greater thermal effect on both the transparent and the substrate metal, thus ablating both. However, the mechanism varies slightly depending upon the distance between the target metal and the glass substrate. Figure 5 describes the mechanism of LIPAA in brief.

As an illustration for the small target to substrate distance, when the laser beam irradiates the target, plasma formed reaches the transparent material on its rear side before the first pulse terminates. This results in a strong interaction between the laser beam, plasma and the transparent material on the rear surface. It thus causes an expansion in the plasma and has greater thermal effect on both the transparent and the substrate metal. For medium distance between target and substrate, plasma generated after the first pulse reaches the transparent material after the termination of the pulse. There is no interaction of plasma with the laser beam during the first pulse. However, target plasma still interacts with the transparent material and forms a thin-film deposition in the rear surface [6]. Thin-film deposition by the preceding laser pulse assists as the absorption site for the upcoming laser pulses which is thought to be dominant mechanism for ablation [39], whereas for large target to substrate distance, no LIPAA effect is observed. As it is carried out in the ambient air, the plasma collides with the air molecules and loses its kinetic energy. Moreover, plasma has a longer flight time. So the plasma does not reach the rear surface of the transparent material and hence no LIPAA effect is produced. The schematic of the experimental set-up of the LIPAA process is shown in Fig. 6.

The LIPAA process has certain advantages over the other fabrication technologies of microchannels. It is because, it can machine transparent materials even at longer wavelengths and with longer pulse width. Moreover, irrespective of the hardness, brittleness and transparency of the material, LIPAA can process any transparent materials. It is a time-saving and an economic microchannel fabrication technique.

Irrespective of the flexibility and user-friendly nature of the process, LIPAA has certain disadvantages. Its primary disadvantage lies in the fact that it can machine only transparent materials. Deposits may be formed on the channel surface from the

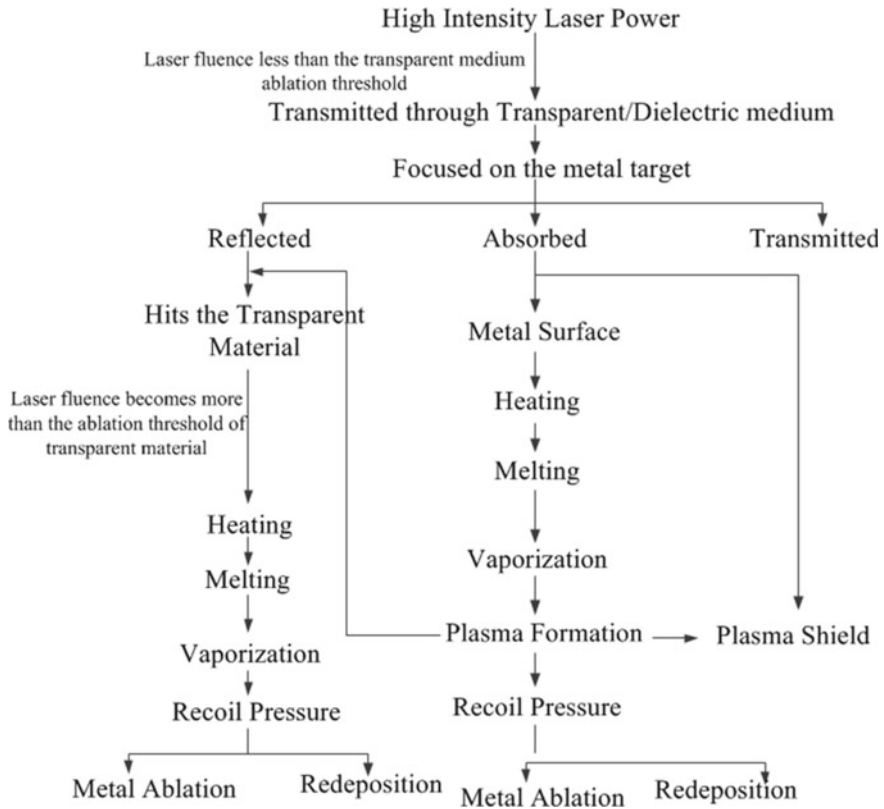


Fig. 5 Mechanism of laser-induced plasma-assisted ablation (LIPAA) concerning the aspect of the reflected and the absorbed beam of laser

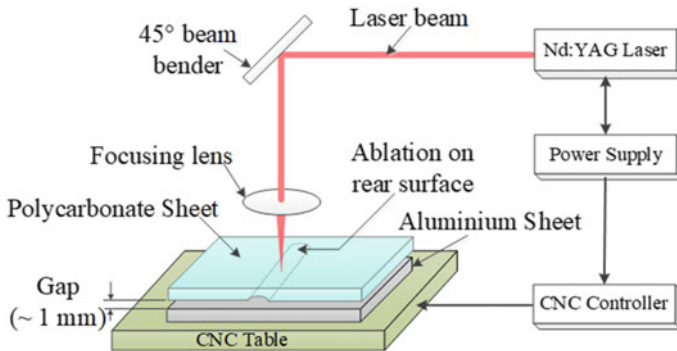


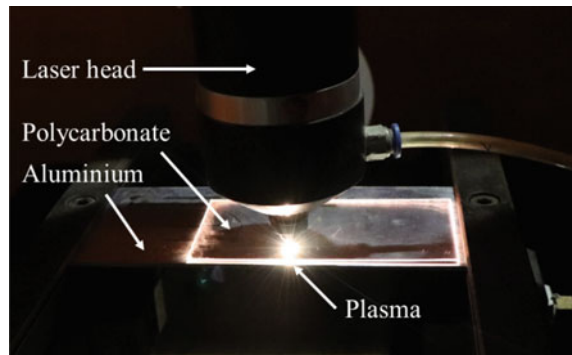
Fig. 6 Schematic representation of the set-up of LIPAA process

metal target sheet used on its rear side. Besides, it requires an additional fixture to maintain the gap between the transparent material and the metal target sheet.

Kim and Park [4] generated circuit patterns on glass by LIBWE for electrosensing devices. They evaluated the circuit patterns by producing a zigzag conductive pattern and then used it to turn on a LED in a simple circuit configuration. Pan et al. [2] proposed the technique of LIPAA to fabricate microchannels with microtexture surface on glass. They further generated a prototype microfluidic device and demonstrated the application of the LIPAA technique for microchannel fabrication. Xu et al. [3] also employed the same technique of LIPAA to fabricate microchannels for microfluidic and electrofluidic devices on glass. They studied the application of the devices as a microheater chip and droplet-based electrofluidic chip, which showed good applicability performance, thus proving the flexibility and feasibility of the LIPAA process. Sarma and Joshi [40] fabricated microchannels on transparent polycarbonate utilizing LIPAA with long pulse duration. They analyzed the presence of any deposits on the channel from the metal substrate and also demonstrated the applicability of the microchannels in a microfluidic device by performing a flow test. Pallav et al. [41] compared the capability of machining during laser direct machining and laser-induced plasma machining. It was discovered that laser-induced plasma process consequences microchannels of depths that are relatively larger than the laser direct ablation process. Similar observations were reported by Bhandari et al. [42]. Malhotra et al. [43] demonstrated the capability and efficiency of laser-induced plasma micromachining in the machining of a wider variety of materials as compared to direct laser ablation.

Microchannel fabrication on transparent polycarbonate (PC) sheet was also carried out in our laboratory using the LIPAA technique. Nd: YAG millisecond pulsed laser was used to generate plasmas on an aluminium substrate which ablates the transparent PC sheet on its rear surface as shown in Fig. 7. The fabricated open channels were then successfully closed by using the thermal bonding technique to make it leak-proof and reduce the uncontrollable spreading of liquids flowing through it. As presented in Fig. 8, the closed channels were then put through a flow test to

Fig. 7 Plasma generation near irradiated zone of aluminium sheet



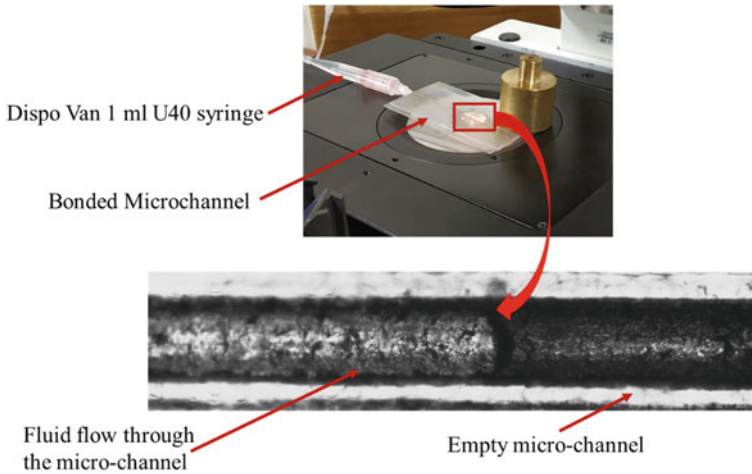


Fig. 8 Flow test of the closed microchannel utilizing a syringe micropump connected to an optical microscope to observe the fluid flow displayed in the computer system attached

check its capability to be used as a microfluidic device and hence, the feasibility of the LIPAA technique was verified.

8 Summary

Microchannels can be fabricated on materials by using various types of fabrication technologies. They allow portability of devices and integrates many processes into a single device called lab-on-a-chip. However, the fabrication of microchannels on different materials and meeting its required precision in dimensions is a challenging task and thus, it requires a significant amount of research. In the present chapter, a study on various technologies for microchannel fabrication has been carried out. From the study, it is observed that microchannels can be fabricated on many materials like glass, metals like stainless steel and polymers like polycarbonate, polydimethylsiloxane, polymethylmethacrylate, etc. Moreover, there are several ways in which the channels can be classified based on their dimensions and the flow conditions. This chapter primarily presents various technologies used for the fabrication of microchannels. A brief discussion on the operation principles of some of the technologies, their process parameters and process capabilities has been presented with respective advantages and disadvantages. It has been found that laser has certain advantages over the other fabrication technologies due to its speed and precision. As such, a comprehensive discussion on the laser fabrication technology of microchannel has been presented in the current chapter. Moreover, some of the experimental results of microchannel formation by the LIPAA process and development of a thermal bonded closed microchannel have also been presented. However, the thermal damage

caused to the materials during laser machining cannot be ignored. Further research is thus necessary to minimize the thermal damage by proper optimization of the laser process parameters.

References

1. Daghighi, Y.: Microfluidic technology and its biomedical applications. *J. Ther. Eng.* **1**(7), 621–626 (2015)
2. Pan, C., Chen, K., Liu, B., Ren, L., Wang, J., Hu, Q., Liang, L., Zhou, J., Jiang, L.: Fabrication of micro-texture channel on glass by laser-induced plasma-assisted ablation and chemical corrosion for microfluidic devices. *J. Mater. Process. Technol.* **240**, 314–323 (2017)
3. Xu, S., Liu, B., Pan, C., Ren, L., Tang, B., Hu, Q., Jiang, L.: Ultrafast fabrication of micro-channels and graphite patterns on glass by nanosecond laser-induced plasma-assisted ablation (LIPAA) for electrofluidic devices. *J. Mater. Process. Technol.* **247**, 204–213 (2017)
4. Kim, H.G., Park, M.S.: Circuit patterning using laser on transparent material. *Surf. Coat. Technol.* **315**, 377–384 (2017)
5. Suryawanshi, P.L., Gumfekar, S.P., Bhanvase, B.A., Sonawane, S.H., Pimplapure, M.S.: A review on microreactors: reactor fabrication, design, and cutting-edge applications. *Chem. Eng. Sci.* **189**, 431–448 (2018)
6. Chandra, P., Segal, E.: *Nanobiosensors for Personalized and Onsite Biomedical Diagnosis*. The Institution of Engineering and Technology (2016)
7. Shirzadfar, H., Khanahmadi, M.: Review on structure, function and applications of microfluidic systems. *Int. J. Biosens. Bioelectron.* **4**(6), 263–265 (2018)
8. Nieto, D., Delgado, T., Flores-Arias, M.T.: Fabrication of microchannels on soda-lime glass substrates with a Nd: YVO4 laser. *Opt. Lasers Eng.* **63**, 11–18 (2014)
9. Singh, S.S., Baruah, P.K., Khare, A., Joshi, S.N.: Effect of laser beam conditioning on fabrication of clean micro-channel on stainless steel 316L using second harmonic of Q-switched Nd: YAG laser. *Opt. Laser Technol.* **99**, 107–117 (2018)
10. Kim, K.R., Kim, H.J., Choi, H.I., Shin, K.S., Cho, S.H., Choi, B.D.: Ultrafast laser micro-fabrication of a trapping device for colorectal cancer cells. *Microelectron. Eng.* **140**, 1–5 (2015)
11. Li, G., Xu, S.: Small diameter microchannel of PDMS and complex three-dimensional microchannel network. *Mater. Des.* **81**, 82–86 (2015)
12. Prakash, S., Kumar, S.: Fabrication of rectangular cross-sectional microchannels on PMMA with a CO₂ laser and underwater fabricated copper mask. *Opt. Laser Technol.* **94**, 180–192 (2017)
13. Kanca, Y., Milner, P., Dini, D., Amis, A.A.: Tribological evaluation of biomedical polycarbonate urethanes against articular cartilage. *J. Mech. Behav. Biomed. Mater.* **82**, 394–402 (2018)
14. Mehendale, S.S., Jacobi, A.M., Shah, R.K.: Fluid flow and heat transfer at micro- and meso-scales with application to heat exchanger design. *ASME. Appl. Mech. Rev.* **53**(7), 175–193 (2000)
15. Kandlikar, S.G., Grande, W.J.: Evolution of microchannel flow passages—thermohydraulic performance and fabrication technology. *Heat Transf. Eng.* **24**(1), 3–17 (2003)
16. Effati, E., Pourabbas, B.: New portable microchannel molding system based on micro-wire molding, droplet formation studies in circular cross-section microchannel. *Mater. Today Commun.* **16**, 119–123 (2018)
17. Kumar, U., Panda, D., Biswas, K.G.: Non-lithographic copper-wire based fabrication of micro-fluidic reactors for biphasic flow applications. *Chem. Eng. J.* **344**, 221–227 (2018)
18. Su, S., Jing, G., Zhang, M., Liu, B., Zhu, X., Wang, B., Fu, M., Zhu, L., Cheng, J., Guo, Y.: One-step bonding and hydrophobic surface modification method for rapid fabrication of polycarbonate-based droplet microfluidic chips. *Sens. Actuators, B Chem.* **282**, 60–68 (2019)

19. Liu, Y., Ganser, D., Schneider, A., Liu, R., Grodzinski, P., Kroutchinina, N.: Microfabricated polycarbonate CE devices for DNA analysis. *Anal. Chem.* **73**(17), 4196–4201 (2001)
20. Xu, J., Locascio, L., Gaitan, M., Lee, C.S.: Room-temperature imprinting method for plastic microchannel fabrication. *Anal. Chem.* **72**(8), 1930–1933 (2000)
21. Yao, P., Schneider, G.J., Prather, D.W.: Three-dimensional lithographical fabrication of microchannels. *J. Microelectromech. Syst.* **14**(4), 799–805 (2005)
22. Hirschbiel, A.F., Geyer, S., Yameen, B., Welle, A., Nikolov, P., Giselsbrecht, S., Scholpp, S., Delaittre, G., Barner-Kowollik, C.: Photolithographic patterning of 3D-formed polycarbonate films for targeted cell guiding. *Adv. Mater.* **27**(16), 2621–2626 (2015)
23. Retolaza, A., Juarros, A., Ramiro, J., Merino, S.: Thermal roll to roll nanoimprint lithography for micropillars fabrication on thermoplastics. *Microelectron. Eng.* **193**, 54–61 (2018)
24. Wu, H.C., Xu, X., He, M., Zhang, M., Ma, K.J., Bao, M.: Fabrication of size-tunable antireflective nanopillar array using hybrid nano-patterning lithography. *Surf. Coat. Technol.* **240**, 413–418 (2014)
25. Chen, P.C., Pan, C.W., Lee, W.C., Li, K.M.: Optimization of micromilling microchannels on a polycarbonate substrate. *Int. J. Precis. Eng. Manuf.* **15**(1), 149–154 (2014)
26. Getu, H., Ghobeity, A., Spelt, J.K., Papini, M.: Abrasive jet micromachining of acrylic and polycarbonate polymers at oblique angles of attack. *Wear* **265**(5–6), 888–901 (2008)
27. Zhang, L., Wang, W., Ju, X.J., Xie, R., Liu, Z., Chu, L.Y.: Fabrication of glass-based microfluidic devices with dry film photoresists as pattern transfer masks for wet etching. *RSC Adv.* **5**(8), 5638–5646 (2015)
28. Kang, J.W., Kim, J.S., Kim, J.J.: Optimized oxygen plasma etching of polycarbonate for low-loss optical waveguide fabrication. *Jpn. J. Appl. Phys.* **40**(5R), 3215 (2001)
29. Jia, Y., Jiang, J., Ma, X., Li, Y., Huang, H., Cai, K., Cai, S., Wu, Y.: PDMS microchannel fabrication technique based on microwire-molding. *Chin. Sci. Bull.* **53**(24), 3928–3936 (2008)
30. McUsic, A.C., Lamba, D.A., Reh, T.A.: Guiding the morphogenesis of dissociated newborn mouse retinal cells and hES cell-derived retinal cells by soft lithography-patterned microchannel PLGA scaffolds. *Biomaterials* **33**(5), 1396–1405 (2012)
31. Laviano, F., Ghigo, G., Mezzetti, E., Hollmann, E., Wördenweber, R.: Control of the vortex flow in microchannel arrays produced in YBCO films by heavy-ion lithography. *Phys. C* **470**(19), 844–847 (2010)
32. Wang, S., Wang, X., Wang, L., Pu, Q., Du, W., Guo, G.: Plasma-assisted alignment in the fabrication of microchannel-array-based in-tube solid-phase microextraction microchips packed with TiO₂ nanoparticles for phosphopeptide analysis. *Anal. Chim. Acta* **1018**, 70–77 (2018)
33. Zhai, H., Li, J., Chen, Z., Su, Z., Liu, Z., Yu, X.: A glass/PDMS electrophoresis microchip embedded with molecular imprinting SPE monolith for contactless conductivity detection. *Microchem. J.* **114**, 223–228 (2014)
34. Lei, J.D., Tong, A.J.: Preparation of Zl-Phe-OH-NBD imprinted microchannel and its molecular recognition study. *Spectrochim. Acta Part A Mol. Biomol. Spectrosc.* **61**(6), 1029–1033 (2005)
35. McCann, R., Bagga, K., Groarke, R., Stalcup, A., Vázquez, M., Brabazon, D.: Microchannel fabrication on cyclic olefin polymer substrates via 1064 nm Nd: YAG laser ablation. *Appl. Surf. Sci.* **387**, 603–608 (2016)
36. Wu, T., Ke, C., Wang, Y.: Fabrication of trapezoidal cross-sectional microchannels on PMMA with a multi-pass translational method by CO₂ laser. *Optik* **183**, 953–961 (2019)
37. Mohammed, M.K., Umer, U., Al-Ahmari, A.: Optimization of Nd: YAG laser for microchannels fabrication in alumina ceramic. *J. Manuf. Process.* **41**, 148–158 (2019)
38. Singh, S.S., Khare, A., Joshi, S.N.: Fabrication of microchannel on polycarbonate below the laser ablation threshold by repeated scan via the second harmonic of Q-switched Nd: YAG laser. *J. Manuf. Process.* **55**, 359–372 (2020)
39. Sugioka, K., Midorikawa, K., Yamaoka, H., Gomi, Y., Otsuki, M., Hong, M.H., Wu, D.J., Wong, L.L., Chong, T.C.: Glass microprocessing by laser-induced plasma-assisted ablation: fundamental to industrial applications. In: *Nonresonant Laser-Matter Interaction (NLMI-11)*, pp. 1–10. St. Petersburg (2003)

40. Sarma, U., Joshi, S.N.: Machining of micro-channels on polycarbonate by using Laser-Induced Plasma Assisted Ablation (LIPAA). *Opt. Laser Technol.* **128**, 106257 (2020)
41. Pallav, K., Saxena, I., Ehmann, K.F.: Comparative assessment of the laser-induced plasma micromachining and the ultrashort pulsed laser ablation processes. *J. Micro Nano-Manuf.* **2**(3), 031001 (2014)
42. Bhandari, S., Murnal, M., Cao, J., Ehmann, K.: Comparative experimental investigation of micro-channel fabrication in Ti alloys by laser ablation and laser-induced plasma micro-machining. *Proc. Manuf.* **34**, 418–423 (2019)
43. Malhotra, R., Saxena, I., Ehmann, K., Cao, J.: Laser-induced plasma micro-machining (LIPMM) for enhanced productivity and flexibility in laser-based micro-machining processes. *CIRP Ann.* **62**(1), 211–214 (2013)

Chapter 7

Droplet Microfluidics—A Tool for Biosensing and Bioengineering Applications



U. Banerjee , R. Iqbal , S. Hazra , N. Satpathi , and A. K. Sen 

1 Introduction

Microfluidics is one of the vast areas of science and technology handling tiny volumes of fluids (10^{-9} – 10^{-18} L) at a length scale of tens to hundreds of micrometers. Microfluidics conjoins basic science and biosciences to address a plethora of real-life challenges, e.g., disease detection [1], therapeutics [2], drug delivery [3], etc. The reduced volume of fluid and length scale results in a high-surface area to volume ratio resulting in high mass and heat transfer, the dominance of viscous forces over inertial forces, and significant surface effects. Droplet microfluidics is the realm of microfluidics handling tiny droplets on a microfluidic platform. Droplets are considered as carrier vessels to execute several processes such as transportation [4], mixing [5], sorting [6], trapping [7]. It offers several attractive features such as—(i) the biological entities are isolated, and the whole process occurs in a closed chamber thus eliminating the possibility of contamination by the external fluid and channel or substrate walls, (ii) the tiny volume of droplets reduce the reagent consumption, (iii) monodispersed droplets enable quantitative comparison and screening applications indicating a high throughput, (iv) convective flow profile inside droplets enable high mass or heat transfer, fast reactions. Droplet microfluidics can be broadly classified as continuous and discrete microfluidics. Continuous microfluidics handles a large number of droplets as compared to discrete microfluidics handling a single droplet at a time. Both of these techniques can be executed either in passive or active manner. Passive techniques utilize the system forces such as the non-inertial lift [8], surface morphology [9] etc. as the prime source of manipulation, whereas active techniques require the presence of an external stimuli such as electrical force [10], optical force [11], magnetic force [12], etc. The microfluidic platform for droplet microfluidics

U. Banerjee · R. Iqbal · S. Hazra · N. Satpathi · A. K. Sen (✉)
Indian Institute of Technology Madras, Chennai, Tamil Nadu 600036, India
e-mail: ashis@iitm.ac.in

can be categorized as in-channel or open surface manipulation techniques. In the case of in-channel manipulations, the droplets are generated and manipulated inside a closed conduit. The open surface microfluidic platform indicates the presence of an engineered surface as the microfluidic platform. This chapter will include a detailed discussion on recent developments in biosensing and bioengineering applications involving droplets on an open surface or in-channel microfluidic platforms. Droplet microfluidics has been exploited to satiate several biochemical applications, e.g., enzymatic reactions [13], proteomics [14], immunoassays [15], single-cell studies [16], etc. In-channel droplet microfluidics exploits fluid properties, channel geometry to achieve several biosensing and bioengineering applications. In the case of open surface droplet microfluidics, extreme wetting surfaces have played a significant role in biosensing and biomedical applications [17, 18] which has enabled a paradigm shift from conventional, flow-based lab-on-a-chip strategy, however ensuring the similar low-sample/reagent consumption, flexibility, and versatility and automation.

2 Open Surface Droplet Microfluidics

Open surface techniques primarily deal with the manipulation of droplets on an open surface and use them for various purposes like disease detection, biological assays, several biological applications. Fabrication techniques play an important role in the case of open surface droplet microfluidics. This section consists of the advantages of open surface droplet microfluidics, a detailed discussion about various fabrication techniques, and lastly, various applications.

2.1 *Advantages of Open Surface Droplet Microfluidics*

Open surface techniques offer several advantages as compared to in-channel methods due to its simple manipulation platforms to perform complex detections. With surface modifications, e.g., by changing the surface wettability or patterning the surface, various existing techniques like Raman Microscopy [19] and Colorimetry can be used in case of high sensitivity for the detection of multiple analytes. On the other hand, several applications of droplet microfluidics include the exploitation of surface wettability to anchor a droplet, to spread the droplet using a hydrophilic surface, or to prevent spreading using a hydrophobic substrate. For biosensing and biomedical applications, the microstructures in the substrate offer enhanced accessibility for probe binding, which is of great benefit for sensitive detection. Exploiting the extreme non-wettable surfaces, the analyte concentration can be significantly enhanced for samples of smaller concentrations. The sensing and detection can be performed using a small volume [20] of 1–10 μL . The system being open allows easier accessibility and further versatile combination with various signal outputting approaches. The

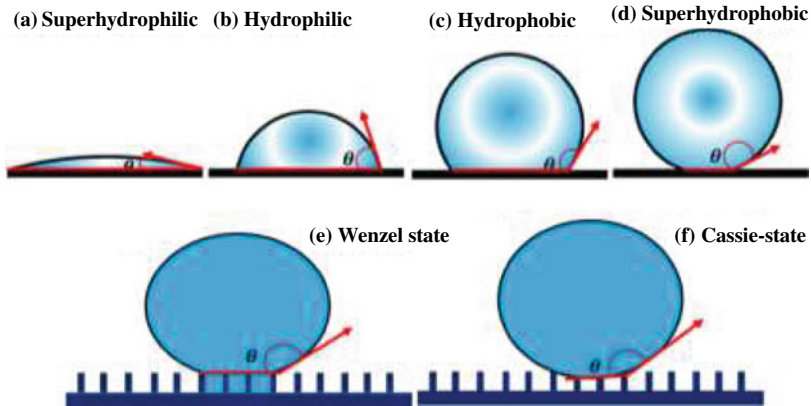


Fig. 1 Schematic of the wetting of a droplet on **a** superhydrophilic, **b** hydrophilic, **c** hydrophobic, and **d** superhydrophobic surface, wetting of a droplet on a real surface having asperities as given by **e** Wenzel, and **f** Cassie-Baxter

substrate can easily be prepared, exploiting several techniques as compared to the closed channels.

Before we dive into the application of open surface microfluidics, it is essential to understand the physics behind various stages of surface wetting. Based on the wettability of the substrate, the droplet will either spread or remain spherical, as shown in Fig. 1. The substrate wettability is characterized into four main categories: (a) superhydrophilic ($0^\circ < \theta < 10^\circ$), (b) hydrophilic ($10^\circ < \theta < 90^\circ$), (c) hydrophobic ($90^\circ < \theta < 150^\circ$), and (d) superhydrophobic ($\theta \geq 150^\circ$). However, other than hydro (water) several different terminologies, for example, oleo (for oil), omni (for oil and water), hemo (for blood), etc. are also being used.

The wettability of a liquid droplet on an isotropic, chemically homogeneous, rigid, perfectly flat surface is given by Young’s contact angle law [21], $\cos \theta = \frac{\gamma_{sv} - \gamma_{sl}}{\gamma_{lv}}$, where γ_{sv} , γ_{sl} , and γ_{lv} are the interfacial tensions of the solid–vapor, solid–liquid, and liquid–vapor interfaces, respectively. However, the surfaces in our daily life applications are far beyond the ideal surfaces, thus understanding of real surfaces are very much needed. This understanding is well proposed by Wenzel [22] and Cassie-Baxter [23] as depicted in Fig. 1e and f, respectively. When a droplet is placed on a rough surface, the effective surface area that it sits upon is not equal to the plane surface area as there is roughness on the surface which affects the equilibrium contact angle. Taking this into account Wenzel gave an expression for the modified contact angle given as –

$$\cos \theta_w = r \times \cos \theta \tag{1}$$

where, θ_w is the Wenzel contact angle, r is the roughness factor defined as the ratio of actual surface area (with surface roughness) and planar surface area (ignoring surface roughness).

In another situation, when the droplet is placed over a surface with chemical heterogeneity, the contact angle is estimated as

$$\cos \theta_{CB} = f_1 \cos \theta_1 + f_2 \cos \theta_2 \quad (2)$$

Here, θ_{CB} represents the Cassie-Baxter angle, f_1 and f_2 are the fractions of the surface area of the respective type of surfaces. If one of the surfaces is an air gap instead then,

$f_2 = 1 - f_1$ and $\theta_2 = 180^\circ$, where subscript 2 is for air. Then the modified equation becomes

$$\cos \theta_{CB} = f_1 \cos \theta_1 - 1 - f_1 \quad (3)$$

2.2 Fabrication Technology of Extreme Wetting Surfaces

There have been several studies focused on the fabrication of extreme wetting surfaces. In general, the process consists of the following steps, creating micro/nanoscale roughness on the substrate, hydrophobic modification, and patterning. Glass and PDMS are the most commonly used hydrophilic and hydrophobic surfaces, respectively. However, efforts are being made in making hierarchical structures on the substrate (creating roughness) to make it extremely non-wetting. The control over roughness over the surface also gives us precise control over the wettability of the surface (Wenzel Equation). It could be achieved in several ways, including lithography, plasma etching, particle assembly, electro-deposition, etc. as depicted in a flow chart in Fig. 2. For a better understanding, the readers are encouraged to read the book by Madou [24]. Here, we will be discussing the various methodologies to fabricate extreme wetting surfaces.

2.2.1 Creating Micro/Nano Roughness

Lithography: This method is employed to generate micro/nanostructures on metals, silicon wafers, and polymers. Essentially, a photoresist layer is exposed and developed to make micro-scale patterns on which a photomask is used for etching. This is a highly efficient method to create micropatterns, although, at times, the structures on polymers do go through a fracture in the peeling-off process [25].

Plasma Etching: This process is used to create micro-scale rough surfaces on a large surface area. Firstly, Oxygen (O_2) Plasma is bombarded on the substrate. This process

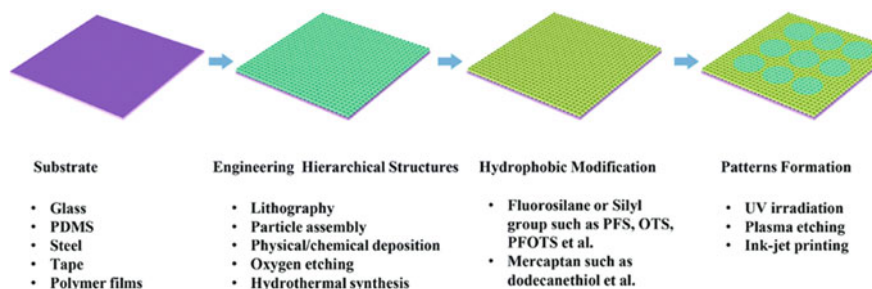


Fig. 2 Schematic of the fabrication of extra-wetting surfaces through various means of hierarchical engineering structures, hydrophobic modification, and pattern formation. The figure is adapted from [18] with permission from the Royal Society of Chemistry

breaks most of the chemical bonds on the substrates and, in turn, makes a rough surface. Although in this process, the control over the shapes of hierarchical structures is minimal. This technique can only be used for particular materials including silica wafers, polymers, etc. [26, 27].

Particle Assembly: This process includes the deposition of micro/nanoparticles on a substrate to create extreme wetting surfaces. This method employs the same idea, micro/nanoparticles are coated over the surface using various methods including spray-coating, spin coating, etc., and then cured to attain certain desired mechanical strength of the integrated substrate. In general, ZnO, silica, and polymer sphere micro/nanoparticles are used. Uniformity of the particle shape and size has always been a challenge and also incurs higher manufacturing costs [28].

Electro-deposition: In this technique, the substrate is treated as an electrode. The process is carried out in a solution where metal ions are transferred to the cathode, which in turn forms a lattice structure. By controlling external inputs like the distance between anode and cathode, voltage, and time, we can control the growth of the crystals on the surface. Even though the process is faster than most other methods, it lags when it comes to stability, morphological control, and mechanical strength, and it can only be used for conductive substrates, thus limiting its large-scale application.

There have also been several other methods that have been developed to create micro/nanoscale roughness on surfaces. However, most of these methods either require a multi-step fabrication process or expensive consumables or high-end equipment. One of the examples being the carbon sooting method [29, 30] which essentially includes exposing a partially cured PDMS substrate to soot particles using a candle and then fully curing the same which leads to the creation of a hierarchical roughness onto the substrate. However, the substrate can be turned hydrophilic by exposing it to an oxygen plasma. This is a cost-effective method that provides excellent surfaces for various applications.

2.2.2 Hydrophobic Modification and Patterning

To introduce hydrophobicity to the substrate, suitable hydrophobic molecules are chosen. Depending on the surface chemical composition, appropriate alkyl groups are chosen, for example, in the case of noble metals thiols, are used. Among the alkyl groups, the fluoroalkyl turns out to be the most hydrophobic as they have the lowest surface energy. For patterning the surface, several methods are employed. The exposure of oxygen plasma to a surface for 2 min makes the exposed portion hydrophilic, and the non-exposed portion remains hydrophobic. Similarly, in the case of UV irradiation, a photomask is used for about 30 min to form a microwell by irradiation. These patterned surfaces have a plethora of applications in sensing technologies, as we will see in the upcoming sections.

2.3 *Some Applications Based on Open Surface Droplet Microfluidics*

The significant applications on open surfaces are by exploiting the wettability of the surfaces. Some of the significant applications are being discussed in this section. We have organized the applications in a way where we present the effect of extreme wetting or extreme non-wetting surfaces separately for biosensing and biomedical applications. Most of the works are being carried out, exploiting either hydrophilic or hydrophobic surfaces. In the next two subsections, we briefly discuss some of the significant works.

2.3.1 Role of Non-wetting Surfaces

In this section, we have briefly discussed some of the recent ongoing activities based on drops on a non-wetting substrate.

Superhemophobic surfaces: The risk of blood clotting and infection in medical implants has remained a perpetual problem over the years. Blood-thinning medications, although being the current state of the art, are not full proof, eventually leading to inflammation, thrombosis, fibrosis, and finally, device failure. Thus, the medical implant technologies need a significant boost in terms of improved biocompatibility, lesser solid–liquid interaction by enabling the surface to be superhemophobic. Nature inspires scientists through its creation of esthetic, functional systems, in which biology meets materials. Enhancing hemocompatibility is the way forward to tackle such problems. To reduce the blood interaction with the substrates, several techniques, for example, diamond-like carbon surfaces, heparin-based coatings [31, 32], modified polymer surfaces, etc. have been proposed. However, none of these surfaces has shown a long-term durable solution. Very recently, metallic materials like titanium have been used as vascular stents. Superhydrophobicity in titanium

is exploited using both anodic oxidation [33–35] and fluorinated coatings. Anodic oxidation introduces the roughness onto the substrate, whereas fluorinated coatings modify the surface chemistry of the substrate. Figure 3 (i) (a) shows images (under scanning electron microscopy) of various titania structures with a fluorinated coating (chemical modification), which makes the structured surfaces superhydrophobic. The resulting nanotubes (100 nm in diameter) dramatically reduces the platelet adhesion from 77/5000 μm^2 on a planar surface to 1/5000 μm^2 on a superhydrophobic surface. Figure 3 (i) (b) shows the fluorescence microscopy of platelets on all these surfaces and respective platelet adhesion. The superhydrophobic surface greatly reduced the platelet adhesion from 81 to 14% between planar and superhydrophobic nanotube topography [36]. In another work, the cell viability is found to be higher on a superhydrophobic surface as compared to the hydrophobic and hydrophilic substrate for a prolonged period [37]. Figure 3 (ii) shows the variation of cell viability (of blood cells and HeLa cells) with time over a period of 75 min. As a summary, the extreme non-wetting surfaces reduce the interaction of the biological samples with the surface, thereby improves the performance either in terms of viability or cell adhesion etc. This may find potential applications in the carrying biosamples in remote areas with prolonged viability.

Blood-plasma separation: In microfluidics, separation of plasma, which contains a lot of biomarkers, has remained a problem for rapid and onsite detection. Most of the techniques reported in the literature use some external force [39] or some other means, which limits its applications for onsite detection. Recently, the separation of plasma from whole blood is achieved using a superhydrophobic surface [2]. The schematic of the device is shown in Fig. 4a, which consists of the superhydrophobic top cover with a separation membrane and a superhydrophobic bottom substrate. Blood samples collected using finger pricking are placed at the bottom of the substrate. Then, the device is closed, and the cells are allowed to sediment at the bottom due to gravimetric settling. After 7–10 min, a transparent layer of plasma is formed at the top of the droplet, which is in contact with the membrane. Thus, the plasma can be collected using a pipette from the top membrane. The blood-in plasma-out device consistently separates 65 μL of plasma from 200 μL of whole blood without any external power input. Further, it is also observed that the separated plasma minimizes biomolecular adhesion to the surface and reduces cell hemolysis and appropriate for the molecular detection of target analytes contained in the blood. It can be used as a stand-alone device in a clinic or resource-limited place without having trained personnel.

2.3.2 Role of Wetting Surfaces

This section discusses some of the vital droplet-based biosensing and biomedical applications using extreme wetting surfaces. Using a wettable surface, disease detection, forensic investigations [40] are being carried out very recently using biological samples [41–45].

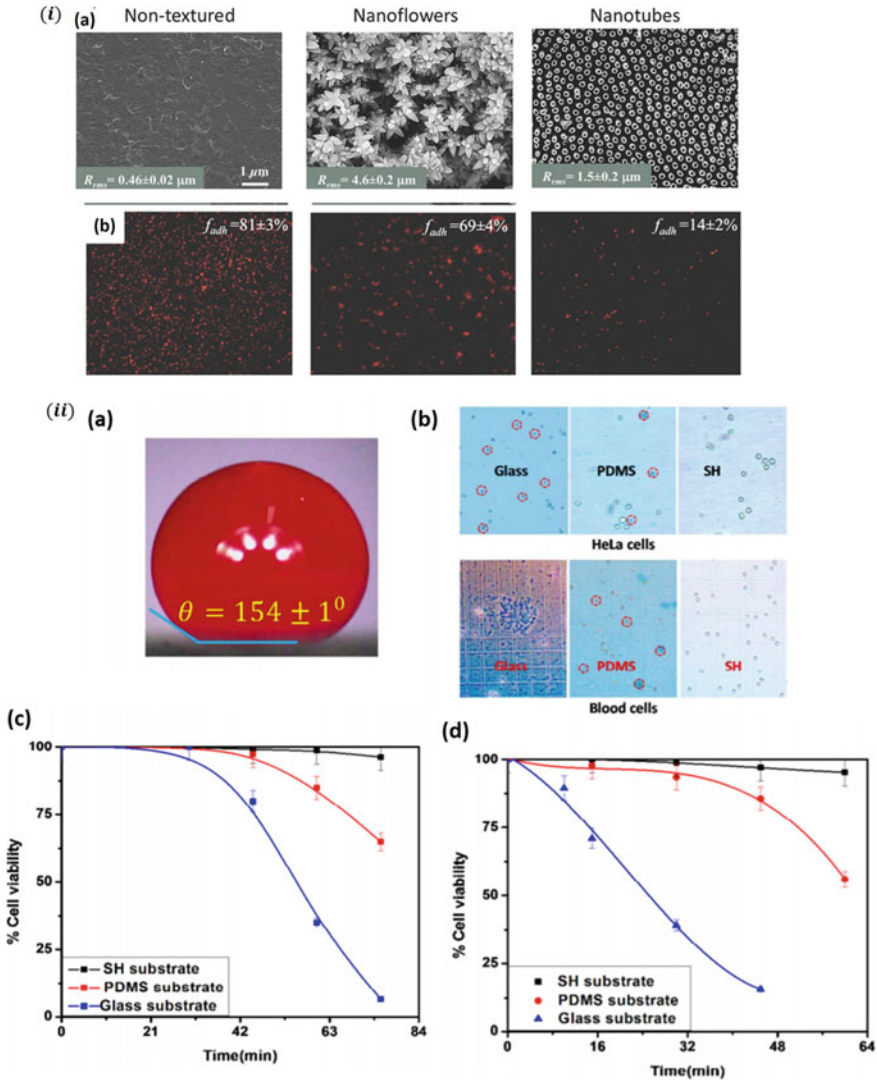


Fig. 3 (i) Sample images of the blood repellent superhydrophobic surface under scanning electron microscopy; **a** non-textured titania, titania nanoflowers, and titania nanotubes obtained using anodic oxidation and fluorinated coating, **b** fluorescent images showing the platelet adhesion for all the textured and non-textured surfaces; adapted with permission from [38], (ii) images of a blood droplet on a candle-soot coated superhydrophobic surface **(a)**, the cell viability (using trypan blue test) of HeLa and blood cells over hydrophilic (glass), hydrophobic (PDMS), and superhydrophobic surface **(b)**, respectively, a variation of cell viability with time for both blood cells and HeLa cells **(c, d)**, adapted with permission from [37]

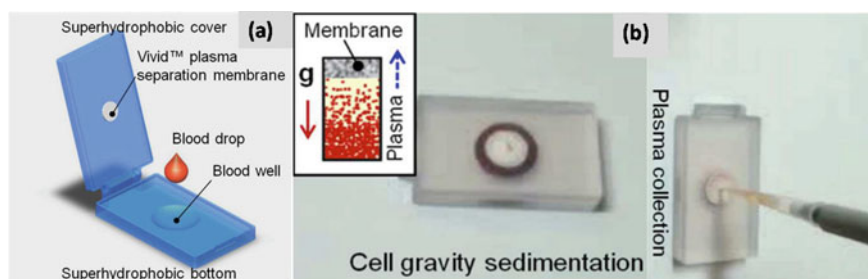


Fig. 4 **a** Schematic of the superhydrophobic plasma separator consisting of a superhydrophobic cover with a separation membrane, and a superhydrophobic bottom with a blood well, **b** images signifying the sequence of the plasma collection; adapted with permission from [2]

Disease detection: The study of blood deposition patterns has emerged as a potential tool for the detection of various diseases [46–52]. Blood droplets are complex colloidal suspensions consisting of plasma, cellular components (RBCs, WBCs, platelets, etc.), inorganic salts, proteins, etc., which carries a numerous biomarker and tons of information about human health. An evaporating droplet dispensed over a glass substrate desiccates and forms several cracks. The final deposition pattern consists of a crack-free peripheral region, RBCs enriched the coronal region with radial and ortho-radial cracks, and a central area with random plaques [50] (see Fig. 5a). However, interestingly the crack patterns are observed to vary from a healthy person to a person with the disease [47, 50]. Figure 5b depicts distinct deposition patterns from both healthy and diseased samples. The crack patterns are observed to differ with the reduction in the number of RBCs. Very recently, an automated platform is developed for the detection of thalassemia carrier samples from the healthy one [53].

Moreover, it is also to be remembered that the deposition pattern depends on several factors, which are biochemical and physio-chemical in nature. Thus, understanding each of these factors would be of utmost importance for further applications. The hematocrit (% RBCs) level in the blood is a vital health index as lower % HCT (hematocrit) than the normal level indicates the lack of RBCs in the blood (i.e., anemia). In contrast, a higher % HCT than the normal level indicates a disorder (polycythemia vera) that causes the production of excessive RBCs inside the body related to dehydration and lung and heart diseases. With the reduction in RBCs, the crack pitch inside the blood droplet is observed to be smaller. Thus, the number of cracks is observed to be more, and in the dilution range of $<2\%$ HCT (hematocrit), a transition from the cracking to the non-cracking regime is observed. This technique could be a potential tool in the preliminary detection of diseases to the places where the basic healthcare facilities are far from their need.

Detection of Malaria biomarker: In another work, exploiting the hydrophilic substrate, a malaria detection platform is developed for *Plasmodium falciparum* histidine-rich protein II (pf-HRP-II) [54]. The set-up consists of an evaporating

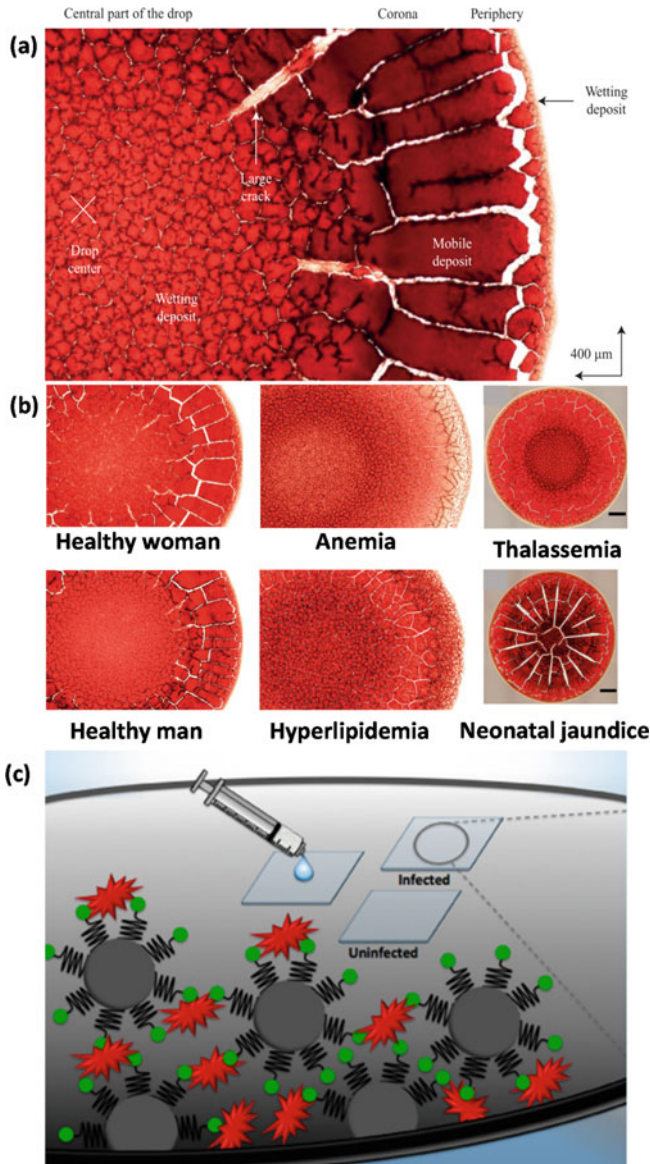


Fig. 5 **a** Evaporative deposition pattern of a blood droplet which consists of the peripheral no-crack region, coronal region, and central region. The coronal region consists of radial and ortho-radial cracks, and the central region consists of random cracks; adapted from [50] with the permission from Elsevier, **b** deposition patterns of various blood samples ranging from healthy to diseased samples (anemia, thalassemia, hyperlipidemia, neonatal jaundice, etc.); adapted from [47, 50] with the permission from Elsevier, **c** schematic of the low-resource platform for the detection of malaria biomarker; adapted from [54] with the permission from American Chemical Society

droplet on a functionalized glass (by Ni (II) nitrilotriacetic acid (NTA), followed by washing. The drop consists of rcHRP-II biomarker functionalized with Ni (II) NTA gold plated polystyrene microspheres. During evaporation, the particle-protein conjugates are driven radially outward due to coffee-ring phenomena [55], where, in the presence of rcHRP-II, particles bind to Ni (II) NTA-functionalized conjugate glass substrate. Post evaporation, the glass substrate is washed under tap water to remove all non-specifically bound materials. Post washing, if a clear ring still exists that confirms the presence of the biomarker due to the interaction of particle-protein conjugate with the functionalized glass substrate (see Fig. 5c). The lowest protein concentration that can be detected is found to be as low as 1 pM. The robust antibody free assay offers a simple user interface and clinically relevant limits of biomarker detection, two critical features required for low-resource malaria detection.

Colorimetry: Colorimetry simply refers to the ability to detect or measure a property by the difference in color or its gradient. It was demonstrated that a superhydrophilic well could hold a pendant droplet as it has strong capillary forces due to its nano-dendritic porous structure [56] as shown in Fig. 6a. Using this capability combined with colorimetry opens up an entirely new avenue for biosensing with visual detection. This method can be used for biosensing under microgravity conditions. It can also be used to differentiate between healthy mouse plasma and diabetic mouse plasma [57]. By taking advantage of the evaporation induced increase in analyte concentration on the superhydrophilic microwell combined with colorimetry has been used as a highly sensitive detector for tracing tetracycline [58]. This sensor shows the colorimetric transition from cyan to red with a detection limit of 2×10^{-9}

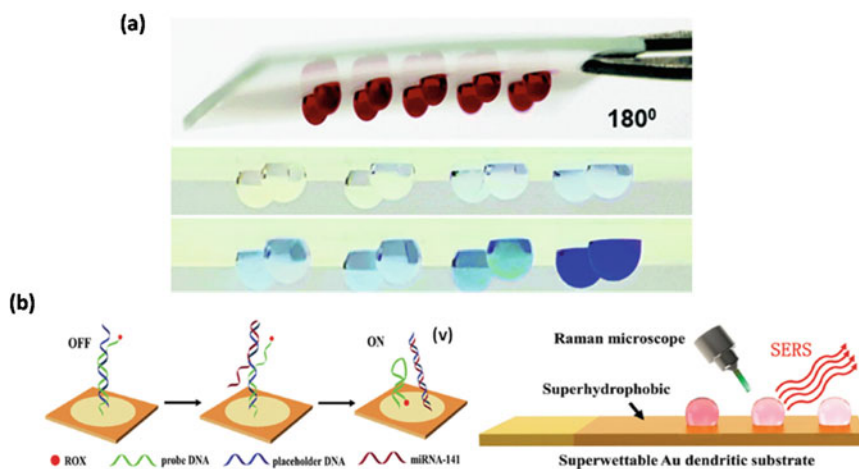


Fig. 6 **a** Superwetable microchips as a platform for upside-down colorimetric biosensing; adapted from [56] with permission from American Chemical Society, **b** superwetable nanodendritic gold substrate for direct miRNA detection; adapted from [63] with permission from Royal Society of Chemistry

M. Furthermore, the Marangoni effect inside a droplet on a microwell was investigated, from this, it was observed that the reactions occurred in the droplet rather than in the well [59]. The Marangoni effect due to natural convection speeded up the mixing of the solution, which in turn speeded up the assay reactions and reduced the assay times. Using superhydrophobic surroundings instead of hydrophobic surroundings also shows a drastic decrease in the coffee ring effect, which again aids in the colorimetric detection process.

SERS: Surface-enhanced Raman Microscopy is utilized for a wide range of applications and experiments. The primary purpose of Raman Microscopy is to give a structural fingerprint of molecules. To enhance the signal strength of Raman Microscopy, various methods are used. SERS is one such method in which signal strength amplification is achieved by coupling between localized Plasmon surfaces. This is generated by the interaction between plasmonic nanostructures and light [60]. Several SERS oriented nano-patterned microchips have been fabricated in recent years, and they provide certain advantages. The nanoscale dendritic structure on metal surfaces ensures a small inter-particle gap, which enhances the Raman signal. The microwell, with its boundary separating the extreme ends of wettability, further improves the Raman signal. The reproducibility of substrates is also enhanced by uniform molecular distribution due to the Marangoni effect on a uniform nanostructure. Due to the enhanced condensation property of superhydrophobic surfaces, they have also become a strong contender for the SERS applications. From a highly dilute solution of 10^{-18} M, analytes have been enriched and detected [61]. The detection of H_2O_2 with concentrations as low as 3 pM has been detected by bioinspired patterning with Ag nanoparticles coated on TiO_2 nanotubes array surface with extreme wettability difference [62]. These examples highlight the ability of SERS in highly sensitive detections. With Electrochemical deposition of Au nanostructure on a superhydrophilic-superhydrophobic patterned substrate which resulted in nano dendritic superhydrophilic SERS hot spots were shown to be useful in trace detection of adenine, dopamine, glucose, and rhodamine with detection limits of 10^{-12} , 10^{-8} and 10^{-15} M, respectively. In the same work, it was also established that with enhanced SERS signal in the superhydrophilic microwells, simultaneous multi-sample detection was possible. Similar fabrication methods were used to detect multiple concentrations of miRNAs. The results of various surfaces (bare Au surface, bare hydrophobic surface, superhydrophilic surface) were compared to the nano dendritic patterned surface, and it was found that it had an enhancement factor of 108 which is far higher than the other surface leading to successful detection of multiple concentrations of miRNAs [63] as shown in Fig. 6b.

3 In-channel Techniques

The flow of two or more immiscible phases (continuous and discrete) inside a microchannel gives rise to the generation of discrete droplets. The generation of droplets can be accomplished in two ways—passive and active. In the case of passive generation, the interface of continuous and discrete phase gets deformed, and pinch-off occurs due to the interfacial instability, which gives rise to droplet generation. On the contrary, active droplet generation requires an external stimulus for interface deformation, and pinch off occurs due to the competition between the hydrodynamic forces and the external force giving rise to droplet generation. The external energy can be electrical, mechanical, magnetic, acoustic, dielectrophoretic, and so on. Based on the channel geometry, droplet generation can be classified as T-junction [64], flow-focusing [65], and co-flow [66] as shown in Fig. 7. In the case of in-channel droplet microfluidics, the fluid flow is characterized using dimensionless numbers [66] such as Reynolds number (Re)—the ratio of inertial force to viscous force, Capillary number (Ca)—the ratio of viscous force to interfacial tension force and Weber number (We)—the ratio of inertial to interfacial tension force. In general, microchannel flows are laminar in nature, which is realized at $Re < 1$. In-channel droplet microfluidics is widely exploited for several applications such as detection of DNA [67], synthetic biology [68], transporting chemical signals [69], and so on. Since the discussion of each application is beyond the scope of the chapter, some prominent applications are discussed in detail in this section.

3.1 Reagent Encapsulation

The droplets are treated as microreactors that can hold various biological, chemical reagents for a plethora of applications [67]. Depending on the application, the encapsulation of reagents has several aspects that need to be satiated. For screening

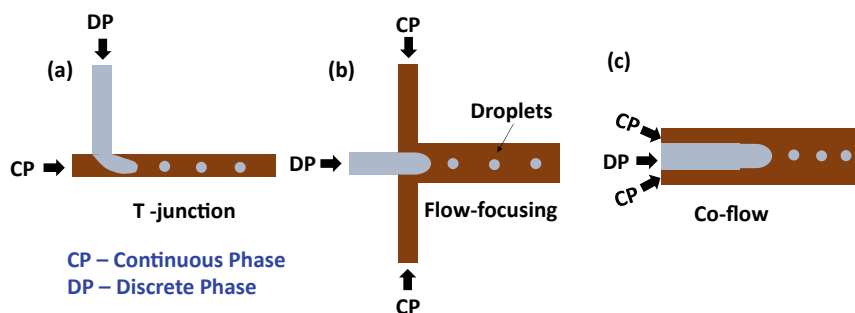


Fig. 7 Schematic of droplet generation **a** T-junction geometry, **b** flow-focusing geometry, **c** co-flow geometry

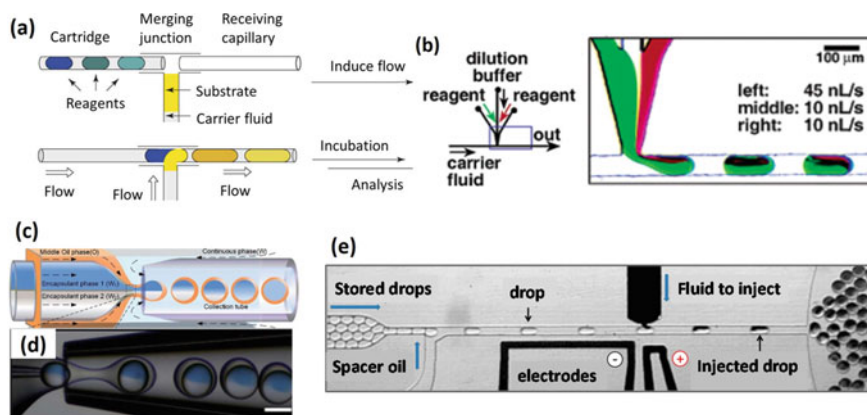


Fig. 8 **a** With preloaded cartridges, the reagents are confined in nanoliter plugs. When the flow is induced, defined nanoliter aliquots of the substrate solution are spontaneously dispensed into the plugs of reagents. Plugs of the reagents and the products are confined in capillaries and are surrounded by an impermeable fluorinated carrier fluid, preventing evaporation; adapted from [70], **b** on-chip dilution was accomplished by varying the flow rates of the reagents, a schematic and experimental image of the microfluidic network; adapted from [71], **c** one-step microfluidic approach for proportional encapsulation of two reagents in W/O/W double emulsion drops, a schematic illustration of the capillary microfluidic device that can encapsulate two different aqueous reagents with required ratios; adapted from [74], **d** optical microscope images showing the one-step generation of double emulsion drops with two encapsulants; adapted from [74], **e** microfluidic device consisting of a droplet spacer and picoinjector. The spacer adds oil from a side channel to space the drops. The picoinjector injects fluid by merging the drops with a pressurized channel containing the reagent. Picoinjection is triggered by an electric field, which is applied by the electrodes; adapted from [73]

purposes, the reagents are confined inside nanolitre plugs and stored in a cartridge. Second, these plugs are merged with a constant volume of the substrate solution at a merging junction. These merged plugs containing both reagent and substrate fluid flows toward the receiving capillary, as shown in Fig. 8a. Finally, the receiving capillary is then detached for post-analysis of the plugs [70]. To obtain a wide range of reagent concentration, on-chip dilution becomes primarily essential. Figure 8b depicts the laminar mixing of two reagents separated by a buffer reagent, which serves as the dilution controller. The final mixture is emulsified into droplets using a T-junction. The concentration of the reagents can be controlled by varying the flow rates of these three streams [71].

Similarly, the encapsulation of two reagents (double emulsion) is achieved using a theta shaped capillary tube, as shown in Fig. 8c and d. On the other hand, when the application demands the accurate control of reagent inclusion, then active techniques [72] become important. A robust method [73] is developed to inject a controlled volume of reagents inside droplets using an electric field. The droplets are allowed to flow in a single streamline inside a channel that consists of electrodes. When the electrodes are energized, the oil–water interface destabilizes, which allows the reagent to enter inside the droplet, as shown in Fig. 8e.

3.2 Cell Manipulation

Cellular heterogeneity has forced the microfluidic community to choose single-cell analysis as a vital tool for cell-based assays [75]. This has enabled several features [76], such as isolation of cells from its environment, analyzing tens of thousands to millions of cells, economical screening of such a large population. In general, encapsulation of cells and their manipulation can be realized using passive or active means inside a microchannel. Passive techniques [77] mainly explore several hydrodynamic forces such as non-inertial lift, dean drag, inertial lift, etc., and channel geometry to achieve encapsulation and manipulation. Confining individual cells in droplets and analyzing those separately can precisely pick the cells of interest and will help to study their influence on the population [78]. Similarly, confining individual cancer cells inside droplets is useful in measuring matrix metalloproteinases (MMPs) activity, population heterogeneity, and disease progression [79]. Jing et al. devised a microfluidic platform combining a droplet jetting generator and a deterministic lateral displacement (DLD) size-sorting channel that is capable of encapsulating individual cancer cells inside picoliter droplets effectively (Fig. 9a). Droplet jetting with cell-triggered Rayleigh-Plateau instability was employed which produced large droplets

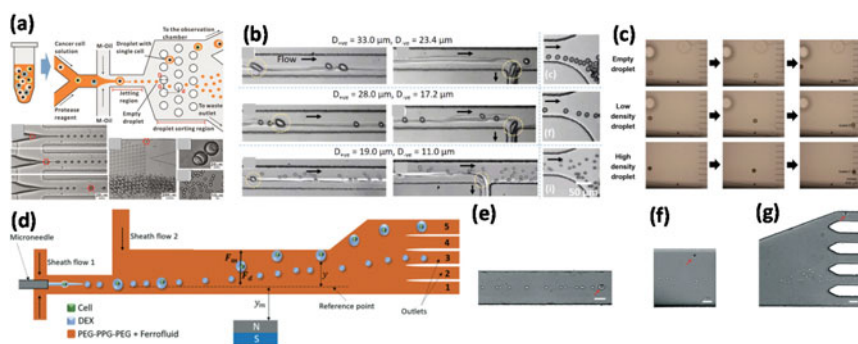


Fig. 9 **a** Schematic representation of the integrated microfluidic device comprising droplet generator and size-based sorting channel. “D”, “G”, and “d” refer to the size, gap, and row shift distance of micropillar array in the sorting channel, respectively. Encapsulation of a cancer cell (indicated by the red-dashed circle) into a droplet with a larger size compared to other empty droplets, the cell containing droplet (indicated by the red-dashed circle) is diverted to the outlet connected to the observation chamber after passing through the sorting channel. In contrast, empty droplets proceed directly to the waste outlet, collection of two droplets with cell encapsulation in the observation chamber, removal of empty droplets from the waste outlet; adapted from [79], **b** sorting of positive droplets encapsulating HeLa cells, MDA-MB 231 and PBMCs across the interface; adapted from [6], **c** the migration of the droplets, the images were taken at 1.34 s interval. Magnetic microdroplets containing different densities of cells showed different migration routes on the magnetic field; adapted from [85], **d** schematic illustration of diamagnetic separation of cell-containing droplets from empty droplets. Representative image frames from experiments showing, **e** the droplet generation region and the size distinction between a particle encapsulating droplet (indicated by a red arrow) and empty droplets, **f** the region of high magnetic field gradient where droplets deflect based on their size, and **g** the sorting of droplets into different outlets; adapted from [86]

capable of cell encapsulation (diameter, 25 μm) and small empty droplets (diameter, 14 μm), which were then size-separated using a DLD size-sorting channel to enrich the single-cell encapsulated droplets (78%), regardless of the cell density of input sample solutions. The droplets containing encapsulated cancer cells were collected in an observation chamber to determine the secretion activity of MMP at a single-cell level. Besides geometry mediated sorting, non-inertial lift induced interfacial migration phenomena have also been employed to sort cell-encapsulating aqueous droplets (positive droplets) from empty droplets (negative droplets) [80]. Utilizing the fact that positive droplets were always larger compared to the negative droplet, positive droplets were migrated across silicone oil-mineral oil interface, and maximum efficiency of $\sim 95\%$ and purity of $\sim 65\%$ was attained (Fig. 9b). On the contrary, active based techniques involve the presence of external source for manipulation. An integration of droplet sorter with fluorescence-activated sorting module was utilized to sort droplets containing single cells [81]. The encapsulation was found to be 94.1%, which is about 200% higher as compared to random compartmentalization. Electric forces [82] were also exploited to sort single or multiple mammalian cells (HePG2) encapsulated inside the droplet with a sorting rate of ~ 100 Hz. Similarly, acoustic force [83] and magnetic force [84] are utilized to extract cells from a droplet into an aqueous stream for further analysis. In one study, microalgal cells are encapsulated inside ferrofluid droplets flowing inside a microchannel. A magnetic field placed near the microchannel separates the empty and non-empty droplets based on the number density of magnetic nanoparticles with an efficiency of 91.2% (empty), 87.12% (low), and 90.66% (high density) droplets [85] as shown in Fig. 9c. Similarly, breast cancer cells (MCF-7) were encapsulated inside aqueous droplets flowing inside a magnetic medium which resulted in a size contrast between the empty (smaller) and non-empty droplets (larger). This size contrast was exploited to achieve size-based sorting, as shown in Fig. 9d, with a purity of 100% in a single pass [86].

3.3 Drug Delivery

Drug delivery is one of the salient features of therapeutics where droplet microfluidics plays a vital role. Droplets engulf the drug, protecting it from environmental conditions, and providing a suitable means for its efficient release. Droplet-based drug encapsulation and release offer several advantageous features as—(i) monodisperse droplets can be generated with the tunable frequency which assures efficient encapsulation, maintaining consistency release rates, (ii) multiple drug encapsulation for several treatments, (iii) by using various matrix materials, different release profiles such as sustained or burst release can be realized. Drug delivery entails two primary steps—drug encapsulation and drug release. Drug molecules can be suspended inside the dispersed phase and can be encapsulated inside droplets using conventional droplet generation techniques discussed at the beginning of Sect. 3. In general, hydrophilic drugs are loaded into a hydrogel-based carrier such as alginate and chitosan. On the contrary, hydrophobic based drugs can be encapsulated inside a

polymer-based carrier [67]. There are therapeutic techniques that demand encapsulation of multiple drug molecules and release at a required proportion. A solvent-free one-step method demonstrates simultaneous encapsulation of a hydrophilic and a hydrophobic drug with high efficiency, ensuring the controlled release of both at a desired concentration and location [87]. The device consists of a core-shell structure comprising a hydrophilic core, which engulfs an aqueous solution of hydrophilic active and a shell that encapsulates the hydrophobic active, as shown in Fig. 10a. A flow-focusing device is utilized to fabricate monodisperse, drug-loaded microparticles (10–50 μm) from biodegradable polymers, as shown in Fig. 10b. An amphiphilic drug (bupivacaine) is encapsulated within the matrix of the particles. The kinetics of drug release, as shown in Fig. 10g reveals three significant features. First, smaller particles release the drug more rapidly as compared to the larger particles due to the larger surface area to volume ratio in the case of smaller particles. Second, particles fabricated using droplet microfluidics release the drugs slowly as compared to the particles prepared using conventional techniques. Lastly, the initial burst release of drug is found to be significantly smaller than the corresponding particles fabricated conventionally.

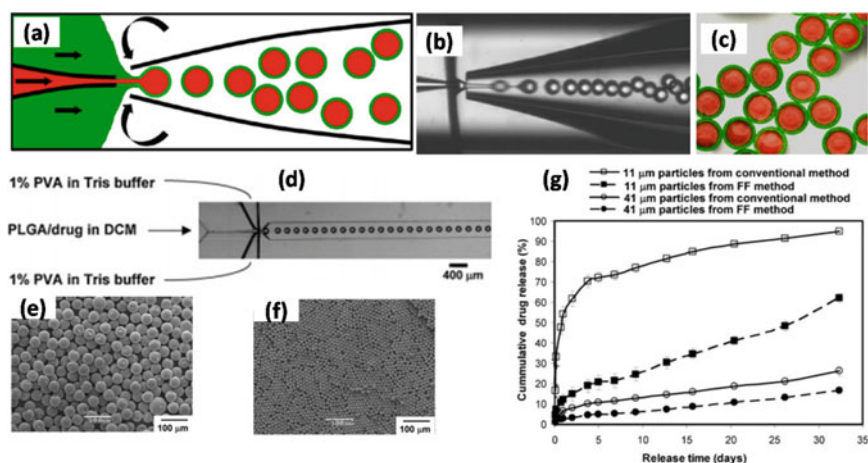


Fig. 10 Generation of double emulsion droplets for the formation of core-shell structures in a microcapillary device. **a** Schematic of the device with two adjacently adjusted cylindrical glass capillaries within a square capillary. The device allows the controlled injection of three different fluids. The inner (red) and middle (green) fluids are hydrodynamically focused by the outer fluid (white). **b** Microscopic image of a running device producing core-shell structures. **c** Fluorescence detection of the encapsulated drugs: doxorubicin (red) in the core liquid and paclitaxel (green) incorporated within the lipid shell structure; adapted from [87]. **d** Optical microscopy image showing the orifice of the flow-focusing region generating droplets of dichloromethane (DCM) in water, SEM images of microparticles prepared via microfluidics of sizes: **e** 41 μm . **f** 11 μm . **g** Drug release profiles from monodisperse microparticles prepared with microfluidic devices and polydisperse microparticles prepared using the conventional single emulsion release technique; adapted from [88]

Similarly, controlled drug release also plays a vital role in therapeutics. On a broader note, drug release can be classified as passive and active. Passive mode relies on diffusion and matrix degradation, and the release depicts an initial burst step following a sustained pattern [67]. The release rate is found to decrease with an increase in particle size and increase with particle monodispersity [88, 89]. Porous particles exhibit a faster rate of release due to their structure. Apart from passive techniques, active techniques [90, 91] involve the presence of external stimuli, e.g., heat, chemical environment, pH, magnetic field, mechanical stress, etc.

3.4 Droplet Screening

Fluorescence-activated screening of cell encapsulated droplets, and subsequent sorting (FADS) is an excellent tool for tracking enzyme activities, protein secretion, metabolite production, single-cell gene expression [68]. This method is robust and yields ultra-high-throughput [92]. Huang et al. [93] employed droplet microfluidics to screen 10^5 – 10^6 of UV-irradiated yeast *S. cerevisiae* variants with desired α -amylase secretion rates (Fig. 11a). The *S. cerevisiae* cell culture was plated on

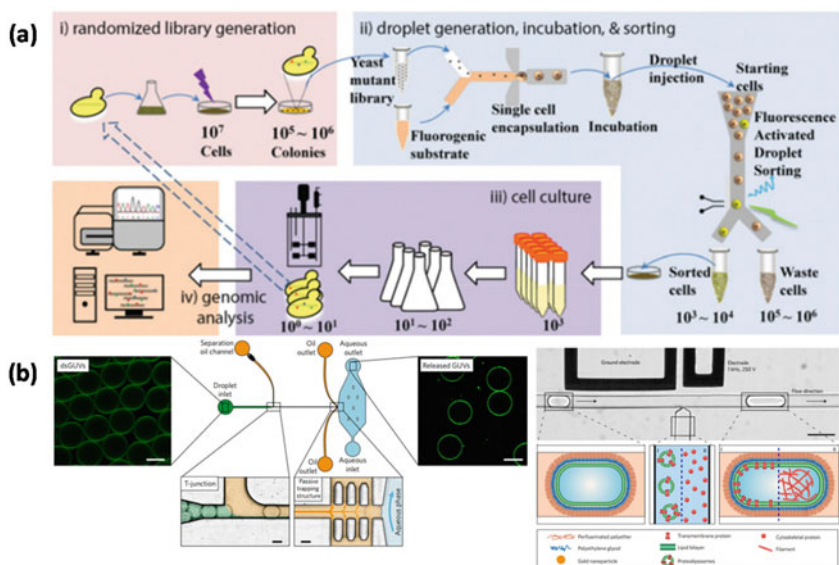


Fig. 11 **a** Workflow for FADS: (i) random library generation by UV irradiation. (ii) Screening for droplet microfluidic sorting. (iii) Validation of amylase production capacity of sorted strains. (iv) Genomic analysis of the selected strains; adapted from [93]. **b** The microfluidic device designed to release the assembled lipid compartments from the surrounding stabilizing polymer droplets into the aqueous phase (left) and picoinjection transmembrane and cytoskeletal proteins into dsGUVs (right); adapted from [94]

an agar plate and irradiated with 254 nm UV light to increase random mutations. These cells were re-suspended and mixed with the α -amylase fluorogenic substrate in a droplet generator, encapsulating a single yeast cell in a droplet. After off-chip incubation, the droplets were screened and sorted using FADS, resulting in 8 clones with high α -amylase secretion rates. These variants were subjected to whole-genome sequencing and identified a total of 330 mutations of interest.

3.5 Artificial Cells

Fully synthesized artificial cells to mimic/model natural systems would be useful not only for the engineering of biological organisms and products but also for reproducible reconstitution studies of biomolecular processes and functional organization in biology without the complicated cellular environment. Although cells are the building blocks of life, with modern biology clarifying many of their structural and biochemical pathways, their complexity is, to a large extent, beyond the understanding of contemporary science [15, 68].

Weiss et al. [94] investigated the merging of lipid vesicles and copolymer-stabilized droplets to generate mechanically and chemically stable cell-like compartments, termed as droplet-stabilized GUVs (dsGUVs) (Fig. 11b). This high-throughput method enables the generation of up to 10^3 functional compartments per second. As a result, it generates a vast number of synthetic cells of unique and precise composition. These compartments can be sequentially loaded with biomolecules utilizing pico-injection technology. This sequential procedure allows for a combination of molecules and organized molecular structures that would not occur spontaneously. This method offers a well-defined micro-environment for the real step-by-step ‘bottom-up’ assembly of intracellular modules with desired features. Moreover, the model systems were released from the oil phase and stabilizing droplets after assembly, thus paving the way toward interactions of these synthetic cells with physiologically relevant environments such as extracellular matrices, cells, or signaling proteins.

3.6 PCR

Absolute quantitation of nucleic acid is of utmost importance for rare mutation detection. The conventional gene sequencing method offers low specificity and fails to detect rare mutations of frequency below 20% [15]. Droplet digital PCR (ddPCR) offers high throughput, robust avenue for rare gene detection limit as low as 0.001% [15]. Hindson et al. [95] studied a ddPCR method where highly diluted DNA Samples and Droplet generation oil are loaded into an eight-channel droplet generator cartridge (Fig. 12a). A vacuum is applied to the droplet well, which draws samples and oil through a flow-focusing nozzle where monodisperse 1 nL droplets are

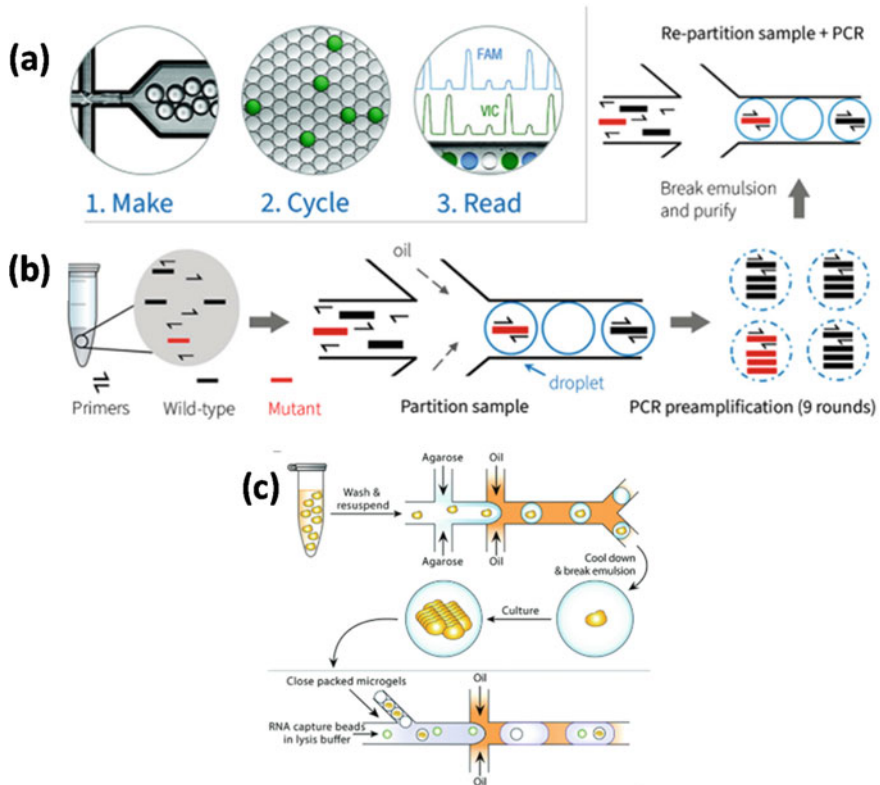


Fig. 12 **a** Workflow for ddPCR: 1. Droplets are formed out of diluted DNA samples in oil using a microfluidic flow-focusing device, 2. PCR amplification using conventional thermal cycle. 3. Detection of DNA containing droplet. **b** Schematic of the workflow of PCR pre-amplification for MED-Amp; adapted from [15]. **c** Single yeast cells are encapsulated inside agarose microgel microdroplets using a flow-focusing device, followed by microgel recovery and colony formation within the microgel; adapted from [15]

formed. In <2 min, eight samples are converted into eight sets of 20,000 droplets. The surfactant-stabilized droplets are pipet transferred to a 96-well PCR plate. Droplet PCR amplification to end-point (3545 cycles) is performed in a conventional thermal cycler. The plate is loaded onto a reader, which sips droplets from each well and streams them single-file past a two-color detector at the rate of ~ 1000 per second. Droplets are assigned as positive or negative based on their fluorescence amplitude. The number of positive and negative droplets in each channel is used to calculate the concentration of the target and reference DNA sequences and their Poisson based 95% confidence intervals.

Molecular detection of circulating tumor DNA (ctDNA) is increasingly used as a tool for cancer surveillance and early detection in oncology [15]. However, for patients with low tumor burdens, ctDNA abundance is extremely low and masked

by large amounts of wild types (wtDNA). In such situations, direct detection via ddPCR can be difficult, and thus, the integration of pre-amplification strategies is desirable. In this regard, Pratt and co-workers [96] developed the ‘Multiplex Enrichment using Droplet pre-amplification’ (MED-Amp) method for the enrichment of ctDNA templates (Fig. 12b). In initial tests, the authors performed nine rounds of high-fidelity polymerase pre-amplification in picoliter-volume droplets, with subsequent ddPCR detection of templates. Through such a strategy, mutation signals could be increased by over 50-fold, with successful detection of KRAS mutant ctDNA in plasma samples from metastatic pancreatic ductal adenocarcinoma patients.

3.7 3D Cell Culture and Cell-Laden Hydrogel Droplets

3D cell culture model provides the environment to emulate the natural context of cell growth in tissue and enables the study of cell development in various matrices. In contrast to traditional monolayer 2D methods, it can simulate more realistic growth morphologies and cell environments (such as tissue-specific structures, intercellular connections, and concentration gradients). In contrast to animal models, 3D cell models are not only cheaper to establish but are also easier to control and standardize. Accordingly, 3D cell cultures are of great significance and hold vast application potential in disease modeling, drug screening, target identification and verification, toxicity testing, and safety evaluation [15].

3D cell culture in microgel droplets has garnered broad interest for appropriate porosity, permeability, mechanical properties, and surface chemistry to artificially generate a 3D network. It offers (i) reduced surface area-to-volume ratios to facilitate the diffusion and exchange of small molecules, (ii) reduced compartment volumes and the control of unit size and cell numbers are favorable when constructing consistent cell culture models on a large scale. (iii) capable of evenly distributing cells and enhancing cell density [15].

Heterogeneity of clonal colonies can be optically investigated through time-lapse fluorescence microscopy single-cell compartmentalization in droplets with subsequent spatial immobilization in 3D hydrogel culture. Kleine-Brueggeny et al. [97] developed a long-term perfusion culture platform for monoclonal embryonic stem cell (mES)-laden hydrogel beads. The workflow integrates cell encapsulation, microgel formation, demulsification, microgel capture, and perfusion culture. A microfluidic device module was developed that performs the de-emulsification of beads, enabling automation and coupling of this module to further microfluidic chips. Subsequently, a chip design was introduced for the spatial immobilization and perfusion of hydrogel beads that are based on a flow dependent trapping mechanism resulting in flow-induced trapping without the need for a bypass channel. By comparing the effect of different perfusion media on the development of mES cells using time-lapse confocal microscopy, the compatibility of the hydrogel bead format with immunohistochemistry and reverse transcription, and quantitative PCR (RT-qPCR) was validated.

The thermosensitivity of agarose gel has attained interest recently. Its ability to switch between liquid and gel state paves the path for performing PCR in liquid-phase agarose droplets at elevated temperatures, then gelling at a lower temperature by cooling to trap amplicons inside the bead for easy washing and collection. Using this key principle, agarose droplets can be used to culture yeast colonies from single cells, which were then subjected to gene expression profiling [98] (Fig. 12c).

Table 1 includes the advantages and quantitative performance of various droplet-based techniques.

Table 1 Summary depicting advantages and quantitative performance of various droplet-based techniques

In-channel droplet microfluidics	The advantage over bulk scale/conventional method	Efficiency/throughput/sensitivity
Reagent encapsulation [71]	<ol style="list-style-type: none"> 1. Compartmentalization due to encapsulation 2. No contamination of reagent 3. Miniaturization of reaction 4. High throughput 	~10 kHz
Cell manipulation [79]	<ol style="list-style-type: none"> 1. Encapsulation of single-cell and thus the single-cell analysis 2. High throughput due to large droplet generation 	~1000 Hz
Drug delivery [87]	<ol style="list-style-type: none"> 1. Controlled encapsulation of drugs inside droplets 2. Controlled release at the desired location 3. Multiple drug delivery at the desired proportion 	~320 mL/h
Droplet screening [92, 93]	<ol style="list-style-type: none"> 1. Ultra-high throughput 2. Cost-effective 3. The investigation is possible at a single-cell level 	~1–30 kHz
Droplet-based artificial cell [94]	<ol style="list-style-type: none"> 1. A tool to unravel complexity by compartmentalizing biochemical reactions 2. Enhanced mechanical and chemical stability compared to lipid-based protocells 	~1 kHz
Droplet PCR [95]	<ol style="list-style-type: none"> 1. Ultra-low reagent volume 2. High sensitivity; detection limit ~0.001%. Conventional method can't detect variants with frequency <20% 	~2 million PCR reactions/hour
3D cell culture and cell-laden microgel [15]	<ol style="list-style-type: none"> 1. Simulation of realistic growth morphology 2. Appropriate porosity, permeability conducive for 3D cell growth 	~5 kHz

4 Conclusion and Perspective

In this chapter, we have discussed both open and closed surface droplet microfluidics. In the case of an open surface, the fundamental of droplet wetting plays a vital role which is briefly discussed. In addition to wetting behavior, fabrication of various surfaces is of paramount importance for efficient droplet manipulation on an open surface platform, which is briefly discussed. Open surface droplet microfluidics has a significant contribution to achieve several disease detections, chemical, and biological assays, which are well covered. On the other hand, in-channel droplet microfluidics requires a better understanding of droplet generation and various dimensionless numbers, as discussed. In addition to the open surface, in-channel droplet microfluidics enables several bioengineering applications, which is widely described. Finally, a comparison table tabulating various applications, advantages, and performance parameters are presented.

Although droplet-based microfluidic tools have profoundly changed the field of high-throughput bioengineering and biosensing experiments, there are some limitations which limit the utility. Microfluidic droplets are soft vessels, which makes it a permeable membrane. Due to this fact, droplets are not perfectly stable despite the usage of surfactants. There is always a possibility of cross-contamination across the droplet wall. To rule out the possibility of cross-contamination, most of the microfluidic devices are not reused, which enhances the cost. Lastly, complexities in various droplet-based microfluidic devices need special attention to minimize operational complications.

References

1. Nematbakhsh, Y., Lim, C.T.: Cell biomechanics and its applications in human disease diagnosis. *Acta Mech. Sin. Xuebao* **31**, 268–273 (2015)
2. Liu, C., et al.: A high-efficiency superhydrophobic plasma separator. *Lab Chip* **16**, 553–560 (2016)
3. Liu, D., Zhang, H., Fontana, F., Hirvonen, J.T., Santos, H.A.: Microfluidic-assisted fabrication of carriers for controlled drug delivery. *Lab Chip* **17**, 1856–1883 (2017)
4. Mandal, C., Banerjee, U., Sen, A.K.: Transport of a sessile aqueous droplet over spikes of oil based ferrofluid in the presence of a magnetic field. *Langmuir* **35**, acs.langmuir.9b00631 (2019)
5. Jiao, L., et al.: Light-actuated droplets coalescence and ion detection on the CAHTs-assisted superhydrophobic surface. *Sensors and Actuators B: Chemical* (2018). <https://doi.org/10.1016/j.snb.2018.11.084>
6. Jayaprakash, K.S., Sen, A.K.: Droplet encapsulation of particles in different regimes and sorting of particle-encapsulating-droplets from empty droplets. *Biomicrofluidics* **13**, 1–11 (2019)
7. Jain, S.K., Banerjee, U., Sen, A.K.: Trapping and coalescence of diamagnetic aqueous droplets using negative magnetophoresis (2020)
8. Jayaprakash, K.S., Banerjee, U., Sen, A.K.: Dynamics of aqueous droplets at the interface of coflowing immiscible oils in a microchannel. *Langmuir* **32**, 2136–2143 (2016)
9. Chowdhury, I.U., Mahapatra, P.S., Sen, A.K.: Self-driven droplet transport: effect of wettability gradient and confinement. *Phys. Fluids* **31** (2019)

10. Srivastava, A., Karthick, S., Jayaprakash, K.S., Sen, A.K.: Droplet demulsification using ultralow voltage-based electrocoalescence. *Langmuir* **34**, 1520–1527 (2018)
11. Park, S.-Y., Kalim, S., Callahan, C., Teitell, M.A., Chiou, E.P.Y.: A light-induced dielectrophoretic droplet manipulation platform. *Lab Chip* **9**, 3228 (2009)
12. Banerjee, U., Raj, A., Sen, A.K.: Dynamics of aqueous ferrofluid droplets at coflowing liquid-liquid interface under a non-uniform magnetic field. *Appl. Phys. Lett.* **113**, 143702 (2018)
13. Lai, S., et al.: Design of a compact disk-like microfluidic platform for enzyme-linked immunosorbent assay. *Anal. Chem.* **76**, 1832–1837 (2004)
14. Wei, W., et al.: Microchip platforms for multiplex single-cell functional proteomics with applications to immunology and cancer research. *Genome Med.* **5**, 1–12 (2013)
15. Ding, Y., Howes, P.D., Demello, A.J.: Recent advances in droplet microfluidics. *Anal. Chem.* (2019). <https://doi.org/10.1021/acs.analchem.9b05047>
16. Gu, S.Q., et al.: Multifunctional picoliter droplet manipulation platform and its application in single cell analysis. *Anal. Chem.* **83**, 7570–7576 (2011)
17. Garcia-Cordero, J.L., Fan, Z.H.: Sessile droplets for chemical and biological assays. *Lab Chip* **17**, 2150–2166 (2017)
18. Xu, T., Xu, L.P., Zhang, X., Wang, S.: Bioinspired superwetable micropatterns for biosensing. *Chem. Soc. Rev.* **48**, 3153–3165 (2019)
19. Ma, X., et al.: Hybrid superhydrophilic–superhydrophobic micro/nanostructures fabricated by femtosecond laser-induced forward transfer for sub-femtomolar Raman detection. *Nanoeng.* **5**, 1–10 (2019)
20. Ebrahimi, A., et al.: Nanotextured superhydrophobic electrodes enable detection of attomolar-scale DNA concentration within a droplet by non-faradaic impedance spectroscopy. *Lab Chip* **13**, 4248–4256 (2013)
21. Young, T.: An Essay on the cohesion of fluids. *Philos. Trans. R. Soc. London* **95**, 65–87 (1805)
22. Wenzel, R.N.: Resistance of solid surfaces to wetting by water. *J. Ind. Eng. Chem. Washington, DC* **28**, 988–994 (1936)
23. Bormashenko, E.: Young, Boruvka-Neumann, Wenzel and Cassie-Baxter equations as the transversality conditions for the variational problem of wetting. *Colloids Surfaces A: Physicochem. Eng. Aspects* **345**, 163–165 (2009)
24. Madou, M.J.: Fundamentals of Microfabrication. CRC Press (2002). <https://doi.org/10.1201/9781482274004>
25. Brittain, S., Paul, K., Zhao, X.-M., Whitesides, G.: Soft lithography and microfabrication. *Phys. World* **11**, 31 (1998)
26. Wang, J.H.: Surface preparation techniques for biomedical applications. In: *Coatings for Biomedical Applications*. Elsevier, pp. 143–175 (2012). <https://doi.org/10.1533/9780857093677.1.143>
27. Luz, G.M., Leite, Á.J., Neto, A.I., Song, W., Mano, J.F.: Wettable arrays onto superhydrophobic surfaces for bioactivity testing of inorganic nanoparticles. *Mater. Lett.* **65**, 296–299 (2011)
28. Rahmawan, Y., Xu, L., Yang, S.: Self-assembly of nanostructures towards transparent, superhydrophobic surfaces. *J. Mater. Chem. A* **1**, 2955–2969 (2013)
29. Majhy, B., Iqbal, R., Sen, A.K.: Facile fabrication and mechanistic understanding of a transparent reversible superhydrophobic–superhydrophilic surface. *Sci. Rep.* 1–11 (2018). <https://doi.org/10.1038/s41598-018-37016-5>
30. Iqbal, R., Majhy, B., Sen, A.K.: Facile fabrication and characterization of a PDMS-derived candle soot coated stable biocompatible superhydrophobic and superhemophobic surface. *ACS Appl. Mater. Interfaces* (2017). <https://doi.org/10.1021/acsami.7b09708>
31. Chou, C.C., et al.: Oxidized dopamine as the interlayer between heparin/collagen polyelectrolyte multilayers and titanium substrate: an investigation of the coating's adhesion and hemocompatibility. *Surf. Coatings Technol.* **303**, 277–282 (2016)
32. Lin, W.C., Liu, T.Y., Yang, M.C.: Hemocompatibility of polyacrylonitrile dialysis membrane immobilized with chitosan and heparin conjugate. *Biomaterials* **25**, 1947–1957 (2004)
33. Sorkin, J.A., Hughes, S., Soares, P., Popat, K.C.: Titania nanotube arrays as interfaces for neural prostheses. *Mater. Sci. Eng. C* **49**, 735–745 (2015)

34. Smith, B.S., Yoriya, S., Johnson, T., Popat, K.C.: Dermal fibroblast and epidermal keratinocyte functionality on titania nanotube arrays. *Acta Biomater.* **7**, 2686–2696 (2011)
35. Smith, B.S., Capellato, P., Kelley, S., Gonzalez-Juarrero, M., Popat, K.C.: Reduced in vitro immune response on titania nanotube arrays compared to titanium surface. *Biomater. Sci.* **1**, 322–332 (2013)
36. Movafaghi, S., et al.: Hemocompatibility of superhemophobic titania surfaces. *Adv. Healthc. Mater.* **6** (2017)
37. Iqbal, R., Majhy, B., Sen, A.K.: Facile fabrication and characterization of a PDMS-derived candle soot coated stable biocompatible superhydrophobic and superhemophobic surface. *ACS Appl. Mater. Interfaces* **9**, 31170–31180 (2017)
38. Jokinen, V., Kankuri, E., Hoshian, S., Franssila, S., Ras, R.H.A.: Superhydrophobic blood-repellent surfaces. *Adv. Mater.* **30**, 1–10 (2018)
39. Maria, M.S., Kumar, B.S., Chandra, T.S., Sen, A.K.: Development of a microfluidic device for cell concentration and blood cell-plasma separation. *Biomed. Microdevices* **17**, 1–19 (2015)
40. Choi, W., Shin, J., Hyun, K.A., Song, J., Jung, H.I.: Highly sensitive and accurate estimation of bloodstain age using smartphone. *Biosens. Bioelectron.* **130**, 414–419 (2019)
41. Chen, R., Zhang, L., Zang, D., Shen, W.: Blood drop patterns: formation and applications. *Adv. Colloid Interface Sci.* **231**, 1–14 (2016)
42. Tomaiuolo, G.: Biomechanical properties of red blood cells in health and disease towards microfluidics. *Biomicrofluidics* **8**, 1–19 (2014)
43. van Oorschot, R.A.H., Szkuta, B., Meakin, G.E., Kokshoorn, B., Goray, M.: DNA transfer in forensic science: a review. *Forensic Sci. Int. Genet.* **38**, 140–166 (2019)
44. Trantum, J.R., Baglia, M.L., Eagleton, Z.E., Mernaugh, R.L., Haselton, F.R.: Biosensor design based on Marangoni flow in an evaporating drop. *Lab Chip* **14**, 315–324 (2014)
45. Yakhno, T.A., Sanina, O.A., Volovik, M.G., Sanin, A.G., Yakhno, V.G.: Thermographic investigation of the temperature field dynamics at the liquid-air interface in drops of water solutions drying on a glass substrate. *Tech. Phys.* **57**, 915–922 (2012)
46. Chen, R., Zhang, L., Zang, D., Shen, W.: Understanding desiccation patterns of blood sessile drops. *J. Mater. Chem. B* **5**, 8991–8998 (2017)
47. Bahmani, L., Neysari, M., Maleki, M.: The study of drying and pattern formation of whole human blood drops and the effect of thalassaemia and neonatal jaundice on the patterns. *Colloids Surf. A: Physicochem. Eng. Aspects* **513**, 66–75 (2017)
48. Zeid, W.B., Brutin, D.: Influence of relative humidity on spreading, pattern formation and adhesion of a drying drop of whole blood. *Colloids Surf. A: Physicochem. Eng. Aspects* **430**, 1–7 (2013)
49. Brutin, D., Sobac, B., Nicloux, C.: Influence of substrate nature on the evaporation of a sessile drop of blood. *J. Heat Transfer* **134**, 1–7 (2012)
50. Brutin, D., Sobac, B., Loquet, B., Sampol, J.: Pattern formation in drying drops of blood. *J. Fluid Mech.* **667**, 85–95 (2011)
51. Sobac, B., Brutin, D.: Desiccation of a sessile drop of blood: cracks, folds formation and delamination. *Colloids Surf. A: Physicochem. Eng. Aspects* **448**, 34–44 (2014)
52. Sobac, B., Brutin, D.: Structural and evaporative evolutions in desiccating sessile drops of blood. *Phys. Rev. E—Stat. Nonlinear, Soft Matter Phys.* **84**, 1–5 (2011)
53. Mukhopadhyay, M., et al.: Interfacial energy driven distinctive pattern formation during the drying of blood droplets. *J. Colloid Interface Sci.* **573**, 307–316 (2020)
54. Gulka, C.P., et al.: Coffee rings as low-resource diagnostics: detection of the malaria biomarker plasmodium falciparum histidine-rich protein-II using a surface-coupled ring of Ni(II)NTA gold-plated polystyrene particles. *ACS Appl. Mater. Interfaces* **6**, 6257–6263 (2014)
55. Deegan, R.D., et al.: Capillary flow as the cause of ring stains from dried liquid drops. *Nature* **389**, 827–829 (1997)
56. Xu, T., et al.: Superwetable microchips as a platform toward microgravity biosensing. *ACS Nano* **11**, 621–626 (2017)
57. Han, H., et al.: Single-droplet multiplex bioassay on a robust and stretchable extreme wetting substrate through vacuum-based droplet manipulation. *ACS Nano* **12**, 932–941 (2018)

58. Hou, J., et al.: Hydrophilic-hydrophobic patterned molecularly imprinted photonic crystal sensors for high-sensitive colorimetric detection of tetracycline. *Small* **11**, 2738–2742 (2015)
59. Hernandez-Perez, R., Fan, Z.H., Garcia-Cordero, J.L.: Evaporation-driven bioassays in suspended droplets. *Anal. Chem.* **88**, 7312–7317 (2016)
60. Li, J.F., Zhang, Y.J., Ding, S.Y., Panneerselvam, R., Tian, Z.Q.: Core-shell nanoparticle-enhanced Raman spectroscopy. *Chem. Rev.* **117**, 5002–5069 (2017)
61. De Angelis, F., et al.: Breaking the diffusion limit with super-hydrophobic delivery of molecules to plasmonic nanofocusing SERS structures. *Nat. Photonics* **5**, 682–687 (2011)
62. Lee, M., et al.: Subnanomolar sensitivity of filter paper-based SERS sensor for pesticide detection by hydrophobicity change of paper surface. *ACS Sens.* **3**, 151–159 (2018)
63. Song, Y., Xu, T., Xu, L.P., Zhang, X.: Superwetable nanodendritic gold substrates for direct miRNA SERS detection. *Nanoscale* **10**, 20990–20994 (2018)
64. Surya, H.P.N., Parayil, S., Banerjee, U., Chander, S., Sen, A.K.: Alternating and merged droplets in a double T-junction microchannel. *Biochip J.* **9**, 16–26 (2015)
65. Hatch, A.C., Patel, A., Beer, N.R., Lee, A.P.: Passive droplet sorting using viscoelastic flow focusing. *Lab Chip* **13**, 1308–1315 (2013)
66. Zhu, P., Wang, L.: Passive and active droplet generation with microfluidics: a review. *Lab Chip* **17**, 34–75 (2017)
67. Shang, L., Cheng, Y., Zhao, Y.: Emerging droplet microfluidics. *Chem. Rev.* **117**, 7964–8040 (2017)
68. Gach, P.C., Iwai, K., Kim, P.W., Hillson, N.J., Singh, A.K.: Droplet microfluidics for synthetic biology. *Lab Chip* **17**, 3388–3400 (2017)
69. Feng, S., Shirani, E., Inglis, D.W.: Droplets for sampling and transport of chemical signals in biosensing: a review. *Biosensors* **9**, 1–14 (2019)
70. Chen, D.L., Ismagilov, R.F.: Microfluidic cartridges preloaded with nanoliter plugs of reagents: an alternative to 96-well plates for screening. *Curr. Opin. Chem. Biol.* **10**, 226–231 (2006)
71. Song, H., Ismagilov, R.F.: Millisecond Kinetics on a Microfluidic Chip Using Nanoliters of Reagents. *J. Am. Chem. Soc.* **125**, 14613–14619 (2003)
72. Sciambi, A., Abate, A.R.: Adding reagent to droplets with controlled rupture of encapsulated double emulsions. *Biomicrofluidics* **7**, 1–7 (2013)
73. Abate, A.R., Hung, T., Mary, P., Agresti, J.J., Weitz, D.A.: High-throughput injection with microfluidics using picoinjectors. *Proc. Natl. Acad. Sci. U.S.A.* **107**, 19163–19166 (2010)
74. Hou, L., et al.: A simple microfluidic method for one-step encapsulation of reagents with varying concentrations in double emulsion drops for nanoliter-scale reactions and analyses. *Anal. Methods* **9**, 2511–2516 (2017)
75. Wen, N., et al.: Development of droplet microfluidics enabling high-throughput single-cell analysis. *Molecules* **21**, 1–13 (2016)
76. Droplet microfluidics—a tool for single-cell analysis.pdf
77. Kemna, E.W.M., et al.: High-yield cell ordering and deterministic cell-in-droplet encapsulation using Dean flow in a curved microchannel. *Lab Chip* **12**, 2881–2887 (2012)
78. Edd, J.F., et al.: Controlled encapsulation of single-cells into monodisperse picolitre drops. *Lab Chip* **8**, 1262–1264 (2008)
79. Jing, T., et al.: Jetting microfluidics with size-sorting capability for single-cell protease detection. *Biosens. Bioelectron.* **66**, 19–23 (2015)
80. Jayaprakash, K.S., Sen, A.K.: Droplet encapsulation of particles in different regimes and sorting of particle-encapsulating-droplets from empty droplets. *Biomicrofluidics* **13** (2019)
81. Wu, L., Chen, P., Dong, Y., Feng, X., Liu, B.F.: Encapsulation of single cells on a microfluidic device integrating droplet generation with fluorescence-activated droplet sorting. *Biomed. Microdevices* **15**, 553–560 (2013)
82. Guo, F., et al.: Droplet electric separator microfluidic device for cell sorting. *Appl. Phys. Lett.* **96** (2010)
83. Hemachandran, E., Laurell, T., Sen, A.K.: Continuous droplet coalescence in a microchannel coflow using bulk acoustic waves. *Phys. Rev. Appl.* **12**, 1 (2019)

84. Banerjee, U., Mandal, C., Jain, S.K., Sen, A.K.: Cross-stream migration and coalescence of droplets in a microchannel co-flow using magnetophoresis. *Phys. Fluids* **31** (2019)
85. Sung, Y.J., Kim, J.Y.H., Choi, H.I., Kwak, H.S., Sim, S.J.: Magnetophoretic sorting of microdroplets with different microalgal cell densities for rapid isolation of fast growing strains. *Sci. Rep.* **7**, 1–11 (2017)
86. Navi, M., Abbasi, N., Jeyhani, M., Gnyawali, V., Tsai, S.S.H.: Microfluidic diamagnetic water-in-water droplets: a biocompatible cell encapsulation and manipulation platform. *Lab Chip* **18**, 3361–3370 (2018)
87. Windbergs, M., Zhao, Y., Heyman, J., Weitz, D.A.: Biodegradable core-shell carriers for simultaneous encapsulation of synergistic actives. *J. Am. Chem. Soc.* **135**, 7933–7937 (2013)
88. Xu, Q., et al.: Preparation of monodisperse biodegradable polymer microparticles using a microfluidic flow-focusing device for controlled drug delivery. *Small* **5**, 1575–1581 (2009)
89. Huang, K.S., et al.: Microfluidic controlling monodisperse microdroplet for 5-fluorouracil loaded genipin-gelatin microcapsules. *J. Control. Release* **137**, 15–19 (2009)
90. Zhang, B., et al.: Multifunctional inverse opal particles for drug delivery and monitoring. *Nanoscale* **7**, 10590–10594 (2015)
91. Zhang, H., et al.: Fabrication of a multifunctional nano-in-micro drug delivery platform by microfluidic templated encapsulation of porous silicon in polymer matrix. *Adv. Mater.* **26**, 4497–4503 (2014)
92. Sciambi, A., Abate, A.R.: Accurate microfluidic sorting of droplets at 30 kHz. *Lab Chip* **15**, 47–51 (2015)
93. Huang, M., et al.: Microfluidic screening and whole-genome sequencing identifies mutations associated with improved protein secretion by yeast. *Proc. Natl. Acad. Sci. U.S.A.* **112**, E4689–E4696 (2015)
94. Weiss, M., et al.: Sequential bottom-up assembly of mechanically stabilized synthetic cells by microfluidics. *Nat. Mater.* **17**, 89–95 (2018)
95. Hindson, B.J., et al.: High-throughput droplet digital PCR system for absolute quantitation of DNA copy number. *Anal. Chem.* **83**, 8604–8610 (2011)
96. Pratt, E.D., et al.: Multiplex enrichment and detection of rare KRAS mutations in liquid biopsy samples using digital droplet pre-amplification. *Anal. Chem.* **91**, 7516–7523 (2019)
97. Kleine-Brüggeney, H., et al.: Long-term perfusion culture of monoclonal embryonic stem cells in 3D hydrogel beads for continuous optical analysis of differentiation. *Small* **15**, 1–11 (2019)
98. Liu, L., Dalal, C.K., Heineike, B.M., Abate, A.R.: High throughput gene expression profiling of yeast colonies with microgel-culture drop-seq. *Lab Chip* **19**, 1838–1849 (2019)

Chapter 8

Advances in Microfluidic Techniques for Detection and Isolation of Circulating Tumor Cells



K. Mirkale , R. Gaikwad , B. Majhy , G. Narendran , and A. K. Sen 

1 Introduction

Cancer is the term for a group of diseases in which some cells of the body start dividing uncontrollably. This uncontrolled growth and division lead to the formation of the tumor. There can be two types of tumors benign and malignant. Benign tumors do not spread; they grow quite large and, once removed, usually do not grow back. On the contrary, malignant tumors can spread all over the body. Circulating tumor cells (CTCs) play a significant role in this process. Circulating tumor cells (CTCs) are cells shed from the primary tumor, circulating through the bloodstream. It has been observed that CTCs can be found in patients even before tumors. Thus, CTCs play a role in the early diagnosis and prognostication of cancer disease [1]. When the tumor starts developing at a particular site of the body, some cells from the tumor may get separated and start flowing through body fluid streams. This gives the disease ability to spread from one side to another for its progression. There can be a growth of secondary tumors at distinct regions in the body initiated by circulating tumor cells. Blood-borne metastasis is directly related to most cancer-related deaths; studies have shown that it is responsible for about 90% of cancer-related deaths [2].

Most cancers remain asymptomatic at the early stages and start showing signs at the lateral stages of the disease. Cancer becomes more and more challenging to treat as it progresses, and at some point, it becomes almost impossible to treat. Hence it is very necessary to detect this disease as early as possible. Detection of CTCs in the bloodstream makes it possible as CTCs serve as an essential part of metastasis. However, the detection of CTCs is not an easy job. It is estimated that one teaspoon of blood may contain just 5–50 CTCs [3]. Therefore, there is a need for analysis of blood at the microscale level. Microfluidics is the field that offers optimum fluid control and

K. Mirkale · R. Gaikwad · B. Majhy · G. Narendran · A. K. Sen (✉)
Indian Institute of Technology Madras, Chennai, Tamil Nadu 600036, India
e-mail: ashis@iitm.ac.in

allows integration with extremely sensitive sensors and actuators. Hence, microfluidics seems to be a promising field for developing state-of-art technologies in CTC detection and isolation. CTC detection and isolation methods can be broadly classified as label-free methods, label-based methods, and nucleic acid-based methods [4]. Label-free methods are based on physical properties of CTCs like size, deformability, compressibility, density, dielectric properties, electric impedance [5], viscosity, etc. which differentiates them from other blood cells. Label-based techniques are based on labeling, specifically CTCs using their unique properties like surface antigens [6], metabolic product [7], etc. optical [8], magnetic [9] elements can be used for labeling purposes. Further, to improve capture efficiency, surfaces are modified. Nucleic acid-based [4] method analyzes DNA/RNA present inside the cell nucleus to determine whether it is CTC or not.

2 Detection and Isolation of CTCs

2.1 Label-Free Techniques

2.1.1 Size-Based

Most of the CTCs are larger than the blood cells [10]; size-based isolation takes advantage of isolating CTCs from the blood cells. Size-based isolation of CTCs using filter membranes is a facile method of isolation which is independent of specific binding to antigens and specific surface makers. Here, we have discussed the size-based isolation of CTCs from the blood cells using microfluidic systems. Microfluidic size-based systems [11–14] aim to achieve superior results as compared to microsize-based conventional filter membranes. Many size-based microfluidics systems have been proposed to isolate CTCs from the blood cells. One main concern in size-based isolation is heterogeneity in CTC size in the patient blood lessens the effectiveness. The selection of a critical size may be suitable for most of the cases but not for all patients. While deciding optimum size, many considerations have to be taken care of, such as the difference in blood sample viscosities and the intended throughput. Also, as the cells are deformable proper care should be taken in operation conditions otherwise, motion through narrow openings may cause potential damage to cell membrane due to shear stress and with high-stress cells may die.

Size-based streamline sorting is an alternative to size-based filtration in which each size cell migrates to a definite streamline due to hydrodynamic forces, which are shown in Fig. 1 [15]. After the separation, each streamline with a particular size cell is collected at an outlet. In advantage, the shear stress level on cells in streamline sorting is negligible as compared to stress developed in constricted passage flow, and hence, there is less chance of physical damage to the cell membrane. But, for

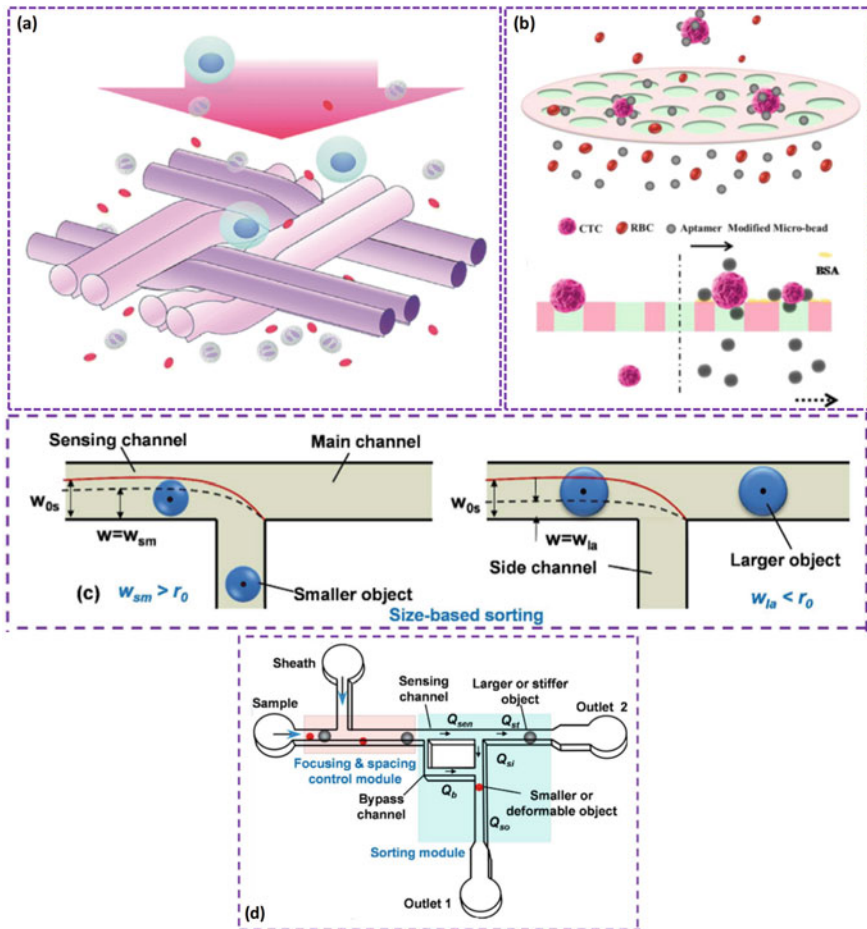


Fig. 1 Size-based sorting of CTCs **a** Hypo-osmotic size-based CTC isolation, and **b** Microbeads enhanced size-based CTC isolation here aptamer modified microbeads get attached to the CTCs results in increasing size of CTCs which improves the capture efficiency of smaller CTCs. (Reprinted from Sun et al. [14] with permission from Elsevier), **c** At low Re, an object tends to flow along the streamline passing through its center of mass, here the main channel bifurcates into two branch channels: straight and side branch channels, with the flow entering these channels separated by a dividing streamline, a bigger particle whose center of mass lies outside the dividing streamline hence particle follows the straight channel, whereas smaller particle goes in the side branch, and **d** schematic illustration of the device with flowrates in the different channel sections (Reprinted from Sajeesh P. [15] with permission from the Royal society of chemistry)

operating the system here, we have to dilute the patient sample with carrier fluids, which may affect the purity of the sample. Also, these devices should be controlled very precisely for achieving efficient sorting.

2.1.2 Deformability-Based

It is a label-free isolation technique, in which target CTC can be separated from blood cells based on deformability despite their nearly equal size. For patients with metastatic castrate-resistant prostate cancer and colorectal cancer, CTCs are nearly identical in size to leukocytes, and CTCs can be isolated based on deformability. CTCs are generally having an enlarged nucleus, and it causes a higher nucleus-to-cytoplasm ratio compared to leukocytes. Young's modulus (E) of the nucleoplasm fluid is approximately three to four times more than cytoplasm fluid and two times more viscous. The deformed cell size can be estimated [16].

$$\frac{r_c^2(4a^2 - \pi r_c^2)U_c}{2\{a^2(\pi\varepsilon - 1) + \pi r_c^2\}} - \frac{\frac{\Delta P}{4\mu_m}(a^2 - r_c^2) + U_c}{4\ln\left(\frac{r_c}{a}\right)} [2(a^2 \ln a - r_c^2 \ln r_c) - (a^2 - r_c^2)] - \frac{U_c \ln a + \frac{\Delta P}{4\mu_m}(a^2 \ln r_c - r_c^2 \ln a)}{2\ln\left(\frac{a}{r_c}\right)} (a^2 - r_c^2) = \frac{\Delta P(a^4 - r_c^4)}{16\mu_m} \quad (1)$$

where ΔP is pressure gradient across the cell, μ_m is media viscosity, a is channel size, r_c is deformed cell size and U_c is cell migration velocity. The tension force acting on the cell membrane as

$$T = \frac{-A\mu_m}{l} \left[\frac{\Delta P r_c}{2\mu_m} + \frac{\frac{\Delta P}{4\mu_m}(a^2 - r_c^2) + U_c}{r_c \ln\left(\frac{r_c}{a}\right)} \right] \quad (2)$$

According to Kelvin–Voigt viscoelastic solid model by considering the cell is a viscoelastic solid, tension force (T) on the cell can be estimated as

$$T = \frac{G}{2} \left(\lambda^2 - \frac{1}{\lambda^2} \right) + \eta_m \frac{2}{\lambda} \frac{\partial \lambda}{\partial t} \quad (3)$$

where λ is the extension ratio of the cell. On replacing shear modulus (G) with Young's modulus (E) as $G = \frac{E_c l}{2(1+\nu)}$, Young's modulus of the cell can be estimated as

$$\frac{E_c l}{4(1 + \nu)} \left(\lambda^2 - \frac{1}{\lambda^2} \right) = \frac{-A\mu_m}{l} \left[\frac{\Delta P r_c}{2\mu_m} + \frac{\frac{\Delta P}{4\mu_m}(a^2 - r_c^2) + U_c}{r_c \ln\left(\frac{r_c}{a}\right)} \right] \quad (4)$$

Figure 2a, b represent a deformability-based microfluidic device for CTC isolation having arrays of tapered constrictions that deform cells, and oscillatory force gives a

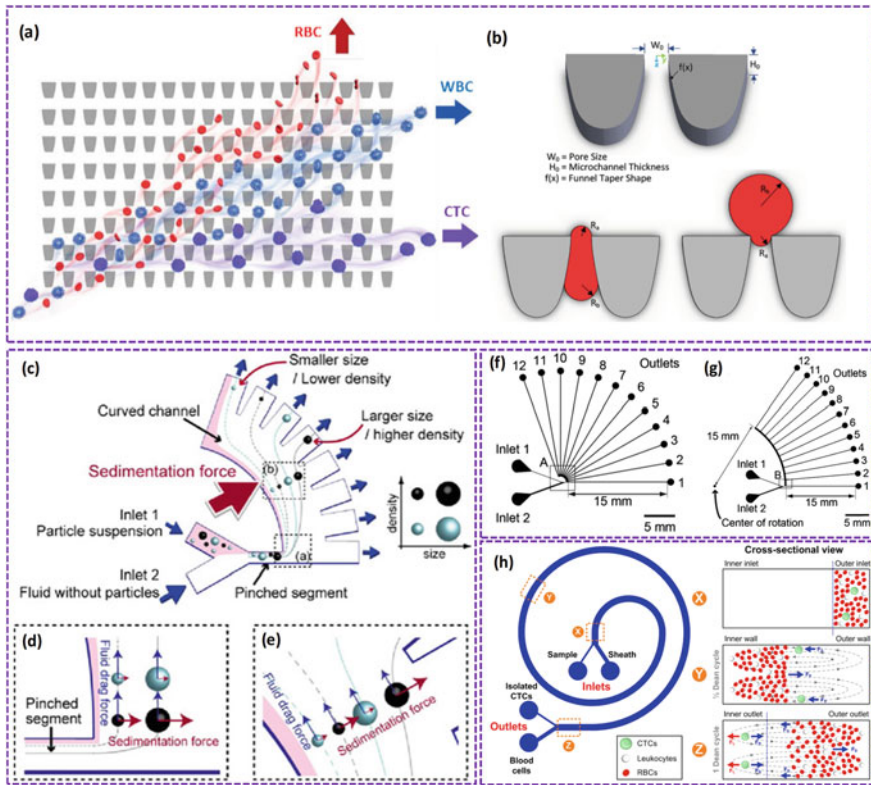


Fig. 2 a Schematic illustration of continuous isolation of CTCs from RBC and WBC based on deformability using an oscillatory flow through tapered arrays of constriction. As RBC are highly deformable, they pass to the top whereas more rigid CTCs move a little diagonal and are collected horizontally, b Size and structure of the micro-tapered constrictions (Adapted from Park et al. [5] with permission from John Wiley and Sons), c Schematically showing the isolation using sedimentation pinched flow, enlarged view of (d) forces acting immediately after the pinched segment, and (e) sedimentation force acting in a curved channel. In the pinched segment, particles are near the upper wall as they move in the curved channel they experience the sedimentation force. The large density particles move away from the streamline and we get density-based sorting. Channel designs for (f) particle inertia (g) device rotation (Adapted from Masumi et al. [18] with permission from American Chemical Society), h schematic illustration of CTCs separation using dean flow fractionation (Adapted from Han Wei Hou et al. [22] from Springer Nature)

continuous motion to the cells. As cells deform in a continuous flow without any accumulation, the hydrodynamic resistance remains constant, which preserves the separation process. Using both size and stiffness properties of cells, MCF-7 and MDA-MB-231 cancer cells have been isolated from PBMCs (peripheral blood mononuclear cells) with the help of non-inertial lift induced lateral migration microfluidics technique [17].

2.1.3 Density-Based

Figure 2c shows sedimentation-based pinched-flow-fraction-action (PFF) technique to achieve density-based CTCs isolation [18]. It is of two types: one is the inertial microfluidics method in which inertial force acts on the particle due to momentum change in the curved shaped channel and the second is the centrifugal microfluidics method in which centrifugal force acts on the particle due to rotation of the device. In the inertial method, the outlets are connected to a small radius (1 mm) curved channel, as shown in Fig. 2f [19–21]. An active pressure-driven flow is employed to give motion to the fluids and particles. When the fluid comes out of the pinched section and enters the curved section, a sediment force acts on the particles due to inertia perpendicular to flow direction, which drives away the particles outward. The higher density particles move more outward than lower density particles. Hence different density particles can be separated even they have the same size.

The sedimentation velocity (U_s) of the particles in the curved section can be estimated as $U_s = \frac{\rho_p}{18\mu r_c} D_p^2 U^2$, where ρ_p is particle density, μ is the viscosity of fluid, r_c is the radius of curvature of the curved channel, D_p is the diameter of the particle, and U is the average velocity of flow. As the migration distance of the particles is directly proportional to the flow rate, hence migration distance will be high at a higher flow rate, but at a lower flow rate separation will be size-based.

In the second centrifugal pinched flow fraction method, the curvature radius of the curved channel is comparatively high 15 mm for achieving higher centrifugal force and to have a long retention time (t) (see Fig. 2g). The device is rotated at 3000 and 750 rpm for a time of 30 and 300 s respectively. The velocity of sedimentation U'_s is a function of both centrifugal force and inertia force which is expressed as:

$$U'_s = U_s + U_c = \frac{\rho_p}{18\mu r_c} D_p^2 U^2 + \left(\frac{\rho_p}{18\mu} - \frac{\rho_f}{18\mu} \right) D_p^2 r_d \omega^2 \quad (5)$$

where U_c is migration velocity due to centrifugal force, ρ_f is the density of the fluid, r_d is the distance between the center of rotation and the particle, and ω is device rotation angular velocity. Due to the centrifugal force, the resolution of particle isolation based on density is improved. Along with, in the centrifugal PFF, external pumps are not required and have high separation efficiency. But the throughput of centrifugal PFF is lower than inertial-based PFF.

For flow through the curved microchannel, due to the centrifugal effect, a secondary flow develops, which is called ‘dean flow’ [22], which is shown in Fig. 2h. The fluid pressure near to inner wall is higher than that near the outer wall for flow through the curved channel. So, the fluid mass from the center of the channel is moved outward, and the fluid near to the bottom and top walls moves inward by satisfying the conservation of mass. This creates a symmetrically swirling two counter-rotating vortices in the channel cross-section. This secondary flow will decide the equilibrium position of the particles along with inertial lift forces. The transverse dean drag force (F_D) carries particles toward the inner wall from the top and bottom. However, the particles placed in the mid-plane between the top and bottom walls are moved toward the outer wall and recirculated. The equilibrium position of the particles depends on the ratio of inertial lift force (F_L) to dean drag force (F_D) and on Reynold’s number. The dean drag force acting on the particle for dean flow can be estimated as $F_D = \rho_m D_h^2 U_m^2 a / r$, where U_m is maximum channel velocity. Microbeads conjugated, which enhances sedimentation rates of different cells, can be used for separating CTCs from blood cells [23].

2.1.4 Compressibility-Based

The unique feature of the tilted-angle standing surface acoustic wave (taSSAW) based system is to carry out CTCs isolation from blood cells based on the compressibility of the cells. By taSSAW, the pressure nodal lines are induced at a particular angle with the flow direction. With this, the particles in the fluid experiences both drag force and acoustic radiation force. The relative magnitude between these two forces decides the position of the particles and motion of the particles along the nodal lines. The primary acoustic radiation force is given below [24]

$$F_{\text{ARF}} = 4\pi a^3 \phi k_y E_{ac} \sin(2k_y y) \quad (6)$$

where, $\phi = \frac{1-\tilde{\beta}}{3} + \frac{\tilde{\rho}-1}{2\tilde{\rho}-1}$, and $\tilde{\beta} = \frac{\beta_p}{\beta_m}$, $\tilde{\rho} = \frac{\rho_p}{\rho_m}$, $\tilde{z} = \frac{z_p}{z_m}$
 $k_p = \frac{1}{\rho_p c_p^2}$, $k_m = \frac{1}{\rho_m c_m^2}$, $z_p = \rho_p c_p$, $z_m = \rho_m c_m$

Where F_{ARF} is primary acoustic radiation force, a is the radius of the particle which is smaller than the wavelength, E_{ac} is acoustic energy density, $k_y = 2\pi/\lambda$ is the wavenumber, y is the distance from the wall, w is the width of the channel, and ϕ is the acoustic contrast factor. ρ_p , β_p and z_p are density, compressibility, and the acoustic impedance of particles respectively. ρ_m , β_m and z_m are density, compressibility, and the acoustic impedance of medium respectively. c_p and c_m is the speed of sound in particle and medium, respectively.

Spatial separation between cells depending on different properties can be estimated as [25].

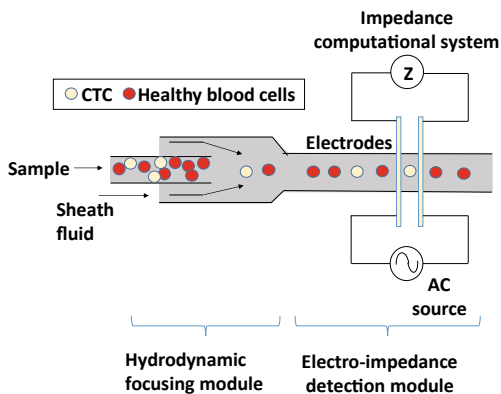
$$u_r = \left(\frac{\pi a^2 p_o^2 \beta_w}{9\lambda\mu} \right) \left(\frac{5\rho_p - 2\rho_m}{2\rho_p + \rho_m} - \frac{\beta_p}{\beta_m} \right) \tag{7}$$

The compressibility of normal leukocytes is $3.99 \times 10^{-10} \text{ Pa}^{-1}$ whereas compressibility of MCF-7 breast cancer cell is $4.22 \times 10^{-10} \text{ Pa}^{-1}$, along with the diameter of normal leukocytes, is $\sim 12 \text{ }\mu\text{m}$ compared to MCF-7 is of $\sim 20 \text{ }\mu\text{m}$ in diameter. Since they have both compressibility and size differences, and both these properties affect isolation. From the expression as we observed compressibility acts against size. Ding et al. 2014 have isolated HL-60 (human promyelocytic leukemia) cell (diameter $\sim 15 \text{ }\mu\text{m}$, density $\sim 1.075 \text{ kg/m}^3$ and compressibility $\sim 4 \times 10^{-10} \text{ Pa}^{-1}$) from polystyrene beads (diameter $\sim 15 \text{ }\mu\text{m}$, density $\sim 1.075 \text{ Kg/m}^3$ and compressibility $\sim 2.16 \times 10^{-10} \text{ Pa}^{-1}$) based on the compressibility.

2.1.5 Electro-impedance Spectroscopy

Electro-impedance spectroscopy is an important tool for several applications varying from simple cell counting to different cell identification. Characterization of dielectric properties can be done in two ways AC electrokinetics and impedance spectroscopy. AC electrokinetics is used to study movement or rotation, etc. related behavior of particles [26]. Electrical impedance spectroscopy measures the dielectric properties of particles suspended in the medium. In different studies, it is observed that the Electric impedance of CTCs is different from other healthy cells at different frequencies [5, 27, 28]. This method is label-free and cost-effective. General electro-impedance-based flow cytometer consists of inbuilt microelectrodes fabricated using a micro-fabrication technique, which can measure the impedance of the particle flowing through the microfluidic stream. Those particle needs to be focused in the flow of the single-particle stream to avoid multiple particle encounter at electrode region, as shown in Fig. 3. Some systems have studied single-cell impedance by trapping it in a particular region [5].

Fig. 3 Schematic of electro-impedance CTC detection consisting of two different modules, one hydrodynamic focusing module where cells are focused and second electro-impedance module where the impedance of a single cell is measured



2.1.6 Inertial Microfluidics

Detection and isolation of the cellular subpopulations is a primary method followed in several biomedical practices. The label-free method is one of the elementary methods of separation by using the mechanical and electrical properties of the cell. Several label-free technologies were demonstrated in the identification of circulating tumor cells (CTCs). The most conventional form of label-free technique is the use of micro-filtration and centrifugation to collect the target cells. Membrane filtration functions by a size exclusion process across a porous matrix capable of retaining larger cells and enabling smaller cells to pass. It is very useful in pre-enrichment treatment to separate cell aggregates, but clogging complicates the process of retrieving larger target cells. Centrifugation is another well sought-after method to separate cells depending on their size and density.

Inertial focusing microfluidics has emerged as the most promising approach for CTCs isolation with better resolution. The earliest interpretation of the particle focusing was reported by Segre [29] in the 1960s. It was observed that along the flow length, the particle tends to distribute between the pipe centerline and the wall circumference. This effect is due to the result of two major inertial forces: the shear-induced lift force and wall induced lift force. Besides the above forces, the stoke drag force induced secondary flow is a major responsible factor for inertial migration and focusing. The presence of secondary flow in the curved channels is reported as dean vortices. It arises as a result of the mismatch in fluid momentum across the channel cross-section due to the centrifugal acceleration. The strength of this secondary flow is characterized by the Dean number (De).

The pioneering work on the inertial focusing effect of the particles in microfluidic devices was reported by Di Carlo's group [30], Di Carlo et al. [31], Papautsky's group [32], etc.

2.1.7 Microfiltration

The earliest form of membrane filter to separate cells and microparticles was introduced during the late 1980s. A two-stage membrane filter was fabricated in a silicon structure to demonstrate the particle separation below 50 nm [33, 34]. The membranes are positioned in such a way that during the filtration process, the flow passes the first membrane, and it reaches the hole by overcoming the gap between the two membranes. This configuration ensures a double filtration by recapitulating membrane filters with a microstructure design. Some have reported particle separation by using a porous medium [35, 36]. For example, a whole blood sample is separated into cell and serum components using the porous filter [36]. Aran et al. [37] demonstrated similar blood plasma separation by a porous polycarbonate using a pore size of 200 nm. Active methods exploit other filtration types such as weir and pillar type microfilter for blood plasma separation [38]. The use of weir filters for the separation of RBC and WBC from the blood was reported by Wilding et al. [39], their results showed that the separation is highly influenced by the weir dimension and the

number of microfilters constructed in the channel. Wu et al. [40] demonstrated the dead-end weir type microfilter for blood plasma separation. The device uses 6 μm holes to prevent RBC clogging and allowed them to move freely to the next chamber.

In the case of pillar type microfilter, the gap between the pillars is very crucial for particle separation. Ji et al. [41] reported a comparative study among different microfilter types for effective separation of RBC and WBCs. According to them, the pillar type filters are more appropriate for genomic studies, and it is better than weir and membrane type filter. A combined two-stage separation process was proposed by Chen et al. [42], in the first stage, cell capture structures are used, and the second stage has pillar type separation for better separation efficiency. Also, induced mechanical oscillations were included in the pillar type filtration to reduce clogging; this enabled the smaller particles to pass through the filter with ease but difficult for larger particles [43]. Subsequently, crossflow techniques are employed for microfluidic trapping devices to avoid clogging [44]. In crossflow devices, the flow is tangential across the membrane cross-sectional filter, and the permeable solution is allowed to pass through the filter. The transmembrane pressure developed in the crossflow device directs the small cells to pass through the gap, while larger cells are targeted in the trapping sites [45].

2.1.8 Dielectrophoresis

A particle in a non-uniform electric field gets polarized and experiences a force due to the electric field. This phenomenon is called dielectrophoresis (DEP). Depending on the polarization of the particle DEP can be divided into two categories: negative dielectrophoresis (nDEP) and positive dielectrophoresis (pDEP). When the particle is more polarized than the medium, the DEP force tends to the particles move toward the higher intensity electric field. Contrarily, the particle is moved toward the lower electric field at higher polarizability of the medium to generate nDEP effect [46]. The particle separation is made possible by controlling DEP forces and Clausius–Mossotti (CM) factor. The CM factor is influenced by the relative permittivity of the particle and the medium; by optimizing the applied voltage the permittivity can be changed. The frequency at which the CM factor switches the sign is termed as the crossover frequency. Applying the frequency in between the crossover frequency, the particles DEP forces can be shifted to opposite directions and the particle can be separated effectively.

The handling of particles has been demonstrated with both continuous and batch forms of DEP [47]. In a simple batch process, a particle is trapped in positive DEP electrodes, and other particles influenced by nDEP are repelled. Hence, the particles affected by the nDEP can be moved and separated from the trapped particles. However, a major limitation is the low separation throughput of the method due to which it is less preferred, nonetheless, the batch process is a simpler platform [48]. Notably, a continuous process is quite popular among researchers, since particles can be manipulated toward a specific target outlet [49, 50]. But compared with the batch process continuous process is more complex due to several dependent factors such as

flow rate, voltage, frequency, and geometry. Later, several researchers demonstrated the DEP technique to isolate CTCs [51–54]. Das et al. [51] simultaneously used nDEP and pDEP to capture HeLa and optimized the design factors to manipulate the cells without electroporation. Chan et al. [54] developed a curved microelectrode for DEP deformation study of Breast cancer cells. The platform is fabricated with an array of DEP microelectrodes in a glass slide over which the cancer cells are pipetted. They observed cell shrinkage and bleeding when the cells are subjected to a higher frequency and peak electric field.

2.2 Label-Based Techniques

There are two types of CTC isolation systems under label-based techniques positive sorting systems and negative sorting systems.

2.2.1 Positive Sorting

In positive sorting, Cells that are of interest are labeled and are isolated. In this case, CTCs are the cell of interest, which can be labeled by various methods. A prevalent method of labeling CTCs is targeting surface antigens present on them. EpCAM is a widely used transmembrane glycoprotein, targeted via antibodies for labeling. There are other different surface antigens like MUC1, HER2, etc. depending on the type of cancer. National Cancer Institute has published a list of 75 prioritized cancer antigens and its comparative study [6]. Once the target cells are detected, they can be separated. In this type of technique, CTCs are detected based on naturally occurring surface proteins. Depending on detection and isolation methods there can be three types of techniques: immunofluorescence technique, immunomagnetic technique, surface adhesion-based techniques.

Immunofluorescence technique

In this technique, CTCs are immunofluorescent-labeled using dyes or nanoparticles [55]. The selectivity of labeling is accomplished by targeting CTCs via antibodies depending on antigen present on their surface. Only cells having those biomarkers are attached to fluorescently labeled antibodies, which upon illumination emits a light signal of a particular wavelength. Detecting this signal indicates the presence of antibodies on the surface of the cell, which indirectly detects CTC. The immunofluorescence technique can detect multiple types of CTCs simultaneously. Shota Izumi et al. demonstrated dual fluorescence imaging at different fluorescence wavelengths using different fluorescent-labeled antibodies, which target two different surface proteins EpCAM and EGFR [8]. Image cytometry is a popular technique through which the advantages of image processing and microfluidics can be combined. Fluorescent-labeled CTCs are detected by image analysis [56]. Nanoparticles-based labeling

represents the state-of-the-art technology in CTC detection using immunofluorescence technique. Nanoparticle probes are most widely used in cancer diagnostic applications. Quantum dots (QDs), polymer dots (PDs), upconversion nanoparticles (UCNPs), and gold nanoparticles (AuNPs) are widely used nanoprobe in cancer diagnosis. Quantum dots are nothing but single crystal semiconductor nanoparticles that are inherently fluorescent due to the bandgap present between their energy levels. Nanoparticles are considered to be highly efficient tagging elements because of their properties like broad absorption spectrum, large molar absorption coefficients, tunable emission wavelengths, longer fluorescence lifetimes (>10 ns) compared to organic dyes (1–5 ns) [55].

Constant detection and separation of cells are achieved by flow cytometry. These flow cytometers are based on fluorescence-activated cell sorting (FACS) technology. The development of micro-flow cytometers introduced the use of micro-optical instruments like optical fibers [57], Fresnel microlenses [58], bARROW [59], etc. This eventually gave rise to the distinct discipline of research micro-optofluidics, which is collaboration microfluidics and optics. The basic micro-flow cytometer consists of 3 sub-units, a Hydrodynamic focusing unit, Optical detection unit, and an Isolation unit.

Hydrodynamic focusing is the initial step in the flow cytometer in which focuses a stream of particles/cells in a jet of fluid in microchannels. The fixing pathway of cells for sensors and actuators plays a vital role as a slight variation in the position of cells can vary the amount of signal reaching sensors and may lead to failure at the isolation unit. Hydrodynamic focusing is generally achieved using sheath fluid. In 2-dimensional hydrodynamic focusing, cells are focused on a single plane, while in 3-dimensional hydrodynamic focusing cells are focused on a single-particle stream.

The optical detection unit is responsible for optical signal detection emitted by fluorescent-labeled cells. It contains optical instruments like a laser, photodetectors, optical filters, etc. As cells flow through the cytometer, they are illuminated by a laser, which results in the scattering of light as well as fluorescence emission. Scattered light provides information about cell morphology, while fluorescence helps us in the detection of the target cell. In a typical flow cytometer, there are three kinds of optical signals: forward scatter (FSC), side scatter (SSC), fluorescence (FL). Forward scatter (FSC) represents the size of the cell, whereas side scatter (SSC) represents information regarding cellular content.

For detecting light signals, various kinds of photodetectors can be used depending on the sensitivity needed. A simple photodetector or avalanche photodetector can be used for detecting signals like FSC or SSC. However, for a small signal like a fluorescence signal from a cell, we may need highly sensitive photodetectors like a single-photon counter. The wavelength of the fluorescence signal depends on the fluorophore we have used for tagging. For detecting fluorescence, we have to focus only on a particular fluorescence wavelength signal avoiding other signals which act as noise. For this purpose, optical filters are used before photodetectors. Even the laser in the system has to be chosen based on the fluorophore we are using in the system. The wavelength of the laser must be smaller than the fluorescence wavelength of the fluorophore. Various other factors like output power, beam quality, the polarization of

output light, etc. are some important factors that need to be taken into consideration while designing the laser system.

The isolation unit takes input from the detection unit and performs segregation. Isolation methods can be broadly classified into two types: direct isolation, droplet-based isolation. In the direct isolation method, cells are separated directly through the stream. Whenever CTC is detected, detection unit generates pulse and isolation unit isolates those cells in different channel outlets. Various forces can be used for separation purposes like dielectrophoretic force [47], magnetophoretic force [60], acoustic force [61], etc. The electrokinetic method used for cell separation is mostly dielectrophoresis, as cells are not charged particles inherently. The magnitude of the DEP force is proportional to the gradient of the electric field. This force, applied by the isolation unit, which depends on input from the detection unit, helps cell changing their path inside the channel according to the electric field. If magnetic beads are used for labeling, simple magnet can be fixed in the system to deviate the path of the target cells (Fig. 4c). Magnetophoresis requires immunomagnetic labeling to which is discussed in the forthcoming section. Force exerted on cells in acoustophoresis is due to applied acoustic signal forming standing waves inside the channel. Acoustic-based

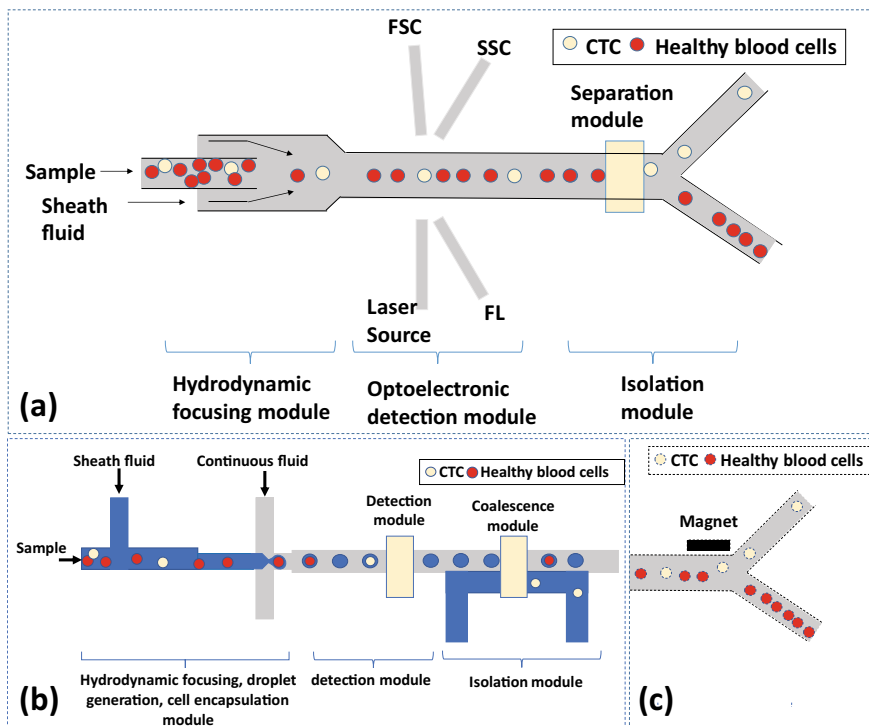


Fig. 4 Schematics of **a** Micro-FACS system showing different modules, and **b** CTC detection and isolation using droplet coalescence, **c** CTC isolation using an immunomagnetic technique where CTCs tagged with magnetic beads are deflected based on magnetic properties

separation offers excellent biocompatibility and high throughput. A schematic of generalized direct particle manipulation-based FACS is shown in Fig. 4a. In droplet-based separation, cells are encapsulated inside droplets, and efforts are made to separate those droplets using conventional droplet microfluidic techniques. Whole droplet manipulation can be done by using SAW [62]. Coalescence techniques like acoustic-coalescence [63], electro-coalescence [64], magneto-coalescence [65], etc. can also be useful for droplet isolation. Figure 4b represents a typical droplet encapsulation isolation technique. The advantage of droplet-based detection and isolation is that the cell remains encapsulated inside the droplet throughout the process, which keeps the cell protected. Thus, these cells can also be used for further processing and analysis.

Immunomagnetic technique

All human tissues are diamagnetic except RBCs because of its iron content [66]. This property opens up the opportunities to use the magnetic field to effectively detect and isolate CTCs. To use the Immunomagnetic detection and separation technique in a microfluidic chip, we have to take care of hydrodynamic flow focusing inside the channel, as mentioned in the immunofluorescence technique. The immunomagnetic technique also uses the principle of antigen–antibody binding. In this method, antibodies are tagged by magnetic microbeads or nanoparticles instead of fluorophores. It does not only detect but also helps in the mechanism of isolation. Using a magnet in a micro-flow cytometer helps in the isolation of the labeled cell, as shown in Fig. 4c, which enhances recovery and purity rate. To further improve effectiveness and selectivity, A wavy-herringbone (wavy-HB) structured microfluidic device can be used. In this type of device, passive turbulence is created, which increases the possibility of tumor cells colliding to the device wall, and consequently, the capture efficiency of CTCs [9]. The performance of an immunomagnetic technique depends on the binding efficiency of magnetic particles. The binding between primary antibody and magnetic particles can be achieved in two ways, one is direct bonding in which primary antibodies are labeled directly by magnetic particles. Another method is through secondary antibodies, in which the primary antibody is labeled using secondary antibodies, which are associated with magnetic particles. These secondary antibodies can bind to the primary antibody using a very specific epitope. Movement of the magnetic particle inside a diamagnetic medium or diamagnetic particle in the magnetic medium (ferrofluid) refers to magnetophoresis. Magnetic susceptibility of labeled cells makes isolation via magnetophoresis possible.

Magnetic particles per unit cell have to be maintained within limit by avoiding interparticle interference. Magnetic particle load per unit cell may increase if already attached magnetic particles try to attract other free particles suspended in the medium. Overexpression of the magnetic particles or the use of large-sized magnetic particles can reduce device performance due to steric hindrance. It can rupture the cell membrane due to the large momentum produced [4]. Thus, more care has to be taken while handling magnetic nanoparticles in microfluidic detection techniques.

Surface adhesion-based CTC isolation

Interaction between solid surfaces and cells has been used as a successful strategy for the separation of CTCs with different kinds of surfaces. Compared to other immunochemical labeling methods, this method requires no or fewer sample preprocessing. Thus, this method is also popular due to its simplicity and accuracy. The basic principle for surface adhesion relies on differential adhesion potential between the target cells and non-target cells. There can be two types of approaches for adhesion-based isolation, implementing specific surface patterns, and immobilizing immuno-affinity binding molecules. Due to the laminar nature of the fluid in microchannels, there are limitations in cell and surface interaction; hence, various approaches are taken like modifying the surface or creating passive turbulence inside the channel [9]. Patterning the nanostructure increases surface area and in some cases, it distributes the flow, enhancing the effective contact area between fluid and surface. This approach can be often combined with other isolation techniques for further enrichment of CTCs. Immune-affinity binding molecules are even attached to silicon surfaces having thousands of micro-posts etched inside the channel for efficient detection and isolation of CTCs [67]. It has been observed that the capture efficiency of CTCs was further improved by the integration of the microfluidic system with a Silicon nanowire (SiNW) array instead of the planar surface in Immunomagnetic isolation [68]. In this method, small numbers of CTCs were first captured after recognizing them by EpCAM-binding magnetic upconversion nanoparticles (MUNPs) and then pulled down on the SiNW-substrate using a magnetic field.

In an immobilizing immuno-affinity binding molecule of CTCs detection technique, CTCs are made immobilized on the surface of the sensor using affinity molecules. Biofunctionalized field-effect transistor (BioFET) based CTCs detection can be classified into this method. Because of the high surface area to volume ratio in the nanostructure, even electrical properties vary drastically for small change, which makes detection of the molecule possible. A field-effect transistor (FET) is an electronic device output whose current varies according to gate potential. Achieving nanoscale gate structures like silicon nanowire (SiNWs) [69], two-dimensional graphene [70], etc. we can develop highly sensitive electrical biosensors. For detection, these cells need to be immobilized, which is done using antibodies. While the fabrication of BioFET, these antibodies are attached to these nanowire structures. Once an affinity molecule captures the antigen, charge transfer takes place to the gate area affecting the output current of the device. The other cells which cannot bind to the surface-immobilized molecule do not affect device output current. This technique avoids pre-labeling and other preprocessing of the sample.

Metabolic labeling

As we have seen antibody-based CTC detection and isolation system provides a very reliable approach, which can accurately detect CTCs by keeping track of their specificity. However, these kinds of methods only work when surface protein expression is sufficient and is in detectable amounts on the cell, e.g., EpCAM is a widely targeted surface protein when it comes to lab-on-chip devices, but it has been observed that

1831 (55%) of 3347 tumors showed EpCAM expression out of which 907 were strong and 926 were moderate to weak. Cancer cells have the ability through which, it can undergo epithelial to mesenchymal transition, which further reduces Existing EpCAM expression on the cell surface [2]. Hence, EpCAM-based CTC detection may not be effective when it comes to detection and isolation of CTCs showing weak to no expression of EpCAM. Hence various efforts are being made to develop a method ideally, which can label all kinds of CTCs. Metabolic labeling is one of the methods which can be used for this purpose. This approach uses the inherent property of cancer cells in terms of glucose metabolism, which can be explained by the Warburg effect [71]. Various detection methods have been developed, which use optical [72], magnetic nanoprobes [73, 74].

2.2.2 Negative Sorting

It is one of the methods of cell sorting in which cells that are not of interest are labeled, detected, and separated. As leucocytes and CTCs are of comparable size, this technique can be used to enrich CTCs after size-based separation. We can target antigens like CD45, CD15, etc., which are present on the surface of leukocytes [75]. This method is also beneficial in the case of the epithelial-mesenchymal transition (EMT) in which the method of tagging EpCAM on the surface of CTCs can become ineffective as EpCAM expression is lost during EMT.

2.3 Nucleic Acid-Based CTC Detection

Nucleic acid-based CTC detection is based on the detection of specific DNA/ RNA sequences (marker) representing CTC-specific genes. These methods also have good specificity in the detection of CTC, but the drawback of this method is that we need to lyse the cell to get nucleic acid and hence cannot retain viable cells after the detection process. The nucleic acid-based approach offers high sensitivity for CTC detection when combined with PCR (polymerase chain reaction) for a very small amount of sample. CTC detection is observed to be more productive using m-RNA than DNA as free DNA molecule analysis may sometimes produce false results [4]. Microelectronic sensors like BioFET are also proved to be very sensitive when it comes to nucleic acid sequence detection [76]. Even though Nucleic acid-based CTC detection has very good specificity, it can reduce the accuracy of detection. Inflamed non-cancerous in the circulation can produce false-positive signals from tissue- and organ-specific markers. Also, none of the markers so far has been assigned as entirely CTC-specific as studies have shown that they can be present inside the blood cells or immune cells [4].

A summary of all label-free and label-based detection and isolation techniques in terms of their limitations and advantages are illustrated in Table 1.

Table 1 Summary of CTC detection and isolation techniques

Techniques	Influencing factor	Limitation	Advantages
Size-based	Size difference	Low recovery rates due to large variations in the size of CTCs, which may overlap with leukocytes, and low purity	High throughput
Deformability-based	Young's modulus of the cells	Stress level is high that can damage the cell membrane	High specificity High purity
Compressibility-based	Compressibility of cells	Stress level is high that can damage the cell membrane	High specificity High purity High throughput
Density-based	Inertia force	It is a time-consuming and labor-intensive process, effective for higher flowrates	High specificity Highly sensitive High throughput
	Centrifugal force	Stress level is high, low throughput	High resolution High separation efficiency No external pumps Very fast process
Electro-impedance technique	The impedance of the cell	Requires addition electrical circuitry for accurate impedance detection	Specificity High throughput Label-free Low cost
Dielectrophoretic	Electrical properties of the cell and medium	Low recovery rate Sometimes generate air bubbles due to high electric field	High throughput Very high sensitivity
Immunofluorescence technique	Fluorescent-labeled antibodies attached to surface antigens of CTCs	Lack of universal surface antigen which can be used to detect all types of CTCs Uses expensive dyes, antibodies, Requires a separated isolation system	High specificity High purity High throughput High post-processed cell viability Multiple-fluorescence technique can detect multiple types of CTCs

(continued)

Table 1 (continued)

Techniques	Influencing factor	Limitation	Advantages
Immunomagnetic technique	Micro-magnetic particles associated antibodies attached to surface antigen of CTCs	Lack of universal surface antigen which can be used to detect all types of CTCs Magnetic beads can induce high momentum which can rupture cells, Uses expensive magnetic beads, antibodies, ferrofluid, etc.	High specificity High purity High throughput Doesn't require separate detection and isolation systems
Adhesion-based CTC isolation	A surface pattern which can trap CTCs after detection	Complex fabrication techniques The expensive fabrication process The cell may get damaged in the micro-array like structure	High specificity High purity High throughput Surface traps enhance capture efficiency
	Immobilized antibodies-CTCs on the surface of the microelectronic sensor	A limited number of CTCs can be detected at a time Different methods like backflow of channel necessary to detach CTCs from surface	High specificity High purity High sensitivity Can detect CTC in a large sample volume Avoids sample pre-labeling and other preprocessing
Metabolic labeling	Cellular metabolism product specific to cancer cells	For detection fluorescence techniques or magnetic nanoparticles are needed which increases the cost of the system For fluorescence detection preprocessing for labeling is required which consumes time	High specificity High purity High throughput Potential universal biomarker for cancer cell
Negative sorting	WBCs are labeled and separated from CTCs-WBCs pool	Reduce purity due to the presence of WBC subtypes with low surface antigen (CD45, CD66b) expression The labeling method increases the cost of the system	High specificity High throughput Higher yield than positive sorting method Can be used to harvest all types of CTCs

(continued)

Table 1 (continued)

Techniques	Influencing factor	Limitation	Advantages
Nucleic acid-based CTC detection	CTC-specific gene marker present in the nucleic acid of the cell	Low accuracy, can give false result due to inflamed, non-cancerous cells CTCs have to be lysed to get nucleic acid hence no postprocessing cell viability, cannot use cells for further analysis High cost	High specificity High sensitivity Can detect CTC in a large sample volume

3 Limitations in Microfluidic-Based CTCs Detection and Isolation

3.1 Lower Abundance of CTCs in Blood Cells

Lower abundance of CTCs as compared to other blood cells is a major challenge in CTC detection. The number of CTCs per unit volume of the cell is as tremendously low as 1–10 CTCs per 7.5 ml of blood [2]. This indicates there are hundreds to few thousands of CTCs per millions of leukocytes (WBCs) or billions of erythrocytes (RBCs) [77]. Hence, even though microfluidics technology has the capability of deriving accurate results from a very small sample size, we need at least 3 ml of blood for testing [2]. Therefore, isolating such a small number of CTCs from the pool of millions and billions of blood cells is challenging.

3.2 Non-specificity

This limitation is mostly faced by label-free approaches of CTC detection and isolation techniques. Size and bio-characteristics of CTCs and leukocytes (WBCs) overlap to a significant extent [2]. Also, CTCs show variation in size among themselves with sizes varying from 4 to 30 μm [4]. Even though size-based isolation of CTCs is label-free and straightforward, the non-specificity reduces accuracy. Acoustic methods have proven to be an efficient approach for cell sorting as it maintains cell viability. It also struggles to differentiate among CTC and WBCs because of the lack of difference in acoustic properties among blood cells [78].

3.3 Epithelial to Mesenchymal Transition (EMT)

Epithelial to mesenchymal transition (EMT) is a biological process in which epithelial cell tends to lose its property of the cell to cell adhesion by changing its phenotype to mesenchymal cells and gain migratory and invasive properties. This process is essential in wound healing, neural tube formation, etc. in healthy cells. However, when CTCs undergo EMT, they cause further progression in cancer by tumorigenesis. EMT increases challenges in label-based CTC detection as it lowers the EpCAM expression on surfaces of CTCs [79].

3.4 Lack of Universal CTC Identification Technique

As mentioned earlier, label-free techniques suffer from non-specificity. Also, as mentioned in the previous label-based detection methods, there is no single cancer cell surface protein or no single dedicated gene marker which can detect CTCs. Even though EpCAM-based labeling method is widely used and one of the reliable methods for CTC detection, there are problems like low/no surface proteins on various kinds of CTCs, reduction in EpCAM expression during the epithelial-mesenchymal transition, etc. Thus multiple efforts are made to find an alternative for EpCAM which leads to a finding of cancer cell markers like VCAM-1, ICAM-1, CEA, CA19-9, CA72-461, pepsinogens62, MUC163, EphB4, CD446, CD133, CD146, CK18, CK195, Ctnnd164, PSMA, HER245, EGFR65, TROP-2, and FAP α , etc. [2]. Most of these markers are specific to only certain types of cancer cells and hence could not be an alternative leaving behind EpCAM as a universal biomarker for CTC.

3.5 Post-processed Cell Viability

One of the vital objectives of CTC detection and isolation is to study and analyze the properties of CTCs. Thus, cells need to be viable after isolation. The various aspects of detection and isolation techniques can damage cells. Physical microstructures like micro-posts, microciliated structures trapping cancer cells, filter microstructures induce large shear stress due to fast flow in the microfluidic chip which may damage cell integrity [2]. As mentioned in the immunomagnetic technique, magnetic beads may produce magnetic momentum large enough to rupture cancer cells [4]. The electroosmosis-based isolation method uses a high electric field, which not only causes the heating problem but also damages cells, which leads to rendering cell viability significantly low after sorting. The use of dielectrophoresis can alleviate this limitation for the use of electric fields in sorting [80].

3.6 Low Throughput and Time-Consuming

In single-cell analysis technology, the sample is required to be diluted and made homogeneous; this leads to low throughput. To alleviate this, we need to use pre-enrichment techniques and hence multiple CTC isolation stages [78]. Even though single-cell analysis is a revolutionary method, it is time-consuming. Further, label-based techniques consume more time (>1 h) for preprocessing, labeling cells with dyes, incubation for proper binding of CTCs and antibodies, etc. As the time for a process increases, the viability of the cells reduces [2]. Thus, for an efficient system, we need detection and isolation techniques consuming less time.

4 Future Scope for Microfluidics-Based CTC Detection and Isolation

CTC count is important not only for diagnosis but also to get an idea about its progression and therapeutic response. Isolation of CTCs is important for further study, including its genetic analysis. Over the past two decades, microfluidic technologies have proved to be promising upcoming technology for lab-on-chip devices for isolating CTCs with more than 90% efficiency. In future, low cost, disposable microfluidic systems like paper-based microfluidics devices forming lab-on-paper [81] have several potential applications, especially in areas having no/low-cost infrastructures. In most cases, the CTC detection and isolation system needs blood about 5–7.5 ml for screening. Increasing the volume of the sample can increase the sensitivity and accuracy of the system [78].

Thus, we can develop *in vivo* or wearable devices that can continuously detect and isolate rare CTCs in the early stages of cancer, as shown in Fig. 5. It is a belief that the development of such technologies will enable breakthroughs not only for cancer treatment but also for the diagnosis, prognosis, and treatment of diseases that remain unconquered by current macroscale approaches [78].

5 Conclusion

In summary, advances in CTC detection and isolation, mainly in microfluidics are reviewed. The methods are broadly classified into two, label-free and label-based techniques. Label-free techniques utilize the physical properties of the CTCs such as size, deformability, density, and dielectric properties. Size-based techniques suffer because of the size overlap between CTCs and PBMCs. Dielectrophoresis depends on the electric conductivity of cells and the frequency of the electric field. The thermal effect induced because of the high electric field affects cell viability. Acoustic-based separation uses surface acoustic and bulk acoustic waves. Label-based techniques

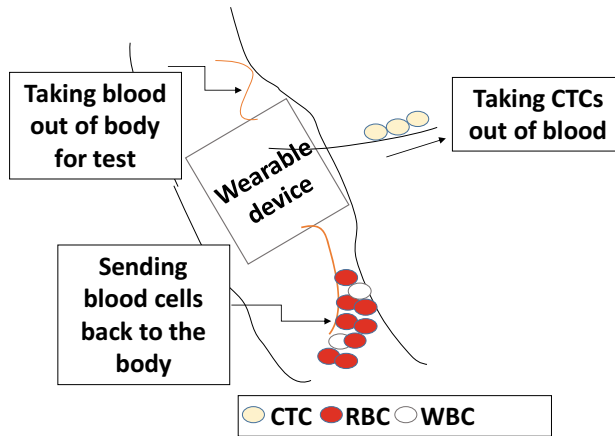


Fig. 5 Schematic of a wearable device for real-time CTC detection and isolation from the bloodstream

mainly depend on affinity binding. Immunofluorescence and immunomagnetic are two main techniques used. Nucleic acid-based CTC detection is another method where CTCs are lysed and a particular sequence in DNA is checked. It is also seen that CTC isolation and detection have some limitations, such as low abundance and non-specificity. The performance of these techniques is evaluated based on purity, throughput, and biocompatibility. These innovative microfluidics techniques have great potential to change the strategy in prognosis and diagnosis of cancer.

References

1. Allard, W.J., et al.: Tumor cells circulate in the peripheral blood of all major carcinomas but not in healthy subjects or patients with nonmalignant diseases. *Clin. Cancer Res.* **10**, 6897–6904 (2004)
2. Zou, D., Cui, D.: Advances in isolation and detection of circulating tumor cells based on microfluidics. *Cancer Biol Med.* **15**(4), 335–353 (2018)
3. Potdar, P.D., Lotey, N.K.: Role of circulating tumor cells in future diagnosis and therapy of cancer. *J Cancer Metastasis Treat.* **1**, 44–56 (2015)
4. Esmailsabzali, H., Beischlag, T.V., Cox, M.E., Parameswaran, A.M., Park, E.J.: Detection and isolation of circulating tumor cells: principles and methods. *Biotechnol. Adv.* **31**, 1063–1084 (2013)
5. Park, Y., et al.: Microelectrical impedance spectroscopy for the differentiation between normal and cancerous human urothelial cell lines: real-time electrical impedance measurement at an optimal frequency. *Biomed. Res. Int.* **2016**, 10 (2016)
6. Hecht, T.T., Mellman, I., Prindiville, S.A., Steinman, R.M., Jaye, L.: HHS Public Access. **15**, 5323–5337 (2018)
7. Wang, H., et al.: Selective in vivo metabolic cell-labeling-mediated cancer targeting. *Nat. Chem. Biol.* **13**, 415–424 (2017)

8. Izumi, S., Yamamura, S., Hayashi, N., Toma, M., Tawa, K.: Dual-color fluorescence imaging of EpCAM and EGFR in breast cancer cells with a bull's eye-type plasmonic chip. *Sensors (Switzerland)* **17** (2017)
9. Shi, W., et al.: Magnetic particles assisted capture and release of rare circulating tumor cells using wavy-herringbone structured microfluidic devices. *Lab Chip* **17**, 3291–3299 (2017)
10. Seal, S.H.: A sieve for the isolation of cancer cells and other large cells from the blood. *Cancer* **17**, 637–642 (1964)
11. Mohamed, H., Murray, M., Turner, J.N., Caggana, M.: Isolation of tumor cells using size and deformation. *J. Chromatogr. A* **1216**, 8289–8295 (2009)
12. Liu, Z., et al.: High throughput capture of circulating tumor cells using an integrated microfluidic system. *Biosens. Bioelectron.* **47**, 113–119 (2013)
13. Au, S.H., et al.: Microfluidic isolation of circulating tumor cell clusters by size and asymmetry. *Sci. Rep.* **7**, 1–10 (2017)
14. Sun, N., Li, X., Wang, Z., Li, Y., Pei, R.: High-purity capture of CTCs based on micro-beads enhanced isolation by size of epithelial tumor cells (ISET) method. *Biosens. Bioelectron.* **102**, 157–163 (2018)
15. Sajeesh, P., Manasi, S., Doble, M., Sen, A.K.: A microfluidic device with focusing and spacing control for resistance-based sorting of droplets and cells. *Lab Chip* **15**, 3738–3748 (2015)
16. Raj, A., Dixit, M., Doble, M., Sen, A.K.: A combined experimental and theoretical approach towards mechanophenotyping of biological cells using a constricted microchannel. *Lab Chip* **17**, 3704–3716 (2017)
17. Hazra, S., et al.: Non-inertial lift induced migration for label-free sorting of cells in a co-flowing aqueous two-phase system. *Analyst* **144**, 2574–2583 (2019)
18. Morijiri, T., Sunahiro, S., Senaha, M., Yamada, M., Seki, M.: Sedimentation pinched-flow fractionation for size- and density-based particle sorting in microchannels. *Microfluid. Nanofluidics* **11**, 105–110 (2011)
19. Burger, R., Ducrée, J.: Handling and analysis of cells and bioparticles on centrifugal microfluidic platforms. *Expert Rev. Mol. Diagn.* **12**, 407–421 (2012)
20. Al-Faqheri, W., et al.: Particle/cell separation on microfluidic platforms based on centrifugation effect: a review. *Microfluid. Nanofluid.* **21** (2017)
21. Burger, R., et al.: Centrifugal microfluidics for cell analysis. *Curr. Opin. Chem. Biol.* **16**, 409–414 (2012)
22. Hou, H.W., et al.: Isolation and retrieval of circulating tumor cells using centrifugal forces. *Sci. Rep.* **3**, 1–8 (2013)
23. Park, J.M., et al.: Highly efficient assay of circulating tumor cells by selective sedimentation with a density gradient medium and microfiltration from whole blood. *Anal. Chem.* **84**, 7400–7407 (2012)
24. Karthick, S., Pradeep, P.N., Kanchana, P., Sen, A.K.: Acoustic impedance-based size-independent isolation of circulating tumour cells from blood using acoustophoresis. *Lab Chip* **18**, 3802–3813 (2018)
25. Carey, T.R., Cotner, K.L., Li, B., Sohn, L.L.: Developments in label-free microfluidic methods for single-cell analysis and sorting. *Wiley Interdiscip. Rev. Nanomed. Nanobiotechnol.* **11**, 1–17 (2019)
26. Sun, T., Morgan, H.: Single-cell microfluidic impedance cytometry: a review. *Microfluid. Nanofluid.* **8**, 423–443 (2010)
27. Chung, Y.K., et al.: An electrical biosensor for the detection of circulating tumor cells. *Biosens. Bioelectron.* **26**, 2520–2526 (2011)
28. Gu, G.: A biosensor capable of identifying low quantities of breast cancer cells by electrical impedance spectroscopy. *Sci. Rep.* **9**, 6419 (2019)
29. Segre, G.: Radial particle displacement in poiseuille flow of suspensions. *Nature* **189**, 209–210 (1961)
30. Di Carlo, D., Irimia, D., Tompkins, R.G., Toner, M.: Continuous inertial focusing, ordering, and separation of particles in microchannels. *Proc. Natl. Acad. Sci. U.S.A.* **104**, 18892–18897 (2007)

31. Di Carlo, D., Edd, J.F., Irimia, D., Tompkins, R.G., Toner, M.: Equilibrium separation and filtration of particles using differential inertial focusing. *Anal. Chem.* **80**, 2204–2211 (2008)
32. Bhagat, A.A.S., Kuntaegowdanahalli, S.S., Papautsky, I.: Continuous particle separation in spiral microchannels using dean flows and differential migration. *Lab Chip* **8**, 1906–1914 (2008)
33. Kittilsland, G., Stemme, G., Nordén, B.: A sub-micron particle filter in silicon. *Sens. Actuators, A: Phys.* **23**, 904–907 (1990)
34. Stemme, G., Kittilsland, G.: New fluid filter structure in silicon fabricated using a self-aligning technique. *Appl. Phys. Lett.* **53**, 1566–1568 (1988)
35. Gu, Y., Miki, N.: A microfilter utilizing a polyethersulfone porous membrane with nanopores. *J. Micromech. Microeng.* **17**, 2308–2315 (2007)
36. Moorthy, J., Beebe, D.J.: In situ fabricated porous filters for microsystems. *Lab Chip* **3**, 62–66 (2003)
37. Aran, K., et al.: Microfiltration platform for continuous blood plasma protein extraction from whole blood during cardiac surgery. *Lab Chip* **11**, 2858–2868 (2011)
38. Sajeesh, P., Sen, A.K.: Particle separation and sorting in microfluidic devices: a review. *Microfluid. Nanofluid.* **17**, 1–52 (2014)
39. Wilding, P., et al.: Integrated cell isolation and polymerase chain reaction analysis using silicon microfilter chambers. *Anal. Biochem.* **257**, 95–100 (1998)
40. Wu, C.C., Hong, L.Z., Ou, C.T.: Blood cell-free plasma separated from blood samples with cascading weir-type microfilter using dead-end filtration. *J. Med. Biol. Eng.* **32**, 163–168 (2012)
41. Ji, H.M., et al.: Silicon-based microfilters for whole blood cell separation. *Biomed. Microdevices* **10**, 251–257 (2008)
42. Chen, J., et al.: Blood plasma separation microfluidic chip with gradual filtration. *Microelectron. Eng.* **128**, 36–41 (2014)
43. Yoon, Y., et al.: Clogging-free microfluidics for continuous size-based separation of microparticles. *Sci. Rep.* **6**, 1–8 (2016)
44. Chen, X., Cui, D.F., Liu, C.C., Li, H.: Microfluidic chip for blood cell separation and collection based on crossflow filtration. *Sens. Actuators, B: Chem.* **130**, 216–221 (2008)
45. Di, H., Martin, G.J.O., Dunstan, D.E.: A microfluidic system for studying particle deposition during ultrafiltration. *J. Memb. Sci.* **532**, 68–75 (2017)
46. Dalili, A., Samiei, E., Hoorfar, M.: A review of sorting, separation and isolation of cells and microbeads for biomedical applications: microfluidic approaches. *Analyst* **144**, 87–113 (2019)
47. Hughes, M.P.: Fifty years of dielectrophoretic cell separation technology. *Biomicrofluidics* **10**, 1–9 (2016)
48. Hughes, M.P.: Strategies for dielectrophoretic separation in laboratory-on-a-chip systems. *Electrophoresis* **23**, 2569–2582 (2002)
49. Alshareef, M., et al.: Separation of tumor cells with dielectrophoresis-based microfluidic chip. *Biomicrofluidics* **7**, 1–12 (2013)
50. Cheng, I.F., et al.: Antibody-free isolation of rare cancer cells from blood based on 3D lateral dielectrophoresis. *Lab Chip* **15**, 2950–2959 (2015)
51. Das, D., Biswas, K., Das, S.: A microfluidic device for continuous manipulation of biological cells using dielectrophoresis. *Med. Eng. Phys.* **36**, 726–731 (2014)
52. Alazzam, A., Mathew, B., Alhammedi, F.: Novel microfluidic device for the continuous separation of cancer cells using dielectrophoresis. *J. Sep. Sci.* **40**, 1193–1200 (2017)
53. Chan, J.Y., et al.: Dielectrophoresis-based microfluidic platforms for cancer diagnostics. *Biomicrofluidics* **12** (2018)
54. Chan, J.Y., et al.: Dielectrophoretic deformation of breast cancer cells for lab on a chip applications. *Electrophoresis* **40**, 2728–2735 (2019)
55. Chinen, A.B., et al.: Nanoparticle probes for the detection of cancer biomarkers, cells, and tissues by fluorescence. *Chem. Rev.* **115**, 10530–10574 (2017)
56. Scholtens, T.M., et al.: Automated identification of circulating tumor cells by image cytometry. *Cytometry Part A* **81 A**, 138–148 (2012)

57. Etcheverry, S., et al.: High performance micro-flow cytometer based on optical fibres. *Sci. Rep.* **7**, 5628 (2017)
58. Siudzi, A., Siudzi, A.: Fluorescent sensing with Fresnel microlenses for optofluidic systems. *Opt. Eng.* **56**(5), 057106 (2017)
59. Wall, T., et al.: Optofluidic lab-on-a-chip fluorescence sensor using integrated buried ARROW (bARROW) waveguides. *Micromachines* **8**, 1–9 (2017)
60. Kang, H., Kim, J., Cho, H., Han, K.H.: Evaluation of positive and negative methods for isolation of circulating tumor cells by lateral magnetophoresis. *Micromachines* **10** (2019)
61. Liang, W., et al.: Microfluidic-based cancer cell separation using active and passive mechanisms. *Microfluid. Nanofluid.* **24**, 26 (2020)
62. Sesen, M., Alan, T., Neild, A.: Microfluidic plug steering using surface acoustic waves. *Lab Chip* **15**, 3030–3038 (2015)
63. Hemachandran, E., Laurell, T., Sen, A.K.: Continuous droplet coalescence in a microchannel coflow using bulk acoustic waves. *Phys. Rev. Appl.* **12**, 044008 (2019)
64. Srivastava, A., Karthick, S., Jayaprakash, K.S., Sen, A.K.: Droplet demulsification using ultralow voltage-based electrocoalescence. *Langmuir* **34**, 1520–1527 (2018)
65. Banerjee, U., Mandal, C., Jain, S.K., Sen, A.K.: Cross-stream migration and coalescence of droplets in a microchannel co-flow using magnetophoresis. *Phys. Fluids* **31**, 112003 (2019)
66. Schenck, J.F.: Physical interactions of static magnetic fields with living tissues. *Prog. Biophys. Mol. Biol.* **87**, 185–204 (2005)
67. Nagrath, S., et al.: Isolation of rare circulating tumour cells in cancer patients by microchip technology. *Nature* **450**, 1235–1239 (2007)
68. Wang, C., et al.: Biomaterials Simultaneous isolation and detection of circulating tumor cells with a microfluidic silicon-nanowire-array integrated with magnetic upconversion nanopropes. *Biomaterials* **54**, 55–62 (2015)
69. Zheng, G., Patolsky, F., Cui, Y., et al.: Multiplexed electrical detection of cancer markers with nanowire sensor arrays. *Nat. Biotechnol.* **23**, 1294–1301 (2005)
70. Thong, J.T.L., Lim, C.T., Loh, K.P.: Flow sensing of single cell by graphene transistor in a microfluidic channel. *Nano Lett.* **11**(12), 5240–5246 (2011)
71. Liberti, M.V., Locasale, J.W.: The Warburg effect: how does it benefit cancer cells? *Trends Biochem. Sci.* **41**, 287 (2016)
72. Ben, F.D., et al.: A method for detecting circulating tumor cells based on the measurement of single-cell metabolism in droplet-based microfluidics. *Angew. Chem. Int. Ed. Engl.* **55**(30), 8581–8584 (2016)
73. Li, Z., Ruan, J., Zhuang, X.: Effective capture of circulating tumor cells from an S180-bearing mouse model using electrically charged magnetic nanoparticles. *J Nanobiotechnol.* **17**, 59 (2019)
74. Chen, B., et al.: Targeting negative surface charges of cancer cells by multifunctional nanopropes. *Theranostics* **6**(11), 1887–1898 (2016)
75. Ozkumur, E., et al.: Inertial focusing for tumor antigen—dependent and—independent sorting of rare circulating tumor cells. *Sci. Transl. Med.* **5**(179), 179ra47 (2013)
76. Li, Z., et al.: Sequence-specific label-free DNA sensors based on silicon nanowires. *Nano Lett.* **2**, 245–247 (2004)
77. Chung, Y., et al.: Silicon nanograss based impedance biosensor for label free detection of rare metastatic cells among primary cancerous colon cells, suitable for more accurate cancer staging Biosensors and Bioelectronics An electrical biosensor for the detection of circul. *Biosens. Bioelectron.* **26**, 2520–2526 (2018)
78. Cho, H., et al.: Microfluidic technologies for circulating tumor cell isolation. *Analyst* **143**, 2936–2970 (2018)
79. Yu, M., Stott, S., Toner, M., Maheswaran, S., Haber, D.A.: Circulating tumor cells: approaches to isolation and characterization. *J. Cell Biol.* **192**, 373–382 (2011)

80. Godin, J., et al.: Microfluidics and photonics for bio-system-on-a-chip: a review of advancements in technology towards a microfluidic flow cytometry chip. *J. Biophotonics* **1**, 355–376 (2008)
81. Li, X., Ballerini, D.R., Shen, W.: A perspective on paper-based microfluidics: current status and future trends. *Biomicrofluidics* **6** (2012)

Chapter 9

Localized Surface Plasmon Resonance Sensors for Biomarker Detection with On-Chip Microfluidic Devices in Point-of-Care Diagnostics



S. Z. Hoque , L. Somasundaram , R. A. Samy , A. Dawane ,
and A. K. Sen 

1 Introduction

Infectious diseases are the deadliest among all other diseases as they can transmit exponentially among the population in a relatively short period. Thus, these types of infections caused by pathogenic microorganisms (viruses, fungus, bacteria, parasites, etc.) are hazardous to the general public health. Even it has the potential to destroy the economic balance of the society [1]. Especially in developing nations where 80% of the population resides, it is becoming eminent to provide health facilities that are affordable and readily available to the general public to counterfeit any pandemic situations due to infectious diseases. Further, predictions have been made for more than half of the world population to be at risk due to infectious diseases [2].

For efficient treatment, accurate and rapid selective sensing assays are of utmost necessity for diagnostics as there is a saying, “without diagnostics medicine are blind” [3]. Further, real-time and rapid detection through a diagnostics tool help in preventing the transmission of infectious diseases. Many current laboratory sensing techniques provide sensitive and specific assays, such as polymer chain reaction (PCR) and mass spectroscopy (MS); however, it insists on large sample volume requirements, time and labor-intensive, complicated instrumentation, and most importantly, too expensive. On the other hand, point-of-care (POC) technology based on affordable, highly sensitive microfluidic devices offers on-site detection that would be an excellent alternative for developing nations [4]. According to the World Health Organization (WHO), for the developing countries, the POC tests for

S. Z. Hoque · L. Somasundaram · R. A. Samy · A. Dawane · A. K. Sen (✉)
Indian Institute of Technology Madras, Chennai, Tamil Nadu 600036, India
e-mail: ashis@iitm.ac.in

infectious diseases should follow the “ASSURED” criteria: (1) affordable, (2) sensitive, (3) specific, (4) user-friendly, (5) rapid and robust, (6) equipment free, and (7) deliverable to end user [5].

With the advent of nanotechnology, a wide variety of biological assays is developed by coupling nanoscale devices with microfluidics, which is more advantageous than the conventional approaches [6]. The pathogenic microorganisms such as viruses, bacteria, and biological cells are of the nanoscale size; therefore, the nanotechnology developed can mimic the complex dynamical process in real time [7, 8]. Most importantly, this has led to the development of nanobiosensors, which dimensionally of the same size as that of the analyte (at the single-cell level) [9]. Nanobiosensors provide versatility, such as multiplexing, portable, and implantable, making the nanosensors unique candidates for use in the POC diagnostics platform [10–13].

Optical and electromagnetic properties of the metallic nanostructure of nanosensors are pertinent for sensing applications [12]. One of the optical characteristics of metallic nanoparticles can be defined as the excitement of free electrons by the incident light due to absorption [14]. When the frequency of oscillation of nanoparticles matches incident light frequency, the phenomenon is known as localized plasmon resonance (LSPR) [12]. LSPR offers sensitive, robust, and facile detection and has surfaced as a leader among label-free biosensing techniques [15–19]. LSPR-based detection sensors combined with microfluidic devices have multiple benefits such as high throughput of label-free biochemical assays, multiplexing, reduction in reagent consumption and reaction time, application to point-of-care (POC) devices [10]. For example, coupling on-chip assays and the on-chip separation of plasma from whole blood would produce a microanalysis system, which would significantly reduce the amount of blood and reagents required for tests [20]. Integrated microfluidic chips would also decrease the necessary amount of time needed to perform an assay, thus minimizing variation in the blood’s biochemical composition between sample collection and assay.

Further, LSPR-based microfluidic bioassays have had significant research rooted in academia over a long period. The proof-of-concept studies that are validated in academia need to be dispatched to produce some practical tools viable for commercialization, which is lacking even recently. This chapter will discuss LSPR biosensors combined with microfluidics devices for miniaturization, such as lab-on-a-chip (LOC) device in POC diagnostics. Firstly, we will be discussing the fundamentals and fabrications related to LSPR biosensors. Then, LSPR functionalization and coupling LSPR with microfluidics platforms are discussed in detail, and finally, some recent applications of on-chip detections of biomarkers using LSPR biosensors are described.

2 Fundamental of LSPR

Surface plasmon resonance (SPR) can be described as the collective resonance oscillation of conduction band electrons in a noble metal triggered by an incident beam of light [21]. Although it can be described as a quantum of plasma oscillations, the plasmon phenomena can be explained based on classical physics. The materials having large negative real and small positive dielectric constant are only capable of supporting surface plasmon (see Fig. 1a). Usually, materials such as gold, silver, copper, and aluminum are used as nanoparticles as they exhibit plasmon resonance. When SPR is confined to nanometer-sized structures, that is, particle sizes are comparable to the wavelength of an incident beam of light as shown in Fig. 1a, b collective oscillation of free electrons of the particles is produced, which is known as localized surface plasmon (LSP) [22].

The frequency of the incident light and the electrons oscillation’s frequency (surface plasmon) matches, i.e., resonance condition, and therefore it is defined as localized surface plasmon resonance (LSPR) [19, 22]. At resonance, a strong absorption band can be observed as the scattering of light, and the electromagnetic field is enhanced on the nanoparticle’s surface. The schematic of the LSPR biosensing system is presented in Fig. 1c. LSPR has certain advantages over SPR [23]. The hardware required for LSPR is much simpler and more affordable since no prism is needed to couple the light. The angle is not an important factor in the LSPR

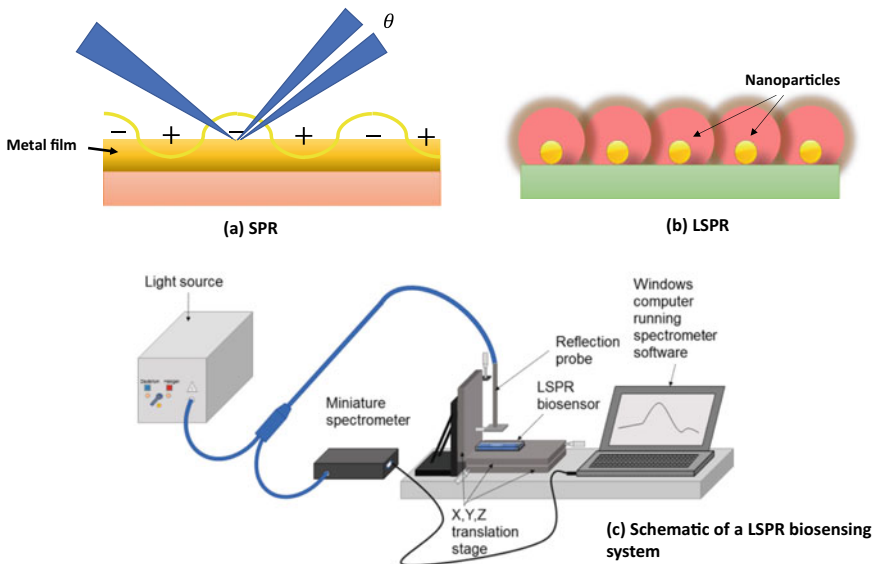


Fig. 1 Schematic depicting, **a** surface plasmon resonance, **b** localized surface plasmon, and **c** LSPR biosensing system (Reprinted from Sunthanthiraraj and Sen [20] with permission from Elsevier)

device; therefore, the instruments are much more robust against mechanical vibrations. Further, the SPR sensor has a large refractive index sensitivity ($\sim 10^6$ nm/RIU) compared to the LSPR sensor, which has modest refractive index sensitivity (10^2 nm/RIU) [24, 25]. Although it seems LSPR sensors are very less (about 1000 times) sensitive compared to SPR, both sensors have comparable sensitivities. Further, the LSPR sensor is much more affordable, easy to use, and maintained than the SPR sensor.

3 Theoretical Concept

In the mid-nineteenth century, for the first time, Michael Faraday reported that a small variation of particle sizes in gold colloid solution gave rise to various colors. Further, he termed the solution as “a beautiful ruby fluid” [22, 26]. Inspired by Faraday’s work, later in the twentieth century, Gustav Mie developed an analytical solution to Maxwell’s equations with spherical boundary conditions, which describe the scattering and absorption of light by spherical particles [27]. Mie’s later work can describe the in-depth theory related to LSPR phenomena.

3.1 Mie Theory

When a plane wave incident on a homogeneous spherical structure, the scattered field results in the following total scattering, extinction, and absorption cross sections [27],

$$\sigma_{sca} = \frac{2\pi}{|k|^2} \sum_{L=1}^{\infty} (2L+1) (|a_L|^2 + |b_L|^2) \quad (1)$$

$$\sigma_{ext} = \frac{2\pi}{|k|^2} \sum_{L=1}^{\infty} (2L+1) (\text{Re}(a_L + b_L)) \quad (2)$$

$$\sigma_{abs} = \sigma_{ext} - \sigma_{sca} \quad (3)$$

where k is the incoming wavevector and $L = 1, 2, 3 \dots$ represents the dipole, quadrupole, and higher-order multipoles of the scattering. The parameters a_L and b_L are composed of complicated Riccati–Bessel functions [28]. To better understand the LSPR phenomena, we can assume the nanoparticle length scale to be very small compared to the length scale, which simplifies Eqs. (1–3) drastically. With the simplification and further taking only up to dipole term (i.e., $L = 1$), we can arrive at the widely quoted expressions of nanoparticle surface plasmon,

$$\sigma_{ext} = \frac{18\pi \varepsilon_m^{3/2} V}{\lambda} \frac{\varepsilon_2(\lambda)}{[\varepsilon_1(\lambda) + 2\varepsilon_m]^2 + \varepsilon_2(\lambda)^2} \quad (4)$$

$$\sigma_{sca} = \frac{32\pi^4 \varepsilon_m^2 V^2}{\lambda^4} \frac{(\varepsilon_1(\lambda) - \varepsilon_m)^2 + \varepsilon_2(\lambda)^2}{[\varepsilon_1(\lambda) + 2\varepsilon_m]^2 + \varepsilon_2(\lambda)^2} \quad (5)$$

where V is the volume of the nanoparticle, λ is the wavelength of the absorbing radiation, ε_m is the medium dielectric constant, ε_1 and ε_2 are the real and imaginary parts of the nanoparticle's dielectric function. Although Eqs. (4) and (5) are derived considering only small nanoparticles (<10 nm), they can predict the dielectric sensitivity even for larger particles accurately [29]. The condition for maximum extinction cross section can be obtained by minimizing the denominator of Eq. (4) and is found to be,

$$\varepsilon_1 = -2\varepsilon_m \quad (6)$$

This relation shows that the LSPR extinction peak is sensitive to the dielectric constant of the surrounding medium. Further, the dielectric constant of the nanoparticles generally expressed in terms of the refractive index of the medium,

$$\varepsilon^2 = n \quad (7)$$

3.2 Refractive Index Sensitivity

Bimolecular binding to the nanoparticle surface offers sensing through the refractive index changes close to the body, which in turn shifts the LSPR maximum extinction wavelength ($\Delta\lambda_{\max}$). The electromagnetic decay length (l_d) of nanoparticles in LSPR is much shorter compared to films used in SPR sensor, thereby confining the shift, $\Delta\lambda_{\max}$ to a smaller sensing volume. Due to this, the sensitivity of biological analyte binding events is similar in both LSPR and SPR, although the SPR sensor has a higher refractive index sensitivity (m). This shift of maximum extinction wavelength to an absorbing layer can be expressed as [30],

$$\Delta\lambda_{\max} = m\Delta n \left[1 - e^{-\frac{2d}{l_d}} \right] \quad (8)$$

where Δn is the change in refractive index between the absorbing layer and the surrounding medium, and d is the thickness of the absorbing layer.

3.3 LSPR Configurations

There are four typical configurations of optical geometries that can be employed to measure LSPR, viz. (1) transmission, (2) reflection, (3) dark-field scattering (DS), and (4) total internal reflection (TIR). The first two types, transmission and reflection, are the simplest models of measurement. The light incident on the sample reflected or transmitted back, which can be monitored through spectroscopy. In dark-field scattering configuration, the spot size of the the nanoparticle's interrogation area can be tuned numerically. However, there are no numerical restrictions placed on the objective aperture in total internal reflection configuration through the prism coupler. A schematic depicting all the four configurations is presented in Fig. 2.

4 Characteristics of LSPR

The plasmon resonance wavelength of the LSPR sensor is a strong function of the shape, size, and materials of the nanoparticles. The LSPR peak wavelength of the silver nanoparticles can be tuned throughout the visible and near-infrared region by their shape, size, and dielectric constant of the space. Further, refractive index

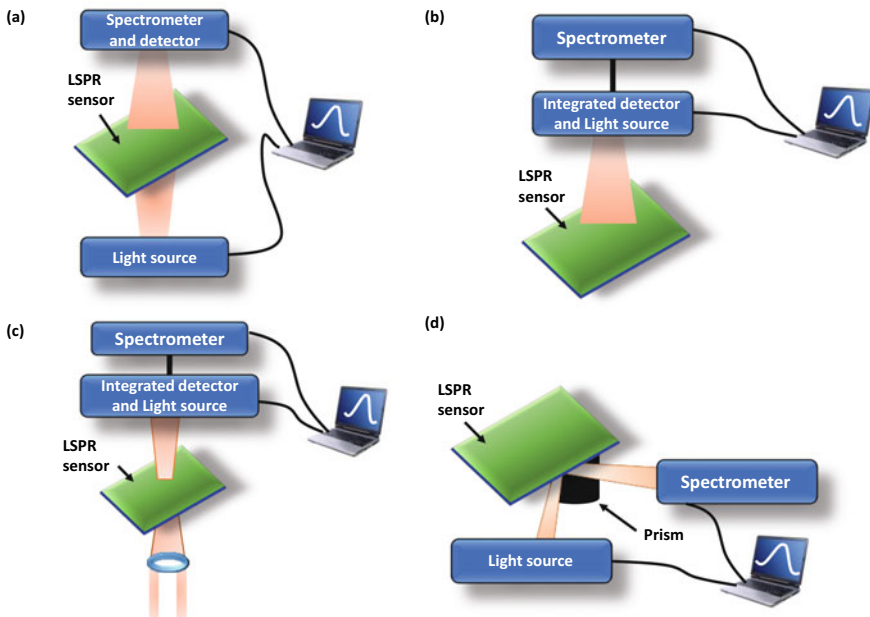


Fig. 2 Schematics of optical measurement configurations, **a** transmission, **b** reflection, **c** dark-field scattering (DS), and **d** total internal reflection (TIR) (Adapted from Bhalla et al. [31] with permission from Elsevier)

sensitivity is not only dependent on the shape, size, and material composition, but also a function of aspect ratio, interparticle separation distance, and nanoparticle environment [6, 19, 22].

4.1 *Material Used*

Among all the materials, silver and gold nanoparticles are used most frequently in LSPR sensing applications. Silver nanoparticles have the strongest affinity toward light and greater scattering cross section, which makes them most important for LSPR sensing [10, 20, 22, 30]. Gold is often preferred as a nanoparticle material since it is chemically stable and less prone to oxidation. Further, it has been shown that the plasmon resonance of silver nanoparticles is at lower wavelengths, and they are more sensitive than those of gold. Yokota et al. fabricated a monolayer of gold and silver nanoparticles by dipping method to realize the control of LSPR energy [32]. The LSPR extinction peak of the monolayer structure was redshifted with decreasing interparticle distance, reflecting plasmon coupling between NPs. Further, the dielectric constant of the nanoparticles has a dependency on the surrounding dielectric environment (see Sect. 3.2), which in turn affects the refractive index, n (see Eq. (8)).

4.2 *Nanoparticles Size and Shape*

For a given shape and metallic composition, Mie's theory predicts a strong variation in LSPR properties with the size of the nanoparticles. If the size of the spherical-shaped nanoparticles of radius R is quite smaller compared to the wavelength of light ($2\pi R < \lambda$), then it can be obtained that the magnitude of the absorption and scattering cross section is proportional to R^3 and R^6 , respectively [22]. Therefore, the LSPR peak can be described by adsorption for smaller particles and as the particle size increases, scattering cross sections come into play. Further, LSPR extinction spectra are sensitive to the changes in nanoparticle shape. Generally, hemispherical particles have LSPR extinction spectra at shorter frequencies than a truncated tetrahedron fabricated with similar parameters.

The dependence of nanoparticles size and aspect ratio on refractive index sensitivity has been widely studied in the literature [6, 19, 22, 23]. For example, changing aspect ratio from 1.0 to 3.4, it has been shown that for elongated nanoparticles (i.e., nanorods) the refractive index sensitivity increases from 157 to 497 nm/RIU [21]. As the nanorods sizes increase by fixing the aspect ratio, it has been found that larger nanorods have higher refractive index sensitivity. Further, it was determined that silver nanotriangles have a much higher refractive index compared to the sphere. Similarly, it was shown that gold nanoshells have a higher refractive index than nanospheres [23].

5 Fabrication Technique

Although depending on specific applications, various materials such as ceramics, glass, polymers, and different metal compounds are used for the fabrication of microfluidics devices; however, the two most frequently used materials for chip fabrications are polymers called polydimethylsiloxane (PDMS) and polymethylmethacrylate (PMMA) [33]. Both of the above-mentioned polymers are inexpensive, and they provide superior optical transparency, along with strong mechanical properties and interesting chemical properties which help in the fabrication of delicate features of the chip [34]. Among a wide range of fabrication techniques, soft lithography is the most commonly used method for the fabrication of PDMS microfluidic prototypes [35].

5.1 PDMS-Based LSPR-Microfluidics Coupling

In a distinctive study, PDMS microfluidic chip was integrated with gold nanoparticles by using an in situ method, as the cross-linking agent of PDMS has excellent reductive properties. In this method, the PDMS microfluidic chip was fabricated using a SU-8 mold, and this low-cost device was further used for the detection of polypeptides [36]. In another study, the fabrication of nanomaterial gold and PDMS as a chip in a macroenvironment, the PDMS samples were fed in the gold precursor solution for different time durations [37]. Finally, it was concluded that the in situ microfluidic synthesis resulted in 8.3 times in size uniformity. Another study discusses the LSPR-based microfluidic chip for the simultaneous monitoring of antigen-antibody reactions [38]. This hypothesis was based on the principle of the gold-capped nanoparticles layer substrate [15]. The microfluidic device which is used to coat the LSPR substrate was fabricated using PDMS (Dow Corning) by standard soft lithography technique [39]. A microfluidic chip integrated with pneumatically controlled valves was developed for multiplexed detection of biomolecules via localized surface plasmonic resonance (LSPR) of a single gold nanorod [40]. This method proved to be fairly cost-effective, and the microfluidic chip was assembled by PDMS layers and glass substrates with precisely controlling its thickness.

A PDMS microfluidic LSPR chip was fabricated using a soft lithography technique. For gauging the functionality of the chip, an antibody-antigen reaction was performed to detect insulin, which is a very crucial hormone and can significantly help in the diagnosis of diabetes [41]. After trapping the antibodies on the surface, real-time monitoring of insulin and anti-insulin antibody immunoreactions was performed. The LSPR responses produced by the biomolecules bonded to the chip were detected and recorded in this study.

PDMS-based microfluidic-nanobiosensors device fabrication process:

1. Initially, using a photoresist, typically like SU-8, a master mold is fabricated with the desired pattern of microchannels on a Si-based substrate.

2. The master mold is treated with Trichloro (1H,1H,2H,2H-perfluorooctyl) silane. This step is performed to significantly decrease the attachment between PDMS and the master mold.
3. PDMS (base) and its curing agent are taken in a 10:1 ratio and mixed in the master mold. The sample is degassed and kept in an oven at 60 °C for 24 h to achieve extensive polymerization of PDMS.
4. The solid PDMS is then smoothly stripped off from the master mold.
5. Then, a biopsy punch is used to generate holes for inlet and outlet tubes which will feed the microchannel continuously.
6. The PDMS channels, after baking, are now patterned and are bonded on a Si or glass substrate, consisting of gold nanostructures (i.e., an LSPR substrate). The equivalent substrate is then exposed to oxygen plasma treatment. In the chamber containing the environment of plasma, it thus creates short-lived loosely swinging –OH groups on the surface of PDMS which quickly reacts with –OH groups on glass or silicon, enabling stable and firm bonding.
7. The above experiment can further be improved by heating the bonded stack at 60 °C for 1 h. Later, the PDMS device is cooled down and can readily be used for fluidic experiments.

5.2 PMMA-Based LSPR-Microfluidics Coupling

PMMA-based microfluidic devices are generally fabricated by commonly used processes like etching, milling, and cutting of large sheets of PMMA. The inlet and outlet ports (called the fluidic ports) are drilled or punched in the corresponding locations which are allotted for fluid entry/exit in the channel. The patterned PMMA can be bonded with glass or silicon, to seal it completely, or multiple layers of PMMA can be piled upon one another with proper surface treatment.

For example, the most common way to bond PDMS and PMMA-based materials is by using oxygen plasma. One noticeable advantage is that it helps to prevent liquid leakage at high flow rates [42–44].

PMMA-based microfluidic-nanobiosensor device fabrication process:

1. Using CAD software like AutoCAD, Creo, SolidWorks, etc. To draw micropatterns as required and design its intricacies layer by layer.
2. After drawing the micropatterns, the next step is to print out each layer on the PMMA substrate using a micromilling machine or laser cutter.
3. When printing of each layer is finished, assemble all PMMA layers and stack them together to constitute a complete microfluidic device
4. Double-sided tape is used to bond the PMMA channels on the Si/glass substrate (combined LSPR substrate) consisting of gold nanostructures. The thickness of the double-sided take defines how thick the channels will be.

PDMS is a hyperelastic polymer with biocompatibility known for its low-cost and easy fabrication [45]. PMMA comes into the picture during conventional translation

microfluidics from laboratory prototypes to commercial products. It is also cost-effective and is versatile to manufacture a wide variety of designs. As PDMS is hydrophobic, surface treatments such as chemical functionalization/oxygen plasma exposure are required for the liquid's capillary flow. In PMMA, it is hydrophilic, and no external treatments are necessary [46]. Many organic solvents can diffuse into PDMS and result in deformation of the channel, whereas PMMA is comparatively stable [47]. Depending on the applications, both PDMS and PMMA-based sensors can be used.

6 Functionalization of LSPR Biosensor

Surface functionalization is an effective way to attract and bind various biomolecules on it and is very commonly used in multiple dimensions of research [48]. This section discusses the method and applications of a few commonly used surface functionalization techniques of LSPR biosensors. Once the fabrication process is completed, the LSPR substrate is functionalized such that the acid group ($-\text{COOH}$) binds with the primary amine group ($-\text{NH}_2$) belonging to various biomolecules like protein, lipids, etc. The annealed substrate went through the process of ultrasonication wherein it was dipped in 5 mL each of acetone, methanol, and isopropanol in a beaker in the following order. In each step, the sample was ultrasonicated for 5 min and then was immersed in 5 mL of acetone boiling at 56 °C over a hot plate. For surface functionalization, the substrate undergoes an oxygen plasma treatment, where the pressure, power, and time duration are set up to ~400 mTorr, 10 W for 5 min, respectively.

Further, the substrate was treated with 5 μL of 2% solution of 3-aminopropyltriethoxysilane (APTES) prepared in ethanol for around 90 min. The unreacted APTES was removed by cleaning the substrate with excess ethanol. The substrate was then treated with 50 μL of 1:9 mixture of 20 mM 11-Mercapto undecanoic acid (MUA) and 3-Mercapto propionic acid (MPA) for 18 h at ambient temperature.

To remove the excess acid, the substrate again was cleansed with excess ethanol. It is then treated with 50 μL of 1:1 mixture of 0.15 M N-(3-dimethyl aminopropyl)-N'-ethyl carbodiimide hydrochloride (EDC) and 0.03 M N-hydroxy succinimide (NHS) for 1 h at ambient temperature. The process is followed to activate the carboxylic acid groups created to bond with the primary amines as discussed before in this section. Finally, to remove the traces of NHS and EDC, the substrate was thoroughly cleansed with phosphate buffer saline (PBS) solution (see Fig. 3a).

A schematic diagram of the functionalization of the monoclonal antibody with the optical fiber is displayed in Fig. 3b [49]. As visible from the scheme given in Fig. 3b, initially, gold particles are immobilized onto the optical fiber along with 3-(mercaptopropyl)-trimethoxysilane (MPTMS), by employing silanization in toluene. Following, a bioactive layer which contains a monoclonal antibody is immobilized by

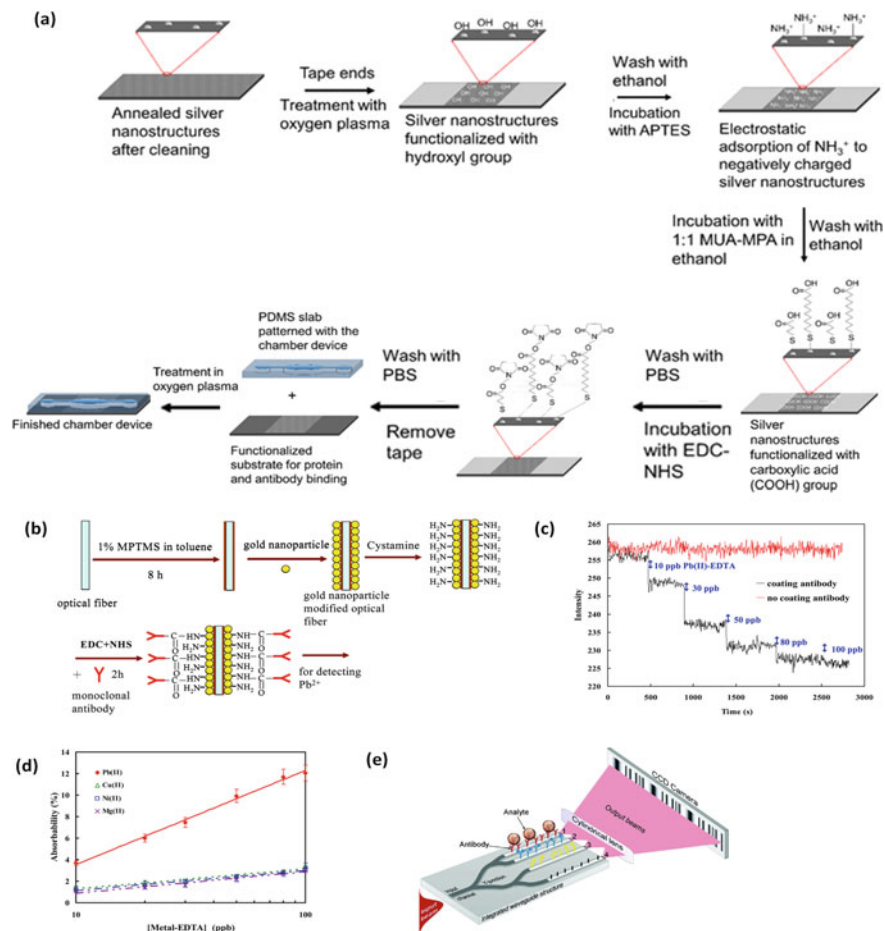


Fig. 3 a Schematic of the procedure for surface functionalization of silver nanostructures for the adsorption of bovine serum albumin (Reprinted from Sunthanthiraraj and Sen [20] with permission from Elsevier), b chemical reaction scheme is shown for covalent binding of monoclonal antibody to the fiber-based LSPR sensor, c response of serial Pb (II)-EDTA complex response signal in the range of 10–100 ppb by two sensors with/without monoclonal antibody coating, d effect of detection temperature on the response for detecting 10–100 ppb Pb (II)-EDTA complex in pH 7.4 PBS buffer solution at 25 °C (Reprinted from Lin and Chung [49] with permission from MDPI), e Schematic of the four-channel integrated optical YI sensor (Reprinted from Ymeti et al. [50] with permission ACS)

covalent coupling onto the gold nanoparticle surface by using a self-assembling technique. Due to this, a self-assembled layer of cystamine is attached for an amine group over the gold nanoparticle substrate. Henceforth, the amine groups of cystamine can bond well with the activated succinimide esters, which are formed after the reaction between antibody and EDC/NHS. Therefore, as a result, the antibodies are efficiently

and flawlessly immobilized upon the optical fiber surface. At room temperature, the responding signals from the modified LSPR sensor decrease with an increase in Pb (II)-EDTA complex concentration (see Fig. 3c). Further, the effect of temperature on monoclonal antibody binding is depicted in Fig. 3d. Although temperature enhancement helps in the increase of both binding and dissociation rate, effects of temperature on the dissociation rate are large compared to that on the binding rate.

Ymeti et al. exhibited an immunosensor with the help of a Young interferometer arrangement. It had a microfluidic chip with integrated waveguides projecting an interference pattern onto a CCD image sensor (see Fig. 3e) [50]. Three distinct waveguides were functionalized in this device with distinctive antibodies, and simultaneously, one waveguide in this device was stored as a reference and thus was not functionalized. When antigens bind to the surface, they interacted with the evanescent wave of the waveguide, thus altering the local refractive index and leading to a variation in the interference pattern.

Many strategies that discuss a similar sensing mechanism by immobilization of metallic gold nanoparticles at the farther end of the optical fiber can be accessed in refs. [51–53]. A fine example regarding this context is that a biosensor is created to identify anti-human IgG. The gold nanorods surface has been functionalized with human IgG [53]. LSPR sensors have a slight tendency of binding with unwanted spurious compounds or analytes of non-interest when it is introduced to biological solutions with complex biomolecules. This may lead to significant and false redshifts in the LSPR frequency. These unwanted molecules may also obstruct the binding of the analyte of our interest. Few methods to evade this are by creating self-assembled monolayers (SAM) on the NP surface, plasmonic coupling, biological scaffolds, and size/shape complementarity. Also, selectivity is largely dependent on the functionalization layer on the nanoparticle surface [54]. These layers are made up of tiny molecules that attract specific proteins of interest to bind. For example, boronic acid ligands are used for the detection of glucose [55].

7 Detection of Various Biomarkers Using LSPR-Based Microfluidic Devices

The integration of microfluidic systems with plasmonic technology has multiple benefits such as the reduction in reagent consumption and reaction time; the capacity to carry out real-time analysis with high-resolution, sensitivity, and detection limits; are cost-effective; and portable [10, 56–59]. Optical biosensor based on plasmonic technology is generally classified into surface plasmon resonance (SPR) and localized surface plasmon resonance (LSPR). The latter has attracted increased interest in recent decades because of its optical label-free biomolecular sensing. However, LSPR is a convenient alternative to SPR, as it has a potential application in the health-care devices, which can detect at the point-of-care (POC) diagnostics. In particular,

the multiplexing, miniaturization, and integration of LSPR into a portable POC diagnostic device would facilitate diagnosis in remote areas, where laboratory facilities are absent or difficult to reach [10, 60].

7.1 LSPR-Based PDMS Microchannel

The study by Hiep et al. was one of the earliest to illustrate the label-free detection of antigen and antibody reaction of insulin in a microfluidic LSPR chip with a collinear optical system [38]. The chip was able to transduce small changes in the refractive index to the changes in glucose solution. This simple collinear optical system used here could overcome the limitations of the Kretschmann configuration and could achieve the detection limit of 100 ng/mL.

Sadabadi et al. proposed an LSPR-based biosensor device that integrated gold nanoparticles into PDMS microchannel by using an in situ method [36]. For the fabrication of the PDMS microchannel, a SU-8 mold was developed using the photolithography process (see Fig. 4a, b). Then the gold solution was injected into the microchannel, where a vinyl silicon compound in the curing agent of PDMS reduces the gold ions to gold nanoparticles as shown in Fig. 4c. The embedded gold nanocomposites are characterized using UV/Vis spectrophotometer and scanning

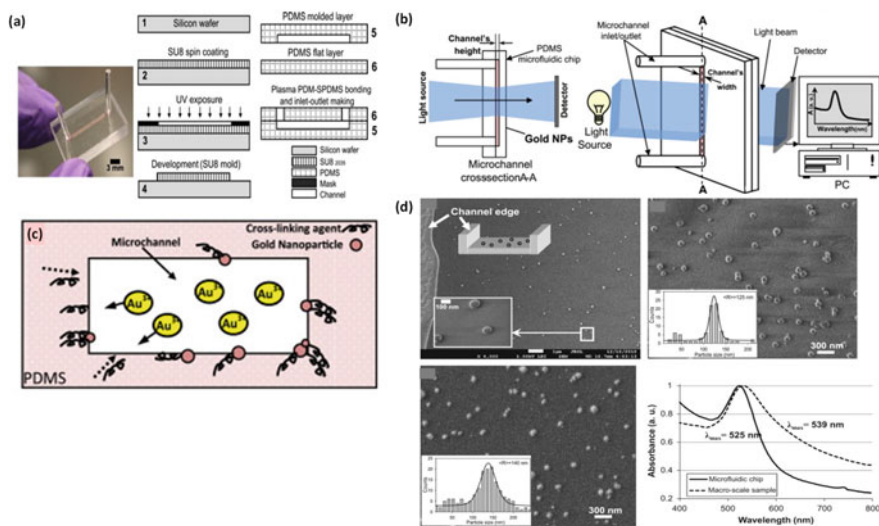


Fig. 4 **a** Illustration of steps involved in PDMS microchannel fabrication. **b** Schematic of UV/Vis spectrophotometer measurement. **c** Illustration of reaction between the cross-linking agent (curing agent) and gold ions in solution **d(a)** SEM images of Au particle size distribution near to channel edge **d(b)**, **c** SEM images of gold nanoparticles formation and distribution in microchannel and macrochannel, respectively; **d(d)** the Au-LSPR band in the macro- and microchannel environment (Reproduced from SadAbadi et al. [36] with permission from Elsevier)

electron microscopy (SEM) (see Fig. 4d). The gold nanoparticles synthesized inside the microchannel had an improved size distribution effect ($\pm 8\%$) when compared with a macroscale environment, where a flat PDMS slab was cut into a particular size and incubated in gold solution. Here, the reductive property of PDMS was exploited to make in situ functionalization of gold nanoparticles in microchannels, which could sense bovine growth hormone (bovine somatotropin) with a limit of detection 3.7 ng/ml.

7.2 Nanoparticles Geometry and Its Influence in Plasmonic Peak Shifts

The surface plasmon wavelengths are strongly dependent on the refractive index of the surrounding medium, which is the base for LSPR devices. The nanoparticles that express high refractive index sensitivity improve the detection by giving a higher redshift to the surface plasmon resonance peaks. The shape and size of the nanoparticles were found to affect the refractive index sensitivities. Either of the two parameters, refractive index sensitivity and figure of merit, is used to characterize the sensitivity of the LSPR chip. The refractive index sensitivity is calculated from the variation of plasmon shift with a change in the refractive index. The figure of merit is obtained by dividing refractive index sensitivity with the full width at half-maximum of the extinction peak. The refractive index sensitivity increases as the size of the nanoparticles is elongated and with the sharp feature of the apex [61]. The study by Chen et al. observed index sensitivity to be lowest for gold spherical particles and highest with gold nanobranched. Gold nanobipyramids have the highest figure of merit [61]. Campu et al. developed a microfluidic LSPR device that has gold nanobipyramids functionalized onto a glass substrate [62]. The device could detect a minimum of 18 nm redshift during the detection of the para-aminothiophenol molecule (p-ATP) in laminar flow. The device could be operated in dual modes with the LSPR and SERS method of detection. Srdjan et al. developed a microfluidic LSPR chip, in which gold nanorods were used for binding the antigen or antibodies [18]. The cancer biomarkers alpha-feto protein and prostate-specific antigen (PSA) were detected with the device even at very low concentrations of 500 pg/mL.

7.3 LSPR in Multiplexing

The key advantage of microfluidics lies in the ability to create a multiplexing platform. Zhang et al. exploited the multiplexing concept to create a microfluidic LSPR device which can detect six analytes in parallel [63]. Further, to minimize the experimental error, an optical bench was designed to load both the test chip and bare microfluidic LSPR chip (Fig. 5a, b). The LSPR chip was made by the microwave plasma method,

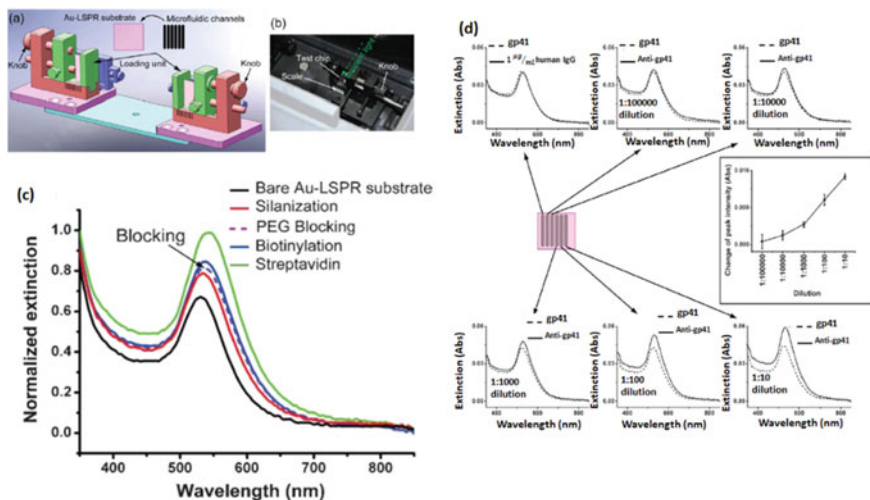


Fig. 5 **a** Schematic of an optical bench to load test chip and bare Au-LSPR chip, **b** the experimental image of optical bench loaded with test chip, **c** extinction curves after functionalization of the surface with different process, and **d** microfluidic chip demonstrated with multiplexing concept, six different dilutions of samples were tested in parallel (Reproduced from Zhang et al. [63] with permission from Royal Society of Chemistry)

and the PDMS layer was made by the photolithography process.

The titration curve showed a positive correlation between the change in peak intensity with an increase in the concentration of antibodies (Fig. 5d), which was attained within 30 min from the introduction of the sample to measurement. The LSPR on-chip detection was found to be faster and simpler than ELISA, and the detection limits of both the methods were found to be approximately the same (1,00,000 times the dilution of serum). LSPR devices are prone to give false readings due to the binding of non-specific proteins. The surface was introduced with PEG-thiol as it has a high resistance to bind proteins on its surface and adding linkers terminated with a biotin moiety aids to immobilize the streptavidin. The measurement of extinction and shift in wavelength after the different processes are shown in Fig. 5c. In a similar work, the multiplexing concept was used to detect three biomarkers thrombin, immunoglobulin E (IgE), and PSA on a pneumatically controlled microfluidic chip [40]. The anti-gp41 antibody that acts as a biomarker for HIV was measured from the microfluidic chip with different dilutions as shown in Fig. 5d.

In a microfluidic LSPR chip, the green light-emitting diode was used as a light source, and a compact quadrant detection scheme was used to monitor the light transmitted through the LSPR chip rather than the conventional spectroscopy method. The device capability to detect biological sensing is demonstrated by detecting the binding of anti-biotin to a self-assembled monolayer immobilized with biotin [64]. Thus, the microfluidic devices provide faster detection in comparison with static conventional LSPR devices. For instance, the incubation of anti-biotin took 3 h in

a conventional case, whereas in microfluidic devices the time could be reduced to ~20 min [64]. This is mainly attributed to the high surface area to volume ratio. Some of the recent publications related to the integration of microfluidic devices with LSPR have been listed in Table 1.

8 Integrated LSPR Biosensors in POC Diagnostics Device: Challenges and Road Ahead

Introducing the LSPR principle into a microfluidic chip holds great promise in application to point-of-care devices. In a recent study, Zhiyuan et al. integrated a microfluidic LSPR chip to a smartphone, within the area of 70 cm², to make portable devices, which will be useful in point-of-care testing [70]. The device was demonstrated to detect the presence of breast cancer biomarkers CA 125 and CA 15–3.

8.1 On-Chip Blood-Plasma Separation Microfluidics Platform

Blood is a complex matrix that has a large amount of cellular material of approximately $4\text{--}6 \times 10^9$ erythrocytes (RBC), $4\text{--}11 \times 10^6$ leucocytes (WBC), and $2\text{--}5 \times 10^8$ platelets per mL [71]. Most diagnostic techniques require the processing of patient blood manually such as the separation of plasma from blood cells, known as plasmapheresis. Despite its ubiquity, the fact that the sample preparation steps are time-consuming, labor-intensive, and prone to red blood cell (RBC) lysis that could interfere with signal sensitivity during medical analysis. Further, the main concern of health operators in the present is to accomplish an early diagnosis. Hence, it is important that the key part of blood-plasma separation needs to be miniaturized to realize point-of-care diagnostics [20, 60, 72–74].

The method of cell-separation principle in microfluidics is classified into active and passive devices, where the former depends primarily on the external force field and the latter depends on channel geometry and hydrodynamic force. One such significant class of passive microfluidic device is, capillarity based as they are self-driven and autonomous, and can process the blood on-chip, and yield real-time information. The integration of on-chip blood-plasma separation with LSPR biosensors yields real-time information regarding the stage of infection and for patients who need regular monitoring of blood [20, 73, 75]. A commercially available asymmetrical membrane was integrated with a microfluidic device to aid the separation of plasma from whole blood.

Our team has reported an LSPR-based biosensor device fabricated with silver nanostructures of a thin silver metal film of 5 nm thickness deposited via electron

Table 1 Lists of some recent research work on LSPR-based detection of various biomarkers in microfluidic on-chip devices

Group	Biomarker detection	Surface	Fabrication method	Limit of detection (LOD)
Campu et al. [62]	Para-aminothiophenol molecule (p-ATP)	Gold bipyramidal nanoparticles (AuBPs)	Anodic aluminum oande (AAO)	18 nm redshift
Wu et al. [40]	Thrombin, Immunoglobulin E (IgE), Prostate-specific antigen (PSA)	Gold nanorods	Seed-mediated growth procedure	10–4 g/mL
Camara et al. [65]	Dengue NS1 antigen	Gold nanoparticles	Sputter deposition and annealing	0.074 μ g/ml
Hiep et al. [38]	Insulin antibody	Gold-capped nanoparticles	Chemical synthesis	100 ng/mL
Huang et al. [64]	Anti-biotin antibody	Gold nanoparticles	Chemical fabrication	270 ng/mL
Guo et al. [66]	Binding of the enantiomer of melagatran to human α -thrombin	Gold nanorods AR ~ 2.6	Seed-mediated growth procedure	0.9 nM
Guo et al. [67]	R-TNA S-TNA	Gold nanorods	Seed-mediated growth procedure	150 nM—R-TNA 100 nM—S-TNA
Qiu et al. [68]	SARS-CoV-2	Dual-functional gold nanoislands (AuNIs) chip	Thermal dewetting	0.22 \pm 0.08 pM
SadAbadi et al. [36]	Bovine growth hormone (bovine somatotropin)	Gold nanoparticles	Reduction property of PDMS used to create in situ synthesis of gold nanoparticles	3.7 ng/mL
Acimovic et al. [18]	Human alpha-feto-protein and prostate-specific antigen. Cancer biomarkers	Gold nanorods	E-beam lithography followed by thermal annealing	500 pg/mL
Austin Suthanthiraraj et al. [20]	Dengue NS1 antigen	Silver nanostructures	E-beam evaporation and thermal annealing	0.06 μ g/mL

(continued)

Table 1 (continued)

Group	Biomarker detection	Surface	Fabrication method	Limit of detection (LOD)
Lv et al. [69]	CD63—Exosomes	Gold nanoellipsoid arrays	Anodic aluminum oxide (AAO)	1 ng/mL
Zhang et al. [63]	Anti-gp41 antibody—HIV	Gold nanoparticles	Microwave plasma method	100,000 times dilution of the original serum
Fan et al. [70]	CA 125 and CA 15-3 Breast cancer biomarkers	Gold nanoparticles	E-beam evaporation and thermal annealing	CA 125—4.2 U/mL CA 15-3—0.87 U/mL

beam evaporation. The biosensor that exploits the LSPR effect of silver nanostructures, could reliably detect dengue nonstructural glycoprotein (NS1) antigen that appears as early as the onset of infection. Here, the separation of plasma from whole blood was demonstrated by pipetting out 10 μ l of blood sample onto the membrane, thus the plasma separates and flows through the channel to the sensing region (see Fig. 6).

A 1.8 μ m asymmetrical pore sized polyethersulfone (polysulfone) membrane of 340 μ m thickness could sufficiently retain the blood cells. The membrane dimension and sample volume are crucial for filtering the blood cells. After repeated cutting and testing, it was found that a 5 mm \times 5 mm dimension of the polysulfone membrane and 10 μ l of the blood sample is ideal for the LSPR device to sense the dengue NS1 antigen. A PDMS slab contains a rectangular channel and a channel inlet was bonded onto the biosensor device by exposing the silver nanostructure LSPR substrate and PDMS channel to oxygen plasma. The channel hydrophilicity and capillary flow are critical in the separation of plasma from other biological cellular components. However, the channel loses its hydrophilicity with time (>15 min), and hence, the capillary flow velocity decreases. Further, the purity of filtered plasma is compared with centrifuged plasma by gray-scale intensity data. The data showed that plasma filtered via polyethersulfone membrane had the highest purity. This blood-plasma separation integrated LSPR device could potentially detect a lower concentration of 0.06 μ g/mL of NS1 dengue antigen with a sensitivity of 9 nm/ μ g/mL.

8.2 Acoustic-Driven Plasmofluidics

Combining different modules in microfluidic chips extend the range of application to wide areas. On that basis, the microfluidic LSPR chip is integrated with acoustics to modulate the LSPR structures by the rapid mixing of two different fluids (Fig. 7a) [76]. The onset of flow in the microchannel traps the bubble (Fig. 7b). The exposure

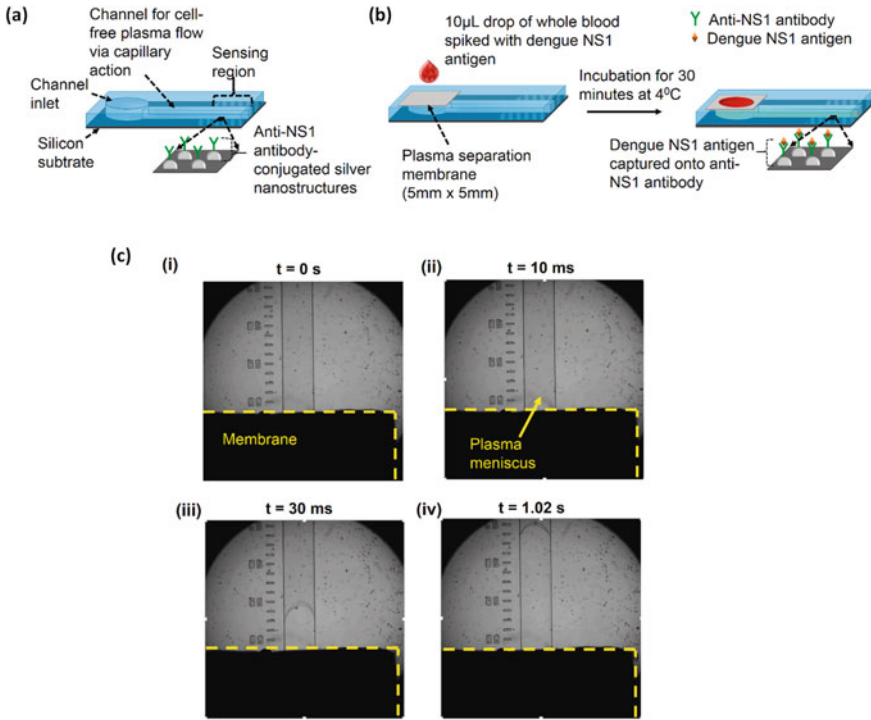


Fig. 6 Steps involved in the separation of on-chip blood-plasma separation. **a** PDMS slab bonded onto the LSPR substrate, **b** on-chip blood-plasma separation and detection of NS1 antigen, **c** images of plasma meniscus after filtration through a polyethersulfone membrane (yellow dotted lines) bonded to glass slide at different time instants (Reproduced from Sunthanthiraj and Sen [20] with permission from Elsevier)

of the bubble to the acoustic field induced oscillations to the trapped bubble. When the frequency of the acoustic wave nears the resonance frequency of the bubble, the amplitude of the liquid–air interface was maximized, which induces the rapid mixing of fluid streams (Fig. 7c–e). The change in refractive index upon mixing of liquid streams gives a shift in peak intensity (see Fig. 7f). This phenomenon could be used to modulate LSPR devices and useful as optical switches and biosensors in lab-on-a-chip devices.

8.3 LSPR Integrated Photothermal Effect

With the outbreak of COVID-19, Qiu et al. developed a dual-functional LSPR biosensor device by combining the photothermal effect and plasmonic sensing transduction for SARS-COVID-2 detection (see Fig. 8) [68]. In this work, the plasmonic

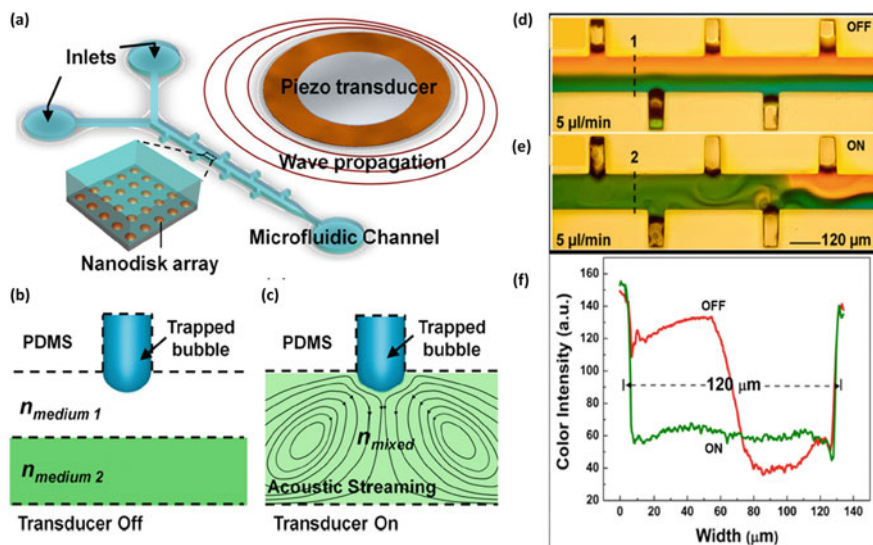


Fig. 7 **a** A schematic of the microfluidic LSPR chip coupled with the acoustic field, **b**, **c** A schematic of the trapped bubble with transducer off and on, respectively, **d** liquid configuration with transducer off and on, respectively, and **e** color intensity plot across the cross section with transducer off and on (Reproduced from Ahmed et al. [76] with permission from AIP)

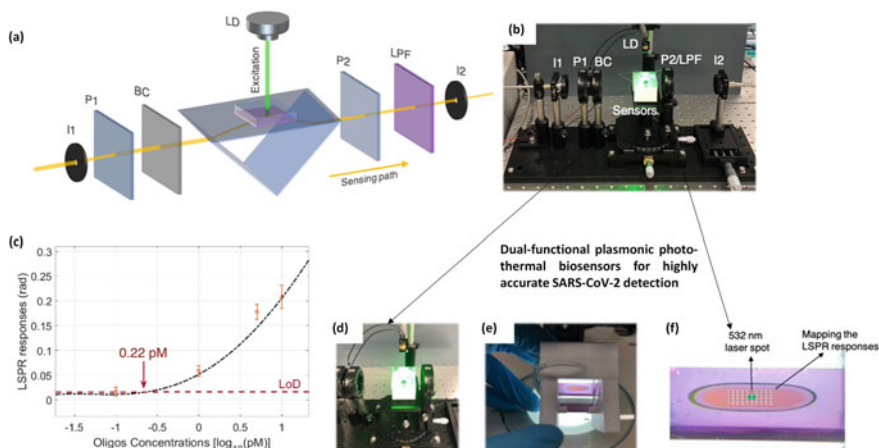


Fig. 8 **a** Schematic and **b** experimental setup of dual-functional PPT enhanced LSPR biosensing, **c** PPT unit and **d** side view of AuNIs sensing chamber **e** scanning illustration of PPT temperature distribution and mapping **f** LSPR response to Rd-Rp COVID oligo-nucleotides concentration (Reproduced from Qiu et al. [68] with permission from American Chemical Society)

chip consists of the two-dimensional distribution of nanoabsorbers (AuNIs), as these plasmonic nanoparticles exhibit large optical cross sections. Upon induction of these plasmonic nanoparticles with a wide spectrum beam, the absorbed light spontaneously converted into significant heat energy, known as the plasmonic photothermal (PPT) effect. This enhanced PPT near the nanoislands could transduce the in situ hybridization for SARS-CoV-2 viral nucleic acid detection. This dual-functional LSPR system exhibited a LOD of 0.22 ± 0.08 pM. The in situ PPT enhanced chip could differentiate the RNA-dependent RNA-polymerase (RdRp) gene of closely related species.

8.4 Aptamer-Induced Sensitivity

The detection limit can be enhanced by the aptamer-antigen-antibody sandwich complex. Aptamers are a short stretch of nucleotides that holds high affinity and specificity toward the target molecule [77]. In a study conducted by Guo et al., an enhanced signal of more than one order of magnitude was found by binding of human α -thrombin to its specific receptor, thrombin binding aptamer (TBA) on a single gold nanorod [66]. Moreover, the sensors can be reused because of the high stability of the aptamer. Here, the proposed apt sensor device could detect a thrombin concentration of 0.1 ng/mL.

9 Challenges and Road Ahead

Although LSPR biosensing features high-end miniaturization, multiplexing, and bio-field applications, multidisciplinary research work needs to be carried out for practical employment. LSPR signal solely depends on the refractive index changes around the metal nanoparticles. Therefore, the size, shape, and interparticle distance have to be reproduced as we transform these laboratory biosensors into robust commercialization tool. Additionally, LSPR is a non-specific technique as the specificity relies only on the biomolecular recognition elements such as antibodies and ssDNA. Also, significant approaches have to be taken in the development of detection limit, sensitivity, nanoparticle degradation, and leaching.

10 Conclusion

In this chapter, we have discussed the principle of LSPR, the method for fabrication of LSPR-based biosensor devices, and its significant role in the detection of biomarkers in the infectious disease diagnosis. Further, the chapter discussed some of the recently developed LSPR-based microfluidic devices and their ability to detect

the lower concentration of various biomarkers. Although the LSPR-based microfluidic on-chip has progressed substantially since its origin, much active research work has to be pursued to achieve a greater detection limit, sensitivity, and reduction of non-specific molecule binding. Besides, the reproducibility of an LSPR biosensor device is another issue in mass production and commercialization. Despite having certain disadvantages, the integration of the LSPR principle with microfluidics system makes them capable of providing personalized health care in developing nations and real-time monitoring. In conclusion, LSPR biosensors could potentially be used in point-of-care diagnostics and could be miniaturized, multiplexed, and integrated with various other microfluidic platforms in the detection of the different analytes.

References

1. Chen, H., Liu, K., Li, Z., Wang, P.: Point of care testing for infectious diseases. *Clin. Chim. Acta* **493**, 138–147 (2019)
2. Hwang, H., Hwang, B.Y., Bueno, J.: Biomarkers in infectious diseases. *Dis. Markers*, 2–4 (2018)
3. García-Basteiro, A.L., DiNardo, A., Saavedra, B., Silva, D.R., Palmero, D., Gegia, M., Migliori, G.B., Duarte, R., Mambuque, E., Centis, R., Cuevas, L.E., Izco, S., Theron, G.: Point of care diagnostics for tuberculosis. *Rev. Port. Pneumol. (English ed.)* **24**, 73–85 (2018)
4. Chen, H., Hagström, A.E.V., Kim, J., Garvey, G., Paterson, A., Ruiz-Ruiz, F., Raja, B., Strych, U., Rito-Palomares, M., Kourentzi, K., Conrad, J.C., Atmar, R.L., Willson, R.C.: Flotation immunoassay: masking the signal from free reporters in sandwich immunoassays. *Sci. Rep.* **6**, 1–8 (2016)
5. Tay, A., Pavesi, A., Yazdi, S.R., Lim, C.T., Warkiani, M.E.: Advances in microfluidics in combating infectious diseases. *Biotechnol. Adv.* **34**, 404–421 (2016)
6. Petryayeva, E., Krull, U.J.: Localized surface plasmon resonance: nanostructures, bioassays and biosensing—a review. *Anal. Chim. Acta* **706**, 8–24 (2011)
7. Velve-Casquillas, G.L., Berre, M., Piel, M., Tran, P.T.: Microfluidic tools for cell biological research. *Nano Today* **5**, 28–47 (2010)
8. Mendes, P.M.: Cellular nanotechnology: making biological interfaces smarter. *Chem. Soc. Rev.* **42**, 9207–9218 (2013)
9. Young, E.W.K., Beebe, D.J.: Fundamentals of microfluidic cell culture in controlled microenvironments. *Chem. Soc. Rev.* **39**, 1036–1048 (2010)
10. Badilescu, S., Packirisamy, M.: Plasmonic biosensors on a chip for point-of-care applications. *Electrochem. Soc. Interface* **28**, 65–69 (2019)
11. Mauriz, E., Dey, P., Lechuga, L.M.: Advances in nanoplasmonic biosensors for clinical applications. *Analyst* **144**, 7105–7129 (2019)
12. Soler, M., Huertas, C.S., Lechuga, M.: Label-free plasmonic biosensors for point-of-care diagnostics: a review. *Expert Rev. Mol. Diagn.* **19**, 71–81 (2019)
13. He, J., Brimmo, A.T., Qasaimeh, M.A., Chen, P., Chen, W.: Recent advances and perspectives in microfluidics-based single-cell biosensing techniques. *Small Methods* **1**, 1700192 (2017)
14. Choi, J.H., Lee, J.H., Son, J., Choi, J.W.: Noble metal-assisted surface plasmon resonance immunosensors. *Sensors (Switzerland)* **20**, (2020)
15. Minh Hiep, H., Endo, T., Kerman, K., Chikae, M., Kim, D.K., Yamamura, S., Takamura, Y., Tamiya, E.: A localized surface plasmon resonance based immunosensor for the detection of casein in milk. *Sci. Technol. Adv. Mater.* **8**, 331–338 (2007)
16. Fujiwara, K., Watarai, H., Itoh, H., Nakahama, E., Ogawa, N.: Measurement of antibody binding to protein immobilized on gold nanoparticles by localized surface plasmon spectroscopy. *Anal. Bioanal. Chem.* **386**, 639–644 (2006)

17. Bae, Y.M., Jin, S.O., Kim, I., Shin, K.Y., Heo, D., and Kang, D.G.: Detection of Biomarkers Using LSPR Substrate with Gold Nanoparticle Array. *J. Nanomater.* 2015, (2015).
18. Acimovic, S.S., Ortega, M.A., Sanz, V., Berthelot, J., Garcia-cordero, J.L., Renger, J., Maerkl, S.J., Kreuzer, M.P., Quidant, R.: Markers in Serum. *Nano Lett.* 6–11 (2014)
19. Hutter, E., Fendler, J.H.: Exploitation of localized surface plasmon resonance. *Adv. Mater.* **16**, 1685–1706 (2004)
20. Austin Suthanthiraj, P.P., Sen, A.K.: Localized surface plasmon resonance (LSPR) biosensor based on thermally annealed silver nanostructures with on-chip blood-plasma separation for the detection of dengue non-structural protein NS1 antigen. *Biosens. Bioelectron.* **132**, 38–46 (2019)
21. Myers, F.B., Lee, L.P.: Innovations in optical microfluidic technologies for point-of-care diagnostics. *Lab Chip* **8**, 2015–2031 (2008)
22. Mayer, K.M., Hafner, J.H.: Localized surface plasmon resonance sensors. *Chem. Rev.* **111**, 3828–3857 (2011)
23. Haes, A.J., Van Duyne, R.P.: A unified view of propagating and localized surface plasmon resonance biosensors. *Anal. Bioanal. Chem.* **379**, 920–930 (2004)
24. Malinsky, M.D., Kelly, K.L., Schatz, G.C., Van Duyne, R.P.: Chain length dependence and sensing capabilities of the localized surface plasmon resonance of silver nanoparticles chemically modified with alkanethiol self-assembled monolayers. *J. Am. Chem. Soc.* **123**, 1471–1482 (2001)
25. Jung, L.S., Campbell, C.T., Chinowsky, T.M., Mar, M.N., Yee, S.S.: Quantitative interpretation of the response of surface plasmon resonance sensors to adsorbed films. *Langmuir* **14**, 5636–5648 (1998)
26. Thompson, D.T.: Michael faraday’s recognition of ruby gold: the birth of modern nanotechnology. *Gold Bull.* **40**, 267–269 (2008)
27. Horvath, H.: Gustav Mie and the scattering and absorption of light by particles: historic developments and basics. *J. Quant. Spectrosc. Radiat. Transf.* **110**, 787–799 (2009)
28. Bohren, C.F., Huffman, D.R.: (Wiley science paperback series) Craig F. (1998)
29. Anderson, L.J.E., Mayer, K.M., Fraleigh, R.D., Yang, Y., Lee, S., Hafner, J.H.: Quantitative measurements of individual gold nanoparticle scattering cross sections. *J. Phys. Chem. C* **114**, 11127–11132 (2010)
30. Hammond, J.L., Bhalla, N., Rafiee, S.D., Estrela, P.: Localized surface plasmon resonance as a biosensing platform for developing countries. *Biosensors* **4**, 172–188 (2014)
31. Bhalla, N., Chiang, H.J., Shen, A.Q.: Cell biology at the interface of nanobiosensors and microfluidics. *Methods Cell Biol.* **148**, 203–227 (2018)
32. Yokota, H., Taniguchi, T., Watanabe, T., Kim, D.G.: Control of localized surface plasmon resonance energy in monolayer structures of gold and silver nanoparticles. *Phys. Chem. Chem. Phys.* **17**, 27077–27081 (2015)
33. Becker, H., Locascio, L.E.: Polymer microfluidic devices. *Talanta* **56**, 267–287 (2002)
34. Fujii, T.: PDMS-based microfluidic devices for biomedical applications. *Microelectron. Eng.* **61–62**, 907–914 (2002)
35. Xia, Y., Whitesides, G.M.: Soft lithography. *Annu. Rev. Mater. Sci.* **28**, 153–184 (1998)
36. SadAbadi, H., Badilescu, S., Packirisamy, M., Wüthrich, R.: Integration of gold nanoparticles in PDMS microfluidics for lab-on-a-chip plasmonic biosensing of growth hormones. *Biosens. Bioelectron.* **44**, 77–84 (2013)
37. SadAbadi, H., Badilescu, S., Packirisamy, M., Wüthrich, R.: PDMS-gold nanocomposite platforms with enhanced sensing properties. *J. Biomed. Nanotechnol.* **8**, 539–549 (2012)
38. Hiep, H.M., Nakayama, T., Saito, M., Yamamura, S., Takamura, Y., Tamiya, E.: A microfluidic chip based on localized surface plasmon resonance for real-time monitoring of antigen-antibody reactions. *Jpn. J. Appl. Phys.* **47**, 1337–1341 (2008)
39. Duffy, D.C., McDonald, J.C., Schueller, O.J.A., Whitesides, G.M.: Rapid prototyping of microfluidic systems in poly(dimethylsiloxane). *Anal. Chem.* **70**, 4974–4984 (1998)
40. Wu, B., Chen, L.C., Huang, Y., Zhang, Y., Kang, Y., Kim, D.H.: Multiplexed biomolecular detection based on single nanoparticles immobilized on pneumatically controlled microfluidic chip. *Plasmonics* **9**, 801–807 (2014)

41. Henry, C.: Getting under the skin: Implantable glucose sensors. *Anal. Chem.* **70**, (1998)
42. Kane, R.S., Takayama, S., Ostuni, E., Ingber, D.E., Whitesides, G.M.: Patterning proteins and cells using soft lithography. *Biomater. Silver Jubil. Compend.* **20**, 161–174 (1999)
43. Qin, D., Xia, Y., Whitesides, G.M.: Soft lithography for micro- and nanoscale patterning. *Nat. Protoc.* **5**, 491–502 (2010)
44. Whitesides, G.M., Ostuni, E., Jiang, X., Ingber, D.E.: Soft lithography in biology. *Annu. Rev. Biomed. Eng.* **3**, 335–373 (2001)
45. Bourbaba, H., Ben Achaiba, C., Mohamed, B.: Mechanical behavior of polymeric membrane: comparison between PDMS and PMMA for micro fluidic application. *Energy Procedia* **36**, 231–237 (2013)
46. Trinh, K.T.L., Zhang, H., Kang, D.J., Kahng, S.H., Tall, B.D., Lee, N.Y.: Fabrication of polymerase chain reaction plastic Lab-on-a-Chip device for rapid molecular diagnoses. *Int. Neurourol. J.* **20**, S38–S48 (2016)
47. Lee, J.N., Park, C., Whitesides, G.M.: Solvent compatibility of poly(dimethylsiloxane)-based microfluidic devices. *Anal. Chem.* **75**, 6544–6554 (2003)
48. Zhang, Y., Yuan, K., Zhang, L.: Micro/Nanomachines: from functionalization to sensing and removal. *Adv. Mater. Technol.* **4**, 1–22 (2019)
49. Lin, T.J., Chung, M.F.: Using monoclonal antibody to determine lead ions with a localized surface plasmon resonance fiber-optic biosensor. *Sensors* **8**, 582–593 (2008)
50. Ymeti, A., Greve, J., Lambeck, P.V., Wink, T., van Hoval, S.W.F.M., Beumer, T.A.M., Wijn, R.R., Heideman, R.G., Subramaniam, V., Kanger, J.S.: Fast, ultrasensitive virus detection using a young interferometer sensor. *Chemtracts* **19**, 350–357 (2007)
51. Wan, M., Luo, P., Jin, J., Xing, J., Wang, Z., Wong, S.T.C.: Fabrication of localized surface plasmon resonance fiber probes using ionic self-assembled gold nanoparticles. *Sensors* **10**, 6477–6487 (2010)
52. Cao, J., Tu, M.H., Sun, T., Grattan, V.: Wavelength-based localized surface plasmon resonance optical fiber biosensor. *Sens. Actuators, B Chem.* **181**, 611–619 (2013)
53. Cao, J., Sun, T., Grattan, K.T.V.: Development of gold nanorod-based localized surface plasmon resonance optical fiber biosensor. In: OFS2012 22nd International Conference on Optical Fiber Sensors **8421**, 84211X-84211X-4 (2012)
54. Raphael, M.P., Christodoulides, J.A., Byers, J.M., Anderson, G.P., Liu, J.L., Turner, K.B., Goldman, E.R., Delehanty, J.B.: Optimizing nanoplasmonic biosensor sensitivity with orientated single domain antibodies. *Plasmonics* **10**, 1649–1655 (2015)
55. Pandya, A., Sutariya, P.G., Menon, S.K.: A non enzymatic glucose biosensor based on an ultrasensitive calix [4]arene functionalized boronic acid gold nanoprobe for sensing in human blood serum. *Analyst* **138**, 2483–2490 (2013)
56. Whitesides, G.M.: The origins and the future of microfluidics. *Nature* **442**, 368–373 (2006)
57. Nge, P.N., Rogers, C.I., Woolley, A.T.: Advances in micro fluidic materials, functions, integration, and applications (2013)
58. Shang, L., Cheng, Y., Zhao, Y.: Emerging droplet microfluidics. *Chem. Rev.* **117**, 7964–8040 (2017)
59. Tadepalli, S., Kuang, Z., Jiang, Q., Liu, K.K., Fisher, M.A., Morrissey, J.J., Kharasch, E.D., Slocik, J.M., Naik, R.R., Singamaneni, S.: Peptide functionalized gold nanorods for the sensitive detection of a cardiac biomarker using plasmonic paper devices. *Sci. Rep.* **5**, 1–11 (2015)
60. Spigarelli, L., Bertana, V., Marchisio, D., Scaltrito, L., Ferrero, S., Cocuzza, M.: A passive two-way micro fluidic device for low volume blood-plasma separation. *Microelectron. Eng.* **209**, 28–34 (2019)
61. Chen, H., Kou, X., Yang, Z., Ni, W., Wang, J.: Shape- and size-dependent refractive index sensitivity of gold nanoparticles. *Langmuir* **24**, 5233–5237 (2008)
62. Campu, A., Lerouge, F., Craciun, A.-M., Murariu, T., Turcu, I., Astilean, S., Focsan, M.: Microfluidic platform for integrated plasmonic detection in laminal flow. *Nanotechnology* (2020)

63. Zhang, Y., Tang, Y., Hsieh, Y.H., Hsu, C.Y., Xi, J., Lin, K.J., Jiang, X.: Towards a high-throughput label-free detection system combining localized-surface plasmon resonance and microfluidics. *Lab Chip* **12**, 3012–3015 (2012)
64. Huang, C., Bonroy, K., Reekman, G., Verstreken, K., Lagae, L., Borghs, G.: An on-chip localized surface plasmon resonance-based biosensor for label-free monitoring of antigen-antibody reaction. *Microelectron. Eng.* **86**, 2437–2441 (2009)
65. Camara, A.R., Gouvêa, P.M.P., Dias, A.C.M., Braga, A.M.B., Dutra, R.F., de Araujo, R.E., Carvalho, I.C.S.: Dengue immunoassay with an LSPR fiber optic sensor. *Opt Express* **21**(22), 27023–27031 (2013)
66. Guo, L., Kim, H.: LSPR biomolecular assay with high sensitivity induced by aptamer-antigen-antibody sandwich complex. *Biosens. Bioelectron.* **31**, 567–570 (2012)
67. Guo, L., Wang, D., Xu, Y., Qiu, B., Lin, Z., Dai, H., Yang, H.H., Chen, G.: Discrimination of enantiomers based on LSPR biosensors fabricated with weak enantioselective and nonselective receptors. *Biosens. Bioelectron.* **47**, 199–205 (2019)
68. Qiu, G., Gai, Z., Tao, Y., Schmitt, J., Kullak-Ublick, G.A., Wang, J.: Dual-functional plasmonic photothermal biosensors for highly accurate severe acute respiratory syndrome coronavirus 2 detection. *ACS Nano* (2020)
69. Lv, X., Geng, Z., Su, Y., Fan, Z., Wang, S., Fang, W., Chen, H.: Label-Free Exosome Detection Based on a low-cost plasmonic biosensor array integrated with microfluidics. *Langmuir* **35**(30), 9816–9824 (2019)
70. Fan, Z., Geng, Z., Fang, W., Lv, X., Su, Y., Wang, S., Chen, H.: Smartphone biosensor system with multi-testing unit based on localized surface plasmon resonance integrated with microfluidics chip. *Sensors (Switzerland)* **20**, 1–13 (2020)
71. Ďurč, P., Foret, F., Kubáň, P.: Fast blood plasma separation device for point-of-care applications. *Talanta* **183**, 55–60 (2018)
72. Kersaudy-Kerhoas, M., Dhariwal, R., Desmulliez, M.P.Y., Jovet, L.: Hydrodynamic blood plasma separation in microfluidic channels. *Microfluid. Nanofluidics* **8**, 105–114 (2010)
73. Maria, M.S., Chandra, T.S., Sen, A.K.: Capillary flow-driven blood plasma separation and on-chip analyte detection in microfluidic devices. *Microfluid. Nanofluidics* **21**, 1–21 (2017)
74. Yang, S., Ündar, A., Zahn, J.D.: A microfluidic device for continuous, real time blood plasma separation. *Lab Chip* **6**, 871–880 (2006)
75. Sivaramkrishnan, M., Kothandan, R., Govindarajan, D.K., Meganathan, Y., Kandaswamy, K.: Active microfluidic systems for cell sorting and separation. *Curr. Opin. Biomed. Eng.* **13**, 60–68 (2020)
76. Ahmed, D., Peng, X., Ozcelik, A., Zheng, Y., Huang, T.J.: Acousto-plasmodfluidics: acoustic modulation of surface plasmon resonance in microfluidic systems. *AIP Adv.* **5**, (2015)
77. Wolter, O., Mayer, G.: Aptamers as valuable molecular tools in neurosciences. *J. Neurosci.* **37**, 2517–2523 (2017)

Chapter 10

Development of Piezoelectric Nanogenerator Based on Micro/Nanofabrication Techniques and Its Application on Medical Devices



Aparna Zagabathuni  and Subramani Kanagaraj 

1 Introduction

Wearable and implantable electronic devices have undergone rapid growth for the treatment and detection of different diseases [1]. These medical devices can improve the quality of life of the patient more efficiently and prolong the lifetime of patients. However, their advancement also faces many obstacles, such as size, weight, flexibility, and durability. Most modern electronic devices need an external power supply for complete functioning which is a major disadvantage. Because of its independence, durability, and maintenance-free existence, self-powered electronics have gained popularity as alternative computing technology. Self-powered electronics are defined as electronics that can be operated without an external power supply.

The rapid development of nanogenerators due to its flexibility, simple structure, lightweight, low cost, and high efficiency have allowed the design of self-powered systems which can operate without external supply. In 2006, Z. L. Wang first proposed the idea of nanogenerators encapsulated in the expression “piezoelectric nanogenerators” [2]. They developed a vertically aligned piezoelectric zinc oxide nanowire arrays that were actuated by the atomic force microscope (AFM) containing Pt-coated tip to transform nano-scale mechanical energy to electrical energy. Since then piezoelectric nanogenerators have been used in several different applications from powering small electronic devices to function as active sensors for human-machine, infrastructural, medical, security, and environmental monitoring [3]. Nanogenerators are capable of harvesting mechanical energy from a range of sources along with

A. Zagabathuni · S. Kanagaraj (✉)
Department of Mechanical Engineering, Indian Institute of Technology Guwahati, Guwahati,
Assam 781039, India
e-mail: kanagaraj@iitg.ac.in

A. Zagabathuni
e-mail: aparnazag@iitg.ac.in

movements of the human body and various types of activities which make them useful for biomedical applications. Nanogenerators can transform minute mechanical energy into electrical energy in body movement, respiration, bone strain, muscle contraction/relaxation, etc. Piezoelectric nanogenerators have the advantages of high sensitivity, lower dimensions, compact structure, durability, and a high response to strain compared with other passive sensors [4].

In this chapter, we first briefly introduce the concept of piezoelectric nanogenerator and then concentrate on the type of materials and device structure for fabricating piezoelectric nanogenerators. Besides, we will present a few case studies on the application of piezoelectric nanogenerators for monitoring blood pressure, heart activity, and also for directly stimulating the brain, and auditory nervous system. Finally, we discuss the challenges and predictions of the potential growth of the piezoelectric nanogenerators. We presume that this chapter of the book will motivate the people who were interested in the production of nanogenerators and their application in medical devices.

2 Working Principle of Piezoelectric Nanogenerator

Maxwell's theory of displacement is the scientific roots for nanogenerators [5]. Piezoelectric nanogenerator working mechanism is based on the piezoelectric potential generated by the presence of electric dipole in the materials under straining. The piezoelectric nanogenerator consists of a piezoelectric material and two electrodes that bind to the piezoelectric material on both sides. Whenever a mechanical force acts on the piezoelectric nanogenerator, the electric dipoles in the piezoelectric material align in a single direction due to a potential difference between the electrodes being formed. This allows the current to flow through an outer circuit from top to bottom electrodes as shown in Fig. 1a. When the force is released, the electrical

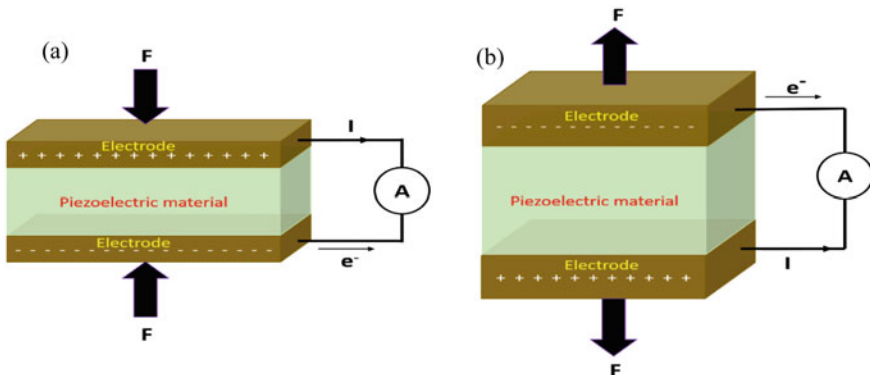


Fig. 1 Working mechanism of piezoelectric nanogenerator

dipoles reverse and cause the current to flow from the bottom to the top as shown in Fig. 1b.

For example, if we consider the wurtzite structure of ZnO crystal which is a piezoelectric material, its root structure can be described as a layer by layer accumulation along the *c*-axis of tetrahedrally coordinated Zn^{2+} and O^{2-} as shown in Fig. 2a [6]. Initially, the center of charge of anions and cations coincides with one another. The system may be extended or squeezed if an external force is applied. Consequently, the positive and negative charge centers are divided and generate an electric dipole that ultimately results in piezoelectric potential. The distribution of piezoelectric potential in a ZnO nanowire under the application of external force is shown in Fig. 2b.

Initially, the ZnO nanowire is in the equilibrium position. If a tensile force is exerted parallel to the *c*-axis on a nanowire surface, the length of the nanowire increases leading to a voltage drop of 0.4 V across the nanowire ends. When the applied force is reversed, i.e., compressive force, the nanowire length decreases, and the piezoelectric potential was reversed with the same voltage difference (0.4 V). The relationship between the piezoelectric potential and the output voltage has been explained in Fig. 2c with the help of a band diagram. The tip (T) of atomic force microscopy has a Schottky interaction with one end of the nanowire and ohmic interaction on the other end, i.e., on the grounded side (G). When the tip slowly moves on the nanowire, a positive piezoelectric voltage is generated on the tensile surface. The electron passes via an external load from the negative electrode (G), and pile up at the tip as the tip keeps moving the nanowire. The electrons were unable to cross the interface because of the reverse-biased Schottky barrier at the tip–nanowire interface. Once the tip hits the middle point of the nanowire during screening, the reverse flow of the collected electrons occurs due to the local potential drop. A considerable increase in the conduction band has been observed once the tip hits the endpoint of the nanowire. If the piezoelectric potential is greatly increased, the electrons in the nanowire will flow over to the tip. This basic method of producing piezoelectric potential applies to different piezoelectric materials.

3 Materials for Piezoelectric Nanogenerators

Piezoelectric nanogenerators can capture energy directly from their natural environment, i.e., in case of medical devices through movements from the human body. Nanogenerators centered on nanoparticles, nanowires, nanosheets, nanotubes, nanorods, etc. are in most cases inserted into different structures to accommodate within the body. There are various nanogenerator materials documented to date [7–10]. The piezoelectric process happens in materials which have a crystal structure without a center of symmetry. Explicitly configured with superior flexibility, lead-free materials, polymers, and composites are mostly preferred for medical applications. The nanogenerators used in medical applications should be highly sensitive and can function efficiently because certain movements of the body, such as heart rhythm,

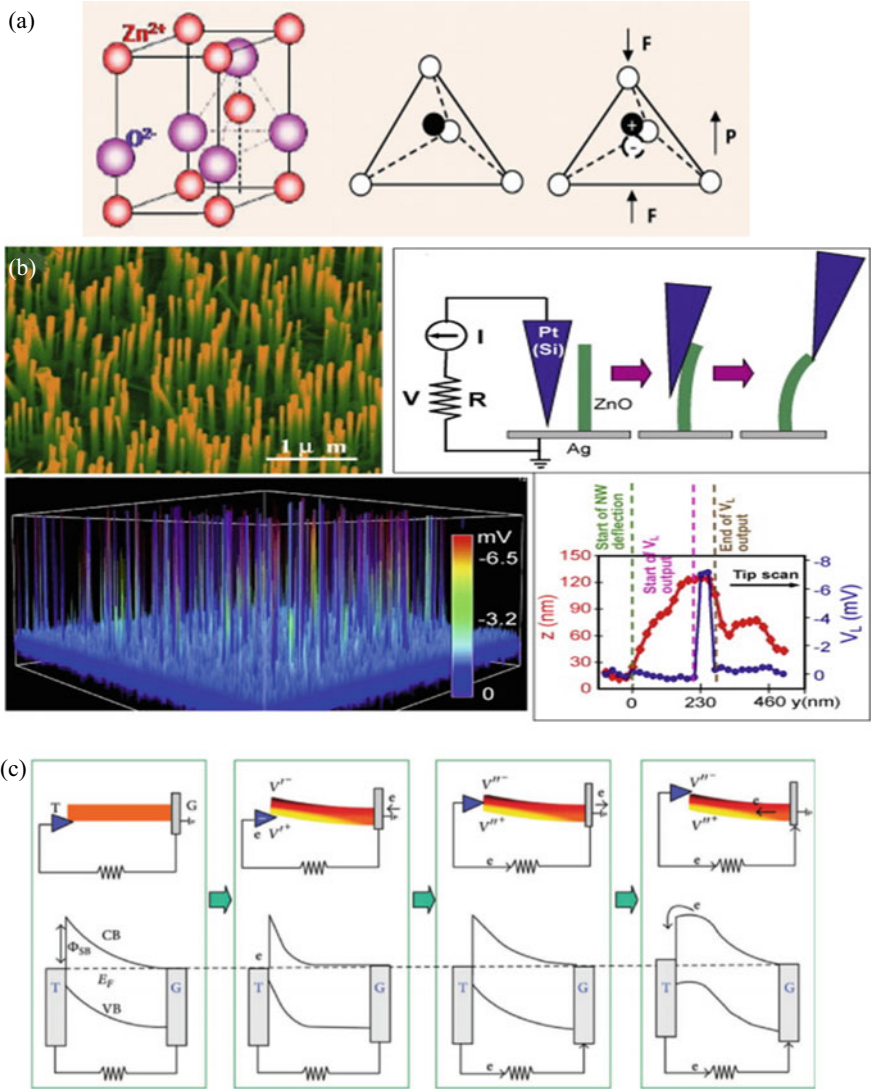


Fig. 2 a Wurtzite crystal structure of ZnO, b output voltage of ZnO nanowire arrays-based piezoelectric nanogenerator once the AFM tip scans through the nanowire arrays, and c flow cycle and charge output band diagrams in nanogenerators [6]. Copyright ©2009, Elsevier

breathing, muscle stretching, etc., are often very mild and make a small amplitude. Nanogenerators require high energy conversion efficiency and adequate output power to be used in the equipment of similar size.

3.1 Lead-Based Materials

Owing to its large output voltage, excellent piezoelectric constant, and high piezoelectric voltage constant, lead-based piezoelectric nanogenerators have received a lot of attention. A flexible piezoelectric nanogenerator was fabricated by transferring a $0.65\text{Pb}(\text{Mg}_{1/3}\text{Nb}_{2/3})\text{O}_3\text{-}0.35\text{PbTiO}_3$ (0.65PMN–0.35PT)-shaped perovskite nanowires produced by hydrothermal process onto a plastic substrate patterned by Au electrode [1]. Electrical poling was performed at 120°C by providing an electric field of 100 kVcm^{-1} for 4 h to enhance the piezoelectric efficiency. The 0.65PMN–0.35PT nanowires-based nanogenerator produced a 1.5 nA current and 9 mV voltage during regular bending and unbending motions. The power density and current density obtained from 0.65PMN to 0.35PT nanowires-based nanogenerator was observed to be 175.4 Wcm^{-3} and 9.7 Acm^2 , respectively.

Recently, Jin et al. [11] synthesized $\text{Pb}(\text{Zr}, \text{Ti})\text{O}_3$ (PZT) nanorod arrays on a pre-oxidized titanium substrate via poly(vinyl alcohol)-assisted hydrothermal process. The PZT nanorod arrays comprise an underlying layer of a PZT film and the nanorods are very well positioned along (001) oriented single-crystalline tetragonal structures that showed strong piezoelectric constant of 1600 pmV^{-1} . The as-synthesized PZT nanorod arrays generated a voltage of 3.3 V when a 10 N force was applied in compression mode by dynamic mechanical analyzer at a frequency of 10 Hz while 8 V was exerted by finger tapping motion. With the external load of $1\text{ M}\Omega$, the average power density generated by compression mode and finger tapping motion were $3.16\text{ }\mu\text{Wcm}^{-2}$ and $5.92\text{ }\mu\text{Wcm}^{-2}$, respectively.

A piezoelectric fiber-type nanogenerator based on PbTiO_3 nanotube on Ti core-shell fiber was fabricated with electrochemical anodization through a hydrothermal process [12]. For acquiring highly crystalline material and also to decrease the oxygen vacant sites, an additional annealing process was conducted. Upon the formation of thin PDMS via spin coating technology, the PbTiO_3 nanotubes/Ti core-shell was housed on an Au/Cr/Polyimide film. While convex and concave bending motions, the piezoelectric nanogenerators based on PbTiO_3 nanotubes/Ti core-shell provided a voltage of 620 mV and current density of 1 nA/cm^2 . In contrast, the dual-core shell piezoelectric nanogenerator displayed constant isotropic energy irrespective of the bending direction.

A single crystal $0.72\text{Pb}(\text{Mg}_{1/3}\text{Nb}_{2/3})\text{O}_3\text{-}0.28\text{PbTiO}_3$ (0.72PMN–0.28PT) thin film was grown on a Si wafer using the Bridgman method [13]. At room temperature, the thin film 0.72PMN–0.28PT was electrically poled with a 1.8 kV/mm electric field. To transfer the thin film on to a plastic substrate, a mechanical exfoliation procedure was adopted using a nickel stress sheet. A polymer binds the free-standing Ni layer onto a polyethylene terephthalate (PET) film, and Ni is etched to reveal the device's top electrode. This thin-film-based piezoelectric nanogenerator provided 8.2 V and $145\text{ }\mu\text{A}$ output voltage and output current, respectively.

Although the piezoelectric constant, of the lead-based piezoelectric nanogenerators, attracts many researchers for various applications, however, due to the toxic Pb concentration, poling, and its brittle nature under the application of force restrict its application in medical electronic devices.

3.2 *Lead-Free Materials*

Khan et al. [14] adopted a simple technique for piezoelectric nanogenerator production, focusing on 3D-ZnO nanosheets. Using the hydrothermal method, the 3D-ZnO nanosheets were manufactured on a thin layer of anodic aluminum oxide (AAO) membrane that serves as an isolating layer. The piezoelectric nanogenerator is comprised of the Al electrode as a base layer, 3D-ZnO on the AAO layer as a piezoelectric material, and Cu thin sheet as the top electrode. The piezoelectric nanogenerator, after applying 3 kgf of mechanical force produced an output voltage, current, and maximum power density of 895 mV, 446 nA, 50 nW/cm², respectively. The fabricated piezoelectric nanogenerator was then used as a load capacitor and noticed that the capacitor reaction affects the piezoelectric nanogenerator's charging capacity. The optimized energy storage value was obtained in 10 nF load capacitor at a constant 3600 cycles that provide a reactant of 2 M Ω . Constant stability was observed in the performance of 3D-ZnO nanosheets-based piezoelectric nanogenerator after continuous activity for a duration of 3 h. It was noticed that the ZnO's sheet-like nanostructure enhances the piezoelectric nanogenerator output performance, robustness, and durability.

A flexible piezoelectric nanogenerator containing an array of ZnO nanorod placed between two layers of silver-coated fabrics was developed by Zhang et al. [15]. A basic screen printing technique has been adapted for plating Ag paste as electrodes upon the fabric surface. This sandwich-like piezoelectric nanogenerator also gives excellent Schottky interaction between Ag electrodes and ZnO nanorods and indeed provides a smooth operational mode in which the outer fabrics behave as base materials and also preserve the ZnO nanorods. This piezoelectric nanogenerator produced 0.8 V of open-circuit voltage and 5 nA of short-circuit current during finger bending, whereas 4 V of voltage and 20 nA of current during palm clapping.

A versatile yarn-based piezoelectric nanogenerator was produced by Maria Joseph Raj et al. [16] based on the brush coating method. Highly crystalline nanoparticles of the Bi₄Ti₃O₁₂ have been produced by using the sol-gel process. The coating layer of the Bi₄Ti₃O₁₂ nanoparticles serves as a piezoelectric layer. A polyvinylidene fluoride (PVDF) layer between the Ag electrodes prevents the device from short-circuiting. The piezoelectric nanogenerator was polarized electrically by setting a constant voltage of 7 kV throughout 12 h. Before the poling phase, the piezoelectric nanogenerator produced a voltage output of 28 V and current output of 150 nA against mechanical stress of 1 N. With the same applied stress (1 N), the poled piezoelectric nanogenerator exhibited a current of 400 nA and voltage of 60 V, respectively. The

output variability may be attributed to creating permanent polarization by aligning the largest number of dipoles along the same path.

An elastic beam in the shape of the tuning fork combined with ZnO nanorods-based piezoelectric nanogenerator was developed by Deng et al. [17]. The robust Kapton substrate has been sliced in the shape of the tuning fork, and a copper layer which serves as a bottom electron was rested on the Kapton substrate using the sputtering technique. By evaporation technique, a thin layer of ZnO was placed on the bottom electrode which acts as a seed layer. Through the hydrothermal process, the ZnO nanorods have been produced on the ZnO seed-coated Kapton film. Later, spin coating has been performed to deposit a thin sheet of polymethyl methacrylate (PMMA) on to the substrate. Finally, the copper electrode which serves as a top electrode was placed on the PMMA layer. To examine the performance of the piezoelectric nanogenerator, a vibrator has been used to produce oscillations. The peak voltage output of 160 mV and peak current output of 11 nA were obtained from the tuning fork-shaped piezoelectric nanogenerator.

3.3 Polymeric Materials

The necessity of biodegradable materials encouraged development in polymeric functional materials for energy storage and as an actuator/sensor in medical devices. Due to better flexibility and elasticity, polymers can be a possible resource for energy-harvesting applications. A PVDF and its copolymers have been adopted for the fabrication of flexible piezoelectric nanogenerators because of their inherent flexibility, mechanical rigidity, and high processability.

A PVDF nanofiber-based nanogenerator was developed by Chang et al. [18]. To generate piezoelectric properties, a near-field electrospinning technique was adopted to position piezoelectric PVDF nanofibers on the working substrate using mechanical in situ expansion and electrical poling. The intense electrical current and the expansion forces from the electrospinning process combine automatically the dipoles in the nanofiber crystal to turn the nonpolar α phase into the polar β phase, which defines the polarity of the electrospun nanofiber. Under mechanical stretching, the piezoelectric nanogenerator produced a peak current and peak voltage of 3 nA, and 30 mV simultaneously. This piezoelectric nanogenerator has demonstrated reproducible and stable electrical outputs with a magnitude higher energy conversion efficiency than those made from thin PVDF films.

Persano et al. [19] illustrated a piezoelectric nanogenerator featuring the highly aligned electrospun fibers of the poly(vinylidene fluoride-co-trifluoroethylene) (PVDF-TrFE) polymer. Under bending condition, this PVDF-TrFE fiber arrays-based piezoelectric nanogenerator displayed an output voltage of 1.5 V and an output current of 40 nA.

To make a flexible piezoelectric nanogenerator, PVDF thin film on the silicon substrate was polarised by Liu et al. [20]. The flexible piezoelectric nanogenerator, when regularly extended by a linear motor, provided a current of 400 nA and

voltage of 1.5 V. This lightweight piezoelectric nanogenerator is used as a portable, self-powered respiratory detector for real-time monitoring of human respiratory conditions via the integration of an elastic band.

3.4 Composite Materials

A versatile hybrid nanocomposite nanogenerator developed with BaTiO₃ nanowire was produced via the hydrothermal process and dispersed in a poly(vinylidene fluoride-co-tri-fluoroethylene) (P(VDF-TrFE)) matrix [21]. This composite material had been sandwiched on a sheet of polyethylene terephthalate (PET) between two electrodes. Because of different poling coefficients of BaTiO₃ and P(VDF-TrFE), a double-sided poling process polarized the resulting system. Owing to high piezoelectricity of BaTiO₃ relative to P(VDF-TrFE), the current and voltage of the nanogenerator increased up to 20 wt.% composition of BaTiO₃ nanowires. With further increase in BaTiO₃ nanowire concentration, both current and voltage were decreased, which could be attributed to the modifications in the electromechanical coupling due to high dielectric constants and aggregation of nanowires resulting from rapid solvent evaporation. This flexible hybrid nanogenerator was mounted on the rear side of a person's hand and observed 8 V and 900 nA voltage and current, respectively.

Moorthy et al. [1] manufactured a nanocomposite piezoelectric nanogenerator with PMN-PT nanowires and a polydimethylsiloxane (PDMS) elastomeric matrix. PDMS elastomeric matrix was initially prepared and a thin layer of PDMS was deposited over Si wafer to develop a dielectric layer between the indium tin oxide electrode (ITO) and the piezoelectric material. The piezoelectric nanocomposite (PN) has been made by mixing the hydrothermally synthesized PMN-PT nanowires without any dispersant into the elastomeric matrix of the PDMS. Using the spin coating process, the piezoelectric nanocomposite layer was mounted on a Si wafer covered with PDMS. The PN/PDMS/Si substrate was coated with a fine layer of PDMS and the Si wafer was eventually removed and the remaining chip was moved to an ITO-coated thick PET substrate. Under periodical bending and unbending motions, this nanocomposite piezoelectric nanogenerator exhibited a current of 400 nA and a maximum output voltage of 4 V, respectively.

Li et al. [22] announced a new piezoelectric nanocomposite based on the nanorods of 0.7Pb(Mg_{1/3}Nb_{2/3})O₃-0.3PbTiO₃ (0.7PMN-0.3PT). The 0.7PMN-0.3PT nanorods have been prepared by the hydrothermal process, and the piezoelectric nanocomposite is prepared by dispersing these nanorods in PVDF that prevents nanorods breakage under mechanical stress. The nanocomposite was then tape-casted onto a glass plate and gradually cured. Upon curing the nanocomposite film, the parts were peeled off and plated on both sides with Ni/Au electrodes. The piezoelectric nanogenerator was then pooled at 100 °C in a silicone oil bath to an electric field of

5 kV/mm. The maximum output current of 46 nA and maximum output voltage of 10.3 V were obtained in the 20 wt.% nanorod samples that were capable to deliver a 13-fold greater voltage and a 4.5-fold greater current than with pure piezoelectric polymer PVDF.

4 Medical Applications

4.1 Blood Pressure Sensor

Hypertension has become a chronic long-term condition and a significant danger aspect for stroke and heart failure [23]. The prevalence of hypertension is rising year after year mostly in the elderly population. An implantable blood pressure monitor can perform a critical task in the early detection and appropriate disease and drug assessment [24, 25]. An effective approach is to directly pulsate the aorta as a source of power for the blood pressure monitor. But the structure needs to be flexible, compact, and robust owing to the delicate characteristics of the aorta and fairly limited heart space.

A piezoelectric nanogenerator developed by Zhang et al. [26] comprises a robust PVDF film coated with the Al layer and enclosed with a polyimide film that is capable of extracting the pulse energy from an upward aorta movement (Fig. 3a). For the *in vitro* procedure, a latex tube was directed to pulsate via an intra-aortic balloon pump to imitate the pulsation of the ascending aorta. To grab the pulsating energy and transform it into electricity, a part of the latex tube was fitted with a piezoelectric nanogenerator. Under the flow pressure of 160/80 mmHg, a maximum current of 400 nA and a peak output voltage of 10.3 V could be obtained from a piezoelectric nanogenerator-dependent PVDF film of 2.5 cm × 5.6 cm × 200 μm. For the *in vivo* test, the manufactured device was wrapped across the elongated aorta of a male domestic porcine as shown in Fig. 3b. As shown in Fig. 3c, under the blood pressure of 160/105 mm Hg and heart rate of 120 bpm, the peak voltage and current achieved from the piezoelectric nanogenerator were 1.5 V and 300 nA, respectively. Within 40 s, the implanted piezoelectric nanogenerator could charge up to 1.0 V for a 1 μF capacitor. Such electrical output signals were strongly synchronous with the signals from electrocardiography, heart rate, and blood pressure.

The earlier research prompted Cheng et al. [27] to investigate a PVDF thin film-centered piezoelectric nanogenerator as a self-operated blood pressure monitor (Fig. 4a). This PVDF thin film-based pressure monitor showed a 173 mV/mm Hg sensitivity and high linearity ($R^2 > 0.99$) for peak output voltage and flow pressure in the *in vitro* study. In the *in vivo* test, the thin film-based piezoelectric nanogenerator was encased around the ascending male porcine aorta and observed a good sensitivity of 14.3 mV/mm Hg with reasonable linearity ($R^2 > 0.97$) measured between peak voltage and the peak systolic blood pressure (Fig. 4b). During the *in vivo* test,

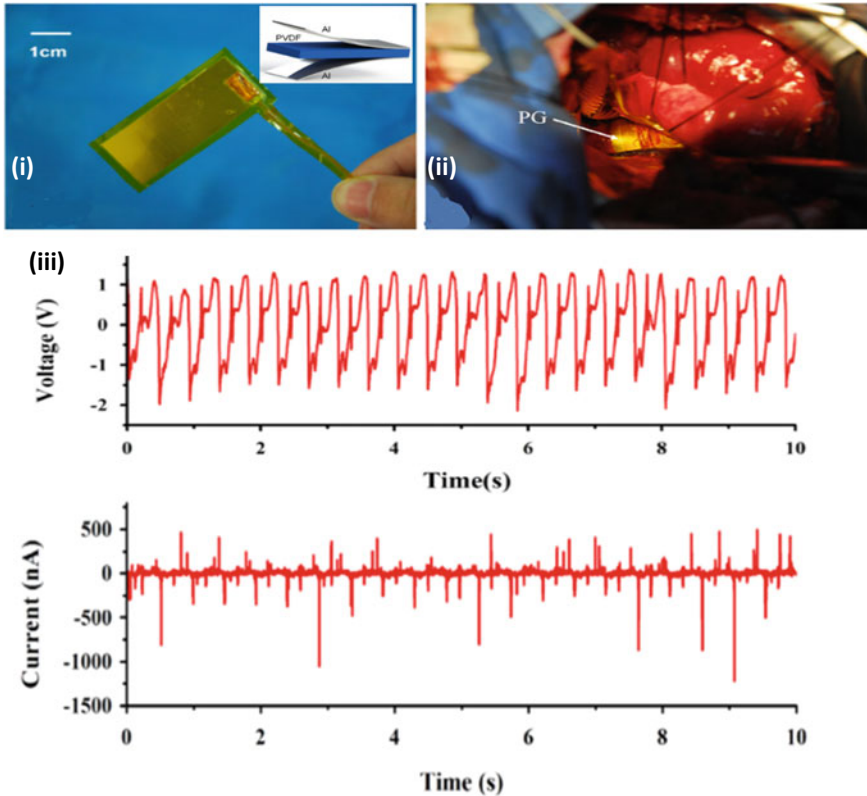


Fig. 3 PVDF film-based piezoelectric nanogenerator. **a** Sealed in a polyimide tape, **b** Encased across the elongated aorta of a porcine, **c** The output voltage and current with flow pressure and ECG signal obtained from the piezoelectric nanogenerator [26]. Copyright ©2015, Elsevier

a highest instantaneous power of 40 nW has been obtained. This device can monitor blood pressure and hypertension in real-time.

4.2 Cardiac Sensor

Cardiac sensors were implanted in the heart to detect arrhythmic symptoms and provide a timely response about the heartbeat condition. With the aid of this implantable cardiac sensor, irregular heart rhythms of the patients with syncope, angina, dizziness, heart failure, etc. can be regulated easily by continuous monitoring with high accuracy [28].

Li et al. [29] fabricated an implantable piezoelectric nanogenerator for capturing the natural energy of the heartbeat and instantly powering the cardiac pacemaker. The piezoelectric nanogenerator is comprised of two piezoelectric composites on

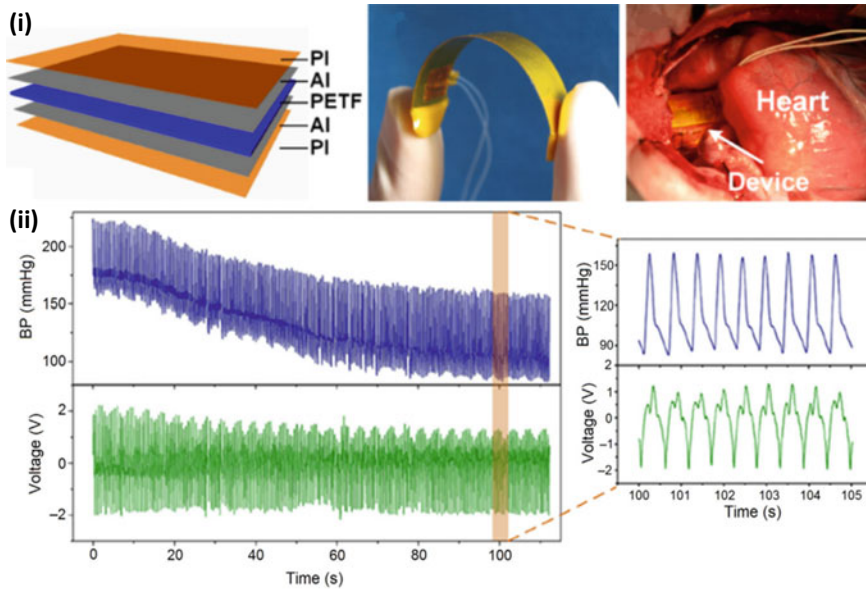


Fig. 4 The piezoelectric nanogenerator as a blood pressure sensor **a** The exploded view of multi-layer thin film piezoelectric nanogenerator that was robust enough to enclose on the porcine aorta, **b** The in vivo output voltage obtained from the multi-layer thin-film piezoelectric nanogenerator [27]. Copyright ©2016, Elsevier

the elastic skeleton as shown in Fig. 5a. The piezoelectric composite consists of beryllium-bronze foil, single crystalline (72%) $\text{Pb}(\text{Mg}_{1/3}\text{Nb}_{2/3})\text{O}_3$ –(28%)– PbTiO_3 piezoelectric layer, and Cr/Au electrodes. The output signal of the piezoelectric generator during compression and expansion by fingers is shown in Fig. 5b. During this cycle, an alternating current is produced, and the piezoelectric generator output hits its positive limit in the compression state and negative in the expansion state. The piezoelectric generator is then implanted in the apex of the pericardial sac as shown in Fig. 5c. When the heart contracts in the systolic phase, the device expands while the heart in the diastolic phase is compressed. The waveforms of the electrocardiogram (ECG) and the corresponding open-circuit voltage (V_{oc}) and the short-circuit current (I_{sc}) of the implanted generator are shown in Fig. 5d. The implanted piezoelectric generator generated the maximum output voltage of 20 V and a short circuit current of 8 μA in series mode, and a voltage and current of 12 V and 15 μA in parallel mode.

Later, a flexible and lead-free LiNbO_3 -doped (K, Na) NbO_3 (LiNN) thin-film based piezoelectric nanogenerator fabricated by Jeong et al. [30] was tested on a porcine heart Fig. 6a. The LiNN piezoelectric nanogenerator exhibited a current of 700 nA and voltage of 5 V from the contraction and relaxation of porcine heart Fig. 6b. For biocompatible and eco-friendly applications, this LiNN thin-film piezoelectric nanogenerator can be an alternative to lead-based piezoelectric materials.

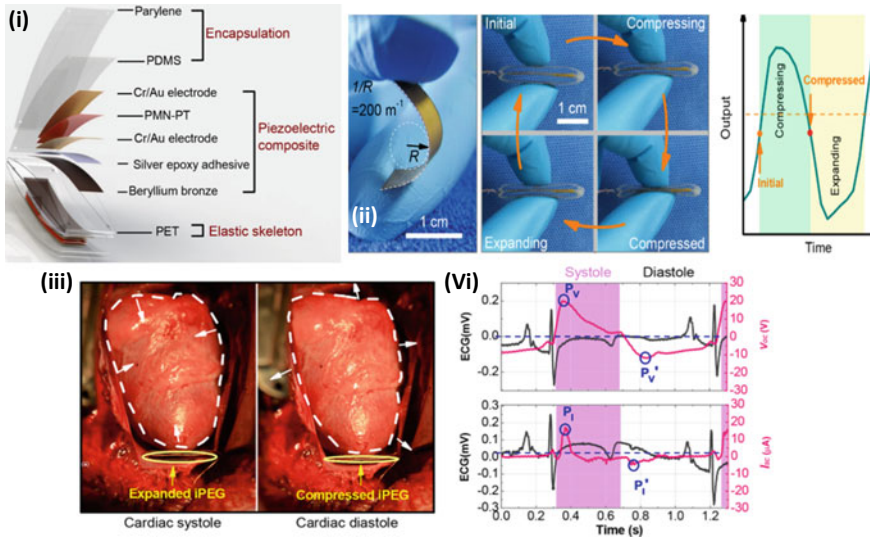


Fig. 5 a Schematic of piezoelectric nanogenerator and the enhanced view of piezoelectric composite on the upper side of the elastic skeleton, b Output signal of piezoelectric composite bent by fingers in one working cycle, c Schematic view of piezoelectric nanogenerator expansion during systolic phase and compressed during diastolic phase, and d ECG, V_{oc} , and I_{sc} waveforms of the piezoelectric nanogenerator at the apex [29]. Reprinted with permission from Li et al. [29]. Copyright ©2019, American Chemical Society

4.3 Auditory Nerve Stimulation in the Cochlea

The hair cells inside the inner ear which are responsible for hearing (connected to the auditory nerves) get damaged by many causes like head trauma, disclose to excessive sound, infections, age, diseases, etc. [30]. With the help of the piezoelectric material, the auditory nerves can be directly stimulated by transforming mechanical stress into electrical energy.

A cochlear implant is a neural prosthetic system that activates auditory nerves circumventing the impaired inner ear part to preserve usable hearing for individuals with moderate to profound hearing loss. A cochlear implant comprises two components: an external sound processor and an internal device. Behind the ear, the external sound processor transforms the sound signal into digital code. These signals are sent to the radiofrequency coil which is held onto the side of the head with a magnet. The radiofrequency coil sends the coded signal through the skin to the receiver which is under the skin. The implant converts the digital code into electrical signal impulses and sends these signals along the electrode array in the inner ear [32, 33]. The main drawback of the cochlear implant is the external processor that requires a continuous power supply, and patients are uncomfortable wearing it. Therefore, a completely implantable nanogenerator-operated cochlear implant can solve this issue.

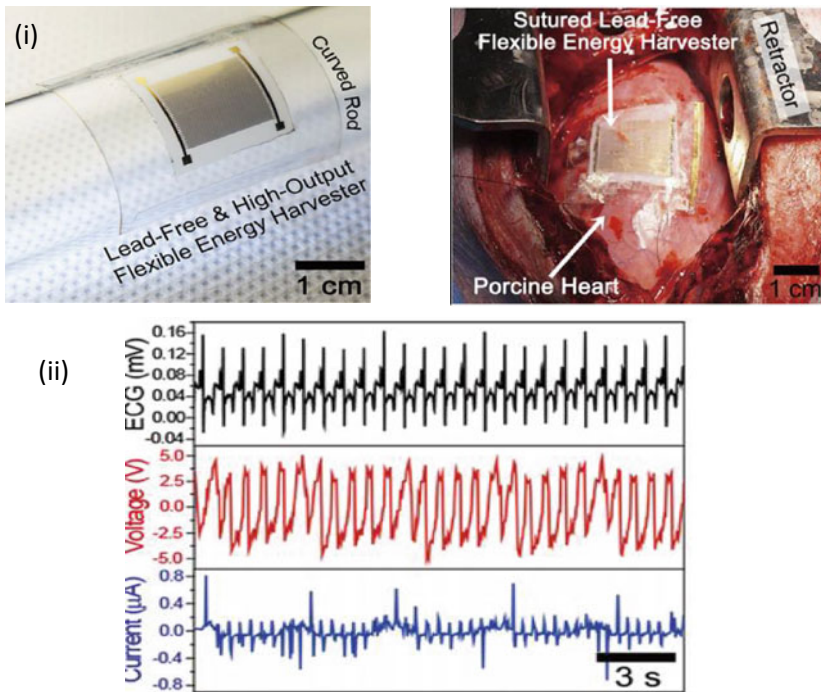


Fig. 6 **a** LiNN thin film, flexible LiNN-based piezoelectric nanogenerator sutured on a porcine heart, and **b** From the in vivo tests output voltage, current, and ECG signals obtained from the LiNN-based piezoelectric nanogenerator [31]. Reprinted with permission from Jeong et al. [31]. Copyright ©2017 APL Materials

Jang et al. [34] developed a micro-electro-mechanical system (MEMS)-based cantilever array beam composed of an aluminum nitride as a piezoelectric material which is sandwiched between Mo layer and Au layers that acts as a bottom electrode and top electrodes, respectively. The fabricated system used eight cantilevers to demonstrate a simple tonotopy within an audible range of 2.92–12.6 kHz. The piezoelectric output signal for the corresponding sound frequency of 42–20 kHz was 0.354–1.67 mV/Pa at 101.7 dB SPL. Deafened guinea pigs have been used to test the device's ability. For auditory neurons, a signal processor has been used to transform the piezoelectric output from the system into an electrical signal that was transmitted by an implantable intracochlear electrode array. For incoming sound pressure ranges of 70.1–94.8 dB SPL, the amplitude of the electrical signal was modulated within the range of 0.15–3.5 V as shown in Fig. 7b. The electrical signal was used to induce an auditory brain stem response (EABR) electrically evoked by deafened pigs (Fig. 7a).

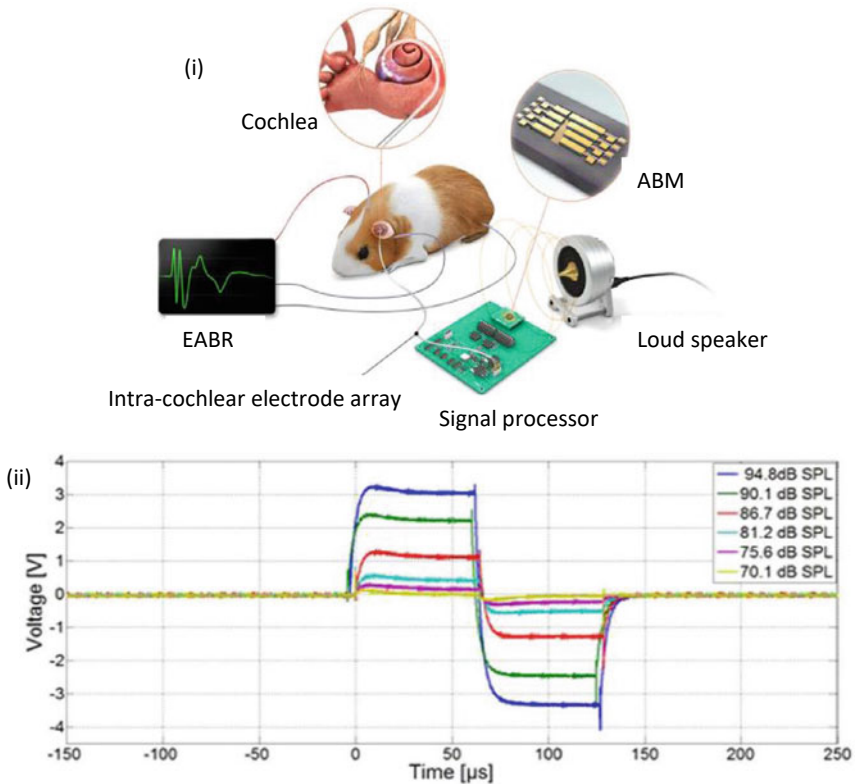


Fig. 7 **a** Artificial basilar membrane (ABM) consisting of an integrated AlN-based cantilever array containing a signal processor and an intracochlear array, **b** The output voltage on the applied SPL (70.1–94.8 dB SPL) from an AlN-based cantilever arrays [34]

4.4 Deep Brain Stimulation

It is a neurosurgical procedure that activates a particular brain portion with electrical stimuli to treat various neurological conditions including mental illness, essential tremor, Parkinson's disease, and epilepsy [35, 36]. An implantable brain stimulator requires 3–5 V, and 130 Hz high processing power having a pulse length of 60 ms, which is several times greater than from a pacemaker which requires 2 V, 1 Hz, and 400 ms pulse length. The biggest challenge of designing a self-powered deep brain stimulator is its design structure, the manufacturing process, and finally, the piezoelectric nanogenerator implantation.

Kim et al. [37] developed a robust single crystal $\text{Pb}(\text{In}_{1/2}\text{Nb}_{1/2})\text{O}_3\text{--Pb}(\text{Mg}_{1/3}\text{Nb}_{2/3})\text{O}_3\text{--PbTiO}_3$ (PIN-PMN-PT) film for deep brain stimulation on plastic PET substrate (Fig. 8a). A voltage of 11 V was observed under mechanical bending, with a maximum output current of 283 μA which can charge a capacitor that can

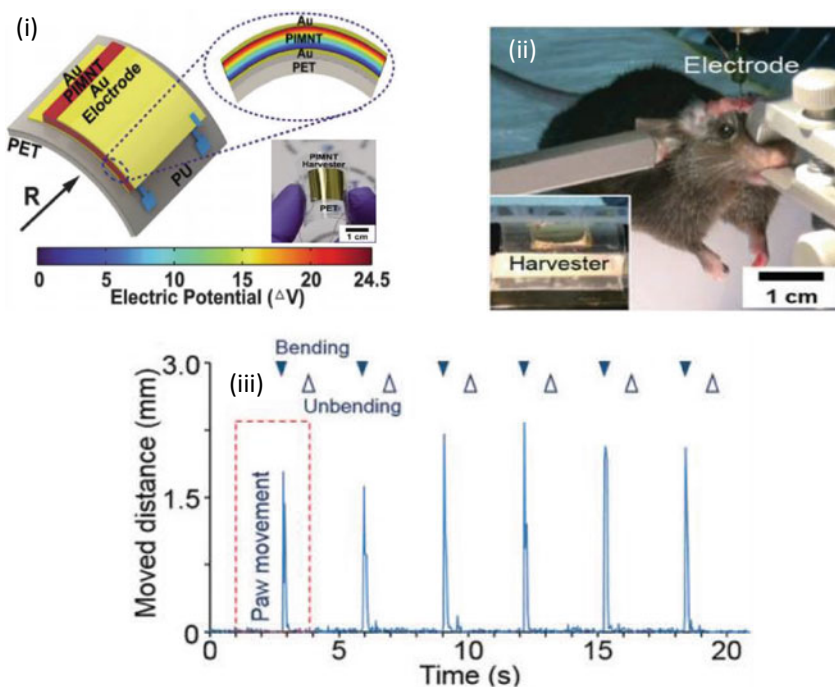


Fig. 8 **a** Flexible PIN-PMN-PT film on PET substrate, **b** The flexible PIN-PMN-PT-based piezoelectric nanogenerator mounted on a fixed anesthetized mouse with a bipolar stimulating electrode located in the M1 cortex, **c** The range of foot movement for six cycles of electric brain stimulation [37]. Copyright ©2015, Royal Society of Chemistry

switch on 120 LEDs. When PIN-PMN-PT-dependent piezoelectric nanogenerator is bent using human fingers, a maximum output current of 0.57 mA and a maximum power of 0.7 mW were observed. This piezoelectric nanogenerator dependent on PIN-PMN-PT has been tested for triggering the primary motor cortex in a live mouse brain (Fig. 8b). The electrical energy produced by this nanogenerator was directly transmitted via metal wires to the stimulating electrode which is exactly placed at the primary motor cortex. For each bending cycle of PIN-PMN-PT-based nanogenerator, the forelimb muscle gets contracted and displacement of 1.5–2.3 mm was observed in the mouse's right paw (Fig. 8c).

4.5 Other Applications

Few other applications of piezoelectric nanogenerator are tabulated in Table 1.

Table 1 Piezoelectric nanogenerator as sensor for biomedical applications

S. No	Application	Piezoelectric nanogenerator material	Output voltage (V)	Output current (μ A)	References
1	Cardiac sensor	0.5 mol.% Mn-doped single crystalline $0.4 \text{Pb}(\text{Mg}_{1/3}\text{Nb}_{2/3})\text{O}_3$ - $0.6 \text{Pb}(\text{Zr}_{0.42}\text{Ti}_{0.58})\text{O}_3$ (Mn-doped PMN-PZT)	17.8 V	1.75	[38]
2	Pulse sensor	$\text{Pb}[\text{Zr}_x\text{Ti}_{1-x}]\text{O}_3$ (PZT) thin film	$V_{oc} = 400 \text{ mV}$ from carotid artery pulse $V_{oc} = 100 \text{ mV}$ from saliva swallowing	–	[39]
3	Gastrointestinal sensor	PZT ribbons	Output voltage varied from 8 to 30 mV when 200 mL water was infused into stomach, and decreased to 15 mV after the water was suctioned	–	[40]
4	Pulse sensor	Single crystalline III-N thin film	$V_{oc} = 8 \text{ mV}$ at posterior tibial $V_{oc} = 10 \text{ mV}$ at finger tip $V_{oc} = 60 \text{ mV}$ at carotid artery $V_{oc} = 6 \text{ mV}$ at radial artery $V_{oc} = 12 \text{ mV}$ at brachial artery $V_{oc} = 3 \text{ mV}$ at femoral artery	–	[4]
5	Respiratory sensor	PVDF thin film	1.5 V	400 nA	[20]

5 Challenges and Future Development

After the very first article of the piezoelectric nanogenerator in 2006, their application has been found in various therapeutic approaches. In reality, their immense uses and potential in implantable and wearable medical devices made piezoelectric

nanogenerators a pivotal resource for energy conversion. However, there are some challenges with these piezoelectric nanogenerators which need to be addressed.

- (1) The property of the material is very crucial for device performance. The piezoelectric nanogenerator's overall output performance is dependent on the piezoelectric constant of the piezoelectric material. Most of the lead-free/polymeric piezoelectric materials have less piezoelectric constant compared to lead-based piezoelectric materials. A material's piezoelectric properties can be enhanced either by doping or by fabricating a hybrid nanogenerator which can enhance its performance.
- (2) The reliability of the implantable devices has to be taken care of. Implantable devices can break before, during, or after surgery due to its design, size, and complexity in reaching the desired location, failure of the device over time due to material deterioration. All the devices therefore should undergo both finite element analysis and extensive real-world testing to evaluate potential failure modes.
- (3) Longevity is a vital determination of the effectiveness of medical devices. Even a successful device can only operate for a given length of time. An optimal implantable device should last much longer than the patient's projected lifespan to avoid or restrict replacement surgery, as this exposes patients to the greater medical risk and it is expensive too. Higher longevity of implantable medical devices requires some of those same analytical steps as long-term failure prevention, but additional electrical design and analysis are required.
- (4) It is important to make the piezoelectric nanogenerators fully flexible and durable to fit as closely as possible into the form of organs in both in vitro and in vivo test conditions to know the efficiency and increase the capability of the device.
- (5) Biocompatibility and biodegradability are the most important requirements for the implantable devices as they require long term stability and durability.
- (6) More robust, durable, and effective encapsulation should be attained to safeguard the piezoelectric nanogenerator from potential rust or oxidation to bodily fluids.
- (7) To test the functionality and efficacy of the piezoelectric nanogenerator, most of the experiments have so far been conducted on rats or porcine. Tests covering both small and large animals and humans are required to successfully produce and market these implantable medical devices.

6 Conclusions

The human body has plenty of resources that can be used to power electronic health care systems. The improvement in nanotechnology can significantly enhance the health care facilities by harvesting these energies. This book chapter mainly focused on the development and application of piezoelectric nanogenerators which can extract energy from the movements of living bodies. We have summarized some examples of

how to use these piezoelectric nanogenerators in medical devices. Recent research on piezoelectric nanogenerators for monitoring blood pressure, heart activity, and also for directly stimulating the brain and auditory nerve system has been detailed. While piezoelectric devices were already being studied thoroughly for years, there is indeed a significant disparity between the anticipated and accomplished performance. Considering the improvements that have already been made, we anticipate significant improvements to obtain the adaptability of implantable piezoelectric nanogenerators in a scalable and sustainable manner in the near future.

References

1. Moorthy, B., Baek, C., Wang, J.E., Jeong, C.K., Moon, S., Park, K.I., Kim, D.K.: Piezoelectric energy harvesting from a PMN-PT single nanowire. *RSC Adv.* **7**, 260–265 (2017). <https://doi.org/10.1039/c6ra24688e>
2. Wang, Z.L., Song, J.: Piezoelectric nanogenerators based on zinc oxide nanowire arrays. *Science* **312**, 242–246 (2006). <https://doi.org/10.1126/science.1124005>
3. Wang, Z.L., Zhu, G., Yang, Y., Wang, S., Pan, C.: Progress in nanogenerators for portable electronics. *Mater. Today.* **15**, 532–543 (2012). [https://doi.org/10.1016/S1369-7021\(13\)70011-7](https://doi.org/10.1016/S1369-7021(13)70011-7)
4. Chen, J., Liu, H., Wang, W., Nabulsi, N., Zhao, W., Kim, J.Y., Kwon, M.K., Ryou, J.H.: High durable, biocompatible, and flexible piezoelectric pulse sensor using single-crystalline III-N thin film. *Adv. Funct. Mater.* **29**, 1–10 (2019). <https://doi.org/10.1002/adfm.201903162>
5. Wang, Z.L.: On Maxwell's displacement current for energy and sensors: the origin of nanogenerators. *Mater. Today.* **20**, 74–82 (2017). <https://doi.org/10.1016/j.mattod.2016.12.001>
6. Wang, Z.L.: ZnO nanowire and nanobelt platform for nanotechnology. *Mater. Sci. Eng. R.* **64**, 33–71 (2009). <https://doi.org/10.1016/j.mser.2009.02.001>
7. Gu, L., Cui, N., Cheng, L., Xu, Q., Bai, S., Yuan, M., Wu, W., Liu, J., Zhao, Y., Ma, F., Qin, Y., Wang, Z.L.: Flexible fiber nanogenerator with 209 V output voltage directly powers a light-emitting diode. *Nano Lett.* **13**, 91–94 (2013). <https://doi.org/10.1021/nl303539c>
8. China, I., Pal, A., Sen, S.: Flexible, hybrid nanogenerator based on Zinc Ferrite nanorods incorporated poly(vinylidene fluoride-co-hexa fluoropropylene) nanocomposite for versatile mechanical energy harvesting. *Mater. Res. Bull.* **118**, 1–11 (2019). <https://doi.org/10.1016/j.materresbull.2019.110515>
9. Yu, Y., Sun, H., Orbay, H., Chen, F., England, C.G., Cai, W., Wang, X.: Biocompatibility and in vivo operation of implantable mesoporous PVDF-based nanogenerators. *Nano Energy* **27**, 275–281 (2016). <https://doi.org/10.1016/j.nanoen.2016.07.015>
10. Chen, C., Bai, Z., Cao, Y., Dong, M., Jiang, K., Zhou, Y., Tao, Y., Gu, S., Xu, J., Yin, X., Xu, W.: Enhanced piezoelectric performance of BiCl₃/PVDF nanofibers-based nanogenerators. *Compos. Sci. Technol.* **192**, 1–7 (2020). <https://doi.org/10.1016/j.compscitech.2020.108100>
11. Jin, W., Wang, Z., Huang, H., Hu, X., He, Y., Li, M., Li, L., Gao, Y., Hu, Y., Gu, H.: High-performance piezoelectric energy harvesting of vertically aligned Pb(Zr, Ti)O₃ nanorod arrays. *RSC Adv.* **8**, 7422–7427 (2018). <https://doi.org/10.1039/c7ra13506h>
12. Lee, Y.B., Han, J.K., Noothongkaew, S., Kim, S.K., Song, W., Myung, S., Lee, S.S., Lim, J., Bu, S.D., An, K.S.: Toward arbitrary-direction energy harvesting through flexible piezoelectric nanogenerators using perovskite PbTiO₃ nanotube arrays. *Adv. Mater.* **29**, 1–6 (2017). <https://doi.org/10.1002/adma.201604500>
13. Lee, S.G., Monteiro, R.G., Feigelson, R.S., Lee, H.S., Lee, M., Park, S.E.: Growth and electrostrictive properties of Pb(Mg_{1/3}Nb_{2/3})O₃ crystals. *Appl. Phys. Lett.* **74**, 1030–1032 (1999). <https://doi.org/10.1063/1.123445>

14. Khan, A., Najma, B., Khan, J., Ra, S.: Fabrication of piezoelectric nanogenerator using 3D-ZnO nanosheets and optimization of charge storage system. *Mater. Res. Bull.* **123**, 1–9 (2020). <https://doi.org/10.1016/j.materresbull.2019.110711>
15. Zhang, Z., Chen, Y., Guo, J.: ZnO nanorods patterned-textile using a novel hydrothermal method for sandwich structured-piezoelectric nanogenerator for human energy harvesting. *Phys. E Low-Dimensional Syst. Nanostruct.* **105**, 212–218 (2019). <https://doi.org/10.1016/j.physe.2018.09.007>
16. Maria Joseph Raj, N.P., Alluri, N.R., Vivekananthan, V., Chandrasekhar, A., Khandelwal, G., Kim, S.J.: Sustainable yarn type-piezoelectric energy harvester as an eco-friendly, cost-effective battery-free breath sensor. *Appl. Energy* **228**, 1767–1776 (2018). <https://doi.org/10.1016/j.apenergy.2018.07.016>
17. Deng, W., Jin, L., Chen, Y., Chu, W., Zhang, B., Sun, H., Xiong, D., Lv, Z., Zhu, M., Yang, W.: An enhanced low-frequency vibration ZnO nanorod-based tuning fork piezoelectric nanogenerator. *Nanoscale* **10**, 843–847 (2018). <https://doi.org/10.1039/c7nr07325a>
18. Chang, C., Tran, V.H., Wang, J., Fuh, Y.K., Lin, L.: Direct-write piezoelectric polymeric nanogenerator with high energy conversion efficiency. *Nano Lett.* **10**, 726–731 (2010). <https://doi.org/10.1021/nl9040719>
19. Persano, L., Dagdeviren, C., Su, Y., Zhang, Y., Girardo, S., Pisignano, D., Huang, Y., Rogers, J.A.: High performance piezoelectric devices based on aligned arrays of nanofibers of poly(vinylidene-fluoride-co-trifluoroethylene). *Nat. Commun.* **4**, 1610–1633 (2013). <https://doi.org/10.1038/ncomms2639>
20. Liu, Z., Zhang, S., Jin, Y.M., Ouyang, H., Zou, Y., Wang, X.X., Xie, L.X., Li, Z.: Flexible piezoelectric nanogenerator in wearable self-powered active sensor for respiration and health-care monitoring. *Semicond. Sci. Technol.* **32**, 1–7 (2017). <https://doi.org/10.1088/1361-6641/aa68d1>
21. Jeong, C.K., Baek, C., Kingon, A.I., Park, K.I., Kim, S.H.: Lead-free perovskite nanowire-employed piezopolymer for highly efficient flexible nanocomposite energy harvester. *Small* **14**, 1–8 (2018). <https://doi.org/10.1002/sml.201704022>
22. Li, C., Luo, W., Liu, X., Xu, D., He, K.: PMN-PT/PVDF nanocomposite for high output nanogenerator applications. *Nanomaterials* **6**, 1–9 (2016). <https://doi.org/10.3390/nano6040067>
23. Chen, L.Y., Tee, B.C., Chortos, A.L., Schwartz, G., Tse, V., Lipomi, D.J., Wong, H.P., McConnell, M. V, Bao, Z.: Continuous wireless pressure monitoring and mapping with ultra-small passive sensors for health monitoring and critical care. *Nat. Commun.* 1–10 (2014). <https://doi.org/10.1038/ncomms6028>
24. Sharma, T., Je, S., Gill, B., Zhang, J.X.J.: Sensors and actuators A: physical patterning piezoelectric thin film PVDF-TrFE based pressure sensor for catheter application. *Sens. Actuators A. Phys.* **177**, 87–92 (2012). <https://doi.org/10.1016/j.sna.2011.08.019>
25. Murphy, O.H., Reza, M., Borghi, A., Mcleod, C.N., Navaratnarajah, M., Yacoub, M.H.: Continuous in vivo blood pressure measurements using a fully implantable wireless SAW sensor. *Biomed Microdevices* **15**, 737–749 (2013). <https://doi.org/10.1007/s10544-013-9759-7>
26. Zhang, H., Zhang, X., Cheng, X., Liu, Y., Han, M., Xue, X., Wang, S., Yang, F., Smitha, A.S., Zhang, H., Xu, Z.: A flexible and implantable piezoelectric generator harvesting energy from the pulsation of ascending aorta: in vitro and in vivo studies. *Nano Energy* **12**, 296–304 (2015). <https://doi.org/10.1016/j.nanoen.2014.12.038>
27. Cheng, X., Xue, X., Ma, Y., Han, M., Zhang, W., Xu, Z.: Nano energy implantable and self-powered blood pressure monitoring based on a piezoelectric thin film: simulated, in vitro and in vivo studies. *Nano Energy* **22**, 453–460 (2016). <https://doi.org/10.1016/j.nanoen.2016.02.037>
28. Dong, L., Jin, C., Closson, A.B., Trase, I., Richards, H.R., Chen, Z., Zhang, J.X.J.: Cardiac energy harvesting and sensing based on piezoelectric and triboelectric designs. *Nano Energy* **76**, 1–19 (2020). <https://doi.org/10.1016/j.nanoen.2020.105076>
29. Li, N., Yi, Z., Ma, Y., Xie, F., Huang, Y., Tian, Y., Dong, X., Liu, Y., Shao, X., Li, Y., Jin, L., Liu, J., Xu, Z., Yang, B., Zhang, H.: Direct powering a real cardiac pacemaker by natural

- energy of a heartbeat. *ACS Nano* **13**, 2822–2830 (2019). <https://doi.org/10.1021/acsnano.8b08567>
30. Morrill, S., He, D.Z.Z.: Apoptosis in inner ear sensory hair cells. *J. Otol.* **12**, 151–164 (2017). <https://doi.org/10.1016/j.joto.2017.08.001>
 31. Jeong, C.K., Han, J.H., Palneedi, H., Park, H., Hwang, G., Kim, S., Shin, H.J., Kang, I., Ryu, J., Lee, K.J.: Comprehensive biocompatibility of nontoxic and high-output flexible energy harvester using lead-free piezoceramic thin film. *APL Mater.* **5**(074102–1), 074102–074109 (2017). <https://doi.org/10.1063/1.4976803>
 32. Woodson, E.A., Reiss, L.A.J., Turner, C.W., Gfeller, K., Gantz, B.J.: The hybrid cochlear implant: a review. *Adv. Otorhinolaryngol.* **67**, 125–134 (2010). <https://doi.org/10.1159/000262604>
 33. Zeng, F.-G., Sun, X., Feng, H., Rebscher, S., Harrison, W.: Cochlear implants: system design, integration, and evaluation. *IEEE Rev. Biomed. Eng.* **1**, 115–142 (2008). <https://doi.org/10.1109/rbme.2008.2008250>
 34. Jang, J., Lee, J., Woo, S., Sly, D.J., Campbell, L.J., Cho, J.H., O’Leary, S.J., Park, M.H., Han, S., Choi, J.W., Hun Jang, J., Choi, H.: A microelectromechanical system artificial basilar membrane based on a piezoelectric cantilever array and its characterization using an animal model. *Sci. Rep.* **5**, 1–13 (2015). <https://doi.org/10.1038/srep12447>
 35. Mayberg, H.S., Lozano, A.M., Voon, V., Mcneely, H.E., Seminowicz, D., Hamani, C., Schwalb, J.M., Kennedy, S.H.: Deep brain stimulation for treatment-resistant depression. *Neuron* **45**, 651–660 (2005). <https://doi.org/10.1016/j.neuron.2005.02.014>
 36. Deuschl, G., Schade-Brittinger, C., Krack, P., Volkmann, J., Schäfer, H., Bötzel, K., Daniels, C., Deuschländer, A., Dillmann, U., Eisner, W., Gruber, D., Hamel, W., Herzog, J., Hilker, R., Klebe, S., Klob, M., Koy, J., Krause, M., Kupsch, A., Lorenz, D., Lorenzl, S., Mehdorn, H.M., Moringlane, J.R., Oertel, W., Pinski, M.O., Reichmann, H., Reuß, A., Schneider, G.H., Schnitzler, A., Steude, U., Sturm, V., Timmermann, L., Tronnier, V., Trottenberg, T., Wojtecki, L., Wolf, E., Poewe, W., Voges, J.: A randomized trial of deep-brain stimulation for Parkinson’s disease. *N. Engl. J. Med.* **355**, 896–908 (2006). <https://doi.org/10.1056/NEJMoa060281>
 37. Kim, S.D., Jae, K., Hwang, G., Kim, Y., Lee, J., Oh, S.: Self-powered deep brain stimulation via a flexible PIMNT energy harvester. *Energy Environ. Sci.* **2**, 2677–2684 (2015). <https://doi.org/10.1039/c5ee01593f>
 38. Kim, D.H., Shin, H.J., Lee, H., Jeong, C.K., Park, H., Hwang, G., Lee, H., Joe, D.J., Han, J.H., Lee, S.H., Kim, J., Joung, B., Lee, K.J.: In vivo self-powered wireless transmission using biocompatible flexible energy harvesters. *Adv. Funct. Mater.* **27**, 1–8 (2017). <https://doi.org/10.1002/adfm.201700341>
 39. Park, D.Y., Joe, D.J., Kim, D.H., Park, H., Han, J.H., Jeong, C.K., Park, H., Park, J.G., Joung, B., Lee, K.J.: Self-powered real-time arterial pulse monitoring using ultrathin epidermal piezoelectric sensors. *Adv. Mater.* **29**, 1–9 (2017). <https://doi.org/10.1002/adma.201702308>
 40. Dagdeviren, C., Javid, F., Joe, P., Von Erlach, T., Bense, T., Wei, Z., Saxton, S., Cleveland, C., Booth, L., McDonnell, S., Collins, J., Hayward, A., Langer, R., Traverso, G.: Flexible piezoelectric devices for gastrointestinal motility sensing. *Nat. Biomed. Eng.* **1**, 807–817 (2017). <https://doi.org/10.1038/s41551-017-0140-7>

Chapter 11

Optical Biosensors Towards Point of Care Testing of Various Biochemicals



Vinoth Edal Joseph and Archana Ramadoss

1 Introduction

Portable point-of-care (PoC) devices provide simple, cost-effective and reliable biosensing platforms for rapid identification and detection of various biomolecules, pathogens, contaminations and chemicals. PoC devices are gaining widespread popularity across various industries such as healthcare systems, in agro-alimentation industry for food safety testing and for the detection of toxins and pollutants in the environment. In 2005, the World Health Organization (WHO) initiated ‘*eHealth*’ and ‘*mHealth*’ (*electronic Health* and *mobile Health*) campaigns that would primarily benefit people across all communities with limited/no access to healthcare facilities [1]. Successful establishment of the ‘*eHealth*’ systems requires intelligent exploitation of portable PoC devices that facilitate medical diagnosis under minimal supervision, i.e. ‘*eDiagnostics*’, coupled with the concept of telemedicine via secure digitally connected platform [2–4]. Thus, WHO recommends the use of compact, handheld devices that can be integrated in hospitals, diagnostic laboratories, doctor’s office and also in remote testing centres [2]. Currently, more than 120 countries have incorporated the ‘*eHealth*’ strategies into their healthcare systems [1]. In other words, from a commercial point of view, the global market for PoC devices in the *in vitro* diagnostics domain has seen a steady increase in market value with a compound annual growth rate of 9.3% from 2013 to 2018 and is predicted to grow at a CAGR of 12% in the next 5-year term world-wide [5, 6]. The steady growth in demand for the design and development of simple and novel PoC devices is well reflected in scientific biosensor research community as it is under intense research.

V. E. Joseph

Department of Biology and Biological Engineering, Chalmers University of Technology, Gothenburg, Sweden

A. Ramadoss (✉)

Department of Research and Development, Nanolane, 72000 Le Mans, France

The WHO recommends that a classical PoC device should meet the following criteria i.e. Affordable, Sensitive, Specific, User-friendly, Rapid and robust, Equipment-free and Deliverable to end users i.e. ASSURED [7]. In other words, PoC devices should be simple, cost-effective, sensitive and portable that can provide real-time diagnostic information of the bio/eco-system studied. Paper-based diagnostics, micro-cell-based sensing, lab-on-chip with integrated microfluidics, wearables integrated into smartphone systems are few examples of PoC devices that offer cost-effective, sensitive and robust diagnosis [2, 8, 9]. Figure 1 is a representative image demonstrating a range of cost-effective PoC devices currently available in market.

The key element that constitutes a portable PoC diagnostic device is the biosensor. In principle, a biosensor converts a biological change into a detectable analytical signal that can be exploited for studying the biological sample being probed.

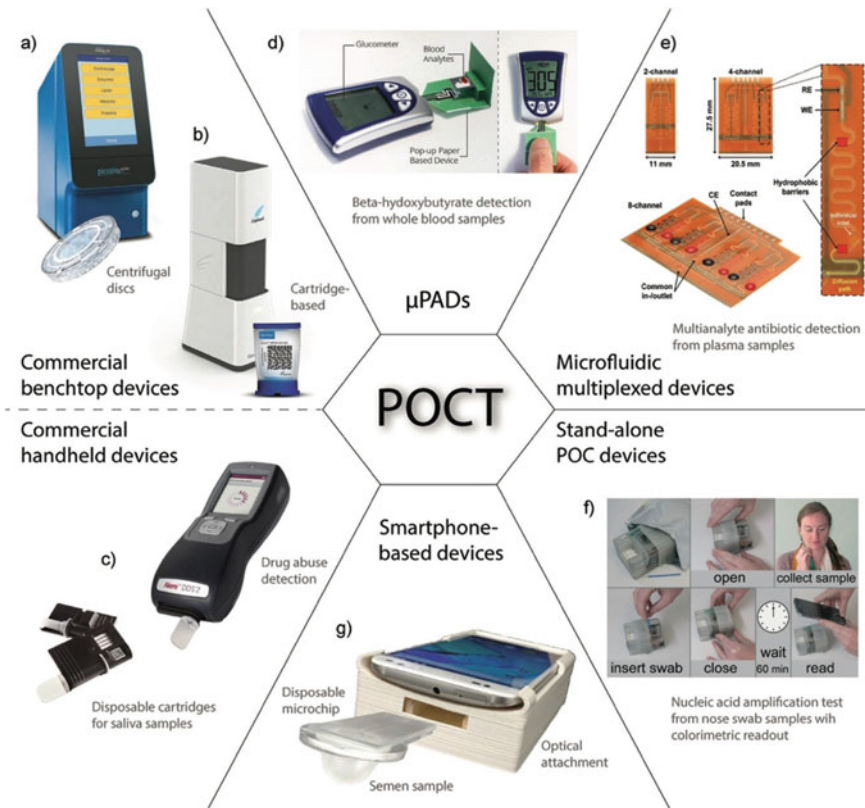


Fig. 1 Overview of the range of PoC devices in in vitro diagnostic market (taken from Dincer et al. [10]: Commercial benchtop devices for PCR and nucleic acid detection: **a** Piccolo Xpress. **b** GeneXpert Omni. Cepheid. Commercial handheld devices: **c** Alere DDS2. PoC testing devices in research stage: **d** paper-based ‘pop-up’ device. **e** Electrochemical microfluidic multiplexed biosensor for multianalyte antibiotic detection. **f** A rapid, instrument-free, sample-to-result nucleic acid amplification test)

Based on the type of the analytical signal generated, a wide range of biosensor classes are described, for instance, optical, electrochemical, mechanical, thermometric or magnetic. Key advantages such as high sensitivity, potential for cost-effective analysis, design simplicity, possibility of device miniaturization and integration of microfluidics technology has made optical biosensors a primary choice for PoC testing applications. Thus, optical biosensors are generally a popular choice of technique for biochemical analyses and show good potential for applications as PoC testing devices [11–13].

This chapter provides a brief overview of currently available label-based and label-free biosensors and discusses the potential and key limitations of the techniques that require further advances in the field to facilitate successful commercialization of such biosensing techniques.

2 Overview of Optical Biosensors

Optical biosensors are the most commonly exploited class of biosensors for detection of various biochemicals [11, 12]. They offer highly sensitive real-time monitoring and detection of biomolecules in both label-based as well as label-free settings. Optical biosensors assess the changes in the optical field parameters of the incident light wave such as its amplitude, frequency, phase, polarization state, reflectance, emission, absorbance, refractive index or interferometric patterns that occur in response to biomolecular interactions that occur in its plane of incidence. Detection of such changes in optical properties of light can be done with very high precision using photodetectors such as CCD camera or a spectrophotometer depending on the technique exploited. Figure 2 shows a detailed schematic overview of an optical biosensor.

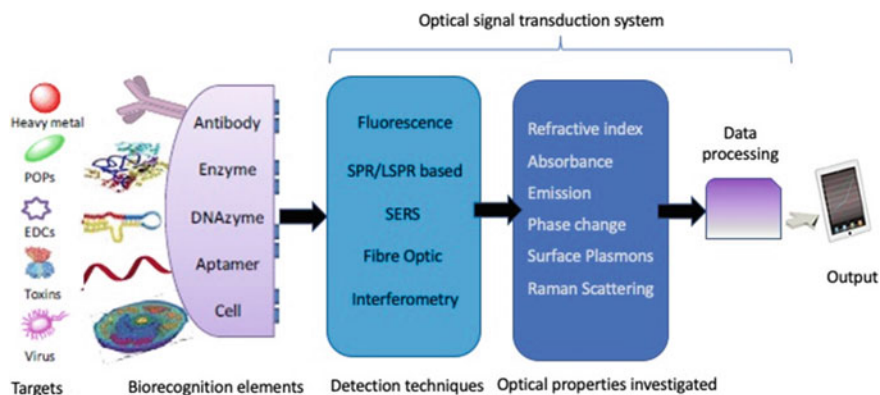


Fig. 2 Schematic overview of new age optical biosensors (modified after Long et al. [14])

The key advantages that have made optical biosensors a popular choice for biochemical analysis are particularly suitable for PoC testing applications that have been listed as follows:

- a. **High sensitivity and very low LOD:** Sensitivity and LOD are crucial aspects that determine the analytical performance of a biosensor device. The sensitivity is defined as the magnitude change obtained in the transduction signal in response to the change in analyte, and LOD is defined as the minimal detectable amount of the analyte by the device. The LOD is commonly expressed in terms of refractive index unit (RIU), or as pgmm^{-2} and/or as ngml^{-1} that determines the surface sensing capacity of the biosensor device. Biosensors with LOD in the range of 10^{-6} – 10^{-8} RIU indicate that a sample concentration of ng ml^{-1} down to pg ml^{-1} can be detected. Biosensors with such sensitivity are highly suitable for PoC-based medical diagnostic applications where sample availability is always limited [11]. The sensitivity of certain optical biosensors such as surface plasmon resonance or interferometry (described in the subsequent sections of this chapter) has been shown to be in the range of $\sim\text{fgmm}^{-2}$, i.e. sensitivity much superior to other biosensing techniques such as amperometry, electrochemical and piezoelectric biosensing techniques [12, 15, 16]. Such a performance of the device allows single molecule detection that is of particular interest in domains of forensic analysis and drug discovery.
- b. **Continuous real-time monitoring** of the optical parameters is made possible by employing photodetectors. This aspect provides the option of continuous monitoring and studying the biomolecular interactions such as binding kinetics or molecular interactions kinetics of the sample analysed.
- c. **Rapid and high-throughput analysis:** The possibility of imaging of the sample under study adds another key advantage to this class of analytical technique as it allows rapid high-throughput detection of samples, i.e. multiple samples can be analysed simultaneously.
- d. **Adaptability to multidisciplinary approach** such as microelectronics, nanotechnology, integrated optics and advanced concepts such as microelectronic mechanical systems (MEMs) and novel surface functionalization techniques based on nanotechnology facilitate miniaturization of the biosensing system [12].
- e. **Compatibility to portable Android systems** such as smartphones or Android tablets. The inbuilt internal memory, quality camera, compatible operating systems, network connectivity, improved and constantly improving hardware and software of smartphones have made smartphones a next-generation PoC device. The user-friendly interface, facile operation and the above-mentioned features make this technology suitable for use in remote settings with little to no skilled healthcare professional. Although this is a highly promising technology, immense research in the field of smartphone technology is underway developing novel signal detecting and decoding algorithms while also to develop miniaturized optical biosensing elements without the loss of sensitivity that can be well integrated into the smart-phone devices for various biochemical detections.

Thus, the above-mentioned advantages of the optical biosensors showcase the potential for such analytical systems in PoC testing applications for use in industrial as well as clinical settings [9, 11, 12].

Efficient ligand immobilization on the sensor surface is an important criterion for the detection of ligand–analyte binding. Optimal immobilization of biorecognition elements such as enzymes, antibodies, synthetic oligonucleotides (aptamers) and cells is a key parameter for efficient detection of the molecular interactions in the sample studied [9, 11]. Surface biofunctionalization is a technique by which the sensor surface is chemically activated after which the biorecognition elements are efficiently immobilized on the sensor surface with better surface coverage. Silicon-based substrates such as SiO_2 , Si_3N_4 and $\text{Si}_x\text{O}_y\text{N}$ are most commonly used for fabricating the optically active sensors [11]. However, silicon surfaces that are compatible with microfluidic integration require expensive fabrication procedures [17]. Paper-based sensor is emerging as a new and promising alternative to silicon-based sensors [18]. The inherent capillary action in the paper provides active fluid flow, unlike the silicon-based sensors that require a pump to ensure the fluid flow in its microfluidic sensing device. This advantage makes paper-based sensors more economical compared to silicon-based sensors. In addition to being cost-effective, abundantly available, easily disposable and biodegradable, the simple surface functionalization procedures make this class of sensors a practical choice for sensor surface. Although paper-based sensors are an attractive sensor surface choice, technical limitations such as autofluorescence especially when such sensor surfaces are used for fluorescence-based optical detection remain to be addressed [17].

Optical biosensors can be broadly classified into label-based (e.g. fluorescence) and label-free (e.g. surface plasmon resonance) biosensors [19]. Label-based biosensors use labels such as fluorescent molecules, dyes or quantum dots attached to the biomolecules for the detection of biochemicals in which case the optical signal is detected using a spectrophotometer. A wide range of optical biosensors are classified as label-based optical biosensors, for instance, colorimetric, luminescence-based, etc. However, a label-free biosensor directly detects the changes in optical parameters of the incident light wave on the biomolecules embedded on sensor surfaces. These techniques are described in detail in the following sections.

2.1 Label-Based Fluorescence Optical Biosensors

Fluorescence-based biosensors are an important class of biosensors as they are among the most commonly employed optical biosensors of the current times for PoC testing applications in the in vitro diagnostic (IVD) market, i.e. for biomarker detection in the healthcare sector, for toxin and contamination detection in food safety and environment sector [20, 21]. Traditionally, fluorescence biosensors have been used to study biomolecular interactions such as antigen–antibody, protein–protein, protein–enzyme, DNA–protein and DNA–DNA/RNA. These techniques have been successfully commercialized, for instance, the commercially available GeneXpert system

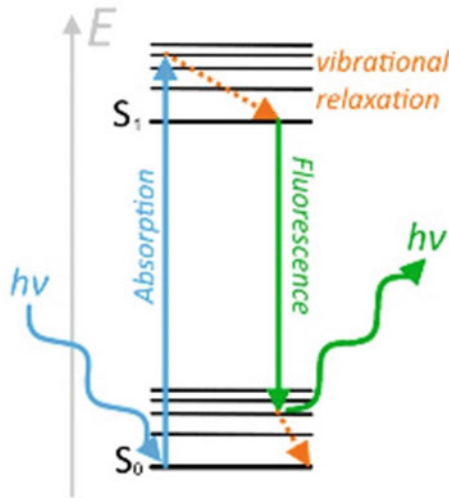


Fig. 3 Principle of fluorescence-based on Jablonski diagram (taken from Hochreiter et al. [23]): Absorption of a photon by an electron in the fluorophore molecule results in the excitation of the electron from a ground state (S_0) to an excited state of energy (S_1) as shown by the blue arrow. Due to vibrational relaxation, the electron drops to the lowest state of energy of S_1 level in a radiationless manner shown by the orange arrow. The unstable excited electron then returns to its ground state S_0 within nanoseconds by emitting a photon of a specific wavelength higher than that of the incident photon containing lesser energy as shown by the green arrow

(a benchtop PCR-based machine) that uses fluorescently labelled DNA probes to rapidly and reliably detect various infectious agents from patient samples including bacterial infections and sexually transmitted diseases [22].

Fluorescence is a short-lived luminescence created by electromagnetic excitation of a fluorophore. The principle of fluorescence-based excitation of a molecule is well explained by the Jablonski diagram (Fig. 3). When an electron present in the fluorophore molecule absorbs a photon emitted from a light source, the molecule is excited from a ground state (S_0) to a higher electronic energy state (S_1) (an event lasting $\sim 10^{-9}$ s). Single electronic state contains multiple vibrational levels and the excited molecule then relaxes to the lowest vibrational energy level of S_1 state through non-radiative transition ($\sim 10^{-12}$ to 10^{-10} s). And finally, the molecule returns to the S_0 ground state of energy by emitting fluorescence ($\sim 10^{-9}$ to 10^{-6} s).

2.1.1 Fluorescence-Based Optical Biosensors

Currently, fluorescence is a popular choice of biosensing technique for PoC devices to perform immunoassays in clinical or laboratory settings for the detection of biomolecules such as DNA/RNA and proteins. This is due to the high sensitivity and selectivity offered by this high-throughput technique [19]. For instance, multiple

Table 1 PoC testing devices that have been developed using fluorescence-based techniques

Biosensor/Assay	Technology used	Detection	References
MoS ₂ nanosheet sensor	FRET aptasensor	Detection of a malarial biomarker, Plasmodium lactate dehydrogenase (pLDH) with high sensitivity around pM	[30]
Microbead-based PoC	Microbeads incorporated with fluorescent particles, dyes, QDs etc.	Multiplexed detections of nucleic acids, proteins, circulating tumour cells (CTCs), and bacteria	[31]
PoC through salivary biomarkers	Fluorescent and Calorimetric measurements	Detection of nucleic acids, human papilloma virus associated cancers	[32]
DNA biomarkers PoC	Solid bridge-based DNA amplification and FRET	Biomarkers in colorectal and lung cancers	[33]
Sandwich Immunoassay	Microcantilevers	Detection of HIV capsid antigen in human serum. The LOD of this immunoassay is 10–17 g/mL that is 5 orders of magnitude better than last generation of approved immunoassays	[34]

commercially available PoC systems use single-use cartridges that are preloaded with fluorescently labelled specific antibodies to perform immunoassays for the diagnostic detection of biomarkers for complex diseases such as cardiovascular diseases, cancer or HIV [24–29]. Table 1 provides a brief overview of a few fluorescence-based optical biosensors developed for point-of-care testing applications.

Despite the unprecedented advantages mentioned above, some major limitations to this technique such as photobleaching, short lifespan of the probe, self-quenching at high concentrations and steric hindrance of the fluorophores, in addition to the fluorophore sensitivity towards environmental factors such as pH and temperature have restricted the use of this system in multiple domains [12, 35, 36]. Fluorescence resonant energy transfer (FRET) is a technique that is relatively insensitive to the external environmental factors and offers relatively stable detection of fluorescently labelled antibodies, especially with the development of new age fluorescent probes such as quantum dots. Extensive research is being conducted to exploit FRET for novel PoC applications. The principle of FRET and recent advances towards FRET-based PoC applications are discussed in detail in the subsequent sections.

2.1.2 FRET-Based Biosensors

Theodor Förster (Foster) was the first to describe the Förster resonance energy transfer (FRET) in 1948 [37]. FRET is a phenomenon in which a non-radiative transfer of energy takes place between a ‘donor’ and an ‘acceptor’ molecules that are in the vicinity of each other (i.e. within the range of ~ 10 nm). Transfer of energy from an excited donor molecule to an acceptor molecule occurs via radiationless dipole–dipole coupling between the donor and acceptor molecules as shown in Fig. 4. As a result of the transfer of energy, a decrease in the fluorescence emission from the donor and subsequent increase in the emission of acceptor fluorescence is observed.

FRET phenomenon occurs when the following conditions are respected: (a) an overlap in the fluorescence emission and the absorption/ excitation spectrum of the of the donor and acceptor, respectively; (b) the distance between the donor and acceptor molecule is in the range of ~ 10 nm; (c) the transition dipole orientations are parallel to each other (i.e. the donor and acceptor molecule); and (d) the duration of fluorescence emission from donor molecule should be long enough to allow FRET to occur.

The efficiency of the energy transfer can be calculated based on the change in intensity of fluorescence emitted and absorbed (Eq. 1). This energy transfer is inversely proportional to the sixth power of the distance between donor and acceptor (Eq. 2). The sensitivity of the technique within distances in the order of 10 – 100 Å makes

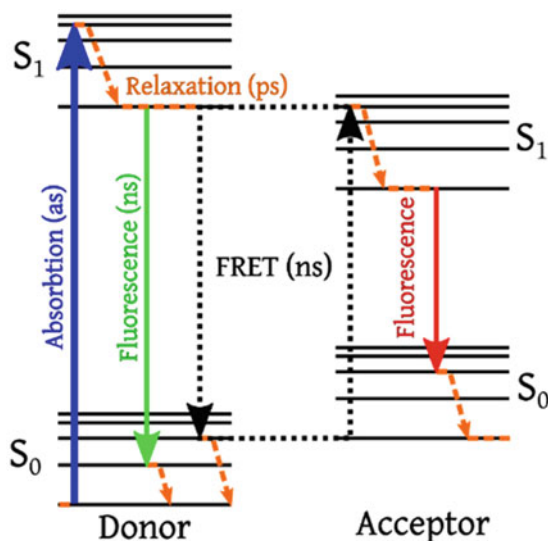


Fig. 4 Schematic of the Jablonski diagram showing the FRET phenomenon (modified after Hochreiter et al. [23]): the fluorescence energy released upon relaxation of an excited donor molecule can be used to excite an acceptor fluorophore molecule present in close proximity in the range of ~ 10 to 100 Å, which in turn releases fluorescence upon the relaxation of the acceptor molecule to its S_0 ground state. This process is visible as quenching of fluorescence is observed on the donor fluorophore and emission of fluorescence is observed on the acceptor molecule

FRET a powerful tool to probe molecular level interaction such as protein–DNA and protein–protein interactions, in addition to quantitative analysis of molecular dynamics such as molecular conformational change. FRET-based biosensors could reach a LOD in the range of pM– μ M depending upon the fluorophore used [20, 38, 39]. The efficiency of energy transfer between donor and acceptor is calculated using,

$$E = 1 - \frac{F_{DA}}{F_D} \quad (1)$$

where F_{DA} is relative fluorescence of donor in the presence of acceptor and F_D is fluorescence intensity of donor in the absence of acceptor. FRET efficiency is also dependent on the distance R_0 between the donor and acceptor and determined using the following equation,

$$E = \frac{R_0^6}{R_0^6 + r^6} \quad (2)$$

where r is the distance between fluorophores, R_0 is Forster distance at which the energy transfer is 50% and is usually in the range of 2–10 nm based on the fluorophores.

FRET phenomenon can be observed with a wide range of fluorescent labels. Quantum dots (QDs) are unique fluorescent labels that can present the FRET effect. These are photoactive semiconductor nanocrystals with much broader absorption spectra and superior photophysical properties compared to common fluorophores [19]. QDs make FRET more robust and reliable as it renders the fluorescent biosensing technique immune to the classical limitations faced (those mentioned in the previous section) by the common fluorophores. Thus, unique advantages of FRET such as high selectivity and detection sensitivity (\sim 10 to 100 Å), simplicity in the biosensor design and robustness of the technique can be well exploited by using quantum dots to probe biomolecular interactions at single cell and single molecule level [40]. This class of biosensors offers reliable time-efficient and high-throughput multiplexed analysis of small quantity of samples [41]. Hence, they have been successfully employed for biosensing applications involving drug screening, studies on molecular dynamics (protein–protein interaction, DNA–protein interactions, protein conformational changes, enzyme–substrate, antigen–antibody) [19, 23, 42]. Some of the FRET-based biosensors that have been developed and commercialized for the detection of biomarkers for cancer, respiratory, pulmonary, cardiovascular and infectious diseases include KRYPTOR/TRACE (BRAHMS/ThermoFisher), HTRF (Cisbio) or LANCE (PerkinElmer) [43].

Recent advances in fluorescence research have demonstrated the compatibility of FRET-based biosensors to MEMs-assisted microfabrication of sensor surfaces, integration of microfluidic technology and integrated optical system that facilitates miniaturization of the system without significant loss of signal-to-noise ratio. This has accelerated the development of FRET-based PoC devices that are rapid, robust

and cost-effective. Novel FRET-based biosensors particularly those developed for application as PoC biosensors are listed in Table 1 and few examples have been discussed in detail in the following sections.

FRET-Based PoC Testing Applications in Agro-Alimentation Industry

Foodborne illness is caused by contaminants like food-borne pathogens (bacteria, virus or parasites), chemicals and toxins resulting in mild gastroenteritis to organ dysfunction or life-threatening syndromes [44]. The analytical technologies used in food industries such as high-performance liquid chromatography (HPLC), gas chromatography (GC) and enzyme-linked immunosorbent assay (ELISA) are expensive, time-consuming and labour-intensive. These roadblocks make these techniques non-viable in developing countries where these infections are predominant. Thus, there is a high demand to develop simple, user-friendly and cost-effective PoC devices to monitor food safety. For a detailed overview of different FRET-based PoC devices, readers are referred to the excellent review by Choi et al. [45]. A few examples of microfluidic-based and/or paper-based PoC devices that have been reported are discussed below.

Morales-Narváez and colleagues developed a paper-based lateral flow immunoassay with a test strip using graphene oxide (GO) to detect pathogens in food products based on resonance energy transfer principle [46]. Antibodies coated with CdSe/Zns QDs were printed on test strips (acts as donor) and GO (acts as acceptor) was added and their interaction between antibodies and GO was monitored. In the absence of pathogens, the interaction between the donor and acceptor was referred to as an 'off' state. However, the presence of the pathogen is detected as it binds to QDs on test strip and thus prevents the binding of GO, leading to the 'on' state which can be detected using a lateral flow reader. The label-free FRET-based PoC immunoassay is used for detection of pathogens like *Salmonella sp.*, and a detection limit of 100 CFUml⁻¹ in water and milk was determined. Similar strategy was used by Zhang and colleagues who developed a simple paper-based microfluidic device to detect different types of chemical contaminants in food. The authors used Cy5 labelled single-stranded DNA (ssDNA) along with GO to detect the heavy metals and antibiotics residues in food. They also extended the use of this device for applications in environmental monitoring [47]. In another example recently demonstrated, Mei and colleagues developed a FRET-based PoC device that used a smartphone and paper-based sensors for the detection of pesticides in food products. The authors demonstrated that the device provided a reliable and user-friendly detection of pesticides with an LOD of 0.1 µM [48].

FRET-Based PoC Testing Applications in Biomedical Diagnostics

FRET-based sensors allow the quantification of different targets like proteins, nucleic acids, drugs, toxins and microbes from various types of clinical specimens, i.e.

complex biological mediums (body fluid, cells and tissues). Thus, FRET-based biosensors are widely used in molecular diagnostics including (a) immunoassays, (b) microarrays, (c) real-time PCR and (d) live cell imaging [43]. Shin and colleagues developed PoC-based molecular diagnostics, utilizing DNA amplification technique that combines solid-phase Bridge PCR and FRET for detection of biomarkers for cancer. The authors used the PoC biosensor to detect the Kristen rat sarcoma (KRAS) gene expressed in colorectal and lung cancers and demonstrated a detection limit of $100 \text{ pg}\mu\text{l}^{-1}$ [33]. In another study, Petryayeva and colleagues developed a multiplexed enzyme activity detection assay that utilized QDs of different photoluminescence range (red, green and blue-emitting QDs), peptides labelled with Alexa Fluor 647 and quenchers, QSY9 and QSY35. The concentration of proteases was detected as changes in RGB intensities during the enzymatic process and which was detected using a smartphone [49]. While Mizutani and colleagues developed a sensitive and specific FRET-based biosensor to detect the activity of BCR-ABL kinase in live animal cells. The biosensor could efficiently detect cancerous and drug-resistant cells, and further, it was used for the evaluation of kinase inhibitor efficacy [50]. Such examples demonstrate the potential for FRET-based biosensors for PoC testing applications to complex diseases such as cancer diagnosis and therapeutics [51].

2.2 Label-Free Evanescence-Based Optical Biosensors

Evanescent wave-based optical biosensors have been widely employed for the detection of nucleic acids in clinical diagnostic settings [52–54]. Label-free biosensing technique offers an undue advantage of probing the sample in its native environment without the influence of labels-based probes on the sample. Therefore, continuous monitoring of the biomolecule interaction process and studies on binding kinetics of molecular interactions can be performed with high degree of accuracy. The sensitivity offered by the technique is much superior to other biosensing techniques such as amperometry etc. The LOD has often been recorded in the range of 10^{-6} – 10^{-8} RIU. This level of sensitivity allows the detection of molecules even in very small amount of samples (in the range of $\sim\text{pgmm}^2$), making this technique very practical for use in medical diagnostics where the sample availability is often limited.

In principle, the evanescent waves are generated when an electromagnetic wave is confined at the interface of an optically active metal–dielectric surface under conditions that satisfy total internal reflection (TIR). When an electromagnetic wave travels from a medium of higher refractive index into a medium of lower refractive index at an incidence angle greater than its critical angle, it undergoes TIR. The confined electromagnetic wave then penetrates through the optically active metal surface, and the evanescent waves are generated as described in Fig. 5. This wave is active up to a few hundreds of nm on an external medium (i.e. from ~ 10 nm to a max ~ 100 nm) and exponentially decays as the distance from the surface increases. This evanescent field is highly sensitive to changes in refractive index of the medium and is therefore

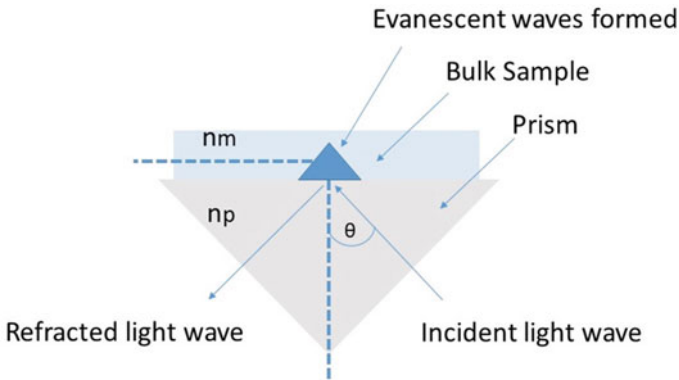


Fig. 5 Principle of TIR and evanescent wave formation: when an incident optical light wave travels from an optically denser medium to a lesser denser medium, i.e. $n_p > n_m$, at an angle greater than critical angle (θ), TIR occurs resulting in the formation of evanescent waves at the metal-dielectric interface, which can be further exploited for biosensing applications for bulk samples

exploited for biosensing applications close to the surface of the optically active metal surface [55].

Advances in the optical biosensor research towards integrated optics, integration of microfluidic technology and microelectromechanical systems-assisted sensor fabrication techniques have significantly contributed to the field as they facilitate the fabrication and development of miniaturized devices that are cost-effective and high-throughput, making them attractive candidates as PoC testing devices require high sensitivity. Most of the evanescent wave-based methods monitor optical properties such as refractive index, phase-shift and resonance-energy transfer. In the following sections, techniques such as surface plasmon resonance (SPR)-based biosensing platforms, and interferometry-based biosensors are discussed in detail.

2.2.1 Surface Plasmon Resonance-Based Biosensors

Surface plasmon resonance (SPR) was first commercially exploited for biosensing application in 1983, and today, SPR is one of the most commonly used label-free optical biosensing techniques [12, 55–57]. It offers high sensitivity (in the range of $\sim 1 \text{ pgmm}^{-2}$) real-time monitoring and detection of biomolecular interactions in label-free settings. SPR occurs when a p-polarized optical wave is incident on a metal interface or passes from a medium of high refractive index (n_1) to a lower refractive index media (n_2), generating evanescent wave at a particular resonance angle called the SPR angle. At this resonance angle, the energy of the electromagnetic wave is transferred on to the sensor surface along which the evanescent wave propagates. This energy then excites the free electrons present on the sensor surface, i.e. the metal–dielectric interface. The excited free electrons tend to oscillate and are now called the surface plasmons. Figure 6a, is a schematic representation of the SPR principle.

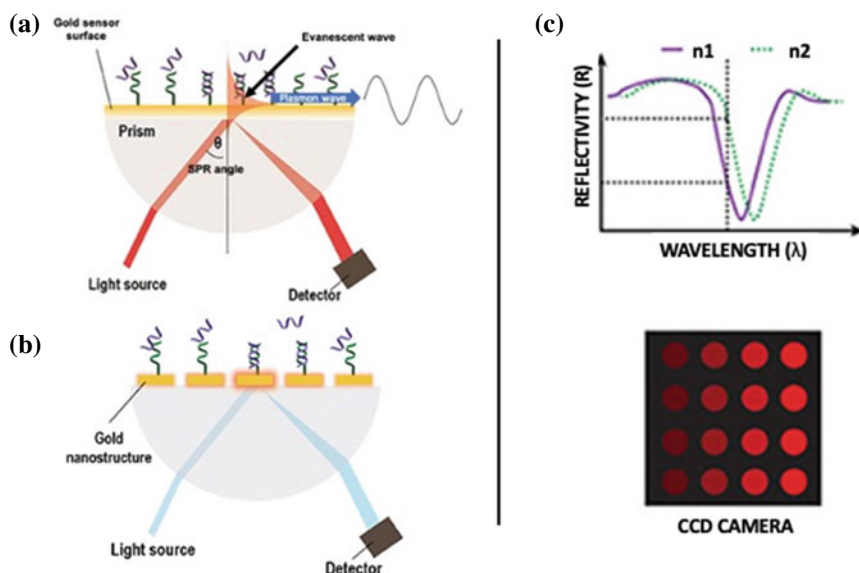


Fig. 6 Principle of SPR and SPR-based biosensors (modified after Huertas et al. [55]): **a** SPR. When an optical wave hits the metal-dielectric interface at an angle greater than critical angle (θ), TIR occurs such that evanescent waves with maximum intensity are formed at this interface. A resonance is observed when the free electrons at the metal-dielectric interface absorb this light energy at a particular SPR angle. Thus, at this SPR angle, a sharp decrease in the intensity of the reflected angle is observed, which can be subsequently measured. **b** LSPR. This is a phenomenon that occurs when surface plasmon resonance is recreated on nanoparticles. In this case, the changes in SPR angle will result in scattering of light in colloidal solutions and thus can be recorded using a spectrophotometer for each of the nanoparticles. **c** SPRi. The SPR effect when is recorded using a CCD camera offers the advantage of rendering this technique into high-throughput multiplex biosensing technique

The collective oscillation of excited free electrons forms the surface plasmon waves and this phenomenon is called the surface plasmon resonance.

Most of the classical forms of SPR techniques use a thin layer or film of a noble metal such as gold in between the metal-dielectric interface in order to enhance the evanescent waves and subsequently to achieve higher sensitivity for the biosensor as described in Fig. 6a. Thus, any biomolecular interactions that occur at the interface of gold surface and sample medium (i.e. air or biological solution) will alter the refractive index of the medium, altering the optical properties of the light which is subsequently detected using a photodetector [58]. For a particular incident angle also known as the SPR angle, the intensity of the reflected light wave steeply decreases, i.e. the total energy of the light wave is transferred to excite the surface free electrons, thus generating the SPR phenomenon or the SP resonance on the gold film-biological solution medium.

The SPR set-up often requires a light coupler that allows p-polarization of the incident light wave and also ensures that the criteria for TIR is met at the metal–dielectric interface. Multiple light coupling configurations or techniques such as prism, grating, fibre and wavelength couplers have been used to create the SPR phenomenon. Of late, fibre-optic-based coupling has shown promising results as it allows the generation of SPR phenomenon with very high signal-to-noise ratio [57]. The limit of detection (LOD) of SPR is calculated based on the bound material on the sensor surface, and it is estimated to be $1 \text{ pg}\cdot\text{mm}^{-2}$. Therefore, antibodies, proteins or DNA can be easily detected. However, low molecular weight targets (typically less than 500 Da), such as mycotoxins, drugs and vitamins low copy number targets, such as bacteria and viruses require increased sensitivity. This can be achieved by using nanostructured substrates and gold nanoparticles (GNPs)-modified tags as SPR sensor surfaces.

Requirement of sophisticated and bulky optical components in addition to perfect optical alignment of the components makes the traditional SPR instruments very expensive and bulky. Therefore, traditional bulky SPR instruments are not suitable for development of PoC devices. However, adaptability of the technology to integrated optics and the potential to generate the SPR phenomenon on a wide range of substrates as sensor surface has facilitated the development of novel SPR-platform-based PoC testing devices for use in medical diagnostics [57].

2.2.2 Localized Surface Plasmon Resonance

Localized SPR (LSPR) is a relatively novel adaptation of the SPR in which the SPR phenomenon is generated using nanoparticles in a colloidal solution. This technique exploits the fact that light is scattered when it incident onto nanoparticles with size comparable or even lesser to that of the wavelength of the incident light. The free electrons present on the surface of the nanoparticles engage in collective oscillation causing absorbance of the light energy while reflecting photons, i.e. observed as scattering of the light and thus generating LSPR (shown in Fig. 6b.). The scattered light generates bright colours in metal colloidal solutions [56]. Thus, changes in the refractive index of the medium studied are observed as spectral changes and can be recorded using the spectrophotometer [36]. This effect is particularly observed in short distances up to 10 s of nm and is highly non-disturbed by changes in bulk solution [36]. Because LSPR is highly sensitive to changes in local refractive index, this technique is particularly useful for label-free DNA sequence analysis for instance studies on DNA mutation and DNA hybridization have become possible [55, 59–62]. Localized surface plasmon resonance (LSPR)-based biosensors have been successfully employed to detect real-time biochemical interactions involving DNA sequences including DNA biomarkers and also DNA hybridizations, proteins such as enzymes, antibodies, including many pathogens [62–65]. The suitability of the technique for PoC testing applications has been shown by numerous research articles and a few such studies have been discussed in the following paragraph.

Roether and colleagues developed a miniaturized biosensor device with LSPR chip integrated with microfluidics in order to demonstrate the real-time monitoring of DNA hybridization and monitoring of the DNA polymerase enzyme activity, i.e. DNA–DNA and DNA–enzyme activity [62]. The authors enhanced the sensitivity of the LSPR technique by incorporating a sensor that was periodically and densely decorated with mushroom-like-nanoplasmonic structure composed of silicon dioxide stems and gold cap heads with average distance of ~ 19 nm. The gold layer was functionalized with ssDNA template (~ 30 bps). The authors used the LSPR chip for real-time monitoring of the binding kinetics of the primers to the ssDNA template and that of the DNA polymerase to the ssDNA template in a label-free and room temperature settings. In another example, Sun and colleagues demonstrated a typical PoC application for sepsis diagnosis using the LSPR-integrated chip [66]. Sepsis is caused as a result of a systemic overreaction of immune system towards an infection. Procalcitonin (PCT) is considered as a highly specific biomarker at a concentration of <1 ngml^{-1} is indicative of 12% likelihood of the disease while at a concentration of 1 mgml^{-1} likelihood of the disease is 96 percent. The authors developed a fully automated LSPR-based PoC system with integrated microfluidics to detect PCT concentration in the patient blood sample. Simple glass-based or PMMA-coated LSPR sensor chips decorated with gold nanoarrays coupled with quantum dots (QD) were used for the detection of PCT as shown in Fig. 8. QD serves as fluorescent probes that enhance the signal in order to facilitate detection by a CCD camera. This PoC system demonstrates a high sensitivity with LOD of 0.5 ngml^{-1} thus meeting the clinical criteria for sepsis diagnosis [66].

2.2.3 Surface Plasmon Resonance Imaging

Surface plasmon resonance imaging (SPRi) is the addition of the imaging aspect to the SPR technique. Steiner Gerald introduced this novel advancement of the traditional SPR technique in 2004 [67]. SPRi provides high-throughput multiplex analysis of the sample, as it allows to image multiple interactions simultaneously using a CCD camera as shown in Fig. 6c. Thus, the imaging aspect clearly offers a big advantage for the technique as it allows real-time temporal and spatial monitoring of the surface-bound molecular interactions in a label-free manner [67].

The technique uses CCD camera to perform image-based analysis of refractive index changes that occur at the sensor surface. Given the fact that sensitivity of the system greatly depends on the resolution of the detection technique which in turn greatly affects the LOD of the system, it is not surprising that SPRi is over 10X times less sensitive compared to traditional SPR technique [68]. Therefore, SPRi has been combined with other techniques to improve the sensitivity and limit of detection [69–72]. For instance, Liu and his colleagues developed a smartphone-based SPR imaging biosensor. The authors used portable and light-weighted optical components with SPR-based biosensors that were connected to the Android mobile platform via fibre-optic cables as shown in Fig. 7. The mobile phone's LED flashlight was used as the source of incident light which was fed into the biosensing system

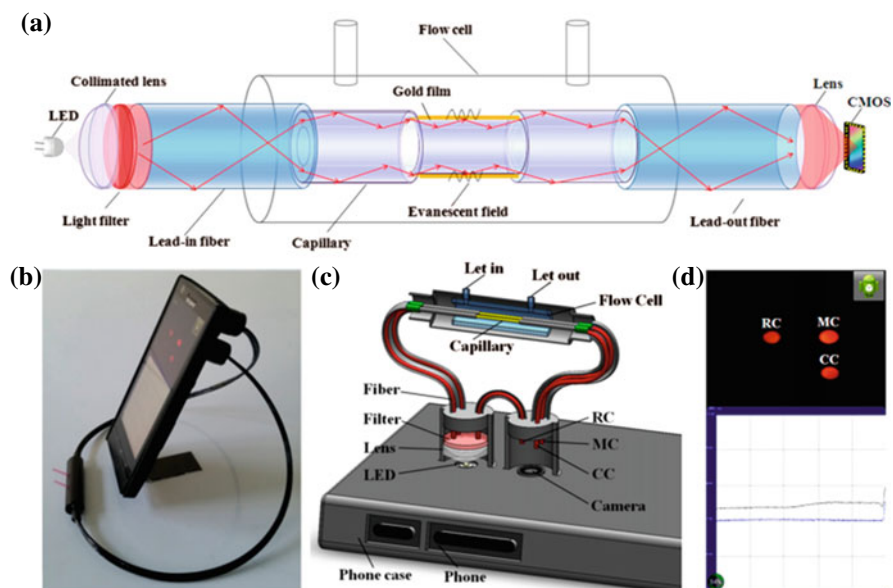


Fig. 7 Instrument set-up of a smartphone-based SPRi biosensor (taken Liu et al. [76]): **a** Schematic representation of the fibre-optic-based SPR sensor. **b** Photograph of the SPR sensor installed on an Android-based smart phone. **c** Schematic representation of the internal structure of the optomechanical attachment of the sensor system displaying the ports that allows the device to be connected to Android smart-phone. **d** The camera of the smart phone captures the images of the measurement channel, control channel and reference channel; then, the images are rapidly processed to obtain the relative intensity. The data points are plotted and displayed on the screen

via lead-in optical-fibres and the reflected light was detected by the phone's camera brought in by the lead-out optical fibres. The biosensing unit was fabricated using a silica capillary and a small testing window was etched on the sensor surface that was covered with gold film (~ 50 nm) as shown in Fig. 7a. The overview of the set-up is shown in Fig. 7b, c. The results were displayed as relative intensity. Figure 7d shows the output as the incident light was fed into three separate channels, i.e. the measurement channel (MC), the reference channel (RC) and the control channel (CC). This set-up was used to detect several antibodies, and an LOD of 47.4 nm was recorded. Such combined SPRi based biosensors have successfully been exploited to study nucleic acid hybridizations, DNA-protein, and their binding kinetics with detection limits in the range of few nMs [73–75]. The inconsistency in the light intensity of the cell phone's LED flashlight source was taken into consideration and suitable image analysis methods were developed and used to correct such influences of light source.

Another approach to improve SPRi sensitivity involves the measurement of the optical phase shifts using the interference patterns. This is an approach that combines the SPRi and interferometry to obtain very high sensitivity [77, 78]. Direct phase shift measurements of optical waves with very high frequency are currently near

to impossible as no detectors are available that could record such fast events [77]. Hence, this technique uses the concept of superimposing two optical waves, i.e. superimposing of a reference wave and a test wave, to generate an interference wave with a low frequency, i.e. to generate a beat signal with beat frequency, that can be detected by the photodetectors. Such an improved SPRi biosensor with capacity to perform simultaneous real-time monitoring of biomolecular interactions in a multiplexed format has gained a lot of attention in the field for PoC-based testing applications. The high-throughput phase shift-based SPRi biosensors further developed using MEMS technology have demonstrated a sensitivity of ~ 1 nM in a classic antigen–antibody interaction studies suggesting a very high clinical relevance for biomarker detection [78, 79].

2.2.4 Surface-Enhanced Raman Scattering

Surface-enhanced Raman scattering (SERS) is a spectroscopy-based detection technique that works on the principle of LSPR. When a light wave is incident on SERS active surfaces such as densely packed nanopatterned surfaces, it results in inelastic scattering of the light wave on the nanopatterned surfaces. This collision results in transfer of a part of the energy to Raman photons which causes the photon oscillation. These oscillating photons scatter the light waves that can be recorded using a spectrophotometer. Unique molecular vibrational spectra based on the structure of every bioanalyte molecule that is structurally different can be well detected using this technique (Fig. 8b). Thus, SERS-based detection helps generate molecular profiling of a single or multiple analytes under investigation primarily based on their structure. Because the photon oscillation is insensitive to water or the medium in which analyte molecules are present, this technique serves with very high sensitivity even for analysis of complex biological samples [80]. SERS has been demonstrated to enhance the Raman scattering by over 10^{11} folds [80]. SERS has been employed in numerous applications that require high sensitivity such as detection of bacteria, and viruses and particularly for detecting and analysing specific molecules in complex biological liquids.

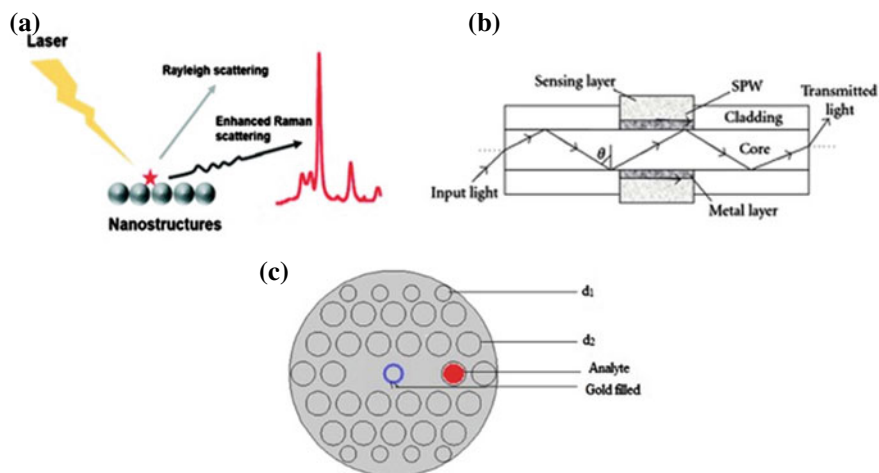


Fig. 8 Principle of other LSPR-based sensors and fibre-optic-based SPR biosensors (modified after [94, 114, 117]): **a** SERS. Based on the principle of LSPR, on a very densely packed periodically arranged nanostructure scatters the incident light in an inelastic scattering. This excites the Raman photons, which can be eventually recorded using a spectrophotometer. **b** A schematic representation of a fibre-guided SPR biosensor displaying a core and a cladding layer. **c** A simplified pictorial representation of the designed PCF structure. (d_1 and d_2 are diameters of 1 and 2, respectively). Analyte is indicated as red filling inside a spot and gold coating is indicated as blue coating over the spot.

One of the major breakthroughs in this field is the development of portable spectrophotometer. Mounting research demonstrates the capacity of SERS to evolve as portable devices for use in PoC applications, particularly for use in applications requiring detection of analytes from very small sample quantities. SERS technology is compatible with a wide range of substrates such as PDMS, hydrogel, PVP, etc. [33]. Recently, a formidable amount of research is being driven towards incorporating MEMs technology and towards developing SERS sensors using flexible and cost-effective substrates such as paper [81–86]. Paper is considered as one of the very important flexible substrates as it is biodegradable, cost-effective, easy to use, and most importantly, they can be custom-tailored to become non-moisture absorbing [18, 88]. For instance, Tian and his colleagues used a specially customized paper composed of 3D nanofibrous structured bacterial nanocellulose (BNC) as SERS sensor substrate with adsorbed gold nanorods to detect *Escherichia coli* (E.coli) from a spinach leaf swab (Fig. 9). Further, the authors also demonstrated the use of paper-based SERS technique for detecting the biomarkers from human tears in PoC testing set-up [88].

Effective ligand adhesion on the functionalized sensor surface is of prime importance and requires detailed inspection as inefficient ligand attachment can result in loss of the sensitivity of the technique. Use of robust flexible surfaces such as silver

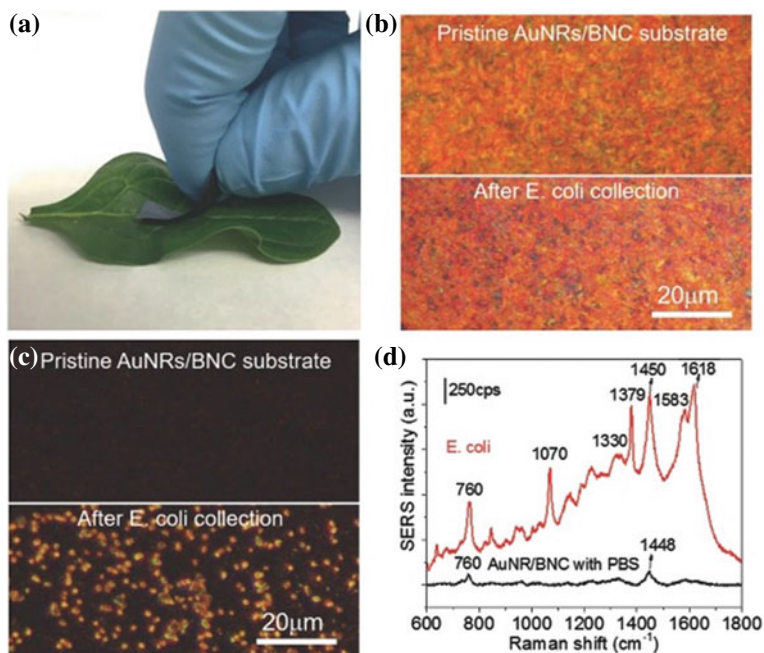


Fig. 9 Portable SERS technique that uses bacterial nanocellulose paper substrate (taken from Tian et al. [88]): **a** Photograph showing a plasmonic BNC SERS substrate swabbed on a intentionally *E. coli* contaminated spinach leaf surface. **b** and **c** Bright field optical images of pristine AuNRs/BNC paper and *E. coli* adsorbed on AuNRs/BNC paper collected by swabbing. **d** Representative SERS spectra collected from *E. coli* adsorbed on the AuNRs/BNC swab showing characteristic Raman bands of *E. coli*

nanorods embedded PDMS-coated SERS sensor substrate that offer very high sensitivity and that are also immune to binding issues is a possible solution for such problems [115, 116, 118, 119]. Another important aspect that requires advances in SERS-based research is the high cost per analysis of the sample as it is a current hindrance to the development and commercialization of SERS-based PoC devices.

2.2.5 Fibre-Optic-Based SPR

Optical waveguide confines the spatial propagation of light waves and guides the lateral propagation of the light waves. In a typical optical waveguide set-up, the light wave is allowed to propagate through wave-guiding platforms that has a core made of thin materials with smaller refractive index (n_1); usually, it is made of silica and its derivatives such as SiO_2 or silicon nitride, and a core-englobing cladding layer composed of materials with slightly higher refractive index (n_2) as shown in Fig. 8b. This arrangement causes the light to be confined in the core at the core-cladding interfaces due to TIR, and the evanescent wave generated penetrates into

the cladding layer. The smaller the thickness of the waveguide and the larger the difference between the refractive indices between guiding and cladding films, the stronger is the evanescent field yielding and subsequently higher is the sensitivity of the biosensor [11, 91]. A small window is etched on the surface of this cladding layer, i.e. a sensor surface is created where the biomolecular interaction occurs which alters the optical properties of the guided optical wave.

Although fibre-optic biosensors have been developed nearly three decades ago, it has only recently gained significant attention for its potential use in PoC devices. Biosensors that use fibre-optic-based SPR sensors demonstrate a key advantage of miniaturization without the loss of sensitivity while particularly maintaining high signal-to-noise ratio [89, 90, 92, 93]. Multiple TIRs are generated as opposed to one observed in traditional SPR systems, and this allows the generation of a spectrum of SPR incidence angle, and hence, the biomolecular interactions can be detected with higher sensitivity [94].

The evanescent wave generated at core-cladding interface propagates along the optical waveguide. Similar to the smartphone-based SPRi, PoC device developed by Liu and colleagues is shown in Fig. 7. The authors developed a compact and economic red-green dual-colour fibre-optic SPR-based sensor for real-time monitoring of the red and green colour channels simultaneously. The portability of fibre-optic sensors by using a convenient SPR adaptor that is attachable to the smartphone via dual-colour optical fibres is shown in Fig. 10. The adapter is equipped with lightweight optical components and SPR sensing element for flexible use. The SPR sensing element is incorporated with a light-guiding silica capillary and a 50-nm-thick gold layer. Light

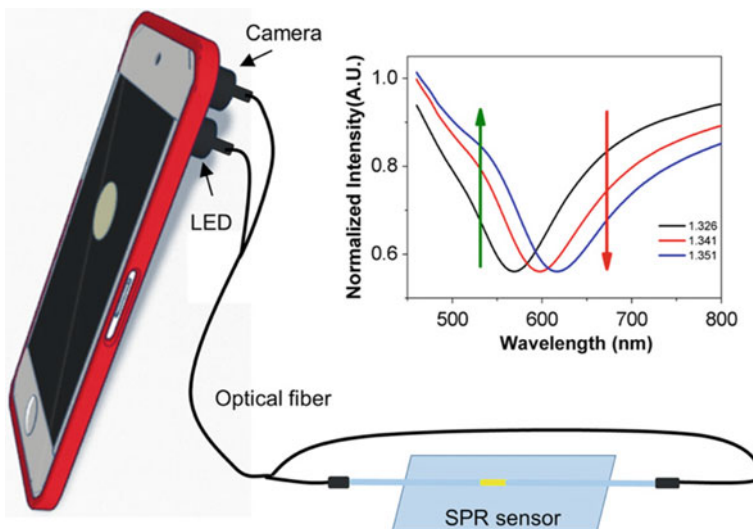


Fig. 10 An example of a fibre-optic SPR-based PoC application (taken from Liu et al. [95]): This is a schematic diagram of smartphone-based dual-colour fibre-optic SPR sensor set-up. The normalized spectrums of the sensor in different RIs obtained by spectrometer is shown as the graph

emitting diode (LED), integrated into the smartphone, is used as the principle source of light that is allowed to pass through three channels, i.e. testing, control and reference channels, which is eventually read using the smartphone camera. A smartphone application is used in order to derive the changes in light intensities and refractive indices observed on the obtained images. The authors immobilized Protein A on the sensor surface, i.e. on gold film surface, and used this system for detection and estimation of bovine IgG concentrations and compared the results obtained with classical SPR experiments. This device has an LOD of $\sim 0.02 \text{ mgml}^{-1}$ with a resolution of 2.3×10^{-4} RIU. Such advancements are a valuable addition to the development of next generation PoC devices [76]. Albeit the advantages of portability, real-time label-free biosensing and simple optics design of the device limitations such as complex image processing algorithm-based data analysis, further improvement in the LOD of the system would require detailed attention of the biosensor research community for successful establishment of the biosensing technique in the PoC testing application market.

2.2.6 PC-Based Biosensors

Photonic crystals (PCs) are a novel class of optical biosensors that were initially described by Yablonovitch E and John S in 1987 [96, 97]. PCs can be considered as an emerging advancement of fibre-optic guided biosensors. PCs offer very high sensitivity (LOD in the range of $\sim \text{pg ml}^{-1}$) and can be easily integrated into PoC testing devices. PCs are composite structures made up of two or more dielectric materials with varying refractive indices arranged in a periodic fashion of alternating high and low refractive indices. This arrangement causes multiple light reflections of the incident light wave from the alternating layers inside the structure as shown in Fig. 8c. Unique structural composition of PCs with varying refractive indices can generate multiple TIRs inside their structures allowing the formation of functional constructive and destructive interference patterns for light waves with different wavelengths. The reflected light waves usually reside at the photonic band gap (PBG). Thus, the PCs allow selective propagation of light waves inside their structures [11]. Introduction of certain structural defects allows to modify the light-controlling properties of the structure. Thus, the propagation of light wave of a certain wavelength can be intricately dictated by carefully orchestrating the structural properties of the PC [11]. The PC effect can be observed in different geometries of the structure. Such geometries include Bragg reflectors, slabs, colloids and microcavities, etc. The geometries of the PC significantly impact the sensitivity of the sensor [16]. Numerous materials such as silicon nitride (Si_3N_4) or silicon-on-insulator have been employed as the core substrate of PCs.

Dinish and colleagues reported a novel type of PC-based biosensor that uses a hollow core waveguide with SiO_2 as the core material. The sensor was employed to detect a cancer biomarker (EGFR), and the authors demonstrated LOD of up to $\sim 100 \text{ pgml}^{-1}$ [98]. PC structures designed with cavities, i.e. slot-waveguide cavities or the slab geometries are able to reach very high sensitivity, i.e. the LOD is down

to $\sim\text{fg ml}^{-1}$. This is because light wave remains well confined in a narrow region with lower refractive index and is surrounded by regions of higher refractive index forming slots with very high signal-to-noise ratio [99, 100]. Dorfner and colleagues, for instance, used slot-waveguide cavities and demonstrated BSA adsorption with LOD down to $\sim 4 \text{ fgmm}^{-2}$ [16, 99].

Recent developments demonstrate that Android mobile phones can be integrated with the PC biosensing system together with microfluidics technology that uses the optical system for spectral analysis of the samples. However, limitations in this system include the fact that the wet sample analysis on mobile phones is not as efficient as the dry sample analysis as yet, suggesting that optical systems and device sophistication need to be improved [16]. In addition, rapid sample analysis using PC-based biosensing systems is another aspect that requires attention as additional sample preparation is needed for proper sample analysis. Thus, research to advance the optical detection systems particularly the read-out for the biosensing system, and the increased sample preparation time needs to be addressed before technical validation of the system for clinical biosensing PoC-based applications is approved [16, 99, 100].

2.2.7 Optical Biosensors Based on Interferometer

This class of biosensors combines the techniques of the waveguide mode and the interferometry for biosensing applications. In an interferometer, optical wave from a monochromatic source of light is split into two light beams and is allowed to pass through two different optical paths, i.e. sensing arm and a reference arm. The light wave that passes through the sensing arm interacts with the sensor surface with the sample studied, while the other is preserved as it is allowed to pass through the reference arm as shown in Fig. 11. The sensor beam undergoes changes in optical phase of the wave due to biomolecular interactions that occur at the sensor surface. Recombination of the two light waves from the sensor arm and the reference arm generates an interference signal that reveals the phase-shift which is detected using a photodetector or a CCD camera. The resulting phase change is directly proportional to

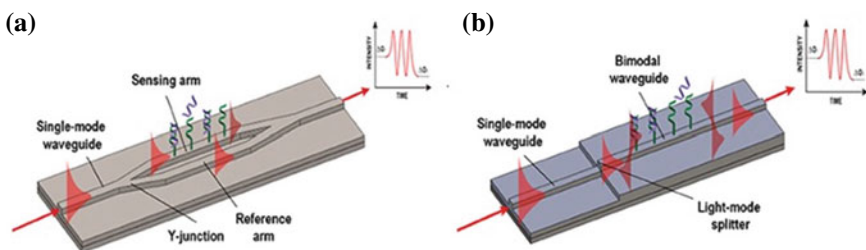


Fig. 11 Optical biosensors based on interferometers (taken from Huertas et al. [55]): The simple working principle of **a** MZI Interferometry, **b** Bimodal waveguide-based biosensor design

the change in the sample state [19]. The combination of waveguide and interferometry techniques offers great potential towards a portable point of care devices as this technique is insensitive to water or fluid-induced disturbances in the system. In addition, phase shift optical interferometry offers the best resolution (LOD up to $\sim 0.05 \text{ pgmm}^{-2}$) among all of the sensors studied so far. In the following sections, the use of classical Mach-Zehnder Interferometry for potential PoC applications and a novel interferometry technique called bimodal waveguide interferometry are discussed in detail.

The Mach-Zehnder Interferometer

The Mach-Zehnder interferometer (MZI) uses a collimated monochromatic source of light that is split into two optical beams. The split two beams are independently allowed to pass through the sensing arm and the reference arm and are recombined again after a certain distance in order to yield an interference pattern. The phase shift induced by changes in the sample state such as biomolecular interactions is interpreted from the interference pattern. MZI-based interferometers offer excellent sensitivity of 10^{-7} RIU [87, 101]. In 2015, Liu and colleagues reported an MZI-based PoC system for the detection of microRNAs in human specimens. Exploiting the optical phase change, the MZI technique was used for rapid profiling of microRNAs and also for the identification of single nucleotide polymorphism from cell line samples. The authors demonstrated the clinical value of this PoC by detecting two types of miRNA from the clinical human samples within 15 min and demonstrated the suitability of the technique for the identification of different miRNA species. The LOD was shown to be in the range of $\sim \text{pM}$. Some recent reports have also shown that the system is also compatible with multiplexing [102]. Such MZI-based PoC systems are very suitable for use in clinical diagnostics and in emergency or any near-patient settings [103].

The sensitivity of the system is both an advantage and a limitation as its high sensitivity also reduces the signal-to-noise ratio. Also, the increased sensitivity comes at a price of miniaturization since sensitivity of the sensor is significantly impacted by changes in temperature of the system and by the length of the sensing arm [87, 101, 104, 105]. The miniaturized MZI sensor chips have also been demonstrated to be highly sensitive to physical disturbances such as vibrations, i.e. they are sensitive to mechanical disturbances [11]. Thus, although MZI interferometers show good potential for PoC applications, significant improvements in the ligand immobilization, sensor fabrication techniques and advanced research to optimize the optical instrumentation for miniaturized device set-up are required for encouraging the use of MZI biosensing technique towards PoC applications.

Young Interferometer

Young interferometer and dual-polarization interferometry: This is a technique that essentially splits a laser beam into two beams that are allowed to pass through the two arms of the interferometer, i.e. the reference and sensor arm, where they are allowed to be super-imposed or mutually interfere in such a way as to produce the interference signal in far-field. Although these interferometers demonstrate far superior sensitivity compared to SPRs and LSPRs, they require a highly sophisticated technical approach to miniaturize. In addition, multiple optical elements must be placed at optimal distances, and it requires a cooling element to maintain a high signal-to-noise ratio. These limitations render them unsuitable for PoC-based devices [11, 106].

Bimodal Waveguide-Based Interferometer

Bimodal waveguide (BiMW)-based interferometer is a new advancement in the field of interferometry. Sensors based on this interferometer are compatible with integration optics and can be integrated into a New Age ultra-high sensitive PoC device. BiMW uses a single straight rib waveguide on Si_3N_4 enclosed in SiO_2 as shown in Fig. 11b. This technique uses two single-mode waveguides. The propagation of fundamental and first-order modes of light in same wavelength and polarization are achieved by increasing the core thickness after a certain distance where light is coupled to the single-mode rib waveguide (Fig. 11). The interference between the two guided modes is collected by a two-sectional photodetector at the end of the device. A sensing window is etched at the top of this bimodal section. This allows the detection of occurrence of biomolecular interactions which subsequently will change the refractive index of the propagating waves. As the propagation constants for the two waves are different, the acquired phase shifts and refractive index changes can be probed using a two-sectional photodetector placed at the end of the device [107]. This system has achieved a sensitivity of 2.5×10^{-7} RIU, similar to that of the MZI biosensor, while particularly allowing miniaturization and development of PoC devices.

Duval and colleagues have demonstrated multiple PoC applications exploiting this BiMW biosensor design [108]. For example, the authors have used BiMW sensors to demonstrate label-free immunodetection of human testosterone stimulating hormone (hTSH) at pM level with high specificity and reproducibility. One of the major challenges with interferometry is the analysis of the output signal. To overcome the complex nature of the analysis, the authors have used an all-optical-wavelength biosensing system to provide a linear response and a direct readout of the phase variation [108]. The following reviews provide a detailed overview and other PoC-based applications of this powerful technology [101, 108–110].

3 Conclusion and Outlook

Increasing demand for rapid and robust PoC devices for various applications has intensified research in the field of optical biosensors. Compatibility of current biosensing technologies to complementary technologies such as microfluidics and mobile platforms has shown that smart-phone based PoC applications hold a bright and promising future. Until recently, PoC devices were majorly used for relatively simpler diagnostic concepts based on glucose detection for monitoring diabetes and hCG hormone detection for monitoring pregnancy [111]. Recent advances in biosensor research and point-of-care testing are addressing the challenges of diagnosing complex diseases such as cancer, stroke, cardiac diseases and many communicable viral infections such as HIV, coronavirus, etc. This is evident as the PoC diagnostics market is estimated to advance at a compound annual growth rate (CAGR) of 11.9% from 2018 to 2023 worldwide [111].

Mounting evidences show that optical biosensors have distinct advantages as these biosensing technologies are compatible with device miniaturization, integration into Android-based platforms and have high sensitivity for detection of biomolecules and pathogens such as proteins, viruses, etc. Currently, label-based optical devices such as the fluorescence-based microarray reader and fluorescence-based glucose monitor, dominate the PoC market in the IVD sector as they offer very high specificity, selectivity and reliable high-throughput detection Table 2 shows an overall summary of the advantages and limitations of all optical biosensing techniques discussed in this chapter.

However, these techniques are expensive due to their dependency on fluorescently labelled probes for detection in addition to being limited because of the environmental influence of the fluorophores/labels used for detection. The limitations such as short lifespan, photobleaching and self-quenching of the fluorophores at high concentrations do not permit long time and constant monitoring of the system investigated. However, New Age labels such as Quantum dots have answered some of the fluorophore stability issues. Another class of optical biosensors that offers label-free optical detection particularly the evanescence-based detection techniques such as classical SPR and interferometry-based techniques has shown serious credulity to merit as PoC devices. Label-free optical biosensors offer high sensitivity and are relatively simpler, cost-effective and faster. They present immense potential as new age nano-biosensors that are compatible with a huge range of cost-effective sensor substrates such as paper-based or silicon-based surfaces. Thus, the class of optical biosensors representing both label-based and label-free systems shows great potential for PoC testing applications.

To fully exploit the versatility of optical biosensors and to develop highly functional PoC devices, a multidisciplinary approach to incorporate advances in the fields of nanotechnology, optoelectronics, surface biochemistry and information technology is indispensable.

Table 2 A detailed overview of optical biosensors that show good potential for PoC testing applications with their advantages and current limitations listed

Technology	LOD	Application towards PoC	Advantages	Limitations	References
FRET with classical fluoroprobes	100 pg μl^{-1} on Au sensor surface	Moderate	High specificity selectivity, and sensitivity and compatibility to microfluidics and device miniaturization	Limitations with fluoroprobes such as: photobleaching, self-quenching at high concentrations, short lifespan and environmental influence such as pH and temperature	[33]
FRET	~5 fM using QDs as sensors	High	High sensitivity, immune to limitations observed with traditional fluoroprobes, compatibility to device miniaturization and microfluidics	QD-QD FRET could create artificial noise in the system	[112]
SPR	1 pg mm^{-2} on Au sensor surface	High	High sensitivity, real-time monitoring of the biomolecular interactions, cost effective, label-free detection	Bulky optical components, high-precision optical component alignment is required	[57]
LSPR	0.5 ngml ⁻¹ using QDs on Au nanoarrays chip	High	High throughput/ multiplexing, compatible with microfluidics, label-free, as well as label-based, cost effective	Selectivity and specificity in complex biological media, sensitivity issues upon device miniaturization need further studies in the field	[66]
SERS	Single molecule detection on Au and Ag nanoparticles embedded on PDMS substrate	High	Rapid, high sensitivity, multiplexing, compatibility to wide range of substrates, immune to problems of sample liquid created interferences	Lack of consistent, expensive detectors, narrow tunable surface plasmon range that leads high SERS signal, special technical considerations are important for SERS instrumentation for PoC-based applications	[80]

(continued)

Table 2 (continued)

Technology	LOD	Application towards PoC	Advantages	Limitations	References
Fibre-optic waveguide-based SPR	$\sim 10 \text{ ng ml}^{-1}$ on Au-coated SiO_2 , Si_3N_4 sensor surface	High	Rapid, reliable, highly sensitive, compact, portable, cost-effective	Challenges regarding optical instrumentation for device miniaturization need to be addressed and complex data analyses process	[113]
Photonic crystals	$\sim 4 \text{ fg mm}^{-2}$ on Si_3N_4 sensors surfaces	High	Compatible with: microfluidics, wide range of smart substrates; extreme high sensitivity, integratable into smart phone system, wearable and flexible sensors possible,	Inefficient for studying labelled samples, high throughput multiplexing requires careful instrumentation considerations, analysis of complex biological samples can be challenging due to interferences from the non-clear liquid, sample preparation before assay is required, i.e. rapid analysis is difficult,	[16]
MZI	0.06 pgmm^{-2} on Si_3N_4 sensor surfaces	High	High sensitivity, multiplex data analysis, device miniaturization possible	Optical instrumentation, temperature and mechanically sensitive sensor, and optimal alignment is important for efficient detection, expensive sample detection and complex image process analysis and data processing are required	[101]
BiModal waveguide	0.05 pgmm^{-2} on Si_3N_4 sensor surfaces	High	Very high sensitivity, rapid and real-time monitoring-based sample analysis	Device miniaturization as the optical alignment is the key to biosensor precision, data read out, i.e. optical detection system could be complex and it can be improved and nature of the sensor and further data analysis are complicated	[110]

References

1. WHO.: Report of the third global survey on eHealth Global Observatory for eHealth Global diffusion of eHealth: Making universal health coverage achievable [Internet]. (2016), <http://apps.who.int/bookorders>
2. Christodouleas, D.C., Kaur, B., Chorti, P.: From point-of-care testing to eHealth diagnostic DEvices (eDiagnostics). ACS Cent. Sci. (2018)
3. Shaw, T., McGregor, D., Brunner, M., Keep, M., Janssen, A., Barnet, S.: What is eHealth (6)? Development of a conceptual model for ehealth: qualitative study with key informants. J. Med. Internet Res. (2017)
4. World Health Organization: Telemedicine: opportunities and developments report on the second global survey on eHealth Global Observatory for eHealth series-Volume 2 Telemedicine in Member States (2010)
5. Konwar, A.N., Borse, V.: Current status of point-of-care diagnostic devices in the Indian healthcare system with an update on COVID-19 pandemic. Sens. Int. **1**, 100015 (2020a). Elsevier BV
6. Vikram, T.: Essence of point-of-care diagnostic testing (POCT) in remote healthcare in India [Internet]. <https://www.linkedin.com/pulse/essence-point-of-care-diagnostic-testing-poct-remote-india-thaploo> (2017)
7. Kosack, C.S., Page, A.L., Klatser, P.R.: A guide to aid the selection of diagnostic tests. Bull. World Health Organ. [Internet]. **95**(9), 639–645 (2017). World Health Organization. <https://pubmed.ncbi.nlm.nih.gov/28867844/>
8. Luppá, P.B.: Point-of-care testing at the interface of emerging technologies and new clinical applications [Internet]. J. Lab. Med. 59–61 (2020). Walter de Gruyter GmbH, <https://doi.org/10.1515/labmed-2020-0020>
9. Purohit, B., Vernekar, P.R., Shetti, N.P., Chandra, P.: Biosensor nanoengineering: design, operation, and implementation for biomolecular analysis. Sens. Int. [Internet]. **1**(July), 100040 (2020), Elsevier Ltd. <https://doi.org/10.1016/j.sintl.2020.100040>
10. Dincer, C., Bruch, R., Costa-Rama, E., Fernández-Abedul, M.T., Merkoçi, A., Manz, A., et al. Disposable sensors in diagnostics, food, and environmental monitoring. Adv. Mater. (2019)
11. Chen, C., Wang, J.: Optical biosensors: an exhaustive and comprehensive review. Anal. Royal Soc Chem. **145**(5), 1605–1628 (2020)
12. Damborský, P., Švitel, J., Katrlík, J.: Optical biosensors. Essays Biochem. **60**(1), 91–100 (2016)
13. Huertas, C.S., Calvo-Lozano, O., Mitchell, A., Lechuga, L.M.: Advanced evanescent-wave optical biosensors for the detection of nucleic acids: an analytic perspective. Front. Chem. 1–25, 7(October). (2019a)
14. Long, F., Zhu, A., Shi, H.: Recent advances in optical biosensors for environmental monitoring and early warning. Sensors (Switzerland) (2013)
15. Dey, D., Goswami, T.: Optical biosensors: a revolution towards quantum nanoscale electronics device fabrication. J. Biomed Biotechnol. (2011)
16. Inan, H., Poyraz, M., Inci, F., Lifson, M.A., Baday, M., Cunningham, B.T., et al.: Photonic crystals: emerging biosensors and their promise for point-of-care applications. Chem. Soc. Rev. (2017)
17. Ulep, T.H., Yoon, J.Y.: Challenges in paper-based fluorogenic optical sensing with smart-phones. Nano Convergence (2018)
18. Mahato, K., Purohit, B., Kumar, A., Chandra, P.: Paper-based biosensors for clinical and biomedical applications: emerging engineering concepts and challenges. Compr. Anal.Chem. (2020)
19. Duque, T., Chaves Ribeiro, A.C., de Camargo, H.S., Costa Filho, P.A., da Mesquita Cavalcante, H.P., Lopes, D.: New insights on optical biosensors: techniques, construction and application. State of the Art in Biosensors—General Aspects [Internet]. (2013), InTech, <https://doi.org/10.5772/52330>

20. Hussain, S.A., Dey, D., Chakraborty, S., Saha, J., Roy, A.D., Chakraborty, S., et al.: Fluorescence resonance energy transfer (FRET) sensor. *BMC Pharmacology* [Internet]. **8**(S1), (2014) Springer Nature, Aug 26 <http://arxiv.org/abs/1408.6559>
21. Zhang, J., Shikha, S., Mei, Q., Liu, J., Zhang, Y.: Fluorescent microbeads for point-of-care testing: a review. *Microchim. Acta* (2019a)
22. Raja, S., Ching, J., Xi, L., Hughes, S.J., Chang, R., Wong, W., et al.: Technology for automated, rapid, and quantitative PCR or reverse transcription-PCR clinical testing. *Clin. Chem.* **51**(5), (2005)
23. Hochreiter, B., Garcia, A.P., Schmid, J.A.: Fluorescent proteins as genetically encoded FRET biosensors in life sciences [Internet]. *Sensors* (Switzerland). 26281–26314 (2015). MDPI AG, /pmc/articles/PMC4634415/?report=abstract
24. A., S.J., C P.L.: Existing and emerging technologies for point-of-care testing—PubMed [Internet]. <https://pubmed.ncbi.nlm.nih.gov/25336761/>
25. D’Auria, S., Ghirlanda, G., Parracino, A., de Champdoré, M., Scognamiglio, V., Staiano, M., et al.: Fluorescence biosensors for continuously monitoring the blood glucose level of diabetic patients. *Glucose Sensing*. [Internet]. pp. 117–130, Springer, US (2006) https://doi.org/10.1007/0-387-33015-1_5
26. Hartman, M.R., Ruiz, R.C.H., Hamada, S., Xu, C., Yancey, K.G., Yu, Y., et al.: Point-of-care nucleic acid detection using nanotechnology. *Nanoscale* [Internet]. **5**(21), 10141–54 (2013). The Royal Society of Chemistry, <https://pubs.rsc.org/en/content/articlehtml/2013/nr/c3nr04015a>
27. Radiometer.: Analyseur d’immunodosage AQT90 FLEX—Radiometer [Internet]. <https://www.radiometer.fr/fr-fr/produits/analyseur-d-immunodosage/analyseur-dimmunodosage-aqt90-flex>
28. Serra, P.A.: Biosensors for health, environment and biosecurity [Internet]. InTech, [cited 9 Nov 2020]. <https://www.intechopen.com/books/biosensors-for-health-environment-and-biosecurity> (2012)
29. Taguchi, M., Ptitsyn, A., McLamore, E.S., Claussen, J.C.: Nanomaterial-mediated biosensors for monitoring glucose [Internet]. *J. Diabetes Sci. Technol.* 403–411 (2014). Diabetes Technology Society, /pmc/articles/PMC4455391/?report=abstract
30. Geldert, A., Kenry, Lim, C.T.: Paper-based MoS₂ nanosheet-mediated FRET aptasensor for rapid malaria diagnosis. *Sci. Rep.* [Internet]. **7**(1) (2017) Nature Publishing Group, <https://pubmed.ncbi.nlm.nih.gov/29235484/>
31. Zhang, X., Hashem, M.A., Chen, X., Tan, H.: On passing a non-Newtonian circulating tumor cell (CTC) through a deformation-based microfluidic chip. *Theor. Comput. Fluid Dyn.* [Internet]. **32**(6), 753–764 (2018). Springer New York LLC, <https://ui.adsabs.harvard.edu/abs/2018ThCFD..32..753Z/abstract>
32. Khan, R., Khurshid, Z., Yahya Ibrahim Asiri, F.: Advancing point-of-care (PoC) testing using human saliva as liquid biopsy. *Diagnostics* (2017)
33. Shin, Y., Kim, J., Lee, T.Y.: A solid phase-bridge based DNA amplification technique with fluorescence signal enhancement for detection of cancer biomarkers. *Sens. Actuators B Chem.* (2014)
34. Kosaka, P.M., Pini, V., Calleja, M., Tamayo, J.: Ultrasensitive detection of HIV-1 p24 antigen by a hybrid nanomechanical-optoplasmonic platform with potential for detecting HIV-1 at first week after infection. *PLoS ONE* (2017)
35. Girigoswami, K., Akhtar, N.: Nanobiosensors and fluorescence based biosensors: an overview. *Int. J. Nano Dimension* (2019)
36. Tokel, O., Inci, F., Demirci, U.: Advances in plasmonic technologies for point of care applications. *Chem. Rev.* **114**(11), 5728–5752 (2014)
37. Förster, T.: Zwischenmolekulare Energiewanderung und Fluoreszenz. *Annalen der Physik.* (1948)
38. Zadran, S., Standley, S., Wong, K., Otiniano, E., Amighi, A., Baudry, M.: Fluorescence resonance energy transfer (FRET)-based biosensors: visualizing cellular dynamics and bioenergetics [Internet]. *Applied Microbiology and Biotechnology*. *Appl. Microbiol. Biotechnol.* 895–902 (2012) <https://pubmed.ncbi.nlm.nih.gov/23053099/>

39. Zhang, X., Hu, Y., Yang, X., Tang, Y., Han, S., Kang, A., et al.: Förster resonance energy transfer (FRET)-based biosensors for biological applications [Internet]. *Biosens. Bioelectron.* (2019c). Elsevier Ltd, <https://pubmed.ncbi.nlm.nih.gov/31096114/>
40. Hellenkamp, B., Schmid, S., Doroshenko, O., Opanasyuk, O., Kühnemuth, R., Rezaei Adariani, S., et al.: Precision and accuracy of single-molecule FRET measurements—a multi-laboratory benchmark study. *Nat. Methods* (2018)
41. Sandbhor Gaikwad, P., Banerjee, R.: Advances in point-of-care diagnostic devices in cancers. *Analyst* (2018)
42. Zhang, J., Shikha, S., Mei, Q., Liu, J., Zhang, Y.: Fluorescent microbeads for point-of-care testing: a review. *Microchim. Acta* (2019b)
43. Qiu, X., Hildebrandt, N.: A clinical role for Förster resonance energy transfer in molecular diagnostics of disease [Internet]. *Expert Rev. Mol Diagn.* 767–771 (2019) Taylor and Francis Ltd, <https://doi.org/10.1080/14737159.2019.1649144>
44. van der Fels-Klerx, H.J., van Asselt, E.D., Raley, M., Poulsen, M., Korsgaard, H., Bredsdorff, L., et al.: Critical review of methods for risk ranking of food-related hazards, based on risks for human health. *Critical Rev. Food Sci Nutr.* (2018)
45. Choi, J.R., Yong, K.W., Choi, J.Y., Cowie, A.C.: Emerging point-of-care technologies for food safety analysis. *Sensors (Switzerland)* (2019)
46. Morales-Narváez, E., Naghdi, T., Zor, E., Merkoçi, A.: Photoluminescent lateral-flow immunoassay revealed by graphene oxide: highly sensitive paper-based pathogen detection. *Anal. Chem.* (2015)
47. Zhang, Y., Zuo, P., Ye, B.C.: A low-cost and simple paper-based microfluidic device for simultaneous multiplex determination of different types of chemical contaminants in food. *Biosens. Bioelectron.* (2015)
48. Mei, Q., Jing, H., Li, Y., Yisibashaer, W., Chen, J., Nan Li, B., et al.: Smartphone based visual and quantitative assays on upconversional paper sensor. *Biosens. Bioelectron.* (2016)
49. Petryayeva, E., Algar, W.R.: Multiplexed homogeneous assays of proteolytic activity using a smartphone and quantum dots. *Anal. Chem.* (2014)
50. Mizutani, T., Kondo, T., Darmanin, S., Tsuda, M., Tanaka, S., Tobiume, M., et al.: A novel FRET-based biosensor for the measurement of BCR-ABL activity and its response to drugs in living cells. *Clin. Cancer Res.* **16**(15), 3964–3975 (2010)
51. Lu, S., Wang, Y.: Fluorescence resonance energy transfer biosensors for cancer detection and evaluation of drug efficacy. *Clin. Cancer Res.* (2010)
52. Carrascosa, L.G., Huertas, C.S., Lechuga, L.M.: Prospects of optical biosensors for emerging label-free RNA analysis. *Trac, Trends Anal. Chem.* (2016)
53. Ermini, M.L., Mariani, S., Scarano, S., Minunni, M.: Bioanalytical approaches for the detection of single nucleotide polymorphisms by Surface Plasmon Resonance biosensors [Internet]. *Biosens. Bioelectron.* 28–37 (2014). Elsevier Ltd, <https://pubmed.ncbi.nlm.nih.gov/24841091/>
54. González-Guerrero, A.B., Maldonado, J., Herranz, S., Lechuga, L.M.: Trends in photonic lab-on-chip interferometric biosensors for point-of-care diagnostics [Internet]. *Anal. Methods.* 8380–8394 (2016) Royal Society of Chemistry, <https://pubs.rsc.org/en/content/articlehtml/2016/ay/c6ay02972h>
55. Huertas, C.S., Calvo-Lozano, O., Mitchell, A., Lechuga, L.M.: Advanced evanescent-wave optical biosensors for the detection of nucleic acids: an analytic perspective. *Front. Chem.* (2019b)
56. Ahn, H., Song, H., Choi, J.R., Kim, K.: A localized surface plasmon resonance sensor using double-metal-complex nanostructures and a review of recent approaches. *Sensors (Switzerland)* **18**(1) (2018)
57. Harpaz, D., Koh, B., Marks, R.S., Seet, R.C.S., Abdulhalim, I., Tok, A.I.Y.: A functionalized gold chip with specific antibody. pp. 1–16, (2019)
58. Tang, Y., Zeng, X., Liang, J.: Surface plasmon resonance: an introduction to a surface spectroscopy technique. *J. Chem. Edu.* (2010)

59. Endo, T., Kerman, K., Nagatani, N., Takamura, Y., Tamiya, E.: Label-free detection of peptide nucleic acid-DNA hybridization using localized surface plasmon resonance based optical biosensor. *Anal. Chem.* [Internet]. **77**(21), 6976–6984 (2005). American Chemical Society, <https://doi.org/10.1021/ac0513459>
60. Mayer, K.M., Hafner, J.H.: Localized surface plasmon resonance sensors. *Chem. Rev.* (2011)
61. Park, K.H., Kim, S., Yang, S.M., Park, H.G.: Detection of DNA immobilization and hybridization on gold/silver nanostructures using localized surface plasmon resonance. *J. Nanosci. Nanotechnol.* [Internet]. 1374–1378 (2009) <https://pubmed.ncbi.nlm.nih.gov/19441528/>
62. Roether, J., Chu, K.Y., Willenbacher, N., Shen, A.Q., Bhalla, N.: Real-time monitoring of DNA immobilization and detection of DNA polymerase activity by a microfluidic nanoplasmonic platform. *Biosens. Bioelectron.* (2019)
63. Bhalla N, Sathish S, Sinha A, Shen AQ. Large-Scale Nanophotonic Structures for Long-Term Monitoring of Cell Proliferation. *Adv. Biosyst.* [Internet]. **2**(4), 1700258 (2018), Wiley. [cited 10 Nov 2020]. <https://doi.org/10.1002/adbi.201700258>
64. Huang, C., Ye, J., Wang, S., Stakenborg, T., Lagae, L.: Gold nanoring as a sensitive plasmonic biosensor for on-chip DNA detection. *Appl. Phys. Lett.* [Internet]. **100**(17), 173114 (2012). American Institute of Physics AIP, <https://doi.org/10.1063/1.4707382>
65. Schneider, T., Jahr, N., Jatschka, J., Csaki, A., Stranik, O., Fritzsche, W.: Localized surface plasmon resonance (LSPR) study of DNA hybridization at single nanoparticle transducers. *J. Nanopart. Res.* [Internet]. **15**(4), 1–10 (2013) Springer, <https://doi.org/10.1007/s11051-013-1531-7>
66. Sun, L.L., Leo, Y.S., Zhou, X., Ng, W., Wong, T.I., Deng, J.: Localized surface plasmon resonance based point-of-care system for sepsis diagnosis. *Mater. Sci. Energy Technol.* **3**, 274–281 (2020). Elsevier BV
67. Steiner, G.: Surface plasmon resonance imaging. *Anal. Bioanal. Chem.* [Internet]. *Anal. Bioanal. Chem.* [cited 10 Nov 2020], **379**(3), 328–331 (2004). <https://pubmed.ncbi.nlm.nih.gov/15127177/>
68. Homola, J.: Surface plasmon resonance sensors for detection of chemical and biological species [Internet]. *Chem. Rev.* American Chemical Society. 462–493 (2008) <https://doi.org/10.1021/cr068107d>
69. Campbell, C.T., Kim, G.: SPR microscopy and its applications to high-throughput analyses of biomolecular binding events and their kinetics. *Biomaterials* (2007)
70. Fu, E., Foley, J., Yager, P.: Wavelength-tunable surface plasmon resonance microscope. *Rev. Sci. Instrum.* [Internet]. **74**(6):3182–3184 (2003). American Institute of Physics AIP, <https://doi.org/10.1063/1.1574603>
71. Shumaker-Parry, J.S., Campbell, C.T.: Quantitative methods for spatially resolved adsorption/desorption measurements in real time by surface plasmon resonance microscopy. *Anal. Chem.* [Internet]. American Chemical Society, Feb 15, **76**(4), 907–917 (2004) <https://doi.org/10.1021/ac034962a>
72. Wang D, Loo JFC, Chen J, Yam Y, Chen SC, He H, et al. Recent advances in surface plasmon resonance imaging sensors. *Sensors (Switzerland)* (2019)
73. Jordan, C.E., Com, R.M.: Surface plasmon resonance imaging measurements of electrostatic biopolymer adsorption onto chemically modified gold surfaces. *Anal. Chem.* (1997)
74. Nelson, B.P., Grimsrud, T.E., Liles, M.R., Goodman, R.M., Corn, R.M.: Surface plasmon resonance imaging measurements of DNA and RNA hybridization adsorption onto DNA microarrays. *Anal. Chem.* (2001)
75. Wegner, G.J., Lee, H.J., Corn, R.M.: Characterization and optimization of peptide arrays for the study of epitope-antibody interactions using surface plasmon resonance imaging. *Anal. Chem.* (2002)
76. Liu, Y., Liu, Q., Chen, S., Cheng, F., Wang, H., Peng, W.: Surface plasmon resonance biosensor based on smart phone platforms. *Sci. Rep.* (2015b)
77. Ho, H.P., Huang, Y.H., Wu, S.Y., Kong, S.K.: Detecting phase shifts in surface plasmon resonance: a review. *Adv. Opt. Technol.* (2012)

78. Lee, K.H., Su, Y.D., Chen, S.J., Tseng, F.G., bin Lee, G.: Microfluidic systems integrated with two-dimensional surface plasmon resonance phase imaging systems for microarray immunoassay. *Biosens. Bioelectron.* (2007)
79. Wang, D., Ding, L., Zhang, W., Luo, Z., Ou, H., Zhang, E., et al.: A high-throughput surface plasmon resonance biosensor based on differential interferometric imaging. *Measur. Sci. Technol.* [Internet]. Institute of Physics Publishing, 2012 May 4, **23**(6), 065701. <https://doi.org/10.1088/0957-0233/23/6/065701>
80. Pilot, R., Signorini, R., Durante, C., Orian, L., Bhamidipati, M., Fabris, L.: A review on surface-enhanced Raman scattering. *Biosensors* (2019)
81. Huang, C.C., Cheng, C.Y., Lai, Y.S.: Paper-based flexible surface enhanced Raman scattering platforms and their applications to food safety. *Trends. Food Sci. Technol.* (2020)
82. Lee, C.H., Tian, L., Singamaneni, S.: Paper-based SERS swab for rapid trace detection on real-world surfaces. *ACS Appl. Mater. Interfaces* (2010)
83. Liu, X., Wang, J., Tang, L., Xie, L., Ying, Y.: Flexible plasmonic metasurfaces with user-designed patterns for molecular sensing and cryptography. *Adv. Funct. Mater.* (2016)
84. Park, M., Jung, H., Jeong, Y., Jeong, K.H.: Plasmonic schirmer strip for human tear-based gouty arthritis diagnosis using surface-enhanced Raman scattering. *ACS Nano* (2017)
85. Qiu, H., Wang, M., Jiang, S., Zhang, L., Yang, Z., Li, L., et al.: Reliable molecular trace-detection based on flexible SERS substrate of graphene/Ag-nanoflowers/PMMA. *Sens. Actuators B Chem.* (2017)
86. Xu, K., Zhou, R., Takei, K., Hong, M.: Toward flexible surface-enhanced raman scattering (SERS) sensors for point-of-care diagnostics. *Adv. Sci.* (2019)
87. Martens, D., Bienstman, P.: Study on the limit of detection in MZI-based biosensor systems. *Sci. Rep.* **9**(1), 1–8 (2019)
88. Tian, L., Jiang, Q., Liu, K.K., Luan, J., Naik, R.R., Singamaneni, S.: Bacterial nanocellulose-based flexible surface enhanced raman scattering substrate. *Adv. Mater. Interfaces* (2016)
89. Rajan, Chand S, Gupta, B.D.: Fabrication and characterization of a surface plasmon resonance based fiber-optic sensor for bittering component-Naringin. *Sens Actuators B Chem.* (2006)
90. Sharma, A.K., Gupta, B.D.: On the sensitivity and signal to noise ratio of a step-index fiber optic surface plasmon resonance sensor with bimetallic layers. *Opt. Commun.* (2005)
91. Zanchetta, G., Lanfranco, R., Giavazzi, F., Bellini, T., Buscaglia, M.: Emerging applications of label-free optical biosensors. *Nanophotonics* (2017)
92. Sharma, A.K., Gupta, B.D.: Absorption-based fiber optic surface plasmon resonance sensor: a theoretical evaluation. *Sens. Actuators B Chem.* (2004)
93. Slavík, R., Homola, J., Tyroky, J., Brynda, E.: Novel spectral fiber optic sensor based on surface plasmon resonance. *Sens. Actuators B Chem.* (2001)
94. Gupta, B.D., Verma, R.K.: Surface plasmon resonance-based fiber optic sensors: principle, probe designs, and some applications. *J. Sens.* (2009)
95. Liu, Q., Yuan, H., Liu, Y., Wang, J.: Real-time biodetection using a smartphone-based dual-color surface plasmon resonance sensor. *J. Biomed. Opt.* (2018)
96. John, S.: Strong localization of photons in certain disordered dielectric superlattices. *Phys. Rev Lett.* (1987)
97. Yablonovitch, E.: Inhibited spontaneous emission in solid-state physics and electronics. *Phys. Rev. Lett.* (1987)
98. Dinish, U.S., Fu, C.Y., Soh, K.S., Ramaswamy, B., Kumar, A., Olivo, M.: Highly sensitive SERS detection of cancer proteins in low sample volume using hollow core photonic crystal fiber. *Biosens. Bioelectron.* (2012)
99. Dorfner, D., Zabel, T., Hürlimann, T., Hauke, N., Frandsen, L., Rant, U., et al.: Photonic crystal nanostructures for optical biosensing applications. *Biosens. Bioelectron.* (2009)
100. Scullion, M.G., di Falco, A., Krauss, T.F.: Slotted photonic crystal cavities with integrated microfluidics for biosensing applications. *Biosens. Bioelectron.* (2011)
101. Zinoviev, K., Carrascosa, L.G., del Río, J.S., Sepúlveda, B., Domínguez, C., Lechuga, L.M.: Silicon photonic biosensors for lab-on-a-chip applications. *Adv. Opt. Technol.* (2008)

102. Scott, A., Florjańczyk, M., Cheben, P., Janz, S., Solheim, B., Xu, D.-X.: Micro-interferometer with high throughput for remote sensing. In: Dickensheets, D.L., Schenk, H., Piyawat-tanametha, W., (eds.) MOEMS and Miniaturized Systems VIII [Internet]. SPIE; 2009 p. 72080G. <https://doi.org/10.1117/12.808271>
103. Liu, Q., Shin, Y., Kee, J.S., Kim, K.W., Mohamed Rafei, S.R., Perera, A.P., et al.: Mach-Zehnder interferometer (MZI) point-of-care system for rapid multiplexed detection of microRNAs in human urine specimens. *Biosens. Bioelectron.* (2015a)
104. Bastos, A.R., Vicente, C.M.S., Oliveira-Silva, R., Silva, N.J.O., Tacão, M., da Costa, J.P., et al.: Integrated optical Mach-Zehnder interferometer based on organic-inorganic hybrids for photonics-on-a-chip biosensing applications. *Sensors (Switzerland)* (2018)
105. Gauglitz, G.: Critical assessment of relevant methods in the field of biosensors with direct optical detection based on fibers and waveguides using plasmonic, resonance, and interference effects. *Anal. Bioanal. Chem.* (2020)
106. Kussrow, A., Enders, C.S., Bornhop, D.J.: Interferometric methods for label-free molecular interaction studies. *Anal. Chem.* (2012)
107. Liang, Y., Zhao, M., Wu, Z., Morthier, G.: Bimodal waveguide interferometer RI sensor fabricated on low-cost polymer platform. *IEEE Photonics J.* (2019)
108. Duval, D., González-Guerrero, A.B., Dante, S., Osmond, J., Monge, R., Fernández, L.J., et al.: Nanophotonic lab-on-a-chip platforms including novel bimodal interferometers, microfluidics and grating couplers. *Lab Chip* (2012)
109. Herranz, S., Gavela, A.F., Lechuga, L.M.: Label-free biosensors based on bimodal waveguide (BiMW) interferometers. *Methods Mol. Biol.* (2017)
110. Zinoviev, K.E., González-Guerrero, A.B., Domínguez, C., Lechuga, L.M.: Integrated bimodal waveguide interferometric biosensor for label-free analysis. *J. Lightwave Technol.* (2011)
111. Konwar, A.N., Borse, V.: Current status of point-of-care diagnostic devices in the Indian healthcare system with an update on COVID-19 pandemic. *Sens. Int.* (2020b)
112. Zhang, C.Y., Yeh, H.C., Kuroki, M.T., Wang, T.H.: Single-quantum-dot-based DNA nanosensor. *Nat. Mater.* (2005)
113. Zeni, L., Perri, C., Cennamo, N., Arcadio, F., D'Agostino, G., Salmona, M., et al.: A portable optical-fibre-based surface plasmon resonance biosensor for the detection of therapeutic antibodies in human serum. *Sci. Rep.* (2020)
114. Arunya Revathi, A., Rajeswari, D.: Surface plasmon resonance biosensor-based dual-core photonic crystal fiber: design and analysis. *J. Opt. (India)* [Internet]. **49**(2), 163–167, (2020), Springer, <https://doi.org/10.1007/s12596-020-00600-y>
115. Eom, H., Kim, J.H., Hur, J., Kim, T.S., Sung, S.K., Choi, J.H., et al.: Nanotextured polymer substrate for flexible and mechanically robust metal electrodes by nanoimprint lithography. *ACS Appl. Mater. Interfaces* (2015)
116. Jiang, J., Zou, S., Ma, L., Wang, S., Liao, J., Zhang, Z.: Surface-enhanced raman scattering detection of pesticide residues using transparent adhesive tapes and coated silver nanorods. *ACS Appl. Mater. Interfaces* (2018)
117. Mungroo, N.A., Neethirajan, S.: Biosensors for the detection of antibiotics in poultry industry—a Review. *Biosensors* (2014)
118. Shu, Y., Tian, H., Yang, Y., Li, C., Cui, Y., Mi, W., et al.: Surface-modified piezoresistive nanocomposite flexible pressure sensors with high sensitivity and wide linearity. *Nanoscale* (2015)
119. Singh, J.P., Chu, H., Abell, J., Tripp, R.A., Zhao, Y.: Flexible and mechanical strain resistant large area SERS active substrates. *Nanoscale* (2012)

Chapter 12

Blood Coagulation System and Carbon-Based Nanoengineering for Biomedical Application



Abhishek R. Panigrahi, Pooja Yadav, Samir K. Beura, and Sunil K. Singh

1 Introduction

Nanotechnology is the most promising field among scientific and engineering bodies in the last few decades due to its huge impact on early diagnosis and therapeutics [1]. Recently nanomaterials have been extensively used as biosensors to detect different types of biomolecules involved in major diseases such as cancer [2]. Nanotechnology comprises the building up of nanometer-scale materials or nanomaterial that display distinctive properties in comparison to its bulk forms such as optical, thermal, electronic, magnetic, mechanical, and catalytic, which are dictated by their shape, size, and composition. Among them, Carbon-based nanomaterials (CBNs) have unique importance owing to its different allotropes ranging from graphite, diamond, and amorphous carbon to newly discovered carbon nanotubes, graphene oxide, fullerenes, and others. CBNs exist in different dimensions such as 0D (fullerene), 1D (SWCNTs, DWCNTs, MWCNTs, carbon nanorods, and carbon nanowires), 2D (graphene nanoribbons, nanofoams, nanosheets, nanoplates), and 3D (carbon nanopillars, graphene nanoflowers) [3]. They can be synthesized via two approaches, including bottom-up and top-down approach. The bottom-up approach includes chemical vapor deposition (CVD), atomic layer deposition, electrodeposition that leads to the self-assembly of smaller components with atomic or molecular dimensions whereas top-down approach [4] starts with a large piece that subsequently converted to smaller structures using finer tools. Thermal methods, electrospinning, high energy methods, arc discharge, laser ablation, and solar flux are common methods of the top-down approach. These approaches and properties of CBNs make them suitable to be exploited for various biomedical applications such as bio-sensing

A. R. Panigrahi · P. Yadav · S. K. Beura · S. K. Singh (✉)
Department of Zoology, School of Basic and Applied Science, Central University of Punjab,
Bathinda, Punjab 151401, India
e-mail: sunil.singh@cup.edu.in

[5, 6], cellular imaging [7], controlled drug delivery [8], and photodynamic therapy, and regenerative medicine [9, 10].

Intravenously injected CBNs, for early diagnosis and controlled delivery of drugs, first interact with complex biological fluid, i.e., blood. This encounter of CBNs with blood components disturbs the normal flow of blood and leads to the pathophysiological processes such as complement activation, platelet aggregation, and thrombosis. The dynamic nature of blood might also modify the CBNs via bio-corona formation that could disturb their pharmacokinetics and therapeutics efficacy [11, 12].

The blood maintains the physiological processes in a healthy state. Any disturbance to balanced blood system leads to the imbalance in its components that activates the coagulation cascade and leads to the thrombus formation and subsequently inflammatory response. Thus, a comprehensive study is required to evaluate the interaction between CBNs and blood coagulation system. There are various research published on the interactions of CBNs with blood components but limited review available on it. Thus, the current book chapter is centered towards the impact of different CBNs on blood coagulation system with subsections describing the coagulation cascade mechanism along with various allotropes of carbon nanomaterials. This chapter also highlighted the effect of CBNs on different platelet function and coagulation proteins along with the brief description of sophisticated techniques used to study the characteristics of CBNs and thrombotic system interaction.

2 Overview of the Blood Coagulation System

The blood coagulation system aids in the prevention of blood loss through clotting of blood that is referred to as hemostasis. This cascade serves as a first line of defense upon vascular injury. This multiplex system consists of various components such as endothelial cells lining the blood vessels, platelets, coagulation proteins. Upon triggering the coagulation cascade via injury, the vWF from endothelial cells make platelet adhere to the damaged site by interacting with them. Further, platelet interacts with coagulation proteins and leads to the fibrin formation and progressively clot the blood. Later, the clot retraction process lead the pathway to completely seal the edges of injured vessel for completion of wound healing. In pathological conditions, the formation of clot occurs in intact blood vessels called thrombi that obstructs the normal flow of blood and disturbs the circulatory system.

2.1 Platelet

Platelets (or thrombocytes) are the essential component of blood coagulation system, which are small, enucleated, colorless, discoid shaped fragments that originate from megakaryocytes of bone marrow under the influence of thrombopoietin (TPO) and

eliminated by reticuloendothelial cells of spleen and liver [13, 14]. Platelets measure 2–4 μm in diameter with a count of 150,000–450,000 per microliter of blood along with a lifespan of about 8–10 days.

The platelet comprises four zones named as (1) peripheral zone, (2) sol-gel zone (3) organelle zone, and (4) membrane zone or system [15]. The peripheral zone consists of plasma membrane and open canalicular system (OCS). The plasma membrane comprises various receptors including G-Protein Coupled Receptors (PAR1, PAR4), integrins ($\alpha\text{IIb}\beta\text{3}$), and glycoproteins (GPVI) that mediate in the signaling cascade of platelets whereas OCS provide a link for externalization of granular component during activation. The sol-gel zone lies beneath the peripheral zone and incorporates actin cytoskeleton and microtubules that support the platelet to maintain its discoid shape during rest and extended filopodial form after its activation. The organelle zone resides in the center of platelet and comprises alpha, dense, lysosomes, and glycogen granules. Among them, alpha granules are the largest (200–500 nm) and most abundant (50–80 granules per platelet) with secretions of vWF, P-selectin, thrombospondin, fibrinogen, factor V, factor XI, protein S, factor XIII, PDGF, EGF, TGF- β , VEGF, fibrinolytic inhibitors and various chemokines [13]. Dense granules are smaller in size and lower in numbers with 3–9 granules per platelet. Its granular content includes bivalent cations (Ca^{2+} , Mg^{2+}), amines (serotonin, histamine), and nucleotides (ADP), and they are responsible for the platelet aggregation and vasoconstriction of blood vessels during damage [16]. Lysosome granules contain glycohydrolases and acid proteases (cathepsins D), which aids in receptor cleavage, breakdown of the extracellular matrix, heparin inactivation, and clearance of platelet thrombi via fibrinolysis [13]. Glycogen granules, along with mitochondria, serve as an energy source for platelets during activation and aggregation [17]. The membrane zone embraces the dense tubular system with Ca^{2+} ions stored in it. Ca^{2+} ions act as a secondary messenger that regulates different platelet function such as activation, adhesion, degranulation, cytoskeleton reorganization, and clot retraction. Platelet cytosolic calcium level is increased via release of Ca^{2+} ions from intracellular store as well as from extracellular compartment of cell that internalize through plasma membrane via SOCE channels. Agonist mediated platelet stimulation results in the activation of phospholipase C (PLC) which further act on phosphatidylinositol 4,5-bisphosphate (PIP₂) and hydrolyze it into inositol trisphosphate (IP₃) and diacylglycerol (DAG). IP₃ mediate the release of Ca^{2+} ions from intracellular store via binding of IP₃ to its receptor, present on the surface of DTS while DAG bring about the internalization of Ca^{2+} ions from extracellular environment [18]. The activation of PLC also activates other receptors such as Orai1 that leads to the activation of STIM. Orai1 and STIM complex activates the SOCE [19] and leads to the increase of Ca^{2+} ions from extracellular environment. Prolonged elevation of Ca^{2+} level can induce the damage to the cells. So, in order to maintain the optimum cytosolic Ca^{2+} level, restoration of Ca^{2+} is required, which is done by using calcium pump i.e. sarcoplasmic/endoplasmic reticulum calcium ATPase (SERCA), present on the surface of DTS.

Platelets play an essential role to maintain the vascular integrity such as hemostatic plug formation, fibrin network formation, and complete healing of injured

vessels. Platelets carried out these function via adhesion, aggregation, activation, and retraction phenomenon to completely seal the injured site.

2.2 Plasma Proteins and Clotting Factors

In blood plasma, protein constitutes 7% of total plasma concentration. Major proteins of plasma include albumin (54%), globulin (38%), fibrinogen (7%), and others (1%). Albumin is the smallest and most numerous protein found in the blood plasma, produced by the liver, and functions in the transport of various steroid hormones and fatty acids. Globulin is synthesized by liver and plasma cells and plays important role in immunity. Fibrinogen (340 kDa) is also produced by the liver and takes part as an essential component in blood clotting [20].

Different blood clotting factors also present but in an inactivated form called zymogen, activated only after stimulus production. They were designated in Roman numerical from I to XIII, and no factor VI is present. After their activation, suffix 'a' is added after the roman numerical (Table 1).

Table 1 Description of coagulation factors [21].

S. No.	Name	Production source
I	Fibrinogen	Liver
II	Prothrombin	Liver
III	Tissue factor (thromboplastin)	Damaged tissue and activated platelets
IV	Calcium ions (Ca ²⁺)	Diet, bones and platelets
V	Proaccelerin or labile factor	Liver and platelets
VII	Proconvertin or stable factor	Liver
VIII	Antihemophilic factor (AHF)	Liver
IX	Christmas factor	Liver
X	Stuart factor	Liver
XI	Plasma thromboplastin antecedent (PTA)	Liver
XII	Hageman factor	Liver
XIII	Fibrin-stabilizing factor	Liver and platelets

*There is no factor VI

*Sequence indicates the order of discovery

2.3 Coagulation Cascade

The coagulation cascade involved the sequence of events that initiates with vascular injury. Normally blood retained the liquid phase as long as it is inside the vessels. Once the vessel damage and blood starts to leak from it, coagulation pathway initiates and proceed through the interaction of platelet with different coagulation factors that ultimately results in a stable clot formation and seal the damaged vessel. Occasionally, the clot formation occurs in an undamaged blood vessels and lead to a pathological condition called thrombosis. The damage in blood vessel leads to different pathways such as activation of platelets, extrinsic pathways, and intrinsic pathway. Platelet activation leads to its shape change, degranulation, and formation of platelet plug at the injured site.

The extrinsic pathway is initiated with the release of tissue factor (or thromboplastin) from the subendothelium tissue of damaged blood vessel. Tissue factor acquires the mixture of lipoproteins and phospholipids, the release of which activates the factor VII and form the complex of TF-VIIa that further converts the factor IX, X into IXa and Xa in the presence of Ca^{2+} ions.

In contrast to extrinsic pathways, intrinsic pathways initiated with factor XII. After activation of factor XII, it is converted into two forms named as α -XIIa and β -XIIa [22]. These converted forms transform the pre-kallikrein to kallikrein that further serves as a factor to activate more factor XII, and elevate the level of XIIa. Factor XIIa followed the sequence and converted the factor XI into XIa. XIa further activates the factor IX and converts the IX into IXa. At this stage, the extrinsic and intrinsic pathways converge and follow a common pathway that activates the prothrombinase, which convert prothrombin into thrombin and ultimately catalyze the formation of insoluble fibrin from soluble fibrinogen. This insoluble fibrin along with platelets forms a complex mesh-like structure that named as 'clot' (Fig. 1).

3 Carbon-Based Nanomaterials

Carbon-based nanomaterials (CBNs) are made of pure carbon with extraordinary properties such as thermal conductivity, longer stability, higher optical and mechanical properties with environment friendliness. Although CBNs have been exploited in electronics and mechanics, the unique properties of CBNs also make them favorable to be used in a biological system. Due to high surface area, ease of surface functionalization and lower toxicity as compared to other nano-scale materials, CBNs are used as nanocarriers for cancer therapy, gene delivery, tissue engineering, drug delivery, probes for biosensors and imaging. Hence, CBNs have captivated huge demand for their manufacturing and research. Nano carbons can be classified as either sp^2 or sp^3 carbon nanomaterials. Depending on their configuration and structure, CBNs are of different types such as carbon nanotubes, graphene nanoparticles, nanodiamonds,

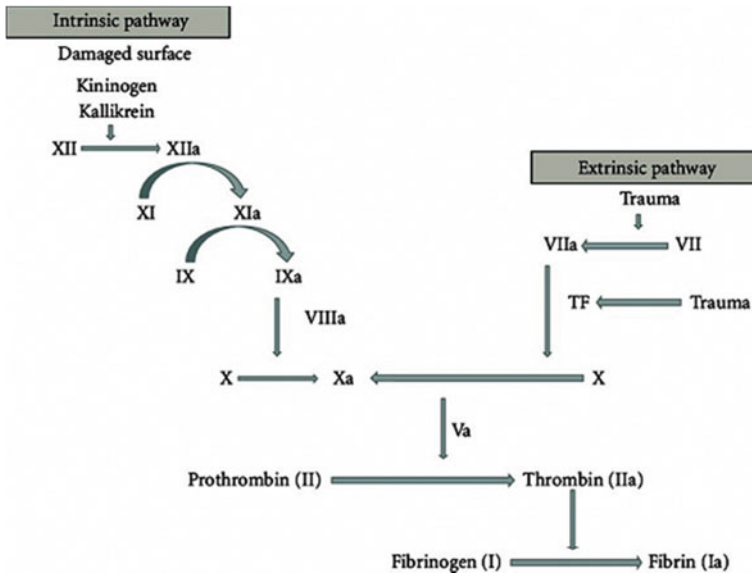


Fig. 1 Schematic representation of blood coagulation cascade reproduced from (“Factor V Leiden and InflammationThrombosis” 2012) reproduced with permission from hindawi [23]

quantum carbon dots (C-Dots), fullerene (C60), and carbon black nanoparticles (CB) [24] (Fig. 2).

3.1 Carbon Nanotubes

CNTs possess high mechanical strength, optoelectronic properties and can also be tuned for different diameter, length, surface functionalization, single-walled or multi-walled, and chirality. [24]. Due to these tunable physical properties, CNTs can be designed in various manners suitable for industrial and biomedical applications. Fortifying military vests, faster electric conductivity, carrying more hydrogen fuel cells, nanosensors in imaging technologies, and nanocarrier for drug and gene delivery in biological systems are some of the practical applications of CNTs. CNTs are the coaxial tubes of graphite sheets of size 2–50 nm. These tubes comprise of hexagonal sp^2 carbon atoms arranged in a helical fashion. They can be single-walled (SWCNTs) with 1–2 nm diameter or multi-walled (MWCNTs) between 10 and 100 nm diameters depending on their synthesis methods. Currently, there are three methods for the synthesis of CNTs. Laser ablation, arc discharge evaporation method, and chemical vapor deposition of which the latter two are most widely used.

CNTs tend to agglomerate as a result of high surface energy and the strong pi-pi interactions among the nanotubes [26]. In this state, CNTs have weak dispersibility and are insoluble in solvents and matrix, which limits their practical applications

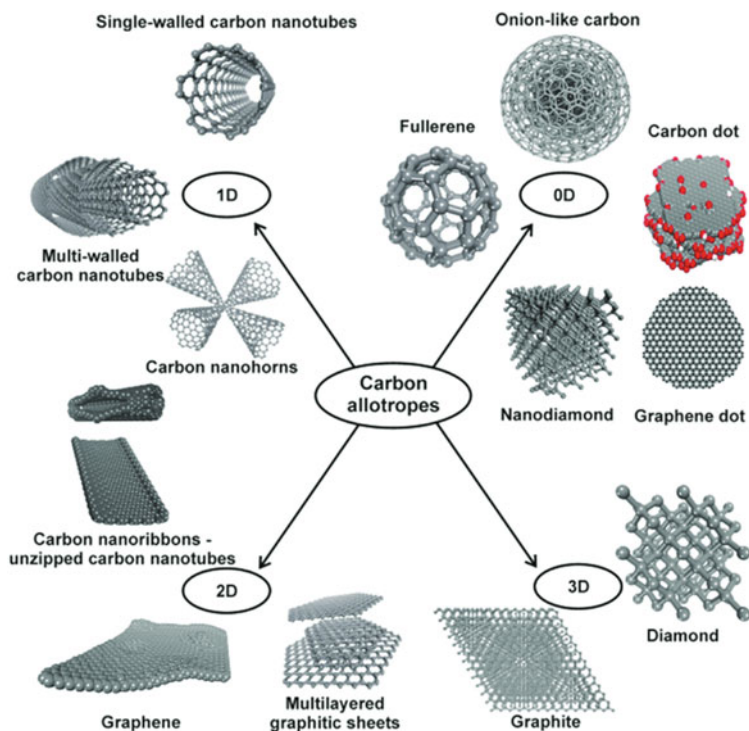


Fig. 2 Different types of carbon-based nanomaterials. Reprinted and adapted from (Georgakilas et al. (2015) <https://pubs.acs.org/doi/10.1021/cr500304f>) copyright© ACS [25]

[9]. Various mechanical and chemical modification techniques have been made to overcome this drawback. Mechanical techniques, namely ultra-sonication, high shear mixing, and grinding, are used to separate nanotube from each other [26]. But these methods are time-consuming and can break nanotubes. Chemical modification on the surface of CNTs alter their surface energy, improves their adhesion or wetting characteristics, and increase dispersion stability. Chemical modifications can be done by either non-covalently or covalently. The non-covalent modification involves surfactants or wrapping with polymers. Covalent functionalization changes the electronic and transport properties of CNTs by changing their translational symmetry. Covalent modification of CNTs can be further categorized into direct covalent sidewall functionalization and indirect chemical modifications [26].

3.2 Graphene

Graphene shows unique properties such as high surface area, low density, tunable electronic band gap, store large amount of charge comparable to conventional Li-ion storage devices, high mechanical strength, high aspect ratio, and high thermal conductivity. In biomedical applications, graphene is used in its oxide form, which has several advantages over pure graphene, including higher solubility [27] hydrophilic functional groups and structural heterogeneity. Graphene oxide (GO) have important applications in transparent conductive films, polymer composite, solar cell manufacturing, biomedicine, fabricating nanoelectronic devices, energy storage devices, biosensors, catalysis, and transparent electrodes. Graphene is the thinnest material consists of sheets of sp^2 carbon atoms in a lattice-like structure.

Carbon, oxygen, and hydrogen are the three main components of GO. Several possible GO structures have been proposed. The most popular Lerf–Klinowski model shows the edge of the GO sheet is hydrophilic which majorly consists of carboxyl and carbonyl groups while the basal plane is hydrophobic and has hydroxyls and epoxides as major groups. There are two distinct regions at the GO plane, one is lightly functionalized sp^2 hybridized carbons and the second region consists of mainly sp^3 carbons [28]. The oxidation and exfoliation of graphite produce GO.

3.3 Nanodiamonds

Nanodiamonds (NDs), have unique properties such as very high stiffness, high thermal conductivity, and are more compatible to biological tissue than other nanocarbons which makes them favorable nanomaterial for industrial manufacturing, biomedical engineering [29].

NDs are made up of tetrahedral sp^3 carbon. They are smaller than 10 nm and commonly manufactured from graphite through the process of detonation. NDs are biocompatible and possess fluorescence and photoluminescence properties like bulk diamond. Conjugated NDs with polyethyleneimine (PEI) are highly effective gene carriers without cytotoxicity of PEI alone [24].

NDs are produced by detonation method. Each ND particle has a diameter of 5 nm. The surface of an ND particle is rich in functional groups with an inert diamond core at the centre. Various wet and gas chemistry methods are utilized on the surface of the ND particles to functionalize them for specific purposes such as in microelectronic devices, cardiovascular devices, and the biomolecular attachment for drug delivery. Lien et al. used fluorescent and magnetic NDs for cell labeling [30].

3.4 Other Carbon-Based Nanomaterials

3.4.1 Fullerene

Fullerenes, C-Dots are some of the less-studied CBNs among others. In addition to various industrial applications (e.g., cosmetics and sports goods), fullerene and its water-soluble derivatives are being exploited for their role in drug delivery, anti-cancer as well as immunomodulatory effects. The Buckminsterfullerene (C₆₀) and its derivatives have been recently explored for their role in pharmacological effects. They are 0.7 nm in diameter and carries 20 six-membered and 12 five-membered rings resembling a soccer ball hence “buckyball.” The density of buckminsterfullerene is very low (1.68 g/cm³) and they are nonconductive as compared to graphite [31].

Fullerenes may be found in natural materials which have been affected by high-energy conditions such as lightning, geological changes, and meteorite striking regions [32]. Traditionally fullerenes were synthesized through condensation of soot generated from vaporization of graphite [33]. The most widely used synthesis method is based on the Krätschmer-Huffman method. In a high-pressure helium environment, an electric arc is produced from graphite electrodes. The carbon soot obtained is dissolved in a non-polar solvent which is dried to obtain C₆₀ and C₇₀ fullerenes [32].

For biomedical applications fullerenes have been functionalized in a variety of methods. Polyhydroxylated fullerenes, also known as “fulleronols,” have antioxidant properties due to their free radical scavenging ability. Fullerene containing amino acids modulate enzyme functions. The lipid membrane incorporates fullerene (LMIC), serum albumen complexed fullerene, PEGylated fullerene, sugar-based polymer encapsulation of fullerene are some of the other methods used to functionalize fullerenes for biomedical applications [34].

3.4.2 Carbon Quantum Dots (CDs)

Carbon Quantum Dots (CDs) possess various properties such as low toxicity, easy to synthesize, good optical properties, and stable in an aqueous environment. These unique properties have allowed CDs to be used in bio applications such as biosensor, drug delivery, catalysis, bioimaging, and therapeutic developments. CDs are fluorescent quasi-spherical, zero-dimensional nanomaterial having a diameter less than 10 nm. There are two methods top-down and bottom-up from which CDs are synthesized [35].

The top-down approach involves the breakdown of carbon through laser ablation [36], arc discharge, electrochemical exfoliation, and oxidative acid treatment [37]. In the bottom-up method, CDs are produced through the process of carbonization [38].

Surface functionalization of CDs can be done with covalent bonding. Amine-containing agents are covalently added to increase the photoluminescence of CDs.

Similarly, functionalization can also be done using Pi-Pi interactions and sol-gel techniques [39].

3.4.3 Carbon Black (CB)

CBs are thermal stable, good electric conductivity, high strength, and surface chemistry can be modified to make it suitable for various bioapplications. CBs contain sp^2 carbon atoms arranged in a grape-like cluster. There are several methods used to produce carbon black but the Furnace Black method is widely used. The particle size ranges from 13 to 95 nm. The surface of CBs contain oxygen atoms attached to acidic or basic functional groups, hydrogen at the edge of the carbon layer and nitrogen atoms are present in the aromatic layer system. Applications for carbon black nanopowder include optoelectronics, rubber manufacturing, conductive material, pigmentation, and bio-sensors.

It has been recently reported that CB nanoparticles induce apoptosis through mitochondrial-dependent intrinsic pathway resulting in caspase activation and DNA fragmentation [40].

4 Interaction of Carbon-Based Nanomaterials and Blood Coagulation System

As previously described, CBNs have biomedical importance so the intravenous administration of CBNs for therapeutics purpose, makes them first encounter with blood. This immediate encounter triggers a cascade of events in the blood vascular system such as biocorona formation, platelet activation, thrombosis, complement activation, and haemolysis. The adsorption of biomolecules such as peptides or proteins, nucleic acids, lipids, metabolites, and others onto the surface of the injected nanomaterials results in the formation of a biomolecular corona (BC) [28]. BC formation is often driven by electrostatic attraction, change of biomolecular conformation due to entropy shifts, and hydrophobicity between the biomolecules and nanomaterials. BC on nanoparticles effectively influence their bio-persistence, biodistribution, cellular uptake, cellular response, and clearance [41].

The encounter of CBNs with blood also modifies the components of the coagulation system such as platelet and coagulation proteins and induces the formation of thrombus.

4.1 Effect of Carbon-Based Nanomaterials on Platelet Functions

Platelet cells are one of the vital components in thrombosis or blood clotting. Interaction of most of the CBNs with platelets resulted in the activation of the platelet. CBNs also modifies other platelet function such as platelet adhesion and aggregation.

4.1.1 Platelet Activation

One of the earliest and reliable methods to detect the in-vitro platelet activation is to determine the expression of CD62P [42]. Interaction of CBNs with platelets resulted in the platelet activation via glycoprotein (GP) integrin receptor GP IIb/IIIa. Previous studies depicted that the particle size plays an essential role in determining the receptor-mediated signaling pathways such as protein kinase C (PKC) is activated by micro-sized particles whereas nano-size materials trigger the integrin receptor without PKC [43].

Carbon nanotubes (SWCNTs, MWCNTs) induces the activation of platelets [19, 44, 45] and also shown increased thrombogenicity in animal models [43, 46]. Platelet activation by CNTs occurs via increased expression of CD62P and open confirmation of glycoprotein IIb/IIIa [46] in 2010 also confirmed the activation of platelets via CNTs. MWCNTs also induces platelets to generate microparticles that further provide stimulation for the activation of other platelets [47], A [48]. MWCNTs enhanced the concentration of intracellular Ca^{2+} ions through its perforation nature, confirmed by electron microscopy [19, 45]. The CNTs could also act as toxic, so to reduce this toxicity and increase their dispersibility, different functional groups attached to the CNTs [49]. SWCNTs modified with different groups such as CONH₂-SWCNT, COOH-SWCNT, OH-SWCNT, and PEG-CNT. Among them, PEG-SWCNTs act as the most effective to activate the platelets, whereas the OH-SWCNTs does not display any significant impact on platelets. Graphene is another CBNs which have the potential to stimulate the platelets for its activation.

Pristine as well as functionalized graphene, both reported to have the possibility for platelet activation, but hydrophobic functionalized graphene (f-G) has more impact on inducing CD62P expression as compared to pristine graphene (p-G). The studies of Singh et al. elucidated that GO induces an integrin RIIbb3-mediated clumping response in human platelets and could also trigger pulmonary thromboembolism in mice. To reduce the toxicity, amine-modified graphene (GO-NH₂) developed, which was better with its biocompatibility and did not activate pulmonary thromboembolism nor any deteriorating effects on human platelets. Another modified form of graphene, i.e., nanoribbons (O-GNR) and amphiphilic polymer PEG-DSPE coated graphene nanoribbon (O-GNR-PEG-DSPE), also examined for its impact on platelet activation via the determination of platelet factor 4 through ELISA test [50]. No significant change was found in the PF4 level in these two graphene-modified forms, indicating no impact on platelet activation.

Among the CBNs, NDs also showed its impact on platelet activation. Like CNTs, they also increased the level of intracellular Ca^{2+} ions, which led to the change in morphology of platelet and its viability. The morphological changes were elucidated by electron microscopy, whereas the reduced platelet viability was confirmed with MTT assay. The results from electron microscopy revealed the spherical shape of normal platelets, and filopodial extension of NDs treated platelets. Elevated ROS levels were also reported to be in NDs treated platelets. Kumari et al. observed the significant platelet activation from carboxylated NDs (cNDs). It was reported that even the small concentration like $1 \mu\text{g/ml}$ of cNDs (4–10 nm in size) could stimulate the platelet activation. Furthermore, during intravenously injected in mice, they had shown to cause the immense pulmonary thromboembolism [51].

Other CBNs such as carbon dots (CDs) interaction with platelets also resulted in increased expression of CD62P, but only at low concentration. At high concentration such as 1 mg/ml , no significant difference was found between test and negative control, which implies the dual nature of carbon dots, i.e., platelet activator and cytotoxicity. The former was due to the presence of hydrophobic structure in CDs that enhance the platelet activation whereas latter, i.e., cytotoxicity caused by disturbed platelet membrane structure. High dosage such as 50 mg/kg did not show any impairment in the blood coagulation function of mice [37].

4.1.2 Platelet Aggregation

Along with platelet activation function, CBNs have also shown their impact on platelet aggregation. CBNs tend to aggregate the platelets via matrix metalloproteinase-dependent pathway [43]. Carbon nanotubes such as SWCNT, MWCNT, mixed carbon nanoparticles (MCNs), and urban particulate matter (SRM1648) were investigated to elucidate their potential in platelet aggregation and were found to follow the series $\text{MCN} > \text{SWCNT} > \text{MWCNT} > \text{SRM1648}$. MCN depicted the strongest capability for platelet aggregation, whereas SRM1648 to be the weakest [52]. Treatment of platelets with MCN led to the release of granular contents such as ATP, P-selectin that eventually results in platelet aggregation. Functionalized CBNs such as PEG-SWCNTs prove to be the most effective for platelet activation as well as aggregation. Among the various CNTs modification as described in the previous section, PE Gylation found to be the best in the context of reduced toxicity and increased pharmacokinetics [53, 54].

Carbon nanodiamond shave also evoked the platelet aggregation in a significant manner. Kumari et al. reported the aggregation of platelets increased in the presence of nanodiamonds. The study was carried out via platelet aggregometer [51].

Graphene oxide also acts in the aggregation of platelets via the release of intracellular Ca^{2+} ions from the dense tubular system and activation of Src kinases whereas reduced GO demonstrated less effect on platelets, could be due to reduced charge density on the surface of grapheme [55].

Other clinically important CBNs such as fullerene (C60) nanocomposites also studied for its effect on platelet aggregation. The solution of C60 in polyvinylpyrrolidone did not show any effect on platelet aggregation, whereas C60 in crown ether and twin-80 solutions inhibited the ADP-stimulated platelet aggregation by 20–30% [56].

4.1.3 Platelet Adhesion

CBNs also responsible for the platelet adhesion but the mechanism lies behind is still poorly understood and more studies required in this context (Fig. 3).

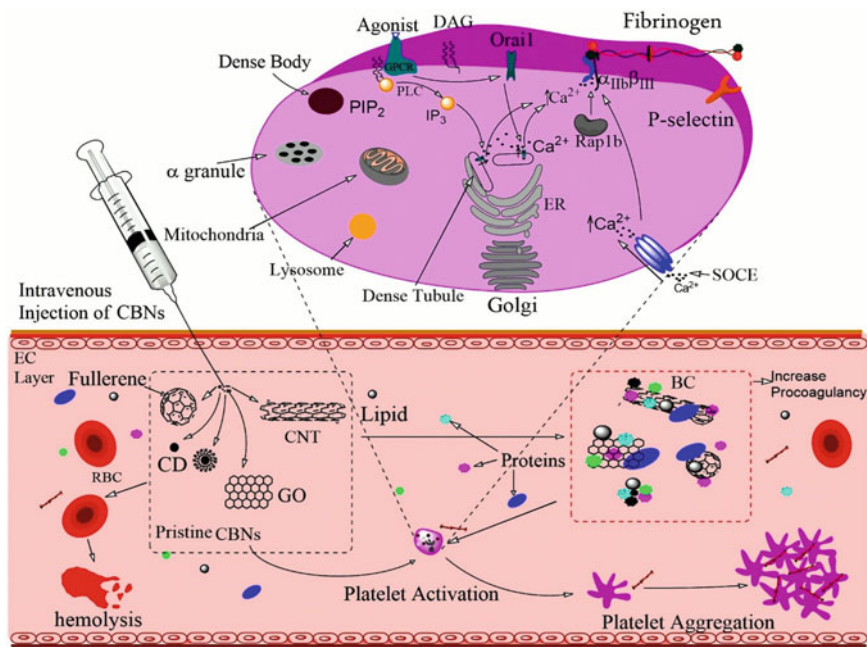


Fig. 3 Schematic representation of carbon-based nanomaterial's interaction with blood components. The formation of biocorona on the surface of injected nanoparticles activates a cascade of events resulting in platelet activation and aggregation, RBC lysis and increased procoagulancy. The events leading to increase in the intra cellular Ca²⁺ of platelet leading to its activation has been depicted (**DAG**—diacylglycerol; **PIP2**—phosphatidylinositol 4,5-bisphosphate; **PLC**—phospholipase C; **IP3**—inositol trisphosphate; **SOCE**—store-operated calcium entry; **ER**—endoplasmic reticulum; **EC**—endothelial cell; **CD**—carbon quantum dot; **CNT**—carbon nanotube; **GO**—graphene oxide; **CBNs**—carbon-based nanomaterials; **BC**—biocorona; **RBC**—red blood corpuscle)

4.2 Coagulation Proteins—Carbon-Based Nanomaterials Interaction

Along with platelet function, CBNs also elicited its impact in other coagulation machinery such as coagulation proteins. Interaction of CBNs with platelets resulted in thrombin generation that stimulated the intrinsic pathway of the blood coagulation system. This interaction also induced the inflammatory response with the release of TNF- α , IL-1 β , IL-8.

Binding of MWCNTs with platelets resulted in up-regulation of IXa enzymatic activity, which played a significant role in intrinsic coagulation cascade [57]. Carbon nanotubes affect coagulation pathways with varied results. The effect of four different lengths MWCNTs was elucidated and were found that fibrin formation was induced by all of them but the effect on clot strength was different such as long-chain CNT-NH₂ resulted in increased clot hardness whereas long-chain CNT-COOH and short-chain CNT-NH₂ outcome in softer clots [58]. The effect of CNTs could be altered due to protein-corona formation such as bare COOH-CNT impact the increased platelet aggregation with the release of PMPs whereas coronated CNT-COOH with fibrinogen and albumin diminished these effects and IgG and Histone-1 (H-1) coated CNT-COOH resulted in fragmentation of platelets and possibly released PMPs. Vakhrusheva et al., demonstrated that reduced thrombogenic potential of SWCNT coronated with albumin [59].

The interaction of NDs with intrinsic and extrinsic pathways resulted that even at high concentrations, no effect was found. This was established via APTT and PT tests [60].

Another CBNs i.e. carbon dots (CDs) interact with fibrinogen and responsible for its quenching that could be due to change in hydrophobic to hydrophilic microenvironment around tryptophan residues but CDs showed least effect on the secondary structure of fibrinogen. The APTT and PT examination of CDs demonstrated that at low concentration (0.1 mg/ml), no interference with intrinsic and extrinsic pathways was exhibited, but strong anticoagulant nature was observed at the concentration of 1 mg/ml [37].

5 Sophisticated Techniques to Characterize Carbon-Based Nanomaterials—Blood Coagulation System Interaction

Several techniques were employed to characterize the interaction between CBNs and the blood coagulation system. Among them, flow cytometry, electron microscopy, and platelet aggregometry are the sophisticated techniques to study the interaction in great detail.

5.1 Flow Cytometry

Flow cytometry is a laser-based technology, which is used to study the characteristics of cells such as count, size, and complexity. It measures the fluorescence intensity developed from fluorescently labeled antibodies that bind with specific protein or marker present on cells. Using this technique, one can study the CBNs-coagulation interaction. In 2011, Singh et al. studied the interaction of GO with platelet function such as activation and secretion with flow cytometer [55]. Platelet activation resulted in degranulation such as alpha granule's release, which was measured by CD62P expression using a fluorescent labeled antibody. Similarly, platelet aggregation occurred via the interaction of soluble fibrinogen with an open conformation of α IIb β 3, which was measured by using PAC1 antibody as PAC1 binds with α IIb β 3. Larger binding with fluorescently labeled antibodies implies higher platelet activation and aggregation. Furthermore, the physical interaction of GO with platelets was also studied via flow cytometer by measuring Side Scatter (SSC). Co-incubation of GO with APC-anti CD41 labeled platelets resulted in a major shift of events to the upper right quadrant of dot plot, suggestive of physical interaction of GO sheet with platelets while the remaining GO that does not shift represents the free GO sheets [55]. So, flow cytometry is also a technique that can be used to deduce that if NPs are physically involved in the binding with cells or they remain in their colloid form and does not show any physical interaction. Fent et al. also characterized the activation and secretion of platelets by surface-modified SWCNTs via flow cytometer [61].

Flow cytometry could also be utilized to study the carbon or other nanomaterial interaction with different cells type to further acknowledge this field. In 2013, Roggers et al., analyzed the magnitude of Mesoporous silica nanoparticle (MSN) and RBC interaction by flow cytometry [62]. In 2018, Njoroge et al. reported the flow cytometric assay to study the internalization of AgNP within the murine macrophage cell line RAW264.7 [63].

5.2 Electron Microscopy

Electron microscopy is a high-resolution image obtaining technique which uses a high-velocity electron beam as a source of illumination that passes through electromagnetic lenses to produce a magnified image. The most common electron microscopes are Transmission electron microscope (TEM) and Scanning electron microscope (SEM). TEM is used to study the ultrathin sections of cells or tissues as electron beam transmitted through the specimen whereas SEM is used to produce the surface image of the specimen as a result of electron deflection from specimen's outer surface.

Kumari et al., showing the presence of localized granules in resending platelets, as well as scattered granules in NDs, treated platelets via electron microscopy [51]. Lacerda et al. used the electron microscopy for the illustration of the ultrastructure

of resting platelets and pristine MWCNTs (M60) treated platelets and revealed internalization of M60, the filopodial extension of platelets, and release of microvesicles from it [19].

5.3 Platelet Aggregometry

Platelet aggregometry is based on a light transmission principle. It is used to study the platelet aggregation induced by various agonist. Whole blood or PRP added to the cuvette at 37 °C and this cuvette placed between the light path and photocell. After addition of agonist, platelets start aggregating, hence the absorption of light decreases whereas the transmission of light increases, detected by a photocell. Singh et al. illustrated the effect of GO on the aggregation of platelets via aggregometer. Addition of GO to the freshly isolated human platelets induced its aggregation in a concentration-dependent manner. It was found that 2 µg/ml GO induced even stronger aggregation than with 1 U/ml thrombin. Fent and colleagues reported the effect of surface-modified SWCNTs on platelet aggregation and found that the carboxylated, pegylated and pristine SWCNTs induce the aggregation of platelets [61]. Vaschenko et al. also demonstrated the impact of fullerene (C60) via aggregometer and found that no effect of C60 in polyvinyl pyrrolidone solution on platelet aggregation whereas C60 in crown ether and Twin-80 solution inhibited ADP-induced platelet aggregation to an extent of 20–30% [56].

6 Summary, Limitations, and Future Perspectives

In summary, carbon-based nanomaterial exist in different allotropic forms such as carbon nanotubes, graphene, nanodiamonds and others. Due to their distinctive properties from its bulk form, they exert its importance in various biomedical applications like bio-imaging, bio-sensing, targeted drug delivery, etc. CBNs administered intravenously for diagnostics and therapeutics purpose first encounters blood fluid system. The blood comprises formed elements and blood plasma. Formed elements include RBC, WBCs, and platelets whereas plasma comprise of the proteins, hormones, electrolytes, etc. The blood plasma proteins includes the blood clotting factor which along with platelets facilitate the coagulation cascade upon injury. In blood, CBNs interacts with these coagulation components and modifies their functions. Encounter of CBNs with platelets induces its activation, aggregation and adhesion properties whereas while interacting with coagulation cascade they mostly affect the intrinsic coagulation pathway and does not show much impact on extrinsic pathways of coagulation. To study the impact of CBNs on blood coagulation system, various sophisticated techniques employed such as flow cytometer used to measure the activation and secretion of platelets as well as physical interaction of NPs with platelets. Electron

microscopy is used to study the ultrastructure of platelets, before and after treatment with CBNs whereas aggregometer is used for the platelet aggregation studies.

CBNs displayed its biomedical importance via diagnostics and therapeutics purposes. But there are certain factors which, if not taken into consideration, can hinder the nanoparticles function and application such as shape, size, concentration, surface charge, and functionalization. Nanotubes due to its cylindrical shape promote more platelet activation and aggregation whereas spherical shape of fullerene (C60) does not show any impact on it [43]. Similarly, concentration level upto an extent might be non-toxic but after that it can act as toxic to cells. Pristine NPs also imparts its limitations due to activation of compliment and immune system. To reduce this toxicity and increase the dispersibility, functionalization of CBNs required such as PEG-modified CBNs does not act as toxic to cells due to masking the charge present on NPs that reduces the interaction of NPs with cells and can be used for biomedical purpose.

Hence, to further imply the biomedical application of CBNs, more work has to be done with its physical interaction with cells, cytotoxicity, and methods to reduce these toxicological effects to make them more biocompatible and dispersible with increased therapeutic value.

References

1. Chandra, P., Das, D., Abdelwahab, A.A.J.: Biostructures: gold nanoparticles in molecular diagnostics and therapeutics **5**(2) (2010)
2. Chandra, P., Noh, H.-B., Pallela, R., Shim, Y.-B.J.B.: & Bioelectronics. Ultrasensitive detection of drug resistant cancer cells in biological matrixes using an amperometric nanobiosensor **70**, 418–425 (2015)
3. Tiwari, J.N., Tiwari, R.N., Kim, K.S.: Zero-dimensional, one-dimensional, two-dimensional and three-dimensional nanostructured materials for advanced electrochemical energy devices **57**(4), 724–803 (2012)
4. Arole, V., Munde, S.J.: Fabrication of nanomaterials by top-down and bottom-up approaches—an overview **1**, 89–93 (2014)
5. Bharath, G., Madhu, R., Chen, S.-M., Veeramani, V., Balamurugan, A., Mangalaraj, D., Ponpandian, N.J.: Enzymatic electrochemical glucose biosensors by mesoporous 1D hydroxyapatite-on-2D reduced graphene oxide **3**(7), 1360–1370 (2015)
6. Chandra, P., Segal, E.: Nanobiosensors for personalized and onsite biomedical diagnosis. *Inst Eng Technol* (2016)
7. Liu, Z., Tabakman, S., Welsher, K., Dai, H.J.N.: Carbon nanotubes in biology and medicine: in vitro and in vivo detection, imaging and drug delivery **2**(2), 85–120 (2009)
8. Chen, J., Chen, S., Zhao, X., Kuznetsova, L.V., Wong, S.S., Ojima, I.J.: Functionalized single-walled carbon nanotubes as rationally designed vehicles for tumor-targeted drug delivery **130**(49), 16778–16785 (2008)
9. Chen, B.: Surface functionalized carbon nanotubes for biomedical applications. In: *Bio-inspired Nanomaterials and Applications: Nano Detection, Drug/Gene Delivery, Medical Diagnosis and Therapy*, pp. 157–179. World Scientific (2015)
10. Cheon, Y.A., Bae, J.H., Chung, B.G.J.L.: Reduced graphene oxide nanosheet for chemophotothermal therapy **32**(11), 2731–2736 (2016)
11. Meng, H., Leong, W., Leong, K.W., Chen, C., Zhao, Y.J.B.: Walking the line: the fate of nanomaterials at biological barriers **174**, 41–53 (2018)

12. Nel, A.E., Mädler, L., Velegol, D., Xia, T., Hoek, E.M., Somasundaran, P., Thompson, M.J.: Understanding biophysicochemical interactions at the nano–bio interface **8**(7), 543 (2009)
13. Jenne, C., Urrutia, R., Kubes, P.J.I.: Platelets: bridging hemostasis, inflammation, and immunity **35**(3), 254–261 (2013)
14. Machlus, K.R., Italiano, J.E.J.J.C.B.: The incredible journey: from megakaryocyte development to platelet formation **201**(6), 785–796 (2013)
15. Geraldo, R., Sathler, P., Lourenço, A., Saito, M., Cabral, L., Rampelotto, P., Castro, H.C.: Platelets: still a therapeutical target for haemostatic disorders **15**(10), 17901–17919 (2014)
16. Zufferey, A., Fontana, P., Reny, J.L., Nolli, S., Sanchez, J.C.: Platelet proteomics **31**(2), 331–351 (2012)
17. Periyah, M.H., Halim, A.S., Saad, A.Z.M.: Research, s.c.: mechanism action of platelets and crucial blood coagulation pathways in hemostasis **11**(4), 319 (2017)
18. Yadav, V.K., Singh, P.K., Sharma, D., Singh, S.K., Agarwal, V.J.: Molecules, diseases: mechanism underlying N-(3-oxo-dodecanoyl)-L-homoserine lactone mediated intracellular calcium mobilization in human platelets **79**, 102340 (2019)
19. De Paoli Lacerda, S.H., Semberova, J., Holada, K., Simakova, O., Hudson, S.D., Simak, J.J.: Carbon nanotubes activate store-operated calcium entry in human blood platelets **5**(7), 5808–5813 (2011)
20. Tortora, G.J., Derrickson, B.H.: Principles of anatomy and physiology, Wiley (2008)
21. Tortora, G.J., Derrickson B.H.: Principles of anatomy and physiology. Wiley (2018)
22. Revak, S.D., Cochrane, C.G., Griffin, J.H.: The binding and cleavage characteristics of human Hageman factor during contact activation: a comparison of normal plasma with plasmas deficient in factor XI, prekallikrein, or high molecular weight kininogen **59**(6), 1167–1175 (1977)
23. Factor V Leiden and Inflammation Thrombosis. Thrombosis (2012). <https://doi.org/10.1155/2012/594986>
24. Cha, C., Shin, S.R., Annabi, N., Dokmeci, M.R., Khademhosseini, A.J.: Carbon-based nanomaterials: multifunctional materials for biomedical engineering **7**(4), 2891–2897 (2013)
25. Georgakilas, V., Perman, J.A., Tucek, J., Zboril, R.: Broad family of carbon nanoallotropes: classification, chemistry, and applications of fullerenes, carbon dots, nanotubes, graphene, nanodiamonds, and combined superstructures. Chem. Rev. **115**(11), 4744–4822 (2015)
26. Mallakpour, S., Soltanian, S.J.R.A.: Surface functionalization of carbon nanotubes: fabrication and applications **6**(111), 109916–109935 (2016)
27. Smith, A.T., LaChance, A.M., Zeng, S., Liu, B., Sun, L.: Synthesis, properties, and applications of graphene oxide/reduced graphene oxide and their nanocomposites **1**(1), 31–47 (2019)
28. Palmieri, V., Perini, G., De Spirito, M., Papi, M.J.: Graphene oxide touches blood: in vivo interactions of bio-coronated 2D materials **4**(2), 273–290 (2019)
29. Bergonzo, P., Jackman, R.B., Loh, K.P., Swain, G.M., Williams, O.A.: Diamond electronics and biotechnology—fundamentals to applications V. Cambridge University Press: Cambridge, UK (2012)
30. Lien, Z.-Y., Hsu, T.-C., Liu, K.-K., Liao, W.-S., Hwang, K.-C., Chao, J.-I.J.B.: Cancer cell labeling and tracking using fluorescent and magnetic nanodiamond **33**(26), 6172–6185 (2012)
31. Bogdanović, G., Djordjević, A.J.S.A.C.L.: Carbon nanomaterials: Biologically active fullerene derivatives **144**(3–4), 222–231 (2016)
32. Siqueira, J., Oliveira, O.N.: Carbon-based nanomaterials. In: Nanostructures, pp. 233–249. Elsevier (2017)
33. Isaacson, C.W., Kleber, M., Field, J.A.: Technology: quantitative analysis of fullerene nanomaterials in environmental systems: a critical review **43**(17), 6463–6474 (2009)
34. Partha, R., Conyers, J.L.: Biomedical applications of functionalized fullerene-based nanomaterials **4**, 261 (2009)
35. Lategan, K., Fowler, J., Bayati, M., Fidalgo de Cortalezzi, M., Pool, E.J.N.: The effects of carbon dots on immune system biomarkers, using the murine macrophage cell line RAW 264.7 and human whole blood cell cultures **8**(6), 388 (2018)

36. Wang, H.D., Niu, C.H., Yang, Q., Badea, I.J.N.: Study on protein conformation and adsorption behaviors in nanodiamond particle–protein complexes **22**(14), 145703 (2011)
37. Li, S., Guo, Z., Zhang, Y., Xue, W., Liu, Z.J.A.: Interfaces: blood compatibility evaluations of fluorescent carbon dots **7**(34), 19153–19162 (2015)
38. Peng, Z., Han, X., Li, S., Al-Youbi, A.O., Bashammakh, A.S., El-Shahawi, M.S., Leblanc, R.: Carbon dots: biomacromolecule interaction, bioimaging and nanomedicine **343**, 256–277 (2017)
39. Wang, Y., Hu, A.J.: Carbon quantum dots: synthesis, properties and applications **2**(34), 6921–6939 (2014)
40. Boland, S., Hussain, S., Baeza-Squiban, A.: Nanobiotechnology: carbon black and titanium dioxide nanoparticles induce distinct molecular mechanisms of toxicity **6**(6), 641–652 (2014)
41. Shannahan, J.J.: The biocorona: a challenge for the biomedical application of nanoparticles **6**(4), 345–353 (2017)
42. Lu, Q., Malinauskas, R.A.J.: Comparison of two platelet activation markers using flow cytometry after in vitro shear stress exposure of whole human blood **35**(2), 137–144 (2011)
43. Radomski, A., Jurasz, P., Alonso-Escolano, D., Drews, M., Morandi, M., Malinski, T., Radomski, M.W.: Nanoparticle-induced platelet aggregation and vascular thrombosis **146**(6), 882–893 (2005)
44. Guidetti, G.F., Consonni, A., Cipolla, L., Mustarelli, P., Balduini, C., Torti, M.: Biology, medicine: nanoparticles induce platelet activation in vitro through stimulation of canonical signalling pathways **8**(8), 1329–1336 (2012)
45. Semberova, J., De Paoli Lacerda, S.H., Simakova, O., Holada, K., Gelderman, M.P., Simak, J.: Carbon nanotubes activate blood platelets by inducing extracellular Ca²⁺ influx sensitive to calcium entry inhibitors **9**(9), 3312–3317 (2009)
46. Bihari, P., Holzer, M., Praetner, M., Fent, J., Lerchenberger, M., Reichel, C.A., Krombach, F.J.T.: Single-walled carbon nanotubes activate platelets and accelerate thrombus formation in the microcirculation **269**(2–3), 148–154 (2010)
47. Khandoga, A., Stampfl, A., Takenaka, S., Schulz, H., Radykewicz, R., Kreyling, W., Krombach, F.J.C.: Ultrafine particles exert prothrombotic but not inflammatory effects on the hepatic microcirculation in healthy mice in vivo **109**(10), 1320–1325 (2004)
48. Khandoga, A., Stoeger, T., Khandoga, A., Bihari, P., Karg, E., Ettehadieh, D.: Haemostasis: platelet adhesion and fibrinogen deposition in murine microvessels upon inhalation of nanosized carbon particles **8**(7), 1632–1640 (2010)
49. Kunzmann, A., Andersson, B., Thurnherr, T., Krug, H., Scheynius, A., Fadeel, B.J.: Toxicology of engineered nanomaterials: focus on biocompatibility, biodistribution and biodegradation **1810**(3), 361–373 (2011)
50. Chowdhury, S.M., Fang, J., Sitharaman, B.J.: Interaction of graphene nanoribbons with components of the blood vascular system **1**(3) (2015)
51. Kumari, S., Singh, M.K., Singh, S.K., Grácio, J.J., Dash, D.J.N.: Nanodiamonds activate blood platelets and induce thromboembolism **9**(3), 427–440 (2014)
52. Frame, M.D., Dewar, A.M., Mullick Chowdhury, S., Sitharaman, B.J.N.: Vasoactive effects of stable aqueous suspensions of single walled carbon nanotubes in hamsters and mice **8**(8), 867–875 (2014)
53. Bottini, M., Rosato, N., Bottini, N.J.B.: PEG-modified carbon nanotubes in biomedicine: current status and challenges ahead **12**(10), 3381–3393 (2011)
54. Heister, E., Lamprecht, C., Neves, V., Tilmaciu, C., Datas, L., Flahaut, E., Silva, S.R.: Higher dispersion efficacy of functionalized carbon nanotubes in chemical and biological environments **4**(5), 2615–2626 (2010)
55. Singh, S.K., Singh, M.K., Nayak, M.K., Kumari, S., Shrivastava, S., Grácio, J.J., Dash, D.J.: Thrombus inducing property of atomically thin graphene oxide sheets **5**(6), 4987–4996 (2011)
56. Vaschenko, V., Samonin, V., Popov, V., Antonenkova, E., Nikonova, V., Vilyaninov, V.: Medicine: Effects of fullerene C⁶⁰ nanocomposites on human platelet aggregation **152**(5), 624 (2012)

57. Burke, A.R., Singh, R.N., Carroll, D.L., Owen, J.D., Kock, N.D., D'Agostino R. Jr., Torti, S.V.J.B.: Determinants of the thrombogenic potential of multiwalled carbon nanotubes **32**(26), 5970–5978 (2011)
58. Meng, J., Cheng, X., Liu, J., Zhang, W., Li, X., Kong, H., Xu, H.J.P.O.: Effects of long and short carboxylated or laminated multiwalled carbon nanotubes on blood coagulation **7**(7), e38995 (2012)
59. Vakhrusheva, T.V., Gusev, A.A., Gusev, S.A., Vlasova, I.I.: Albumin reduces thrombogenic potential of single-walled carbon nanotubes **221**(2), 137–145 (2013)
60. Mona, J., Kuo, C.-J., Perevedentseva, E., Priezhev, A., Cheng, C.-L.J.D., Materials, R.: Adsorption of human blood plasma on nanodiamond and its influence on activated partial thromboplastin time **39**, 73–77 (2013)
61. Fent, J., Bihari, P., Vippola, M., Sarlin, E., Lakatos, S.J.T.: In vitro platelet activation, aggregation and platelet–granulocyte complex formation induced by surface modified single-walled carbon nanotubes **29**(5), 1132–1139 (2015)
62. Roggers, R., Kanvinde, S., Boonsith, S., Oupický, D.J.A.P.: The practicality of mesoporous silica nanoparticles as drug delivery devices and progress toward this goal **15**(5), 1163–1171 (2014)
63. Njoroge, J.M., Yourick, J.J., Principato, M.A.: A flow cytometric analysis of macrophage–nanoparticle interactions in vitro: induction of altered Toll-like receptor expression **13**, 8365 (2018)

Chapter 13

Opportunities and Challenges in Medical Robotic Device Development



Neha Khatri , Mukesh Kumar , and Ranjan Jha 

1 Introduction

The world and its biodiversity are changing at a faster pace due to unprecedented surge in industrialization, rapid economic development and the growing needs of the mankind to meet its unending desire. Though such activities are still considered as an advancement in the quality of life and betterment of mankind, it cannot be denied that all of this has negatively affected the global climate including water and air quality as well as the overall health of most of its inhabitants. With changing lifestyle and related behavioral pattern, the mankind is constantly threatened by newer diseases and pandemics. Though human race has managed to control and limit the spread of some of these diseases earlier like in the case of Flu, Polio, Leprosy, Measles, Mumps, Rubella and Guinea worm, etc., some of the newer ones like Ebola and SARS including the COVID-19 viruses has exposed the limitations of healthcare systems and challenges in dealing with such diseases. The situation becomes further challenging in developing countries and nations with low-resource settings. Consequently, development of medical devices is now required to be more affordable but with higher accuracy and precision. With some of the contagious diseases, it has also become essential to innovate medical devices and tools for remote diagnostics and minimally invasive surgical procedures.

Medical devices play a significant role in the delivery of many health care services [1]. Broadly, medical devices are basically used for the diagnosis, cure, mitigation,

N. Khatri (✉) · M. Kumar

Department of Optical Devices and Systems, CSIR-CSIO, Sector 30 C, Chandigarh 160030, India
e-mail: nehakhatri@csio.res.in

R. Jha

Department of Biomedical Instrumentation, CSIR-CSIO, Sector 30 C, Chandigarh 160030, India

N. Khatri · M. Kumar · R. Jha

Academy of Scientific and Innovative Research (AcSIR), Ghaziabad 201002, India

treatment or prevention of disease and are not absorbed or metabolized by the body. Such devices range from common medical supplies such as latex gloves and syringes to advanced imaging equipment and implantable devices such as cardiac defibrillators. The development of new medical devices is essential as it can improve the ability to diagnose and treat illness [2, 3]. The future of medical device faces a new world that is full of opportunities, however, many uncertainties lie ahead as well with emerging of new standards and regulations, evolving of health care dynamics with increasingly competitive scenario. The emerging trends in medical device development are shown in Fig. 1. Globally, the manufacturing of medical devices is shifting from transaction-based approach to an approach that focuses on creating value for the patients and practitioners by providing the surgical instruments and the medical tools that are highly innovative and cost-effective.

Over the last few decades, General Surgery has evolved toward using Minimally Invasive Surgery (MIS) than the conventional larger open incisions for various medical procedures. It allows the surgeons to make few small incisions in the patient, rather than making one large incision for access. The incline toward minimally invasive or when possible, non-invasive procedures is greatly because of the patient benefits that come with it such as reduced post-operative pain and faster recovery. With the incisions and access ports becoming lesser and smaller, inclusion of robotics

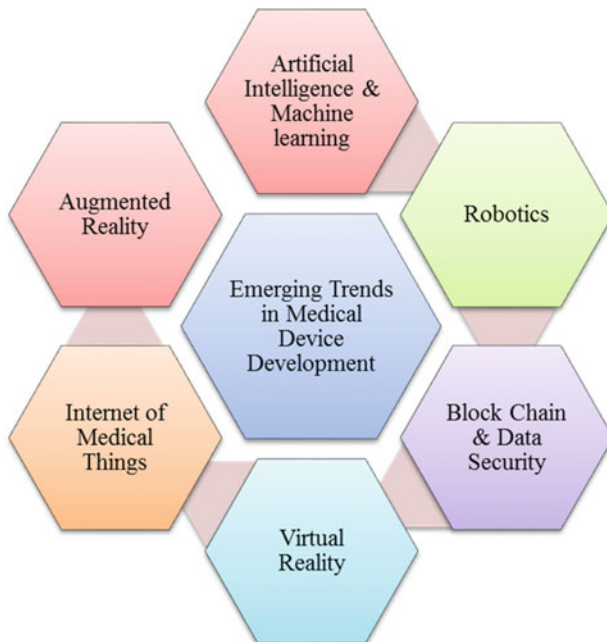


Fig. 1 Emerging trends in medical device development. The revolution in the emerging applications of medical devices with artificial intelligence, machine learning, medical Internet of things have unlocked the promising possibilities in health care technologies

into surgical procedures was initiated. Thus, the development of a series of robotic manipulators to assist the surgeon with medical interventions started [4].

Robotic surgical systems have successfully provided several key advantages over standard minimal access surgery, there are a number of challenges that have prevented this technology from reaching its full potential. Foremost among these is the loss of force feedback (haptics) [5]. Another significant challenge of robotic technology is the extremely high (and recurring) cost of instruments and maintenance. Lastly, the robotic systems are large and bulky and have complex, time-consuming setup, which requires additional specialized training for the entire operating room team.

Artificial intelligence (AI) and machine learning coupled with advancements in electro-mechanical systems have provided a paradigm shift in medical device development through deployment of robotic tools, intelligent patient carts, remote diagnostics and consultation and other automated patient monitoring devices. This chapter mainly focuses on AI-powered and software-driven medical devices and associated research opportunities and challenges in those domains.

2 Opportunities in Medical Device Development

Over the last decade, the medical device manufacturing industry has shifted its focus on developing simple, intuitive and intelligent assistive and therapeutic devices with a faster deployment and commercialization modalities. As a result, software-driven medical devices have emerged as a major thrust area for delivering smart medical solutions for the masses. Starting from wearable health monitoring devices to more sophisticated imaging and surgical medical tools to contact tracing apps, the power of software-driven medical devices has started to touch every aspect of healthcare infrastructure and is expected to remain a key area for times to come [6, 7]. Similarly, surgical robots have recently gained much importance for offering more secure, flexible and efficient manipulators for various complex medical procedures and they provide accuracy levels which are mostly beyond human capability. A description of such fascinating trends in medical device development is presented in this section.

2.1 Software-Driven Medical Devices

Software is becoming increasingly essential as well as pervasive in today's healthcare system. With increasing availability of technology platforms such as smartphones, tablets, laptops, and network servers and with increasing ease of access with the help of Internet and cloud, software tools customized for medical applications are widely used in today's healthcare system. Such software-driven and easy to access medical devices primarily encourages healthy lifestyle and promotes digital healthcare system. Nowadays, most life-saving medical devices function using some kind of embedded software for processing of acquired data or for performing a certain

assigned assistive task. Such devices include life sustaining implantable pacemakers to life support devices like infusion pumps, defibrillators and insulin pumps [8]. Many of these software tools interface with other hardware equipment or connect to hospital's information system, thus demanding a higher computational efficiency which eventually pose development challenges for the designers and manufacturers.

As all these devices are directly related to a patient's safety, developing regulatory framework for such software leading to safe commercialization is another opportunity for medico-legal professionals and certification agencies [9, 10]. In most of the countries, medical devices undergo rigorous scrutiny before they are launched into the market. Such scrutiny is essential to have assurance and confidence that the product is safe and fit for its purpose [8]. To define the role and interaction of a software with hardware or in stand-alone mode, Software-Driven Medical Devices (SDMD) have been classified as "Software as a Medical devices" (SaMD) and "Software in Medical devices" (SiMD) depending on whether the software operates on stand-alone mode without needing any hardware or it is used in conjunction with a hardware to improve and support the hardware's functionality respectively [11, 12]. Some examples of SaMDs are the mobile applications installed onto a smartphone such as smartphone-enabled arrhythmia detector, calorie counter, and drug dose reminder as well as all the mobile-enabled fitness trackers also fall under the category of SaMD as the functionality and features of these software codes are not directly related to the operation of the parent hardware system like the smartphone in this case. Similarly, all the computer and mobile applications that maintain and transfer electronic patient care data to the physician come under SaMD category. This includes sending scheduled electronic patient charts to a designated doctor to relaying results of CT scans of the patient from the equipment to the monitor of an observing physician. On the other hand, example of SiMD includes that of a software which controls the motors of an infusion pump or which encrypts the radiation data to digital image form for a CT scanner [13].

2.2 Surgical Robots and Minimally Invasive Surgery (MIS)

An operation technique, Minimally Invasive Surgery (MIS), was established in the 1980s. The surgeon works with long instruments through small incisions without any direct access to the operation field, thereby differentiating it from the open surgery. Usually, four small incisions are made: two for the surgical instrument, one for laparoscope (rigid endoscope) and one for insufflating CO₂.

Laparoscopic Surgery

During the late 1980s, breakthroughs in technology brought about an increased development in MIS. This resulted in a shift from traditional open surgeries to laparoscopic procedures. As instrumentation improved, the number of different laparoscopic procedures expanded. Nearly every general procedure previously performed by traditional methods has been performed using laparoscopic techniques. Although more

difficult than open surgery, laparoscopic surgery has demonstrated multiple patient benefits. The opportunity in this area still lies in further reducing the invasiveness of surgical procedure by limiting the number and size incisions [14, 15].

Minimally Invasive Robotic Surgery (MIRS)

To overcome the disadvantages of the manual MIS, MIRS plays an important role. MIRS systems help the surgeon to overcome barriers such as the patient's chest or abdomen, which separate him from the operating area. The distance between the surgeon and patient is overcome even if they are located in different rooms or hospitals. MIRS system is divided into three parts according to physical components of a system: Slave, Master and communication between slave and master. Slave system consists of several sub-systems. The minimally invasive instruments should be very small having diameter less than 10 mm to reduce pain and trauma. To have full manipulability inside the body the instruments should have addition 2° of Freedom (DoF) [5]. The tactile information along with the force should be measurable thereby providing information to the surgeon in order to increase the quality of immersion and for more intelligent control laws for surgical robots. The instruments should be lightweight so that they can be handled by single person in the emergency situation when a person needs to be operated without access to the robotic instruments. The master system has to provide high quality feedback, both in terms of tactile and kinesthetic. The tactile would help the surgeon to find the invisible structures such as blood vessels under the muscles by feeling the palpations whereas the kinesthetic lets the surgeon have a direct access to the forces at the operating area thereby increasing the quality of the operation [16]. The other additional factors that are important include the scaling of the surgeon's and filtering the surgeon's tremor to increase the safety and accuracy of the MIRS system.

The communication between the master and the slave should be flexible so that different master stations can be connected so that surgeons can get help from expertise or the training of the surgeons can be enhanced for better usage of the system. So, the communication system should be safe and secure. The communication system should not get affected from the underlying networks or other radiations produced within the premises, thereby acquiring a Quality of Service. Thus, these efforts would make the MIS surgery safer and faster, thereby reducing the cost and post-operative complications for the patients. The tasks such as automatic camera guiding [18, 19], holding needles, positioning of instruments, grasping of tissues, automatic cutting and suturing should be handled by the robot autonomously. To realize the autonomous functions special attention should be made to the organs that are in motion induced by the patient's respiration and heartbeat. These motions are to be detected and compensated accordingly. With the development of surgical robots like "da Vinci" as shown in Fig. 2, many surgical procedures are being conducted remotely through tele-robotics [17, 20].

Robotic Cardiac Catheterization

As the human resource in the field of medicine is scared, their welfare is one of the major priorities of healthcare industries. The device manufacturers are striving hard



Fig. 2 Da Vinci Robotic surgical system (from Intuitive Surgical, Inc.): It is designed to facilitate surgery using a minimally invasive approach, controlled by a surgeon from a console [17]

to offer cutting-edge advanced products with more safety and regulatory compliance. For example, the X-ray machines which were developed few decades back are now considered hazardous in view of stringent radiation leakage norms and larger procedural time. Many other medical procedures like surgeries, transplants have also been made safer with the availability of better sterilization methods and higher precision equipment.

But, with such advancements in the field of robotic surgery, there are some procedures which are still being performed manually in hazardous situations and one of them is cardiac catheterization. Cardiac catheterization is a process where a small tubular structure called “catheter” is inserted into a major blood vessel through the groin area and is threaded through the vascular system to reach the human heart. This procedure is used for several diagnostic and treatment purposes such as angiography, angioplasty, valvuloplasty, and arterial fibrillation. The procedure is very effective as it is minimally invasive, safer and with very low recovery time. The only downside of this procedure is that it has to be performed under a fluoroscope. Fluoroscopes is an x-ray imaging device which provides real-time continuous x-ray imaging by which the physician tracks the movement of the catheter and adjust its direction so that it reaches its desired destination. The radiation emitted by the fluoroscope is very harmful for the human body if absorbed in large quantities [21–23]. Though for the patients, the radiation dosage is regulated, a physician performing 5–6 procedures in a day is highly vulnerable to radiation side effects. To prevent the radiation absorption, the medical staff uses lead aprons and similar headwear which absorbs most of the leaked radiation and protects the person. But many studies aimed at measuring the level of such protection found that the lead apron and accessory gear is not fully efficient and only protects the torso and forehead leaving eye, throat and palms still vulnerable [24]. To mitigate the radiation side effects, many researchers



Fig. 3 CorPath GRX by Corindus Vascular Robotics Inc. [29]

worldwide have reported development of robotic catheterization systems [25–28]. Such systems enable the physician to perform the cardiac catheterization procedure away and protected from the hazardous radiation zone. Several multinational companies like Corindus Vascular Robotics Inc. and Hansen medical Inc. have developed commercially available robotic catheterization systems.

However, these robotic devices are designed for a specific procedure only. For example, CorPath GRX of Corindus Inc. (shown in Fig. 3) can only perform angioplasties and angiography primarily by manipulating a hard metal guide wire. Similarly, Sensei X and Magellan of Hansen Medicals can only be used for atrial fibrillation procedure. One of the limitations of the existing systems is the limiting length in linear travel, i.e., the catheter can be moved up to and in between a fixed distance only.

There is another important component of this robotic cardiac catheterization system that helps in rotating the catheter around its own axis. This turning of the catheter has to be very precise as it determines in which vessel the catheter will enter into. If the movement is not precise, either the catheter will enter into a different artery which can lead to non-desired locations or due to the rotating motion, the catheter can scar or rupture the interiors of the blood vessels which can be life threatening for the patient under procedure. This situation can be resolved by implementing a driving mechanism instead of the conventional geared mechanism as it helps improving the accuracy in rotation of the catheter. Also, there is one more prospect of research which is still relatively untouched as compared to other aspects of such systems, i.e., the catheter tactile sensor. Conventionally, during manual cardiac catheterization procedures, physicians used to rely on the sensation of touch to determine whether the tip of the catheter is hitting any arterial wall or is facing some resistance in travel path. After the movement of the catheter is mechanized, there should be some way to replicate the human sensation judgment during the procedure. Development of this kind of a sensor is a major task in itself because of its size, accuracy and reusability. Development of such haptic feedback system-based robotic systems has already opened up new avenues of robotic research in this field. There is also a need to develop robotic devices that can perform other common procedures like valvuloplasty which uses a soft off-the-shelf catheter.

Haptics in Robotic Systems

Haptic refers to the sense of touch. Ancient psychologists referred haptesthai (Greek origin of word haptic) to tactile sensations. However contemporary psychology treats somatic senses to be working synergistically. Haptic could therefore be effectively referred to proprioception, kinesthesia and the vestibular sense as somatic senses of touch. “Haptic” has been deployed in various contexts (art history, aesthetics and architecture) and most frequently in the psychology of perception and technologies of touch engineering. Various aspects of embodied tactile namely scientific, psychological and engineering aspects find use from the term haptic. However, implications arise while handling spatial access and mobility problems of people with sensory or motor impairments, especially the blind and visually impaired.

Our skin has touch receptors which transfers the sensory information through neuronal firings to brain and help the human being in responding to the information accordingly. This haptic technology is also a mimicking of similar process so as to transfer the information of touch to the central processor. The device mainly measures the stress occurring during any kind of linear or non-linear motion giving signals corresponding to the surface profile on which it is moved. This kind of technology finds its direct application in robotic surgery and several applications which require monitoring the direct interaction of robotic arm/instrument on human subject. The haptic technology consists of device configuration to receive sensory signal corresponding to the sense of touch, and vary with the level of roughness on a surface. It mainly consists of a miniaturized accelerometer and a force sensor, embedded in an elastomeric sheet mimicking the human skin.

Human–machine interaction (HMI) has become an integral component of artificial intelligence and computer vision, required for automation in several applied sectors. However, HMI is not an easy task as still many limitations exist in the behavior of humanoid robots. Mimicking human being completely has always been the target of several researchers, but is a difficult task to make it really possible. Machine vision-based approaches to interact with real world are limited by environment condition, calibration procedures and several other man-made factors. In order to overcome these problems, the sense of touch has been incorporated along with the sense of sight to add on to the amount of information available to a machine for decision-making process. It can be lucidly illustrated through a situation, when a person touches an object to obtain more accurate idea of the shape and texture of the object, when visual clues do not provide enough information, like in dark environments or when object of interest is occluded. Added to it, few researchers have also looked into the aspects of tactile sensor alignment with respect to measured surface and error induced into the system due to the deformation in tactile array [30]. It has been also speculated that a special device if added in between the robot end effector and the tactile sensor to compensate for misalignments would ensure uniform force distribution on the tactile probe. Use of haptic technology to detect geometrical profiles has been used extensively and aids in the task of object recognition, and thus helping in automation-based system [31].

Fig. 4 PHANTOM, commercially available Haptic device, which accurately models the surface and textures of materials used in CAD/CAM [32]



Applications of Haptic Feedback Systems

As haptic systems aim to reproduce tactile sensations and engage the user with “force feedback”, they have found applications in a wide range of areas ranging from the coarse rumble and vibrations in gadgets and domestic technologies such as mobile phones, intuitive robotic surgery and videogame controllers, to the more refined and specialized design and engineering interfaces such as the PHANToM (Personal Haptic iNterface Mechanism), which more accurately models the surfaces and textures of materials used in computer-aided design and manufacture (CAD/CAM) as shown in Fig. 4 [32].

Furthermore, included within an increasing array of consumer technologies, haptics is reaching near ubiquity by being included in everything from vibrating mobile phones, rumbling controllers for videogame consoles, the distribution of touchscreens throughout our urban environments. On the other hand, more specialized haptic technologies are refining the human–computer interface and changing the way that virtual sculpting and virtual prototyping is achieved simply by offering more intuitive, tactile engagement with the computer. Haptic devices are widely used in different applications such as gaming and multimedia.

As mentioned earlier, a lot of activities are being reported worldwide with respect to integration of haptic feedback with robotic systems for better human–machine interaction and ease of remote surgical procedures [33–35].

3 Major Challenges in Medical Device Development

3.1 *Data Security and Product Safety*

With abundant use of software-driven medical devices now-a-days and over-dependency on such tools at crucial decision-making points, it becomes highly essential to ensure adequate product safety and security, more so when a human life is at stake. Therefore, there are certain regulatory issues specific to SDMDs such as dynamic software development processes, product safety and security, data collection and privacy and payment-related issues. The dynamic software development process mainly deals with the design, development and application of the software. A software is always developed in an evolving environment as it is regularly edited, modified, maintained and updated with deployment of improved versions over a period of time. In such a scenario, there must not be any product rollout or version upgrade at the expense of planning and documentation, both of which are necessary and critical for all the medical devices. Apart of development, distribution of such software is also a concern for regulation [36]. As conventional medical devices are operationalized by formal healthcare system, this software tools can be accessed personally outside the traditional medical supply chain. For example, for a patient, who cannot access traditional medical equipment approved only for usage within a specific geographical area, he/she can easily download and use the tool if it is only based on a software bypassing local regulations and approvals.

The product safety and security also include software vulnerability and bugs that also need to be carefully addressed [37]. As regular updates will be rolled out periodically for a software, there is always a possibility of introduction of a bug or defect with a recent update which can hamper the smooth running of existing medical device. There are also cybersecurity risks associated with the functioning of the SDMDs with extending network capabilities of such software for remote monitoring and control of devices. This also exposes the vulnerability of the device to a cyber-attack to hinder the working of such systems. There is also an issue of maintaining, managing and supporting SDMDs beyond the lifespan of the manufacturer. For example, if a company manufacturing pacemakers and control software application shuts down after a while, then the patients implanted with those specific pacemakers would be adversely affected due to lack of software updates or maintenance of existing software. As such concerns are directly related to a human life, they have to be properly regulated in medical device manufacturing sector [8, 38, 39].

3.2 *Process and Product Validation*

In a bid to outpace competitors, medical device manufacturers often rush their products into commercialization without much background validation of the process

or/and the product. US Food and Drug Administration (FDA) has issued many warnings in the past to such manufacturers for inadequate process validation. According to FDA, process validation is defined as “*the collection and evaluation of data, from the process design stage through commercial production, which establishes scientific evidence that a process is capable of consistently delivering quality product*” [40]. Validation refers to the end-product or process and how effectively it does its intended application. Validating a certain process almost always requires a dedicated team of R&D, process and quality assurance engineers along with a target user group. Small and medium scale industries often find it economically untenable to carry out such activities before launching a product. In case of computer-assisted devices, the challenge is to identify the output system parameters to validate the efficacy of a certain procedure with respect to unassisted human procedures. In complex assistive surgical devices having many submodules, several variability like patient anatomy, different data acquisition modalities, differing reference coordinates and subjective surgical approaches and procedures to do a certain task, makes it difficult to evolve a validation protocol to assess the quantitative improvements of maneuverability of the assistive device [41, 42]. As the field of surgical robots and software-driven medical devices are evolving very rapidly, there are also challenges for the regulatory authorities to reach a consensus with the industry regarding the method of validation and the specific parameters to be looked into.

With respect to medical cyber-physical (MCP) systems that are networked and intelligent systems to provide continuous care solutions with remote assistance, the challenges of system validation become further challenging due to data security and privacy issues. MCPs usually have a host of patient data acquisition tools connected to an intelligent server that continuously monitors the acquired data and issues warnings to the healthcare professionals if any of the monitored data exceeds some preset threshold [43]. Some of the major challenges associated with validation of MCPs are as below [43–47]:

- **Compliance with the EU/US and other local regulatory requirements**—Development of a safe and reliable cyber-physical system requires compliance to norms of local regulatory authorities such as US Food and Drug Administration (FDA), European Medicines Agency of the European Union, Health Canada, and The Central Drugs Standard Control Organisation (CDSCO) of India depending on the geographical market of the product or process. Inadequacies and failure to meet the regulatory requirements can attract legal actions leading to suspension or complete ban on product marketing. Actions such as lack of documentation for a software version upgrade, failure to perform monitored pre-clinical and human trials or inadequate process validation methodologies can amount to regulatory violation and can subsequently lead to blacklisting by concerned agencies.
- **Maintaining traceability records**—As per USFDA regulations for software validation, it is mandatory that the software codes and any subsequent version changes are required to be mapped to requirement specifications and test cases at each development stages [48]. But, many a time, changes are incorporated in the medical products and associated software codes without proper justification and

traceability to the change in requirement specifications. This leads to poor software integrity and other issues related to testing and fixing of probable software bugs.

- **Identifying and recognizing cases where product cannot be validated**—There can be disagreements between a certifying agency and the manufacturer regarding the scope and extent of product validation with respect to certain market segments. For example, in additive manufacturing, 3D printing, welding and sterilization of components, it may not be feasible and appropriate to inspect the end-product and it may require the regulators to look into the process itself to validate the outcomes.
- **Verifying and certifying mobile apps for user safety**—Of late, smartphone based applications for monitoring health parameters have emerged as a popular tool among the masses for tracking their daily activities. As per a guidance document released by USFDA in 2011, such apps are defined as software tools that is either used as an accessory to already regulated medical device or transforms a mobile platform into a regulated medical device [44, 49]. To assure consumers of the clinical validity as well as practical utility of medical mobile apps, both the software developers as well as the regulators need to evolve a comprehensive framework for assessing the performance characteristics of such applications. While hardware-based products are relatively easier to assess and validity owing to ease of observability, regulating and validating medical apps for treating and diagnosing diseases becomes challenging.

4 Conclusion

With the rise in infectious diseases and the evolution of chronic comorbidities, the world is constantly looking upon the medical industries with high expectations for affordable and intelligent healthcare solutions. This has given rise to many game-changing medical innovations such as robotics, wearable health monitors, networked medical systems for telemedicine, and remote consultations. The preference and acceptability of minimally invasive or when possible, non-invasive procedures are also increasing rapidly because of the patient benefits and ease of surgical procedures. Thus, the opportunities related to development of a series of robotic manipulators to assist the surgeons during medical interventions are also opening up newer avenues for biomedical researchers and manufacturers. There has been a renewed focus on preventive medication including vaccine research as well as e-healthcare and community care systems. At the same time, stricter regulatory compliance regime has also posed challenges for the manufacturers to get approval and necessary clearances for a product/service launch. The situation becomes trickier when a product is envisaged to launch in multiple global markets as the regulatory framework in each of those constituent countries can be significantly different. Though all such regulations are primarily aimed at ensuring safety and enhanced utility of the products, these can be resource-exhaustive for small industries as the number and type of qualification tests

can differ from one country to the other. Considering all such trade-offs between faster product development and product security, it is high time all the stakeholders put their best effort in evolving a dedicated product development methodology for medical devices. Such a methodology should also include post-development market analysis and incorporation of user feedback for enhancing the product efficacy. There is also a need to relook at the global risk management and quality control practices so that they are in all sync with the larger idea of better quality of life with adequate safety measures without unnecessarily delaying a product launch. As former American politician, educator and author Shirley Anita Chisholm, once famously said, “*Health is a human right, not a privilege to be purchased*”, the medical industries, researchers, regulators and even consumers need to rise to the occasion to cooperate, codevelop, collaborate and formulate a way forward for a better tomorrow.

References

1. Blumenthal, D., Tavenner, M.: The “meaningful use” regulation for electronic health records. *N. Engl. J. Med.* **363**(6), 501–504 (2010)
2. Alexandru, A., et al.: Healthcare, big data and cloud computing. *Management* **1**, 2 (2016)
3. Raghupathi, W., Raghupathi, V.: Big data analytics in healthcare: promise and potential. *Health Inf. Sci. Syst.* **2**(1), 1–10 (2014)
4. Wall, J., Chandra, V., Krummel, T.: Robotics in general surgery. In: *Medical Robotics*. IntechOpen (2008)
5. Ghodoussi, M., Butner, S.E., Wang, Y.: Robotic surgery—the transatlantic case. In: *Proceedings 2002 IEEE International Conference on Robotics and Automation* (Cat. No. 02CH37292). IEEE (2002)
6. Gordon, W.J., Stern, A.D.: Challenges and opportunities in software-driven medical devices. *Nat. Biomed. Eng.* **3**(7), 493–497 (2019)
7. Wang, S., Ding, S., Xiong, L.: A new system for surveillance and digital contact tracing for COVID-19: spatiotemporal reporting over network and GPS. *JMIR mHealth uHealth* **8**(6), e19457 (2020)
8. Fu, K.: Trustworthy medical device software. *Public Health Effectiveness FDA* **510**, 102 (2011)
9. Burleson, W., et al.: Design challenges for secure implantable medical devices. In: *DAC Design Automation Conference 2012*. IEEE
10. Clark, S.S., Fu, K.: Recent results in computer security for medical devices. In: *International Conference on Wireless Mobile Communication and Healthcare*. Springer, Berlin (2011)
11. Group, I.S.W.: Software as a Medical Device (SaMD): key definitions. **9**, 9. Published online December (2013)
12. Digital Health Criteria (FDA, 2018): (2018). Available from: <https://www.fda.gov/medical-devices/digital-health/digital-health-criteria>
13. Developing Software Precertification Program: A Working Model US Department of Health and Human Services Food and Drug Administration (2018)
14. Horgan, S., Vanuno, D.: Robots in laparoscopic surgery. *J. Laparoendosc. Adv. Surg. Tech.* **11**(6), 415–419 (2001)
15. Bass, E.B., Pitt, H.A., Lillemoie, K.D.: Cost-effectiveness of laparoscopic cholecystectomy versus open cholecystectomy. *Am. J. Surg.* **165**(4), 466–471 (1993)
16. Wagner, C.R., Howe, R.D., Stylopoulos, N.: The role of force feedback in surgery: analysis of blunt dissection. In: *International Symposium on Haptic Interfaces for Virtual Environment and Teleoperator Systems*. Citeseer (2002)

17. Lobontiu, A.: The da Vinci surgical system performing computer-enhanced surgery. *Osp Ital Chir* **7**, 367–721 (2001)
18. Wei, G.-Q., Arbter, K., Hirzinger, G.: Automatic tracking of laparoscopic instruments by color coding. In: *CVRMed-MRCAS'97*. Springer, Berlin (1997)
19. Arbter, K., Wei, G.-Q.: Method of tracking a surgical instrument with a mono or stereo laparoscope. Google Patents (1998)
20. Wilson, E.: The evolution of robotic general surgery. *Scand. J. Surg.* **98**(2), 125–129 (2009)
21. Kim, K.P., Miller, D.L.: Minimising radiation exposure to physicians performing fluoroscopically guided cardiac catheterisation procedures: a review. *Radiat. Prot. Dosimetry.* **133**(4), 227–233 (2009)
22. Sandblom, V., et al.: Evaluation of the impact of a system for real-time visualisation of occupational radiation dose rate during fluoroscopically guided procedures. *J. Radiol. Prot.* **33**(3), 693 (2013)
23. Kesavachandran, C.N., Haamann, F., Nienhaus, A.: Radiation exposure and adverse health effects of interventional cardiology staff. In: *Reviews of Environmental Contamination and Toxicology*, pp. 73–91. Springer (2013)
24. Goni, H., et al.: Investigation of occupational radiation exposure during interventional cardiac catheterisations performed via radial artery. *Radiat. Prot. Dosimetry.* **117**(1–3), 107–110 (2005)
25. Moll, F.H., et al.: Methods using a robotic catheter system. Google Patents (2010)
26. Guo, J., Guo, S., Yu, Y.: Design and characteristics evaluation of a novel teleoperated robotic catheterization system with force feedback for vascular interventional surgery. *Biomed. Microdevice* **18**(5), 76 (2016)
27. Moll, F.H., et al.: Instrument driver for robotic catheter system. Google Patents (2011)
28. Guo, S., et al.: A novel robot-assisted endovascular catheterization system with haptic force feedback. *IEEE Trans. Rob.* **35**(3), 685–696 (2019)
29. Rafii-Tari, H., Payne, C.J., Yang, G.-Z.: Current and emerging robot-assisted endovascular catheterization technologies: a review. *Ann. Biomed. Eng.* **42**(4), 697–715 (2014)
30. Pasca, C., et al.: Intelligent haptic sensor system for robotic manipulation. In: *Proceedings of the 21st IEEE on Instrumentation and Measurement Technology Conference. IMTC 04* (2004)
31. Kirkpatrick, A.E., Douglas, S.A.: Application-based evaluation of haptic interfaces. In: *Proceedings of 10th Symposium on Haptic Interfaces for Virtual Environment and Teleoperator Systems, 2002. HAPTICS 2002*. IEEE (2002)
32. Massie, T.H., Salisbury, J.K.: The phantom haptic interface: A device for probing virtual objects. In: *Proceedings of the ASME Winter Annual Meeting, Symposium on Haptic Interfaces for Virtual Environment and Teleoperator Systems*. Kluwer (1994)
33. Bethea, B.T., et al.: Application of haptic feedback to robotic surgery. *J. Laparoendosc. Adv. Surg. Tech.* **14**(3), 191–195 (2004)
34. Tiwana, M.I., Redmond, S.J., Lovell, N.H.: A review of tactile sensing technologies with applications in biomedical engineering. *Sens. Actuators A* **179**, 17–31 (2012)
35. Girão, P.S., et al.: Tactile sensors for robotic applications. *Measurement* **46**(3), 1257–1271 (2013)
36. Hanna, S., et al.: Take two software updates and see me in the morning: the case for software security evaluations of medical devices. In: *HealthSec* (2011)
37. Rakitin, S.R.: Networked medical devices: essential collaboration for improved safety. *Biomed. Instrum. Technol.* **43**(4), 332–338 (2009)
38. Alsubaei, F., Abuhussein, A., Shiva, S.: Security and privacy in the internet of medical things: taxonomy and risk assessment. In: *2017 IEEE 42nd Conference on Local Computer Networks Workshops (LCN Workshops)*. IEEE (2017)
39. Lee, I., et al.: High-confidence medical device software and systems. *Computer* **39**(4), 33–38 (2006)
40. Guidance for Industry, Process Validation: General Principles and Practices (US Food Drug Administration). Center for Biologics Evaluation and Research. US Department of Health and Human Services, Rockville, MD (2011)

41. Janda, M., Buch, B.: The challenges of clinical validation of emerging technologies: computer-assisted devices for surgery. *JBJS* **91**(Supplement_1), 17–21 (2009)
42. Haidegger, T.: Surgical robots: system development, assessment, and clearance. In: *Prototyping of Robotic Systems: Applications of Design and Implementation*, pp. 288–326. IGI Global (2012)
43. Lee, I., et al.: Challenges and research directions in medical cyber–physical systems. *Proc. IEEE* **100**(1), 75–90 (2011)
44. Hrgarek, N.: Certification and regulatory challenges in medical device software development. In: *2012 4th International Workshop on Software Engineering in Health Care (SEHC)*. IEEE (2012)
45. Vogel, D.A.: *Medical device software verification, validation and compliance*. Artech House (2011)
46. Gatouillat, A., et al.: Internet of medical things: a review of recent contributions dealing with cyber-physical systems in medicine. *IEEE Internet Things J.* **5**(5), 3810–3822 (2018)
47. McHugh, M., McCaffery, F., Casey, V.: Barriers to adopting agile practices when developing medical device software. In: *International Conference on Software Process Improvement and Capability Determination*. Springer, Berlin (2012)
48. *General Principles of Software Validation. Final Guidance for Industry and FDA Staff, USFDA*, pp. 33–34 (2002)
49. Shuren, J., Patel, B., Gottlieb, S.: FDA regulation of mobile medical apps. *JAMA* **320**(4), 337–338 (2018)

Chapter 14

Flexible Organic Field-Effect Transistors for Biomimetic Applications



Vivek Raghuwanshi and Shree Prakash Tiwari 

1 Introduction

In the current fast-growing electronic world, computers are acting as the backbone for our efficient and comfortable work experience. On average, today a working person is surrounded by more than 1000 processors. This all started with the invention of the transistor in 1948 by John Bardeen, William Shockley, and Walter Brattain at Bell Labs and since then the semiconductor industry is growing expeditiously. In the year 1965, Gordon Moore predicted that the number of transistors will double in an integrated circuit every two years [1]. With the need for miniaturization of chips, the statement became the roadmap to the growing semiconductor industries and the number of transistors on chips has tremendously increased over time, where the count was ~8000 in 1974 which is now 39.54 billion transistors in a commercially available microprocessor. The technology node has immense advancement where it was ~8000 nm process in 1974 and which has reached to 7 nm in 2019.

Silicon electronics has solved many challenges related to our increased electronics use, but there are limitations to what silicon electronics can do. There is a need for alternative electronics that can be used for large-area flexible electronics without using costly fabrication tools and can be processed at low temperatures so that the application area can be broadened. In addition, the methodologies and resources use in silicon electronics manufacturing concerns the negative environmental impact and there is a need for technology that can reduce the electronic waste at the end of the life span of the devices. Considering the need, organic electronics seems to be the best possible alternative to conventional silicon technology in terms of solving the problems discussed above. The use of organic materials will provide a platform for

V. Raghuwanshi · S. P. Tiwari (✉)

Department of Electrical Engineering, Indian Institute of Technology Jodhpur, Jodhpur, Rajasthan 342037, India

e-mail: sptiwari@iitj.ac.in

the electronic world to be more environmentally friendly and reducing production costs. In this chapter, the salient feature of organic electronics and its importance in today's electronics world is discussed.

In the last few decades, electronics based on electroactive organic compounds has gained a lot of attention and is termed as organic electronics. The special electronics uses organic materials and their properties for the world of electronics in a way that was unimaginable until now with the silicon technology. The ability to tailor the electrical, optical, and mechanical properties of the electroactive organic materials has broadened the application area to a wide range.

The capability to process at low temperature with simple solution processing techniques makes the production of organic-based electronic devices feasible even in the resource-limited regions of the world where necessary infrastructure is unavailable. The organic devices are not comparable to the conventional silicon technology when high electrical performance and stability of the devices are of prime importance. However, in the applications where the nominal electrical performance with low-temperature processing and low production cost is required, organic electronics is dominating and the best replacement to conventional silicon technology has the potential to change the way how our society interacts with electronics.

1.1 Historical Perspective

Up to the mid of the twentieth century, the semiconducting properties, metallic conductivity, and superconductors were the domain of inorganic science and solid-state inorganic science only, and organic materials were considered only as insulators with a wide range of application in the insulating and packaging industry. Inspiring from the discovery of the transistor, there were initial reports on the organic semiconductor with decent dim conductivity in the 1950s [2, 3]. Later in 1963, McNeill and coworkers reported high electrical conductivity in polypyrrole [4]. The blue light emission from anthracene single crystal was reported by pope and coworkers in the same year [5]. The materials used in their studies have shown semiconducting behavior but with very low performance and at that time they were considered to have a low potential for future applications.

In 1964, articles published by William Little on the possibility of excitonic superconductivity gave inspiration to the researches in the field and organic electronics thus advances with various findings from semiconductors to metals to superconductors [6, 7]. In 1977, the finding on the variable electrical conductivity of the conjugated polymer polyacetylene played a huge role in revolutionizing organic electronics [8]. In the year 2000, for the discovery of conductive polymers, the Chemistry Nobel Committee awarded A. J. Heeger, A. G. MacDiarmid and H. Shirakawa Nobel prize in chemistry [8, 9]. The electroactive organic materials thus developed have been used in various potential applications and devices. The high-performance electroluminescent organic vacuum evaporated dye films [10, 11], organic field-effect transistors with polythiophene [12, 13], and small conjugate oligomers were demonstrated in

the late 1980s [14]. The first conjugated polymer-based light-emitting diode (PLED) was demonstrated by Burroughes and coworkers in 1990 [15]. Apart from organic light-emitting diodes, organic field-effect transistors (OFETs) [16, 17] and circuits based on OFETs [18–20], solar cells [21, 22], photodiodes [23–25], and lasers [26] with organic materials have been widely explored, and the technology has been developed a lot. These findings were the stepping stones toward the development of organic electronics to the commercial level. Today using organic electronic devices in the commercially available product is no more a dream, rather the industry has already left its footprints in the organic electronic device industry with cellphones using organic light-emitting displays which is one of its examples. Printed electronics, flexible large-area electronics, polymer electronics, plastics electronics, etc., are some of the names today used for organic electronics. The technology is using a combination of low-cost materials, printing technology, and large-area processing capabilities with environmentally friendly processes to open up new fields of application. Radiofrequency identification (RFID) tags, flat panel display drivers, solar cells, smart packaging, printable batteries, foldable displays, flexible sensors, and printable circuits are examples of the advancement of organic electronics technology till date [16, 21, 27–33]. The technological achievements in the field in such a short span shows the interest of the research community in this fast-growing field and its development. The success and growth of particular technology can be said by its revenue generated in the real world. The organic electronics market is expected to reach USD 87.21 billion by 2024, and the organic displays are the largest revenue-generating segment of the technology with 65–75% of the total market revenue. The main devices where the organic light-emitting displays used are TVs, tablets, cell phones, etc. The graph of revenue generation and demand for organic electronics based devices are continuously growing. An example of which is shown in Fig. 1, which is as per the 2011–2021 forecast report from IDTechEx, where the market capture by printed electronics components and the future estimation of the 3D printed electronics is shown. Such a high demand for the commercial market shows why researchers around the world are putting continuous efforts into the development of this technology. The foldable organic light-emitting diodes and printable light-emitting diodes are capturing huge attention and are on a verge of commercial growth. Organic electronics technology has traveled a long way and there is huge scope for the industry to grow with an immense number of products to come in the future and is thus called the futuristic technology.

1.2 Flexible Electronics Advantages

Some of the major advantages of flexible electronics technology, where organic semiconductors are mostly utilized as the active material, are listed below:

Solution Processability. The major advantage of this technology is the solution processability of most of the organic materials. The organic semiconductors can

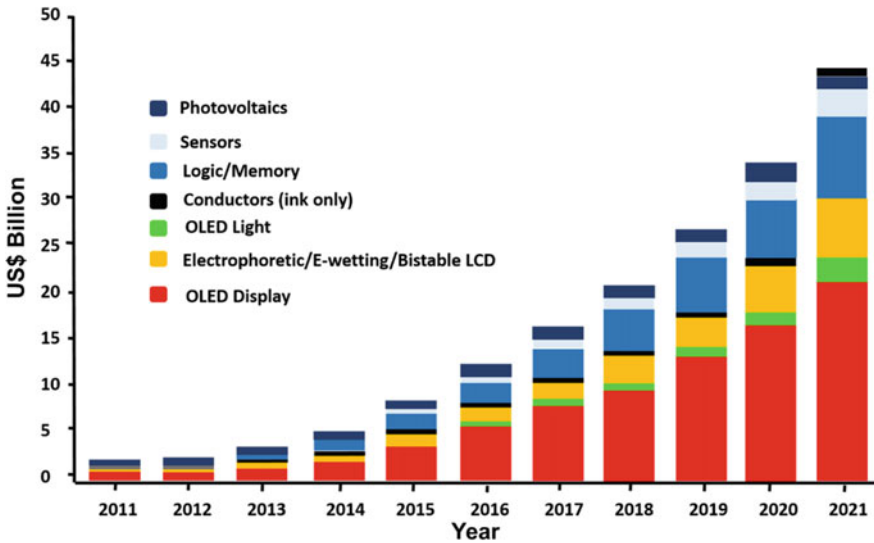


Fig. 1 Graph showing continuous growth in the printed electronics market and expected demand in the future [34]

also be processed through a high vacuum deposition system like sputtering, thermal evaporation systems, organic molecular beam deposition, and organic physical vapor deposition. But utilizing such a sophisticated instrument does not fulfill the core motive of the organic electronics that is producing electronic devices at low cost. Solution processability allows the organic semiconductors to convert in the form of inks by dissolving in various solvents, and the obtained inks can easily be patterned in various ways with the use of printers to obtain various circuits. Imagine plotting a drawing of a particular circuit on software and developing it using a printer. Such easy processing of semiconductors is a major factor in obtaining high throughput, easily processed electronic devices. The solution casting of organic material can be done in numerous ways like spin coating, dip coating, blade coating, spray coating, and screen printing etc.

Low-temperature processing. Organic electronics is also termed as printed and foldable electronics. Thus, the technology mainly focuses on substrates like plastics, paper, cloth, etc. The glass transition temperature of most of these flexible substrates is $<150\text{ }^{\circ}\text{C}$. This means processing over $150\text{ }^{\circ}\text{C}$, the substrate loses its integrity. The processing temperature for most of the organic electronic devices fabrication is $<100\text{ }^{\circ}\text{C}$, which makes these substrates compatible with this futuristic technology and the temperature processing requirements are much lesser compared to the single-crystalline Si ($>800\text{ }^{\circ}\text{C}$), polycrystalline Si ($\sim 600\text{ }^{\circ}\text{C}$), and the hydrogenated amorphous Si ($\sim 300\text{ }^{\circ}\text{C}$). The organic materials thus can be processed from room temperature to $100\text{ }^{\circ}\text{C}$ and do not require complex processing equipment.

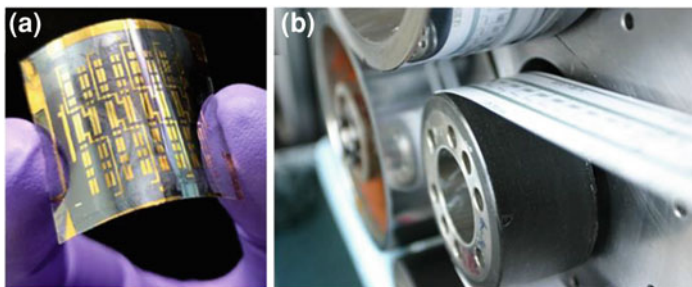


Fig. 2 **a** A typical device fabricated in the laboratory. **b** Gravure printing of electronic structures on paper. *Source* Wikipedia, Creative Commons CC BY-SA 3.0

Flexibility and roll-to-roll processing. The soft nature of the organic semiconductors allows them to be processed on bendable and foldable plastic and other flexible substrates. The mechanical flexibility itself highly broadens the application area of organic electronics. The flexibility properties are used to make electronic skin with tactile sensing properties that can be used in robotics and other applications where flexible touch sensors are required that were impossible to be built by existing silicon technology. The soft nature of these carbon-based materials makes them compatible with various curved and movable surfaces. The flexible nature also favors the production of organic devices through the roll-to-roll processing, where the fabrication is almost similar to printing a newspaper with high speed. The roll-to-roll processing cuts down the processing cost to a large extent and allows the bulk production at a faster rate. The organic devices fabricated on a flexible PET substrate and gravure printing of electronic components on paper are shown in Fig. 2.

Low manufacturing cost. Technology is said to be successful not only by its nature of producing products with ease but also by the development of products that are accessible to the common population and are affordable in their budget. Organic electronics not only changes the way how people look at the technology but also promises to reach the sector of the population that cannot afford basic facilities by producing products at a much cheaper cost. This technology does not necessarily require a cleanroom with sophisticated instruments. In addition, it requires simple processing techniques like spin coating, drop-casting, printing, etc., that reduce the budget requirement. Also, the materials used in the process are nowadays available in bulk, which further reduces the manufacturing cost. This low-cost processing allows the manufacturing of the organic electronic devices even in resource-limited regions of the world. Around 1.2 billion people in the world do not have access to electricity and they rely on batteries or kerosene. The development of organic electronics is fruitful in such areas. One of the examples of such low-cost technological advancement is the indigo program run by Elight19 a UK-based company that works on the organic solar cell. In the program, the company has provided solar power energy to rural areas with organic printed solar cells. The program was named as pay-as-you-go which eliminates the high initial cost of solar power systems. The consumers

have to pay in the week by week system until they own the system and the cost per week was less than their cost that was put on kerosene for a week and also environmentally friendly than kerosene. Once the total product cost is paid, the usage was free of cost. The advantages of low-cost productivity and various other advantages discussed above are the motivation of the researchers to carry out research in this futuristic technology.

1.3 Applications

The soft nature of organic electronics made it possible to be processed at a variety of substrates that have the benefit of mechanical flexibility. This core advantage broadens the application area of the technology and changes the perspective of the world to this growing technology. Some of the major applications are organic light-emitting diodes (OLEDs), flexible displays, radio frequency identification tags (RFIDs), intelligent packaging, energy-efficient lightning, organic memory devices, etc.

Organic electronics opens up new possibilities and applications in the field, and one of the most important applications is the use of organic thin-film transistors in the flexible active matrix display circuitry. Organic transistors are most crucial to the basic building block for organic electronics circuits. Brief details of some of the important applications of flexible electronics where organic field-effect transistors used are following.

OLED Displays. OLEDs are emissive displays; they do not require any backlight to work rather they produce their own light via electroluminescence to display images. These displays are more energy-efficient and consume less power when compared to the displays that require a backlight. TFTs-based pixel driver circuits allow them to be fabricated on a variety of flexible substrates which broadens the application area of these displays with the aid of transparency, foldability, and rollability in the displays. These displays are commercially utilized all around the world. For example, the Samsung galaxy cellphone series uses OLED displays and it covers a large cellphone sector. The latest example of this technology is the foldable smartphone launched by Samsung (Samsung galaxy fold) that utilizes the AMOLED display.

RFIDs. Radio frequency identification tag is a device used to transmit information from a transponder to the reader device. RFIDs are used in tracking of consumer goods, electronics product codes for logistics, identification cards of employees, electronic ski-pass, and many other automation applications. It is a passive device, which means it does not contain any power source, rather it gets activated when it comes in a range of particular frequency of the reader (high radio frequency of 13.56 MHz) and the stored information is thus transmitted from the RFID tag to the reader. The RFID tags are the combination of integrated digital logic circuitry and memory, which is connected to an antenna for transmitting the information. The RFID market is very large and its cost-effectiveness is a major concern in further expansion

of its use. Printed RFIDs can be very cost-effective and a good substitute to the standard RFID tags where a silicon chip is mounted on the substrate and connected to the antenna. The antenna can be printed using conductive inks. If the internal circuitry uses organic thin-film transistors, then the complete RFID tag can be printed. Along with the advantage of low cost, the printed RFID will also have flexibility, smaller thickness, and better ecological properties compared to the standard RFID tags. Researchers are working on the development of printed organic RFID tags. The first printed RFID tag was presented by PolyIC in the year 2007, which was working at a high frequency of 13.56 MHz. Since then many researchers came up with improve performance of printed RFID tags. Along with the advantage of printing, there are many challenges in printed RFIDs in terms of performance, memory size reading distance, etc. Thus, a lot of research is still needed in improving the performance of organic field-effect-based printed RFID tags and with the maturity of the technology the application areas of printed RFID tags are increasing and the performance is expected to meet that of the conventional RFID tags.

Sensors. Organic electronics has a wide range of application in low-cost sensors. Sensors are the means of detecting any stimuli. They detect some physical quantity (any stimuli), and the detected parameter is seen in terms of change in the electrical signal. Flexible electronics sensors can be used in a variety of applications like mounting flexible sensors on the body of the athletes, continuous health monitoring of patients, etc. To understand the relation between the wide organic electronics technology and the sensors, let us understand what is required for a sensor. The sensor consists of material that reacts to particular stimuli that can be either environmental change, temperature, pressure, etc. Thus, the organic flexible electronics uses materials that are compatible with the printed technology to develop low cost printed sensors. Organic thin-film transistor-based biological, temperature, pressure, chemical and environmental sensor have shown promising results in the field. These sensors have advantages of mechanical flexibility, affordable cost, low-temperature deposition, and the ability to be produced by the roll-to-roll processing to produce in high volumes. These advantages are the motivation for the researchers to develop further low-cost and easily processable sensors based on organic TFTs.

2 Organic Field-Effect Transistors

An organic field-effect transistor or thin-film transistor (OFET/OTFT) is an electronic device that uses organic semiconductor material for the active layer. OFETs are the main elements in organic electronic devices and are the basic building blocks for many applications namely the RFID tags, active-matrix displays, circuits, and various low-cost environmental and biological sensors. OFETs are receiving much attention for flexible electronic applications because of their solution processability, low manufacturing cost, low-temperature processing, and ability to be processed in large areas. Initial work on OFETs was started in 1983 by Ebisawa where the device

was made using polyacetylene as an active semiconductor. A couple of years later Tsumura demonstrated an OFET with polythiophene as an active layer and a large modulation in current was observed in these devices. These initial OFETs were based on polymeric semiconductor films which were deposited by spin coating or screen printing. The achieved mobility was of the order of $10^{-5} \text{ cm}^2 \text{ V}^{-1} \text{ s}^{-1}$. In terms of electrical performance, OFETs have traveled a long way and today the mobility values higher than $10 \text{ cm}^2 \text{ V}^{-1} \text{ s}^{-1}$ are achievable. Although the performance of OFETs is much lower compared to Si-based devices, however, this future technology is in high demand because of its broad range of applications and its ability to be fabricated on various unconventional and bendable substrates.

2.1 Device Structure

The cross-sectional view of four different types of OFET architectures is shown in Fig. 3. The device architecture of OFETs is much simpler as compared to the conventional MOSFET. It is a three-terminal device namely gate, source, and drain. Based on the position of these terminals with respect to the organic semiconducting film, the OFET device structures can be classified and they can either be coplanar or with staggered architecture. The first architecture is known as bottom gate top contact (BGTC), the second one is called bottom gate bottom contact (BGBC), and the other two are top gate bottom contact (TGBC) and top gate top contact (TGTC), respectively. In the bottom contact devices, the organic semiconductor is deposited over the gate insulator and source–drain electrode, whereas in top contact devices source–drain electrodes are generally deposited over organic semiconductors through a shadow mask. OFETs with the same materials but with different structures can show a drastic change in their electrical performance.

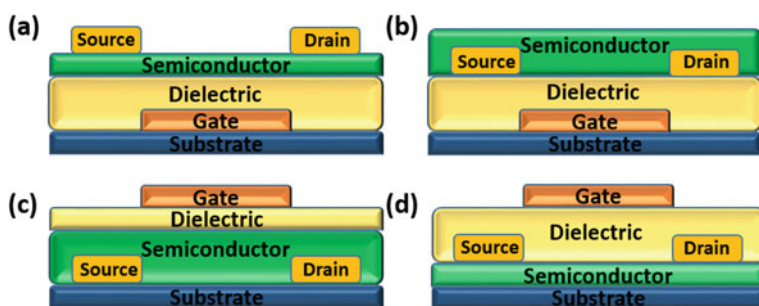


Fig. 3 OFET device architectures: **a** Bottom gate top contact. **b** Bottom gate bottom contact. **c** Top gate bottom contact. **d** Top gate top contact

2.2 Operation

For understanding the operation of the devices, the lowest unoccupied molecular orbital (LUMO) and highest occupied molecular orbital (HOMO) of the organic semiconductor are considered similar to the conduction and valence band of inorganic crystalline semiconductors. Let us consider a metal–insulator–semiconductor (MIS) structure with a hole transport organic semiconductor (similar to p-type), and when a negative gate voltage is applied ($V_{GS} < 0$), in a device, holes are accumulated in the semiconductor near dielectric. A p-type transistor operates when we apply a negative voltage at the drain ($V_{DS} < 0$). Just to remind, in conventional MOSFETs, the transistor operation is achieved in inversion mode.

In addition to the analysis of the MIS structure, we can also understand the charge injection process from source to semiconductor separately. Charge injection from metal to semiconductor is dependent on energy level alignment between the Fermi level of metals and HOMO or LUMO levels of the organic semiconductors. For p-type organic semiconductors (hole conduction), the HOMO level of the organic semiconductors should match with the Fermi level of a high work function metal like gold or platinum. Similarly, for n-type organic semiconductors (electron conduction), the LUMO level should match with the Fermi level of a low work function metal like calcium or magnesium. This is schematically illustrated in Fig. 4. The injection barrier (amount of energy level mismatch between HOMO/LUMO and Fermi energy of metal) has to be overcome by appropriate means for efficient charge injection and high performance in devices.

Since there are fewer stable options available for source–drain metals (Ca, Al, etc.) for n-channel transport, other available options that are suitable for p-channel operation (such as Au) are widely used for both types of devices. However, n-channel devices suffer from a high injection barrier due to this reason, leading to higher contact resistance. Contact resistance in the devices can be extracted using various methods including the transmission line method.

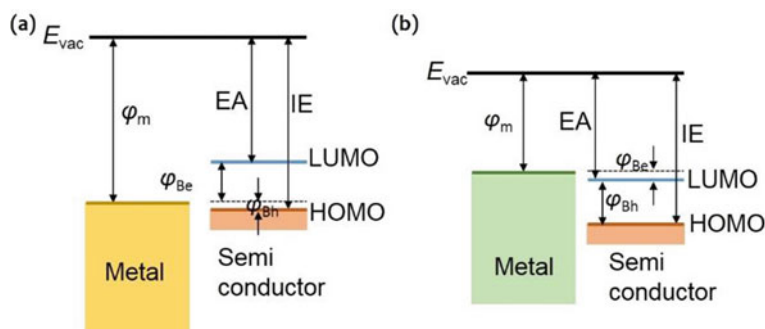


Fig. 4 Schematic representation of metal–semiconductor junction for a hole transport semiconductor **a** and electron transport semiconductor **b**

2.3 Flexible OFETs

One of the core advantages associated with organic electronics is its flexible nature, which broadens the application area of the devices. OFETs fabricated on flexible substrates have a wide range of applications as they can be used in wearable sensors, foldable displays, biomedical devices, smart identification cards, and other emerging applications with the potential of the roll-to-roll processing. In the last few decades, a lot of research has been carried out focusing on the high performance and operational stability of OFETs fabricated on various flexible substrates.

Plastic has the advantage of smooth surface suitable for organic device fabrication, thus in spite of being costlier than its other counterparts, it is widely explored globally. However, plastic suffers from a disadvantage of a negative impact on the environment. In recent years, with increasing awareness on environmental pollution, researches have tried making devices on substrates which can leave fewer footprints at the end of their lifespan. Paper is one of the most common unconventional substrates which are available at low cost and is naturally renewable. Summary of some selected studies reporting high-performance OFETs on plastic substrates, as well as on biodegradable substrates such as paper is given in Table 1. It is important to note that fabricating devices on paper are challenging because it suffers from severe microscopic surface non-uniformities. Thus, to overcome the high surface non-uniformities, a planarization layer is generally required before the fabrication of devices on paper. Despite the high surface roughness of the paper substrate, high performing OFET devices can be fabricated by utilizing planarizing techniques. However, despite so many reports on

Table 1 Summary of some selected studies reporting high-performance OFETs on plastic substrates, as well as on biodegradable substrates such as paper. Subs: Substrate; Dev. Str.: Device Structure; OSC.: Organic semiconductor; Op. Vol.: Operating Voltage

Subs	Dev. Str	Dielectric	OSC	Op. Vol. (V)	μ (cm ² V ⁻¹ s ⁻¹)	V _{TH} (V)	References
PES	TGBC	CYTOP /Al ₂ O ₃	TIPS-pen:PTAA	8	0.24 ± 0.08	-1.3 ± 0.1	[35]
PET	BGTC	HfO2 /PVP	TIPS-pen	10	0.12	-0.2	[36]
PEN	BGBC	PVC	TIPS-pen:PS	5	0.37	-	[37]
Polyester	BGTC	PMMA	TIPS-pen	40	0.062	~-4 V	[38]
PET	BGTC	HfO2	TIPS-pen: PS	5	0.5 ± 0.3	-0.5 ± 0.3	[39]
PEN	BGTC	PMMA	TIPS-pen: PMMA	5	0.87	-0.81	[40]
Kapton Tape	BGTC	PVA/ HfO2	TIPS-pen: PS	10	0.4 ± 0.2	-0.6 ± 0.7	[41]
Paper	TGBC	Cytop /Al ₂ O ₃	TIPS-pent: PTAA	10	0.1	-2.1 ± 0.7	[42]
Paper	BGTC	PVA/HfO2	TIPS-pen: PS	10	0.2 ± 0.1	0.2 ± 0.6	[43]

a paper substrate, the study of the device on paper with external stress remains under-explored. Extensive investigation of this facet of device performance is imperative to address for productive fostering of the field and to cater the increasing demand of solutions to futuristic applications by the route of the unconventional substrate. In the recent study [43], the optimized device's components were utilized and the devices were fabricated on a low-cost paper substrate with PVA as a planarizing layer. The devices were then studied for performance stability under environmental and electrical stress.

2.4 Operational Stability

Along with achieving high performance in OFETs, operational stability is another major concern for OFETs to be deployed in practical applications. Many efforts have been made in the last few decades to improve the long term stability of devices. Various organic semiconductors with high mobilities were developed which have an air-stable nature. However, utilizing air-stable semiconductors is not the only requirement of stable OFETs, various other factors affect the stability of OFETs. The first factor is the material used for semiconductor, dielectric, and metal contacts. All these materials should have an intrinsic stable nature. A material which itself degrades with time or bias cannot be a good candidate for the overall stable device. The second factor is the quality of films and functional interfaces in the devices. For OFETs, smoother and uniform the quality of films, better will be the performance and stability of the device. The various functional interfaces such as the dielectric–semiconductor and metal–semiconductor interface play a crucial role in determining the stability. As most of the charge carriers are accumulated in the few monolayers at the dielectric–semiconductor interface, the interface plays a crucial role in defining the stability of the device. The poor quality dielectric–semiconductor interface provides a large number of trapping sites to the charge carriers, which get trapped to the sites and the phenomenon eventually leads toward unstable device performance. Similarly, the quality of the metal–semiconductor interface defines the barrier to the injecting charge carriers from metal to semiconductor and limits the amount of charge carrier injection which also limits the stability of the device. Hence, efforts need to put on improving the uniformity of various films and reducing the barrier height for maximum charge injection. The third factor is the processing techniques used for the deposition of the various layer in device fabrication. The quality of the films obtained varies drastically with the processing technique. For instance, a semiconducting layer can be deposited by various methods such as drop-casting, spin coating, and dip coating. However, the same material deposited with different techniques provides different device performance and stability. The process parameters also change the stability by a large margin. All these factors such as the processing techniques or process parameters eventually affect the interfacial conditions of the device, which define stability. Another major factor is the architecture of the device used. The device fabricated with the same materials in different architecture provides

different performance and stability. For example, a semiconducting film in a BGTC architecture is more exposed to the environment compared to the same film in a TGBC architecture and thus the different environmental exposure results in different stability conditions.

For all the factors affecting the stability, their remedies need to be taken care of before fabricating a stable device. The chosen semiconducting material should be less prone to environmental conditions. Dielectric material with hydroxyl groups may lead to charge trapping at the dielectric–semiconductor interface, thus utilizing hydroxyl free dielectrics or strategies through which the direct contact of the hydroxyl group with the charge carriers is avoided, should be used, which limits the charge trapping at the interface and provide a stable device. The devices will also encounter various external stimuli such as humidity, temperature, and electrical stress applied, which affect the performance and stability. One example of this is when an external bias is applied in OFET their electrical characteristics changes with time. Say if we use an OFET that is used to switch ON a current, for example, to drive a pixel in a display, will switch OFF in some time. The problems arise due to the change in threshold voltage of the OFETs due to charge trapping at various regions of the active layer film. The effect is called the bias stress effect. Various remedies to improve the stability of OFETs are used. In the case of TIPS–pentacene, which is inherently air-stable, it is also blended with insulating polymer PS to improvise the dielectric–semiconductor interface and helps in decreasing the interfacial traps. Other factors affecting the stability can be considered to obtain high performance and operationally stable OFET devices.

2.5 Low Voltage Operation

Another critical issue in OFETs for practical application is the operational voltage. The major target applications of OFETs are dedicated to low-cost RFID tags and the electrophoretic displays which require low threshold voltage. In addition, to use these devices in the portable application, where the devices run through a battery, the operating voltage needs to be lowered. Lowering the operating voltage is the pursuit of the goal because the operating voltage is still high that leads to high power consumption in these devices. To understand what are the possibilities through which the operating voltage can be reduced let us understand the standard drain current equation of OFETs

$$I_{DS} = \mu C_{ox} \frac{W}{L} \left[(V_{GS} - V_{TH}) V_{DS} - \frac{V_{DS}^2}{2} \right] \quad (1)$$

where μ is the field-effect mobility, C_{ox} is the capacitance density, V_{TH} is the threshold voltage of the device, and W and L are the channel width and length, respectively. Looking at the equation it can be observed that the operating voltage at

a given drain current can be reduced by three paths: either the dimension factor (W/L) or the capacitance density or the mobility of the device must increase accordingly. The first cannot be altered much as the channel length is limited with processing techniques such as shadow mask or printing. Also, with reducing channel length, the contact resistance starts dominating over the channel resistance and the device inhibits saturation. Channel width, on the other hand, cannot be increased above an extent because with time the dimensions of the device are shrinking to accommodate a large number of devices in a small area. Mobility is the inherent property of the material and that cannot be increased above a particular limit. The only and important parameter left in hand to reduce the operating voltage is by increasing the capacitance density of the dielectric stack, which in turn is directly proportional to the dielectric constant of the material used and inversely proportionally to the thickness of the dielectric stack. The use of an ultrathin dielectric stack may lead to a high leakage current, which eventually degrades the device performance and undesirable for practical applications. Utilizing a high- k organic, inorganic, or hybrid dielectric stack is one of the most efficient means to reduce the operating voltage requirement.

Polymeric dielectrics are the first choice for OFETs because of their solution-processable nature and the ability to provide better quality semiconductor–dielectric interface. Some of the most common polymeric dielectric used are poly(4-vinylphenol) (PVP), polyvinyl alcohol (PVA), polymethylmethacrylate (PMMA), etc., which provide high performance in devices but the operating voltage still remains high because of their low dielectric constant. On the other hand, high- k inorganic dielectrics which are typically deposited by atomic layer deposition, chemical vapor deposition, or sputtering can significantly increase the surface charge density at the dielectric–semiconductor interface but these dielectrics also suffer from poor quality dielectric–semiconductor interface. Thus, to obtain high performing and low operating voltage devices, procedures need to be adopted that utilize the benefits of both the solution-processable polymeric dielectrics and high- k inorganic dielectrics.

3 OFETs for Smart Applications

An accurate information collection and prompt decision making is the key feature of the various modern day smart devices. Thanks to the flexible nature of OFETs they are reasonable for various smart applications, encouraging futuristic usage in smart medical service-related IoT. The OFETs serve as the information collector, i.e., sensor because of the various privileges that it possesses. The precise variation of channel current with the gate voltage gives room to a variety of dedicated detection possibilities. The logic functionality can also be enhanced by coupling one organic transistor with another or by tuning the source–drain voltage to overstep the gate voltage to achieve the amplification effect. In addition, access to its multiple parameters like threshold voltage, mobility, current on–off ratio is extra parameters for more comprehensive and accurate analyte detection. However, there are various

challenges that need to be addressed to use these devices in real-time health monitoring systems. Hence, comprehensive consideration is required to apply flexible OFETs for biomimetic applications. Primarily the selected materials must conform to the human body, and biocompatibility is much needed when these systems are embedded in the body for continuous sensing. Other challenges include improving the electrical performance and operational stability to ensure prompt and accurate response toward a specific stimulus. Further, the flexible nature of these devices needs to be improved because flexibility and stretchability are the prerequisite for the integration of electronics into many biological applications and are as important as high performance. Reducing power consumption (operating voltage) is another essential aspect that allows them to be used in portable and small battery-operated applications.

3.1 OFETs as Sensors for Biomimetic Applications

Wearable sensors-based health monitoring systems that can detect and diagnose various health parameters related to body homeostasis like the body temperature, breathing rate, heart rate, blood pressure, blood sugar, strain at various body parts, fluid balance, etc., can significantly improve the human health by reducing the spatial barriers between the medical centers and humans. Real-time health monitoring systems use sensors to detect these abnormalities and collect the information. OFETs are basic sensors that can be used to detect the stimuli and store the information. Figure 5 depicts the use of OFETs in detecting various stimuli.

In the human body, homeostasis is maintained. In other words, it maintains a constant internal environment irrespective of the external conditions. This homeostasis includes body temperature and cardiovascular system parameters like the heart rate, breath rate, blood pressure, body fluids such as glucose and several ions (calcium, pH levels, sodium, potassium, etc.). However, when there are health issues, the homeostasis cannot be maintained. OFETs detect various body parameters and the information collected can be used by the healthcare specialist for timely diagnosis of the disease. In addition, with the additional feature of data storage, the use of OFETs in wearable sensors not only helps in health improvisation but also contribute to the improvement of medical technology by collecting a large amount of human health information in one system.

3.2 OFETs Toward Green Electronics

To reduce the impact of E-waste on the environment, there is a need to develop electronic products that leave minimum footprints on earth at the end of their lifespan. Organic and flexible electronics technology offers advantages over conventional electronics on this aspect with the possibility of fabrication on unconventional substrates

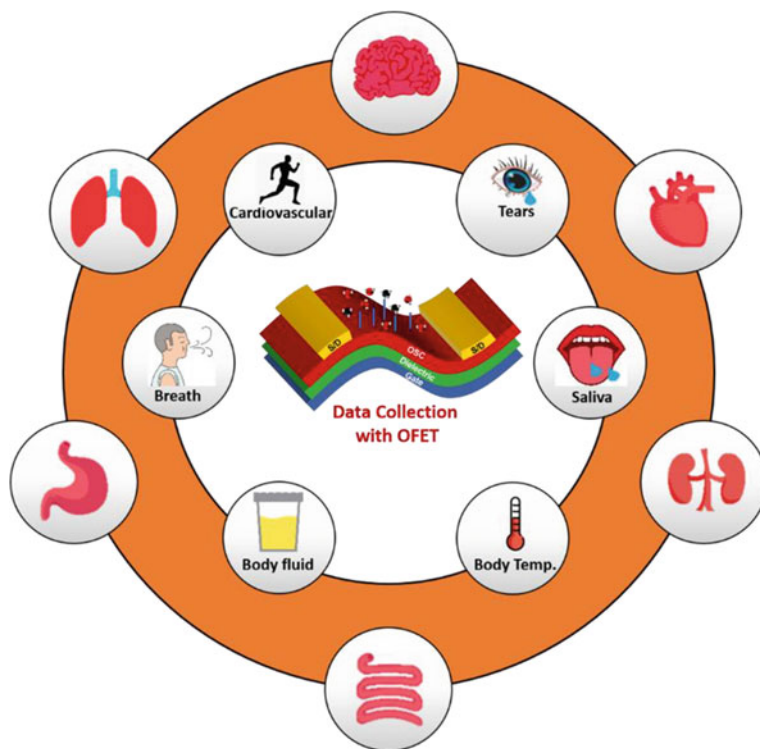


Fig. 5 OFET as sensor for detecting various body analytes

and using materials that can have biodegradable nature. In recent years, various biocompatible and biodegradable materials like natural proteins have been used for high-performance OFETs. The materials if used properly can simplify the OFET fabrication process, reduce the production cost, and improve the performance of the devices. Along with biodegradable nature, natural proteins have unique properties that are difficult to achieve through conventional organic and inorganic insulating materials. Some of the natural proteins used for high-performance OFETs are silk fibroin, chicken albumen, cross-linked DNA, collagen, etc. [44–51]. Among these, gelatin is another low-cost natural protein used for high-performance OFETs with vacuum evaporated p-type semiconductors, and it can easily be extracted from bone, skin, cartilage, and connective tissues [52–54]. Gelatin is most commonly used in capsules for oral drug ingestion. It is biocompatible and biodegradable. Electronic devices built with hard gelatin may be easily ingested for various specific biomedical applications targeting short interrogation time, utilizing the biodegradable nature. Gelatin films are hydrophobic in nature but have the unique property that even a small amount of water molecules absorbed can change the electrical properties of OFETs hugely. The device formed with such biodegradable and highly sensitive material

can be used to sense stimuli like human breath and the devices can be used in real-time health monitoring systems along with the advantage of biodegradability [55]. In the futuristic approach of organic electronics, the idea is to develop healthcare electronics along with reducing electronic waste. To fulfill the purpose, the materials inspired by nature which will have the biocompatible nature and the processes that are environmentally friendly should be used for the purpose. For example, polylactide is one of the material from nature and is obtained by natural plant sugars and is also approved by food and drug administration. It has a biodegradable nature and its derivatives are used in flexible substrates and/or dielectrics [56]. Silk fibroin is another splendid material that comes from nature and is a resource obtained from domesticated silkworms. It is one of the strongest fibers in need and has a very high dielectric constant, thus these natural dielectrics can be used in OFETs. The nature-inspired materials not only serve as substrate or dielectric but their biodegradable nature also helps in reducing electronic waste.

4 Summary

Flexible electronics is an emerging technology that offers ways to replace conventional electronic devices and the technology refers to the devices that can be bent, rolled, or folded without losing the functionality. Flexible electronics have a wide product range with low production costs, low energy consumption, and environmentally friendly processes. The basic building blocks for the said technology are the organic field-effect transistors and researchers around the globe are working on achieving high performance in these devices, and significant endeavors have been made by the researchers in the last few decades that today the best performing OFETs outperform the widely used amorphous silicon transistors. In addition, specific research is focusing on developing OFETs for smart health monitoring systems. The research in this domain focuses on developing sensors that can detect variation in human body homeostasis and store the information. It is an ideal type of device for sensing due to the diverse functional materials used for various sensing functions. A large number of sensing devices based on organic FETs have been reported that can detect chemical, pressure, biological, or photosignals. Flexibility is one of the core requirements of these devices when used in wearable sensors as these devices need to be placed in scenarios where the working conditions confront unusual external interferences. Organic FETs are the best replacement for the conventional FETs in applications where moderate electrical performance is required along with the additional feature of flexibility, low cost, and biodegradability.

References

1. Moore, G.: Cramming more components onto integrated circuits, **86**, 82–85 (1998)
2. Akamatu, H., Inokuchi, H., Matsunaga, Y.: Electrical conductivity of the perylene-bromine complex. *Nature* **173**, 168–169 (1954)
3. Gutman, F., Lyons, L.E.: *Organic Semiconductors*. Wiley, New York (1967)
4. McNeill, R., Siudak, R., Wardlaw, J.H., Weiss, D.E.: Electronic conduction in polymers. I. The chemical structure of polypyrrole. *Aust. J. Chem.* **16**, 1056–1075 (1963)
5. Pope, M., Kallmann, H.P., Magnante, P.J.: Electroluminescence in organic crystals. *J. Chem. Phys.* **38**, 2042–2043 (1963)
6. Little, W.A.: Superconductivity at room temperature. *Sci. Am.* **212**, 21–27 (1965)
7. Little, W.A.: Possibility of synthesizing an organic superconductor. *Phys. Rev.* **134**, A1416–A1424 (1964)
8. Chiang, C.K., Fincher, C.R., Jr., Park, Y.W., Heeger, A.J., Shirakawa, H., Louis, E.J., Gau, S.C., MacDiarmid, A.G.: Electrical conductivity in doped polyacetylene. *Phys. Rev. Lett.* **39**, 1098 (1977)
9. Shirakawa, H., Louis, E.J., MacDiarmid, A.G., Chiang, C.K., Heeger, A.J.: Synthesis of electrically conducting organic polymers: halogen derivatives of polyacetylene, (Ch) X. *J. Chem. Soc. Chem. Commun.* 578–580 (1977)
10. Tang, C.W., VanSlyke, S.A.: Organic electroluminescent diodes. *Appl. Phys. Lett.* **51**, 913–915 (1987)
11. Tang, C.W., VanSlyke, S.A., Chen, C.H.: Electroluminescence of doped organic thin films. *J. Appl. Phys.* **65**, 3610–3616 (1989)
12. Koezuka, H., Tsumura, A., Ando, T.: Field-effect transistor with polythiophene thin film. *Synth. Met.* **18**, 699–704 (1987)
13. Tsumura, A., Koezuka, H., Ando, T.: Polythiophene field-effect transistor: its characteristics and operation mechanism. *Synth. Met.* **25**, 11–23 (1988)
14. Garnier, F., Horowitz, G., Peng, X., Fichou, D.: An all-organic “soft” thin film transistor with very high carrier mobility. *Adv. Mater.* **2**, 592–594 (1990)
15. Burroughes, J.H., Bradley, D.D.C., Brown, A.R., Marks, R.N., Mackay, K., Friend, R.H., Burns, P.L., Holmes, A.B.: Light-emitting diodes based on conjugated polymers. *Nature* **347**, 539–541 (1990)
16. Mannsfeld, S.C.B., Tee, B.C.K., Stoltenberg, R.M., Chen, C.V.H.H., Barman, S., Muir, B.V.O., Sokolov, A.N., Reese, C., Bao, Z.: Highly sensitive flexible pressure sensors with microstructured rubber dielectric layers. *Nat. Mater.* **9**, 859–864 (2010)
17. Meager, I., Nikolka, M., Schroeder, B.C., Nielsen, C.B., Planells, M., Bronstein, H., Rumer, J.W., James, D.I., Ashraf, R.S., Sadhanala, A.: Thieno [3, 2-B] thiophene flanked isoindigo polymers for high performance ambipolar ofet applications. *Adv. Func. Mater.* **24**, 7109–7115 (2014)
18. Di, C.A., Zhang, F., Zhu, D.: Multi-functional integration of organic field-effect transistors (Ofets): advances and perspectives. *Adv. Mater.* **25**, 313–330 (2013)
19. Khim, D., Han, H., Baeg, K.J., Kim, J., Kwak, S.W., Kim, D.Y., Noh, Y.Y.: Simple bar-coating process for large-area, high-performance organic field-effect transistors and ambipolar complementary integrated circuits. *Adv. Mater.* **25**, 4302–4308 (2013)
20. Li, M., Mangalore, D.K., Zhao, J., Carpenter, J.H., Yan, H., Ade, H., Yan, H., Müllen, K., Blom, P.W.M., Pisula, W.: Integrated circuits based on conjugated polymer monolayer. *Nat. Commun.* **9**, 1–8 (2018)
21. Liu, J., Chen, S., Qian, D., Gautam, B., Yang, G., Zhao, J., Bergqvist, J., Zhang, F., Ma, W., Ade, H.: Fast charge separation in a non-fullerene organic solar cell with a small driving force. *Nat. Energy* **1**, 1–7 (2016)
22. Chen, Y., Ye, P., Zhu, Z.G., Wang, X., Yang, L., Xu, X., Wu, X., Dong, T., Zhang, H., Hou, J.: Achieving high-performance ternary organic solar cells through tuning acceptor alloy. *Adv. Mater.* **29**, 1603154 (2017)

23. Ng, T.N., Wong, W.S., Chabinyk, M.L., Sambandan, S., Street, R.A.: Flexible image sensor array with bulk heterojunction organic photodiode. *Appl. Phys. Lett.* **92**, 191 (2008)
24. Rauch, T., Böberl, M., Tedde, S.F., Fürst, J., Kovalenko, M.V., Hesser, G., Lemmer, U., Heiss, W., Hayden, O.: Near-infrared imaging with quantum-dot-sensitized organic photodiodes. *Nat. Photon.* **3**, 332 (2009)
25. Lamprecht, B., Thünauer, R., Ostermann, M., Jakopic, G., Leising, G.: Organic photodiodes on newspaper. *Physica Status Solidi (a)* **202**, R50–R52 (2005)
26. Gaal, M., Gadermaier, C., Plank, H., Moderegger, E., Pogantsch, A., Leising, G., List, E.J.W.: Imprinted conjugated polymer laser. *Adv. Mater.* **15**, 1165–1167 (2003)
27. Myny, K., Steudel, S., Smout, S., Vicca, P., Furthner, F., Van Der Putten, B., Tripathi, A.K., Gelinck, G., Genoe, J., Dehaene, W.: *Org. Electron* **11**, 1176–1179 (2010)
28. Dodabalapur, A., Bao, Z., Makhija, A., Laquindanum, J.G., Raju, V.R., Feng, Y., Katz, H.E., Rogers, J.: Organic smart pixels. *Appl. Phys. Lett.* **73**, 142–144 (1998)
29. Sirringhaus, H., Tessler, N., Friend, R.H.: Integrated optoelectronic devices based on conjugated polymers. *Science* **280**, 1741–1744 (1998)
30. Tang, C.W.: Two-layer organic photovoltaic cell. *Appl. Phys. Lett.* **48**, 183–185 (1986)
31. Wu, H., Shevlin, S.A., Meng, Q., Guo, W., Meng, Y., Lu, K., Wei, Z., Guo, Z.: Flexible and binder-free organic cathode for high-performance lithium-ion batteries. *Adv. Mater.* **26**, 3338–3343 (2014)
32. Sekitani, T., Yokota, T., Zschieschang, U., Klauk, H., Bauer, S., Takeuchi, K., Takamiya, M., Sakurai, T., Someya, T.: Organic nonvolatile memory transistors for flexible sensor arrays. *Science* **326**, 1516–1519 (2009)
33. Zang, Y., Huang, D., Di, C.A., Zhu, D.: Device engineered organic transistors for flexible sensing applications. *Adv. Mater.* **28**, 4549–4555 (2016)
34. 3DPI Webpage <https://3dprintingindustry.com/news/3d-printing-stock-pe-40-meet-mgi-23869/>. Last accessed on 21 Oct 2020
35. Hwang, D.K., Fuentes-Hernandez, C., Kim, J.B., Potscavage, W.J., Jr., Kippelen, B.: Flexible and stable solution-processed organic field-effect transistors. *Org. Electron.* **12**, 1108–1113 (2011)
36. Raghuwanshi, V., Bharti, D., Tiwari, S.P.: Flexible organic field-effect transistors with tips-pentacene crystals exhibiting high electrical stability upon bending. *Org. Electron.* **31**, 177–182 (2016)
37. Ding, L., Zhao, J., Huang, Y., Tang, W., Chen, S., Guo, X.: Flexible-blade coating of small molecule organic semiconductor for low voltage organic field effect transistor. *IEEE Electron Device Lett.* **38**, 338–340 (2017)
38. Yu, X., Zhou, N., Han, S., Lin, H., Buchholz, D.B., Yu, J., Chang, R.P.H., Marks, T.J., Facchetti, A.: Flexible spray-coated tips-pentacene organic thin-film transistors as ammonia gas sensors. *J. Mater. Chem. C* **1**, 6532–6535 (2013)
39. Bharti, D., Raghuwanshi, V., Varun, I., Mahato, A.K., Tiwari, S.P.: High performance and electro-mechanical stability in small molecule: polymer blend flexible organic field-effect transistors. *IEEE Electron Device Lett.* **37**, 1215–1218 (2016)
40. Onojima, N., Akiyama, N., Mori, Y., Sugai, T., Obata, S.: Small molecule/polymer blends prepared by environmentally-friendly process for mechanically-stable flexible organic field-effect transistors. *Org. Electron.* **78**, 105597 (2020)
41. Raghuwanshi, V., Bharti, D., Mahato, A.K., Varun, I., Tiwari, S.P.: Operationally stable organic fet's with bilayer dielectrics on low-cost flexible polyimide substrate. *IEEE Trans. Electron Devices* **66**, 4915–4920 (2019)
42. Wang, C.-Y., Fuentes-Hernandez, C., Liu, J.-C., Dindar, A., Choi, S., Youngblood, J.P., Moon, R.J., Kippelen, B.: Stable low-voltage operation top-gate organic field-effect transistors on cellulose nanocrystal substrates. *ACS Appl. Mater. Interfaces* **7**, 4804–4808 (2015)
43. Raghuwanshi, V., Bharti, D., Mahato, A.K., Varun, I., Tiwari, S.P.: Solution-processed organic field-effect transistors with high performance and stability on paper substrates. *ACS Appl. Mater. Interfaces* **11**, 8357–8364 (2019)

44. Chang, J.-W., Wang, C.-G., Huang, C.-Y., Tsai, T.-D., Guo, T.-F., Wen, T.-C.: Chicken albumen dielectrics in organic field-effect transistors. *Adv. Mater.* **23**, 4077–4081 (2011)
45. Wang, C.-H., Hsieh, C.-Y., Hwang, J.-C.: Flexible organic thin-film transistors with silk fibroin as the gate dielectric. *Adv. Mater.* **23**, 1630–1634 (2011)
46. Kim, Y.S., Jung, K.H., Lee, U.R., Kim, K.H., Hoang, M.H., Jin, J.-I., Choi, D.H.: High-mobility bio-organic field effect transistors with photoreactive Dnas as gate insulators. *Appl. Phys. Lett.* **96**, 103307 (2010)
47. Hsieh, C.-Y., Hwang, J.-C., Chang, T.-H., Li, J.-Y., Chen, S.-H., Mao, L.-K., Tsai, L.-S., Chueh, Y.-L., Lyu, P.-C., Hsu, S.S.H.: Enhanced mobility of organic thin film transistors by water absorption of collagen hydrolysate gate dielectric. *Appl. Phys. Lett.* **103**, 023303 (2013)
48. Ko, J., Nguyen, L.T.H., Surendran, A., Tan, B.Y., Ng, K.W., Leong, W.L.: Human hair keratin for biocompatible flexible and transient electronic devices. *ACS Appl. Mater. Interfaces* **9**, 43004–43012 (2017)
49. Zhu, B., Wang, H., Leow, W.R., Cai, Y., Loh, X.J., Han, M.-Y., Chen, X.: Silk fibroin for flexible electronic devices. *Adv. Mater.* **28**, 4250–4265 (2016)
50. Tsai, L.-S., Hwang, J.-C., Lee, C.-Y., Lin, Y.-T., Tsai, C.-L., Chang, T.-H., Chueh, Y.-L., Meng, H.-F.: Solution-based silk fibroin dielectric in N-Type C60 organic field-effect transistors: mobility enhancement by the pentacene interlayer. *Appl. Phys. Lett.* **103**, 233304 (2013)
51. Lee, J.H., Kwak, H.W., Park, M.H., Hwang, J., Kim, J.W., Jang, H.W., Jin, H.-J., Lee, W.H.: Understanding hydroscopic properties of silk fibroin and its use as a gate-dielectric in organic field-effect transistors. *Org. Electron.* **59**, 213–219 (2018)
52. Lee, C., Chang, Y., Wang, L., Wang, Y.: Biodegradable materials for organic field-effect transistors on a paper substrate. *IEEE Electron Device Lett.* **40**, 236–239 (2019)
53. Mao, L.-K., Hwang, J.-C., Chang, T.-H., Hsieh, C.-Y., Tsai, L.-S., Chueh, Y.-L., Hsu, S.S.H., Lyu, P.-C., Liu, T.-J.: Pentacene organic thin-film transistors with solution-based Gelatin dielectric. *Org. Electron.* **14**, 1170–1176 (2013)
54. Mao, L.-K., Hwang, J.-C., Tsai, J.-C.: Operation voltage reduction and gain enhancement in organic Cmos inverters with the Ttc/Gelatin bilayer dielectric. *Org. Electron.* **16**, 221–226 (2015)
55. Raghuvanshi, V., Saxena, P., Rahi, S., Mahato, A.K., Varun, I., Tiwari, S.P.J.A.A.E.M.: Solution processed flexible organic field-effect transistors with biodegradable gelatin as dielectric layer: an approach towards biodegradable systems (2020)
56. Bettinger, C.J., Bao, Z.: Organic thin-film transistors fabricated on resorbable biomaterial substrates. *Adv. Mater.* **22**, 651–655 (2010)

Chapter 15

Methods for Surface Superfinishing of Prosthesis



Atul Singh Rajput, Sajan Kapil, and Manas Das

1 Introduction

The continuous upsurge in modern people's living patterns and faster growth of medical sciences consequence in an extended life span. However, the human living machine hasn't been designed for so long period. Our sinews, linkages of bones, "pumps" and "hinges" are subject to wear. As a consequence of a person's movement, significant tension is applied to his joints and spine. At a higher age, due to wrong postures and heavy workload, wear in the joints starts. These fallouts in inflammatory situations and, common in old age human beings, require medical involvement by implanting prostheses [1–4]. However, the implantation technique in medical science was introduced in the first half of the twentieth century, and a few of the prostheses are shown in Fig. 1.

These prostheses are produced with the help of different machining operations such as milling and turning. The friction associated with the tool and workpiece's relative movement leads to micro-cutting marks. Friction also causes heat emission, which changes the metallurgical properties of the workpiece and generates residual stresses. The tensile residual stresses may cause micro-cracks at the topmost layer of the workpiece surface. These micro-cracks may lead to the failure of the prosthesis [5]. After the machining period's culmination, prostheses are exposed to polishing or grinding to improve surface quality. However, the grinding operation may fail

A. S. Rajput · S. Kapil · M. Das (✉)

Department of Mechanical Engineering, Indian Institute of Technology Guwahati, Guwahati, India

e-mail: manasdas@iitg.ac.in

A. S. Rajput

e-mail: atulsingh@iitg.ac.in

S. Kapil

e-mail: sajan.kapil@iitg.ac.in

© The Author(s), under exclusive license to Springer Nature Singapore Pte Ltd. 2022

335

S. N. Joshi and P. Chandra (eds.), *Advanced Micro- and Nano-manufacturing*

Technologies, Materials Horizons: From Nature to Nanomaterials,

https://doi.org/10.1007/978-981-16-3645-5_15

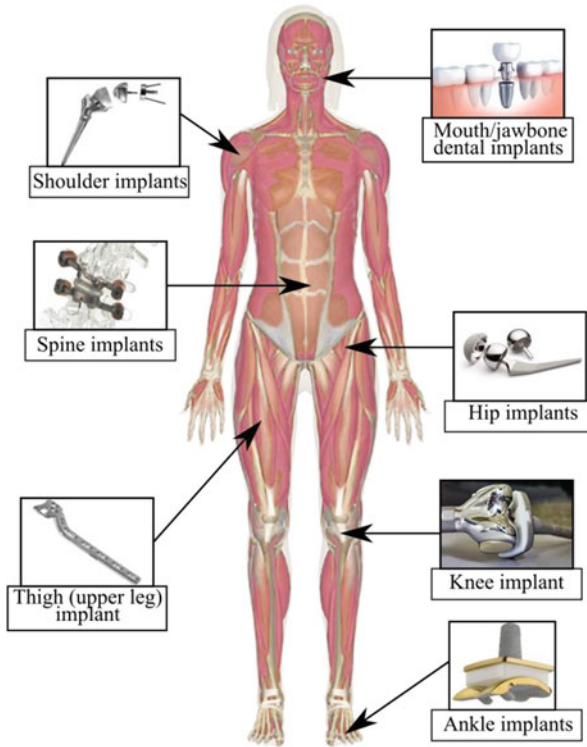


Fig. 1 Biomedical prostheses for different body parts

to eliminate these micro-cracks. Because of these unfavorable conditions, the prosthesis is subjected to quicker wear, leading to a reduced life span [6]. For many reasons, grinding followed by a polishing operation such as electropolishing, chemical–mechanical polishing, and abrasive flow finishing seems favorable. The unevenness attained employing polishing is considerably lesser than grinding, leading to a reduction in the friction and upsurge in the product life. A better carrying ratio can be achieved in polishing as compared to grinding, which generates low wear and tear on the interfacing surface. Further, the polishing operations provide a better corrosion resistance.

In Total Hip Arthroplasty (THA), metal on polyethylene is the most common prosthesis type. Several studies were also made to develop some other kind of bearing couple, including ceramic on polyethylene, ceramic on ceramic, and metal on metal. The wear rate in metal on metal was lower than metal on polyethylene [7]. It is observed that the wear rate in the case of metal-on-metal bearing couple is low, with minimal debris size; hence, the number of debris produced is very high as compared with other bearing couples [8]. These small metal particles cause Aseptic losing or Adverse Reactions to Metal Debris (ARMD), which may instigate Pseudotumours

or Aseptic Lymphocytic Vasculitis and Associated Lesions (ALVAL), metal hypersensitivity, and inflammatory masses [9, 10]. Metal hypersensitivity can also occur. Lower wear and osteolysis were found in ceramic on ceramic bearing and ceramic on polyethylene compared with metal-on-polyethylene bearing in some long-term studies [11, 12]. In the ceramic-based bearing couple's case, the debris particles' size is in the nanometer range. Still, their adverse effect on the human body is relatively less compared with the metal-based bearing couple. However, ceramics are expensive, brittle, so fracture risk increases, sensitive to component mal-positioning, which may cause impingement damage and edge loading wear [13, 14]. High pitched sounds were also reported in the case of ceramic prostheses [15]. A 930 random hip prosthesis study found that the metal-on-metal bearing couple's survival rate is 96.8%, which is higher compared with metal-on-polyethylene bearing couples [16].

Several experiments are performed to find the relation between the wear rate and the prostheses' surface roughness. It was noticed that if the initial surface roughness is high, then wear will be increased in the prostheses. Dowson et al. [17] formulated mathematical modeling, which describes the relation between wear and tear factor (k) with surface roughness as shown in Eq. 1.

$$k = a(R_a)^b \quad (1)$$

where R_a is the average of the peaks and valleys generated during the finishing of the surface, a and b are material-dependent constant. For stainless steel sliding against polyethylene, the value of a and b is 4×10^{-5} and 1.2, respectively. Wang et al. [18] have established a theoretical relation between wear per cycle, $\frac{\Delta V}{N}$ and surface roughness as shown in Eq. 2,

$$\frac{\Delta V}{N} \propto L^{1.5} R_a^{1.5} \frac{1}{\sigma_u^{1.5} \epsilon_u} \quad (2)$$

where the load is defined by L , ultimate tensile strength is determined by σ_u and elongation of the material at failure is defined as ϵ_u . This relation shows that the surface roughness (R_a) has a significant contribution over wear. Several experiments were performed regarding prosthesis's in vivo surface degradation [19–24]. It has been noticed that surface quality is a prime concern irrespective of the different mechanisms used to engage the joints with the femoral head or the kind of metal used to manufacture the femoral head [23]. However, to enhance the prosthesis's surface quality, an appropriate surface superfinishing process is required. A detailed analysis of the surface superfinishing processes existing for the prosthesis is provided in the subsequent sections.

2 Surface Superfinishing Operations for Prostheses

Various surface finishing processes were developed from the last few decades such as *Magnetorheological Fluid Assisted Finishing (MFAF)*, *Abrasive Flow Finishing (AFM)*, *Electropolishing (EP)*, *Large Area Electron Beam (LAEB) irradiation*, *Electrolytic in-process dressing (ELID)*, *Grinding*, and *Chemical–Mechanical Polishing (CMP)* to provide better surface quality for prostheses. However, the energy utilized to perform the surface finishing for different techniques depends upon the processes' requirement. Electrical energy is required to achieve improved surface quality with high material removal rate, whereas to achieve enhanced biocompatibility of the prosthesis, mechanical and chemical energy is utilized. Hence, these surface superfinishing processes can be classified based on energy used, as shown in Fig. 2. In this section, a detailed discussion is made on the mechanism involved during these surface finishing processes. However, these finishing processes' key capabilities are also discussed along with their limitations, and a comparative study is made to provide an overview at a glance.

2.1 Magnetorheological Fluid Assisted Finishing Processes

The major challenge in the field of surface finishing of prostheses is to achieve high surface quality without affecting the topography of the prosthesis's material; one of the remedies to this problem is the utilization of magnetorheological (MR) fluid in the surface finishing operation. The smart behavior of MR fluid helps to get the unbonded form of the polishing tool, which aid in providing high surface quality without ruining the surface contour. Different MFAF processes were developed in the last few decades to provide better surface quality to the prostheses.

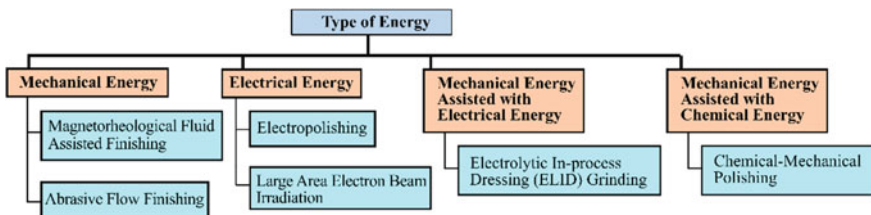


Fig. 2 Different finishing processes based on the utilization of energy

2.1.1 Magnetorheological Fluid (MR Fluid)

MFAF process uses the MR fluid's rheological properties to enhance the surface quality of the prosthesis. First time MR fluid was introduced at the *National Aeronautics and Space Administration (NASA)* to utilize its property to carry fuel in gravity-free space. However, MR fluid composed of abrasives and metal powder circulated in the viscoelastic plastic solid base of carrier fluid [25–30]. As MR fluid comes under the impact of external magnetic fluxes, magnetic particles arranged themselves in a chain-like structure in which abrasives were embedded in between them. This supple act of magnetorheological fluid is functional to regulate the different forces exerted during the polishing process and perform the surface finishing operation [31]. However, initially, MFAF enhances the brittle material's surface quality, such as glass and quartz [32]. With further development in the MFAF process, the surface quality of ductile materials such as stainless steel and copper also gets enhanced. The following analytical model can describe the MR fluid's behavior under the external magnetic field's influence.

Bingham plasticity model

This model is used to determine the shear stress exerted by MR fluid under the influence of external magnetic field and can be represented as the function of magnetic field strength as shown in Eqs. (3) and (4) [33].

$$\tau = \tau_0(H) \operatorname{sgn}(\dot{\gamma}) + \eta\dot{\gamma}; |\tau| > |\dot{\tau}| \quad (3)$$

$$\tau = 0; |\tau| < |\dot{\tau}| \quad (4)$$

where yield stress generated in an external field is defined as τ_0 , the shear strain rate is termed as $\dot{\gamma}$; external field strength is termed as H , the slope of the curve in the Bingham plastic model is defined as η . The modes through which MR fluid assists in the surface finishing process are as follows:

Flow mode: Utilization of constant velocity flow of MR fluid to finish workpiece; this mode is used in *Magnetorheological Abrasive Flow Finishing (MRAFF)* and *Rotational-Magnetorheological Abrasive Flow Finishing (R-MRAFF)*.

Squeeze mode: Concentrated and focused magnetic field is used to squeeze the MR fluid between the magnet and workpiece and used as a finishing tool; this mode is used in *Ball End Magnetorheological Finishing (BEMRF)*, or *Magnetic Field Assisted Finishing (MFAF) process*.

2.1.2 MRAFF and R-MRAFF

MRAFF is used to provide a uniform surface roughness to the prostheses with the aid of MR fluid. Jha and Jain developed the MRAFF process in 2004 [34]; it is

a hybrid process that utilizes the benefits of *Abrasive Flow Finishing (AFF)* and *Magnetorheological Finishing (MRF)*. Herein, the MR fluid's reciprocating motion is generated through pistons' synchronized action, which helps to create the shear stresses required to plow out the materials from the workpiece and provide better surface quality. The magnetic field is provided in the region where the workpiece is placed, and other areas were kept unaffected. However, to increase the efficiency and effectiveness of the MRAFF process, Das and Jain developed R-MRAFF process; this process's working principle is very much similar to the MRAFF process. In R-MRAFF [35], the magnet fixture is rotated to increase an abrasive impact during the finishing operation [36]. With the increase in the effectiveness of abrasive particles, surface finishing time reduces. The surface finishing time obtained while finishing knee joint prosthesis made of Co-Cr alloy was 2 hours through R-MRAFF [37]. However, through the MRAFF process, the surface finishing time was 64.7 hours. Satish et al. [38] performed some finishing operations on the knee joint prosthesis made of stainless steel and achieved a surface roughness (R_a) of 35 nm, as shown in Fig. 3. It was observed that in the case of R-MRAFF, to achieve uniform surface quality, the constant velocity of MR fluid is crucial along with constant magnetic field distribution. However, to achieve a constant MR fluid velocity, a flow restrictor is provided. Nagdeve et al. [39] use a negative replica of the outer surface of knee joint prosthesis as a flow restrictor to achieve surface roughness (R_a) of 25 nm during the surface finishing operation with the least standard deviation (1.04–1.87) on all four faces of the knee joint. However, alteration in the workpiece fixture design is required with a slight change in the workpiece shape, which is a big drawback of the MR fluid (flow mode) based finishing processes (Fig. 4).

2.1.3 Magnetorheological Ball End Finishing Process (BEMRF)

To overcome the problem associated with the MR fluid's flow mode, a squeeze mode-based finishing process was developed. Herein, a concentrated and focused

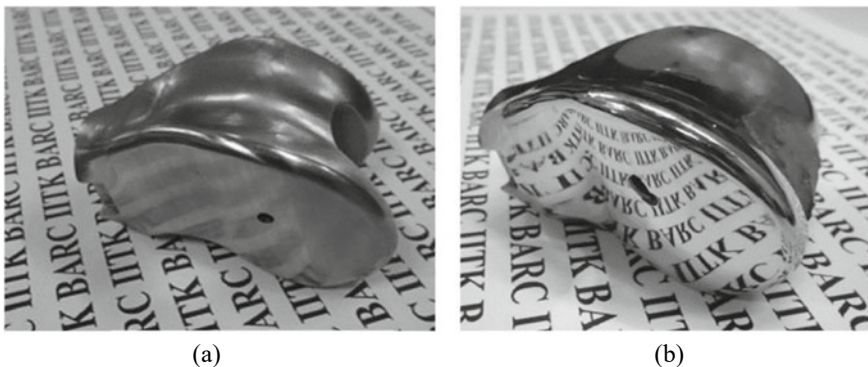
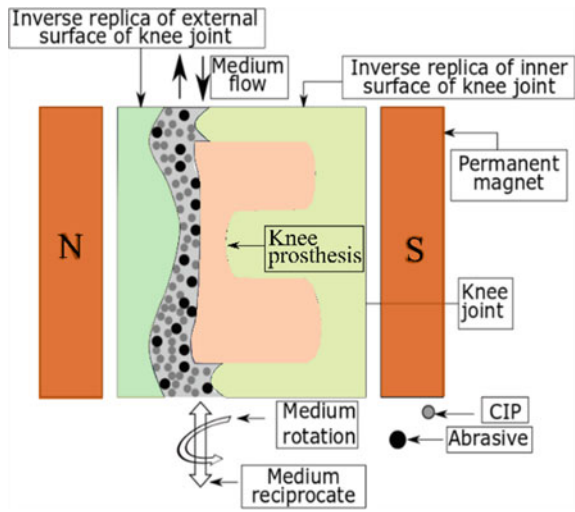


Fig. 3 Knee joint prosthesis **a** before polishing, **b** after polishing [38]

Fig. 4 Workpiece fixture for knee prosthesis in R-MRAFF; Inner workpiece fixture as an inner replica of knee joint prosthesis, outer workpiece fixture with an outer replica of knee joint prosthesis [40]



magnetic field is used to squeeze the MR fluid between the magnet and workpiece and is applied as a finishing tool. The magnetic field can be generated with the help of a permanent magnet or electromagnet. Singh et al. [41] developed the BEMRF process to finish 3D complex shapes; herein, the electromagnet is used to generate the magnetic field instead of a permanent magnet. Here, a semi-solid ball-shaped MR fluid at the electromagnet core’s tip is generated to perform finishing operations. The system controls the table’s motion in the X–Y direction, where the workpiece is placed, and the polishing tool motion is provided in the Z direction. MR fluid with different compositions is used to achieve a better surface quality, as shown in Table 1. To finish a semi-permanent implant (i.e., prostheses engaged in relative

Table 1 Compositions of MR fluids [42]

Constituents of MR fluid	MR fluid 1 (% by Vol.)	MR fluid 2 (% by Vol.)
Carbonyl Iron Particles (CIPs)	40	40
Abrasive (diamond)	7.1	7.1
Hydrogen peroxide (H ₂ O ₂)	–	1.3
Hydrofluoric acid (HF)	1.17	–
Deionized water	41.1	43.6
Nitric acid (HNO ₃)	2.33	–
Glycerol	8	8

motion with other body parts like the knee joint, hip joint, etc.), MR fluid 1 is suitable; it increases the hydrophilicity of prostheses. To finish a permanent implant, MR fluid 2 is advisable, as it increases the hydrophobicity of prostheses. Surface roughness (R_a) of 10 nm and 70 nm is achieved with MR fluids 1 and 2, respectively [42]. Furthermore, to analyze the effect of carrier fluid over the surface quality, water and oil-based MR fluid are examined. It was noticed that it is beneficial to use water-based MR fluid after performing with oil-based MR fluid. Water-based MR fluid removes the chemical layer generated during oil-based MR fluid finishing and provides a glaring surface, with surface roughness (R_a) of 28 nm on artificial knee joint [43].

During the BEMRF process, the normal force generated due to the magnetic field helps to indent the abrasive particles into the workpiece. Meanwhile, the shear force generated due to the polishing tool's rotation helps remove the workpiece's material and provide better surface quality. However, it was found that the impact of normal force over surface roughness is more significant than other forces. Meanwhile, a higher polishing tool's rotational speed leads to increased normal and shear force, caused by an increase in Coriolis force. However, a significant decrease in the normal and tangential force is noticed when the MR polishing tool's contact area with the workpiece decreases. However, with an increase in the feed rate of the workpiece and rotational speed of the tool over a specific limit, the CIP-chain-structure's strength decreases, leading to reduced surface quality [44]. While performing the surface finishing process on Ti alloy's knee prosthesis, the optimized process parameters and the output variable are listed in Table 2 [45]. BEMRF enhances the functionality, i.e., the knee joint prosthesis's condyle surface's wettability and tribological properties. With the assistance of the MR fluid, the dimensional accuracy of the condyle surface is maintained. Specified lays are also attained with extended cutting marks at 78.1° , 20.3° , and 5.7° as designed, shown in Fig. 5 [46]. A surface roughness (R_a) of 31.7 nm is obtained.

Table 2 Optimized process parameters [45]

Parameters	Values
Rotational speed of the tool	901 rpm
Working gap	0.6 mm
Surface finishing time	4.30 h
S_a	11.32 nm
S_{pk}	15.82 nm
S_k	6.51 nm
S_{vk}	41.1 nm

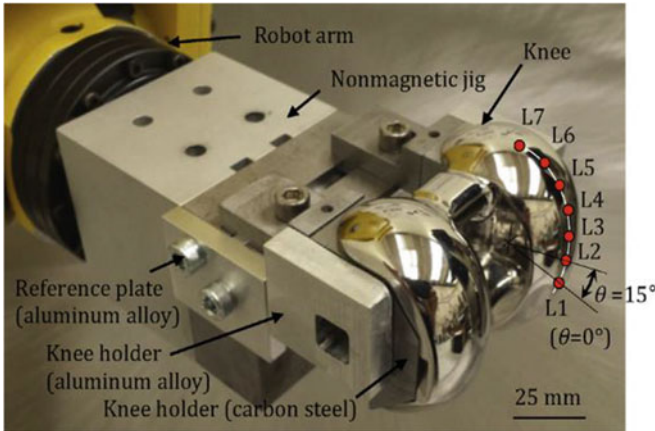


Fig. 5 Experimental setup for magnetic field analysis while finishing knee implant [46]

2.2 Abrasive Flow Finishing

In 1960, Extrude Hone Corporation, USA developed Abrasive Flow Finishing (AFF) process. In the initial development phase of AFF, three different experimental setups were established.

1. One-way Abrasive Flow Finishing [47]
2. Two-way Abrasive Flow Finishing [48]
3. Orbital Abrasive Flow Finishing [49].

Two-way Abrasive Flow Finishing is the most efficient one among all the variants. Herein, the workpiece is placed between two vertical cylinders, which are placed opposite to each other [50]. This two-cylinder movement is synchronized so that they always move in the opposite direction having the same velocity. Because of moving fluid, shear stress is generated in the workpiece's targeted region, where the surface finish is required. AFF is used to achieve a high surface finish on any freeform surfaces using the abrasive embedded medium having unique rheological properties. The abrasive embedded medium must have superior self-deformability, easy flowability, and well abrading ability.

With the assistant of AFF, the minimum removed layer thickness is around 1–10 μm , and surface roughness up to 50 nm can be attained with $\pm 0.5 \mu\text{m}$ tolerance. In AFF, tooling is crucial throughout this progression, as it is a fluidic medium; it is quite easy to finish inaccessible areas. It can generate factual round radii on intricate surfaces with a reduction of 70–90% of initial surface roughness. Although AFF upholds suppleness; it reduces the human efforts and time required to finish a prosthesis; produces uniform, precise and accurate products on an influential variety of surface finishing operations. The significant advantage of AFF, which distinguishes it from other finishing processes, is that with the proper design of workpiece fixture and varying process parameters, it is conceivable to control and select the strength





Faces	Initial R_a (nm)	Final R_a (nm)	% Reduction
 Face-1	187.5	46.6	75.15
 Face-2	192.4	47.3	75.42
 Face-3	184.8	42.9	72.86
 Face-4	186.1	50.5	72.86

Fig. 6 Surface roughness improvement of the knee implant at different faces

and position of abrasion. However, surface finishing operation is performed on the knee prosthesis and achieved a roughness (R_a) within 42.9–62.5 nm over different surfaces. During this process, the total reduction in the surface roughness was around 75% of its initial value, as illustrated in Fig. 6 [51].

Apart from prostheses, AFF is used to finish air cooling holes on a turbine disk, like dies and molds, aerospace, and automotive industries. However, to analyze the mechanism behind the surface finishing process, different analytical models were proposed. A linear relationship is noticed between shear stress applied on the prosthesis surface due to medium flow and material removal [52]. Meanwhile, a capillary rheometer is used to obtain the relationship between the polyborosiloxane medium's viscosity and wall shear stress. However, it was found that during the flow of medium through restricted areas (reduced cross-sectional area), its shear rate increases. Meanwhile, the polyborosiloxane medium's viscosity decreases with increased shear rate, leading to a rise in the material removal rate.

Similarly, with an increase in the piston stroke duration, finishing action increases due to higher wall shear stress [53]. To optimize the process parameters during AFF, neural network simulation forecasts workpiece surface quality and structural modification. Meanwhile, these neural network models are combined with a heuristic search algorithm to choose essential process parameters for AFF [54]. Lam and Smith [55, 56] practiced Cascade-Correlation neural network modeling; with this algorithm, the time required to achieve the desired output, i.e., the required workpiece surface finish, can be determined.

Apart from several advantages of the AFF process, some limitations are associated with it; the productivity is very low compared to other polishing techniques. The

time required to achieve the surface finish is high. To overcome these limitations and increase AFF efficiency, some hybridization is needed for this process [57–60].

2.3 Large Area Electron Beam Irradiation

Electron beam (EB) irradiation utilizes a focused energy source (electron beam) on the workpiece, which causes melting, evaporation, and solidification of the workpiece [61]. With high heat transfer due to the focused energy source, the phase of the material changes and provides enhanced mechanical properties, which cannot be attained by the available surface treatment processes [62]. This method was developed by Proskurovsky et al. in 1997 [63]; after that, lots of modifications were made in this experimental setup [64–66]. However, to enhance electron beam irradiation performance, *Large Area Electron Beam (LAEB) irradiation* is developed. Meanwhile, apart from the conventional electron beam irradiation performed in a vacuum, in LAEB irradiation, argon gas is provided inside the chamber with a pressure of $(5–15) \times 10^{-2}$ Pa before the experiment. Initially, with a solenoid coil's help, magnetic flux was created to beset the compartment's external surface. However, the pulse voltage is laden to the anode at the moment of maximum generated magnetic flux. Because of the peening effect, the electron is generated inside the chamber and moves in the anode direction. However, at the same time, the electron also moves spirally because of Lorentz's force. After the collision of these energized electrons with argon atoms present inside the chamber, argon atoms get ionized and create plasma near the anode [67].

Meanwhile, at the instant when the intensity of plasma is maximum, the pulse voltage is applied to the cathode. Consequently, because of the formation of a double electric layer at the cathode, electrons are accelerated by a high field. Then, EB with high energy density is exposed to the material. From the Langmuir equation, as shown in Eq. (5), the current density of EB can be calculated as

$$J_e = j_i \left(\frac{M}{m} \right)^{0.5} \quad (5)$$

where J_e represents the electron current density, J_i is the current density associated with ions, the mass of the ion defines M , and m is the electron's mass. However, it can be analyzed that with an increase in ion mass and ionic current density, the current density of EB increases. When an electron passes through the plasma region, Coulomb's force acting between them gets weaker, and consequently, the straightness of LAEB is frequently enhanced. Hence, plasma improves the effectiveness of LAEB. All through this system, a series of pulses are generated to cause EB irradiation. The surface quality of different orthopedic tools made of stainless steel was improved as shown in Fig. 7 with LAEB irradiation [68]. The surface quality variation was compared with varying quantities of pulses for various energy densities; it was found

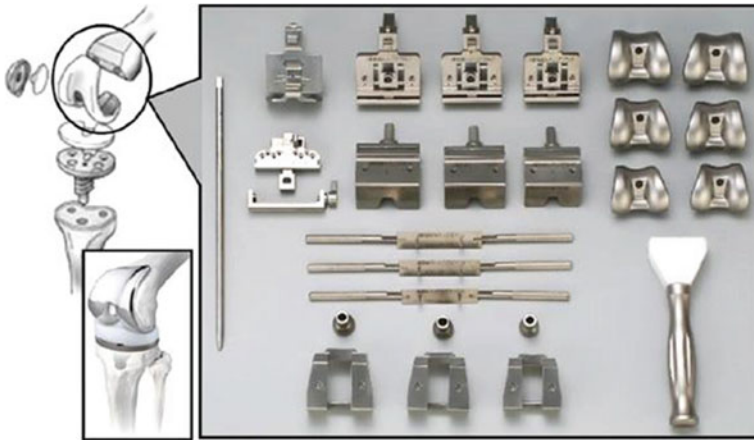


Fig. 7 Different parts of a knee prosthesis with surgical tools [68]

that with an upsurge in energy density, the surface quality of the prosthesis gets enhanced.

From different experiments, it was observed that with an increase in the electron beam's energy density, the prosthesis's surface quality and shininess improve. Meanwhile, by controlling the process parameters, the surface roughness between 10 and 1 μm can be achieved within few minutes by this process, which is infeasible by any other existing techniques. The material's corrosion resistance improves after finishing, and high surface finish and modification can be attained on bio-titanium alloy by LAEB irradiation [69].

The benefit of LAEB is that the time required to achieve better surface quality is relatively low; in a few minutes, the prosthesis's surface finish improves. The limitation of LAEB is that surface roughness can be improved up to 1 μm ; However, further improvement in the surface quality is impossible. Another problem associated with LAEB irradiation is the formation of the recast layer on the bio-titanium alloy after finishing.

2.4 Electropolishing

Electropolishing comprises of electrochemical reaction, which helps to reduce unevenness from the metallic surface at the micro-level by anodic dissolution. However, the potential difference applied between workpiece and tool generates an electric current, which leads to the formation of a viscous layer at the interface of electrolyte and workpiece. Meanwhile, at the peak of the unevenness on the material, the viscous layer is thinner and provides dissolution of the material at the micro-level. As a consequence of the phenomenon mentioned above, with a reduction in the surface's

coarseness, surface quality gets enhanced. The advantages of using electropolishing are easiness in automation and polishing multiple prostheses simultaneously. Hence, it is economically feasible with better surface quality and enhanced mechanical properties [70]. In mechanical polishing, normal stress is generated in the workpiece that initiates micro-cracks because of the mechanical action. The use of electropolishing overcomes this problem. This advantage of electropolishing is best suited for surface improvement of biological prostheses [71].

The electric current is supplied in the form of a pulse with different characteristics. The control module in the workbench controls the various parameters of electric current characteristics. More than one electrode is used to manage the surface finishing process better to enhance its efficiency. Graphite is often selected as the electrode because it does not dissolve under the electrolyte. Hence, it reduces the chance of electrolyte contamination [72]. Different electrolytes are examined to perform the surface finishing process on titanium alloys' biomedical components, as shown in Table 3 [73–79]. The selection of these electrolytes is based on their effectiveness, difficulties associated with the chemical composition, and easiness in process execution.

However, to perform finishing operations, materials having high hardness (Co-Cr alloys, Ti alloys), Perchloric acid, chromium oxide, and hydrofluoric acid are the most commonly used electrolytes [81]. These electrolytes are highly toxic or destructive. Often the circumstances essential to experiment are challenging to obtain. For example, some electrolytes need a negative temperature range, i.e., $-72\text{ }^{\circ}\text{C}$, to experiment. Meanwhile, for steel and titanium alloy, the maximum surface quality achieved with electropolishing is $0.05\text{--}0.15\text{ }\mu\text{m}$. Approximately 25–30% enhancement in the surface quality with the help of electropolishing was obtained on the prosthesis surface [82].

Shape error build-up in the material is associated with the electropolishing; to overcome this problem, two appropriately formed and located electrodes were used [83]. However, after surface finishing of the prosthesis, some uncomplimentary consequence of electrolytes is noticed on the finished surface, e.g., in electrolytes containing hydrofluoric acids, local defilement was observed while removing the prosthesis material. To eliminate the adverse effect, a suitable finishing and speedy extinction of the electrolyte action is required. Meanwhile, it was observed that the

Table 3 Different compositions of electrolytes to finish on Titanium alloy in biomedical components [80]

Electrolytes	1	2	3	4	5
H ₂ SO ₄	20–40%	–	60–65%	60%	–
HF	10–18%	160 ml	20–25%	30%	3–4%
HClO ₄	–	–	–	–	–
Other	CH ₃ COOH 42–62%	CrO ₃ 500 g, H ₂ O to 11	Glycerine 10–20%	Glycerine 10–20%	Ethylene glycol to 100%

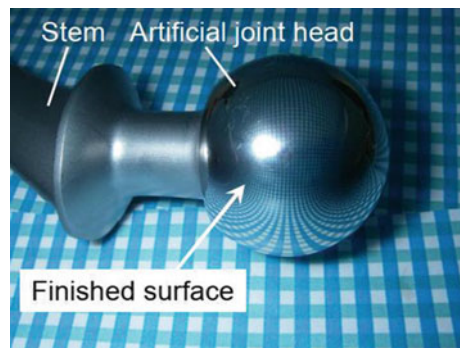
pulsed current's surface quality is better than the direct current in electropolishing. Because of the high surface quality obtained through electropolishing and the ability to finish multiple workpieces simultaneously, it is mostly suggested for biomedical prostheses' superfinishing [84]. However, because of the use of chemicals in electropolishing, a long-term impact can be seen on the finished surface.

2.5 Electrolytic In-Process Dressing (ELID) Grinding

In conventional fixed abrasive grinding, the wheel requires dressing before initiating grinding of the particular workpiece. However, this dressing aims to make sure that new sharp grit is protruding from the wheel surface. Meanwhile, Ohmori et al. [85] introduced Electrolytic In-process Dressing (ELID) as a significant improvement on this traditional method. Herein, continuous dressing of the wheel occurs during the grinding cycle. The axis of a metal-bonded abrasive wheel is connected to the electric power supply with a brush. One side of the wheel performs grinding on the prosthesis, while the opposite side undergoes electrochemical dressing inside a little gap (usually around 0.1 mm) crammed with alkaline liquids. These liquids generally serve both as electrolyte and coolant. The electrolytic reaction causes stripping of the metal bond, thus continuously revealing fresh and sharp grit, which will perform in the ductile regime. However, one of the biggest challenges of this process is controlling the grinding wheel's shape since the wheel diameter reduces continuously during machining. Nevertheless, ELID grinding has been tested with suitable materials and shapes (including freeform) of the workpiece [86].

Surface finishing operation is performed on biocompatible Co-Cr alloy to analyze its grinding characteristics and surface modifying effects. Co-Cr alloy is the most reliable material to produce biomedical prostheses because of its properties to resist corrosion, wear, and better biocompatibility. The final surface roughness (R_a) of a hip prosthesis achieved is 7 nm, as shown in Fig. 8 with the following process parameters and machining conditions [85]:

Fig. 8 Hip implant after ELID grinding [85]



- *Grinding Wheel*—8000 average grain size made of copper and chromium—diamond abrasive with resinoid hybrid bonding.
- *Grinding Fluid*—A chemical solution-based grinding fluid with 5% dilution of water and pH 8.2.
- *Process Parameters*—Rotational speed of wheel: 100 min^{-1} , Rotational speed of workpiece: 100 min^{-1} .
- *Electrical condition*—Pulse wave: square, pulse timing (on/off): $2/2 \text{ } \mu\text{s}$, Open voltage: 90 V.

Further investigation was made to analyze hip implants' biocompatibility on biological tissue through animal experiments, as shown in Fig. 9. It was found that ELID grinding is very useful and efficient for long-term living body safety [87]. The cytokines' concentration, the confrontation to implant pull out, and histopathology at the implant site was assessed. It was found that implants processed using the ELID method performed well compared to the other surface finishing processes [88].

The ELID grinding forms a diffused oxygen and carbon layer due to the biomaterial Ti alloy's electrochemical reaction. The modified layer causes improved surface characteristics, such as mechanical properties and corrosion resistance. Further improvement in the corrosion resistance through a hybrid process is proposed, i.e., ELID grinding/ thermal oxidation (TO) on Co-Cr-Mo alloy. It was observed that the oxide layer formed on the specimen through ELID grinding/ thermal oxidation hybrid process is thicker. Another advantage that comes out from ELID/TO process is that the percentage of cobalt within the specimen decreases, which reduces metal implant's corrosion level [89]. While experimenting on efficient-ground Alumina and zirconia ceramics used for dental application, the surface roughness (R_a) of 130 nm was achieved on glass-impregnated and sintered ceramics. While processing the prosthesis through ELID grinding, iron was not spotted in sintered and glass-impregnated ceramics. It was observed that sintered and glass-impregnated ceramics is more appropriate than semi sintered ceramics for dental prosthesis [90]. The problem associated with ELID grinding is to retain the grinding wheel shape accuracy throughout the finishing process.

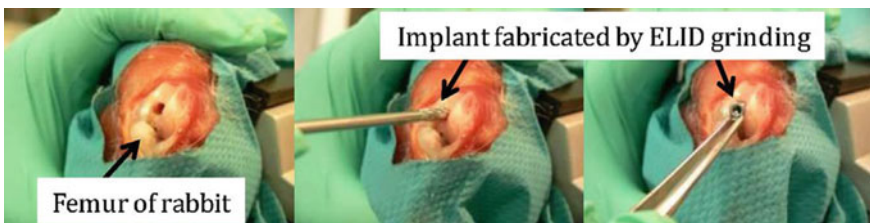


Fig. 9 Placing ELID grinding processed implant in animal [87]

2.6 Chemical Mechanical Polishing

Chemical mechanical polishing (CMP) was developed at IBM in 1986 to achieve the superfinishing on electronics materials made of silicon oxide. The first time this process was utilized to finish metal-based workpieces in 1988 [91]. Afterward, lots of efforts were made to improve this finishing process for several decades [92, 93]. In CMP, mechanical and chemical actions simultaneously improve the prosthesis's surface quality with an enhanced material removal rate [94]. Material removed from the prosthesis is in the form of micro-, nano-, or atomic level. Hence, any desired surface quality can be achieved with this finishing process with a controlled finishing rate as both mechanical forces in the form of abrasive polishing and chemical forces in the form of etching are responsible for material removal from prosthesis [95].

The CMP media is a colloidal solution of chemical slurry and abrasive, combined with a polishing pad and retaining ring, whose diameter is higher than the workpiece [96]. With the dynamic polishing head, the wafer and the pad were pressed together and placed undisturbed through the retaining ring. Rotational motion is provided to the dynamic polishing head with eccentric axes of rotation; because of this action, irregularity is removed from the workpiece surface, and surface quality is enhanced [97]. However, dimensional accuracy obtained through CMP during surface finishing of prostheses is high compared with other processes [98]. Basically, four different kinds of experimental setup were developed in the CMP process:

1. A wafer carrier assisted rotatory type polisher with an oscillation motion.
2. A carrier assisted rotatory type polisher with an oscillation motion.
3. A platen is having orbital motion in an orbital type polisher.
4. A linear motion polishing bed with a liner type polisher.

Meanwhile, different experiments were performed to determine the impact of oxidizer in CMP on Ti alloy's prosthesis. It was found that when 3–5 wt% of H_2O_2 (oxidizer) was added to the chemical slurry, the material removal rate of the prosthesis increases because of the formation of a passive oxide layer. This oxide layer also limits bacterial growth on the prosthesis surface, as shown in Fig. 10 [99, 100]. It is identified that the adhesion of bio-species on implant surface improves with the increased surface oxidation. Wettability, one of the crucial parameters to determine the prosthesis's better biocompatibility, is enhanced through the CMP [101]. However, the non-uniformity in the surface roughness produced through CMP is one of the primary concerns.

3 Selection of a Suitable Surface Superfinishing Process

The selection of an appropriate superfinishing process for a prosthesis mainly depends on the process's final achievable surface roughness with enhanced biocompatibility. However, the selection of the finishing process can be made based on surface finishing parameters and biocompatibility.

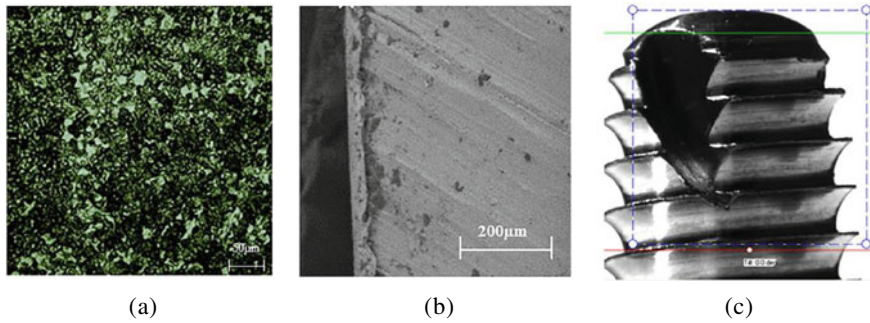


Fig. 10 Surface modification of titanium dental implant **a** SEM image showing the oxide layer to prevent the bacterial growth, **b** implant without any surface treatment, and **c** dental implant [100]

Surface finishing parameters

The output parameters required to perform well for a prosthesis mainly depend upon the surface finishing parameters such as minimum surface roughness that can be attained through the finishing process, surface finishing time to enhance the productivity, and uniformity of the surface roughness over the entire surface.

Biocompatibility

It is always essential to determine how a prosthesis will interact with the biological tissue after the implantation. The parameters that define a prosthesis's biocompatibility are (a) formation of an oxide layer on the prosthesis surface to prevent bacterial growth and (b) hydrophilicity or hydrophobicity to determine the prosthesis interaction with the biological tissue and corrosion resistance. The key capabilities of each surface superfinishing process with their limitations are listed in Table 4. However, a comparative study is made between different surface superfinishing processes based on these parameters and is demonstrated in Table 5.

4 Conclusions

Different super finishing techniques to enhance metallic prostheses' surface quality for enhanced functionality have been discussed in this chapter. It is essential to achieve a smooth finish surface for implant prostheses; otherwise, it may lead to Pseudotumours or Aseptic Lymphocytic Vasculitis and Associated Lesions (ALVAL), metal hypersensitivity, and inflammatory masses. However, from the study, it can be concluded that.

- *Magnetorheological Fluid Assisted Finishing (MFAF)* process can be used to enhance prostheses' roughness with close tolerances without damaging the surface integrity. The MFAF process can improve the surface roughness of freeform

Table 4 Key capabilities of various superfinishing process with their limitations

Process		Benefits	Limitations
MFAF	MRAFF and R-MRAFF	Almost uniform surface quality can be achieved	Every time change in the workpiece fixture is required with a slight change in the workpiece design
	BEMRF	Freeform surfaces can be finished	Low surface finishing rate
AFF		Provides uniform surface roughness throughout surface	Low productivity
LAEB Irradiation		Low surface finishing rate	Formation of recast layer on prostheses surface
EP		The surface quality of multiple prostheses can be enhanced simultaneously	Chemical reaction may ruin the surface quality
ELID grinding		Provides an oxide layer on the prosthesis's surface to limit the bacterial growth	Very difficult to enhance the surface quality of freeform surface
CMP		Highly smooth surface can be obtained	Low efficiency due to low surface finishing rates

surfaces of hard materials such as titanium, steel, and cobalt-chromium. However, for freeform surface finishing, a tool with higher degrees of freedom is required in the machinery. Meanwhile, different experimental setups are modified to accommodate the prostheses and enhance process performance.

- *Abrasive Flow Finishing (AFF)* process is feasible to control and select the intensity and position of abrasion, enhancing the surface quality of inaccessible areas and complex internal passages. However, low productivity is a primary concern in AFF.
- The surface finishing time required during *Large Area Electron Beam (LAEB) irradiation* is relatively low; in a few minutes, the prostheses' surface roughness improved. However, surface roughness can be improved up to 1 μm ; further improvement in the surface roughness is not possible with this process. Meanwhile, the formation of the recast layer on the prostheses surface is a significant drawback of LAEB.
- *Electropolishing (EP)* provides the benefits of enhancing the surface quality of multiple prostheses simultaneously. However, because of the use of chemicals used in electrolytes, a long-term impact can be seen on prostheses' finished surface.

Table 5 Overview of different surface superfinishing processes for prostheses

Serial no.	Energy required to finish	Magnetic field assisted finishing process		Abrasive flow finishing	Large area electron beam irradiation	Electropolishing	Electrolytic in-process dressing (ELID) grinding	Chemical–mechanical polishing	
		MRAFF and R-MRAFF	BEMRF-based finishing techniques						
1	Energy required to finish	Mechanical energy	Mechanical energy	Mechanical energy	Electrical energy	Electrical energy	Mechanical energy assisted with electrical energy	Mechanical energy assisted with chemical energy	
2	Surface Finishing parameters	Surface roughness (minimum)	10 nm	42.9 nm	Up to 1 µm	40.9 nm	7 nm	300 nm	
		Material removal rate	69.3 nm/h	32.5 nm/h	9.04 nm/h	2 µm/h	N.A	16 mm	20 nm/min
		Time required to finish	2.05 h	6.30 h	15 h	Few minutes	N.A	N.A	N.A
3	Biocompatibility	Surface accuracy	50 nm	19.6 nm	N.A	2.5 nm	16 nm	N.A	
		Formation of oxide layer to prevent bacterial growth	N.A	12.8 wt% enhanced	N.A	N.A	1.46 wt% enhanced	enhanced	enhanced
		Hydrophobicity/hydrophilicity	N.A	77.5° Hydrophilic in nature	N.A	74° blood repellency enhanced	70°	N.A	35° Hydrophilic in nature
	Corrosion resistance	N.A	Improved	N.A	Improved	Improved	Improved with improvement in cytotoxicity	0.049 (mm/year)	

(continued)

Table 5 (continued)

Serial no.	Workpiece		Type of prosthesis	Material	Magnetic field assisted finishing process		Abrasive flow finishing	Large area electron beam irradiation	Electropolishing	Electrolytic in-process dressing (ELID) grinding	Chemical–mechanical polishing
					MRAFF and R-MRAFF	BEMRF-based finishing techniques					
4					Knee joint	Knee joint	Knee joint	Knee joint	Bone plates	Hip joint	Dental implant
					Co-Cr–Mo alloy	Ti–6Al–4 V	Ti–6Al–4 V	Stainless steel	Ti–6Al–4 V	Co-Cr alloy	Ti alloy
5	Process parameters				Extrusion pressure, no. of finishing cycles, and rpm of magnet	Tool rpm, concentration of abrasive and CIPs, and working gap	Extrusion pressure, no. of finishing cycles, and mesh size of abrasive	Energy density and number of pulses	Electrode gap, electrolyte, and voltage	Rotational speed of wheel, and rotational speed of workpiece	Rotational speed of platen, and Concentration of H ₂ O ₂ in slurry
6	References				[37]	[45]	[51]	[68]	[102]	[85]	[97]

- *Chemical Mechanical Polishing (CMP)* can reduce the surface roughness to the nanometers. Still, it has certain disadvantages, i.e., low efficiency due to low removal rates, nonuniform surface finish due to the variation in relative cutting speed across the prosthesis surface, and relatively high cost involved in this process.
- *Electrolytic in-process dressing (ELID)* is an efficient method that eliminates wheel loading and glazing problems generated during the grinding process and provides an oxide layer on the prostheses surface to prevent bacterial growth. However, finishing operation on the freeform surface is very tough through this process.

Acknowledgements We acknowledge Science & Engineering Research Board (SERB), New Delhi, India, for financial support for project No. EEQ/2017/000597 entitled “Fabrication of Prosthetic Implants and further Nanofinishing Using Magnetic Field Assisted Finishing (MFAF) Process.”

References

1. Dental Implants Market Analysis | United States | COVID19 | 2021–2027|. [Online]. Available: <https://idataresearch.com/product/dental-implants-market-united-states/>. Accessed 22 Jan 2021
2. Total Hip Replacement—OrthoInfo—AAOS. [Online]. Available: <https://orthoinfo.aaos.org/en/treatment/total-hip-replacement/>. Accessed 27 Oct 2020
3. Total Knee Replacement—OrthoInfo—AAOS. [Online]. Available: <https://orthoinfo.aaos.org/en/treatment/total-knee-replacement/>. Accessed 22 Jan 2021
4. Kroemer, K.H.E.: Anthropometry and biomechanics: anthromechanics. In *Biomechanics in Ergonomics*, pp. 59–106. CRC Press (2007)
5. Nowicki, B.: Elektropolerowanie, W: Obróbka skrawaniem ścierna i erozyjna. In Dąbrowski, L., Marciniak, M., Nowicki, B. (Eds.) *Praca zbiorowa pod. Oficyna Wydawnicza Politechniki Warszawskiej Warszawa* (2001)
6. Zaborski, S., Sudzik, A., Wołyńiec, A.: Electrochemical polishing of total hip prostheses. *Arch. Civ. Mech. Eng.* **11**(4), 1053–1062 (2011)
7. Jacobsson, S.-A., Djerf, K., Wahlström, O.: 20-year results of McKee-Farrar versus Charnley prosthesis. *Clin. Orthop. Relat. Res.* **329**, S60–S68 (1996)
8. Doorn, P.F., Campbell, P.A., Worrall, J., Benya, P.D., McKellop, H.A., Amstutz, H.C.: Metal wear particle characterization from metal on metal total hip replacements: transmission electron microscopy study of periprosthetic tissues and isolated particles. *J. Biomed. Mater. Res. An Off. J. Soc. Biomater. Japanese Soc. Biomater. Aust. Soc. Biomater.* **42**(1), 103–111 (1998)
9. Willert, H.-G., et al.: Metal-on-metal bearings and hypersensitivity in patients with artificial hip joints: a clinical and histomorphological study. *JBJS* **87**(1), 28–36 (2005)
10. Pandit, H., et al.: Pseudotumours associated with metal-on-metal hip resurfacings. *J. Bone Joint Surg. Br.* **90**(7), 847–851 (2008)
11. Urban, J.A., et al.: Ceramic-on-polyethylene bearing surfaces in total hip arthroplasty: seventeen to twenty-one-year results. *JBJS* **83**(11), 1688–1694 (2001)
12. Hannouche, D., Hamadouche, M., Nizard, R., Bizot, P., Meunier, A., Sedel, L.: Ceramics in total hip replacement. *Clin. Orthop. Relat. Res.* **430**, 62–71 (2005)
13. Yoon, T.R., Rowe, S.M., Jung, S.T., Seon, K.J., Maloney, W.J.: Osteolysis in association with a total hip arthroplasty with ceramic bearing surfaces. *JBJS* **80**(10), 1459–1467 (1998)

14. Nam, K.W., Yoo, J.J., Kim, Y.L., Kim, Y.-M., Lee, M.-H., Kim, H.J.: Alumina-debris-induced osteolysis in contemporary alumina-on-alumina total hip arthroplasty: a case report. *JBJS* **89**(11), 2499–2503 (2007)
15. Jarrett, C.A., Ranawat, A.S., Bruzzone, M., Blum, Y.C., Rodriguez, J.A., Ranawat, C.S.: The squeaking hip: a phenomenon of ceramic-on-ceramic total hip arthroplasty. *JBJS* **91**(6), 1344–1349 (2009)
16. Mesko, J.W., D'Antonio, J.A., Capello, W.N., Bierbaum, B.E., Naughton, M.: Ceramic-on-ceramic hip outcome at a 5-to 10-year interval: has it lived up to its expectations? *J. Arthroplasty* **26**(2), 172–177 (2011)
17. Dowson, D., Diab, M., Gillis, B., Atkinson, J.: Influence of countersurface topography on the wear of UHMWPE under wet or dry conditions: polymer wear and its control. American Chemical Society, Washington DC (1985)
18. Wang, A., Sun, D.C., Stark, C., Dumbleton, and JH, Wear mechanisms of UHMWPE in total joint replacements. *Wear* **181**, 241–249 (1995)
19. Hall, R.M., Unsworth, A., Siney, P., Wroblewski, B.M.: The surface topography of retrieved femoral heads. *J. Mater. Sci. Mater. Med.* **7**(12), 739–744 (1996)
20. Hall, R.M., Siney, P., Unsworth, A., Wroblewski, B.M.: The effect of surface topography of retrieved femoral heads on the wear of UHMWPE sockets. *Med. Eng. Phys.* **19**(8), 711–719 (1997)
21. Drabu, K.J., Michaud, R.J., McCullagh, P.J.J., Brummitt, K., Smith, R.A.: Assessment of titanium alloy on polyethylene bearing surfaces in retrieved uncemented total hip replacements. *Proc. Inst. Mech. Eng. Part H J. Eng. Med.* **208**(2), 91–95 (1994)
22. Jasty, M., Bragdon, C.R., Lee, K., Hanson, A., Harris, W.H.: Surface damage to cobalt-chrome femoral head prostheses. *J. Bone Joint Surg. Br.* **76**(1), 73–77 (1994)
23. Bauer, T.W., Taylor, S.K., Jiang, M., Medendorp, S.V.: An indirect comparison of third-body wear in retrieved hydroxyapatite-coated, porous, and cemented femoral components. *Clin. Orthop. Relat. Res* **298**, 11–18 (1994)
24. Kusaba, A., Kuroki, Y.: Femoral component wear in retrieved hip prostheses. *J. Bone Joint Surg. Br.* **79**(2), 331–336 (1997)
25. Phillips, R.W.: Engineering applications of fluids with a variable yield stress D. Eng. Thesis (1969)
26. Carlson, J.D.: What makes a good MR fluid? *J. Intell. Mater. Syst. Struct.* **13**(7–8), 431–435 (2002). <https://doi.org/10.1106/104538902028221>
27. Carlson, J.D., Catanzarite, D.M., Clair, K.A.S.: Lord Corporation, Cary, NC 27511 USA. In Commercial Magneto-Rheological Fluid Device, Proceedings of the 5th International Conference on ER Fluids, MR Fluids and Associated Technology, U. Sheffield, UK, pp. 20–28 (1995)
28. Huang, J., Zhang, J.Q., Yang, Y., Wei, Y.Q.: Analysis and design of a cylindrical magnetorheological fluid brake. *J. Mater. Process. Technol.* **129**(1–3), 559–562 (2002). [https://doi.org/10.1016/S0924-0136\(02\)00634-9](https://doi.org/10.1016/S0924-0136(02)00634-9)
29. Wong, P.L., Bullough, W.A., Feng, C., Lingard, S.: Tribological performance of a magnetorheological suspension. *Wear* **247**(1), 33–40 (2001). [https://doi.org/10.1016/S0043-1648\(00\)00507-X](https://doi.org/10.1016/S0043-1648(00)00507-X)
30. Rajput, A.S., Prasad, D., Mondal, A.K., Bose, D.: 2D computational fluid dynamics analysis into rotational magnetorheological abrasive flow finishing (R-MRAFF) process. In *Advances in Materials and Manufacturing Engineering*, Springer, pp. 67–73 (2020)
31. Menapace, J.A., Dixit, S.N., Génin, F.Y., Brocious, W.F.: Magnetorheological finishing for imprinting continuous-phase plate structures onto optical surfaces. *Proc. SPIE* **5273**, 5273–5273–11 (2004). <https://doi.org/10.1117/12.527822>
32. Rabinow, J.: The magnetic fluid clutch. *Electr. Eng.* **67**(12), 1167 (1948)
33. Yang, G., Spencer, B.F., Carlson, J.D., Sain, M.K.: Large-scale MR fluid dampers: modeling and dynamic performance considerations. *Eng. Struct.* **24**(3), 309–323 (2002). [https://doi.org/10.1016/S0141-0296\(01\)00097-9](https://doi.org/10.1016/S0141-0296(01)00097-9)

34. Jha, S., Jain, V.K.: Design and development of the magnetorheological abrasive flow finishing (MRAFF) process. *Int. J. Mach. Tools Manuf.* **44**(10), 1019–1029 (2004)
35. Das, M., Jain, V.K., Ghoshdastidar, P.S.: The out-of-roundness of the internal surfaces of stainless steel tubes finished by the rotational–magnetorheological abrasive flow finishing process. *Mater. Manuf. Process.* **26**(8), 1073–1084 (2011)
36. Das, M., Jain, V.K., Ghoshdastidar, P.S.: The out-of-roundness of the internal surfaces of stainless steel tubes finished by the rotational–magnetorheological abrasive flow finishing process. *Mater. Manuf. Process.* **26**(8), 1073–1084 (2011). <https://doi.org/10.1080/10426914.2010.537141>
37. Nagdeve, L., Jain, V.K., Ramkumar, J.: Optimization of process parameters in nano-finishing of Co-Cr-Mo alloy knee joint. *Mater. Manuf. Process.* **00**(00), 1–8 (2020). <https://doi.org/10.1080/10426914.2020.1750633>
38. Kumar, S., Jain, V.K., Sidpara, A.: Nanofinishing of freeform surfaces (knee joint implant) by rotational–magnetorheological abrasive flow finishing (R-MRAFF) process. *Precis. Eng.* **42**, 165–178 (2015)
39. Nagdeve, L., Jain, V.K., Ramkumar, J.: Experimental investigations into nano-finishing of freeform surfaces using negative replica of the knee joint. *Procedia CIRP* **42**, 793–798 (2016). <https://doi.org/10.1016/j.procir.2016.02.321>
40. Nagdeve, L., Jain, V.K., Ramkumar, J.: Development of inverse replica fixture for nano-finishing of knee joint using R-MRAFF process. *J. Micromanufacturing* **2**(1), 35–41 (2019). <https://doi.org/10.1177/2516598418811460>
41. Singh, A.K., Jha, S., Pandey, P.M.: Design and development of nanofinishing process for 3D surfaces using ball end MR finishing tool. *Int. J. Mach. Tools Manuf.* **51**(2), 142–151 (2011). <https://doi.org/10.1016/j.ijmachtools.2010.10.002>
42. Barman, A., Das, M.: Nano-finishing of bio-titanium alloy to generate different surface morphologies by changing magnetorheological polishing fluid compositions. *Precis. Eng.* **51**, 145–152 (2018). <https://doi.org/10.1016/j.precisioneng.2017.08.003>
43. Sidpara, A.M., Jain, V.K.: Nanofinishing of freeform surfaces of prosthetic knee joint implant. *Proc. Inst. Mech. Eng. Part B J. Eng. Manuf.* **226**(11), 1833–1846 (2012). <https://doi.org/10.1177/0954405412460452>
44. Sidpara, A., Jain, V.K.: Analysis of forces on the freeform surface in magnetorheological fluid based finishing process. *Int. J. Mach. Tools Manuf.* **69**, 1–10 (2013). <https://doi.org/10.1016/j.ijmachtools.2013.02.004>
45. Barman, A., Das, M.: Magnetic field assisted finishing process for super-finished Ti alloy implant and its 3D surface characterization. *J. Micromanufacturing* **1**(2), 154–169 (2018). <https://doi.org/10.1177/2516598418785506>
46. Yamaguchi, H., Graziano, A.A.: Surface finishing of cobalt chromium alloy femoral knee components. *CIRP Ann. Manuf. Technol.* **63**(1), 309–312 (2014). <https://doi.org/10.1016/j.cirp.2014.03.020>
47. Rhoades, L.J., Kohut, T.A.: Reversible Unidirectional AFM. Google Patents (1991)
48. Suppression, N., For, C.: United States Patent [19], no. 16, pp. 2–6 (2000)
49. Kumar, S.S., Hiremath, S.S.: A review on abrasive flow machining (AFM). *Procedia Technol.* **25**, 1297–1304 (2016). <https://doi.org/10.1016/j.protcy.2016.08.224>
50. Sankar, M.R., Jain, V.K., Ramkumar, J.: Abrasive flow machining (AFM): an overview. *Dep. Mech. Eng. Indian Inst. Technol. Kanpur, India*, no. September, pp. 1–8 (2011)
51. Sarkar, M., Jain, V.K.: Nanofinishing of freeform surfaces using abrasive flow finishing process. *Proc. Inst. Mech. Eng. Part B J. Eng. Manuf.*, **231**(9), 1501–1515 (2017). <https://doi.org/10.1177/0954405415599913>
52. Rajeshwar, G., Kozak, J., Rajurkar, K.P.: Modeling and computer simulation of media flow in abrasive flow machining process. In: *Proceedings of the 1994 International Mechanical Engineering Congress and Exposition*, pp. 965–971 (1994)
53. Fletcher, A.J., Hull, J.B., Mackie, Trengove, S.A.: Computer modelling of the abrasive flow machining process. In: *Surface Engineering*, Springer, pp. 592–601 (1990)

54. Petri, K.L., Billo, R.E., Bidanda, B.: A neural network process model for abrasive flow machining operations. *J. Manuf. Syst.* **17**(1), 52–64 (1998)
55. Lam, S.S.Y., Smith, A.E.: Process monitoring of abrasive flow machining using a neural network predictive model. In: *Industrial Engineering Research Conference Proceedings*, pp. 477–482 (1997)
56. Slaughter, W.S., Smith, A.E.: *Neural Network Modeling of Abrasive Flow Machining*
57. Sankar, M.R., Jain, V.K., Ramkumar, J., Joshi, Y.M.: Rheological characterization of styrene-butadiene based medium and its finishing performance using rotational abrasive flow finishing process. *Int. J. Mach. Tools Manuf.* **51**(12), 947–957 (2011). <https://doi.org/10.1016/j.ijmachtools.2011.08.012>
58. Sankar, M.R., Jain, V.K., Ramkumar, J.: Rotational abrasive flow finishing (R-AFF) process and its effects on finished surface topography. *Int. J. Mach. tools Manuf.* **50**(7), 637–650 (2010)
59. Sankar, M.R., Jain, V.K., Ramkumar, J.: Nano-finishing of cylindrical hard steel tubes using rotational abrasive flow finishing (R-AFF) process. *Int. J. Adv. Manuf. Technol.* **85**(9–12), 2179–2187 (2016)
60. Sankar, M.R., Jain, V.K., Ramkumar, J.: Experimental investigations into rotating workpiece abrasive flow finishing. *Wear* **267**(1–4), 43–51 (2009)
61. Dumitru, G., Romano, V., Weber, H.P., Haefke, H., Gerbig, Y., Pflüger, E.: Laser microstructuring of steel surfaces for tribological applications. *Appl. Phys. A* **70**(4), 485–487 (2000)
62. Hecke, M., Schomburg, W.K.: Review on micro molding of thermoplastic polymers. *J. Micromechanics Microengineering* **14**(3), R1 (2003)
63. Proskurovsky, D.I., Rotshtein, V.P., Ozur, G.E.: Use of low-energy, high-current electron beams for surface treatment of materials. *Surf. Coatings Technol.* **96**(1), 117–122 (1997). [https://doi.org/10.1016/S0257-8972\(97\)00093-5](https://doi.org/10.1016/S0257-8972(97)00093-5)
64. Proskurovsky, D.I., Rotshtein, V.P., Ozur, G.E., Ivanov, Y.F., Markov, A.B.: Physical foundations for surface treatment of materials with low energy, high current electron beams. *Surf. Coatings Technol.* **125**(1–3), 49–56 (2000). [https://doi.org/10.1016/S0257-8972\(99\)00604-0](https://doi.org/10.1016/S0257-8972(99)00604-0)
65. Okada, A., Uno, Y., Raharjo, P., Furukawa, T.: Surface modification of EDMed surface by wide-area electron beam irradiation. In: *Proceedings of ASPE Annual Conference*, vol. 18, pp. 172–175 (2003).
66. Uno, Y., Okada, A., Uemura, K., Raharjo, P., Furukawa, T., Karato, K.: High-efficiency finishing process for metal mold by large-area electron beam irradiation. *Precis. Eng.* **29**(4), 449–455 (2005)
67. Murray, J.W., Kinnell, P.K., Cannon, A.H., Bailey, B., Clare, A.T.: Surface finishing of intricate metal mould structures by large-area electron beam irradiation. *Precis. Eng.* **37**(2), 443–450 (2013). <https://doi.org/10.1016/j.precisioneng.2012.11.007>
68. Okada, A., et al.: Surface finishing of stainless steels for orthopedic surgical tools by large-area electron beam irradiation. *CIRP Ann. Manuf. Technol.* **57**(1), 223–226 (2008). <https://doi.org/10.1016/j.cirp.2008.03.062>
69. Okada, A., Uno, Y., Yabushita, N., Uemura, K., Raharjo, P.: High efficient surface finishing of bio-titanium alloy by large-area electron beam irradiation. *J. Mater. Process. Technol.* **149**(1–3), 506–511 (2004). <https://doi.org/10.1016/j.jmatprotec.2004.02.017>
70. Landolt, D.: Fundamental aspects of electropolishing. *Electrochim. Acta* **32**(1), 1–11 (1987)
71. Carlsson, L., Röstlund, T., Albrektsson, B., Albrektsson, T.: Removal torques for polished and rough titanium implants. *Int. J. Oral Maxillofac. Implants* **3**(1) (1988)
72. Andreaacchi, A.: *Apparatus for electropolishing a stent*. Google Patents (2004)
73. Tajima, K., Hironaka, M., Chen, K.-K., Nagamatsu, Y., Kakigawa, H., Kozono, Y.: Electropolishing of CP titanium and its alloys in an alcoholic solution-based electrolyte. *Dent. Mater. J.* **27**(2), 258–265 (2008)
74. Piotrowski, O., Madore, C., Landolt, D.: Electropolishing of titanium & titanium alloys in perchlorate-free electrolytes. *Plat. Surf. Finish.* **85**(5), 115–119 (1998)
75. Han, W., Fang, F.: Fundamental aspects and recent developments in electropolishing. *Int. J. Mach. Tools Manuf.* **139**, 1–23 (2019)

76. Lausmaa, J., Kasemo, B., Mattsson, H., Odelius, H.: Multi-technique surface characterization of oxide films on electropolished and anodically oxidized titanium. *Appl. Surf. Sci.* **45**(3), 189–200 (1990)
77. Piotrowski, O.: The mechanism of electropolishing of titanium in methanol-sulfuric acid electrolytes. *J. Electrochem. Soc.* **145**(7), 2362 (1998). <https://doi.org/10.1149/1.1838644>
78. Peighambardoust, N.S., Nasirpouri, F.: Electropolishing behaviour of pure titanium in perchloric acid–methanol–ethylene glycol mixed solution. *Trans. IMF* **92**(3), 132–139 (2014)
79. Huang, C.A., Hsu, F.-Y., Yu, C.H.: Electropolishing behavior of pure titanium in sulfuric acid–ethanol electrolytes with an addition of water. *Corros. Sci.* **53**(2), 589–596 (2011)
80. Piotrowski, O., Madore, C., Landolt, D.: The mechanism of electropolishing of titanium in methanol-sulfuric acid electrolytes. *J. Electrochem. Soc.* **145**(7), 2362 (1998)
81. Eliaz, N., Nissan, O.: Innovative processes for electropolishing of medical devices made of stainless steels. *J. Biomed. Mater. Res. Part A Off. J. Soc. Biomater. Jpn. Soc. Biomater. Aust. Soc. Biomater. Korean Soc. Biomat.* **83**(2), 546–557 (2007)
82. Wagner, C.: Contribution to the theory of electropolishing. *J. Electrochem. Soc.* **101**(5), 225–228 (1954)
83. Rowe, M.S., Harper Jr. C.E., Underwood, C.R.: Computer controlled electropolishing system. Google Patents (1990)
84. Datta, M., Romankiw, L.T.: Electrochemical tool for uniform metal removal during electropolishing. Google Patents (1993)
85. Ohmori, H., Katahira, K., Akinou, Y., Komotori, J., Mizutani, M.: Investigation on grinding characteristics and surface-modifying effects of biocompatible Co-Cr alloy. *CIRP Ann. - Manuf. Technol.* **55**(1), 597–600 (2006). [https://doi.org/10.1016/S0007-8506\(07\)60491-0](https://doi.org/10.1016/S0007-8506(07)60491-0)
86. Rahman, M., Senthil Kumar, A., Biswas, I.: A review of electrolytic in-process dressing (ELID) grinding. *Key Eng. Mater.* **404**, 45–59 (2009). <https://doi.org/10.4028/www.scientific.net/KEM.404.45>
87. Ohmori, H., et al.: Surface generating process of artificial hip joints with hyper-hemispherical shape having higher smoothness and biocompatibility. *CIRP Ann. Manuf. Technol.* **62**(1), 579–582 (2013). <https://doi.org/10.1016/j.cirp.2013.03.027>
88. Okada, Y., et al.: Verification of implant surface modification by a novel processing method. *Acta Med. Okayama* **71**(1), 49–57 (2017). <https://doi.org/10.18926/AMO/54825>
89. Hamada, M., Komotori, J., Mizutani, M., Kunimura, S., Katahira, K., Ohmori, H.: Corrosion resistance of Co-Cr-Mo Alloy treated by electrolytic in-process dressing (ELID) grinding/thermal oxidation hybrid process. *J. Solid Mech. Mater. Eng.* **6**(6), 504–511 (2012). <https://doi.org/10.1299/jmmp.6.504>
90. Kasuga, H., Ohmori, H., Watanabe, Y., Mishima, T.: Surface characteristics of efficient-ground alumina and zirconia ceramics for dental applications. *Key Eng. Mater.* **404**, 69–75 (2009). <https://doi.org/10.4028/www.scientific.net/kem.404.69>
91. Ryan, J.G., Geffken, R.M., Poulin, N.R., Paraszczak, J.R.: The evolution of interconnection technology at IBM. *IBM J. Res. Dev.* **39**(4), 371–381 (1995)
92. Nanz, G., Camilletti, L.E.: Modeling of chemical—mechanical polishing: a review. *IEEE Trans. Semicond. Manuf.* **8**(4), 382–389 (1995). <https://doi.org/10.1109/66.475179>
93. Et, B., Usoo67873o8e32, A.: (12) United States Patent, **2**(12) (2010)
94. Bai, A., et al.: A 65nm logic technology featuring 35nm gate lengths, enhanced channel strain, 8 Cu interconnect layers, low-k ILD and 0.57/spl mu/m/sup 2/SRAM cell. In: *IEDM Technical Digest. IEEE International Electron Devices Meeting, 2004*, pp. 657–660 (2004)
95. Zantye, P.B., Kumar, A., Sikder, A.K.: Chemical mechanical planarization for microelectronics applications. *Mater. Sci. Eng. R Reports* **45**(3–6), 89–220 (2004)
96. Zhao, D., Lu, X.: Chemical mechanical polishing: theory and experiment. *Friction* **1**(4), 306–326 (2013). <https://doi.org/10.1007/s40544-013-0035-x>
97. Alsaeedi, R., Ozdemir, Z.: Evaluation of chemical mechanical polishing-based surface modification on 3D dental implants compared to alternative methods. *Materials (Basel)* **11**(11) (2018). <https://doi.org/10.3390/ma11112286>

98. Kahng, A.B., Samadi, K.: CMP fill synthesis: a survey of recent studies. *IEEE Trans. Comput. Des. Integr. Cir. Syst.* **27**(1), 3–19 (2007)
99. Chathapuram, V.S., Du, T., Sundaram, K.B., Desai, V.: Role of oxidizer in the chemical mechanical planarization of the Ti/TiN barrier layer. *Microelectron. Eng.* **65**(4), 478–488 (2003). [https://doi.org/10.1016/S0167-9317\(03\)00177-1](https://doi.org/10.1016/S0167-9317(03)00177-1)
100. Ozdemir, Z., Ozdemir, A., Basim, G.B.: Application of chemical mechanical polishing process on titanium based implants. *Mater. Sci. Eng. C* **68**, 383–396 (2016). <https://doi.org/10.1016/j.msec.2016.06.002>
101. Basim, G.B., Ozdemir, Z., Mutlu, O.: Biomaterials applications of chemical mechanical polishing. *Icpt* **2012**, 15–17 (2012)
102. ur Rahman, Z., Pompa, L., Haider, W.: Influence of electropolishing and magnetoelectropolishing on corrosion and biocompatibility of titanium implants. *J. Mater. Eng. Perform.* **23**(11), 3907–3915 (2014). <https://doi.org/10.1007/s11665-014-1205-3>

Chapter 16

Principles of Advanced Manufacturing Technologies for Biomedical Devices



G. L. Samuel, Lingxue Kong, Y. Arcot, and Pavan Pandit

1 Introduction

This chapter summarizes the advanced manufacturing processes that are being used to fabricate the biomedical devices and systems. The chapter includes the concepts of machining, forming, joining, additive manufacturing, and micro/macro scale process. For all the concepts mentioned the significant applications and the physical science behind these concepts are outlined. Biomedical manufacturing can be defined as the process of fabrication, joining, functionalizing, measurement of the systems, arrays, and the devices. The systems can be the surgical equipment, the microfluidic arrays, prosthetics, cell and tissue culture equipment, genetic engineering apparatus, development of bio sensors, therapeutics, and biomaterials. Biomedical manufacturing bridges the gap between the healthcare sector and the production industries. Today the advent of advanced manufacturing and product development is integrated with CAD/CAE packages and product lifecycle management solutions. Product development, new product manufacturing cycle time has been greatly reduced as the management of information became global through product development and carried from the stage of requirements gathering to the development of maintenance strategy as shown in Fig. 1 [1, 2].

Computer-Aided manufacturing and seamless flow of information is a part of global product management solution for every product in any field. Customization of the product is becoming a new normal in the solutions provided by the biomedical product manufacturers. Adaptation of the devices according to the patient-specific

G. L. Samuel (✉) · Y. Arcot · P. Pandit

Department of Mechanical Engineering, Indian Institute of Technology Madras, Chennai, India
e-mail: samuelgl@iitm.ac.in

L. Kong · Y. Arcot

Institute of Frontier Materials, Deakin University, Geelong, Australia
e-mail: lingxue.kong@deakin.edu.au

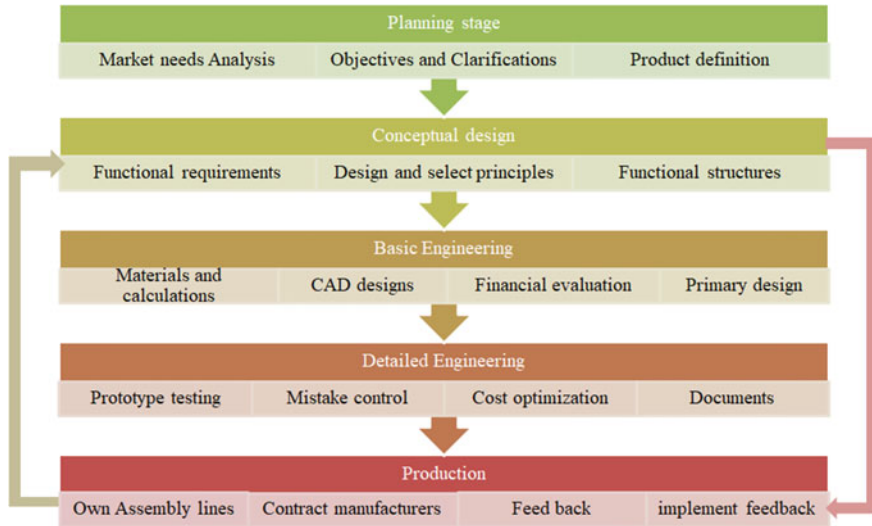


Fig. 1 Modern-day product development cycle and flow of information in all stages of product development

morphology is promoting enhanced diagnostic capabilities. For example, combination of medical imaging and CAM are promoting personalized prosthesis implants. CAM became an integrated part of the advanced manufacturing technologies like additive manufacturing and is widely being used by dentistry. Today placing order for personalize dental implants is quite easier because of the collaboration between the dental clinics and other laboratories. These laboratories are equipped with the digital scanners, CAD resources for designing, compact milling machines. This became a part of academic curriculum in dentistry, and the doctors are already equipped with the knowledge of manufacturing personalized implants and biomimetic materials. Similarly, research is focusing towards other medical procedures related to knee replacements, hip prostheses, and other devices [3, 4]. Fabrication of these devices either personalized or generic involves gamut of technologies as shown in Fig. 2 and are classified into methods like additive, subtractive and net-shape manufacturing and their combination in the product life cycle. The primary aim of this chapter is to provide an introduction of the considerations in the current manufacturing process towards biomedical applications, benefits, and opportunities.

2 Subtractive Manufacturing

Metals such as stainless steel, cobalt-chromium-molybdenum alloys, Ti and Ti-Ni alloys are the primary materials used in biomedical implant manufacturing. Biocompatible metals have superior mechanical properties, high corrosion resistance and

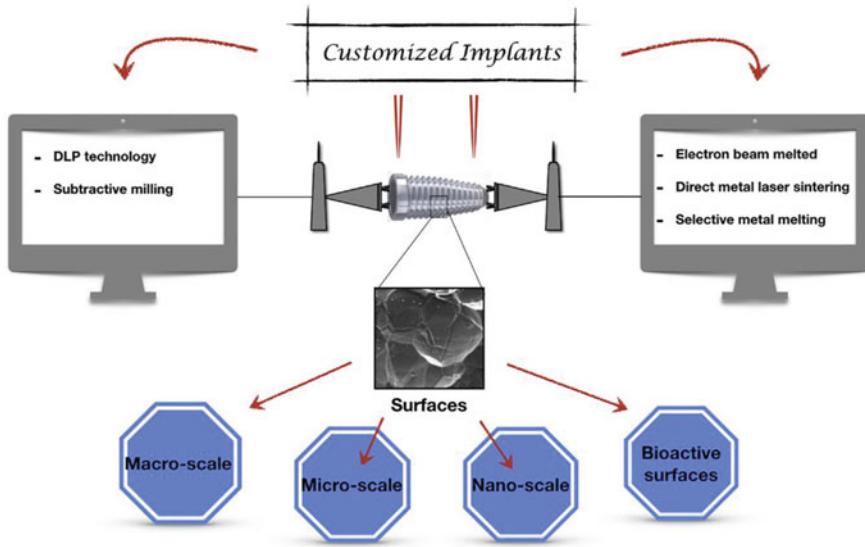


Fig. 2 Various methodologies are involved in developing a single implant. *Image courtesy Ferreira [3]*

work in complex environments. Subtractive manufacturing is extensively used to change the surface properties of the devices and are also used to fabricate micron-sized textures [5] on the biomedical implants for increased osseointegration as shown in Fig. 3. Many micron size range devices are equipped into medical devices such as microfluidic devices (LOC), pumps, valves, and thermal devices [6, 7]. The main

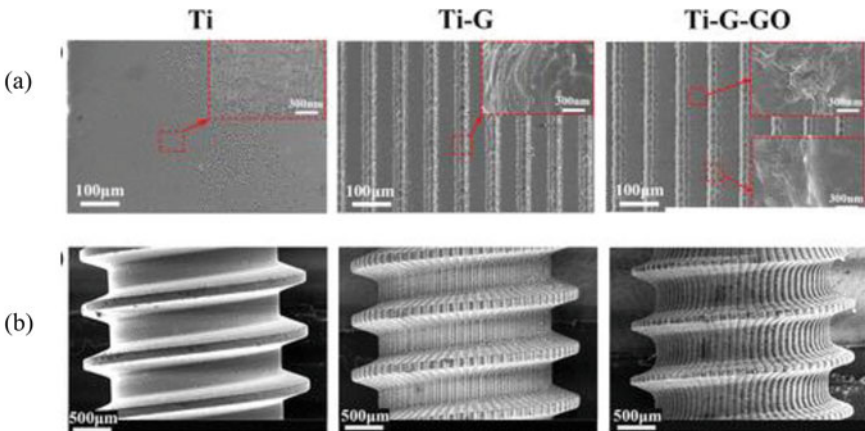


Fig. 3 Laser engraved microgrooves on titanium alloy implants. **a** SEM images of three different plates; **b** SEM images of three bone screws. *Image courtesy Wang et al. [5]*

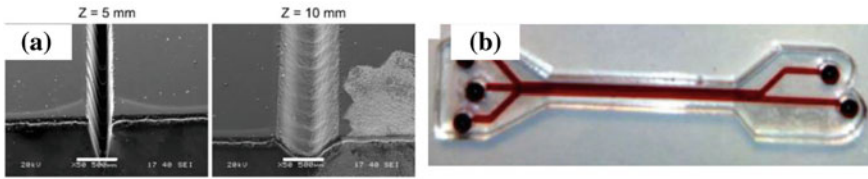


Fig. 4 **a** Morphology of microfluidic channels laser-engraved at varying distance-to-focus; **b** PMMA microfluidic devices. *Image courtesy Matellan et al. [8]*

advantage of these devices is reduced material consumption and faster analysis which directly affects the cost of the device and the analysis performed. Especially microfluidic devices consist of fluidic channels ranging in 10s of microns which handle volumes in nano-liters. These devices are used for DNA/RNA amplification, immunoassays, particle sorting, and genomic identifications. The limiting capabilities of these processes depend upon the tool dimensions and work-piece materials. Subtractive manufacturing includes Computer Numeric Controlled (CNC) machines for micromilling, electrode discharge machining, laser machining, and other advanced methods as shown in Fig. 4 [8]. Most consumer goods and ordinary metals require ISO 9001 quality management certification, but for medical parts the standards used to measure is ISO 13485 and are recognized by regulators like FDA.

While it has to be clearly understood no one part is made of single manufacturing process. There is process engineering involved for every single product at various stages where the material is subjected to various manufacturing processes like machining, joining, coating, etc., to achieve the desired shape and functionality. For example, a hip implant is formed using forming operations, machined for suitable tolerances, and coated to achieve its functionality. Also a particular process may directly or indirectly involve in process engineering at any stage in the manufacturing the product. Like, CNC machining will be used to fabricate the mould, and later the product is fabricated using that mould. Biomedical devices designed are suited to complex shapes of bones, joints and complex structures which make the manufacturing process complex and requires conglomerate of processes. CNC machining is a vitally important method in medical industry where machined parts are found through the health care as given in Table 1.

Basic requirements for medical CNC machining include:

- Machining capability with tight tolerances (Micro to Nano meter ranges)
- Multi-axis machining centres for complex geometries
- Ultra-high level cleanliness suitable for an implant manufacturer
- Ability to machine-wide materials
- Superior surface finishing capabilities.

Table 1 Medical equipment and Medical devices that are usually used in hospitals

S. no.	Equipment	Medical devices
1	Machined implants	Hip implants
		Spine implants
		Knee implants
2	Surgical instruments	Handles
		Cutters
		Forceps
		Saws
		Holders
		Clamps
		Spacers
3	Electronic medical equipment	Monitor housings
		Switches
		Buttons
		Leveres
4	Micro-machined medical parts	Stents
		Catheters
		Pacemakers
		Drug delivery systems
		Screws and tubes

2.1 Mechanical Machining

The two broad categories of machining are cutting and grinding, under which there are myriad of operations like sanding, drilling, facing, turning, grinding, etc. The underlying process for all these operations is material removal with the help of a tool with cutting edges [9] as shown in Fig. 5. To optimize this material removal there is a variety of parameters of which speed of the tool, feed to the tool, and depth-of-cut are considered primary. Cutting speed refers to the speed of the machine similar to speed of spinning the end mill/drill tool-bit, feed rate is how fast the operator is pushing the

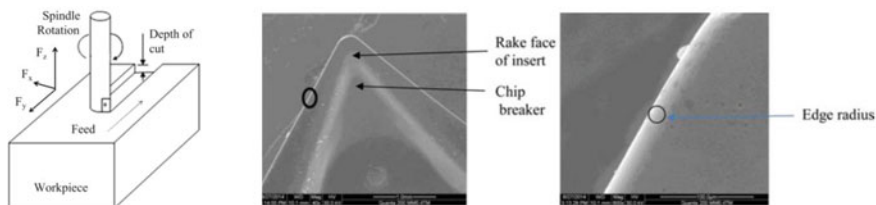


Fig. 5 Geometry of tool insert with the cutting edges. *Image courtesy* Shunmugam [11] and Jagadesh and Samuel [9]

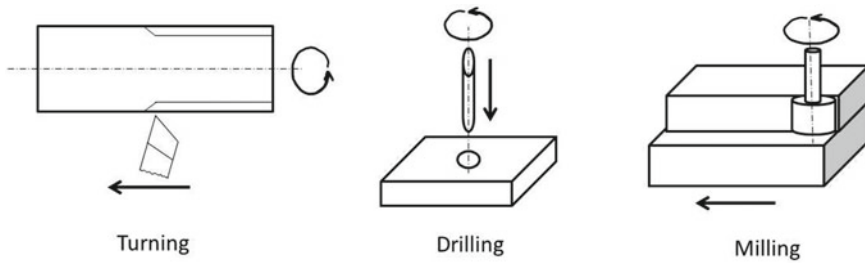


Fig. 6 The most common types of machining processes

tool into work-piece, and depth of cut is the amount of material in contact. Also, the material removal happens depending upon the mechanical properties of the materials and their reaction to the forces produced by the tool. Figure 6 shows different tools for each process and the each tool is specifically designed with cutting edges according to the functionality or particular purpose [10].

Cutting involves applying one sharp edge in line with the required direction also tool may have multiple sharp edges termed as teeth/flutes. Grinding involves using many sharp edges arranged disparately in every direction. Tools used for material removal must be harder than the material they cut and are made of different grades of tool steel and grinding tools use a variation of abrasives. In machining process, you bring the tool surface and part (work-piece) surface together and break the molecular bonds and remove on the part through a predefined tool path and thus creating the required shape. This produces an incredible amount of heat and a by-product called Chips [10]. These chips are either thrown away or recycled but give valuable information about the efficiency of material removal. Generally, this information is used to trouble shoot the machining process. Cutting fluids are used to remove the heat during machining and provide enough lubrication. It is important to select cutting fluids judiciously as they extend tool life and improve the surface finish of the work piece. By using these principles bio-devices like knee implants and micro-textures on surfaces as shown in Fig. 7 were fabricated [12, 13].

These cutting principles discussed above remain same for micromachining process and can be considered as a downscaled process for conventional machining process [11]. The tool geometries in mechanical micro machining are in sub millimetre ranges and can be used either to fabricate micro devices or used in surface finishing operations. Research in micromachining for biomedical devices has gained momentum in the last decade with the increased availability of the cutting tools. The edge radius of the micro tools are in the range of 1–10 μm . Due to these microscale dimensions the effects of edge radius, material strengthening and other microstructural effects become more prominent in mechanical micromachining. As shown in Fig. 8, the edge radius creates a large negative rake angles and makes material flow more complex and is termed as edge radius effect [9, 11]. Also when the depth of cut is very small, the material exhibits higher strength. Due to this, specific cutting energy required for machining also increases causing material strengthening due to

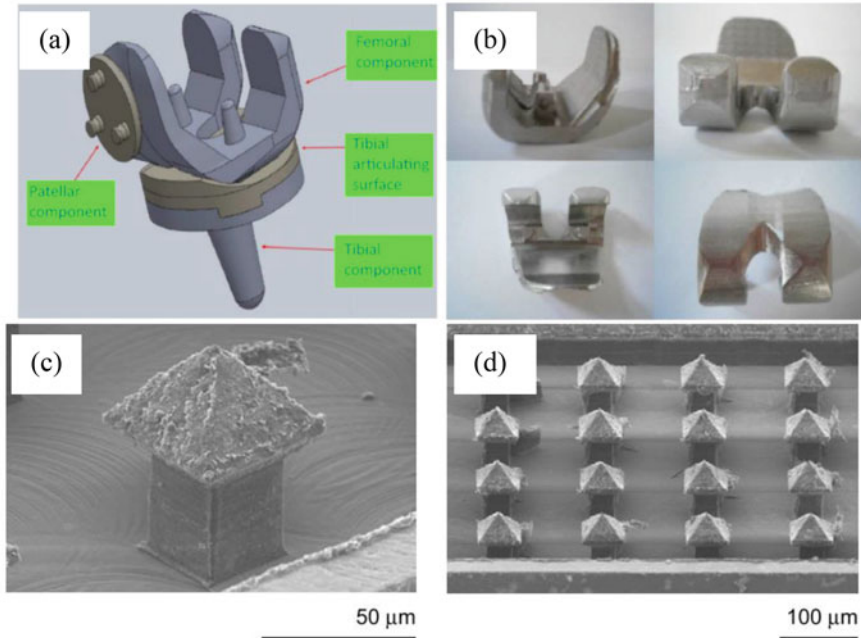


Fig. 7 **a** 3d drawing of Femoral Component of Knee Implant, **b** Precision CNC Machined Femoral Component of Knee Implant, **c** Micro-barbs with sizes (68 mm head width and 84 mm overall height), and **d** an array of smaller micro-barbs. *Image courtesy* Markopoulos et al. [12] and Filiz et al. [13]

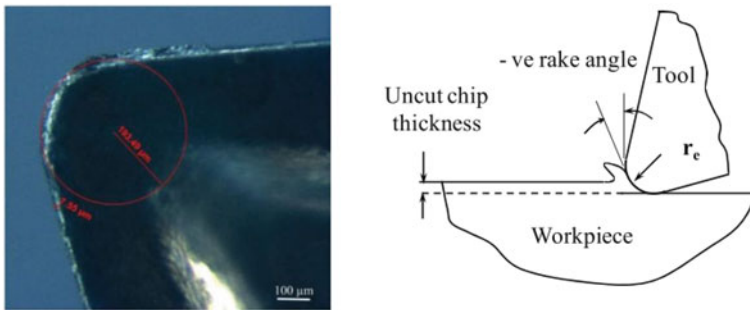


Fig. 8 Cutting tool insert with edge radius and schematic of negative rake angles while machining. *Image courtesy* Jagadesh et al. [9] and Shunmugam [11]

size effect. Different approaches [14] were used to propose exponents to accommodate these effects and reduce the difference between the predicted and actual values as shown in Fig. 9. The rotational speed required to achieve recommended is very high due to the size of the tool. Higher feed rate, tool run out, and unpredictable cutting action makes micro-cutting more complex. Mechanistic models with minor

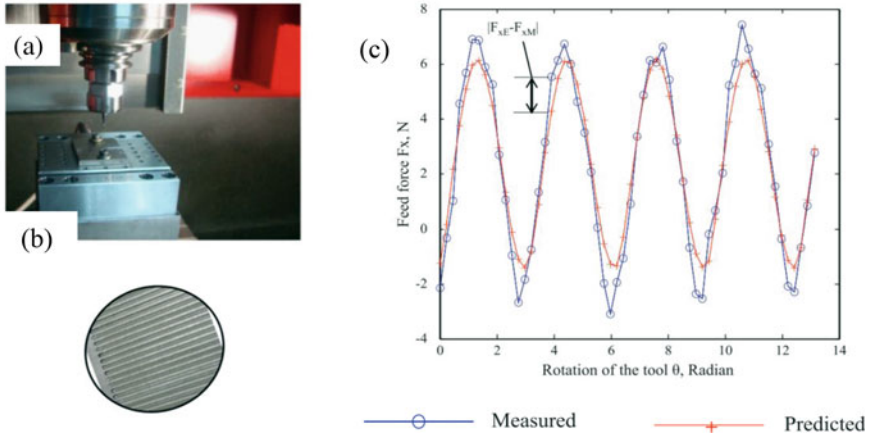


Fig. 9 a Kern Evo micro-machining setup used for prediction of cutting forces for micro-end milling. b Micro-channels machined using the setup. c Predicted forces in red color matching with measured forces in blue color. *Image courtesy* Srinivasa et al. [16]

prediction error were developed for predicting the cutting forces considering edge radius and material strengthening effects [9, 15, 16].

2.2 Photolithography

This is one of the most common and versatile methods, these days for fabricating printed circuit boards, microprocessors, and miniature robots. It uses light to transfer patterns from a photo mask to light-sensitive material (Photoresist) onto a substrate and the whole process is performed in clean rooms. Though there are different protocols and chemicals are used to fabricate, a basic common procedure is presented in Fig. 10 [17]. Photoresist is of two types: Soluble and insoluble after treating with light and are termed as positive and negative resist respectively. The photoresist can

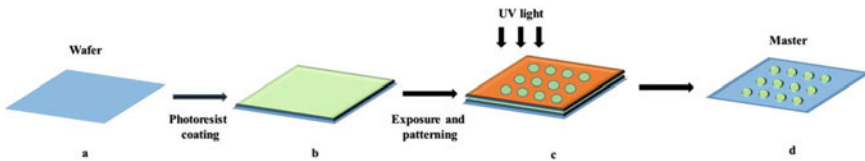


Fig. 10 Schematic of photolithography process. a The wafer is cleaned to remove any unwanted contaminants. b The photoresist is spin-coated onto the wafer. c The photo-mask is placed above the photoresist. UV light is exposed through the mask. d The unexposed part is removed by solvents leaving the desired patterns. *Image courtesy* Tran et al. [17]

be coated on different substrates like Silicon, Glass, and Polymer wafers which are generally 100 μm to 1 mm thick. The basic procedure is as follows:

1. Photo mask is prepared with the required pattern depending upon type of the resist.
2. Wafers are cleaned with acetone, alcohol, and water to remove any contaminants on the wafer surface.
3. Photo resist is coated on the cleaned wafers using spin coating methods. The thickness of the coating is controlled by speed and time that can be adjusted in the spin coaters, Usually 10–100 μm .
4. The coated wafer is baked on a heating plate for required time depending upon the resist used. Usually in 50–150 s.
5. The wafer is cooled to room temperature and transferred to mask aligner where the photo mask is placed on the coated wafer and flooded with UV light of required wave length. Here the area on which the light is exposed gets hardened.
6. The wafer is then dipped or flooded with developer solution to remove the photoresist forming a pattern. This pattern is then taken to either etching platform and to further improve the depth of the pattern or coating methods.
7. For microfluidic devices: The obtained pattern from etching is transferred to PDMS by pouring PDMS along with curing agent onto the patterned silicon wafer. It is then cured at 65–85 $^{\circ}\text{C}$ temperature and stripped off to get micro-features on the PDMS as shown in Fig. 10.

While this is the basic common procedure, there are many variations in this procedure depending upon the requirements. For example, microfluidic devices can be fabricated using positive photoresist and Negative photoresist. Photolithography for bio-medical devices are used for drug delivery systems for fabricating the particles to required sizes potentially to cross the barriers [18], Nano imprinting polymers [19], Transdermal delivery using micro-needles [20], Microfluidic devices [21] and Tissue engineering [17] as shown in Fig. 10. In our preliminary work [22] we used Ni electroplating to fabricate a mould master to fabricate PMMA microfluidic devices using Hot-embossing. Many micro-features ranging from 100 μm to 1 mm were imprinted on PMMA wafer using a mould-master in four steps: 1. Pre-master Fabrication using Si master (ii) Ni-Master fabrication (iii) Hot- embossing, as shown in Fig. 11. The Si-master was fabricated using the basic common procedure described above but using SU8-2025 negative resist and coated upto 50um thick. To promote adhesion between layers Si and SU8 2025 resist extra thin layers of SU8-2005 was coated for 5 μm and baked. The pre-master is then sputtered with Cr and Ni for 10 min and then plunged into Ni-Electroplating bath for about 6 h. Later the Ni-master is stripped of from the Si master and SU-8. This master with micro-features is used as insert for hot embossing of PMMA wafers. PDMS is the most commonly used material for fabricating microfluidic devices using SU8 resist and dry etching methods. Combination of UV-Lithography, etching, coating is used for developing various micro-devices, Research is being performed on the interaction between these microstructures and cells/proteins [23]. The objective of these micro-devices is to provide better sensing, targeting, and response to stimuli (Fig. 12).

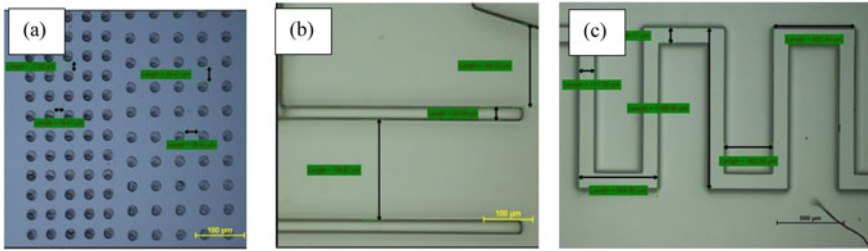


Fig. 11 Microfluidic device on PDMS. **a** Micro-pillars with 20 μm diameter, **b** Walls with 25 μm thickness, **c** Microfluidic channels which are 100 μm in width approximately. *Image courtesy Author's research group at Deakin University, Australia*

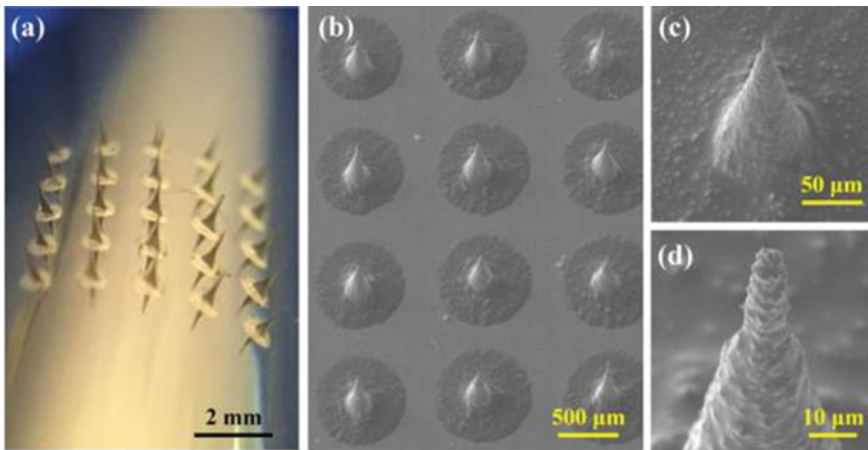


Fig. 12 **a** FMA coated with Ti/Au film. SEM images of **b** FMA, **c** Microneedle, and **d** Microneedle tip. *Image courtesy Chen et al. [20]*

2.3 Replication Technologies

Efforts are continually made to increase the capability of the replication technologies for variety of sizes for micro devices and materials. LIGA, casting, injection moulding, hot embossing, roll-to-roll imprinting, nano-imprint lithography, etc., are industrially well-established processes and can produce high resolutions and in Nanometer ranges. These technologies can be a combination of different MEMS process and Moulding process. The replication technologies are a two-stage process (1) Fabrication of the required pattern onto a mould master. (2) Replication of the pattern onto a required substrate. The mould masters are fabricated using different technologies like Lithography techniques and machining techniques. These techniques are generally linked to mass production techniques and tailored according to the materials. The moulds are composed of two halves: a fixed half and a moving half and are strongly

pressed against each other. Plastic pellets are plasticised using a rotating screw in a heating chamber. The plastic pellets are transformed into molten plastic is then injected into the mould until it is completely filled. The mould is then cooled either using cooling fluids or air cooled and later ejected. These can be generalized into four stages: Filling, maintaining pressure between platens, cooling and demoulding stage. The most important process parameters for this process include Time, Temperature and Pressure [24] (Fig. 13).

New applications of biomedical devices are trending towards smaller devices like microfluidic devices, laparoscopic instruments for grasping, cutting, and suturing tissues, superficial micro, and nano structures. This shift towards the smaller devices led to development of micro injection moulding, micro hot-embossing techniques. To produce high-quality parts, optimization of the cavity filled is crucial. The complexity of the attainable geometries depends upon mould designing and quality control of the material indeed. For micro-parts variety of fabrication processes like laser machining, Electric-discharge machining, 3D printing, lithography and mechanical micromachining processes. Few methods for analysis of micro-cavities include short-shot methods, flow visualization methods, and flow length tests. Conventional injection moulding, a leaching technique was used for fabricating porous scaffolds for preliminary mesenchymal stem cells for tissue engineering applications [25] as in Fig. 14. In this study, the author’s injection moulded PCL/NaCl, PCL/Sucrose composites and found Moulded PCL/Sucrose scaffolds were good candidates for tissue engineering. In another similar study microcellular injection molding was combined with particle

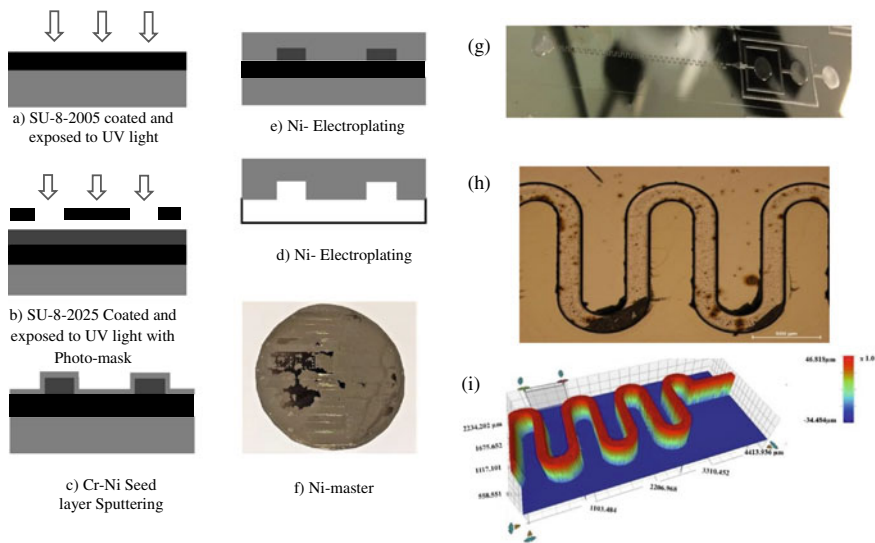


Fig. 13 a–e Schematic of Ni-Master fabrication with various stages of lithography, f, g and h Ni-master with micro-features, i 3d topography of the Ni-master with serpentine channels. *Image courtesy Arcot et al. [22]*

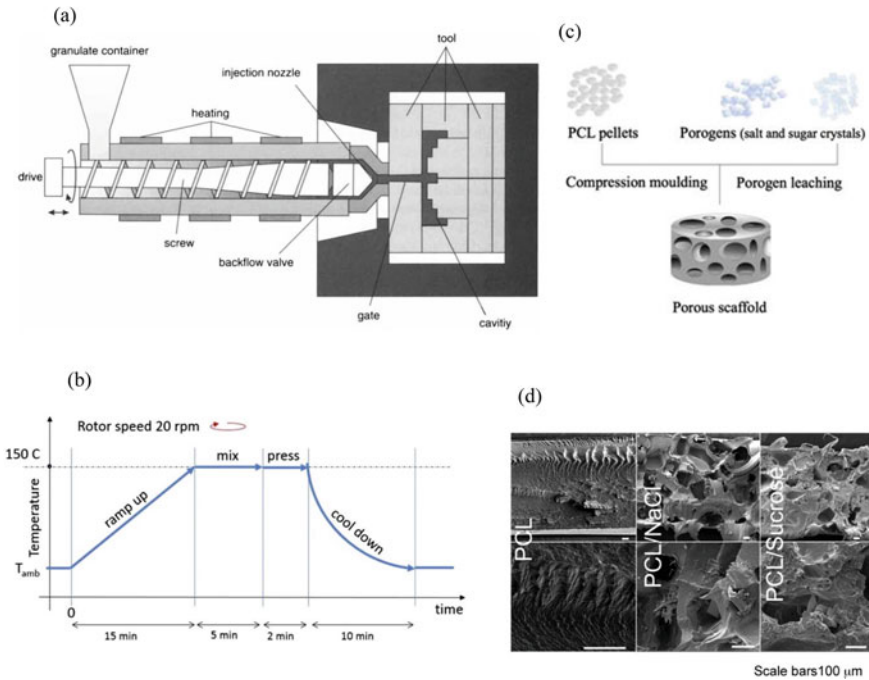


Fig. 14 **a** Injection moulding process, **b** Cycle for fabricating scaffolds, **c** Mixing of injection moulding and porous leaching, **d** Porous Scaffold after leaching. *Image courtesy* Limongi et al. [25] and Yi [27]

leaching to produce porous scaffolds for thermoplastic polyurethane using water-soluble polyvinyl alcohol (PVOH) and sodium chloride (NaCl) as porogens [26]. This shows that Microcellular injection moulding is a process capable of producing complex plastic parts at large scales and when coupled with other methods can lead to scalable soft tissue scaffold fabrication methods.

The other remarkable technology for imprinting microstructures is hot-embossing process which can imprint microstructures with 1 μm resolution [28, 74]. In embossing, tool and the substrate are heated to required temperature under vacuum and moved towards each other. The polymers are heated above the glass transition temperature and the mould master with required pattern is held against the material with a pressure. The mould master and substrate material are held in contact for certain period of time called holding time and the cavities are filled. Later the pressure is released slowly and the temperature is decreased simultaneously and tool is de-embossed for obtaining final part. Similar to injection moulding the process parameters to be controlled in embossing are pressure (load), temperature, and time as shown in Fig. 15. The hot-embossing is not limited to heating and pressing as there are different process variations like thermoforming, roller embossing, hot punching through holes, multi-layer moulding, etc.,

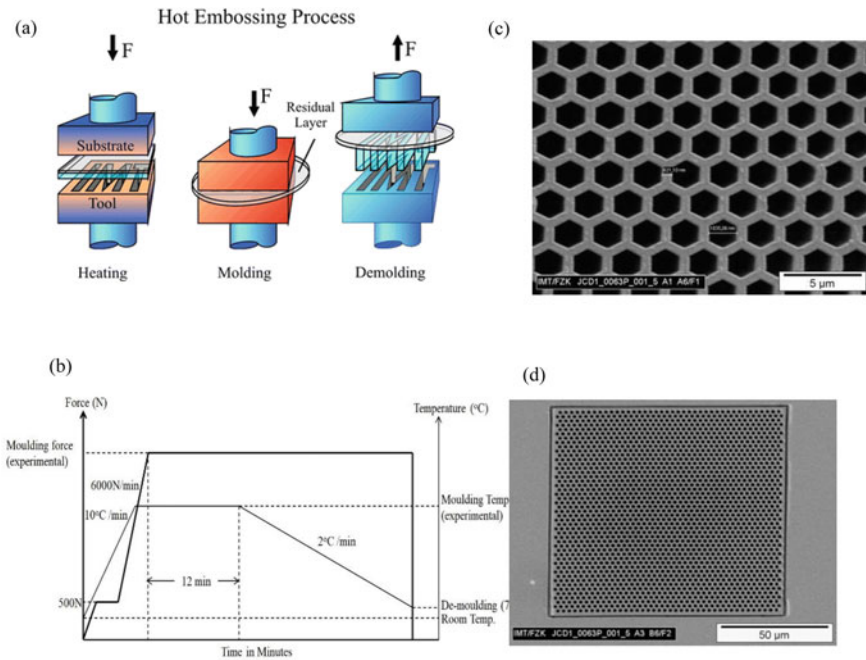


Fig. 15 **a** Hot-embossing process, **b** Embossing cycle for fabricating PMMA microfluidic devices **c, d** Honey comb structure on PMMA. *Image courtesy* Worgull et al. [28] and Arcot et al. [22]

The advanced version of this replication technique is Nano-imprinting lithography (NIL) where nanostructures are patterned [19]. This can be classified into Thermal NIL, UV-NIL, laser-assisted NIL, and electrochemical nano imprints. These processes are well established for fabricating electronic devices and are yet to industrially establish for fabricating biomedical devices as shown in Fig. 16. Thermal NIL is similar to the hot embossing processing process where a polymer film is spin-coated onto a wafer and load is applied for a time period. Other NIL processes slightly differ as described below:

UV NIL: The substrate material is coated with UV curable resist and exposed to UV light for solidification. Upon solidification, a transparent mould is pressed against the resist material and later etched for obtaining the required features.

Laser-assisted NIL: This method doesn't require etching. A silicon substrate is melted to liquid using a single pulse excimer laser exposed through a transparent quartz mould which is in contact with the substrate. The mould is released after the substrate has cooled down and nano structures with 10 nm range can be imprinted using this technique.

Electrochemical nano imprints: In this process, voltage is applied between the mould and substrate and current flow between them. Due to the presence of moisture

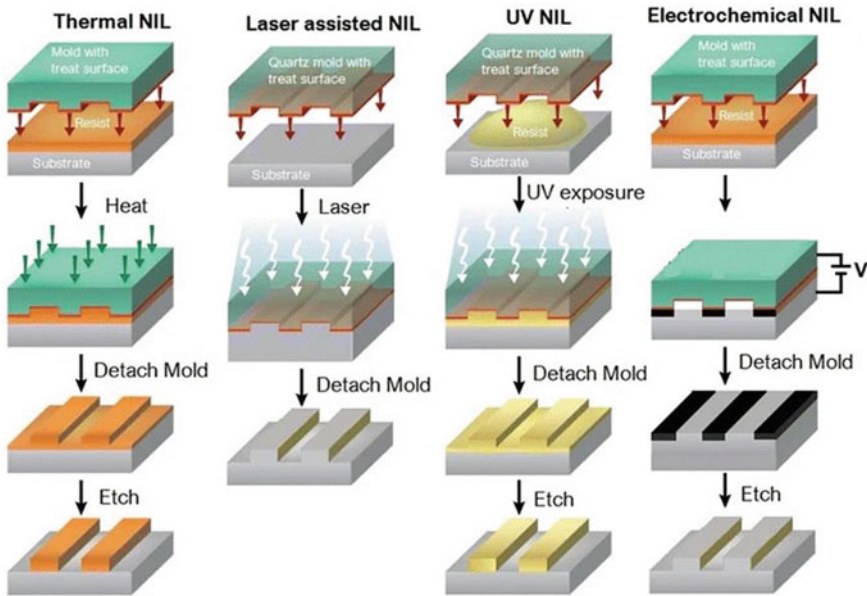


Fig. 16 Basic process steps for different NIL techniques. *Image courtesy* Hasan et al. [19]

between them a strong anodic oxidation at corresponding protrusive parts takes place resulting in nano-structures.

2.4 Other Important Fabrication Technologies

Any other advanced fabrication techniques are an improvement or variations of the above-discussed processes but not limited. The research in manufacturing technology has been largely focused to develop techniques to fabricate Micro/Nano structures for biomedical application that industrially applicable. Electronic devices manufacturing techniques like spinning, plasma etching, physical vapor deposition (PVD), chemical vapor deposition (CVD), electron beam lithography (EBL), and focussed ion beam lithography (FIBL) are being adapted to fabricate micro/nano devices. While PVD, CVD processes are sub-processes involved in photolithography, EBL and FIBL can be considered as subtractive manufacturing processes.

2.4.1 E-Beam Lithography

Modern EBL machines can write nanostructures on a substrate material and the working principle is relatively simple and similar to Photolithography [29]. A

focussed beam of electrons are scanned over a substrate covered with resist material. According to the tone of the resist the areas exposed or not exposed are developed. EBL is similar to SEM where the electrons in EBL are scanned according to a pattern generator while in SEM electrons are raster scanned and collect secondary electrons. The SEM's have a working voltage of 30 kV while EBL has a working voltage of 100 kV. Similar to EBL, FIBL uses ion beams to hit the substrate as shown in Fig. 17. When ions hit the substrate the possible reactions are (1) sputtering of neutral ionized and excited surface atoms, (2) electron emission, (3) displacement of atoms in the solid, (4) emission of photons, and (5) chemical reactions. Based on these FIBL systems are also used for deposition of tungsten, platinum, and carbon. These two process areas also called as mask-less lithography processes.

An EBL system consists of a chamber maintained at high vacuum. It consists of a column through which the electrons are accelerated using optical elements as shown in Fig. 18. The area exposed to the electron beam is called as writing field which ranges from tens of microns to millimetres. The writing field is subdivided into exposure elements (EXEL) which is determined by Digital to Analog converter (DAC). For example, a 15bit DAC subdivides each field into a writing grid of 32,768 EXELs per side, meaning that for a 327.68 μm field, the EXEL dimension is 10 nm. There can be multiple writing fields and can be stitched which depends upon the quality of the stage on which the substrate is locked. Acceleration voltage and current are fixed for a single exposure, called as exposure dosage measured in current deposited per unit area. The EBL is characterized by the writing speed which depends upon the hardware and ranges from 1 to 50 MHz. As the electrons undergo multiple scatterings a finite of them get deposited few microns away. This is called as proximity effect and can be eliminated by higher acceleration of the electron beam. Also the resolution depends upon the beam current which is defined as the number of electrons is impinging on the sample each second (range: 0.05–0.5 pA). The pattern is designed using suitable CAD software's and the GDSII is the industry-accepted

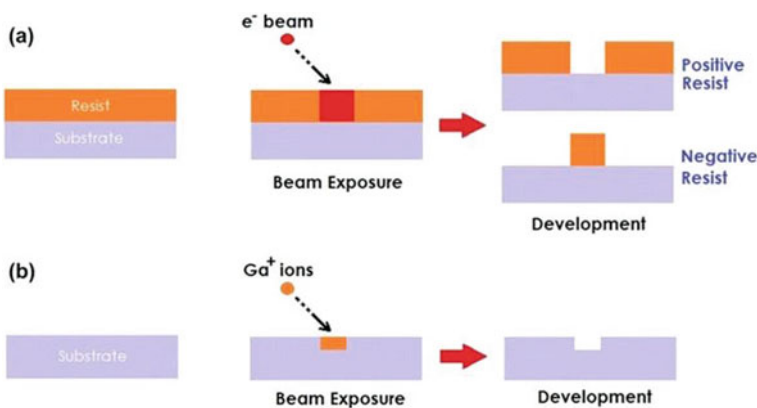


Fig. 17 Process steps for Electron beam lithography (EBL) and Focused ion beam lithography (FIBL). *Image courtesy Hasan et al. [19]*

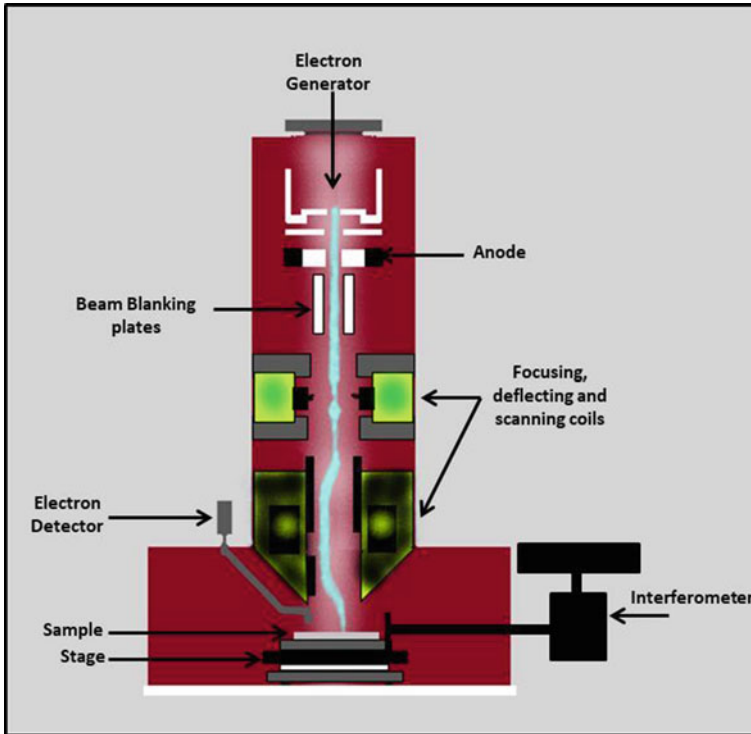


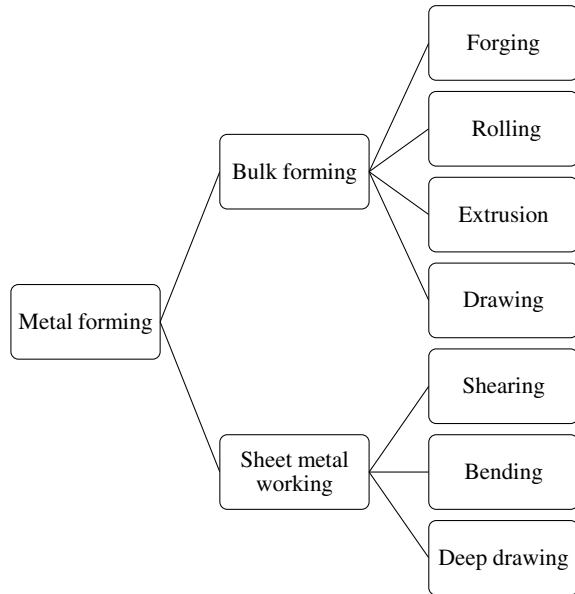
Fig. 18 Block diagram of electron beam lithography

format. Proprietary software converts this GDSII files into instructions necessary for the pattern generator to direct an scan the beam as required. Implementation of correct exposure dosages eliminates the proximity effects. As the desired features are in range of nano-meters, the sample needs to be prepared before exposure which includes cleaning with acetone, alcohol, and blow drying. The samples are then coated with the required resist material and then coated with insulating materials like Al or Au in order to avoid charging effects. The coated samples are mounted in loading dock for exposure to Electron beam and later developed carefully.

2.4.2 Forming Techniques

This technique has been used by the blacksmiths since a very long time for making agricultural equipment's and weapons. Forming techniques are used for shaping sheet metals and can be divided into two groups as shown in Fig. 19 that impart the required shape onto the materials. Material is subjected to shear stress and principal of plastic deformation using punch and die. The working principles are even same for the micro forming process but largely depend upon the material properties. Material

Fig. 19 Basic forming procedures used in manufacturing technology



properties on which effect the sheet metal forming significantly include stress–strain relationship, grain size, work-hardening, residual stresses, orientation of the grain sizes, etc., Most of the forming processes are used at room temperature but when heated metals have less resistance to deformation. Temperature-induced hot forming changes the properties by easing the material flow and decreases the punching force. Biomaterials like Ti, Mg and Co-alloys are difficult to deform and make use of hot forming conditions. Industries which manufacture small components such as dental implants and hearing aids use bulk forming techniques. Micro-tubes, needles, and other tubular parts are fabricated using techniques like hydroforming where pressure is applied using water or oil emulsions within a range of 100–400 Mpa.

Metal forming process is a general term for a wide variety of process where the metal can be compressed, stretched, and bent depending upon the force applied. Apart from the material properties the typical process parameters that affect the forming process are Temperature, Flow stress, Strain and Strain-rate and other tribology factors. The objective of these parameters is to deform the sheet metal to desired shape, avoid part breakage and develop required microstructure. Hot forming is used for large components like orthopaedic implants made of Ti or Co-alloys while micro components are formed in room temperature conditions. The average stress at which the material deforms is called Mean flow stress. By increasing the temperature on the material, flow stress decreases and hence lesser energy will be required to deform the material. In cold working condition, work hardening will take place and products become stronger and produce better finish. Plastic deformation takes place between the approach section of punch and die. The total energy required for this deformation

is the summation of energy required in plastic deformation and energy required in overcoming friction.

For different metal forming process flow stress analysis is different depending upon the process. For example, extrusion is continuous deformation process while forging is intermittent deforming process. Stress and strain guide the material flow during deforming while response of the material depends upon the strain rate. Strain rates affect the deformation process. It is the speed of deformation process and is related to particular metal forming process. The response of the material depends on the strain rate. Also a minimum amount of friction is required for the metal forming processes. Excessive amounts are undesirable and lubricants are used to avoid excessive friction. The advanced forming methods like hydroforming, incremental sheet forming and micro-forming are revolutionary approaches of the previously discussed forming operations. Hydroforming is the process where the tube/sheet is clamped in a hydro-former and fluid pressure is applied to deform the tube/sheet for a required shape as shown in Fig. 20 [30]. This process has the ability to create enhanced mechanical properties, better surface finish and fewer components required in an assembly, and less required rework. Incremental forming was used for fabricating clavicle implants using medical-grade titanium sheets as shown in Fig. 21 [31]. In incremental forming a hemispherical tool controlled by computer program for movement plastically deforms material moving from one counter to another incrementally. Here no die is needed during the process and is more suitable for the customization production compared to other forming processes.

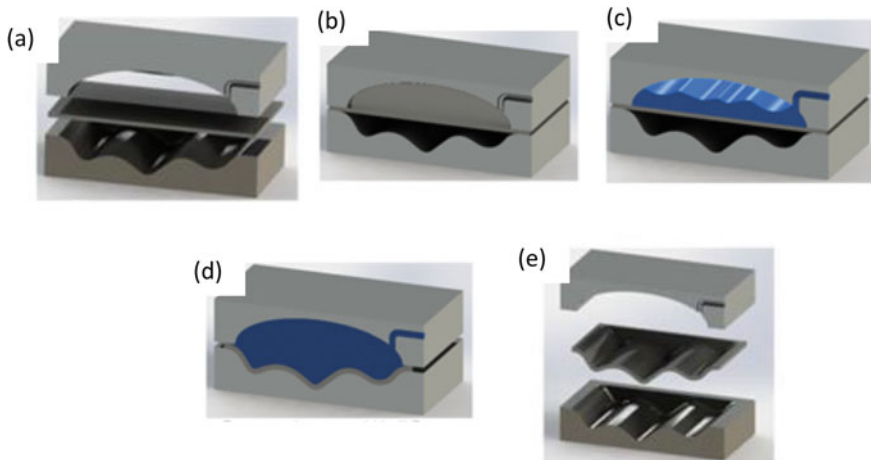
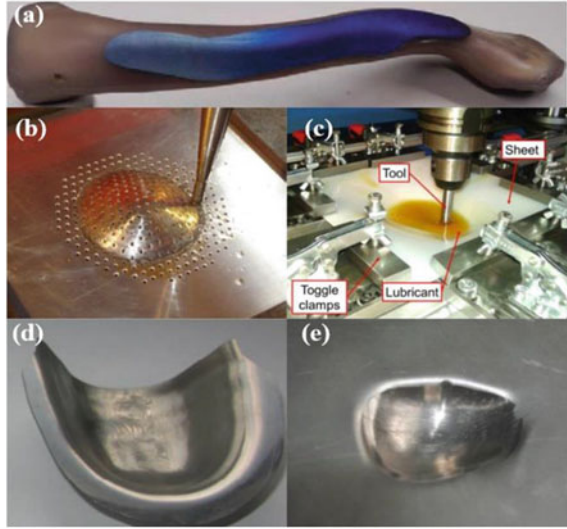


Fig. 20 Process showing sheet hydroforming. **a** Sheet metal inserted to hydroforming equipment, **b** Sheet metal clamped into place, **c** Fluid inserted into hydroforming equipment, **d** Increase in pressure until the part is formed, **e** Part ejected. *Image courtesy Bell et al. [30]*

Fig. 21 Different implants and materials formed by Incremental sheet forming process. **a** clavicle implant of pure titanium, **b** skull prosthesis of meshed titanium plate, **c** cranial implant of polymer material, **d** denture base of stainless steel, **e** knee joint of titanium. *Image courtesy Cheng [31]*



3 Biomedical Additive Manufacturing

The field applications of additive manufacturing popularly known as 3D printing include medical instruments, haptic, tissue engineering and bioprinting, dentistry, personalized equipment, automatic models, and pharmacy-related applications. This process can be broadly classified into bio-printing additive manufacturing of soft constructs, silicones, metallic and ceramic materials, polymeric and composite materials, pharmaceutical applications.

3.1 Bio-Printing

The normal additive manufacturing technique is basically a layer-by-layer material deposition process where the geometry and the shape of the models are constructed with the aid of Computer-Aided Design. This process consists of model construction, slicing the model into layers, preparation of the building material, construction of the modeled design, and sintering for binding of the layers. Bio-printing is broadly classified as bio-printing of soft constructs and hard materials depending on the material which is printed. Hard structures are generally load-bearing members, especially in medical equipment or implants. Soft constructs/structures are the members used in the functionalization of the muscles, neurons, cells, and tissues which are readily deformable on application of forces [32].

Bio-printing of soft constructs is further categorized as indirect and direct bioprinting. In direct bio-printing, the build materials are living cells whereas in indirect printing the materials are acellular. In the process of direct printing the

materials which have already been successful printed are endothelial and epithelial cells, fibroblasts, keratinocytes, smooth muscle cells, articular and nasospetal chondrocytes, interstitial cells, hepatocytes, stromal cells, and various progenitor and stem cells according to Zhang et al. [33]. The crucial mechanical and chemical properties of the 3D bio-printed model are achieved by the combination of various hydrogels and their precursors. Based on the origin of the hydrogels, they are classified as natural and synthetic hydrogels. The natural hydrogels include collagen, gellan, chitosan, hyaluronic acid (HA), fibrin, silk fibroin, alginate, and agarose; similarly the synthetically derived hydrogels include poly acrylic acid (PAA) and the derivatives of the same such as poly ethylene oxide (PEO) and its co-polymer, poly vinyl alcohol (PVA), Polypeptides and polyphosphazene.

Bio-printing types include filament-based extrusion, inkjet 3D printing (i3DP), laser induced forward transfer vat polymerisation, photopolymerisation, stereolithography (SLA)/digital light processing (DLP) process. The processes such as vat polymerisation, photopolymerisation, stereolithography (SLA)/digital light processing (DLP) are not so commonly used in bioprinting since incorporating living cells and high stiffness materials are difficult to incorporate during printing.

3.2 Extrusion-Based Bioprinting

This method is the most common method to print silicones and soft materials. The printing system is simple, consisting of a syringe extruder, a 3D platform, and a curing mechanism. Here, the silicone is extruded through a nozzle onto a substrate. By maneuvering the 3D platform with the help of the drives, the required geometry is printed. After printing it is cured at a desired temperature for a particular period of time depending on the chemical property of the material being printed. Figure 21a shows the representation of the process.

Various research groups and also commercial products have demonstrated that depending on the chemical characteristics, silicones can be cured by heat, ultraviolet light, humidity or catalyst [34]. The solidification rate is determined by the intensity of the curing mechanism, except in case of catalyst method. Unavailability of support structures is a major challenge in silicone printing as controlling the deformation becomes difficult without support structures [35]. Alternatively, Jin et al. [36] proposed 3D printing of PDMS directly in a hydrophobic fumed silica suspension for support.

Extrusion-based bioprints are accompanied with material anisotropy and optical intransparency due to the presence of extrusion marks, layer interfaces, and internal voids.

In this process, the nozzle size determines the dimensional accuracy and the resolution of the print.

3.3 Inkjet Printing

This process is capable of producing ultra-fine components with good surfaces. To ensure the stability of the printed part, UV curable and soluble support material can be used in the process. The process is similar to extrusion, but here the ink is dispensed using a micro-sized channel which works based on piezoelectric mechanism. Since, this uses a micro-sized channel, printing of high viscous fluids is difficult. The most essential properties in this process are fluid properties such as surface tension, viscosity, and density since these are very much essential in the formation of the droplet.

Ink printing needs suitable materials for printing, here the materials should account for mechanical features and fluid compatibility. The silicones should be used in such a way that the additives do not increase the viscosity too much so that the micro channels will not be able to dispense the material. Figure 22b shows the schematic representation of the droplet on drop extrusion process. Figure 23 shows the schematic of the photopolymer-based inkjet printer.

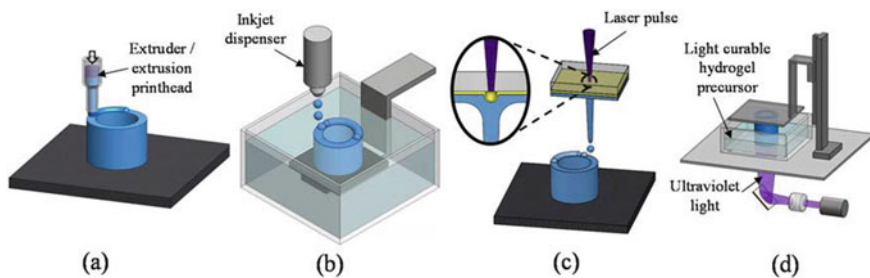


Fig. 22 Representative soft construct printing techniques. **a** extrusion, **b** inkjet printing, **c** laser-induced transfer, and **d** stereolithography. *Image courtesy* Huang et al. [37]

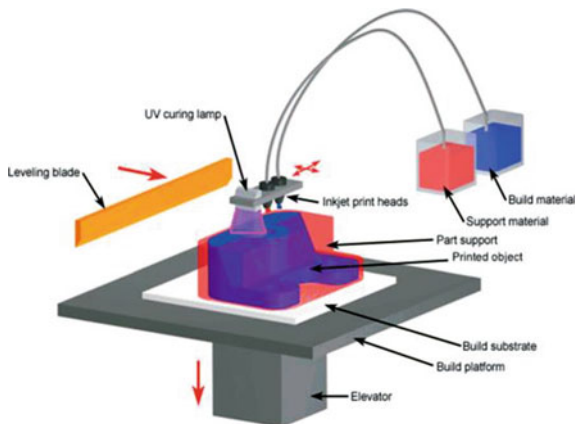


Fig. 23 Photopolymer-based inkjet printer. *Image courtesy* Custompartnet/3D printing [38]

3.4 *Laser Bioprinting*

In this process, bioink is prepared as a thin-film coating on the bottom side of a transparent quartz support, which is usually called a ribbon as a whole. Laser pulses are made to pass through the top side of the ribbon perpendicularly and are focussed at the interface of the bioink and coating the quartz support. The resulting localise heat due to laser matter interaction creates sublimation of a small portion of the coating to form a high-temperature, high-pressure vapor bubble. This pressure pulse ejects a part of the bioink from the ribbon forming different types of jets and several droplets are formed. The ejected droplets form the basic structures for tissue constructs. The schematic representation of the process is shown in Fig. 22c.

This technique can handle a wide range of viscosities as it is orifice-free and non-contact printing process [39] and the bioink transferred has less chances of contamination.

Laser bioprinting is used in printing variety of biological materials including hydrogels, peptides, DNA, and living cells [40–42]. It is also used in making cellular and acellular constructs.

It is still difficult to achieve good printing quality when printing bioinks with relatively low viscosity, which has been partially addressed by introducing a sacrificial energy absorbing layer such as a gelatin layer [43].

3.5 *Vat Photopolymerisation*

The most commonly used 3D printing technique, Stereolithography and Direct Light Photopolymerisation are the two widely used conventional techniques of Vat polymerisation. This process is strictly applicable to photopolymers. Photopolymers are those species of polymers which change their properties when exposed to heat and light mainly their crystallinity and hardness.

In this process, the polymer to be 3D printed is taken in a tank commonly known as Vat, a 3D platform is used for printing. The platform submerged in the vat is moved in such a way that the required geometry of the layer is produced, then the platform is lowered and is exposed to laser light such that the subsequent layer is formed. The process is repeated until all the layers are formed and then the part fabricated is cured. Figure 22d represents the schematic representation of SLA.

Vat photopolymerisation produces better quality prints when compared with extrusion based methods. The main challenge faced in this method is adhesion of material to the vat when exposed to the laser (Fig. 24).

These techniques are used in the fabrication of dental and surgical implements. These offer high resolution and smooth surface finish when compared with other additive manufacturing techniques [45]. Various research groups have worked on the improvement of this process since it is a promising technique in the manufacturing of the implants. Novel advanced resins are developed so that the range of the materials

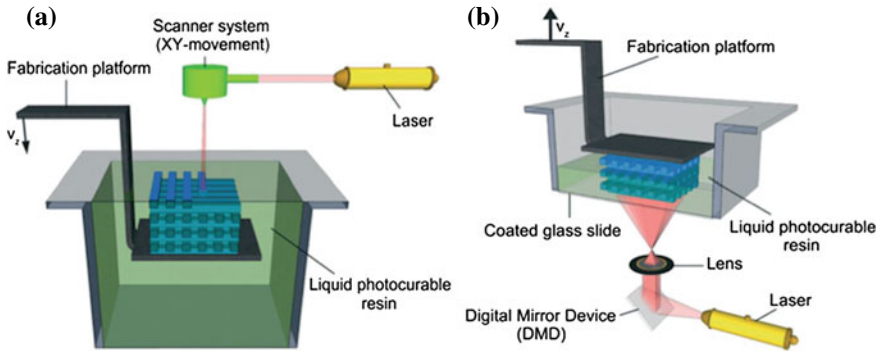


Fig. 24 **a** Laser-scanning SL with the free surface/bath configuration. **b** DLP SLA with the constrained-surface/bath configuration. *Image courtesy* Billet et al. [44]

that can be printed is enhanced, the resolution and the surface finish of the products are improved. This process is used in the printing of ceramics, shape memory polymers, carbon fibers, and magnetic particles.

3.6 Laser Micromachining

Femtosecond laser micromachining is the most recently found technique in Laser Micromachining. In this technique, laser with pulse duration of 1–100 femtoseconds is used to remove or even join the sample. This finds applications in laser surgery, 3D optical waveguide writing, 3D optical data storage, and direct laser joining. The intensity of the femtosecond laser pulses is so high that it is capable of producing localized structural modifications [76].

This process works on the principle of localized melting and re-solidification of the materials only around the focal volume. Near-infrared femtosecond lasers are useful in cell biology, these lasers are used in imaging and modifying subcellular structures. As these lasers offer localized energy absorption and intracellular ablation around a focal volume, these are used in site specific dissection, removal, or disruption of organelles [46].

A femtosecond laser produces various features such as voids, cracks, color centers change in the refractive indices and modification in bi-refringement depending on various conditions like focusing parameters, materials and laser parameters such as wavelength, pulse duration, energy, and repetition rate.

3.6.1 Effect of Repetition Rate

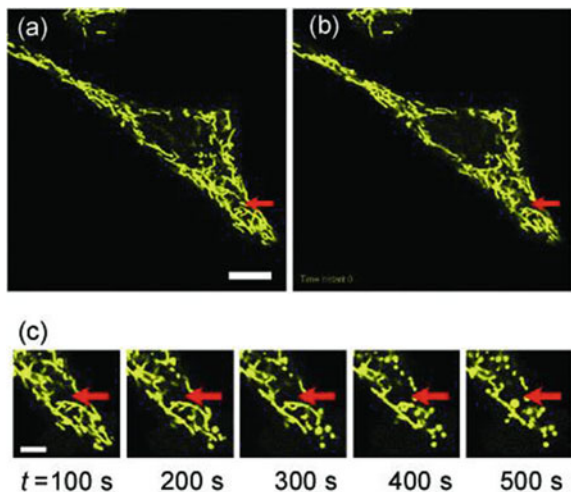
There are two regimes in Laser microprocessing namely low and high repetition rate processing depending on the time required for heat to diffuse away. In low repetition rate regime, single pulses are used to modify the properties of the sample being focused. Here, the pulses are separated by milliseconds, so that it exceeds the time required for heat diffusion, thus the sample returns to normal temperature before the next pulse is focused. But, in high repetition rate regime, multiple pulses are used to produce the cumulative thermal effect. Here, the pulses act as a heat source acting at a point accumulating heat at a point hence increases the heat-affected zone. At low repetition rate, the energy deposition is diffused before the preceding pulse but at high repetition rate, the heat gets accumulated into the system.

The high repetition rate laser micromachining has advantages over the low rate regime.

- i. Much higher processing speeds.
- ii. Better control over the structural modification, as it is influenced by the number of pulses and writing speed.

Near-infrared femtosecond lasers are used for intracellular surgery, since femtosecond laser allows noninvasive intracellular ablation at sub-diffraction resolution with submicron size damaged region in the cell. The surgery on mitochondrial cells was carried out by Shimada et al. [47] and the induction of mitochondrial fragmentation in the HeLa cells is shown in Figs. 25 and 26.

Fig. 25 Mitochondrial fragmentation in HeLa cells induced by femtosecond laser pulses. Stacked three-dimensional confocal images obtained **a** before and **b** after irradiation with 0.53 nJ/pulse (exposure time: 32 ms). The red arrow indicates the irradiation point. Scale bar: 10 μm . **c** Time-lapse confocal images after irradiation. Scale bar: 5 μm . *Image courtesy Shimada et al. [47]*



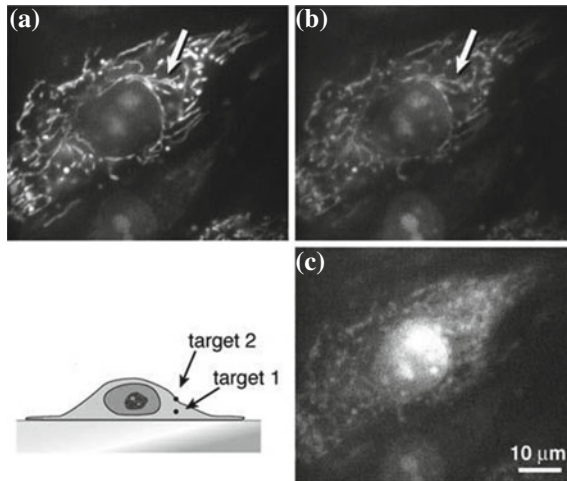


Fig. 26 Ablation of a mitochondrion in a live cell without compromising cell viability. Fluorescence microscopic images of a live cell containing EYFP-labeled mitochondria in a cultured medium containing ethidium bromide ($4 \mu\text{m}$). **a** before femtosecond laser irradiation, **b** after ablation of a single mitochondrion within its cytoplasm (target 1 in diagram at bottom left), and **c** after irradiation of the apical cell membrane (target 2). *Image courtesy Shen et al. [48]*

4 Characterization of Micro and Nano Biological Samples

The fabrication techniques used in the production of these micro-nano components are different from the conventional manufacturing process. Hence, there develops a challenge of having newer techniques to characterize the produced components. The characterization techniques used in the macro regime can be applied to the micro-scale with certain modifications. There is always a chance that the stresses might be induced in the components during the measurement process, so care needs to be taken while choosing the characterization technique. The range of parameters is extreme small in the micro features, hence becomes the most challenging part of the study. Quantification of the output results of the characterization process becomes difficult as the size of the sample becomes tiny and the characteristics of the material vary with size due to the size effect. The functionality of the materials change with size and that has to be taken into account while characterizing the micro or nano scale components.

The materials can change their electrical properties at nanoscale from conductors in bulk form to semiconductors or poor conductors at the nanoscale. Certain materials that are semiconductors might become conductors or superconductors. The compact arrangement of electrons results in the change of electrical properties at the nanoscale.

Optical properties also depend on the size of the material. Electrons become restricted and cannot move as freely as in bulk when compared to nanoscale. The compact arrangement of electrons causes them to react to light differently. Gold for

example will appear yellowish at the macro scale. However, it appears red in color as nanosized particles. In sun blocks, large zinc-oxide particles are used to scatter visible light appearing white. Nanosized zinc-oxide particles will not scatter visible light, which causes sun block to appear transparent. Quantum dots also have unique optical appearance as the size of the particles decreases, the colors emitted are totally different.

Some properties of the materials are dependent on the surface area namely rate of reaction, melting point, adhesion and capillary action. For example, at macro scale, the melting point of Gold is 1064 °C. As its particle size decreases to the 100–10 nm diameter its melting temperatures drops to 100 °C. As the size reduces to 2 nm, the melting point decreases to half of the melting point at the macro scales level. Gold acts as an electrical insulator when it becomes less than 10 nm.

5 Nanometrology

Nanometrology deals with the coordinates and identities of all the constituent atoms of a nanoscale structure. This can be categorized into imaging and non-imaging and further each can be categorized as contact and noncontact types. These techniques involve topographical and chemical characterization by identifying regularities. Biological characterization is the most challenging field of metrology as the field of study is unfamiliar to most of the metrologists (Table 2).

Some of the challenges for nanometrology are:

1. Three-dimensional characterization of the structures as the existing technologies provide 2.5D analysis systems. Avoid the trade-off between spatial resolution and measurement sensitivity.

Table 2 Various microscopy techniques and the physical form and particle sizes of the samples. Courtesy: T. Linsinger, et al. [77]

Microscopy technique	Analyte form	Particle size (nm)
Atomic force microscopy	Dry, deposited on substrate	8.5 ± 0.3
Scanning electron microscopy	Dry, deposited on substrate	9.9 ± 0.1
Transmission electron microscopy	Dry, deposited on substrate	8.9 ± 0.1
Differential mobility analysis	Dry, aerosol	11.3 ± 0.1
Dynamic light scattering	Liquid suspension	13.5 ± 0.1
Small-angle X-ray scattering	Liquid suspension	9.1 ± 1.8

2. The measurement strategy or technique to characterize the structures falling in the transition range between micro and nanoscale metrology.
3. Reference value mean size and expanded uncertainty \times Average particle size of gold nanoparticle (diameter), in nm [49].
4. Collection of multiple parameters, i.e., physical, spatial, chemical, and mechanical data, simultaneously by integrating the techniques such as scanning with spectroscopic analysis, functionalized probe tips capable of picking both chemical and mechanical features.
5. Correlation of functionality and dimensional metrology by developing an international database.
6. Meeting the demands of the medical and healthcare industries, as new challenges and developments have been taking place.
7. Characterization of next-generation nanostructures, as the second-generation nanostructures are more complex.
8. Application of non-linear optical microscopy and spectroscopy, single-molecule Fluorescence Resonance Energy Transfer (FRET), and X-ray scattering in validating accuracy to characterize the biological environment.

5.1 *Bio Characterization*

The main challenges in characterizing biological samples are.

1. The range of the ambient conditions in which the living things can be analyzed is very narrow.
2. The living samples usually consist of soft, irregular structures, free-form surfaces that keep evolve in different scales.
3. The living samples, even the simplest structures are capable of changing their environment through secretions.

The list of the characterization techniques is mentioned in Table 3.

5.2 *Confocal Microscopy*

Confocal Microscopy is one of the most widely used microscopic techniques. It is well suited to image thick specimens like embryonic cells or tissues. Here, Laser light is focused on a particular spot at a specific depth inside the specimen. And the pinhole located in the microscope blocks the signals which are out of focus and only the fluorescence signals are allowed to enter the light detector, hence providing a sharp image at the end of the raster scan.

The sample image scanned using Confocal Microscope is shown in Fig. 27, the images of the bovine pulmonary endothelial cells and pyramid cell dendrites of a rat visual cortex are analyzed.

Table 3 Various characterization techniques that can be used for biological samples

Confocal microscopy	X-ray absorption spectroscopy	Transmission electron microscopy
Atomic force microscopy	Small angle X-ray scattering	Capacitance microscopy
X-ray diffraction	Scanning tunneling microscopy	Polarisation spectroscopy
Auger electron spectroscopy	Small angle neutron scattering	Cyclic voltammetry
Raman spectroscopy	Scanning electron microscope	Linear sweep voltammetry
Nuclear magnetic resonance	Photoluminescence spectroscopy	Secondary ion mass spectrometry
Mossbauer spectroscopy	Electroluminescence spectroscopy	Cathodoluminescence spectroscopy
Fourier transform infrared spectroscopy	Differential scanning calorimetry	Electron energy loss spectroscopy
Energy-dispersive X-ray spectroscopy	X-ray photoelectron Spectroscopy	Single-molecule spectroscopy
Four-point probe and I-V technique	Scanning near field optical microscopy	Neutron diffraction
Interference microscopy	Laser interferometry	–

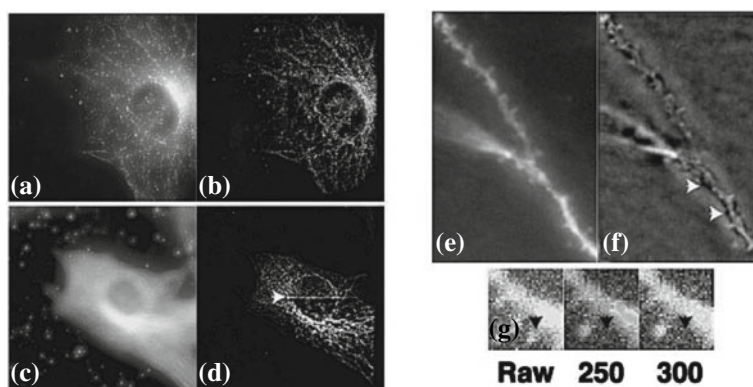
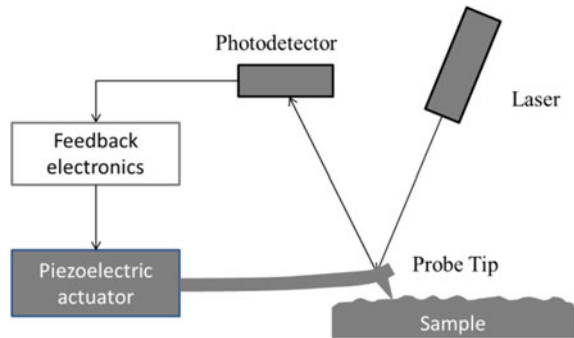


Fig. 27. **a–d** Images of bovine pulmonary endothelial cells from a prepared slide, **e, f** Pyramid cell dendrites from sections of rat visual cortex, fixed and then injected with Lucifer Yellow (emission max = 533 nm). **g** Detail of a similar sample to panel E before deconvolution (Raw) and after deconvolution by increasing numbers of iterations (250 and 300). A small feature disappears (black arrow). *Image courtesy* Wallace et al. [50]

5.3 Atomic Force Microscopy (AFM)

First found in the year 1986 by Binnig, Quate and Gerber. This involves scanning the surface with a probe tip. The force originating between the surface's atoms and the probe tip results in the deflection of the probe as shown in Fig. 28. The deflection

Fig. 28 Schematic representation of Atomic Force Microscope (AFM)



is picked up by the laser beam, cantilever and photo-detector the lateral resolution is also a function of the vertical resolution and the tip size [51]. The typical depth range of AFM is 0.5–5 nm and the lateral resolution is 0.2–130 nm.

This technique is used in the measurement of properties such as surface roughness, surface topography, elasticity, grain size, magnetic features, surface friction, surface molecular interactions, and the density of electron states. AFM is highly recommended for characterizing Carbon Nano Tubes (CNT), nano-crystals, nanoparticles, nanowires, and dendrimers.

In a recent study by Piras et al. [46], 150 nm thick and 1 μm wide aluminum features on a silicon substrate buried under a 300 nm thick photoresist and 50 nm thick titanium layers were characterized using AFM with blunt (Nominal radius of 80 nm) and sharp (Nominal radius of 8 nm) diamond tips. The results of the scans are represented in Fig. 29.

AFM is used in the characterization of biological soft tissues [73], though some modifications have to be made to the conventional AFM equipment. As shown in Table 4, the young's moduli of biological samples are much smaller than the metals and polymers. Further, when compared to the bone tissue (Young's modulus—10 GPa), the living cells are way too soft (Young's modulus—100 kPa), i.e., 10^{-6} times softer.

AFM is used to characterize the cancer cells and Fig. 30 shows the comparison of the AFM images of normal and cancerous cells [52].

5.4 Scanning Tunneling Microscopy (STM)

First found in the year 1982 by Binnig et al. [53]. This involves scanning the surface with a metal tip, unlike AFM, an electric voltage is applied between the tip and the surface resulting in a tunneling current as shown in Fig. 31. The intensity of this current is used for analysis of the surface. The typical depth range of STM is 1-5 nm and the lateral resolution is 2–10 nm.

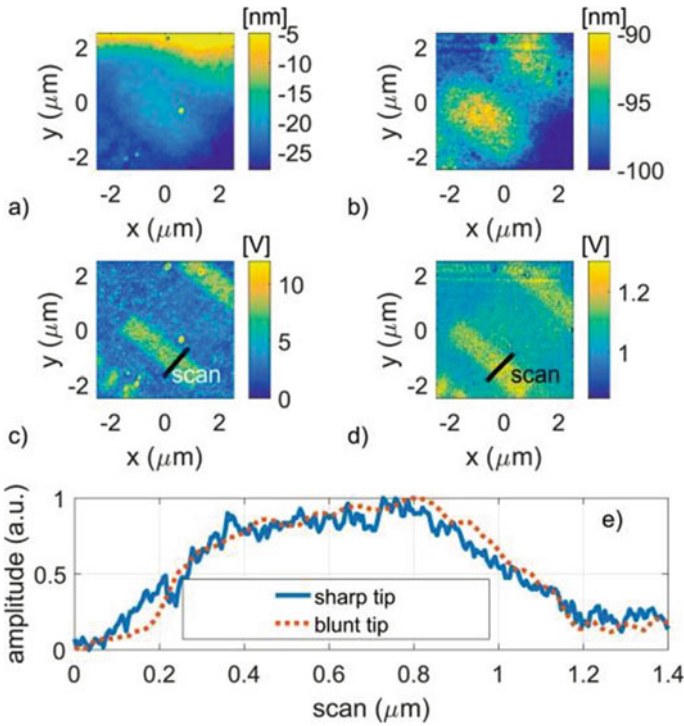


Fig. 29 **a** Topography and **c** subsurface AFM amplitude scan with blunt (Adama AD-40, 80 nm nominal radius) diamond tip performed with an AFM Bruker system equipped for subsurface imaging. **b** Topography and **d** subsurface AFM amplitude with a sharp (Adama AD-40 s, 8 nm nominal radius) diamond tip of the same sample. In **e**, the normalized subsurface profiles from the area marked with black lines in **c** and **d** are shown [scan axis in (**c**) and (**d**) runs from left to right]. *Image courtesy Piras [51]*

Table 4 Elastic properties of materials [42]

Material	Young's Modulus
Steel	200 GPa
Glass	70 GPa
Bone	10 GPa
Silk	10 GPa
Collagen	1 GPa
Protein crystal	0.2–1 GPa
Rubber	1.4 MPa
Living Cells	1–100 kPa

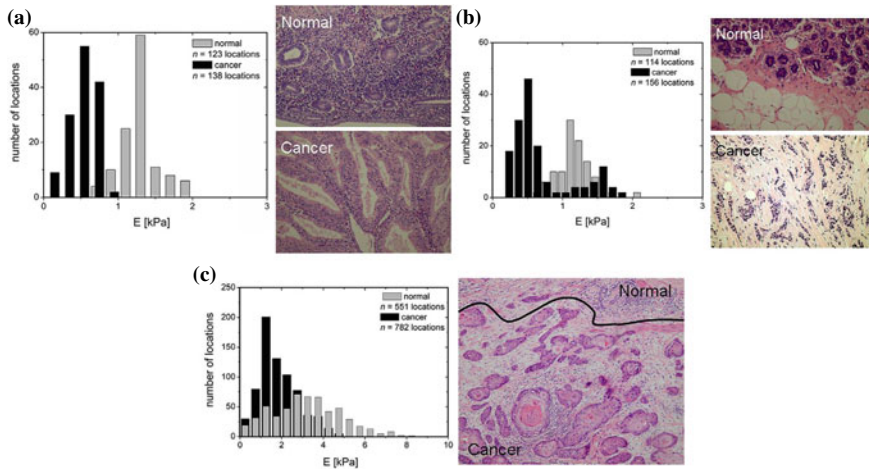


Fig. 30 Stiffness distributions in tissues sections accompanied by the corresponding histological staining (hematoxylin–eosin, 400×). **a** Non-neoplastic endometrium (gray columns) and well-differentiated endometrioid carcinoma (black columns) of the uterine corpus. **b** Non-neoplastic breast tissue (gray columns) and infiltrating ductal carcinoma (black columns). **c** Vulvar cancer—black columns denote cancer while gray ones—non-neoplastic parts of the tissue section separated by black line in the histological image. *Image courtesy* Lekka et al. [52]

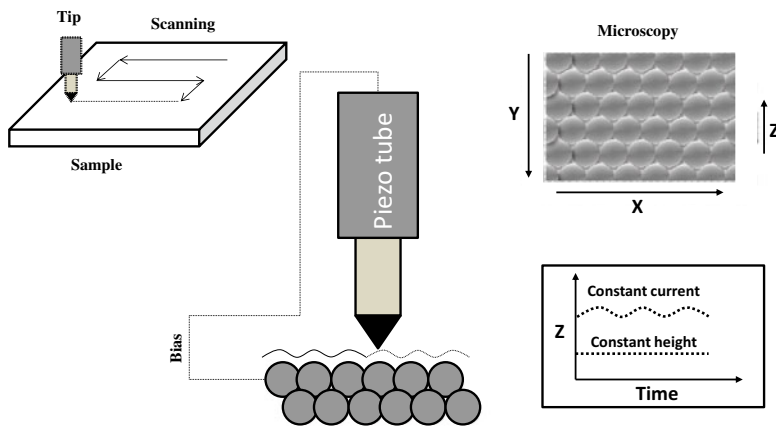


Fig. 31 Schematic representation of scanning tunneling microscopy

This technique is used in obtaining the 3D topology, defects, electronic structure, size, shape, roughness, and the density of electron states. STM has been used in the characterization of chemoreceptive areas of the olfactory organ of the shark and the Fd virus as shown in Figs. 32 and 33 respectively.

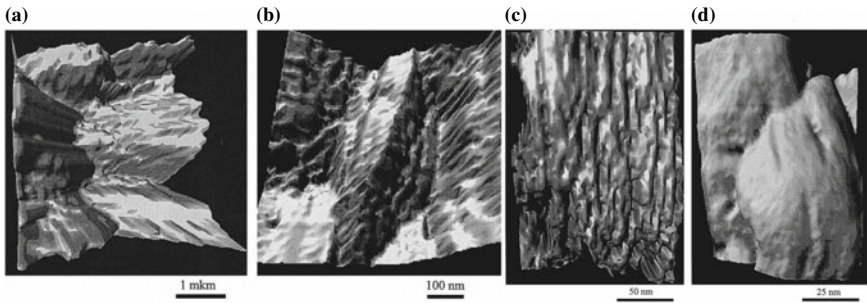


Fig. 32 Investigation of biological samples by the scanning tunneling microscope. **a** A surface of chemoreceptive areas of the olfactory organ of the shark *Carcharhinus longimanus*. **b** Outlet of differentiating receptive cell to the surface of olfactory organ. **c** Lateral surface of support cell microvilli. **d** Apical surface of support cell microvilli. *Image courtesy Permjakov [54]*

5.5 Scanning Near-Field Optical Microscopy (SNOM)

First found in the year 1984. SNOM is a combination of scanning-probe microscopy and optical microscopy. The resolution of SNOM is 50–100 nm.

This is used in the analysis of chemical structure, refractive index, and local stress. This technique has been used to characterize quantum dots, nanospheres, and nanowires.

The heart of the near-field optical microscope is the near-field probe that interacts with the sample at nanometer distance and determines contrast, resolution, and sensitivity. Due to the small illumination volume of confocal microscopy ($\sim 10^8 \text{ nm}^3$) it has become an important tool in single-molecule biophysics.

Total internal reflection fluorescence microscopy (TIRFM) is a successful technique to reduce the intracellular background and a common method to image single molecules. This uses an induced evanescent field to illuminate and excite fluorophores selectively in a sample region just adjacent to a glass-water interface as is shown in Fig. 34a [55].

The restrictions of TIRFM are overcome by NSOM, this conserves the advantages of the near-field excitation. Since it has high spatial resolution and small penetration depth, the excitation volume provided by NSOM is the smallest compared to other optical techniques, e.g. $\sim 10^5 \text{ nm}^3$. NSOM excitation volume versus $\sim 10^8 \text{ nm}^3$ obtained with confocal microscopy. This technique is useful in reducing intracellular auto-fluorescence background and also in imaging the closely packed molecules (max. 100 molecules/ μm^2).

Single-molecule studies on complete cells using NSOM have not been reported so far, mainly due to:

- (1) The complexity of the technique, which requires reliable and reproducible probe fabrication and accurate control of sample-probe distance.
- (2) The slow frame rate, which is inherent to scanning probe techniques.
- (3) The fact that NSOM does not work reliably under liquid conditions.

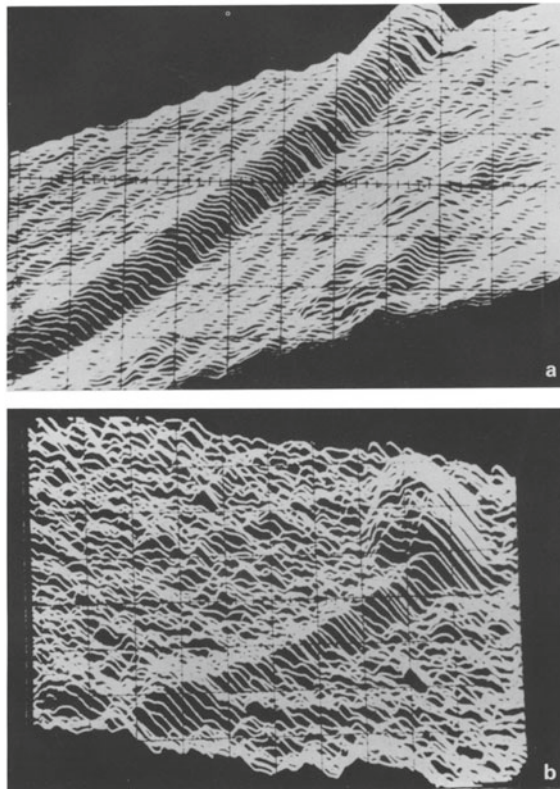


Fig. 33 STM images of Fd virus. **a** Deposition time 2 min, concentrations 3×10^{12} particles/ml. Lateral scales 173 Å/div x and 265 Å/div y. Vertical scale 165, ~div. The ends of the virus cannot be seen, but the apparent diameter is about 100, ~, in agreement with the width of a coated Fd virus. **b** Deposition time 2 min, concentration 3×10^{12} particles/ml. Lateral scales 130, ~div x and 184, ~div. Vertical scale 97, ~div. The virus seems to double back on itself at the top of the image. Two viruses cross each other at the bottom. *Image courtesy Garcia [32]*

The most relevant results of NSOM studies on cells include fluorescence imaging of cytoskeletal actin on fixed mouse fibroblast cells [56], (co-)localization of host and malarial proteins on malaria-infected cells [57], imaging of membrane lipids and proteins on fibroblasts, both dried and in saline [58, 59] and visualization of lectins binding to cell surface proteins [60]. Two of the few NSOM studies under liquid conditions have been performed on antibody-labeled nuclear pore complexes visualized on an isolated nucleus membrane [61] and on fluorescently labeled human leukocyte antigens present on fibroblast cells [62].

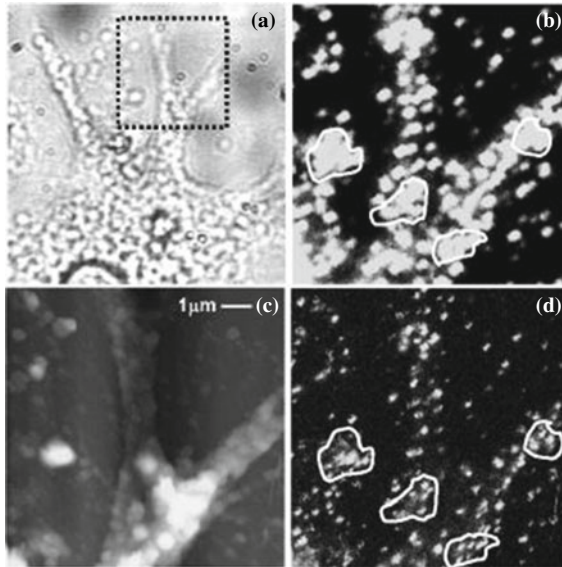


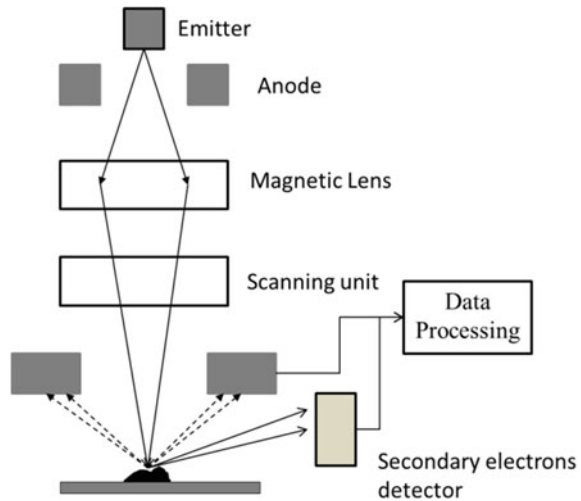
Fig. 34 Fluorescence image of a dendritic cell in buffer solution collected in confocal (a) and NSOM (b) modes. The white circles indicate the position of the line traces through single molecules (recognized by their unique dipole emission, red or green color) in c and d. These line traces demonstrate the superior resolution of NSOM (100 nm) in d as compared to the diffraction-limited confocal resolution (300 nm) in c. The intensity scale is locally changed in the confocal image [indicated by the white box in (a)] in order to visualize the individual molecule. *Image courtesy Koopman [63]*

5.6 Scanning-Electron Microscopy (SEM)

First found in the year 1937. Here a probe of highly focused electrons with energies ranging upto 40 keV is focused on the specimen, and scanned in a raster method. The resulting outputs such as secondary electrons, auger electrons, back-scattered electrons, and X-rays are detected by the appropriate detectors and hence the data analysis is carried out.

The beam is scanned by a set of coils in a raster method. As shown in Fig. 35, the objective lens focuses the scanning beam onto the sample in investigation, one point at a time. The surface topography information of the nanomaterial sample is shown when the electron beam strikes the surface materials and interacts with its atoms, generating signals in the form of backscattered electrons (BSEs), secondary electrons (SEs), and characteristic X-rays [64]. Back scattered electrons are more sensitive to heavier elements than secondary electrons. Energy-dispersive X-ray spectroscopy technique can be used to identify specific elements by detecting the X-ray radiations [65, 66].

Fig. 35 Schematic representation of Scanning Electron Microscope (SEM)



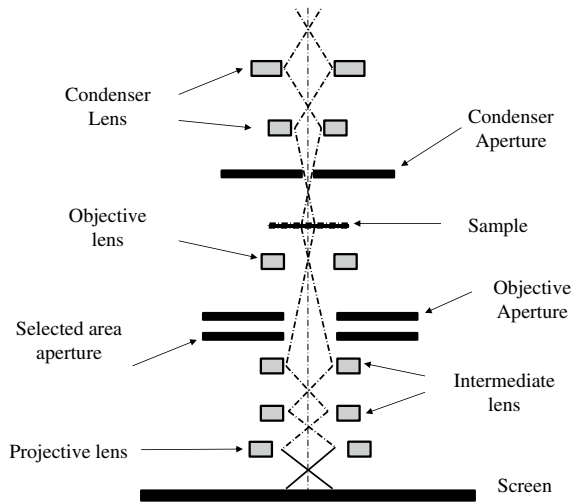
Scanning electron microscopy damages the delicate biostructures during the necessary sample preparation, dehydration and impregnation with heavy metal ions are significant problems.

5.7 Transmission Electron Microscopy

First found in the year 1931 by Ruska and Knoll. In this type of microscopy, the electrons have to pass through the sample and hence the samples are formed into thin foils (less than 100 nm) especially using Focused Ion Beam machining. This technique is used to analyze and capture the atomic structures in a sample. This technique can be used for structural and chemical characterization at a spatial resolution upto 0.1 nm.

When a focused beam of electrons interacts with the sample, various signals are generated and the transmitted electrons form the basis of Transmission Electron Microscope (Fig. 36). Here the electrons interact with the sample mostly through diffraction generating elastic and inelastic, scattered, and unscattered electrons. This technique is used in capturing the crystallographic material at atomic scale on the basis of phase contrasting imaging. The deflection of the diffraction is reliant on the orientations of the planes of atoms in a crystal relative to the electronic beam.

Fig. 36 Schematic representation of Transmission Electron Microscope (TEM)



5.8 Auger Electron Microscopy

This provides significant elemental and chemical characterization of nanostructures with a depth resolution of a few nanometers and a lateral spatial resolution better than 10 nm [67]. When an electron is bombarded on a substrate, an excited atom with an inner shell vacancy is created. And when an electron from the outer shell fills the inner vacancy, an auger electron is emitted. By measuring the intensities of the auger electrons all the elements can be detected with this technique as shown in Fig. 37. The typical sampling depth of AES is 2–5 nm, making it a surface-sensitive analytical technique [63].

Auger Electron Spectroscopy can be used for determining the surface elemental composition of the sample, this technique is difficult to use for soft materials such as cells and tissues as the high-energy electrons might damage the integrity of the biological tissues.

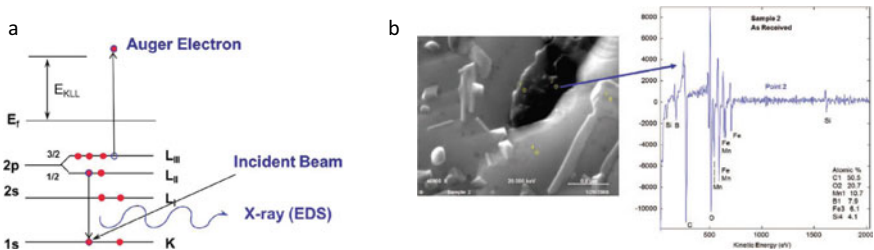
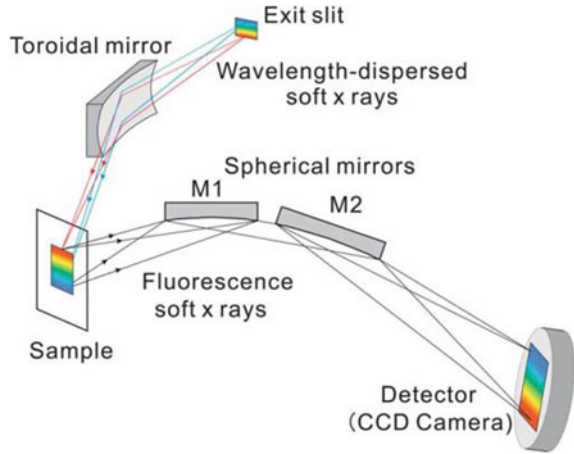


Fig. 37 **a** Schematic representation of emission of an Auger Electron. **b** Auger spectrum of oxidized area, which is enriched in Mn and B. *Image courtesy* Raman et al. [67]

Fig. 38 Schematic representation of X-ray absorption spectroscopy. *Image courtesy Amemiya et al. [68]*



5.9 X-Ray Absorption Spectroscopy

See Fig. 38.

5.10 Flow Cytometer

Flow Cytometry is a technique in medicine and biology, by which the suspended particles are measured and classified. This technique is used to analyze the geometric properties, physiological properties, and quantities of DNA, RNA, cytokines, antigens, enzymes, and proteins [31]. This device is used in the rapid analysis of DNA, cellular marker expression, and electronic sorting of cells of interest for further investigations. These are increasingly used in cellular DNA monitoring, drug transport, phenotype expression, calcium flux, proliferation, and apoptosis. This has been a significant tool as it is used in the diagnostic and therapeutic analysis of leukemic cells. This device is also extended for monitoring hormone receptor expression in solid tumors and also in the human genomic studies.

Flow cytometry is also used in the analysis of cell populations, chromosome sorting, intracellular cytokines, small animal oncology, drug resistance, host–pathogen interactions, and analysis of electronic nuclear volume and DNA content in normal and abnormal human tissue [69, 70].

As shown in Fig. 38, flow cytometer works on the principle of fluorescence of the samples, every particle when incident with high energy white light absorbs a certain amount of energy, raises to a higher energy level which is known as a metastable level, then it emits the absorbed energy and collapses back to the normal level. During this process, the energy is emitted in the form of light, hence it is called Fluorescence.

The wavelength of the emitted energy determines the color of the emitted light. The wavelength thus emitted is used to characterize the sample.

The flow cytometer consists of three important parts, namely, the fluidic part, the optical part, and the electronic part as shown in Fig. 39. The fluidic system is used to create a flow path for the sample so that the cells in investigation are exposed to the high energy light. The cells in contention emit the radiations in different wavelength ranges. The radiations emitted flow through the optical fibers and are then picked up by the photodetectors. The optical fibers and the photodetectors form the optical system of the flowcytometer [72]. The output of the photosensors are then amplified and displayed on the computer (Table 5).

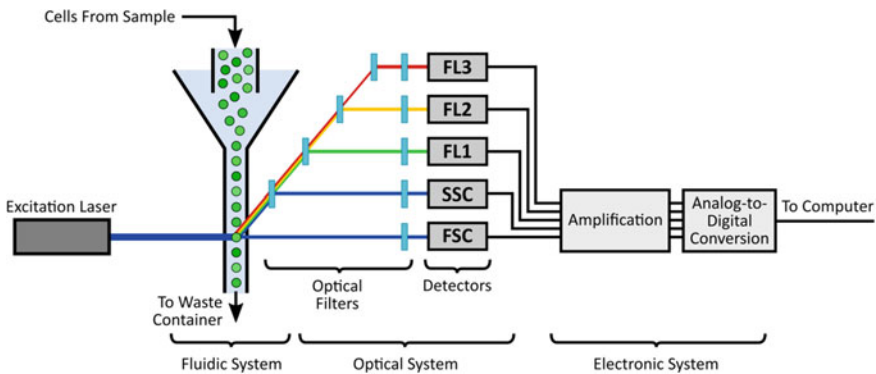


Fig. 39 Schematic representation of flow cytometer, illustrating the fluidic, optical, and electronic systems. *Image courtesy* AAT Bioquest [71]

Table 5 The size range of particles analyzed in a flow cytometer [70]

Particle Size (micrometer)	Particle
100,000	Larger planktons
10,000 = 1 cm	Zooplankton Algae Encapsulated cells/bacteria
100	Multicellular spheroids, Bioreactors Cell aggregates, Plant protoplasts, Microenvironments
10	Mammalian cells Microspheres, Cell nuclei
1	Chromosomes, Bacteria Cellular vesicles. Picoplankton
0.1	Liposomes DNA fragments
0.01	Virus particles
0.001	Phycoerythrin Other individual molecules
0.0001 = 1 Å	

6 Conclusions

Together an overall view of the advanced methodologies in manufacturing biomedical devices was presented in this chapter. The capability of the fabricated devices in various fields like surgery, microfluidic arrays, prosthesis, tissue culture, genetic engineering, pharmacy, sensing, and therapeutics has increased four folds. The advanced processes mentioned in this chapter consider materials with a wide range of stiffness values varying from titanium to human cells. Hence, offer a wide range of materials for fabrication of the devices in turn increasing the scope of their applications. With CAD/CAM and imaging aiding the additional possibility are enabling custom and complex manufacturing according to the patient needs by ease in flow of information at every stage of modern product development. This chapter lays emphasis on describing the basic principles of manufacturing process and its connection to develop advanced manufacturing systems focused towards bio medical devices. The progress in micro-manufacturing technologies aided the growth and development of novel microsystems and their applications in biomedical-devices effecting at cellular level. An important few of enormous variety of methods in developing micro and nano structures using lithographic methods were discussed to impart basics of the processes to the reader. Advancements in mass fabrication methods like injection molding and hot embossing are enabled with the development of mold inserts fabricated using lithographic methods, laser machining, and mechanical micromachining methods. Forming methods are extensively used in fabricating metal implants since a long time, but processes like hydroforming and incremental sheet forming procedures are used nowadays especially for custom manufacturing. In this chapter, it is made to clearly understand that in the lifecycle of biomedical device fabrication involves myriad of processes and steps. The advances in the measurement equipment, the integration of the equipment with computer unit, processors have led to the development of more intricate biomedical devices. The development of bio-printing has opened an entirely new area for exploration; it has led to the development of artificial organs and organelles with all the functions of the human organs. Biomimetic exploration has increased the robustness of the health care equipment and the development of novel measurement and characterization techniques has increased the scope of manufacturing high precision devices and applications.

References

1. Thewes, R., Polla, D.: Biomedical Devices (2007)
2. Handbook on Advanced Design and Manufacturing Technologies for Biomedical Devices
3. Ferreira, M.: Bioprinting customized dental implants: manufacturing processes, topography, osseointegration and future perspectives of 3D fabricated implants. *Bioprinting* **20**(August), e00107 (2020)
4. Lee, J.-A., Koh, Y.-G., Kang, K.-T.: Biomechanical and clinical effect of patient-specific or customized knee implants: a review. *J. Clin. Med.* **9**(5), 1559 (2020)

5. Wang, C., et al.: Enhanced osseointegration of titanium alloy implants with laser microgrooved surfaces and graphene oxide coating. *ACS Appl. Mater. Interfaces* **11**(43), 39470–39483 (2019)
6. Guckenberger, D.J., De Groot, T.E., Wan, A.M.D., Beebe, D.J., Young, E.W.K.: Micromilling: A method for ultra-rapid prototyping of plastic microfluidic devices. *Lab Chip* **15**(11), 2364–2378 (2015)
7. Amirouche, F., Zhou, Y., Johnson, T.: Current micropump technologies and their biomedical applications. *Microsyst. Technol.* **15**(5), 647–666 (2009)
8. Matellan, C., Armando, E., Hernández, R.: Cost-effective rapid prototyping and assembly of poly (methyl methacrylate) microfluidic devices, pp. 1–13 (2018)
9. Jagadesh, T., Samuel, G.L.: Mechanistic and finite element model for prediction of cutting forces during micro-turning of Titanium Alloy. *Mach. Sci. Technol.* **19**(4), 593–629 (2015)
10. Rodríguez, J.M., Carbonell, J.M., Jonsén, P.: Numerical methods for the modelling of chip formation. *Arch. Comput. Methods Eng.* **27**(2), 387–412 (2020)
11. Shunmugam, M.S.: Machining challenges: macro to micro cutting. *J. Inst. Eng. Ser. C* (2015)
12. Markopoulos, A.P., Galanis, N.I., Karkalos, N. E., Manolakos, D.E.: Precision CNC machining of femoral component of knee implant: a case study. *Machines* **6**(1) (2018)
13. Filiz, S., Xie, L., Weiss, L.E., Ozdoganlar, O.B.: Micromilling of microbarbs for medical implants. *Int. J. Mach. Tools Manuf.* **48**(3–4), 459–472 (2008)
14. Joshi, S.S., Melkote, S.N.: An explanation for the size-effect in machining using strain gradient plasticity. *J. Manuf. Sci. Eng. Trans. ASME* **126**(4), 679–684 (2004)
15. Rahamathullah, I., Shunmugam, M.S.: Mechanistic approach for prediction of forces in micro-drilling of plain and glass-reinforced epoxy sheets, pp. 1177–1187 (2014)
16. Srinivasa, Y.V., Shunmugam, M.S.: Mechanistic model for prediction of cutting forces in micro end-milling and experimental comparison. *Int. J. Mach. Tools Manuf.* **67**, 18–27 (2013)
17. Tran, K.T.M., Nguyen, T.D.: Lithography-based methods to manufacture biomaterials at small scales. *J. Sci. Adv. Mater. Devices* **2**(1), 1–14 (2017)
18. Guan, J., Ferrell, N., James Lee, L., Hansford, D.J.: Fabrication of polymeric microparticles for drug delivery by soft lithography. *Biomaterials* **27**(21), 4034–4041 (2006)
19. Hasan, R.M.M., Luo, X.: Promising lithography techniques for next-generation logic devices. *Nanomanufacturing Metrol.* **1**(2), 67–81 (2018)
20. Chen, Z., et al.: Rapidly fabricated microneedle arrays using magnetorheological drawing lithography for transdermal drug delivery. *ACS Biomater. Sci. Eng.* **5**(10), 5506–5513 (2019)
21. Di Carlo, D., Edd, J.F., Irimia, D., Tompkins, R.G., Toner, M.: Equilibrium separation and filtration of particles using differential inertial focusing. *Anal. Chem.* **80**(6), 2204–2211 (2008)
22. Arcot, Y., Samuel, G.L., Kong, L.: Micro hot-embossing of serpentine channels on PMMA based microfluidic devices, pp. 1044–1047 (2017)
23. Yuan, Y., Hays, M.P., Hardwidge, P.R., Kim, J.: Surface characteristics influencing bacterial adhesion to polymeric substrates. *RSC Adv.* **7**(23), 14254–14261 (2017)
24. Becker, H., Gärtner, C.: Polymer microfabrication technologies for microfluidic systems. *Anal. Bioanal. Chem.* **390**(1), 89–111 (2008)
25. Limongi, T., et al.: Laboratory injection molder for the fabrication of polymeric porous poly-epsilon-caprolactone scaffolds for preliminary mesenchymal stem cells tissue engineering applications. *Microelectron. Eng.* **175**, 12–16 (2017)
26. Mi, H.Y., Jing, X., Salick, M.R., Turng, L.S., Peng, X.F.: Fabrication of thermoplastic polyurethane tissue engineering scaffold by combining microcellular injection molding and particle leaching. *J. Mater. Res.* **29**(8), 911–922 (2014)
27. Yi, Q.: *Micro-Manufacturing Engineering and Technology* (2010)
28. Worgull, M., Héту, J.F., Kabanemi, K.K., Heckeles, M.: Modeling and optimization of the hot embossing process for micro- and nanocomponent fabrication. *Microsyst. Technol.* **12**(10–11), 947–952 (2006)
29. Altissimo, M.: E-beam lithography for micro-/nanofabrication. *Biomicrofluidics* **4**(2), 2–7 (2010)
30. Bell, C., Corney, J., Zuelli, N., Savings, D.: A state of the art review of hydroforming technology: Its applications, research areas, history, and future in manufacturing. *Int. J. Mater. Form.* **13**(5), 789–828 (2020)

31. Cheng, Z., Li, Y., Xu, C., Liu, Y., Ghafoor, S., Li, F.: Incremental sheet forming towards biomedical implants: a review. *J. Mater. Res. Technol.* **9**(4), 7225–7251 (2020)
32. Garcia, R., Keller, D., Panitz, J., Bear, D.G., Bustamante, C.: Imaging of metal-coated biological samples by scanning tunneling microscopy. *Ultramicroscopy* **27**, 367–374 (1989)
33. Zhang, Z., Jin, Y., Yin, J., Xu, C., Xiong, R., Christensen, K., Ringeisen, B.R., Chrisey, D.B., Huang, Y.: Evaluation of bioink printability for bioprinting applications. *Appl. Phys. Rev.* **5**(4), 041304 (2018)
34. Liravi, F., Toyserkani, E.: Additive manufacturing of silicone structures: a review and prospective. *Addit. Manuf.* **24**, 232–242 (2018)
35. Muthusamy, M., Safaee, S., Chen, R.: Additive manufacturing of overhang structures using moisture-cured silicone with support material. *J. Manuf. Mater. Process.* **2**(2), 24 (2018)
36. Jin, Y., Song, K., Gellermann, N., Huang, Y.: Printing of hydrophobic materials in fumed silica nanoparticle suspension. *ACS Appl. Mater. Interfaces* **11**(32), 29207–29217 (2019)
37. Huang, Y., Schmid, S.R.: Additive manufacturing for health: state of the art, gaps and needs, and recommendations. *J. Manuf. Sci. Eng.* **140**(9), 094001 (2018).
38. <http://www.custompartnet.com/wu/3d-printing>. Accessed on 9 Oct 2020
39. Lin, Y., Huang, Y.: Laser-assisted fabrication of highly viscous alginate microsphere. *J. Appl. Phys.* **109**(8), 083107 (2011)
40. Christensen, K., Compaan, A., Chai, W., Xia, G., Huang, Y.: In situ printing-then- mixing for biological structure fabrication using intersecting jets. *ACS Biomater. Sci. Eng.* **3**(12), 3687–3694 (2017)
41. Barron, J.A., Wu, P., Ladouceur, H.D., Ringeisen, B.R.: Biological laser printing: a novel technique for creating heterogeneous 3-dimensional cell patterns. *Biomed. Microdevices* **6**(2), 139–147 (2004)
42. Gruene, M., Pflaum, M., Hess, C., Diamantouros, S., Schlie, S., Deiwick, A., Koch, L., Wilhelm, M., Jockenhoovel, S., Haverich, A., Chichkov, B.: Laser printing of three-dimensional multicellular arrays for studies of cell-cell and cell-environment interactions. *Tissue Eng. Part C Methods* **17**(10), 973–982 (2011)
43. Xiong, R., Zhang, Z., Chai, W., Chrisey, D.B., Huang, Y.: Study of gelatin as an effective energy absorbing layer for laser bioprinting. *Biofabrication* **9**(2), 024103 (2017)
44. Billiet, T., Vandenhoute, M., Schelfhout, J., Van Vlierberghe, S., Dubruel, P.: A review of trends and limitations in hydrogel-rapid prototyping for tissue engineering. *Biomaterials* **33**, 6020–6041 (2012)
45. Melchels, F.P.W., Feijen, J., Grijpma, D.W.: A review on stereolithography and its applications in biomedical engineering. *Biomaterials* **31**(24), 6121–6130 (2010)
46. Watanabe, W., Tamaki, T., Itoh, K.: Femtosecond laser micromachining and biological therapy. *Laser Phys* **18**(3), 263–269 (2008)
47. Shimada, T., Watanabe, W., Matsunaga, S., Higashi, T., Ishii, H., Fukui, K., Isobe, K., Itoh, K.: Intracellular disruption of mitochondria in a living HeLa cell with a 76-MHz femtosecond laser oscillator. *Opt. Express* **13**, 9869–9880 (2005)
48. Shen, N., Datta, D., Schaffer, C.B., LeDuc, P., Ingber, D.E., Mazur, E.: Ablation of cytoskeletal filaments and mitochondria. *MCB* **2**(1), 17–25 (2005)
49. Seah, M.P.: Quantitative auger electron spectroscopy and electron ranges. *Surf. Sci.* **32**, 703–728 (1972)
50. Wallace, W., Schaefer, L.H., Swedlow, J.R.: A workingperson’s guide to deconvolution in light microscopy. *Biotechniques* **31**(5), 1076–1078, 1080, 1082 (2001)
51. Piras, D., van Neer, P.L., Thijssen, R.M., Sadeghian, H. (2020). On the resolution of subsurface atomic force microscopy and its implications for subsurface feature sizing. *Rev. Sci. Instrum.* **91**(8), 083702
52. Lekka, M., Gil, D., Pogoda, K., Dulinska-Litewka, J., Jach, R., Gostek, J., Klymenko, O., Prauzner-Bechcicki, S., Stachura, Z., Wiltowska-Zuber, J., Okon, K., Laidler, P.: Cancer cell detection in tissue sections using AFM. *Arch. Biochem. Biophys.* **518**, 151–156 (2012)
53. Binning, G., Rohrer, H., Gerber, C., Weibel, E.: Surface studies by scanning tunneling microscopy. *Phys. Rev. Lett.* **49** (1982)

54. Permjakov, N.K., Ananyan, M.A., Luskinovich, P.N., Sorokovoi, V.I., Saveliev, S.V.: Use of STM for analysis of surfaces of biological samples. *Appl. Surf. Sci.* **144–145**, 146–150 (1999)
55. de Bakker, B.I.: Single Molecule Detection on the Cell Membrane with Near-Field Scanning Optical Microscopy (2004)
56. Betzig, E., Chichester, R.J., Lanni, F., Taylor, D.L.: Near-field fluorescence imaging of cytoskeletal actin. *Bioimaging* **1**, 129 (1993)
57. Enderle, T., Ha, T., Ogletree, D.F., Chemla, D.S., Magowan, C., Weiss, S.: Membrane specific mapping and colocalization of malarial and host skeletal proteins in the *Plasmodium falciparum* infected erythrocyte by dual-color near-field scanning optical microscopy. *Proc. Natl. Acad. Sci. U.S.A.* **94**, 520 (1997)
58. Hwang, J., Gheber, L.A., Margolis, L., Edidin, M.: Domains in cell plasma membranes investigated by near-field scanning optical microscopy. *Biophys. J.* **74**, 2184.
59. Edidin, M.: Near-field scanning optical microscopy, a siren call to biology. *Traffic* **2**, 797 (1998)
60. Subramaniam, V., Kirsch, A.K., Jovin, T.M.: Cell biological applications of scanning near-field optical microscopy (SNOM). *Cell Mol. Biol.* **44**, 689 (1998)
61. Hoppener, C., Molenda, D., Fuchs, H., Naber, A.: Scanning near-field optical microscopy of a cell membrane in liquid. *J. Microsc.* **210**, 288 (2003)
62. Gheber, L.A., Hwang, J., Edidin, M.: Design and optimization of a near-field scanning optical microscope for imaging biological samples in liquid. *Appl. Optics* **37**, 3574 (1998)
63. Koopman, M.: *Nanoscale Cell Membrane Organization: A Near-Field Optical View* (2006)
64. Jores, K., Mehnert, W., Drechsler, M., Bunjes, H., Johann, C., Mäder, K.: Investigations on the structure of solid lipid nanoparticles (SLN) and oil-loaded solid lipid nanoparticles by photon correlation spectroscopy, field-flow fractionation and transmission electron microscopy. *J. Control. Release.* **95**(2):217–27 (2004)
65. Hanada, N., Hirotochi, E., Chikawa, T., Akiba, E., Fuji, H.: SEM and TEM characterization of magnesium hydride catalyzed with Ni nano-particle or Nb₂O₅. *J. Alloy Comp.* **450**, 395e9 (2008).
66. Adeola, T., Kola-Mustapha: *Microscopy of nanomaterial for drug delivery*. In *Characterization and Biology of Nanomaterials for Drug Delivery*, Elsevier, vol 20
67. Raman, S., Paul, D., Hammond, J., Bomben, K.: Auger electron spectroscopy and its application to nanotechnology. *Microscopy Today* **19**(2), 12–15 (2011)
68. Amemiya, K., Sakata, K., Suzuki-Sakamaki, M.: Development of fluorescence yield wavelength dispersive X-ray absorption spectroscopy in the soft x-ray region for time resolved experiments. *Rev. Sci. Instrum.* **91**, 093104 (2020)
69. Solti, R.C., Krishan, A.: *Advanced Flow Cytometry: Applications in Biological Research*. Springer, Medicine, Oncology & Hematology (2003)
70. Cram, L.S.: Flow cytometry, an overview. In *Methods in Cell Science*, vol. 24, pp. 1–9. Kluwer Academic Publishers (2002)
71. Flow cytometry, AAT Bioquest, Inc.
72. Biotech, M.: Flow cytometry instrumentation—an overview. *Curr Protocols Cytometry* **87**(1) (2018)
73. Radmacher, M.: Measuring the elastic properties of biological samples using AFM. *IEEE Eng. Med. Biol. Mag.* **16**(2), 5568142, 47–57 (1992)
74. Pawell, R.S., Inglis, D.W., Barber, T.J., Taylor, R.A.: Manufacturing and wetting low-cost microfluidic cell separation devices. *Biomicrofluidics* **7**(056501), 1–8 (2013)
76. Gattass, R.R., Cerami, L.R., Mazur, E.: Micromachining of bulk glass with bursts of femtosecond laser pulses at variable repetition rates. *Opt. Express* **14**, 5279–5284 (2006)
77. Linsinger, T.P.J., Roebben, G., Solans, C., Ramsch, R.: Reference materials for measuring the size of nanoparticles. *TrAC* **30**(1), 18–27 (2011)